MID-AMERICA TRANSPORTATION CENTER

Report # MATC-KSU: 453

Final Report
25-1121-0001-453

Determining the Transfer Length in Prestressed Concrete Railroad Ties Produced in the United States

Robert Peterman, Ph.D.
Martin K. Eby Distinguished Professor
Department of Civil Engineering
Kansas State University

Rob Murphy
Graduate Research Assistant
Weixin Zhao, Ph.D.
Postdoctoral Research Associate
B. Terry Beck, Ph.D.
Professor of Mechanical and Nuclear Engineering

2012

A Cooperative Research Project sponsored by the U.S. Department of Transportation Research and Innovative Technology Administration

**Determining the Transfer Length in Prestressed Concrete
Railroad Ties Produced in the United States**

Rob Murphy
Graduate Research Assistant
Department of Civil Engineering
Kansas State University

Weixin Zhao, Ph.D.
Postdoctoral Research Associate
Department of Mechanical Engineering
Kansas State University

Robert Peterman, Ph.D.
Martin K. Eby Distinguished Professor in Engineering
Department of Civil Engineering
Kansas State University

B. Terry Beck, Ph.D.
Professor
Department of Mechanical and Nuclear Engineering
Kansas State University

A Report on Research Sponsored by

Mid-America Transportation Center

University of Nebraska–Lincoln

May 2012

Technical Report Documentation Page

1. Report No.
25-1121-0001-453

2. Government Accession No.

3. Recipient's Catalog No.

4. Title and Subtitle
Determining the Transfer Length in Prestressed Concrete Railroad Ties Produced in the United States

5. Report Date
May 2012

6. Performing Organization Code

7. Author(s)
Rob Murphy, Weixin Zhao, Robert Peterman, and Terry Beck

8. Performing Organization Report No.
25-1121-0001-453

9. Performing Organization Name and Address
Mid-America Transportation Center
2200 Vine St.
PO Box 830851
Lincoln, NE 68583-0851

10. Work Unit No. (TRAIS)

11. Contract or Grant No.

12. Sponsoring Agency Name and Address
Research and Innovative Technology Administration
1200 New Jersey Ave. SE
Washington, D.C. 20590

13. Type of Report and Period Covered
Draft Report October 2009-January 2012

14. Sponsoring Agency Code
MATC TRB RiP No. 28507

15. Supplementary Notes

16. Abstract
This paper presents results from transfer length measurements on prestressed concrete railroad ties. Results are shown from the four main producers of concrete ties in the United States. Six prestressed concrete tie plants were visited by the research team to measure transfer length on ties with various mix designs and prestressing reinforcement. After all plants had been visited, a total of nine concrete-mix designs and 10 reinforcement variations were tested. Overall, 220 transfer length measurements were conducted on prestressed concrete railroad ties during the duration of this research project. This was the first coordinated effort to measure transfer lengths in concrete railroad ties ever conducted in the industry. Concrete strains were monitored using the standard Whittemore gage, as well as a non-contact procedure called laser-speckle imaging (LSI). This method to measure transfer lengths was developed at Kansas State University (KSU).
Ties measured using the Whittemore gage were sent back to the civil engineering structural laboratory at KSU for the long-term measurement of transfer lengths.

17. Key Words
Prestressed Concrete Railroad Ties, Crossties, Indented Wire Bond, Indented Strand Bond, Transfer Length, Transmission Length

18. Distribution Statement

19. Security Classif. (of this report)
Unclassified

20. Security Classif. (of this page)
Unclassified

21. No. of Pages
254

22. Price

Table of Contents

List of Figures

List of Tables

List of Abbreviations

American Railway Engineering and Maintenance-of-Way Association (AREMA)
Average Maximum Strain (AMS)
Detachable Mechanical (DEMEC)
Federal Highway Administration (FHWA)
Kansas State University (KSU)
Laser-Speckle Imaging (LSI)
Linear Variable Differential Transformer (LVDT)
Mid-America Transportation Center (MATC)
Self-Consolidating Concrete (SCC)
Standard Deviation (Std. Dev.)
Universal Testing Machine (UTM)
Water-to-Cementitious Ratio (W/C)

Acknowledgements

I would like to thank Dr. Robert Peterman for his extensive help on this project. His knowledge of prestressed concrete, as well as his assistance during the long hours at each plant, helped tremendously. I would also like to thank Dr. Kyle Riding and Dr. Asad Esmaeily. Many thanks also go out to the Mid-America Transportation Center (MATC) for funding this project.

I would also like to thank all of the prestressed concrete tie plants for their cooperation. Without their help, this project would not have been possible. I would especially like to thank Pelle Duong and Vince Petersen from LB Foster/CXT Concrete Ties, Steve Mattson from voestalpine Nortrak Inc., Rusty Croley and Tom Waskosky at Rocla Concrete Ties, and Scott Craig and Ed Sullivan at KSA Concrete Ties. These individuals assisted our research team during visits to each of their plants, and their help was much appreciated.

I would also like to recognize the graduate students that assisted with this research project: Steven Hammerschmidt, Narendra Bodapati, Matthew Arnold, Brandon Bortz, and Joseph Holste; as well as Dr. Weixin Zhao, postdoctoral research associate at Kansas State University, for all his help throughout this project. These individuals took time out of their schedules to help with the research at the various plants. I would also like to thank civil engineering students Rachel Spicer and Becca Greif for their help with the long-term transfer length measurements and shop work. Lastly, I would like to thank research technologist Ryan Benteman for all of his help with machine work and troubleshooting.

Disclaimer

The contents of this report reflect the views of the authors, who are responsible for the facts and the accuracy of the information presented herein. This document is disseminated under the sponsorship of the Department of Transportation University Transportation Centers Program, in the interest of information exchange. The U.S. Government assumes no liability for the contents or use thereof.

Abstract

This project presents the results from transfer length measurements on prestressed concrete railroad ties. Results from the four main producers of concrete ties in the United States are shown. Six prestressed concrete tie plants were visited by the research team to measure transfer length on ties with various mix designs and prestressing reinforcement. After all plants had been visited, a total of nine concrete-mix designs and 10 reinforcement variations were tested. Overall, 220 transfer length measurements were conducted on prestressed concrete railroad ties during the duration of this research project. This was the first coordinated effort to measure transfer lengths in concrete railroad ties ever conducted in the industry.

Concrete strains were monitored using the standard Whittemore gage, as well as a non-contact procedure called laser-speckle imaging (LSI). This method to measure transfer lengths was developed at Kansas State University (KSU).

Ties measured using the Whittemore gage were sent back to the civil engineering structural laboratory at KSU in order to monitor their long-term transfer lengths. After a certain period of time, the ties were load-tested according to the American Railway Engineering and Maintenance-of-Way Association (AREMA) loading specifications of the rail-seat positive moment test.

Chapter 1 Introduction

1.1 Background

Railroad ties are structural members that hold the steel track in place on railroad lines. Typically the ties are made out of wood; however, concrete ties have become increasingly popular in the United States over the past 25 years. Concrete ties have many environmental and economic benefits over wood ties. Wood ties are normally treated with creosote to eliminate their susceptibility to rot and decay. However, one disadvantage of creosote is that it is a flammable material. The absence of creosote is a desirable feature of concrete ties, as is their longer life expectancy. Further, concrete ties have more mass, and are less likely to move under thermal and mechanical loads induced on the steel rails. This rigidity increases train fuel economy and makes for a smoother ride along the track. Concrete ties also provide excellent gauge holding power and lateral load resistance.

Concrete ties have become the preferred choice for many railway lines in the Midwest, where heavy freight movement occurs. This is especially true for extreme tonnage lines, which are the primary routes used to transport coal from the Powder River Basin to the rest of the country.

To meet the structural demands imposed by intense dynamic loading conditions found on the railroad, concrete ties are produced by prestressing the members. By prestressing each individual tie, large compressive forces are introduced into the concrete member. This compressive force increases the load-carrying capacity. However, for prestressed concrete ties to perform efficiently, the prestressing force must be fully introduced into the tie at a location closer to the tie end than the rail load is applied. In most cases, the rail-seat is 21 in. from the end of the tie; however, in some specialty ties, such as those used in railway switches, the rail-seat is 24 in.

from the end of the tie. The length required to transfer the prestress force into the concrete is known as the “transfer length.”

Because concrete ties are relatively short and the rail seat is close to the end of the member, adequate wire or strand bond is critical to tie performance. For this reason, most concrete tie producers utilize indented wire or indented strand, as opposed to the traditional seven-wire, smooth prestressing strands. Although little information is known about the various indented-wire and indented-strand patterns, there is general agreement that indentations improve bond performance between the steel and concrete. This feature of indentations is thought to reduce the transfer length of prestressed concrete ties.

However, because the use of indented prestressing reinforcement is so limited, there are no recommended design assumptions for transfer length in the current U.S. design codes. Also, there is currently no standardized indention pattern (shape, size, depth of indent, etc.) used by all indented-wire manufacturers. This lack of knowledge regarding prestressing reinforcement causes concrete tie producers to use a variety of indented strands and wires in their day-to-day operations.

Since the transfer length is critical to the performance of prestressed concrete ties, this project involved taking transfer length measurements at all four major concrete tie producers in the U.S. This was the first coordinated effort to measure the transfer length of concrete ties in the industry. Taking transfer length measurements at all producer plants helped quantify differences in transfer lengths that currently occur with indented strands and indented wires for a variety of concrete mixes. The concrete tie producers, where transfer lengths were measured, are listed below, in alphabetical order by city:

Cheyenne, Wyoming – voestalpine Nortrak Inc.

Denver, Colorado – Rocla Concrete Ties

Grand Island, Nebraska – CXT Concrete Ties

Sciotoville, Ohio – KSA Concrete Ties

Spokane, Washington – CXT Concrete Ties

Tucson, Arizona – CXT Concrete Ties

Due to the sensitive nature of the information contained in this report, each of the above companies was assigned a random letter corresponding to its results. However, each participating company was made aware of its own letter designation and results. The lettering was random, and does not reflect the alphabetical list above or the order in which each plant was visited.

Transfer length measurements were conducted on concrete ties using a Whittemore gage, as well as a new, non-contact technique utilizing laser-speckle imaging (LSI). This method was developed at Kansas State University (KSU).

1.2 Plant Information

The six prestressed concrete tie plants were visited by the research team over the course of a 15-month period. After traveling to all of the plants, a total of nine concrete-mix designs and 10 reinforcement variations were tested. Some of the participating concrete tie producers wished to view changes in transfer length that occurred when the concrete-mix design was altered or the reinforcement was changed.

1.2.1 Plant A

One concrete-mix was tested using two different reinforcements. Over the course of two days, 16 transfer lengths were recorded using the Whittemore gage, and 24 transfer lengths were recorded using LSI.

1.2.2 Plant B

Two different concrete-mixes were tested using a single reinforcement in all the ties. Over the course of two days, 12 transfer lengths were recorded using the Whittemore gage, and 27 transfer lengths were recorded using LSI.

1.2.3 Plant C

Measurements at Plant C were taken on two separate occasions. During the first visit, six transfer lengths were measured using the Whittemore gage. During the second trip, seven transfer lengths were measure using LSI. One concrete-mix was tested using one type of reinforcement in all ties.

1.2.4 Plant D

One concrete-mix was tested using two different reinforcements. Over the course of two days, 12 transfer lengths were recorded using the Whittemore gage, and 50 transfer lengths were recorded using LSI.

1.2.5 Plant E

Two concrete-mixes were tested using a single type of reinforcement. Over the course of two days, ten transfer lengths were recorded using the Whittemore gage, and 21 transfer lengths were recorded using LSI.

1.2.6 Plant F

Two different concrete-mixes were tested using three different reinforcements. Over the course of two days, 12 transfer lengths were recorded using the Whittemore gage, and 23 transfer lengths were recorded using LSI.

1.3 Scope

Chapter 2 reviews literature that discusses transfer length measurements and factors that affect the transfer length of prestressed concrete members. Chapter 3 explains how the LSI device works, and discusses research conducted to get the LSI device to work on concrete ties**.** Following, chapter 4 discusses procedures used to measure transfer length; both the Whittemore method and LSI method are explained in detail. Chapter 5 provides details on mix designs and the number of reinforcements each plant tested in the prestressed concrete ties. Next, chapter 6 reports transfer length values obtained from each plant; the average transfer length, standard deviation, and minimum and maximum values are shown for each mix design from each of the six plants. Chapter 7 reports results from the rail-seat positive moment test on the concrete ties sent back to KSU for long-term transfer length measurement; results from this test are correlated with transfer length values from each of the ties. Finally, chapter 8 discusses the conclusions and recommendations developed from this research project.

Chapter 2 Literature Review

Oh and Kim (2000) reviewed the important parameters affecting the transfer length of prestressed concrete members. The authors pointed out that the ACI 318 design code considers only the diameter of prestressing strands and intensity of the prestress force to calculate transfer lengths. The authors took the strand diameter, prestress force, concrete strength, concrete cover around the steel, and time-dependent effects such as creep and shrinkage into consideration when determining transfer lengths. The experiment consisted of 36 prestressed beams with 200 mm depths and 3000 mm lengths. Beams were cast with both mono strand and twin strand, and the compressive strength, bottom steel cover, and strand diameter were altered to view the difference in transfer length values. The concrete compressive strengths at transfer were 35 and 45 MPa, and the prestressing steels used were uncoated, low-relaxation, stress-relieved, seven-wire strands. The strands used were 12.7 mm and 15.2 mm in diameter. Detachable mechanical (DEMEC) strain gage points were mounted 50 mm apart along the length of each beam at strand height. Transfer lengths were measured using a DEMEC gage to record the distance between points before and after transfer of the prestress force. The data was smoothed by averaging values over three consecutive gage points, and transfer lengths were determined using the 95% average maximum strain method. The authors found that transfer lengths decreased with an increase in concrete compressive strength. Also, transfer lengths increased as the concrete cover decreased. The ACI code assumes a linear relation between strand diameter and transfer length. This testing proved that transfer length increases with an increase in strand diameter; however, the increase is not linear as assumed by the ACI code. The authors also found that sudden release of prestress force at the cut end resulted in higher transfer lengths than at the dead-end. The live-end transfer lengths were found to have approximately 15% larger transfer length values than that of dead-ends. It was also determined that an increase of strand spacing resulted in shorter transfer lengths. The authors determined that transfer length values increased about 5% over 90 days due to creep effects.

Steinberg et al. (2001) used three pretensioned concrete beams to monitor concrete strains during the cutting of the strands. The three beams were 32 ft long and had a 5½ x 23-in. cross section. The concrete used in the beams was 6000 psi, and each beam had four, ½-in. diameter, uncoated, seven-wire strands. The strand pattern consisted of two rows of two strands spaced 2 in., both horizontally and vertically. A 4.375 in. strand eccentricity was used. To measure the transfer length, the authors used end-slip measurements of the strands, internal strains determined by strain gages, and DEMEC points mounted on the surface of the beam to measure surface strains. End-slip values were recorded using linear variable differential transformers (LVDT). Strain gages were embedded and placed on the surface of the beams to monitor concrete response during transfer. The DEMEC points were mounted at each end of the beam at a 2 in. spacing. The points extended from the end of the beam to a location that was 8 ft from the end. A gage distance of 10 in. was used, and the points were manually measured twice by different persons to eliminate error. Average transfer lengths on Beam 1, using the DEMEC points, were 40 in. on the live-end and 43 in. on the dead-end. Beam 2 transfer lengths were 34 in. on the live-end and 48 in. on the dead-end. DEMEC points were not mounted on Beam 3. Transfer length values using LVDTs to monitor end slip were 27 in. on the live-end and 29 in. on the dead-end for Beam 1. For Beam 2, the live-end transfer length was 45 in., and on the dead-end it was measured as 40 in. The live-end transfer length for Beam 3 was 46 in., and the dead-end was 42 in. Both of these measurement procedures resulted in higher transfer length values than the calculated 25 in. transfer length. Using strain gages, it was determined that longitudinal tensile strains of 50 to 150 microstrain existed due to the release procedure. The authors determined that longitudinal tensile strains caused by the release procedure can be significant enough to cause cracking at the end of the members.

Russell and Burns (1997) investigated the ability of a 15.2 mm prestressing strand to produce an acceptable transfer length in concrete beams. This research was conducted in response to the Federal Highway Administration (FHWA) disallowing the use of 15.2 mm strands for pretensioned applications due to extremely large transfer length values determined through research at North Carolina State University in 1986. Eight beams were cast at the Ferguson Structural Engineering Laboratory at The University of Texas at Austin, using 12.7-mm, seven-wire, low-relaxation strands. Ten beams were cast using 15.2 mm strands. Each beam had a rectangular cross section 102 mm wide and 127 mm tall. No transverse reinforcement was used in the beams. The concrete-mix was specified to have a release strength of 28 MPa and a 28-day strength of 41 MPa. To determine the transfer length of the specimens, DEMEC points were mounted longitudinally across each beam. The distance between the points was measured before detensioning the strand, and measured again after detensioning. The DEMEC readings were taken by two people to reduce error. The transfer length was taken as the intersection of the strain profile and the 95% average maximum strain (AMS). The researchers determined the AMS did not significantly change if a few data points were excluded from the average. The authors determined an average transfer length at the cut end of the beam, with the 12.7 mm strand, was 978 mm (38.5 in.). The average transfer length at the dead-end was 730 mm (28.7 in.). At the cut end of the beam with the 15.2 mm strand, the average transfer length was 1,020 mm (40.2 in.). The average transfer length at the dead-end was 998 mm (39.3 in.). It was determined that, on average, for the 12.7 mm strand, transfer lengths on the cut ends were 34%

larger than transfer lengths measured on the dead-ends. Two of the beams made by the researchers were damaged at the release of the prestress force. Longitudinal cracks were produced at the cut end of the beams due to the dynamic shock of the sudden release. The authors concluded that a new transfer length expression was needed to replace the existing assumption of $50d_b$, and that the recommended expression to estimate transfer length should be changed to $80d_b$ to provide a greater factor of safety. The authors also concluded that the 15.2-mm strand could effectively transfer the prestressing force into the concrete, and use of the 15.2-mm strand was recommended for pretensioned uses.

Oh et al. (2006) developed a theoretical analysis of the transfer length of pretensioned concrete members. The authors noted the current design code considered only prestress force and strand diameter. In actuality, many factors affect transfer length, such as concrete strength and steel cover. The author's theory considered the concrete surrounding the steel strand as a hollow cylinder and the steel strand as a solid cylinder. Due to Poisson's ratio, the steel strand would increase in diameter as the prestressing force was relieved. The compatibility expression developed by the authors uses Poisson's ratio, and is imposed at the steel-concrete interface. This compatibility expression is used hand-in-hand with a three-dimensional equilibrium equation that members must satisfy. The equilibrium equations are solved successively throughout the member in the longitudinal direction. Solving these equations generates a strain development curve starting from the end of the concrete member. Using these strain development curves, the authors were able to determine transfer length values. Once the theoretical expressions were determined, the authors compared their calculations to actual transfer length measurements. Transfer lengths were determined from concrete members with various concrete strengths, strand spacings, strand diameters, and strand covers. The theoretical transfer lengths and experimental measurements were comparable. For the majority of the measurements, the theoretical transfer lengths fell between the dead-end measurements and live-end measurements of the beams. This data proves that the theoretical determination of the transfer length can be applied to various beam designs.

Krishnamurthy (1972) determined a relationship between transmission length and diameter of prestressing tendons based on research conducted by present tests as well as past data. Tests conducted by the author included taking transmission lengths on 80 I-sections using 5-mm diameter indented wires. Transmission lengths were determined from the strain profiles using a DEMEC strain gage. Strength of the concrete and method of transfer were varied to obtain more data. Methods of force transfer included a gradual force release and a sudden release of the prestress force into the concrete. Tests conducted by British Railways were carried out on 2 mm and 5 mm plain wires. Concrete strengths at transfer ranged from 270 to 550 kg/cm^2. Tests conducted at Leeds University included recording transmission lengths on 2 mm, 5mm, and 7-mm plain wire. Rusch and Rehm conducted tests on various German-produced wires. The wires had diameters of 3, 4, and 5 mm. These tests varied the concrete strength, level of prestress, method of force transfer, and type of wire. Wire types used included ribs and indents. Arthur and Ganguli included taking 19 transmission length measurements using 5 mm diameter wire. These tests used the Belgian B-type indented wire, and concrete strength ranged from 158 to 435 kg/cm^2. The force transfer in all of these measurements was gradual. Based on all data gathered by past researchers, as well as present data gathered by the author, the author determined some relationships between transmission length and diameter of the wires. For wire diameters of 2, 5, and 7 mm, under gradual-force release conditions, the transmission length can be determined from the following equation:

$$l_t = 100d \quad (2.1)$$

where,

d is the diameter of the wire.

For a wire diameter of 5 mm and a sudden release of the prestress force, the transmission length can be calculated using the following equation:

$$l_t = 120d \quad (2.2)$$

where,

d is the diameter of the wire.

The author stated that further research is needed to determine an expression for other wire diameters. For 9.52, 12.70, and 17.80 mm diameter strands under gradual-force transfer conditions, the following equation can be used to determine transmission length:

$$l_t = 10d + 1.2d^2 \quad (2.3)$$

where,

d is the diameter of the strand.

The author stated that further research was needed to determine an expression for sudden transfer-release situations.

Rose and Russell (1995) investigated the feasibility of correlating the bond strength from pull-out tests to the measured transfer length in prestressed concrete members. The authors noted that several previous studies had explored many different variables of prestressed concrete members, including concrete strength, strand spacing, strand diameter, etc. Although past researchers attempted to maintain consistency among their tests in order to obtain similar transfer length measurements, transfer length data was consistently scattered. Rose and Russell determined the surface condition of the strand could have been the reason past researchers obtained scattered data. To compare transfer length to the bond performance of pull-out tests, the authors obtained strand samples from three different manufacturers, A, B, and C. Strand from manufacturers A and B was not modified in any way before testing. Strand from producer C was tested with four different surface conditions: as received, weathered, lubricated, and cleaned. To weather strand C, the authors cleaned the surface with muriatic acid and rinsed with water. The strand was then placed in a damp environment for three days to rust. The lubricated strand was cleaned with muriatic acid, rinsed with water, dried, and finally sprayed with silane. The cleaned strand was cleaned with muriatic acid, rinsed with water, and dried with paper towels. For each strand surface condition, three prestressed beams were poured to measure the transfer length. Also, a large pull-out specimen was poured containing 12 strands of the wire being tested. Finally, two tensioned pull-out specimens were made for each wire type. To measure transfer length, the authors used a DEMEC gage to measure surface strain on each side of the concrete beam at the height of the prestressing steel. Each beam was 17 ft long and had two strands. For the pull-out tests, 6 ft strands were laid out in a grid 9 in. apart. The large pull-out block was 4 ft x 3 ft x 2 ft. The tensioned pull-out tests consisted of placing the strand through a 5.5 in. x 5.5 in. x 12 in. concrete specimen. The tension was reduced at one end of the specimen. This caused the strand to slip in the concrete. The strand slip and tensile forces were measured at each end of the concrete specimens. After obtaining the transfer length measurements, direct pull-out stress, and tension pull-out data, the authors commented that a statistical analysis will be performed. If the researchers find a correlation between pull-out strengths and transfer length, a standard and repeatable test could be developed to determine the bond performance of prestressing strand.

Srinivasa et al. (1977) studied the transmission length of ribbed bars and plain wires in pre-tensioned concrete. The authors focused specifically on the transfer mode of the stress and the steel surface characteristics. The concrete compressive strength and prestressing force were kept constant during the testing. For transmission length measurements, eight concrete specimens measuring 10 cm x 10 cm x 250 cm were cast. Four of these specimens contained four, 5 mm diameter plain wires; the other four beams contained two, 10 mm diameter ribbed wires. All of the beams were concentrically loaded. To view the effects the method of transfer had on transmission length, some of the beams were gradually relieved of their prestress, and some were released suddenly. To measure surface strains of the concrete, a Pfender mechanical gage was used. The authors determined that the transmission length of the specimens occurred at a point where 80% of the maximum concrete strain had occurred. It was determined that the two specimens with 5 mm plain wire and a sudden release had an average transmission length of 85 cm. The two specimens with 5 mm plain wire and a gradual release had an average transmission length of 62 cm. The specimens with the ribbed bars and a gradual release had an average transmission length of 33 cm, and the specimens with a sudden release had an average transmission length of 30 cm. The authors concluded that ribbed bars achieved a high bond by mechanical interlocking without any significant change of shape. The plain bars, on the other hand, showed an enlargement of diameter toward the specimen ends, a phenomenon called the

Hoyer effect. It was also noted that the method of prestress transfer significantly changed the transmission length of specimens cast with plain bars. Transmission lengths of the ribbed bars, however, were comparable between the two methods of prestress transfer.

Hanna (1979) discussed prestressed concrete ties used in North American railroads. The author explained the various methods of tie fabrication, design considerations, and material requirements for ties. Laboratory testing of ties and the advantages of prestressed concrete ties were also discussed. According to the author, concrete ties are advantageous over wood ties because concrete ties are more economical and their structural properties add considerably to the overall performance of the track structure. The track structure includes everything from the steel rails, to ties, fastenings, and ballast. It was noted that the first use of prestressed concrete ties in America was in 1960, when 500 ties were installed on the Atlantic Coast Line Railroad and 600 ties were installed on the Seaboard Air Line Railroad. However, the first major use of prestressed concrete ties was in 1966, when 74,000 were installed on the Florida East Coast Railway. According to the author, there are three methods of producing prestressed concrete ties: long-line, stress-bench, and individual-form methods. The long-line method consists of several forms set up end to end on a prestressing bed. These beds can span a few hundred feet, depending on the producer. Prestressing tendons are tensioned by two abutments placed on the ends of the bed. Once the tendons are tensioned, concrete can be poured in the forms. After the concrete cures, the abutments relieve the stress in the tendons and the ties are individually cut. The stress-bench method uses mobile benches that accommodate forms of four or five ties. These benches can move in both longitudinal and transverse directions. Movement of the benches allows operations such as preparation, tensioning of the tendons, placement and vibration of the concrete, and curing to be conducted at different stations. In the individual-form method, the tendons are tensioned against the forms. According to the author, the long-line method is used the most in North America due to the fact that fewer man hours are required to produce a concrete tie; it also provides better uniformity in tie quality, and a larger quantity of ties can be produced. The author goes on to describe the materials necessary to produce prestressed concrete ties. Use of high-strength concrete must be used in ties because the ties can be detensioned at a much earlier time than with conventional concrete; prestressing losses are also reduced, and the high flexural capacity improves resistance to cracking under service loads. To obtain high-strength concrete and to have freeze-thaw durability, the ties must follow these specific guidelines:

1. Maximum size of the coarse aggregates should not exceed ¾ in.
2. Cement content should be greater than 650 pounds per cubic yard.
3. Water-cement ratio should be less than 0.4. Water-reducing admixtures should be used to achieve this number.
4. Vibration should be used to ensure proper consolidation of the concrete.
5. Air-entraining admixtures should be used to improve freeze-thaw resistance.

The prestressing tendons used in concrete ties should obtain adequate bond with the concrete to reduce the transfer length. Maximum prestress should transfer before the rail seat region. To achieve this, the prestressing tendons should adhere to the following qualities:

1. Strands should have a strength of 225 ksi or more and be stress-relieved.
2. Diameter of the tendons should not exceed 3/8 in.
3. Tendons should be indented wires or indented wire strands.

The author noted that under critical loading, tensile stresses occur on the top surface at the center of the tie and at the bottom surface at the rail-seat locations. To accommodate these tensile stresses, the center of the ties has a more shallow section than the ends. This permits locating the prestressing strands towards the tensile surface at both locations. The author then described the laboratory testing conducted on prestressed concrete ties, as follows:

1. The rail-seat moment test evaluates the ties' ability to carry a specified positive bending moment at the rail seat.
2. The tie-center moment test evaluates the ties' ability to carry a specified negative bending moment at the center.
3. The bond development test evaluates the ability of the tie to be overloaded without the prestressing tendons slipping.
4. The tie-center moment and torsion test evaluates the ties' performance when a combination of a bending moment and torque are applied at the tie center.
5. The repeated-load test evaluates the ability of the tie to withstand repeated loading.

Finally, the author described the advantages of using concrete ties over conventional wood ties. The advantages are that they provide better stiffness in the track; they settle more uniformly and thus provide a smoother, safer ride; the track maintains alignment for a longer period of time and thus reduces the risk of derailment; the estimated service life is twice as long as wood ties; there are fewer irregularities among the ties; and they have a lower life-cycle cost than wood ties.

Barnes et al. (2003) discussed the variables that affect the transfer length of prestressed concrete members. The authors noted that concrete strength has a direct effect on the transfer length because the strand introduces radial compressive stresses into the concrete via the Hoyer effect. This causes a pressure between the concrete and strand, and the greater the concrete strength, the greater the bond anchorage. The authors also determined from previous research that transfer length increases over time due to creep, shrinkage, and relaxation of the strand. The authors stated that "some time-dependent softening of the concrete grip on the tendon is possible due to stable radial crack growth and stress redistribution." Another variable that affects transfer length is the strand surface condition. Research has shown that bond performance is increased when the strand has surface weathering. This is caused by an increase in frictional resistance. Although weathered strand produces shorter transfer lengths, previous researchers argue that using weathered strand is impractical due to the fact that it is difficult to evaluate the degree of rust needed. Also, prestress plants process the strand so quickly that weathering of strand is unreasonable. The final variable commented upon by the authors that affects transfer length is the method of prestress release. Previous studies show that sudden prestress release results in larger transfer lengths. This is caused by the dynamic effects of the transfer of energy from the strand to the concrete. To test these variables affecting the transfer length, the researchers casted 36 full-scale AASHTO Type 1 girders. The beams had varying strand surface conditions, concrete strengths, and prestress release methods. Two strand-cutting procedures were used for this study: one method cut the strand on each end of the prestress member at the same time, and the second method cut only one end of the strand. This test created a sudden release in some members and a gradual release in others. The transfer length of the members was determined using the 95% average maximum strain method. Gage points were placed at 1.97 in. spacing on each side of each end of the beams. All measured transfer lengths were less than the AASHTO LRFD value of 60 bar diameters, and only three of the 85 transfer lengths were greater than the 50 bar diameter value prescribed in ACI 318-02. It was determined the transfer lengths increased approximately 10 to 20% over time. Almost all of the increase occurred in the first 28 days after release. Average transfer length values of the weathered strand were shorter than that of the clean, bright strand. However, the weathered strand provided inconsistent measurements; some of the transfer lengths were even larger than that of the clean strand. It was concluded that surface weathering of the strand could not be relied upon to reduce the transfer length. The authors also determined the method of prestress release had no significant impact on specimens with a concrete release strength greater than 7000 psi.

Staton et al. (2009) investigated the transfer length of beams cast with self-consolidating concrete (SCC), comparing their results to beams cast with conventional concrete. The research team cast 20 prestressed beams; 14 of them were cast using two different SCC mixes, and the remaining six used conventional concrete. Each beam was 18 ft long, 6.5 in. wide, and 12 in. tall. Two 0.6-in. diameter, 270 ksi, low-relaxation seven-wire strands were in each beam, and were located 2 in. from the bottom of the beams. The strands were relieved of their stress using a slow-release method. DEMEC points were glued at 4-in. spacing along both sides of the beam at the center of gravity of the strand. Distance between these points was measured using a DEMEC gauge before and after detensioning to monitor the change in strain. Measurements were taken at three days, five days, seven days, 14 days, and 28 days after release to view the increase of transfer length over time. The research group used the 95% average maximum strain (AMS) method to determine the transfer length of each beam. At 28 days, the average transfer length of the first SCC mix at the live-end was 21.8 in., with a standard deviation of 3.8 in., and the dead-end was 21.1 in., with a standard deviation of 3.8 in. For the second SCC mix, the average transfer length at the live-end was 19.6 in. with a standard deviation of 3.6 in., and the dead-end was 19.8 in. with a standard deviation of 4.1 in. The average transfer length for the conventional concrete-mix at the live-end was 24 in., with a standard deviation of 2.9 in., and the dead-end was 23.5 in. with a standard deviation of 4.4 in. From these results, the research group concluded there were no clear correlations between the live and dead-ends of the beams. Previous researchers had found that live-end transfer lengths were larger than dead-end measurements. The research group also found their results were considerably lower than the transfer lengths estimated by ACI 318-05 and AASHTO LRFD. The ACI 318-05 equation estimated the transfer length to be 30 in., based on the equation $50d_b$, where d_b is the diameter of the prestressing strand. The AASHTO LRFD equation estimated the transfer length to be 36 in., based on the equation $(1/3)f_{se}d_b$, where f_{se} is the stress of the steel after all losses. Concrete strength at the transfer of prestress ranged from 6.8 ksi to 9.9 ksi. The researchers plotted the transfer length values versus the concrete strength at transfer. Previous research had shown that larger concrete compressive strengths caused the transfer lengths to be lower. However, the researchers found no correlation between compressive strength and transfer length.

Peterman (2007) investigated strand bond as a function of cast depth and concrete fluidity on prestressed concrete members. The study consisted of three parts. During the first part, six prestressed concrete plants were visited, and each cast identically-sized members that were load tested to failure. One beam used for this project was 10 in. wide and 15 in. deep. The prestressing strand was located 13 in. from the top of the member. The second beam had a cross section identical to the first member; however, the strand was located 2 in. from the top of the member. The last member was 8 in. wide and 6 in. deep, and the prestressing strand was located 4.5 in. from the top of the member. All steel used was ½ in. diameter, 270 ksi unweathered strand, and was sent to each plant prior to casting. From the first test, it was found that the transfer length was reduced as the strand depth increased. The second part of the test consisted of casting two beams of different cross sections with strand located at various heights. The beams were 4 in. wide. One beam was 28 in. deep and had one strand placed at 2 in. from the top of the member.

Four more strands were placed in this member at 6 in. increments; leaving 2 in. of cover below the bottom strand. The second beam was 16 in. deep, and had one strand placed 2 in. from the top of the member. Two more strands were placed at 6 in. increments; leaving 2 in. of cover below the bottom strand. These test specimens were specifically designed to decouple the effects of strand height from the top and bottom of the specimen. For these members, both conventional and high-fluidity concrete mixtures were tested. A coefficient of determination R^2 of 0.83 was found between the measured transfer length and the amount of concrete placed over the strand. This indicated that the primary variable contributing to the observed top-strand effect was the amount of fresh concrete cast above the strands. For the third and final test conducted for this study, prestressed concrete members were cast that were 4 in. deep and 24 in. wide. Two strands were placed 2.5 in. from the top and six in. from each side. The objective of this test was to load test the specimens and monitor end-slip of the strands. Embedment lengths of 30, 45, and 60 in. were tested by varying panel lengths. Both conventional and high-fluidity (SCC) mixes were tested. After load testing, it was determined that the nominal moment capacity of SCC panels averaged 30% lower than the conventional mix. Also, transfer lengths of the SCC panels averaged 30% longer than the conventional mix. In conclusion, the author determined that the amount of fresh concrete above strands was more influential to bond than was concrete below the strand. Also, it was found that longer transfer lengths were introduced as the fluidity of concrete increased.

Kaar and Hanson (1975) tested 108 prestressed concrete beams under simulated loading similar to that experienced on railroad crossties. These tests were conducted to provide an indication of the effect of repeated loading near the end of cracked prestressed members. Strand surface condition and prestress release method were varied to produce members with a wide range of transfer lengths. All beams had a 3.5 in. by 7 in. cross section, and a single 3/8 in., seven-wire strand at a depth of 4 2/3 in. Each specimen was 8 ft 6 in. long, and a load was applied at a distance of 18, 21, 24, or 27 in. from the end. To measure the transfer length of each specimen, brass points were attached at 5 in. spacings along the beam at the steel depth. A Whittemore gage was used to measure the length between points before and after detensioning. For this test, the transfer length was defined as the distance required for the measured strain to build up a 95% average plateau strain. Transfer lengths evaluated for smooth strand and a gentle release ranged from 12-37 in. Transfer lengths evaluated for smooth strand and a sudden release ranged from 17-54 in. Transfer lengths evaluated for lightly rusted strand and a sudden release ranged from 9-21 in. Transfer lengths evaluated for sand-blasted strand and a sudden release ranged from 11-28 in. A cracking load of 5,800 lb. was determined for a beam without a crack former. At this load, a crack of approximately 0.001 in. was developed. A ram force was initially applied to the members until a desired load level was reached. Pulsating loads were then applied at a rate of 250 cycles per minute, with the load varying in a sine wave from 10-100% of the planned maximum load. After load testing all specimens, the authors concluded that in order to obtain a bond fatigue life of three million cycles under a severe loading causing an existing crack to open more than 0.001 in., the load could not be applied nearer the end than 2.2 times the transfer length. Also, it was found that weathered strand could sustain a load at a distance equal to the transfer length. The authors recommended that a tie be designed so that any existing crack would not be opened by expected repeated loading. Moreover, concrete ties should be constructed with prestressing tendons that produce short transfer lengths. Transfer lengths can be reduced by roughening the strand or by using small-diameter strand.

Larson et al. (2007) investigated the bond performance of SCC for prestressed bridge girders. Because ACI 318 and AASHTO design requirements did not address the use of SCC in pretensioned applications, various prestressed SCC members were produced, and the researchers measured the transfer length and development length. Twelve single-strand development-length specimens with different embedment lengths were fabricated and tested. These specimens used two cross sections so that the "top-strand" effect could be evaluated. The first cross section had dimensions of 8 in. by 12 in., and a prestressing strand placed at a depth of 10 in. The top-strand effect beams had dimensions of 8 in. by 24 in., and strand was placed 22 in. from the bottom of the member. End-slip measurements were used to evaluate the transfer length of each member. For all beams with strand located at the bottom, no members had a longer transfer length than was assumed by AASHTO and ACI. Transfer lengths of these members increased approximately 10-20%. Transfer lengths of strand located at the top increased about 40-45%. These large increases were attributed to the top-strand effect. All flexural tests resulted in member failure due to strand rupture. In every case, the failure moment exceeded the calculated nominal moment capacities by 10-20% for an embedment length of 6 ft 1 in. Specimens with an embedment length of 4 ft 10 in. had an increase of 25-35% in nominal capacity. The authors concluded that the current ACI 318 and AASHTO equations for strand development length were conservative for the SCC mix and specimen geometry used in the study. Transfer lengths estimated from 21-day strand end-slip measurements were in accordance with AASHTO and ACI 318. The average transfer lengths for the top-strand beams were approximately 50% larger than transfer lengths measured for bottom-strand members.

Chapter 3 Implementation of the Laser-Speckle Imaging Device

This section discusses how the LSI device functions, and how the LSI technique was made robust enough to function in the harsh conditions of the concrete tie plants. The LSI device works well in laboratory conditions, and is very accurate. However, the concrete tie plants introduce water, dust, and temperature effects that change surface conditions of the concrete that are not present in laboratory conditions.

3.1 Laser-Speckle Methodology

As digital-image recording and processing have become widely available, optical speckle techniques have evolved into powerful tools for the measurement of surface strain. When utilizing optical speckle, almost any rough surface can be used, with the advantage that minimal surface preparation is needed (Zhao 2012).

Speckle is generated by illuminating a rough surface with a coherent light source, as shown in figure 3.1. The random reflected waves interfere with each other, resulting in a grainy image, as shown in figure 3.2.

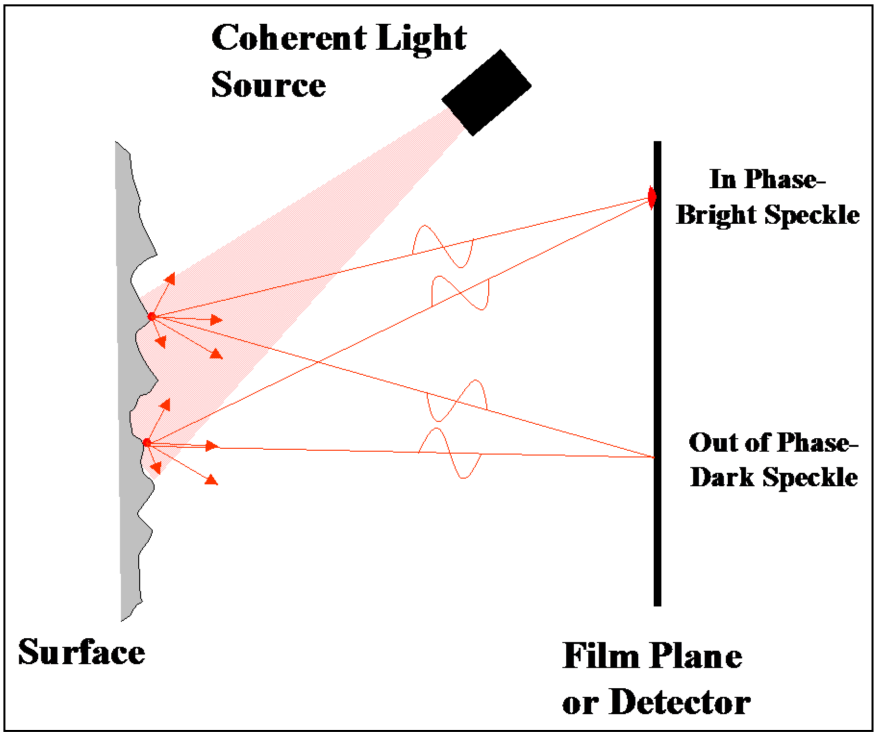

Figure 3.1 Illustration of the laser-speckle concept (Zhao 2011)

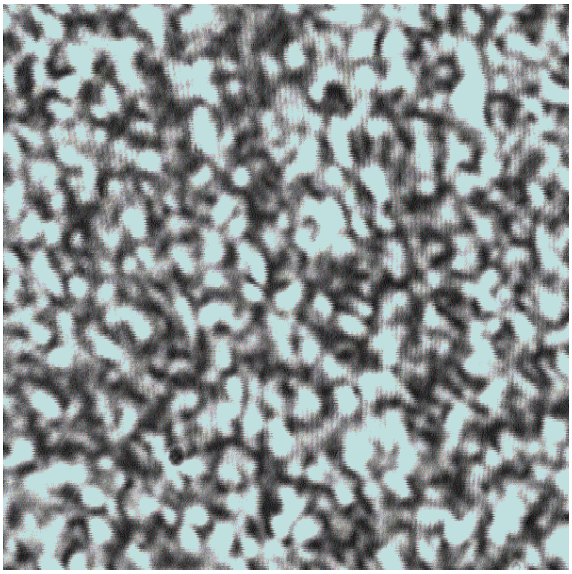

Figure 3.2 Image of speckle pattern generated by concrete surface (Zhao 2011)

The speckle pattern of the member's surface serves as a "fingerprint" of the unique location (Zhao 2012). As the member undergoes deformation due to stress increases, the speckle pattern will also move. This deformation in the surface can be converted to a change in strain by measuring the speckle-pattern movement.

To detect surface strain, the grainy speckle-pattern image is recorded before stress is applied to the member, and once again after the member undergoes its stress deformation. The deformation or displacement components can then be extracted by comparing the shift of the speckle patterns before and after deformation. This is typically done statistically, using a cross-correlation technique to measure the speckle displacement. In particular, phase correlation that mainly relies on the phase information for matching the image pairs is used in the software implement (Zhao 2004).

To determine the accuracy required from the LSI device, results were compared to those obtained via a mechanical hand-held gage typically used to measure the transfer length of pretensioned concrete members. Using a laboratory interferometer as a controlled calibration technique (fig. 3.3), accuracy of an experienced user was approximately +/- 0.0002 in. If using the standard 8 in. gage length, this value corresponds to a strain level of +/- 25 microstrain. Using this information, the design team concluded that the optical system must have an accuracy of at least +/- 25 microstrain (Zhao 2012).

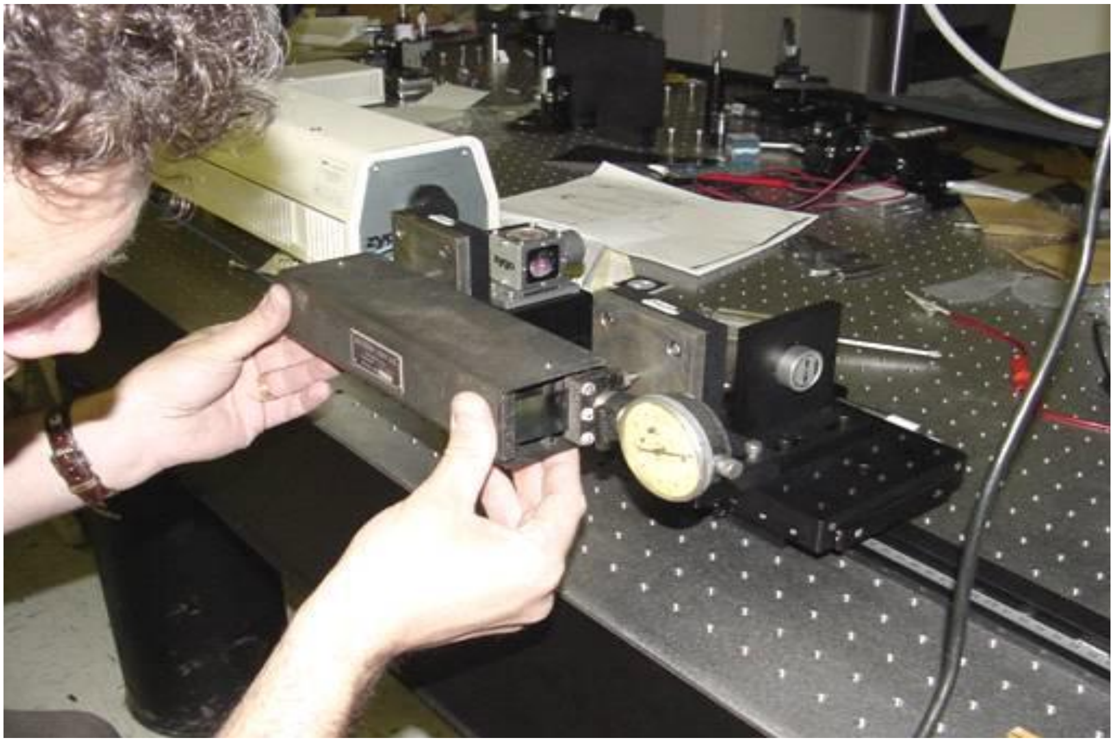

Figure 3.3 Determining accuracy of a standard mechanical gage (Zhao 2011)

A prototype of the optical strain sensor was fabricated in a portable, light-weight, self-contained unit for field testing, as shown in figure 3.4. It has two identical modules attached rigidly to each other in a mirror setup, with each module capable of detecting surface movement independently. This unique modular design provided several preferable features, including flexible adjustment of the gauge length, easy upgradeability to automatic operation, robustness, and higher accuracy (Zhao 2011).

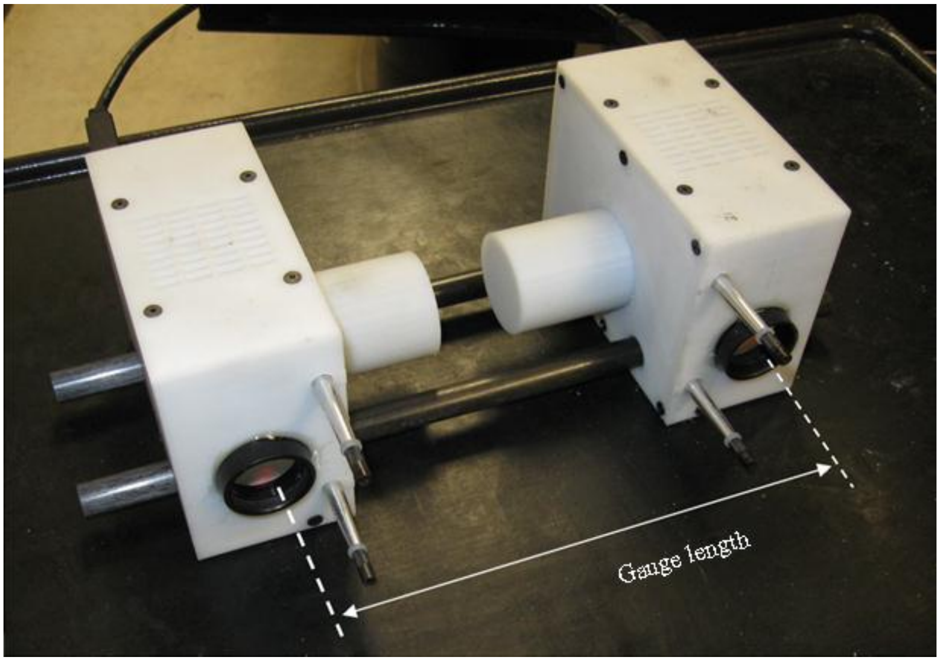

Figure 3.4 Laser-speckle prototype (Zhao 2011)

For surface strain measurement, the optical strain sensor is first positioned onto the concrete surface before applying any load. The two cameras in the left and right modules capture a pair of speckle images generated by points A and B, respectively. These two speckle images are denoted as A1 and B1, and are referred to as the base readings. The sensor is then removed from the concrete surface. After detensioning the prestressing strands, the optical sensor is positioned back onto the surface in the exact location the base readings were taken. The cameras capture another pair of speckle images, which are denoted as A2 and B2. By applying a cross-correlation technique to the pair of speckle images A1 and A2, displacement ΔA can be extracted. Displacement ΔB can be extracted from images B1 and B2 in a similar fashion. As shown in figure 3.5, axial surface strain (ε) between point A and point B can thus be determined by $\varepsilon = (\Delta B - \Delta A) / L$, where L is the gage length of 8 in. for the current setup (Zhao 2011).

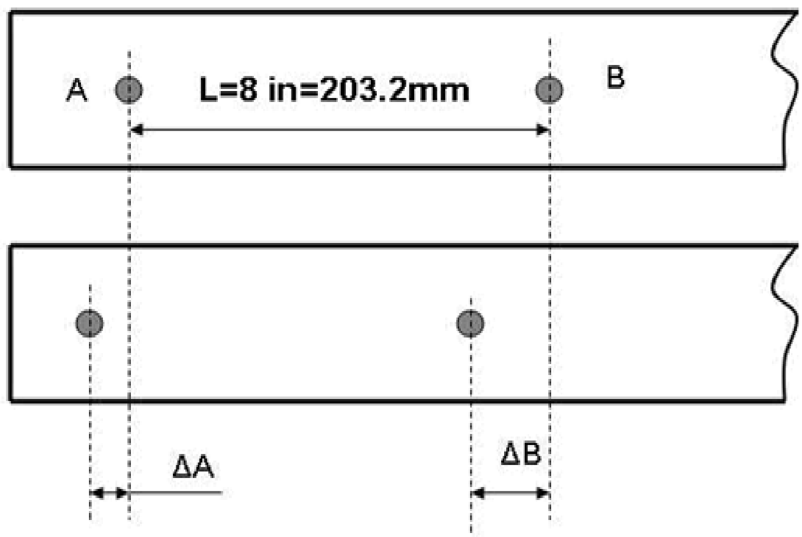

Figure 3.5 Visualization of strain measurement (Zhao 2011)

3.2 Laboratory Verifications of LSI Technique

In order to test the accuracy and sensitivity of the LSI methodology, a laboratory setup was fabricated and used to conduct comparisons between the optical sensor and a manual gage. The capability of the optical sensor-strain measurement was validated by using a manual motion system, as shown in figure 3.6. Two small concrete blocks were positioned side by side approximately 8 in. apart. The concrete block shown on the left was attached to a manual traverse system, and displacement was measured by a digital dial gage with a resolution of 0.001 mm (Shars 303-3506), while the concrete block on the right was held stationary. This system was used to create a relatively linear displacement between the two concrete blocks.

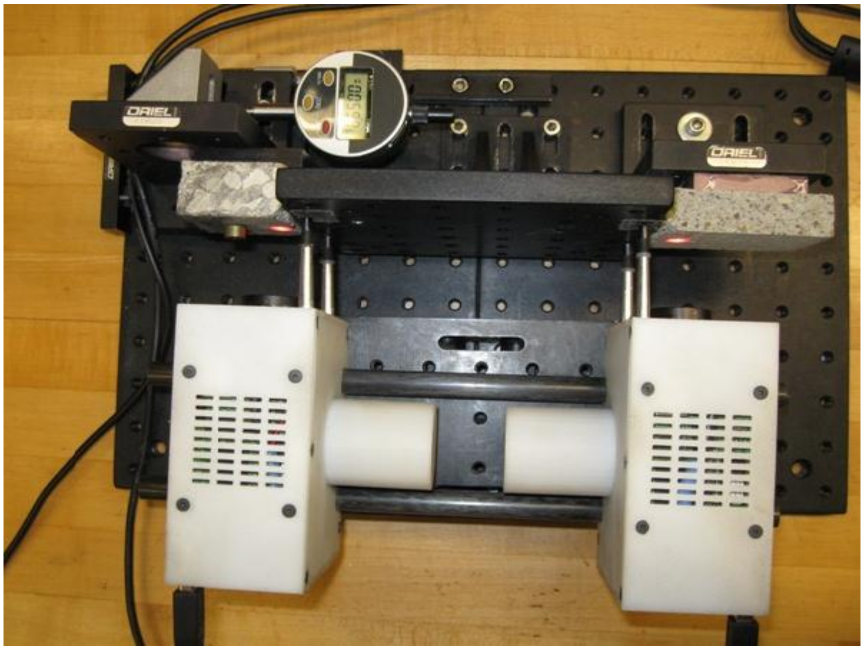

Figure 3.6 Concrete block system used to validate LSI measurements (Zhao 2011)

The relative displacement between the two concrete blocks was increased from 0 mm to 2 mm with 0.1 mm increments. Displacements were measured by both the digital dial gage and the laser-speckle strain sensor. Results from this test are shown in figure 3.7, and prove the readings from the two devices have excellent correlation (Zhao 2011).

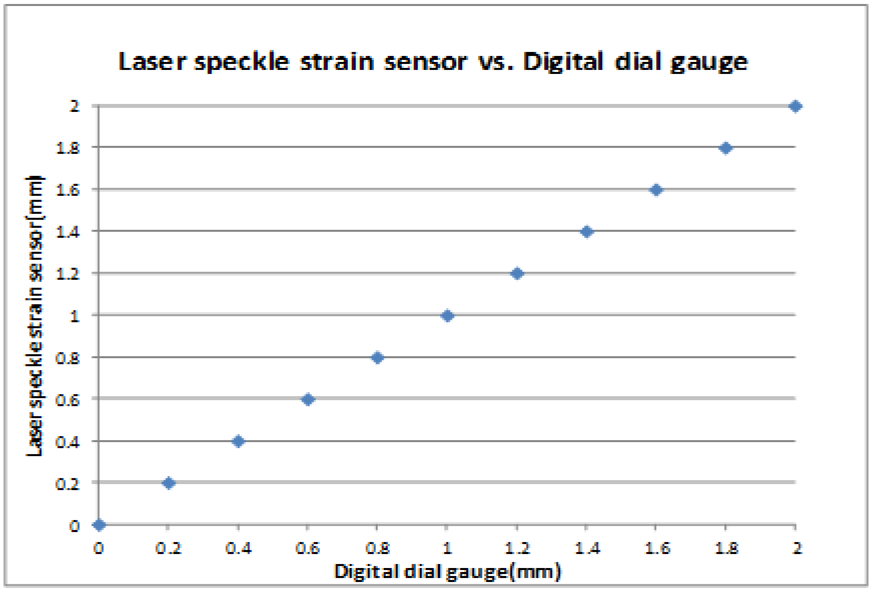

Figure 3.7 Comparison of laser-speckle strain sensor and digital dial gage (Zhao 2011)

3.3 Problems with Surface Correlation

In order for the laser-speckle device to function properly, the surface of the concrete must remain perfectly consistent throughout the measurement process. Once the base readings are taken on the concrete surface, the surface must remain unchanged, otherwise secondary readings cannot be taken. This is caused by the speckle pattern not recognizing the "fingerprint" for each individual location. This is a major problem when taking measurements at a prestressed concrete tie plant. The plant introduces many factors that alter the concrete surface. These include water, dust, handling of the ties by machines and vacuums, and early release of the prestressing force.

All of the tie plants visited produced their ties in a similar fashion. The ties were cast upside down in a continuous bed, and the prestressing force was released as soon as the concrete reached a specified strength. Once the prestressing force was released, the individual ties were cut with a diamond saw blade, using a wet-cutting procedure. After cutting, the ties were then either vacuum lifted out of place or relocated using a forklift.

This harsh environment caused many problems with preserving the surface for laser-speckle measurements. First, the prestressing force was released when the concrete was only 8 to 12 hrs. old. The surface of the concrete was still changing on a microscopic level at that point in time due to surface drying. Also, the wet-saw cutting procedure covered the surface of the concrete tie with slurry (fig. 3.8) from the water and dust. This slurry was thick, and dried on the surface rather quickly. Lastly, the vacuum-lifting procedure (fig. 3.9) and forklift handling scraped the ties, causing major damage to the concrete surface. All of these factors caused surface changes to the concrete that made laser-speckle readings impossible on the bare concrete surface.

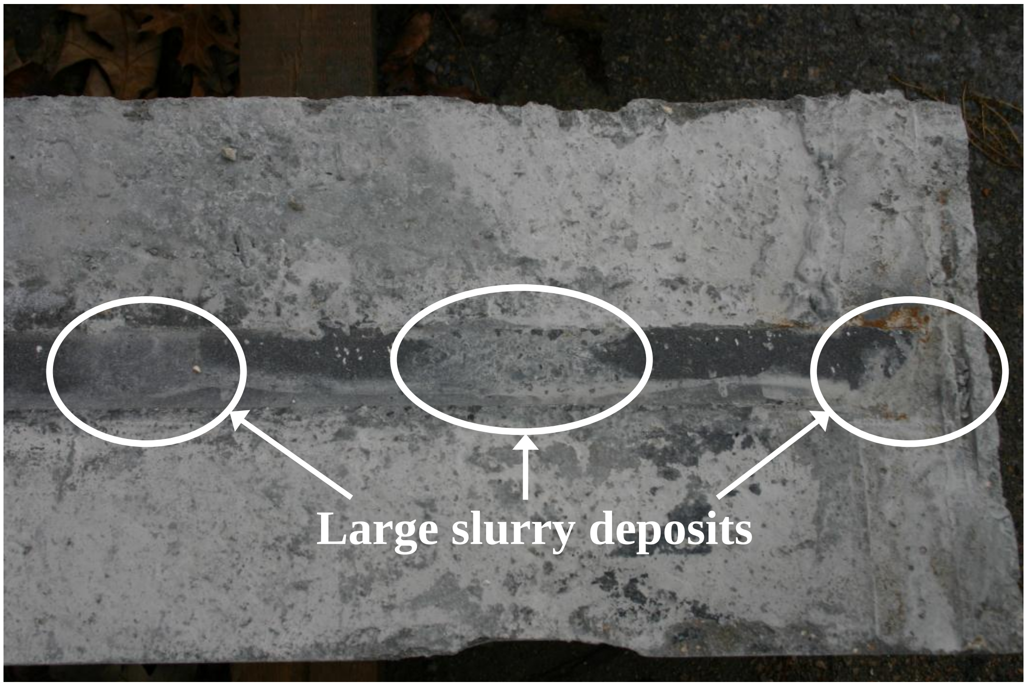

Figure 3.8 Slurry covering tie from saw cutting

Figure 3.9 Vacuum lifting of ties

3.3.1 Painted Concrete Surface

To mitigate surface changes, paint that contained a speckled pattern was applied to the concrete surface, as shown in figure 3.10. The speckled pattern contained small reflective particles that bonded to the surface and created an artificial speckle (Zhao 2011). The paint masked the microscopic changes to the concrete surface, and measurements were able to be taken at the early release times required by the plants. Also, the slurry created during the wet-saw cutting procedure could be wiped off, revealing the clean painted surface. With the paint applied to the concrete surface, the strain sensor was able to obtain correlation between the speckle-image pairs, and to extract the necessary surface-strain information.

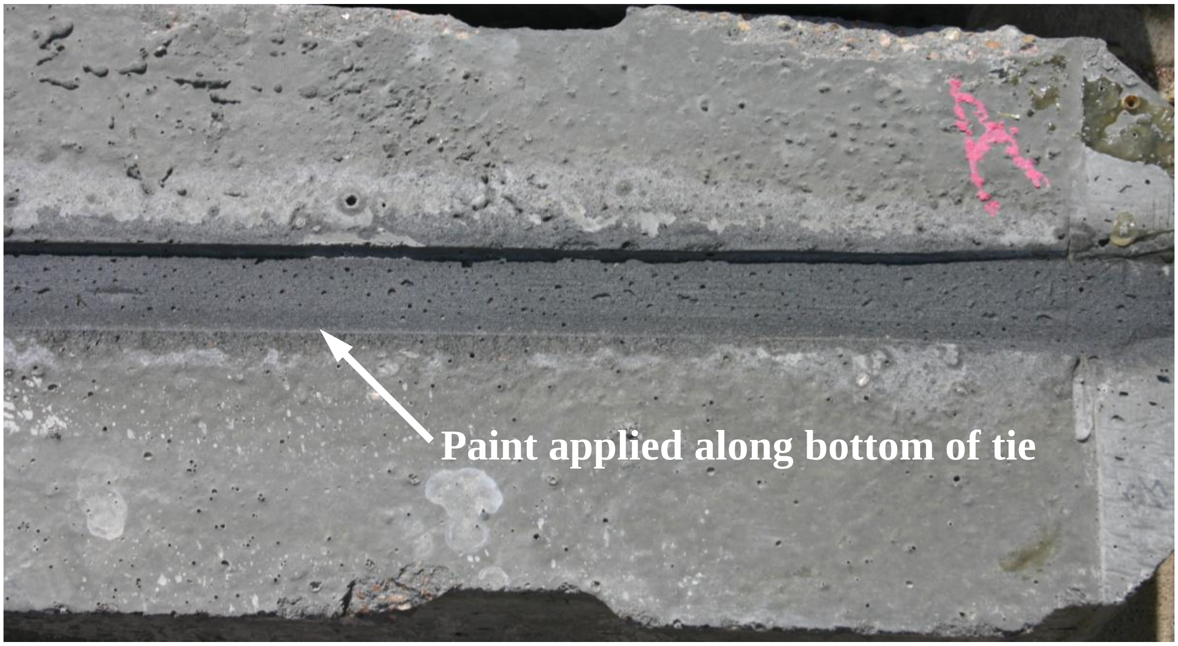

Figure 3.10 Protective paint applied to concrete tie surface

3.4 Laser-Speckle Rail Mount

In order for the laser-speckle device to work properly, secondary readings must be taken at precisely the same location as the base readings. To make the system rigid and precise enough to accomplish this, a traversable rail was constructed, to which the laser-speckle was connected. This rail is pictured below in figure 3.11.

The rail rested on three points to mitigate the possibility of an unstable surface. A ruler was mounted on the back side of the rail, and a magnifying lens was used to ensure the laser was traversing along the concrete tie at the correct location. This setup is pictured below in figure 3.12.

Figure 3.11 Traversable rail with laser attached

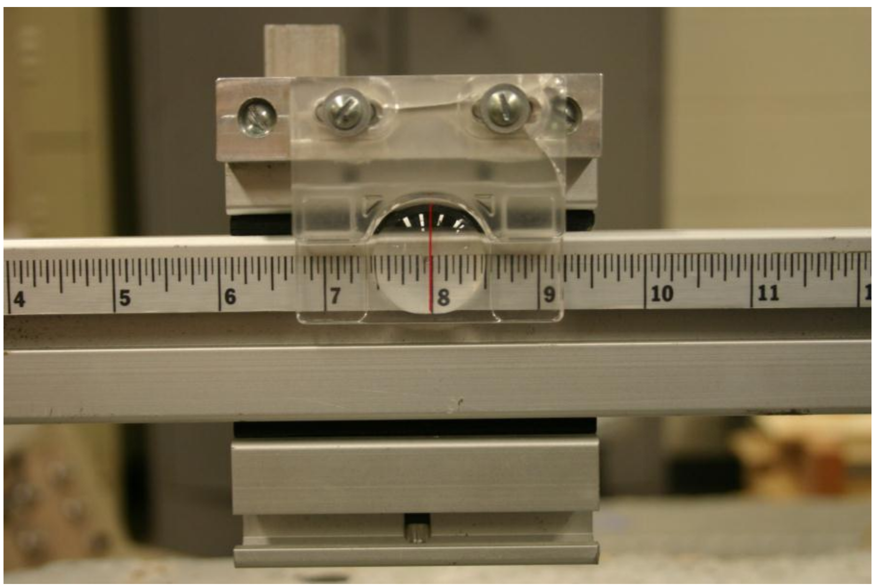

Figure 3.12 Ruler and lens device on traversable rail

Steel bars were also made to assist with the laser-speckle measurements. The bars were placed in the concrete during casting (fig. 3.13). Once the concrete had cured, the bars were removed. These steel bars accomplished three things: First, brass points were screwed to the bars at three locations where the feet of the traversable rail would sit.

Figure 3.13 Steel bars cast in fresh concrete

When the steel bars were removed from the dried concrete, the brass points would be embedded in the concrete (fig. 3.14). This allowed the traversable rail to be placed on the three brass points in a consistent location.

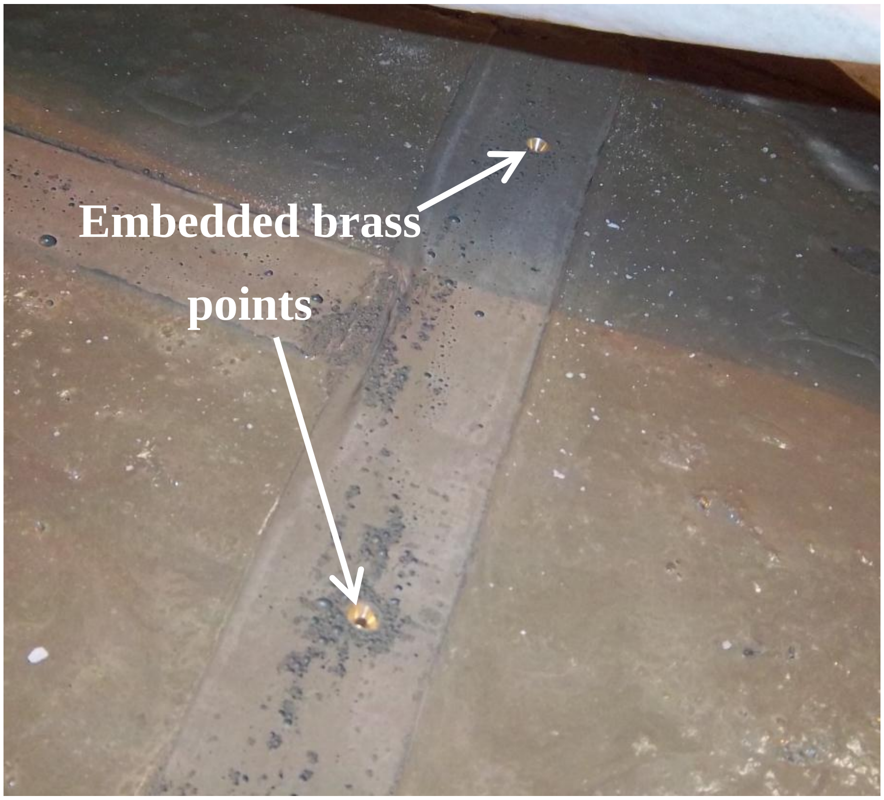

Figure 3.14 Embedded brass points used for traversable rail

The second benefit of the steel bars is that they provided a smooth surface from upon which the laser could take measurements; because the bars were cast in concrete, the concrete was able to flow around the bars and take the smooth shape of the steel. Finally, the steel bars created a notch approximately 1/8 in. deep into the bottom of the concrete ties. This notch protected the surface from the vacuum lifting and forklift handling. The smooth notched surface is shown below in figure 3.15.

Figure 3.15 Notch created by steel bar inserts

Chapter 4 Transfer Length Procedures

Transfer lengths of the prestressed concrete railroad ties were measured using a Whittemore gage and the LSI device. Zhao et al. (2012) conducted research revealing that concrete surface strain measurements using the laser-speckle compared favorably to the Whittemore gage. The Whittemore gage was used so that long-term transfer lengths could be measured at KSU. The laser-speckle device was used in the plants to obtain the majority of the data; however, long-term measurements could not be taken using this method due to the problem of surface preservation.

4.1 Whittemore Gage Measurements

To measure the transfer length using a Whittemore gage, brass points were screwed into a steel bar at 1-in. spacings (fig. 4.1). This bar was then placed into the concrete at the end of the ties during the time of casting at each plant. Placing the bars as close to the end of the tie as possible ensured that strain readings were being monitored near the edge of the tie.

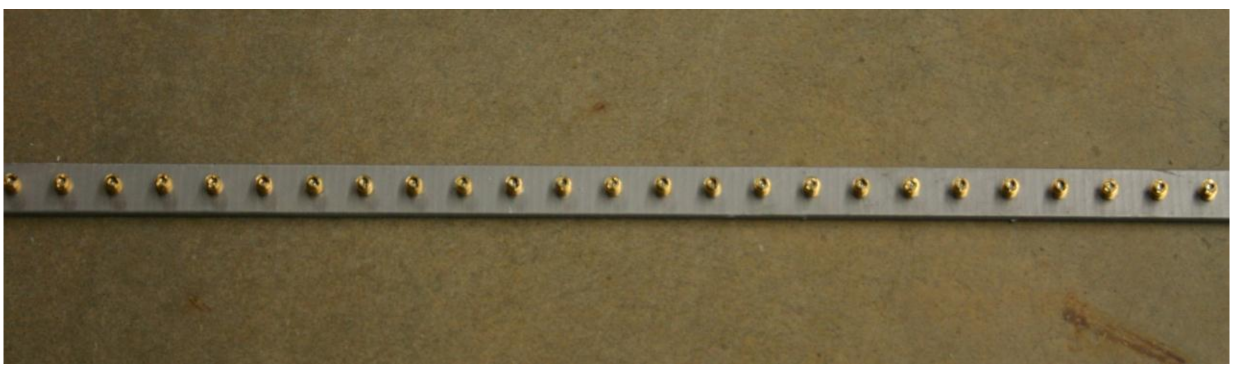

Figure 4.1 Brass points at 1-in. spacing used for Whittemore readings

Before the ties were detensioned, the screws were removed and the bar was pulled from the hardened concrete, leaving the brass points embedded, as shown in figure 4.2. The distance between each point was measured before and after detensioning, using the Whittemore gage shown in figure 4.3. Readings were taken by two different researchers to eliminate any errors.

Figure 4.2 Embedded brass points used for Whittemore readings

Figure 4.3 Whittemore gage used to take readings

After the prestressing force is released, the concrete develops strain throughout the member. The strain is zero at the end of the tie and increases until it reaches a constant strain value. When the strain becomes constant in the member, the prestressing force is transferred. To determine the transfer length value, the data was smoothed using the 3-point average technique, and the 95% AMS was applied (Russell and Burns 1993). Most of the ties tested at the plants using the Whittemore gage were sent back to KSU so that the long-term transfer length could be monitored.

4.2 Laser-Speckle Measurements

To measure the transfer length on concrete ties using the laser-speckle, the steel bars described in section 3.4 were cast into the concrete at the time of pouring. Once the concrete had had time to cure, the bars were removed. These bars left three brass points embedded in the concrete and created a smooth surface from which the laser could read. A thin layer of protective paint was applied to the concrete at the location where the steel bar rested. The laser was then used on the traversable rail to take an initial set of readings before the ties were detensioned. Readings were taken with the laser-speckle at an interval of 0.5 in. By taking readings at this spacing, more accurate transfer lengths could be determined.

After the ties were detensioned and saw-cut, readings were taken once more. The secondary readings were compared to the initial readings to extract the strain information at each location. These strain readings were used to plot the strain profile of the railroad tie for the transfer length determination.

Because the laser-speckle was used to take readings every 0.5 in., it was concluded that a different approach was needed to obtain transfer length values. Traditionally, strain measurements are taken at 2 in. spacings on the surface of the concrete, using a mechanical gage (Russell and Burns 1997; Oh and Kim 2000; Steinberg 2001; Barnes et al. 2003). This mechanical gage typically has a gage length of 8 in. Previous researchers constructed the surface strain profile by averaging three consecutive points to smooth the data (Russell and Burns1993). By averaging three consecutive points with an 8 in. gage length, the surface strain is effectively being averaged over a 12 in. length (gage length plus 4 in.), as shown in figure 4.4.

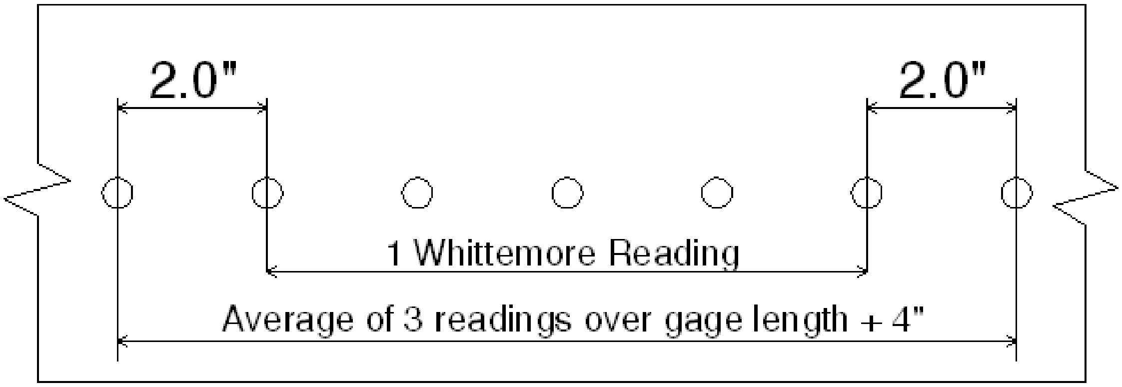

Figure 4.4 12 in. length created using the 3-point average method

To obtain a similar average over a 12 in. length for the laser-speckle readings, the average of nine consecutive speckle readings was used, as shown in figure 4.5. The transfer length was then determined based off of the 95% AMS method of this smoothed strain profile (Russell and Burns 1993).

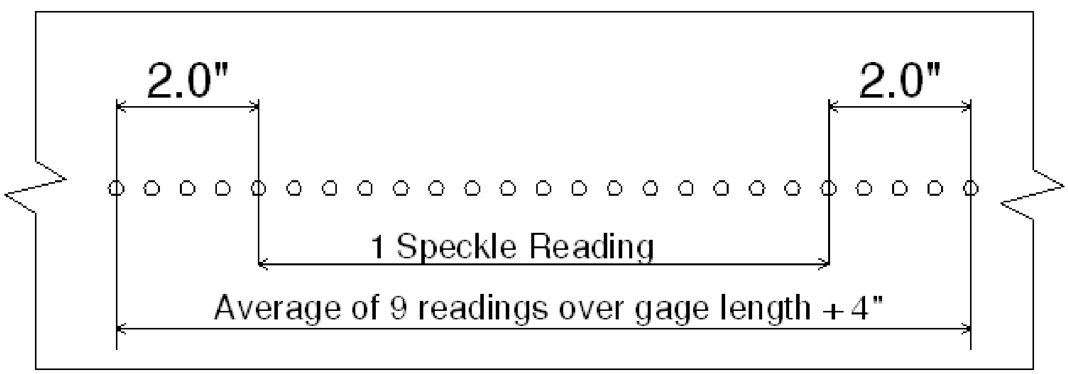

Figure 4.5 12 in. length created using the 9-point average method

A sample of the 9-point average technique can be seen below. Figure 4.6 shows a transfer length graph produced by the laser-speckle device. The surface strain measurements were smoothed using a 3-point average method and the transfer length was determined by the 95% AMS method.

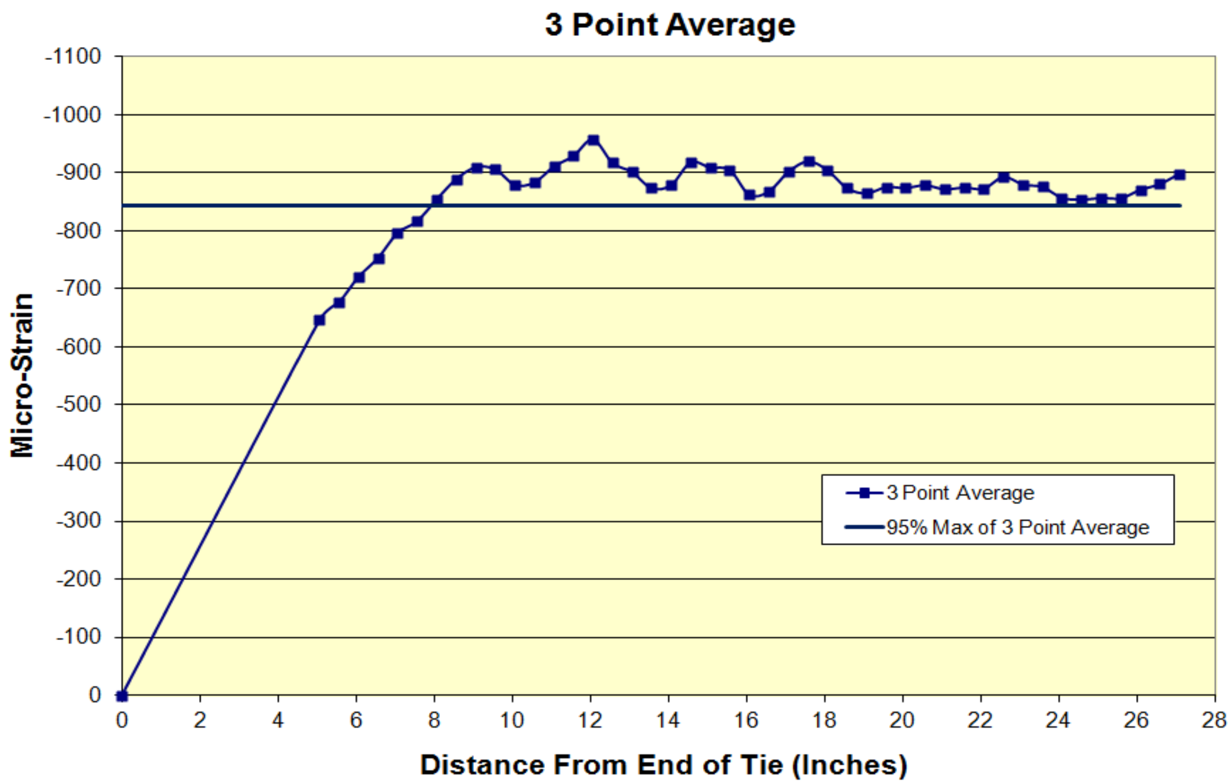

Figure 4.6 Surface strain measurements smoothed by the 3-point average method

The strain profile of figure 4.6 was smoothed even further using the 9-point average technique. This change can be seen in figure 4.7 (below). The transfer length of the 9-point average technique was also found by the 95% AMS method.

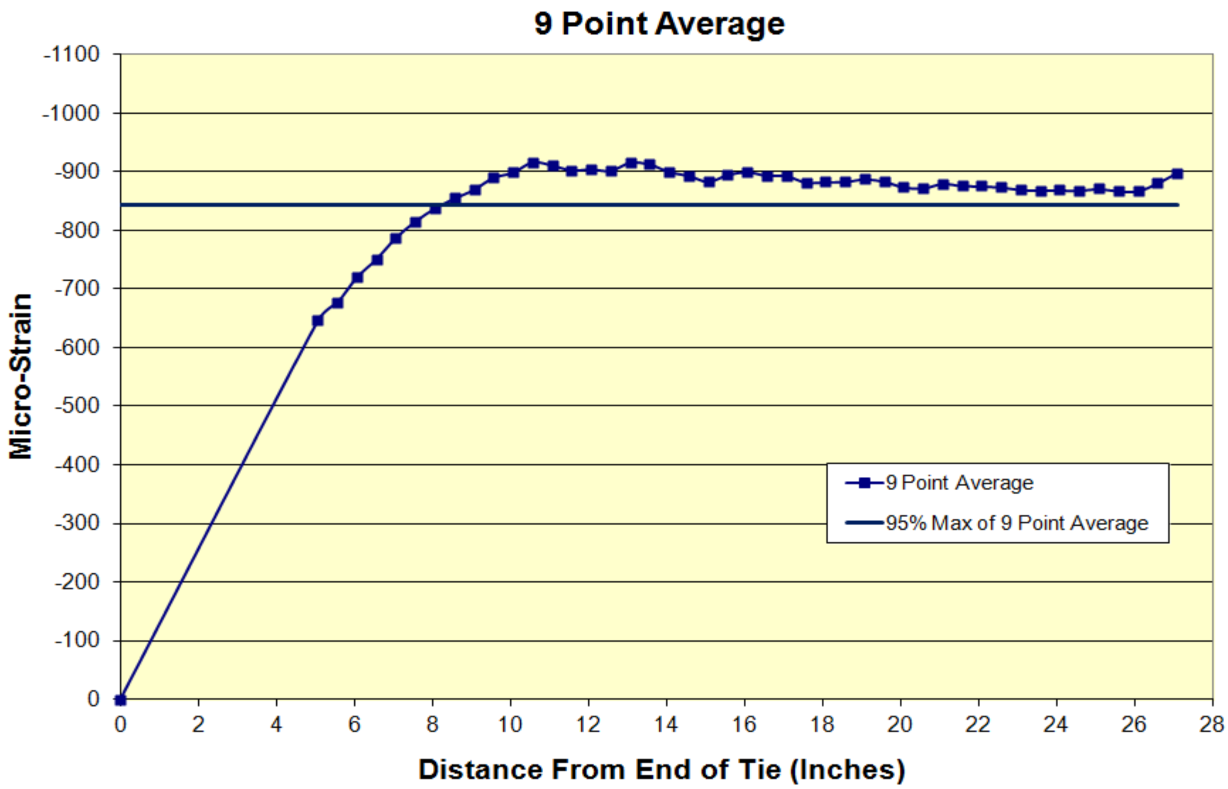

Figure 4.7 Surface strain measurements smoothed by the 9-point average method

By comparing the two graphs, it can be seen that the 9-point average method produces smoother strain profiles. These profiles are easier to work with and give more consistent results of the transfer length. Also, in some extremely high transfer length situations where there are only a few points in the strain-plateau, it is easier to see which points to include in the 95% AMS.

Chapter 5 Concrete-Mix and Reinforcement Variations

At the time the six prestressed concrete tie plants were visited by the research team, a total of nine mix designs and 10 reinforcements were used. The reinforcements consisted of nine indented wires and one indented strand. This section discusses the concrete-mix designs that each plant used, as well as the number of reinforcements evaluated. Because of the sensitivity of this information, consistent data regarding the mix designs is shown for each plant. Also, the type of reinforcement used by each plant is not shown. Instead, the information is reported as reinforcement 1, reinforcement 2, etc.

Information regarding the concrete-mix designs includes the water-to-cementitious ratio (W/C), air content percentage, average compressive strength at release, tensile strength at release, total cementitious weight, and average 28-day compressive strength. The total cementitious weight includes fly ash that may have been added to the concrete-mix.

5.1 Plant A

Tables 5.1, 5.2, and 5.3 below show information regarding the concrete-mix designs and reinforcements used at Plant A. One mix design was tested using two reinforcements. In the following tables, Mix 1 and Mix 1A are the same mix design; however, release strengths are considerably different.

Table 5.1 Mix design 1 and reinforcement 1 used at Plant A

Mix 1/Reinforcement 1	
W/C Ratio	0.36
Air Content (%)	5.8
Average Compressive Strength at Release (psi)	6240
Split Tensile Strength (psi)	515
Total Cementitious Weight (lb/yd^3)	600
28-Day Compressive Strength (psi)	9530

Table 5.2 Mix design 1A and reinforcement 1 used at Plant A

Mix 1A/Reinforcement 1	
W/C Ratio	0.36
Air Content (%)	5.2
Average Compressive Strength at Release (psi)	4520
Split Tensile Strength (psi)	600
Total Cementitious Weight (lb/yd^3)	600
28-Day Compressive Strength (psi)	11220

Table 5.3 Mix design 1A and reinforcement 2 used at Plant A

Mix 1A/Reinforcement 2	
W/C Ratio	0.36
Air Content (%)	5.2
Average Compressive Strength at Release (psi)	4520
Split Tensile Strength (psi)	600
Total Cementitious Weight (lb/yd^3)	600
28-Day Compressive Strength (psi)	11220

5.2 Plant B

Tables 5.4 and 5.5 below show information regarding the concrete-mix designs and reinforcement used at Plant B. Two mix designs were tested using only one type of reinforcement.

Table 5.4 Mix design 2 and reinforcement 3 used at Plant B

Mix 2/Reinforcement 3	
W/C Ratio	0.38
Air Content (%)	3.6
Average Compressive Stength at Release (psi)	3760
Split Tensile Strength (psi)	380
Total Cementitious Weight (lb/yd^3)	600
28-Day Compressive Strength (psi)	8400

Table 5.5 Mix design 3 and reinforcement 3 used at Plant B

Mix 3/Reinforcement 3	
W/C Ratio	0.38
Air Content (%)	3.6
Average Compressive Stength at Release (psi)	5600
Split Tensile Strength (psi)	420
Total Cementitious Weight (lb/yd^3)	600
28-Day Compressive Strength (psi)	9160

5.3 Plant C

Tables 5.6 and 5.7 below show information regarding the concrete-mix design and reinforcement used at Plant C. Two separate concrete pours using one mix design were tested using one type of reinforcement.

Table 5.6 Cast 1, mix design 4, and reinforcement 4 used at Plant C

Cast 1 - Mix 4/Reinforcement 4	
W/C Ratio	0.31
Air Content (%)	5.9
Average Compressive Strength at Release (psi)	5940
Split Tensile Strength (psi)	480
Total Cementitious Weight (lb/yd^3)	720
28-Day Compressive Strength (psi)	10630

Table 5.7 Cast 2, mix design 4, and reinforcement 4 used at Plant C

Cast 2 - Mix 4/Reinforcement 4	
W/C Ratio	0.30
Air Content (%)	5.6
Average Compressive Strength at Release (psi)	7080
Split Tensile Strength (psi)	585
Total Cementitious Weight (lb/yd^3)	720
28-Day Compressive Strength (psi)	11720

5.4 Plant D

Tables 5.8, 5.9, 5.10, and 5.11 below show information regarding the concrete-mix designs and reinforcement used at Plant D. One concrete-mix was tested in four separate pours using two different reinforcements.

Table 5.8 Cast 1, mix design 5, and reinforcement 5 used at Plant D

Cast 1 - Mix 5/Reinforcement 5	
W/C Ratio	0.28
Air Content (%)	4.2
Average Compressive Strength at Release (psi)	5520
Split Tensile Strength (psi)	580
Total Cementitious Weight (lb/yd^3)	780
28-Day Compressive Strength (psi)	10040

Table 5.9 Cast 2, mix design 5, and reinforcement 5 used at Plant D

Cast 2 - Mix 5/Reinforcement 5	
W/C Ratio	0.28
Air Content (%)	4.4
Average Compressive Strength at Release (psi)	5820
Split Tensile Strength (psi)	630
Total Cementitious Weight (lb/yd^3)	780
28-Day Compressive Strength (psi)	10400

Table 5.10 Cast 3, mix design 5, and reinforcement 6 used at Plant D

Cast 3 - Mix 5/Reinforcement 6	
W/C Ratio	0.28
Air Content (%)	4.5
Average Compressive Strength at Release (psi)	5360
Split Tensile Strength (psi)	520
Total Cementitious Weight (lb/yd^3)	780
28-Day Compressive Strength (psi)	9570

Table 5.11 Cast 4, mix design 5, and reinforcement 6 used at Plant D

Cast 4 - Mix 5/Reinforcement 6	
W/C Ratio	0.28
Air Content (%)	4.5
Average Compressive Strength at Release (psi)	5790
Split Tensile Strength (psi)	610
Total Cementitious Weight (lb/yd^3)	780
28-Day Compressive Strength (psi)	9900

5.5 Plant E

Tables 5.12 and 5.13 below show information regarding the concrete-mix designs and reinforcement used at Plant E. Two concrete-mixes were used with one type of reinforcement.

Table 5.12 Mix design 6 and reinforcement 7 used at Plant E

Mix 6/Reinforcement 7	
W/C Ratio	0.27
Air Content (%)	4.2
Average Compressive Strength at Release (psi)	5830
Split Tensile Strength (psi)	440
Total Cementitious Weight (lb/yd^3)	935
28-Day Compressive Strength (psi)	12300

Table 5.13 Mix design 7 and reinforcement 7 used at Plant E

Mix 7/Reinforcement 7	
W/C Ratio	0.27
Air Content (%)	4.9
Average Compressive Strength at Release (psi)	5520
Split Tensile Strength (psi)	440
Total Cementitious Weight (lb/yd^3)	915
28-Day Compressive Strength (psi)	11760

5.6 Plant F

Tables 5.14, 5.15, 5.16, and 5.17 below show information regarding the concrete-mix designs and reinforcement used at Plant F. Two concrete-mixes were tested and three reinforcements were used in four separate pours.

Table 5.14 Mix design 8 and reinforcement 8 used at Plant F

Mix 8/Reinforcement 8	
W/C Ratio	0.29
Air Content (%)	5.3
Average Compressive Strength at Release (psi)	5200
Split Tensile Strength (psi)	655
Total Cementitious Weight (lb/yd^3)	750
28-Day Compressive Strength (psi)	10440

Table 5.15 Mix design 8 and reinforcement 9 used at Plant F

Mix 8/Reinforcement 9	
W/C Ratio	0.29
Air Content (%)	5.2
Average Compressive Strength at Release (psi)	6110
Split Tensile Strength (psi)	630
Total Cementitious Weight (lb/yd^3)	750
28-Day Compressive Strength (psi)	11260

Table 5.16 Mix design 8 and reinforcement 10 used at Plant F

Mix 8/Reinforcement 10	
W/C Ratio	0.29
Air Content (%)	5.0
Average Compressive Strength at Release (psi)	4730
Split Tensile Strength (psi)	655
Total Cementitious Weight (lb/yd^3)	750
28-Day Compressive Strength (psi)	11840

Table 5.17 Mix design 9 and reinforcement 10 used at Plant F

Mix 9/Reinforcement 10	
W/C Ratio	0.31
Air Content (%)	4.8
Average Compressive Strength at Release (psi)	5700
Split Tensile Strength (psi)	580
Total Cementitious Weight (lb/yd^3)	700
28-Day Compressive Strength (psi)	11910

Chapter 6 Transfer Length Results

This section discusses transfer length results obtained at each of the six prestressed concrete tie plants. Transfer length measurements are shown after the prestressing force was released and the ties were individually saw-cut. Concrete strengths, at release, both compressive and tensile, were graphed against transfer length values to whether any correlation was present. Long-term transfer length results are shown for the concrete ties sent back to KSU for further measurements.

6.1 Transfer Length Measurements at Release

The transfer length results are summarized in table 6.1 (below). This table reports the measurements recorded immediately after the concrete ties were detensioned and saw-cut. Results from each plant are separated by the concrete-mix designs and reinforcements described in chapter 5. In this table, reinforcements are denoted as “RF.” Transfer lengths measured using the Whittemore gage were determined using the 3-point average and 95% AMS method (Russell and Burns 1993). Because Whittemore readings were taken at 1 in. spacings, strain profiles could have been graphed using a 5-point average method. However, there was minimal error with the Whittemore method, and strain profiles were acceptable using the 3-point method. Transfer lengths measured using the LSI device were determined with the 9-point average technique described in section 4.2 and the 95% AMS method. The table shows the average transfer length, standard deviation (std. dev.), minimum (min), and maximum (max) obtained for each concrete-mix design in inches.

Table 6.1 Transfer length information for various mix designs and reinforcements

		Average	Std. Dev.	Min	Max
Plant A	Mix 1/RF 1	9.5	1.1	7.2	11.4
	Mix 1A/RF 1	10.0	1.1	8.3	12.0
	Mix 1A/RF 2	11.4	1.1	8.8	12.9
Plant B	Mix 2/RF 3	19.6	3.2	15.0	26.8
	Mix 3/RF 3	14.6	1.8	11.0	18.3
Plant C	Cast 1 - Mix 4/RF 4	7.6	1.1	6.3	9.5
	Cast 2 - Mix 4/RF 4	6.6	0.7	6.0	8.0
Plant D	Cast 1 - Mix 5/RF 5	10.8	1.0	9.1	11.9
	Cast 2 - Mix 5/RF 5	11.7	1.8	8.5	16.3
	Cast 3 - Mix 5/RF 6	11.7	1.9	8.2	15.3
	Cast 4 - Mix 5/RF 6	12.1	2.4	7.7	16.4
Plant E	Mix 6/RF 7	18.6	1.4	16.0	21.0
	Mix 7/RF 7	18.3	2.5	14.4	22.8
Plant F	Mix 8/RF 8	9.4	2.9	4.5	14.0
	Mix 8/RF 9	9.4	2.2	7.4	14.7
	Mix 8/RF 10	7.8	1.3	5.2	9.7
	Mix 9/RF 10	8.1	1.8	5.1	11.0

Table 6.1 reports transfer length values for various concrete-mix designs and reinforcements used. However, previous researchers have determined that longer transfer lengths often exist on the live-end of prestressed concrete members due to the dynamic shock of the sudden release (Russell and Burns 1997). Table 6.2 shows transfer length values separated by the dead- and live-end of the ties. All plants had a slow release method that detensioned using prestressing rams. However, at two of the plants, a sudden release was experienced at both ends of the ties. The live-end of the tie is considered as the side of the bed where prestressing force is released. This table does not show a consistent difference between the dead-end and live-end of the prestressed concrete ties. This could be caused by high concrete strengths and slow release of

prestressing force used in the concrete tie industry. A slow release of prestressing force reduces the dynamic shock present in sudden releases.

Table 6.2 Transfer length measurements, including dead and live-ends of ties

		Dead End				Live End				Live/Dead
		Avg.	St. Dev.	Min	Max	Avg.	St. Dev.	Min	Max	End Ratio
Plant A	Mix 1/RF 1	9.7	1.1	7.2	11.4	9.2	1.0	7.8	10.5	0.95
	Mix 1A/RF 1	9.7	0.8	8.3	10.2	10.2	1.4	8.3	12.0	1.05
	Mix 1A/RF 2	11.2	1.4	8.8	12.3	11.6	0.8	10.8	12.9	1.03
Plant B	Mix 2/RF 3	18.9	2.1	15.0	21.8	20.3	4.1	15.4	26.8	1.07
	Mix 3/RF 3	14.3	2.0	11.0	18.0	14.9	1.4	13.3	18.3	1.04
Plant C	Cast 1 - Mix 4/RF 4	7.0	0.8	6.3	7.8	8.1	1.2	7.3	9.5	1.16
	Cast 2 - Mix 4/RF 4	7.0	0.9	6.5	8.0	6.3	0.3	6.0	6.5	0.89
Plant D	Cast 1 - Mix 5/RF 5	10.9	1.1	9.1	11.9	10.1	---	10.1	10.1	0.93
	Cast 2 - Mix 5/RF 5	11.9	2.1	10.1	16.3	11.4	1.5	8.5	12.8	0.96
	Cast 3 - Mix 5/RF 6	11.0	1.7	8.2	14.7	12.6	1.8	9.7	15.3	1.14
	Cast 4 - Mix 5/RF 6	11.3	2.4	7.7	16.1	12.7	2.3	10.0	16.4	1.13
Plant E	Mix 6/RF 7	18.8	1.0	17.5	20.5	18.3	1.7	16.0	21.0	0.98
	Mix 7/RF 7	18.6	1.9	15.0	22.2	18.0	3.2	14.4	22.8	0.97
Plant F	Mix 8/RF 8	8.9	1.9	6.0	11.0	10.1	4.1	4.5	14.0	1.14
	Mix 8/RF 9	9.7	3.0	7.4	14.7	9.0	1.0	7.5	9.6	0.93
	Mix 8/RF 10	7.6	1.8	5.2	9.7	8.0	0.7	7.0	8.7	1.06
	Mix 9/RF 10	7.8	2.1	5.1	11.0	8.5	1.5	6.8	10.5	1.08

A visual representation of table 6.1 can be seen below in figure 6.1. This figure clearly illustrates the average transfer length and minimum and maximum values obtained for each concrete-mix design and reinforcement combination. Also, the common distance to the rail seat (21 in.) is shown as the solid red line, and the turnout tie distance to the rail-seat (24 in.) is shown as the solid green line. Any ties with transfer length values above these lines will not have full prestress force at the rail seat. However, if the ties are designed with an excess capacity, then a reduced prestress force may not be detrimental to the performance in track. The transfer lengths measured per mix and reinforcement combination are also shown in the graph under each of the bars and are given the notation "TL" for number of transfer lengths measured.

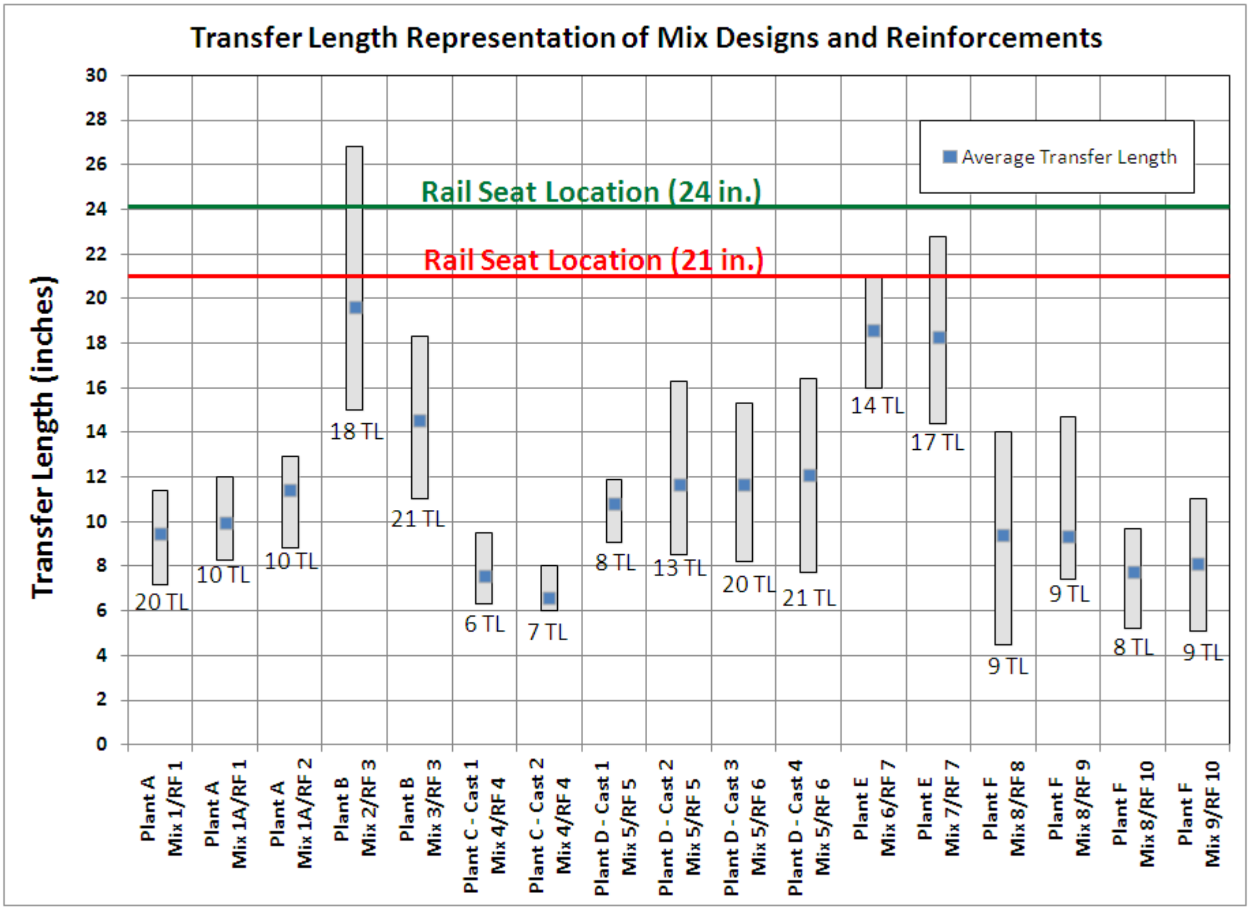

Figure 6.1 Transfer length data from table 6.1

In Figure 6.1, the blue square dot is the average transfer length at release for each specific mix design. The top of each bar is the maximum transfer length and the bottom of each bar is the minimum transfer length measured for each concrete-mix and reinforcement combination. From this diagram, it is easy to see the smallest transfer length measured was 4.5 in., while the largest transfer length measured was about 27 in. It is obvious that some of the transfer lengths measured were longer than the 21 or 24 in. to the rail seat. Ties with transfer lengths above 21 or

24 in. do not have full strength capacity at the rail-seat, and are not as efficient or conservative as ties with shorter transfer lengths. This diagram indicates that some concrete-mixes and reinforcements produce transfer length data that are very consistent, while others result in a more scattered range of transfer lengths.

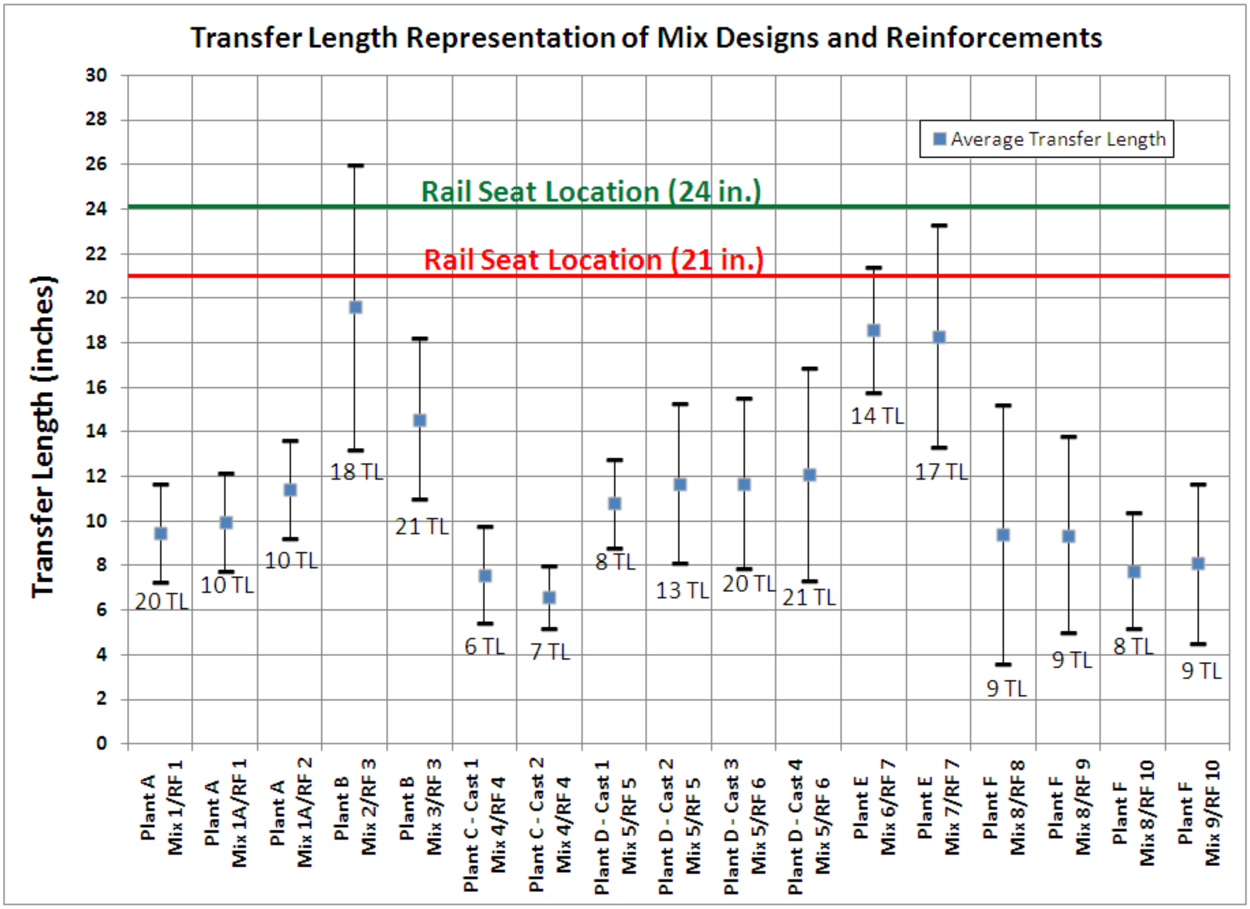

Figure 6.2 Transfer length data showing 95% confidence interval

Figure 6.2 (above) shows average transfer length values with the 95% confidence intervals. This technique was used to show two standard deviations from the average, rather than the minimum and maximum values used in figure 6.1. Figure 6.3 (below) shows a visualization of the transfer length values measured for each cast. This figure clearly shows each individual measured transfer length, and points out the outliers in the data. Both figures 6.2 and 6.3 show the distance to the rail seat, as well as the individual plant and cast information.

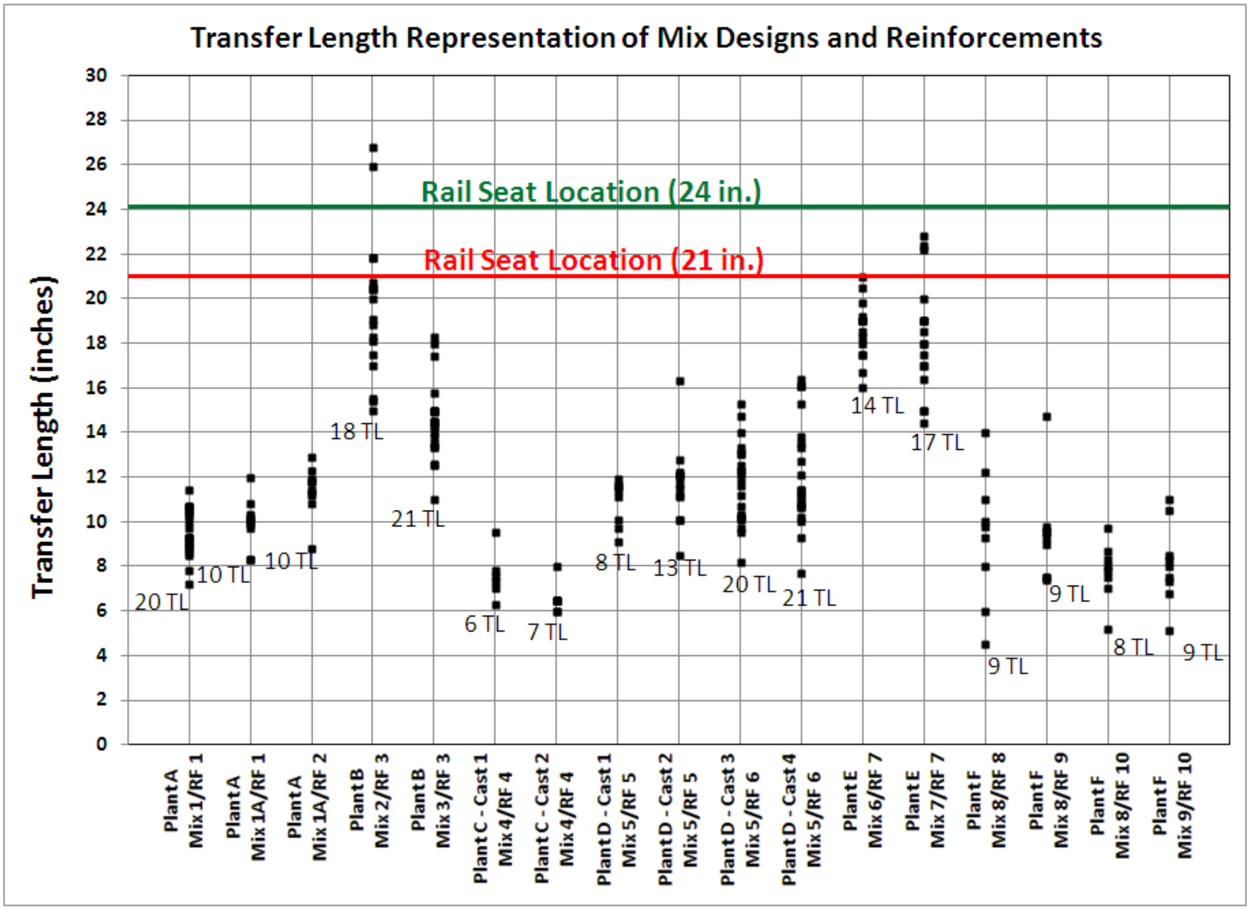

Figure 6.3 Transfer length values presented for each cast

Each of the short-term transfer length measurements for Plant A can be seen in Appendix A. Transfer length values after prestress release and saw-cutting, as well as the method used to measure the transfer length, are shown in table A.1 in appendix A. All figures in Appendix A show the strain profile and 95% AMS line plotted for each tie end that was measured at the plant. Each tie was assigned a number, and the ends were labeled either A or B. This labeling system helped with documentation of each concrete tie. Transfer length graphs for Plants B, C, D, E, and F are shown in appendices B, C, D, E, and F, respectively.

6.2 Transfer Lengths Correlated with Compressive Strength of Concrete

Previous research has found that the release strength of the concrete is a major factor influencing transfer length. Generally, transfer length will become shorter as the compressive strength of the concrete increases (Barnes 2003); this is caused by the prestressing reinforcement introducing radial compressive stresses into the concrete due to the Hoyer effect. This creates a pressure between the steel and concrete, and the greater the compressive strength of the concrete, the greater the bond performance. Figure 6.4 shows the average transfer length measured for each cast, correlated with average release strength of the concrete of each cast. The trend line illustrates the decrease in transfer length as the concrete strength increases. However, the coefficient of determination R^2 for these data points with respect to the theoretical line of perfect correlation is only 0.15. This lack of correlation may be caused by the variations of mix design and reinforcement type used at each plant.

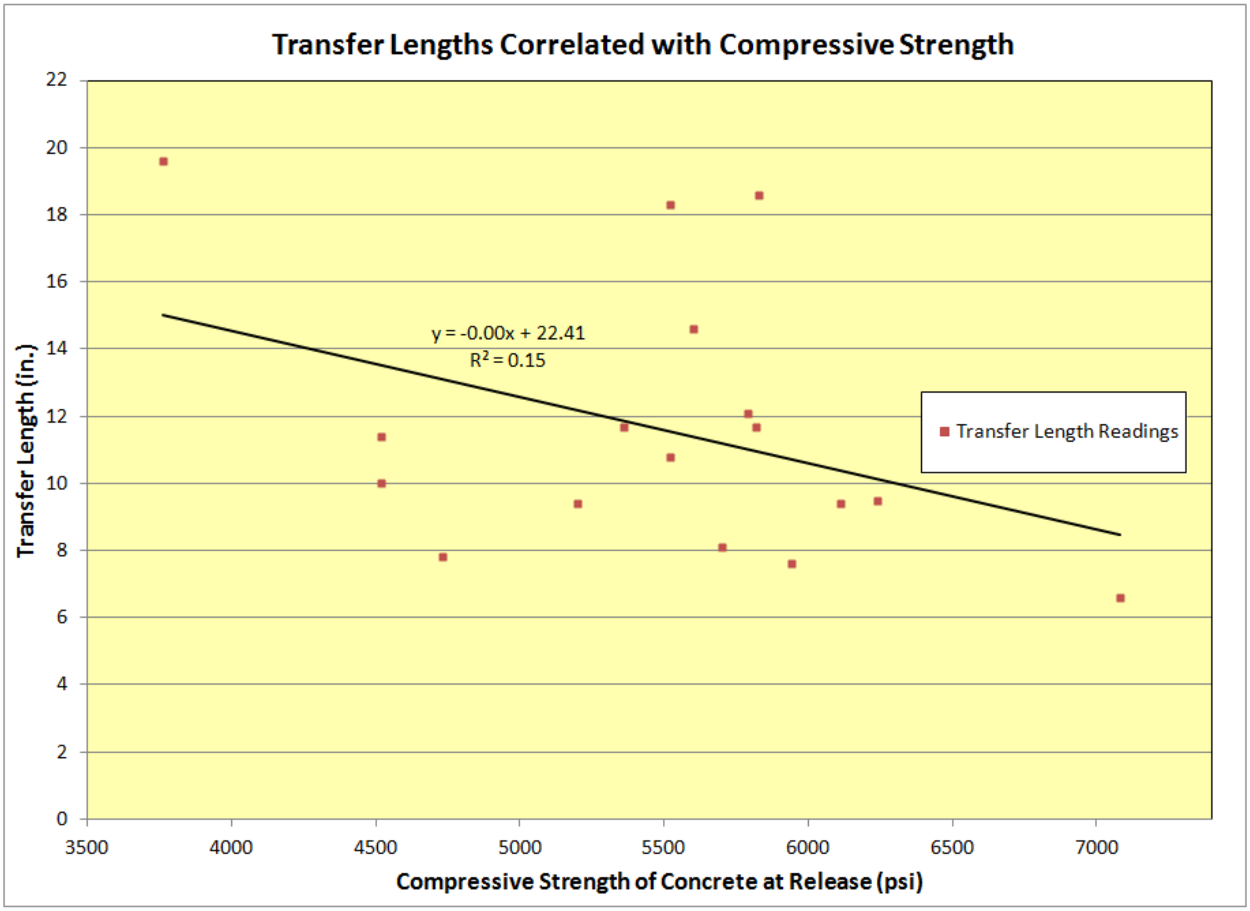

Figure 6.4 Transfer lengths correlated with compressive strength of concrete at release

6.3 Transfer Lengths Correlated with Tensile Strength of Concrete

The ACI 318-11 equation for the tensile strength of concrete is shown below:

$$f_{ct} = 6.7\sqrt{f_c^{'}} \tag{6.1}$$

In this equation, f_{ct} is the split tensile strength and f'_c is the compressive strength of the concrete. This equation implies that, as the compressive strength of concrete increases, so does the tensile strength. Transfer lengths of prestressed concrete members should decrease as the tensile strength increases. Figure 6.5 below shows the average transfer length for each cast at the time of saw-cutting, correlated with the average tensile strength from each cast of the concrete at release. The trend line decreases as the tensile strength increases. This indicates that larger concrete tensile capacities are desired during the time of release. The R^2 value of the trend line is 0.53. This indicates that the transfer lengths have better correlation with split tensile strengths than with compressive strengths at release.

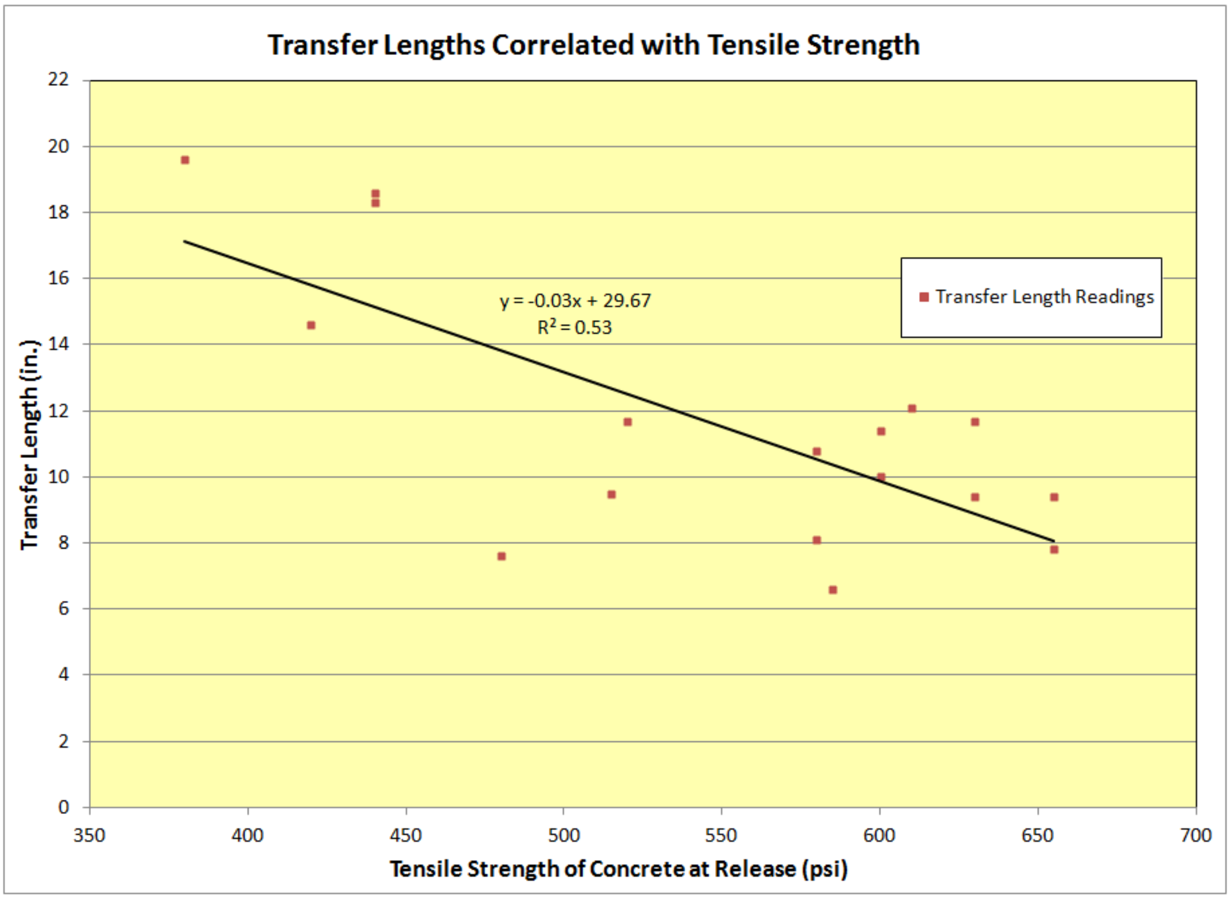

Figure 6.5 Transfer lengths correlated with tensile strength of concrete at release

6.4 Transfer Length Results of 3-Point Average and 9-Point Average

As mentioned in section 4.2, the 9-Point Average method was used to determine transfer lengths of ties measured using the laser speckle. This section presents transfer lengths using both the 3-point average and 9-point average methods for laser speckle measurements. The tables below indicate the similarity of the results obtained for each method. The last column in each table represents the absolute value of the difference between the two measurement procedures.

Table 6.3 Transfer lengths obtained for 3-point and 9-point average for Plant A measurements

	Tie Label	3 Pt Avg (in.)	9 Pt Avg (in.)	Difference of 3 Pt Avg and 9 Pt Avg (in.)
Plant A Mix 1/RF 1	1B	10.2	10.7	0.5
	2A	7.5	7.8	0.3
	4B	10.7	10.6	0.1
	5A	9.5	10.0	0.5
	6A	9.7	10.5	0.8
	7B	7.0	7.2	0.2
	11B	9.8	8.9	0.9
	12A	7.7	8.5	0.8
	13B	10.4	10.7	0.3
	14A	8.4	8.8	0.4
	15B	9.0	9.1	0.1
	16A	8.7	8.6	0.1
Plant A Mix 1A/RF 1	4A	10.1	10.3	0.2
	4B	7.9	8.3	0.4
	8A	8.6	8.3	0.3
	8B	10.3	9.9	0.4
	12A	10.9	12.0	1.1
	12B	9.5	10.2	0.7
Plant A Mix 1A/RF 2	1A	12.8	12.9	0.1
	1B	11.6	11.8	0.2
	6A	10.4	10.8	0.4
	6B	12.7	11.9	0.8
	9A	11.3	11.8	0.5
	9B	8.2	8.8	0.6

Table 6.4 Transfer lengths obtained for 3-point and 9-point average for Plant B measurements

	Tie Label	3 Pt Avg (in.)	9 Pt Avg (in.)	Difference of 3 Pt Avg and 9 Pt Avg (in.)
Plant B Mix 2/RF 3	1A	20.1	20.7	0.6
	1B	18.9	19.1	0.2
	3A	22.1	21.8	0.3
	5B	25.7	25.9	0.2
	6A	18.1	18.1	0.0
	6B	21.4	21.8	0.4
	7A	20.1	20.4	0.3
	7B	19.5	20.0	0.5
	11A	14.6	15.0	0.4
	13A	16.2	17.0	0.8
	13B	15.1	15.4	0.3
	15B	15.4	15.5	0.1
Plant B Mix 3/RF 3	18A	10.2	11.0	0.8
	18B	13.0	13.3	0.3
	19A	17.7	17.4	0.3
	19B	12.7	13.4	0.7
	20A	14.5	14.5	0.0
	20B	18.2	18.3	0.1
	21A	15.0	15.0	0.0
	21B	15.3	15.8	0.5
	24A	18.4	18.0	0.4
	26A	13.4	13.5	0.1
	26B	13.9	13.8	0.1
	27A	13.7	14.0	0.3
	27B	15.0	15.0	0.0
	28A	13.0	12.5	0.5
	28B	14.6	14.5	0.1

Table 6.5 Transfer lengths obtained for 3-point and 9-point average for Plant C measurements

	Tie Label	3 Pt Avg (in.)	9 Pt Avg (in.)	Difference of 3 Pt Avg and 9 Pt Avg (in.)
Plant C Mix 4/RF 4 Cast 2	1A	6.0	6.5	0.5
	2A	6.0	6.0	0.0
	2B	6.0	6.5	0.5
	3A	6.0	6.0	0.0
	3B	6.5	6.5	0.0
	4A	6.0	6.5	0.5
	4B	7.5	8.0	0.5

Table 6.6 Transfer lengths obtained for 3-point and 9-point average for Plant D measurements

	Tie Label	3 Pt Avg (in.)	9 Pt Avg (in.)	Difference of 3 Pt Avg and 9 Pt Avg (in.)
Plant D Mix 5/RF 5 Cast 1	4A	11.3	11.6	0.3
	5A	10.9	11.6	0.7
	8A	9.8	9.7	0.1
	9A	10.1	11.9	1.8
	10A	10.5	11.1	0.6
Plant D Mix 5/RF 5 Cast 2	12A	9.2	10.1	0.9
	13A	11.1	12.2	1.1
	14A	11.4	12.0	0.6
	14B	12.8	12.8	0.0
	15A	10.2	10.1	0.1
	15B	11.9	12.1	0.2
	16A	9.7	11.1	1.4
	16B	12.0	12.1	0.1
	22A	16.5	16.3	0.2
	22B	12.1	11.7	0.4

Table 6.7 Transfer lengths obtained for 3-point and 9-point average for Plant D measurements

	Tie Label	3 Pt Avg (in.)	9 Pt Avg (in.)	Difference of 3 Pt Avg and 9 Pt Avg (in.)
Plant D Mix 5/RF 6 Cast 3	23B	12.0	12.5	0.5
	24B	12.2	13.1	0.9
	25A	10.5	10.7	0.2
	25B	11.9	11.9	0.0
	26A	10.0	10.1	0.1
	27A	8.0	8.2	0.2
	28A	9.0	10.3	1.3
	30A	12.0	12.2	0.2
	30B	13.3	13.3	0.0
	31A	14.9	14.7	0.2
	31B	13.2	14.0	0.8
	32A	12.1	11.6	0.5
	32B	9.8	10.2	0.4
	33A	10.9	12.3	1.4
	33B	12.1	13.0	0.9
	34A	10.7	11.2	0.5
	34B	16.0	15.3	0.7
Plant D Mix 5/RF 6 Cast 4	35B	11.2	12.1	0.9
	36A	11.3	11.1	0.2
	36B	10.6	10.2	0.4
	37B	10.8	10.8	0.0
	38A	6.6	7.7	1.1
	38B	12.4	13.5	1.1
	39B	10.0	10.8	0.8
	40A	10.0	10.7	0.7
	40B	9.4	10.0	0.6
	42A	13.9	13.3	0.6
	42B	13.0	12.7	0.3
	43A	10.8	11.4	0.6
	43B	15.0	15.3	0.3
	44A	15.9	16.1	0.2
	44B	14.0	13.8	0.2
	45B	15.9	16.4	0.5
	46A	11.4	11.4	0.0
	46B	15.7	16.1	0.4

Table 6.8 Transfer lengths obtained for 3-point and 9-point average for Plant E measurements

	Tie Label	3 Pt Avg (in.)	9 Pt Avg (in.)	Difference of 3 Pt Avg and 9 Pt Avg (in.)
Plant E Mix 6/RF 7	1A	18.5	18.5	0.0
	1B	20.0	21.0	1.0
	2A	18.0	18.0	0.0
	2B	19.0	19.0	0.0
	3A	19.0	19.0	0.0
	3B	17.0	17.5	0.5
	5A	18.8	20.5	1.7
	5B	15.5	16.0	0.5
	6A	15.5	17.5	2.0
	6B	19.0	19.0	0.0
Plant E Mix 7/RF 7	11A	17.0	17.5	0.5
	11B	18.0	19.0	1.0
	12A	19.0	18.0	1.0
	12B	23.0	22.4	0.6
	13A	19.0	20.0	1.0
	13B	16.0	17.0	1.0
	14A	18.0	18.0	0.0
	15A	18.0	18.5	0.5
	15B	16.0	17.0	1.0
	16A	20.0	19.0	1.0
	16B	18.1	22.8	4.7

Table 6.9 Transfer lengths obtained for 3-point and 9-point average for Plant F measurements

	Tie Label	3 Pt Avg (in.)	9 Pt Avg (in.)	Difference of 3 Pt Avg and 9 Pt Avg (in.)
Plant F Mix 8/RF 8	1A	9.5	10.0	0.5
	1B	14.5	14.0	0.5
	2A	7.0	8.0	1.0
	2B	4.5	4.5	0.0
	3A	6.0	6.0	0.0
	3B	9.5	9.8	0.3
Plant F Mix 8/RF 9	1A	8.5	9.0	0.5
	1B	8.2	9.6	1.4
	2A	13.4	14.7	1.3
	2B	8.5	9.5	1.0
	3A	7.6	7.5	0.1
	3B	8.0	7.5	0.5
Plant F Mix 8/RF 10	1B	6.5	7.0	0.5
	2A	8.0	7.5	0.5
	2B	7.7	8.3	0.6
	3A	5.1	5.2	0.1
	3B	7.5	8.0	0.5
Plant F Mix 9/RF 10	1A	5.0	5.1	0.1
	1B	8.0	8.0	0.0
	2A	10.5	11.0	0.5
	2B	8.7	10.5	1.8
	3A	7.5	7.5	0.0
	3B	8.0	8.5	0.5

Tables 6.3-6.9 (above) indicate that the 3-point average and 9-point average methods are very comparable. Also indicated is that the 9-point average method produces smooth strain profiles that are easy to use and interpret; for these reasons, this method was preferred for the determination of transfer lengths when using the laser speckle imaging device.

6.5 Long-term Transfer Length Results

Long-term transfer lengths were monitored on the concrete ties with embedded Whittemore points. Problems with surface preservation make long-term measurements difficult using the laser-speckle. Tables 6.10-6.15 show initial and long-term transfer length measurements in inches. A percent increase in transfer length was also calculated with this information. Due to the fact that six prestressed concrete tie plants were visited over the course of a 15-month period, long-term data varied from plant to plant. The extensive long-term data collected from the first few plants that were visited was obviously not obtainable from the last of the plants visited. However, all ties were at least 60 days old, and previous research has shown that almost all of the transfer-length increases occur during the first 28 after de-tensioning (Barnes et al. 2003). Long-term measurements in tables 6.10-6.15 correspond to the last time transfer length readings were taken on the set of ties. To reduce the effects of thermal strains, the concrete ties were placed inside at room temperature a few days prior to taking the final set of measurements.

The tie plants made the final decision on which ties would be sent back for long-term measurements. Since each plant only sent a few ties to KSU for long-term measurements, not all concrete-mix designs and reinforcements were monitored for long-term transfer lengths.

Table 6.10 Long-term transfer length data for Plant A

	Tie	Initial (in.)	Long Term (in.)	Percent Increase
Plant A Mix 1A/RF 1	3A	10.8	10.8	0.0
	3B	10.1	10.6	5.0
	7A	9.7	10.6	9.3
	7B	10	11.2	12.0
Plant A Mix 1A/RF 2	2A	11.3	11.7	3.5
	2B	11.4	13.2	15.8
	5A	11.2	12.8	14.3
	5B	12.3	13.7	11.4

Table 6.11 Long-term transfer length data for Plant B

	Tie	Initial (in.)	Long Term (in.)	Percent Increase
Plant B Mix 2/RF 3	4A	20.4	21.6	5.9
	9A	18.3	19.1	4.4
	9B	20.5	20.5	0.0
	14A	18.8	18.9	0.5
	14B	17.5	18.4	5.1
Plant B Mix 3/RF 3	17A	14.3	15.3	7.0
	17B	14.9	14.9	0.0
	23A	12.6	13.5	7.1
	23B	14.4	14.4	0.0
	25A	14.3	15	4.9
	25B	14.5	14.7	1.4

Table 6.12 Long-term transfer length data for Plant C

	Tie	Initial (in.)	Long Term (in.)	Percent Increase
Plant C Mix 4/RF 4 Cast 1	1A	7	8.1	15.7
	1B	7.6	9.5	25.0
	2A	7.8	9.3	19.2
	2B	7.3	10.2	39.7
	3A	6.3	8.3	31.7
	3B	9.5	10.3	8.4
Plant C Mix 4/RF 4 Cast 2	1A	6.5	7.5	15.4
	2A	6	8.5	41.7
	2B	6.5	8.5	30.8
	3A	6	9.2	53.3
	3B	6.5	10	53.8

Table 6.13 Long-term transfer length data for Plant D

	Tie	Initial (in.)	Long Term (in.)	Percent Increase
Plant D Mix 5/RF 5 Cast 1	1A	9.1	11	20.9
	7A	11.4	11.6	1.8
	7B	10.1	10.9	7.9
Plant D Mix 5/RF 5 Cast 2	12B	8.5	9.9	16.5
	19A	11.5	13.4	16.5
	19B	11.2	11.9	6.3
Plant D Mix 5/RF 6 Cast 3	23A	9.5	10.2	7.4
	29A	10.2	11.2	9.8
	29B	9.7	10.9	12.4
Plant D Mix 5/RF 6 Cast 4	35A	9.3	10.5	12.9
	41A	10.6	12	13.2
	41B	11.2	11.4	1.8

Table 6.14 Long-term transfer length data for Plant E

	Tie	Initial (in.)	Long Term (in.)	Percent Increase
Plant E Mix 7/RF 7	9A	22.2	22.6	1.8
	9B	15	15.2	1.3
	17A	19	19.4	2.1
	17B	14.4	14.9	3.5

Table 6.15 Long-term transfer length data for Plant F

	Tie	Initial (in.)	Long Term (in.)	Percent Increase
Plant F Mix 8/RF 8	4A	9.3	11.8	26.9
	4B	12.2	12.5	2.5
Plant F Mix 8/RF 9	4A	7.4	10.9	47.3
	4B	9.3	12.4	33.3
Plant F Mix 8/RF 10	4A	9.7	10.4	7.2
	4B	8.7	10.1	16.1
Plant F Mix 9/RF 10	4A	7.3	8.3	13.7
	4B	6.8	8.7	27.9

Table 6.16 (below) demonstrates the average increase and standard deviation of the long-term transfer length measurements. These values represent the transfer length increase that can be expected due to creep and shrinkage of the concrete over time. TL in this table represents transfer length.

Table 6.16 Average long-term increase of transfer length and standard deviation of increase

	Average TL Increase (in.)	Std. Dev. (in.)
Plant A Mix 1A/RF 1	0.65	0.52
Plant A Mix 1A/RF 2	1.30	0.62
Plant B Mix 2/RF 3	0.60	0.52
Plant B Mix 3/RF 3	0.47	0.45
Plant C Mix 4/RF 4 Cast 1	1.70	0.75
Plant C Mix 4/RF 4 Cast 2	2.44	1.00
Plant D Mix 5/RF 5 Cast 1	0.97	0.86
Plant D Mix 5/RF 5 Cast 2	1.33	0.60
Plant D Mix 5/RF 6 Cast 3	0.97	0.25
Plant D Mix 5/RF 6 Cast 4	0.93	0.64
Plant E Mix 7/RF 7	0.38	0.13
Plant F Mix 8/RF 8	1.40	1.56
Plant F Mix 8/RF 9	3.30	0.28
Plant F Mix 8/RF 10	1.05	0.49
Plant F Mix 9/RF 10	1.45	0.64

The long-term transfer length measurements for Plant A can be seen in appendix A under the section titled "Long-term Transfer Lengths." Each strain profile is labeled according to the number of days after casting. The strain profiles for the Whittemore readings were smoothed using the 3-point average technique, and the transfer length was determined using the 95% AMS method. The 95% AMS line is shown on each of the graphs for each strain profile. The color of the 95% AMS line is the same color as its corresponding strain profile. Long-term transfer length graphs for Plants B, C, D, E, and F can be seen in appendices B, C, D, E, and F, respectively. Long-term measurements were taken using the laser-speckle on ties from Plant C Mix 4/RF 4 Cast 2. However, measurements were only taken for 52 days due to surface preservation problems. Differences in the time of measurements were caused by the scheduling of plant visits.

Chapter 7 Rail Seat Positive Moment Tests

After long-term transfer length data had been measured, two ties from each plant were tested for the rail seat positive moment test in accordance with the AREMA chapter 30 Section 4.9.1.8 loading specification. Two ties were chosen from each plant, having considerably different long-term transfer length values. This was done to determine whether the transfer length would affect the load-carrying performance. The ties were load-tested in the civil engineering structural laboratory at Kansas State University using either MTS hydraulic testing equipment or a Baldwin universal testing machine (UTM). Each tie was loaded according to the following requirements:

1) With the tie supported as shown in figure 7.1, a load was applied at a rate no larger than 5 kips per minute until a load of 1.5P was obtained. This load corresponds to 150% of the design moment capacity.

2) If there was no more than 0.001 in. tendon slippage at this load, requirements of the test were met. Tendon slippage was measured on the outermost steels tendons of the lower layer. The load was then increased until ultimate failure occurred or the maximum actuator force was applied.

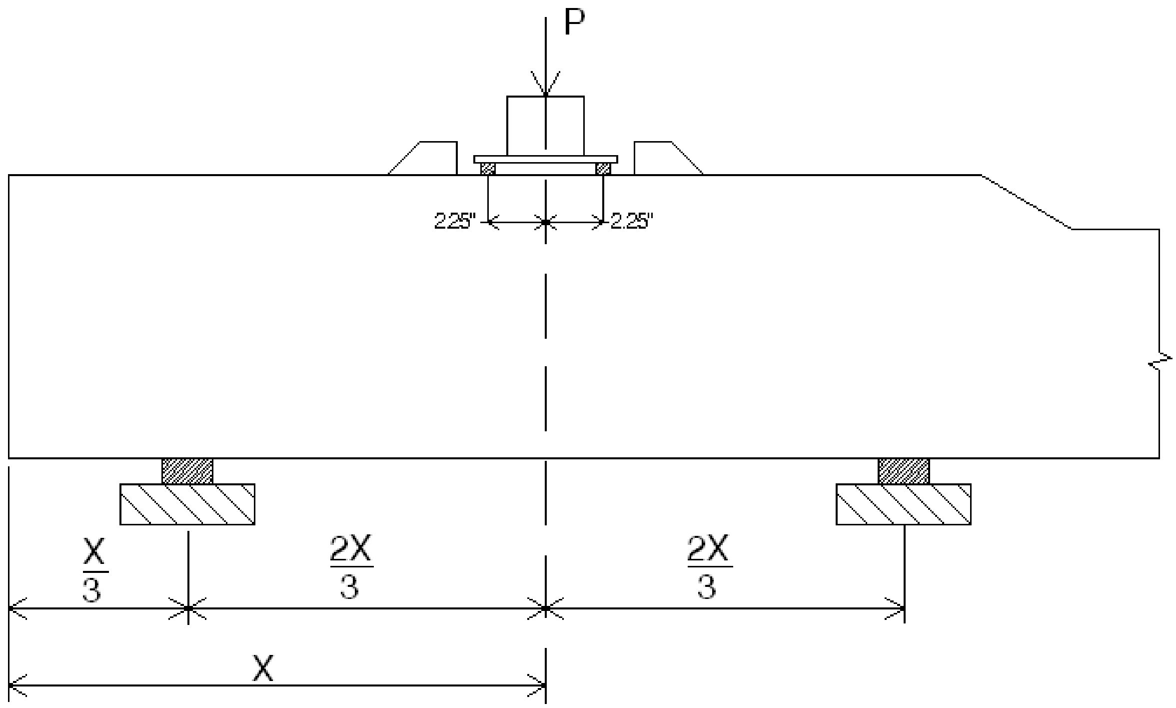

Figure 7.1 Typical layout of rail-seat positive moment test (AREMA 2010)

The value of P was calculated according to the following equation:

$$P = \frac{2M}{\frac{2X}{3} - 2.25"}$$

In this equation, X was determined from figure 7.1, and M is the positive design moment at the rail seat as required by AREMA Article 4.4.1. The positive moment capacity is dependent on the tie spacing and tie length. The design moment is considered as the moment required to produce a crack up to the first layer of prestressing steel. According to contacts at each of the plants, for each of the ties sent back to KSU for long-term measurements, the tie spacing was 24 in. Ties were either 8 ft 6 in. or 9 ft 6 in. long. With this information, a moment capacity of 300 kip-in. and 400 kip-in. was found for the 8 ft 6 in. ties and 9 ft 6 in. ties, respectively. These capacities were determined using a figure found in AREMA section 4.4 Flexural Strength of Prestressed Monoblock Ties. This figure is used to determine the unfactored bending moment at the centerline of the rail-seat. Factored bending moments can be determined by increasing the moments by 10% according to AREMA section 4.4.1.2.

For the 8 ft 6 in. and 9 ft 6 in. ties, it was determined that the tendons could not slip more than 0.001 in. at a load of 84 kips and 96 kips, respectively. If the tendon slippage was greater than 0.001 in. at this load, requirements of the test were not met.

7.1 Rail-Seat Positive Moment Test Setup

The ties were loaded with a 28 in. span, as shown in figure 7.2, and the distance to the rail seat was either 21 in. or 24 in. A load was applied directly at the rail-seat location.

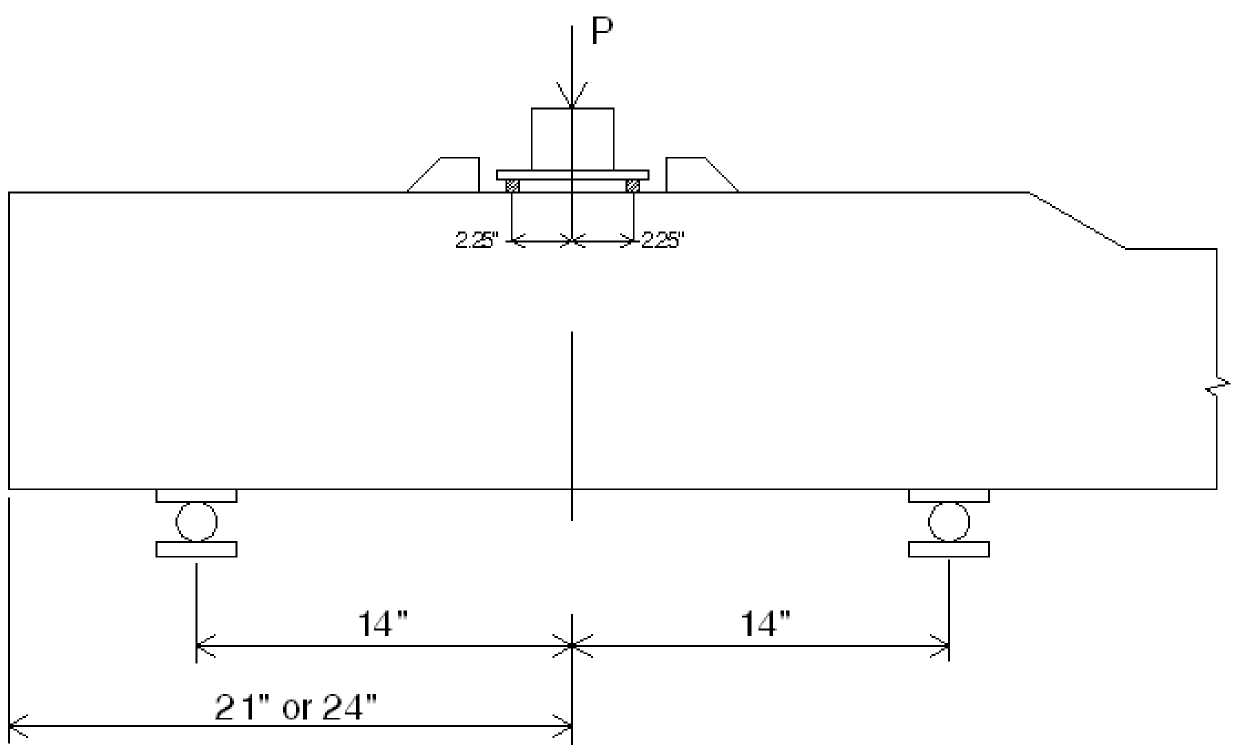

Figure 7.2 Layout of load tests conducted at KSU (AREMA 2010)

Tendon slippage was monitored by two LVDTs. The LVDTs were placed on the outermost reinforcing wires of the lower layer, as shown in figure 7.3.

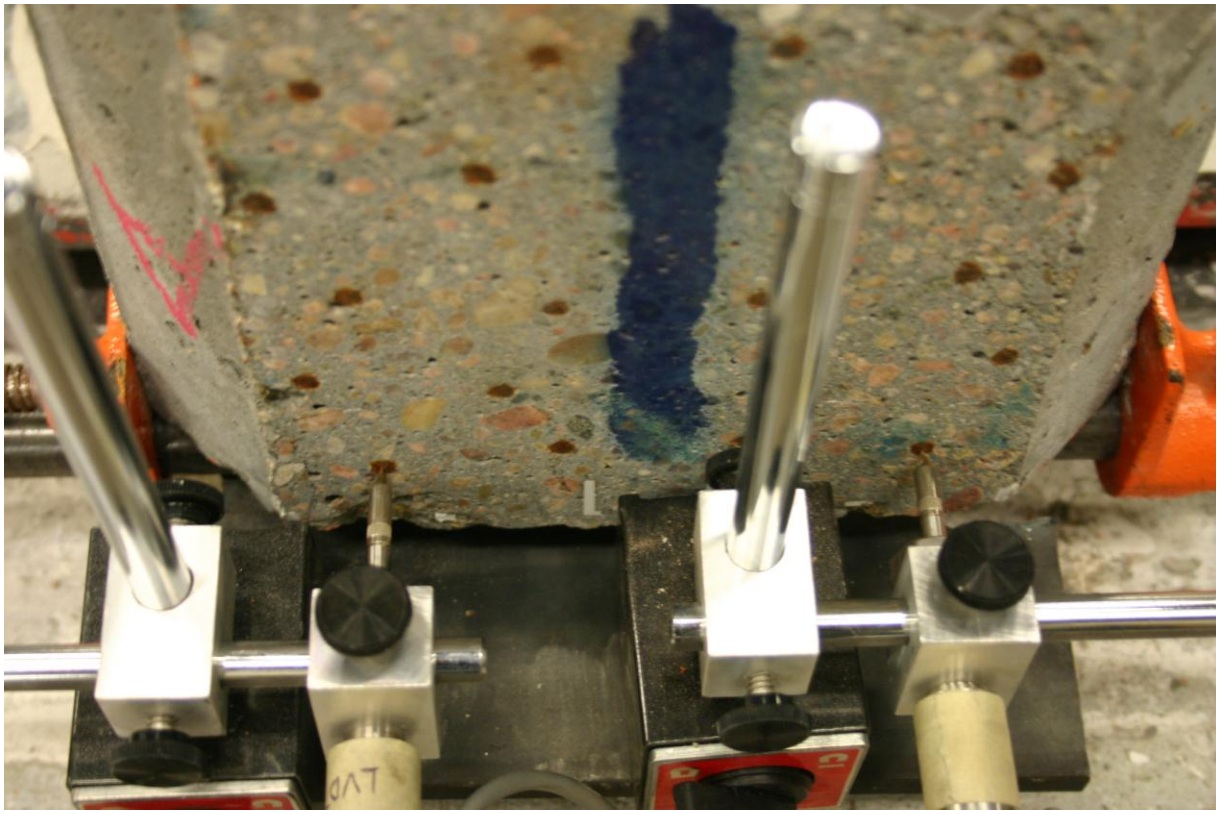

Figure 7.3 LVDT placement on outermost wires of lower layer

In addition to measuring the wire end slip, the midspan deflection was measured during the duration of testing. This procedure is not included in the AREMA loading specifications of chapter 30 section 4.9.1.8; however, the data was collected to observe any variations between the ties. Because the midspan deflection was monitored as well, the ties were set on steel rollers, as shown previously in figure 7.2. The rollers were capped with steel plates, and hydrocal was used to eliminate any instability. This system created a rigid system that would not allow extra deflection during loading. Two LVDTs were then placed at the midspan of the ties to measure deflection. The LVDTs rested on steel brackets held in place by epoxy, as shown below in figure 7.4.

Figure 7.4 LVDT placement at midspan of ties

The entire test setup can be seen in figure 7.5. This includes the load head, two LVDTs at midspan, and the two LVDTs measuring end slip.

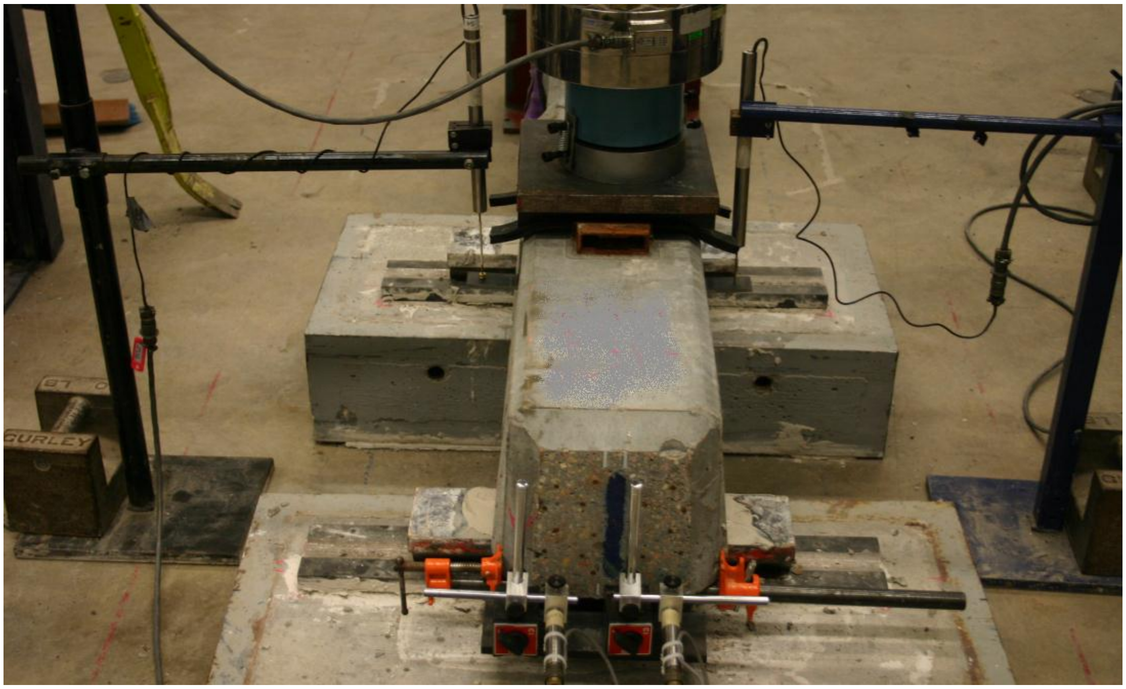

Figure 7.5 Setup of rail seat positive moment test

7.2 Rail-Seat Positive Moment Test Results

Results from the rail-seat positive moment test are shown in table 7.1. In this table, the two end-slip values are shown from the LVDT readings at 150% of the design moment capacity. Any slip value greater than 0.001 in. at this load does not meet the requirements of this test. Two different hydraulic presses were used for load testing the ties. The first press used had a capacity of 155 kips. Due to this stipulation, some of the ties did not reach their ultimate moment capacity. A few of the ties were tested using a press with a capacity of 400 kips. This system had more than enough capacity to bring ties to their ultimate capacity. Table 7.1 is illustrative of how the ties performed and their failure mode. The maximum percentage of the design moment capacity that was reached during load testing is also shown.

Table 7.1 Results of rail-seat positive moment tests

Plant	Tie	Long-Term TL (in.)	End Slip 1 (in.)	End Slip 2 (in.)	Pass/Fail Bond Test	Percentage of Design Capacity	Failure Mode
A	5A	12.8	0	0	Pass	290	No Failure
	5B	13.7	0.0001	0	Pass	290	No Failure
	7A	10.6	0.0004	0.0004	Pass	286	Shear
	7B	11.2	0.0005	0.0001	Pass	267	Shear/longitudinal cracks
B	9A	19.1	0.0021	0	Fail	234	Strand slip and shear
	9B	20.5	0.0001	0.0001	Pass	201	Shear
	23A	13.5	0.0001	0.0002	Pass	235	Shear
	23B	14.4	0.0002	0.0001	Pass	228	Shear
C	1A	8.1	0	0.0001	Pass	237	No Failure
	1B	9.5	0.0004	0.0003	Pass	238	No Failure
	3A	8.3	0.0025	0.0026	Fail	208	Shear
	3B	10.3	0.0001	0.0002	Pass	238	No Failure/large cracks
D	19A	13.2	0.0010	0.0081	Pass	266	Shear
	19B	11.9	0.0002	0.0001	Pass	278	No Failure
	29A	11.2	0.0008	0.0008	Pass	278	Compression/Shear
	29B	10.9	0.0001	0	Pass	279	No Failure
E	9A	22.6	0.0001	0	Pass	373	Shear
	9B	15.2	0	0	Pass	362	Shear
	17A	19.4	0	0	Pass	341	Shear
	17B	14.9	0	0	Pass	335	Shear
F	4A Cast 1	11.8	0	0.0002	Pass	241	No Failure
	4B Cast 1	12.5	0	0.0002	Pass	241	No Failure/large cracks
	4A Cast 4	8.3	0.0002	0.0001	Pass	240	No Failure
	4 B Cast 4	8.7	0	0	Pass	240	No Failure

The graphs from load-testing each tie can be seen in the appropriate sections below. Each graph shows the percentage of design moment capacity versus the mid-span deflection, as well as the two end-slip readings throughout the testing period. End-slip values were only needed up to 84 kips or 96 kips; however, the values were recorded during the entire test, up to the maximum load. Each graph also gives the value for the long-term transfer length of each tie.

7.2.1 Plant A

Every tie from Plant A passed the end-slip requirement. Tie 5 ends A and B did not fail during the load test. However, tie 7 ends A and B both failed due to shear cracking.

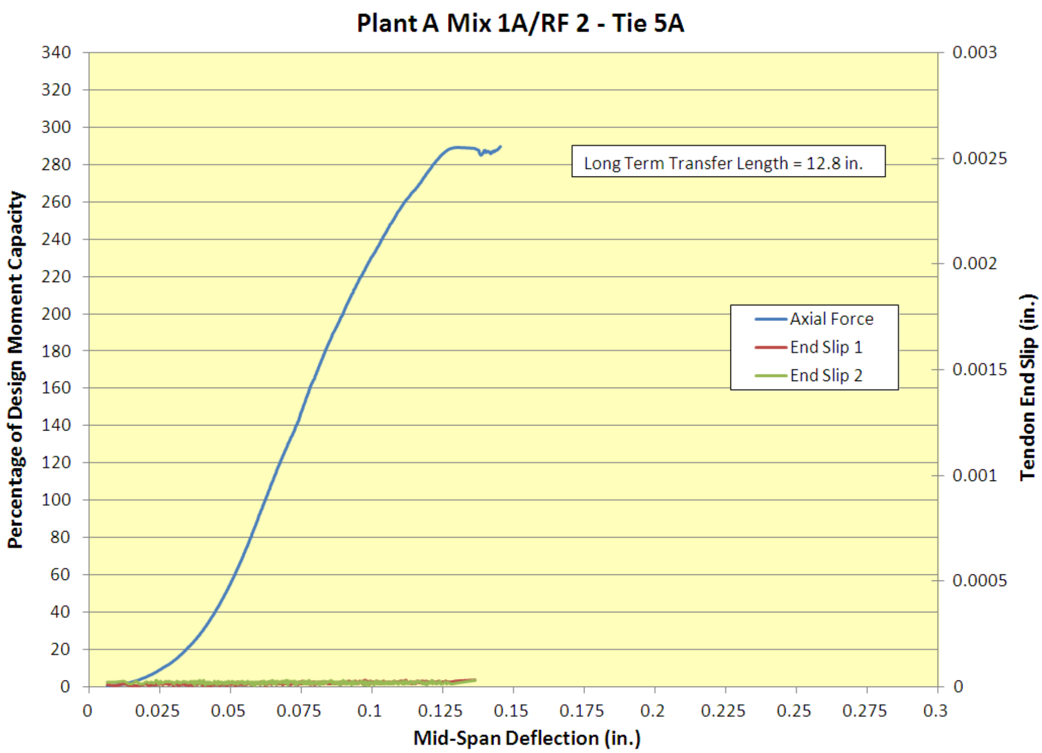

Figure 7.6 Load test results of Plant A Mix 1A/RF 2 Tie 5A

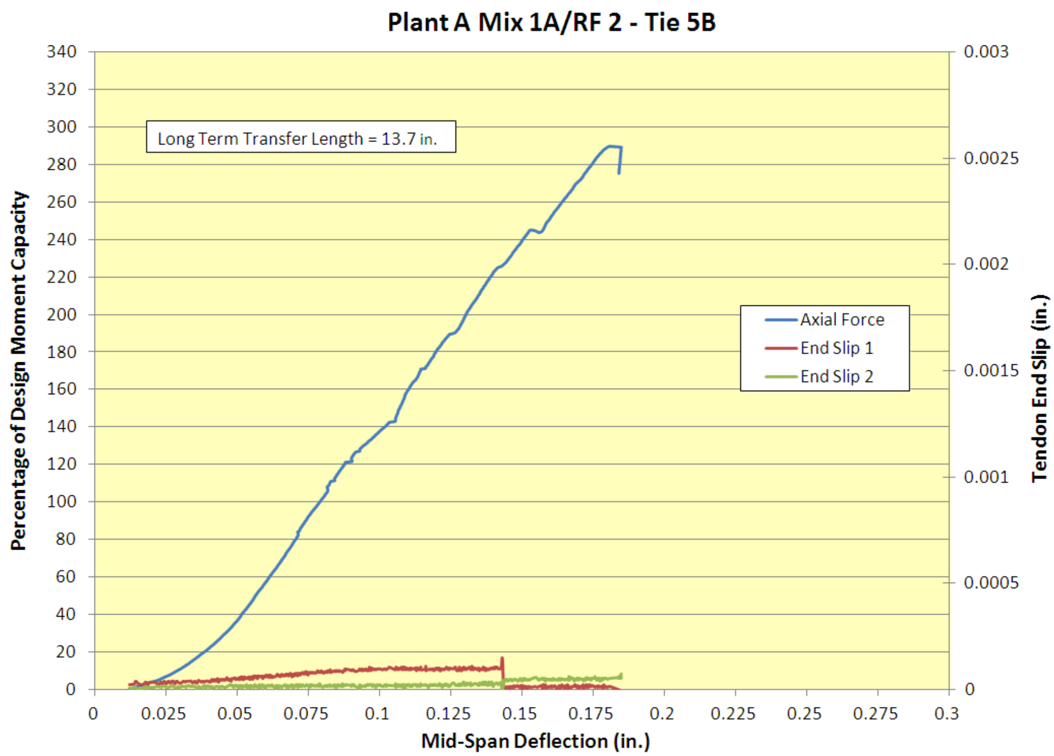

Figure 7.7 Load test results of Plant A Mix 1A/RF 2 Tie 5B

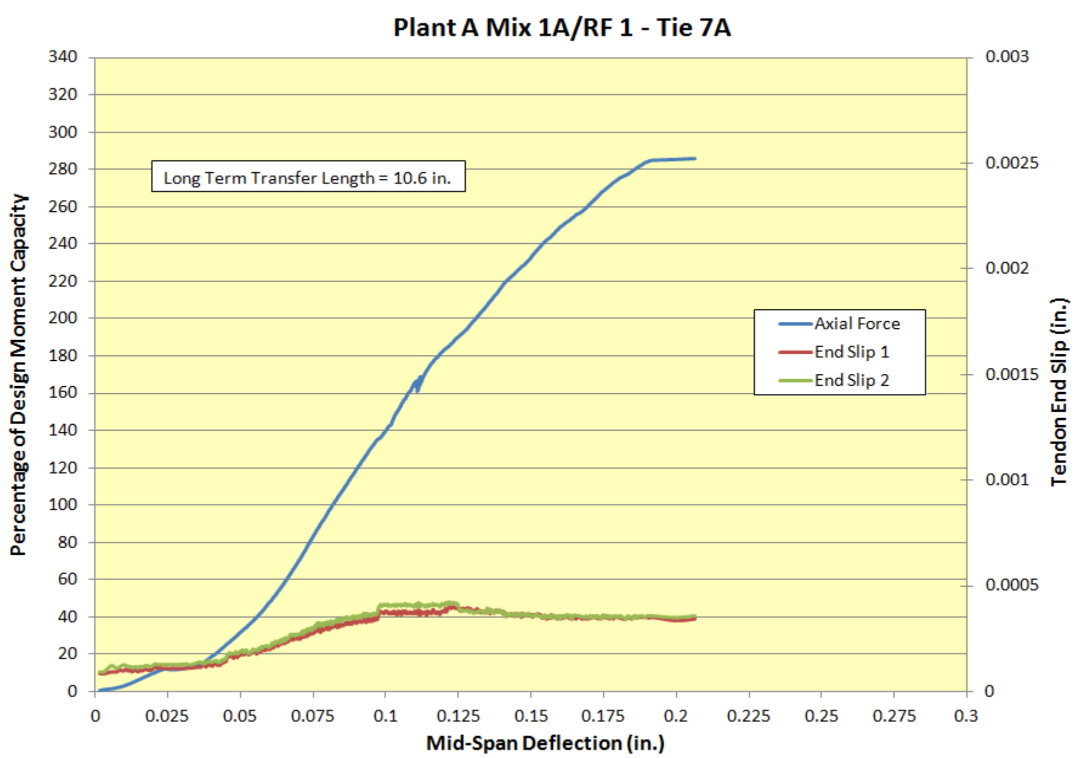

Figure 7.8 Load test results of Plant A Mix 1A/RF 1 Tie 7A

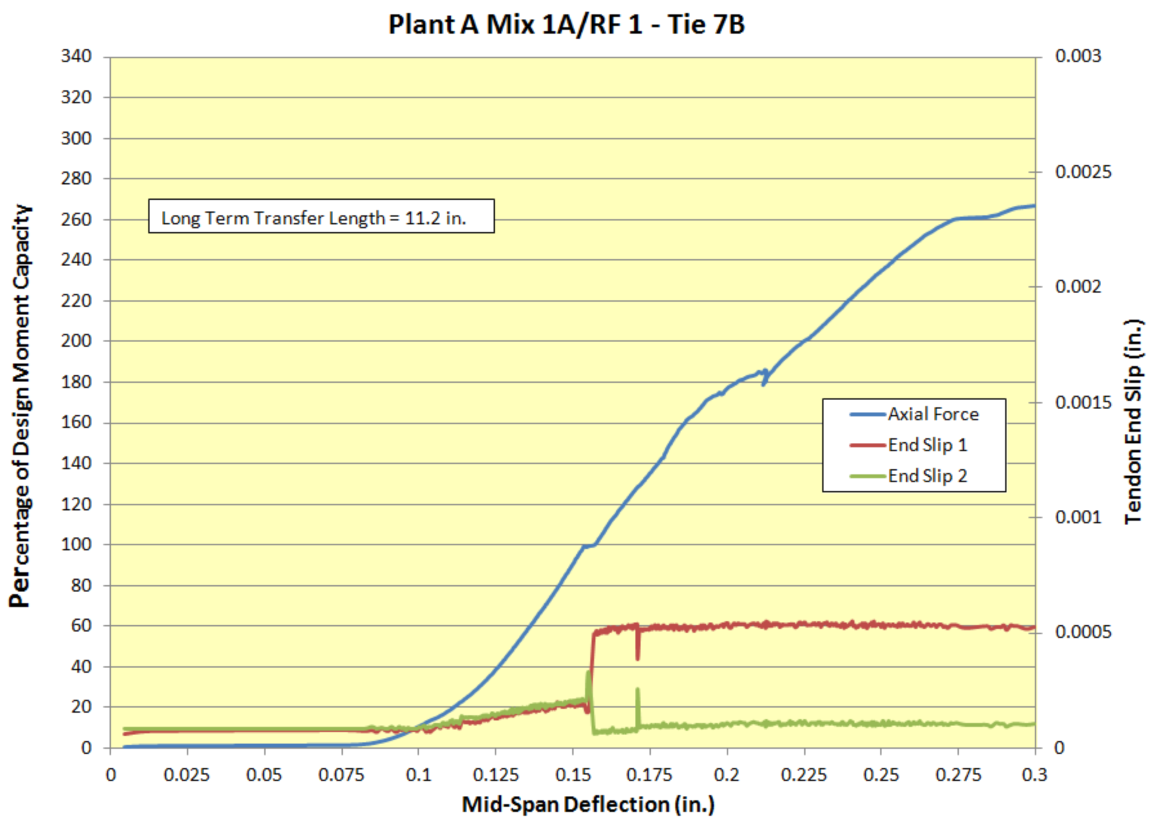

Figure 7.9 Load test results of Plant A Mix 1A/RF 1 Tie 7B

7.2.2 Plant B

Tie 9A failed the bond test with an end slip of 0.0021 in. Every other tie from Plant B passed the bond test. All ties from Plant B failed in shear during load testing.

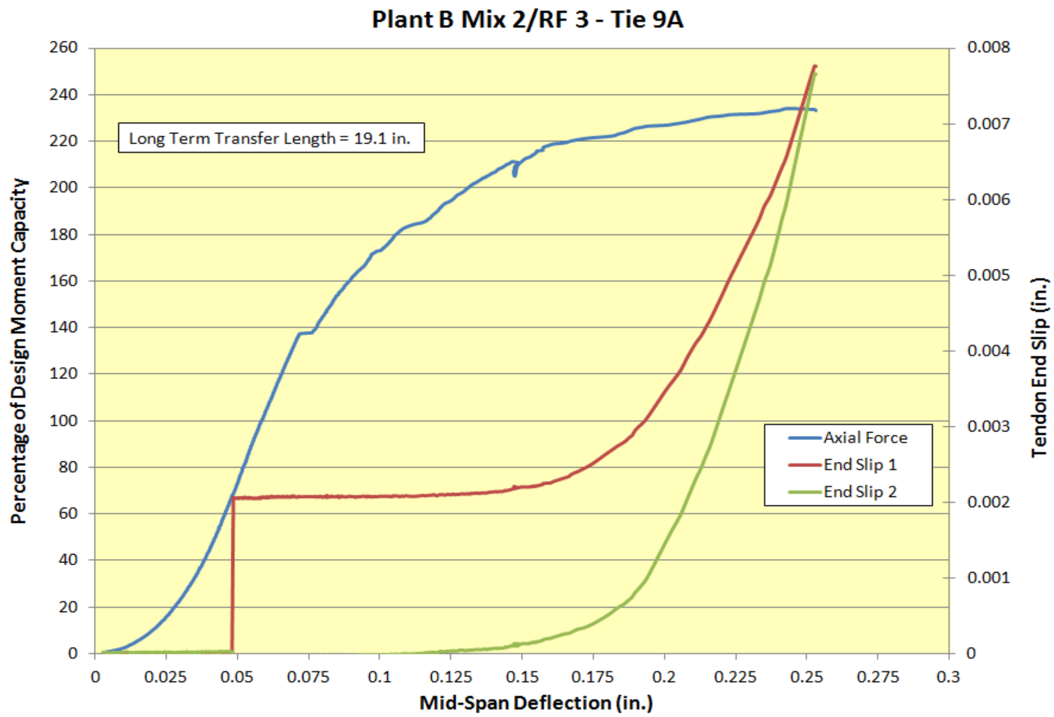

Figure 7.10 Load test results of Plant B Mix 2/RF 3 Tie 9A

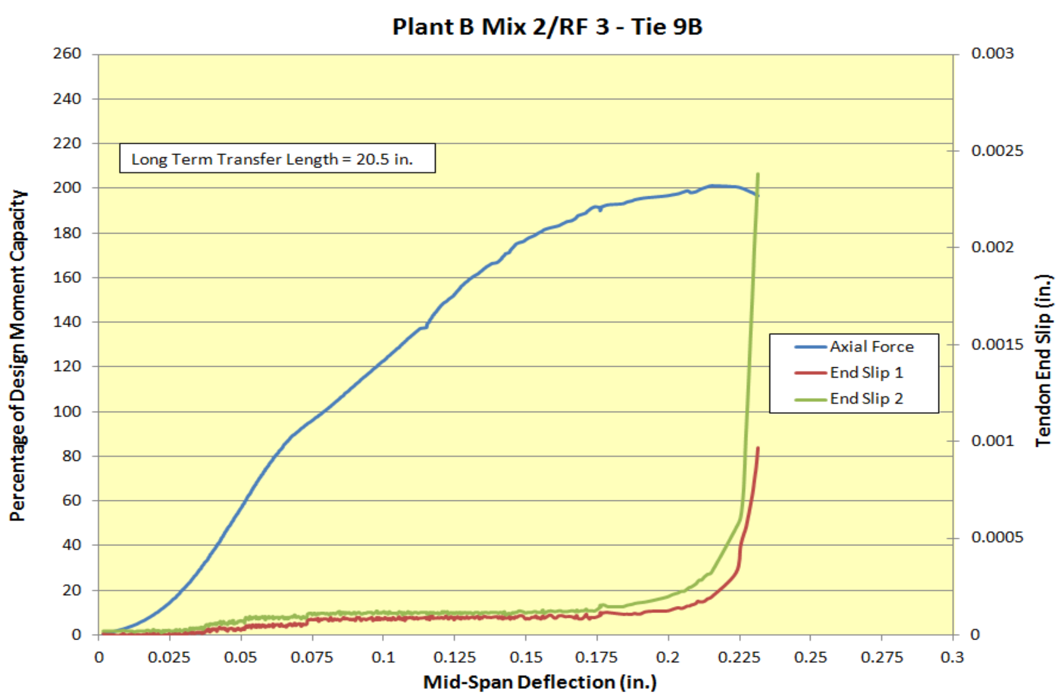

Figure 7.11 Load test results of Plant B Mix 2/RF 3 Tie 9B

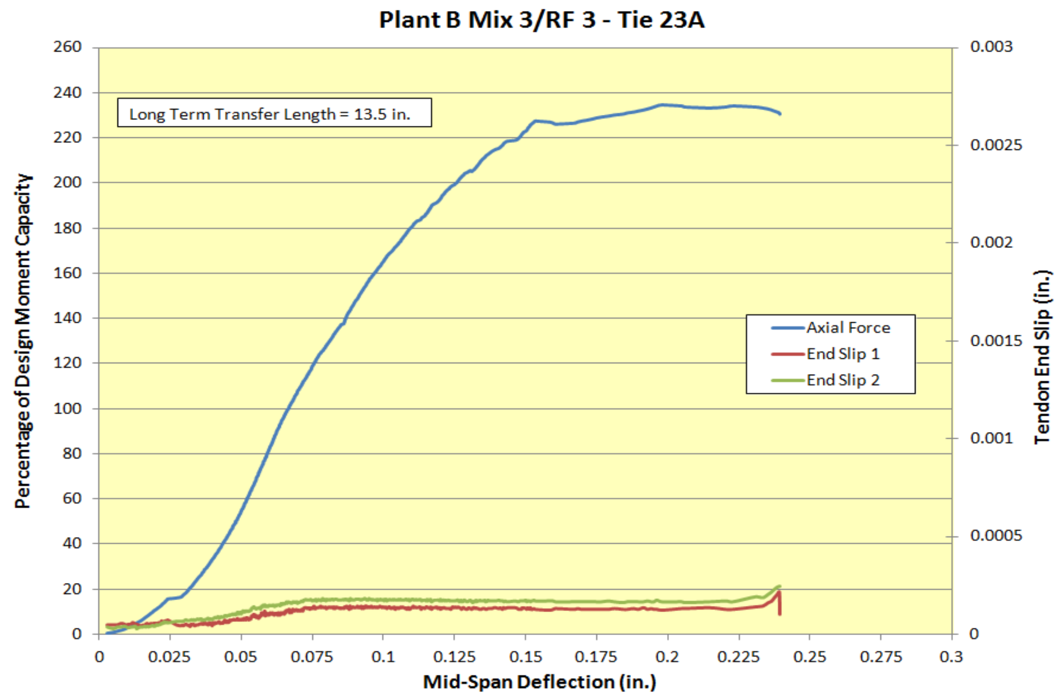

Figure 7.12 Load test results of Plant B Mix 3/RF 3 Tie 23A

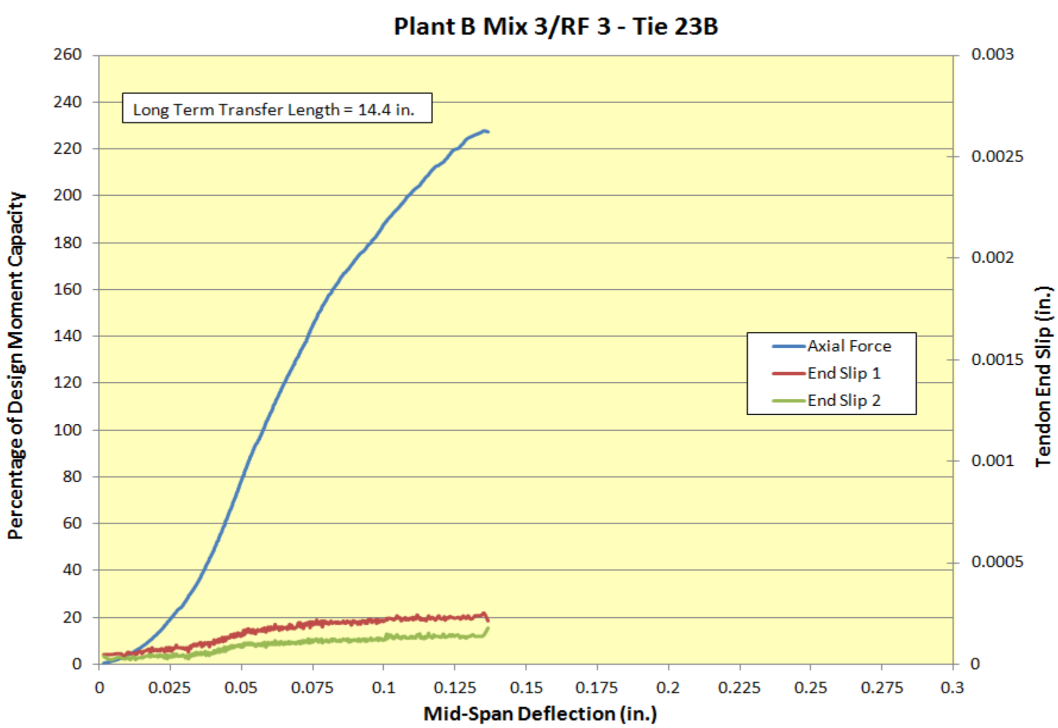

Figure 7.13 Load test results of Plant B Mix 3/RF 3 Tie 23B

7.2.3 Plant C

Tie 3A failed the bond test with an end slip of 0.00251 and 0.00262 in. from the LVDTs, and it was the only tie end to fail in shear during loading. Every other end from Plant C passed the end-slip requirement and did not fail during the load test.

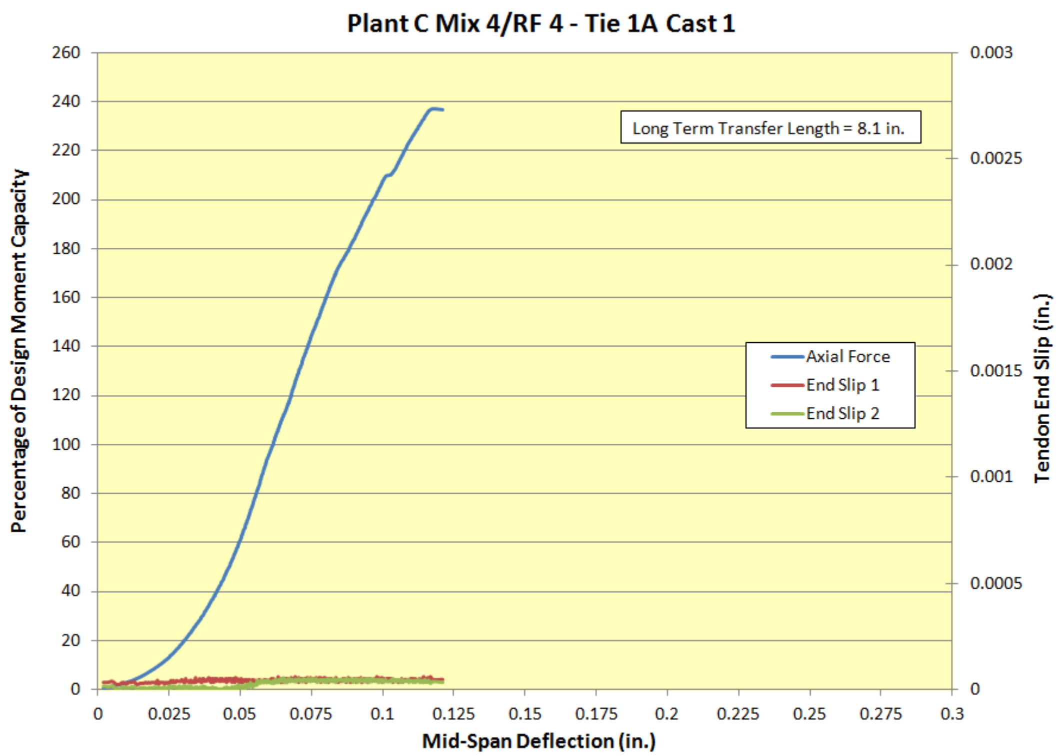

Figure 7.14 Load test results of Plant C Mix 4/RF 4 Tie 1A Cast 1

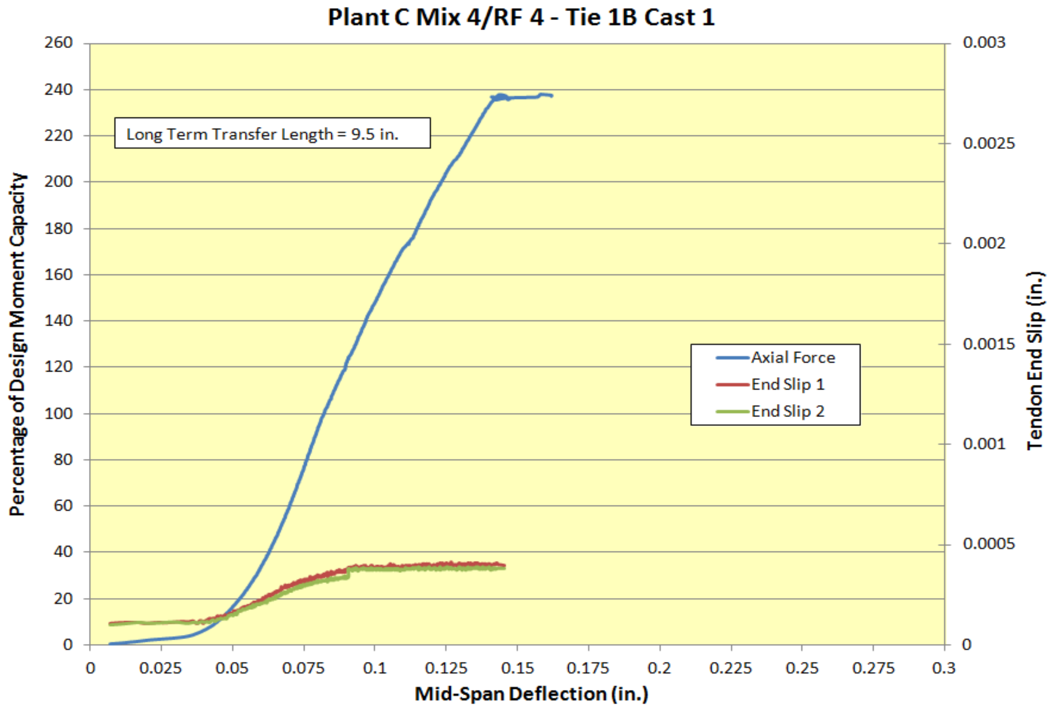

Figure 7.15 Load test results of Plant C Mix 4/RF 4 Tie 1B Cast 1

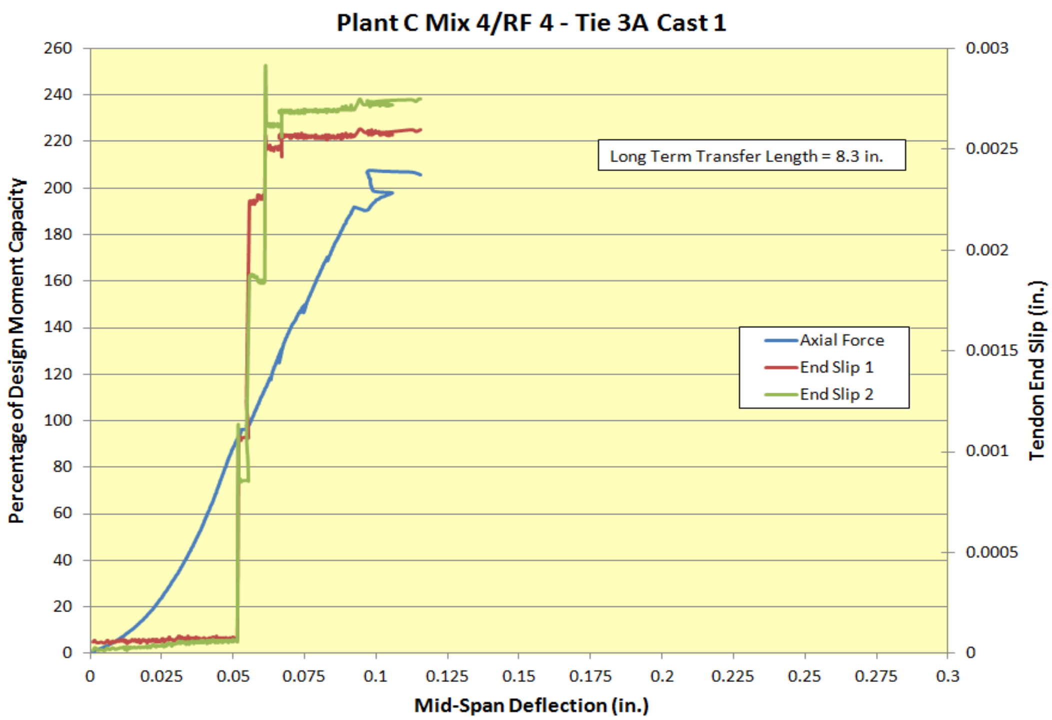

Figure 7.16 Load test results of Plant C Mix 4/RF 4 Tie 3A Cast 1

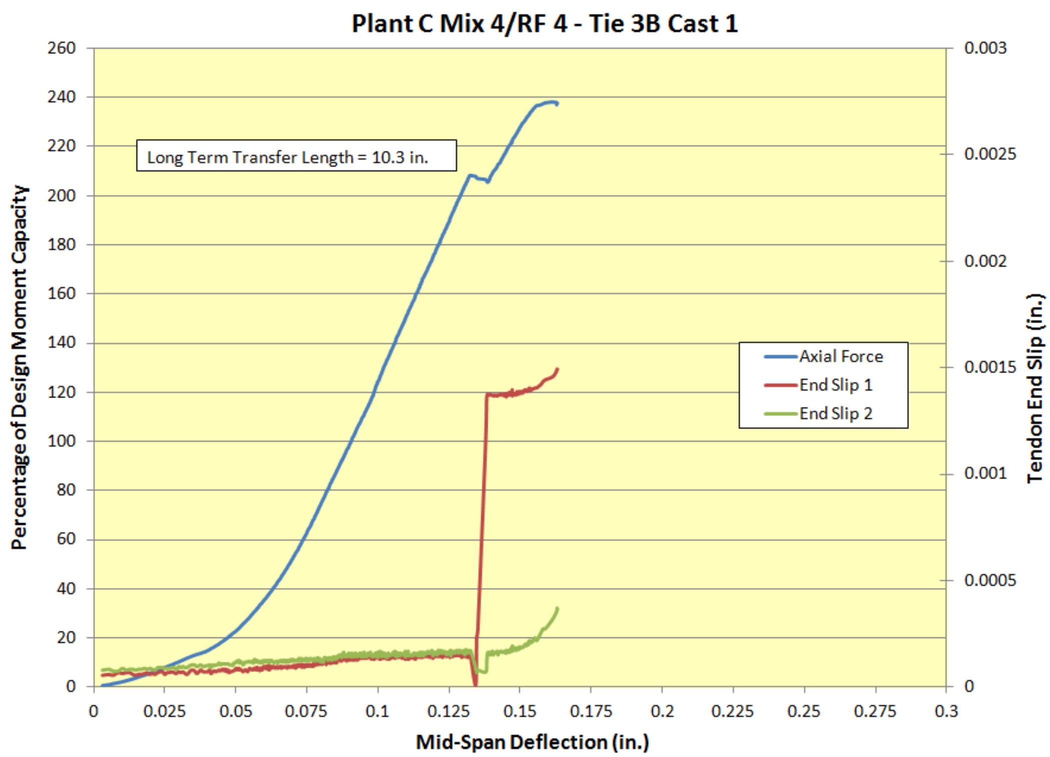

Figure 7.17 Load test results of Plant C Mix 4/RF 4 Tie 3B Cast 1

7.2.4 Plant D

Every tie from Plant D passed the end-slip requirement. Ties 19A and 29A failed in shear during load testing. Ties 19B and 29B did not fail during the load test.

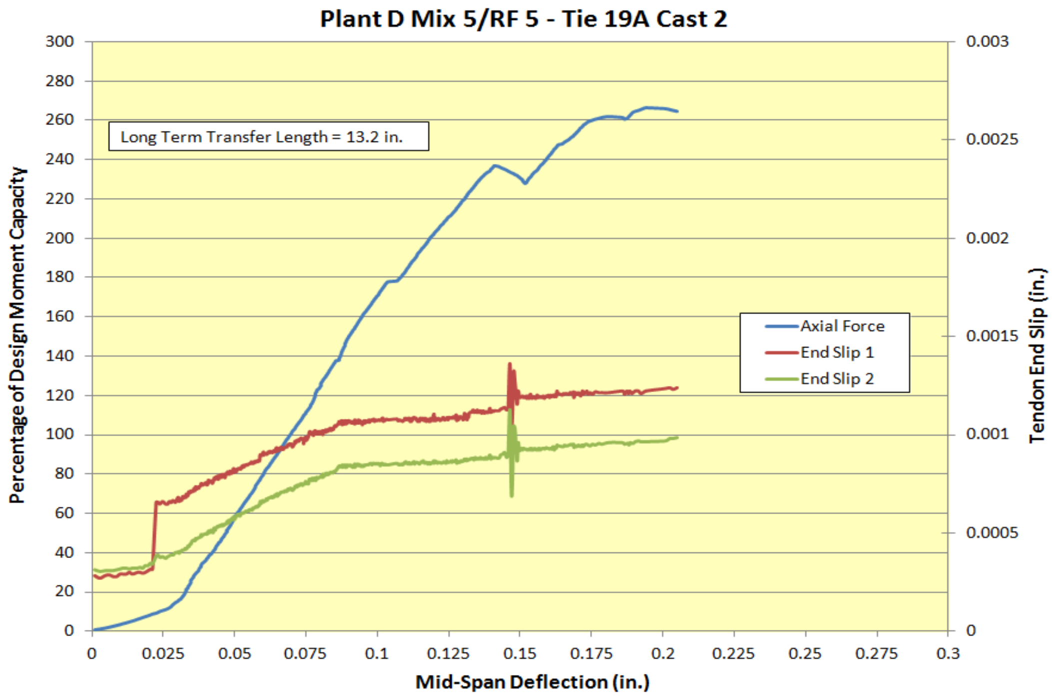

Figure 7.18 Load test results of Plant D Mix 5/RF 5 Tie 19A Cast 2

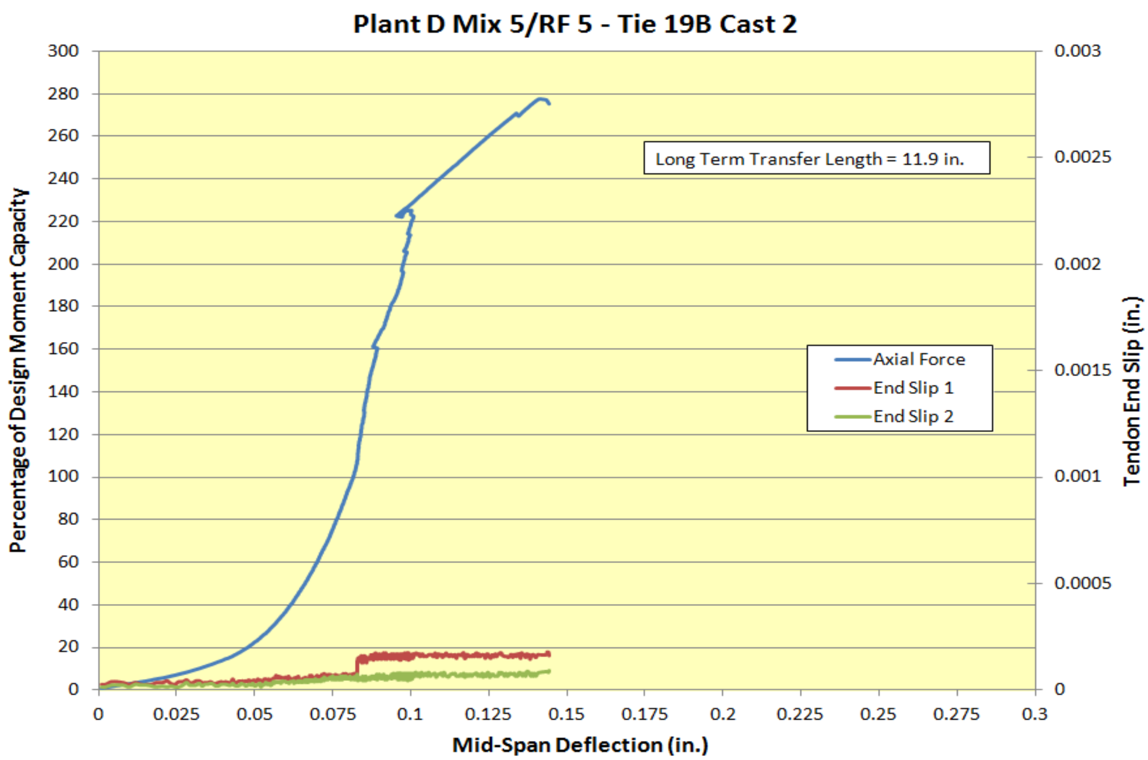

Figure 7.19 Load test results of Plant D Mix 5/RF 5 Tie 19B Cast 2

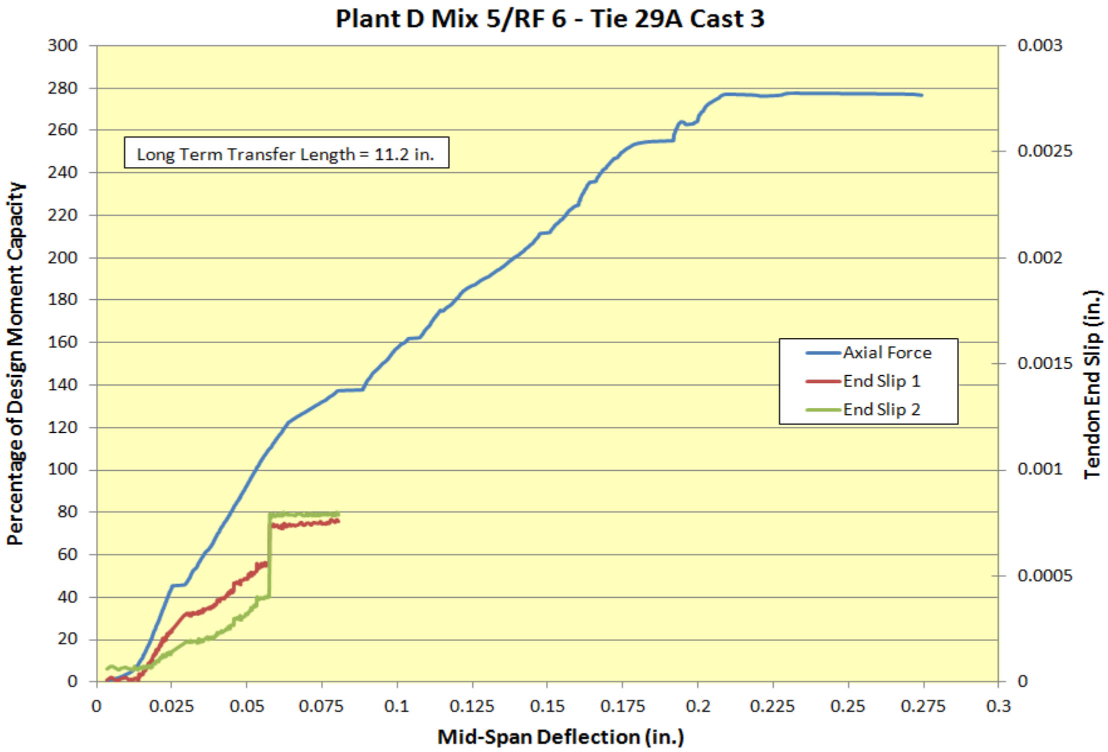

Figure 7.20 Load test results of Plant D Mix 5/RF 6 Tie 29A Cast 3

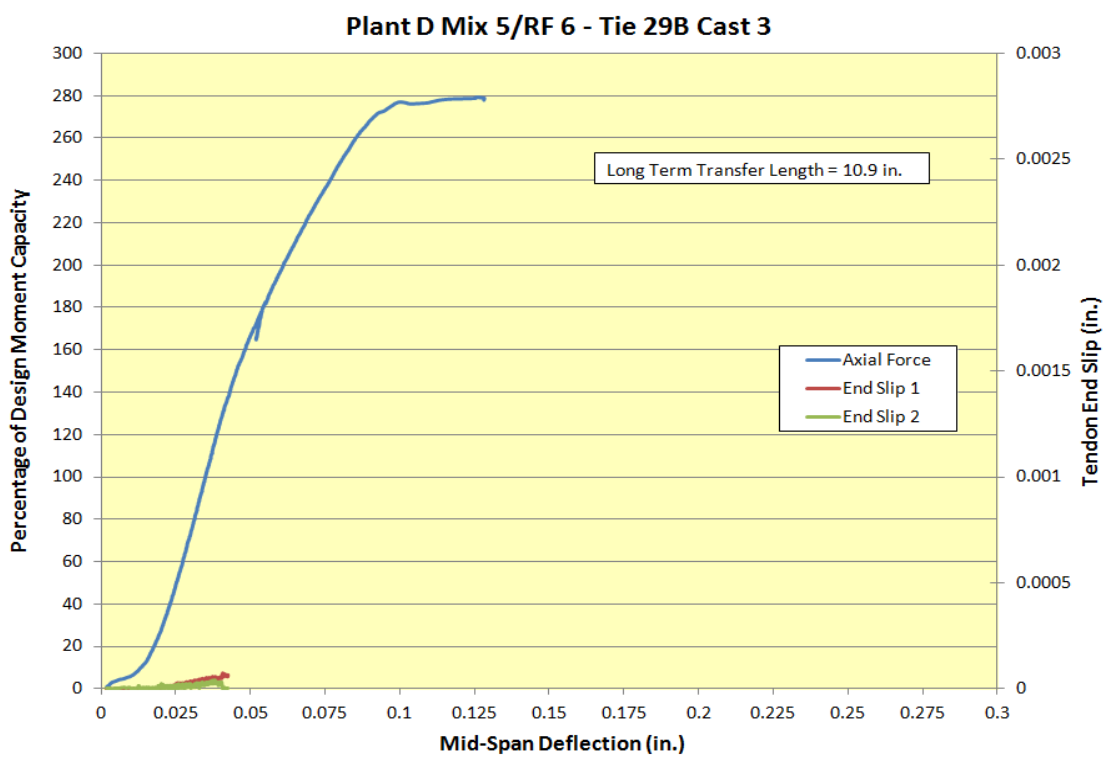

Figure 7.21 Load test results of Plant D Mix 5/RF 6 Tie 29B Cast 3

7.2.5 Plant E

Every tie from Plant E passed the end-slip requirement and ultimately failed in shear.

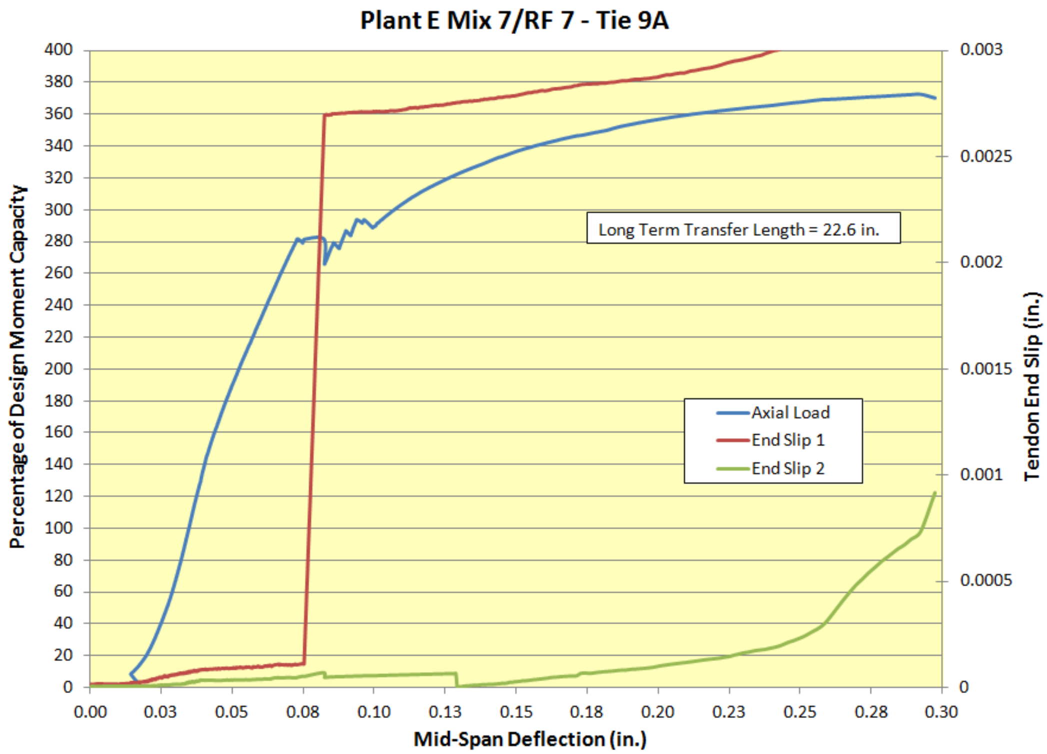

Figure 7.22 Load test results of Plant E Mix 7/RF 7 Tie 9A

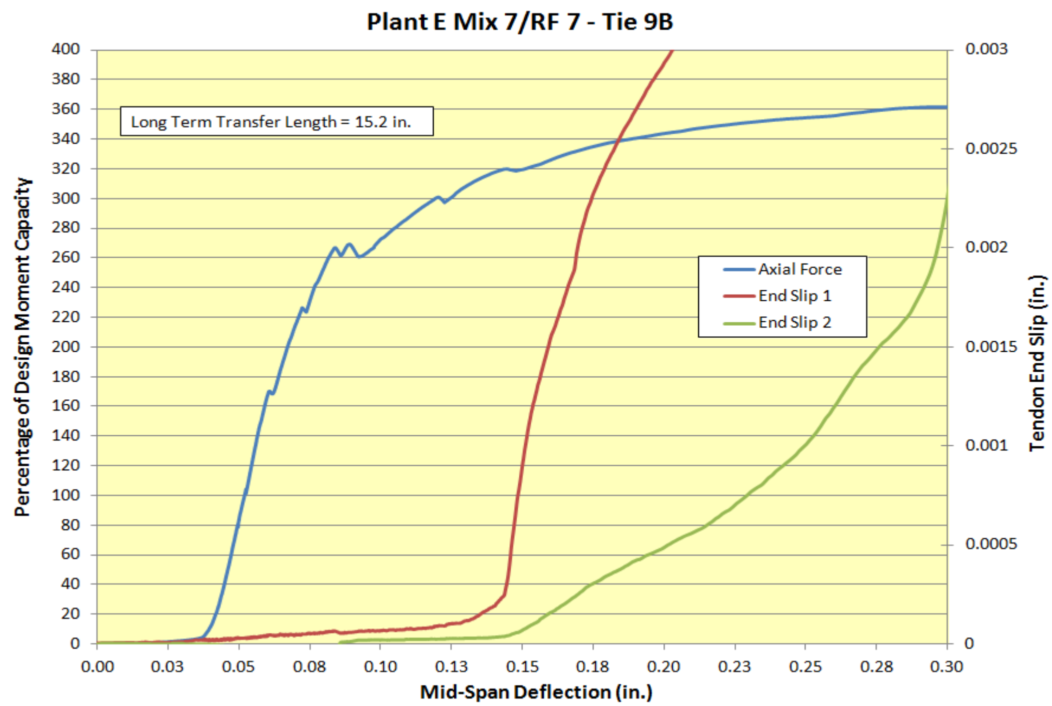

Figure 7.23 Load test results of Plant E Mix 7/RF 7 Tie 9B

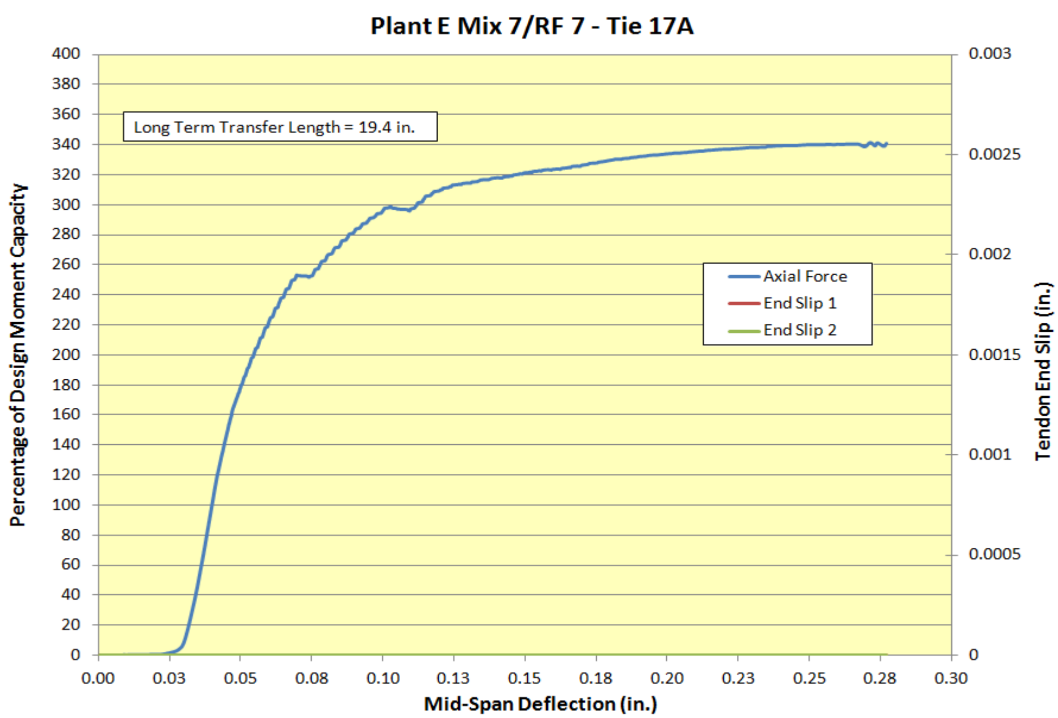

Figure 7.24 Load test results of Plant E Mix 7/RF 7 Tie 17A

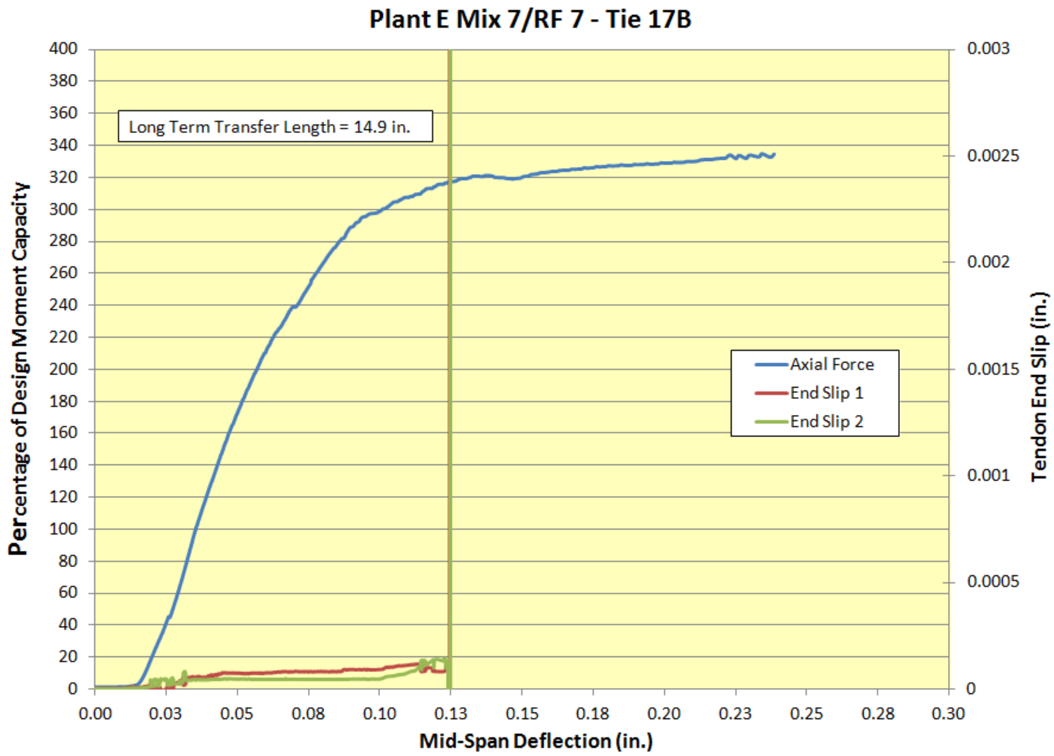

Figure 7.25 Load test results of Plant E Mix 7/RF 7 Tie 17B

7.2.6 Plant F

Every tie from Plant F passed the end-slip requirement. None of the tie ends failed during load testing. However, heavy cracking was present in tie 4B from mix 8 reinforcement 8.

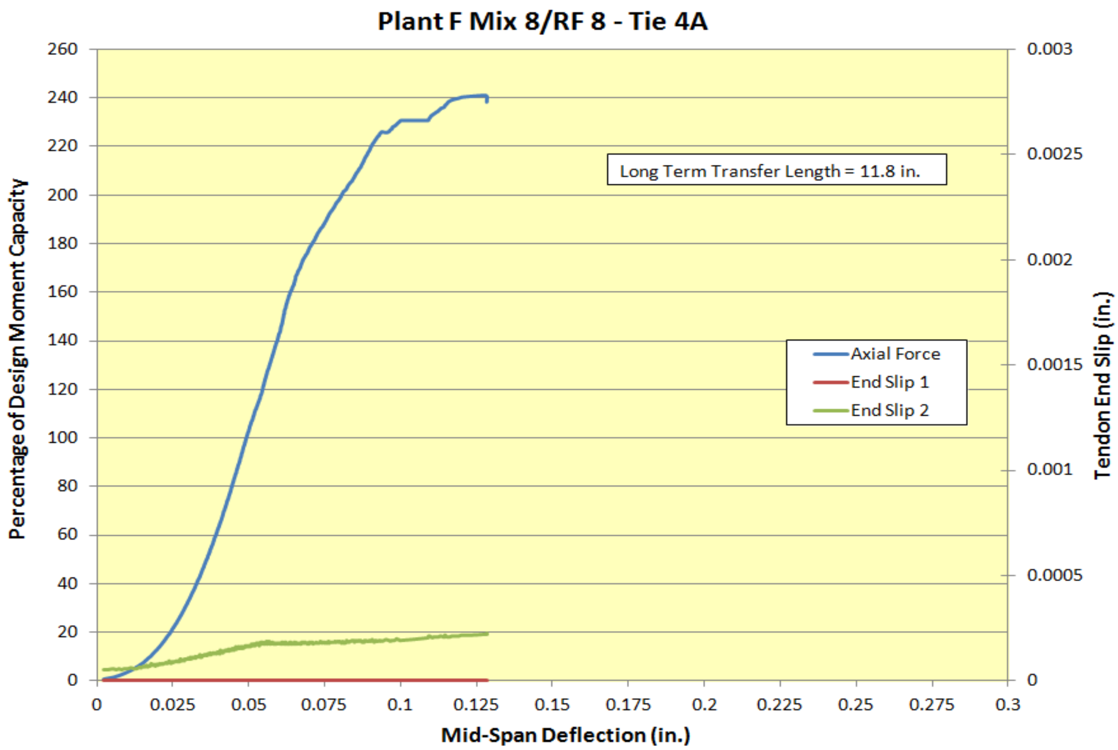

Figure 7.26 Load test results of Plant F Mix 8/RF 8 Tie 4A

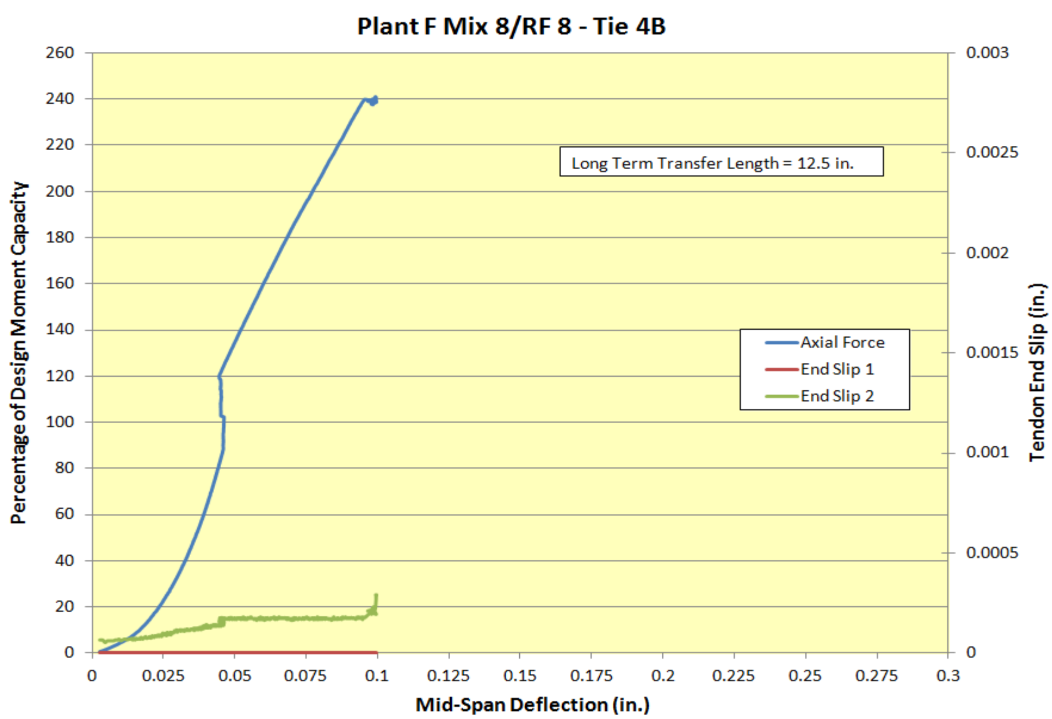

Figure 7.27 Load test results of Plant F Mix 8/RF 8 Tie 4B

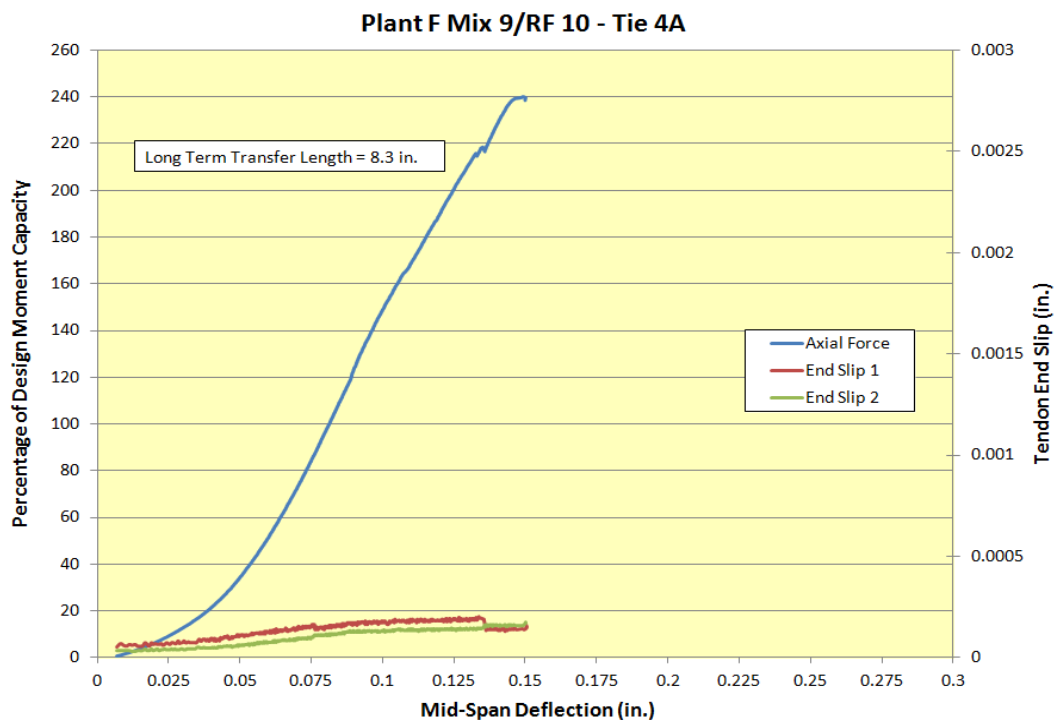

Figure 7.28 Load test results of Plant F Mix 9/RF 10 Tie 4A

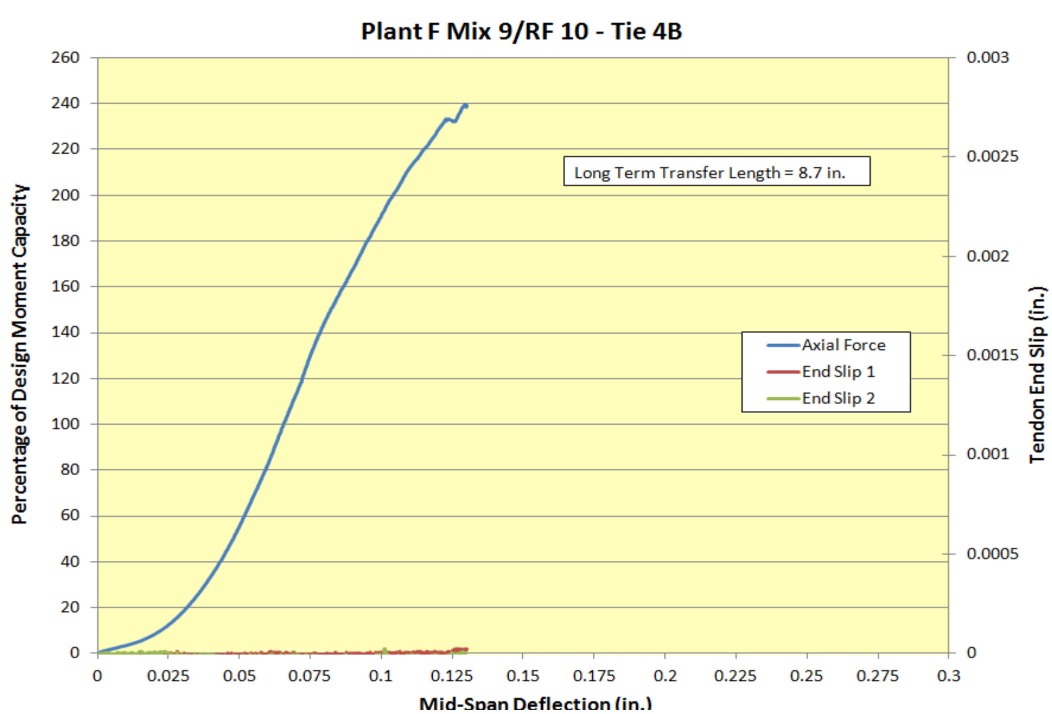

Figure 7.29 Load test results of Plant F Mix 9/RF 10 Tie 4B

Due to the fact that all ties were not the same age, different reinforcements were used in the ties, and the ties all had different cross sectional dimensions, it was difficult to relate the long-term transfer length to the performance of the ties. Also, just over half of the ties were able to be tested to their full capacity. If all ties could have been taken to full moment capacity, better correlation between the maximum load and transfer length may have been found.

Chapter 8 Conclusions and Recommendations

8.1 Conclusions

Because this was the first coordinated effort to measure the transfer length of concrete ties produced by railway tie manufacturers in the United States, this project led to many interesting conclusions about the transfer length of prestressed concrete railroad ties.

1. Although the prestressed concrete ties were all produced using a long-line production technique at the tie plants, variables are introduced that lead to a wide variety of transfer lengths. Examples of these variables include different reinforcement indentation patterns being utilized, concrete-mix designs and aggregate sources, placement techniques, and various concrete release strengths.
2. This project confirmed conclusions by Zhao et al. (2012) that the LSI device measured transfer lengths comparable to the Whittemore gage measurements. The LSI was used to measure transfer lengths consistently and quickly. This is a significant breakthrough in transfer length measurement procedures.
3. The 9-point average method is a viable technique to plot the strain profile when taking strain measurements at every 0.5 in. This method produces smooth strain profiles that are easy to analyze, and the 95% AMS line can be established with minimal error.
4. The water to cementitious ratio varied from 0.27 to 0.38; the total cementitious weight varied from 600 to 935 pounds per cubic yard; the air content varied from 3.6% to 5.9%; the release compressive strengths varied from 3760 psi to 7080 psi; and the split tensile strengths at release varied from 380 psi to 655 psi for all the concrete mix designs encountered.

5. 220 transfer length measurements were taken during the duration of this project. The shortest transfer length measured during the research project was 4.5 in., and the longest transfer length was 26.8 in.
6. In some instances, the transfer length was longer than 21 or 24 in., the distance from the end of the tie to the rail-seat.
7. There was not a consistent difference in the live-end and dead-end transfer lengths measured at the six plants.
8. Transfer length had much better correlation with split tensile strength at release than with the compressive strength at release.
9. Most ties experienced an increase in transfer length over time. Only four out of 54 tie ends experienced no transfer length increase over time.
10. Some ties had a large transfer length percentage increase over time but still had a small overall increase. The percent increase of long-term transfer lengths ranged from 0 to 53.8%.
11. The average transfer length increase over time was found to range between 0.4 and 3.3 in.
12. Due to test apparatus limitations, only 13 of the 24 concrete tie ends were loaded to failure during the rail-seat positive moment tests. If all of the ties could have been tested to their full capacity, better correlation in regards to the transfer length and the load may have been possible.
13. Only two tie ends failed the end-slip requirement during the rail-seat positive moment tests. One of these ends was from Plant B, and had a transfer length of 19.1 in. The other tie was from Plant C and had a transfer length of 8.3 in.

8.2 Recommendations

Results of this research project led to many questions that future research could help to answer. This project focused on measuring the transfer length of ties produced in the U.S. Further research is recommended in the following areas:

1. Transfer lengths should be measured on prestressed concrete members using various reinforcements and a consistent concrete-mix design. This will determine which reinforcement performs the best. Also, long-term transfer length measurements could be monitored to view any changes over time.
2. Once the most desirable indent pattern has been selected, changes to the concrete-mix can then be fully evaluated.
3. Transfer lengths should be periodically measured at the prestressed concrete tie plants to ensure quality control. The transfer length should be measured in the plants when a new concrete-mix design or reinforcement is being considered for use; this would provide each plant with immediate feedback on the performance of the concrete-mix or reinforcement.
4. The transfer length could increase due to the dynamic loading effects of trains. Transfer lengths should be measured on ties during production, and then once more after a period of being in service. This could help place a numerical value on the increase in transfer length of concrete railroad ties after being heavily loaded.
5. The prestressed concrete ties should be load-tested using a system able to take all of the ties to failure. This may lead to a better correlation between the long-term transfer length and the load-carrying capacity of each tie.

References

1. ACI Committee 318. 2011. *Building code requirements for structural concrete (318-11*). Farmington Hills, MI: American Concrete Institute.

2. American Railway Engineering and Maintenance-of-Way Association. 2010. *AREMA manual for railway engineering.* Lanham, MD: author.

3. Barnes, Robert W., J. W. Grove, and N. H. Burns. 2003. “Experimental assessment of factors affecting transfer length.” *ACI Structural Journal*, 100, no. 6: 740-748.

4. Hanna, Amir N. 1979. “Prestressed concrete ties for North American railroads.” *PCI Journal, 24,* no. 5: 32-61.

5. Kaar, Paul H., and N. W. Hanson. 1975. “Bond fatigue tests of beams simulating pretensioned concrete crossties.” *PCI Journal, 20*, no. 5: 65-80.

6. Krishnamurthy, D. 1972. “Relationship between transmission length and diameter of prestressing tendons.” *Journal of the Institution of Engineers. Civil Engineering Division, 52*, no. 9: 243-247.

7. Larson, K. H., R. J. Peterman, and A. Esmaeily. 2007. “Bond characteristics of self-consolidating concrete for prestressed bridge girders.” *PCI Journal, 52,* no. 4: 44-57.

8. Oh, Byung Hwan, and E. S. Kim. 2000. “Realistic evaluation of transfer lengths in pretensioned, prestressed concrete member.” *ACI Structural Journal, 97*: 821-830.

9. Oh, Byung Hwan, E. S. Kim, and Y. C. Choi. 2006. “Theoretical analysis of transfer lengths in pretensioned prestressed concrete member.” *Journal of Engineering Mechanics, 132*, 10: 1057-1066.

10. Peterman, R. J. “Effects of as-cast depth and concrete fluidity on strand bond.” *PCI Journal, 52*, no. 3: 72-101.

11. Rose, Dallas R., and B. W. Russel. 1995. “Measurement of bond performance; correlation of pull-out strength with transfer length.” *Restructuring—America and Beyond,* 2: 1474-1477.

12. Russell, B. W., and N. H. Burns. 1993. "Design guidelines for transfer, development and debonding of large-diameter seven-wire strands in pretensioned concrete girders." *Report No. 1210-5F*, Center for Transportation Research, the University of Texas at Austin, Austin, TX.

13. Russell, Bruce W., and N.H. Burns. 1997. "Measurement of transfer lengths on pretensioned concrete elements." *Journal of Structural Engineering*, 123, no. 5: 541-549.

14. Srinivasa Rao, P., P. Kalyanasundaram, and M. F. Sharief. 1977. "Transmission length of ribbed bars in pre-tensioned concrete." *The Indian Concrete Journal, 51*, no. 5: 149-153.

15. Staton, Blake W., N. H. Do, E. D. Ruiz, and W. M. Hale. 2009. "Transfer lengths of prestressed beams cast with self-consolidating concrete." *PCI Journal, 54,* no. 2: 64-83.

16. Steinberg, E., J. T. Beier, and S. Sargand. 2001. "Effects of sudden prestress force transfer in pretensioned concrete beams." *PCI Journal, 46,* no. 1: 64-75.

17. Zhao, W., B. T. Beck, and J. Wu. 2004. "A novel optical technique for measuring 5-axis surface movement." In Kevin G. Harding (editor), *Two and three-dimensional vision systems for inspection, control, and metrology II*. Proceedings of the SPIE, 5606: 66-73.

18. Zhao, W., K. Larson, R. Peterman, T. Beck, and J. Wu. 2012. "Development of a laser-speckle imaging device to determine the transfer length in pre-tensioned concrete members." *PCI Journal, 57,* no. 1: 135-143.

19. Zhao, W. 2011. "Development of a portable optical-strain sensor with applications to diagnostic testing of prestressed concrete." (Ph.D. Dissertation) Kansas State University, Lawrence, KS.

Appendix A Plant A Transfer Lengths

A.1 Short-term Transfer Lengths

Table A.1 Plant A transfer length data

	Tie Label	Measurement Method	Transfer Length (in.)
Plant A Mix 1/RF 1	1B	Laser Speckle	10.7
	2A	Laser Speckle	7.8
	3B	Whittemore Gage	11.4
	4B	Laser Speckle	10.6
	5A	Laser Speckle	10
	6A	Laser Speckle	10.5
	7B	Laser Speckle	7.2
	8B	Whittemore Gage	8.9
	9A	Whittemore Gage	10.3
	9B	Whittemore Gage	9.7
	10B	Whittemore Gage	10.3
	11B	Laser Speckle	8.9
	12A	Laser Speckle	8.5
	13B	Laser Speckle	10.7
	14A	Laser Speckle	8.8
	15B	Laser Speckle	9.1
	16A	Laser Speckle	8.6
	17A	Whittemore Gage	9.3
	17B	Whittemore Gage	9.3
	18B	Whittemore Gage	9.3
Plant A Mix 1A/RF 1	3A	Whittemore Gage	10.8
	3B	Whittemore Gage	10.1
	4A	Laser Speckle	10.3
	4B	Laser Speckle	8.3
	7A	Whittemore Gage	9.7
	7B	Whittemore Gage	10
	8A	Laser Speckle	8.3
	8B	Laser Speckle	9.9
	12A	Laser Speckle	12
	12B	Laser Speckle	10.2
Plant A Mix 1A/RF 2	1A	Laser Speckle	12.9
	1B	Laser Speckle	11.8
	2A	Whittemore Gage	11.3
	2B	Whittemore Gage	11.4
	5A	Whittemore Gage	11.2
	5B	Whittemore Gage	12.3
	6A	Laser Speckle	10.8
	6B	Laser Speckle	11.9
	9A	Laser Speckle	11.8
	9B	Laser Speckle	8.8

Note: Side A = Live-end of tie

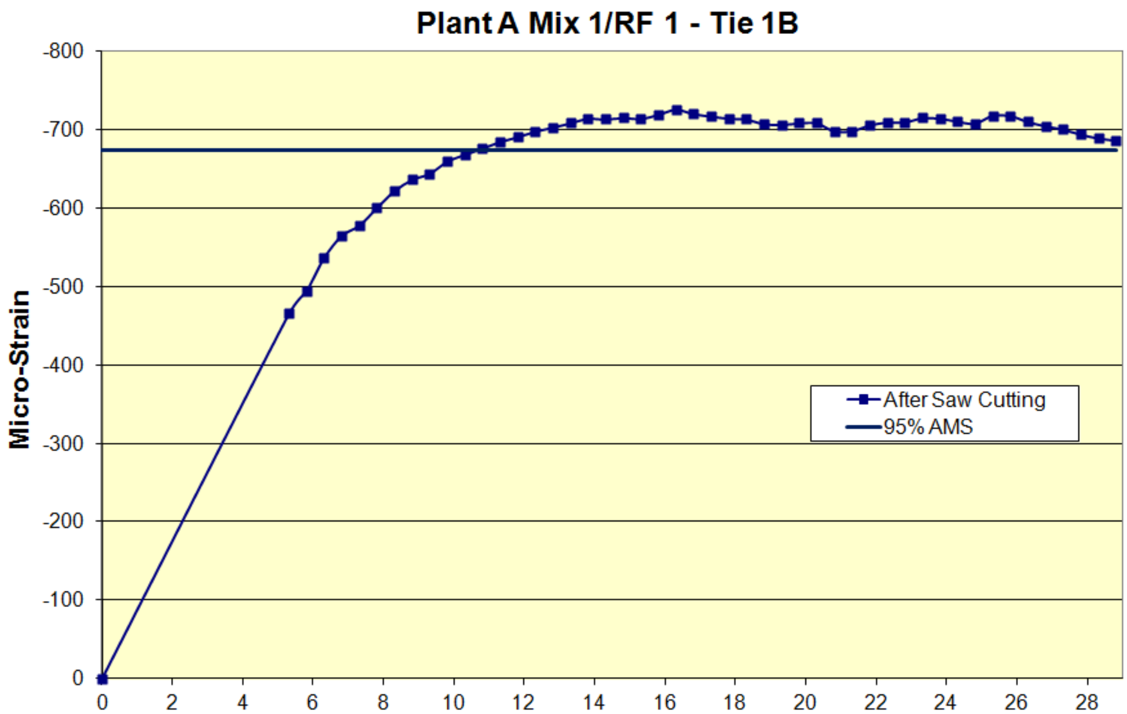

Figure A.1 Transfer length of Plant A Mix 1/RF 1 Tie 1B

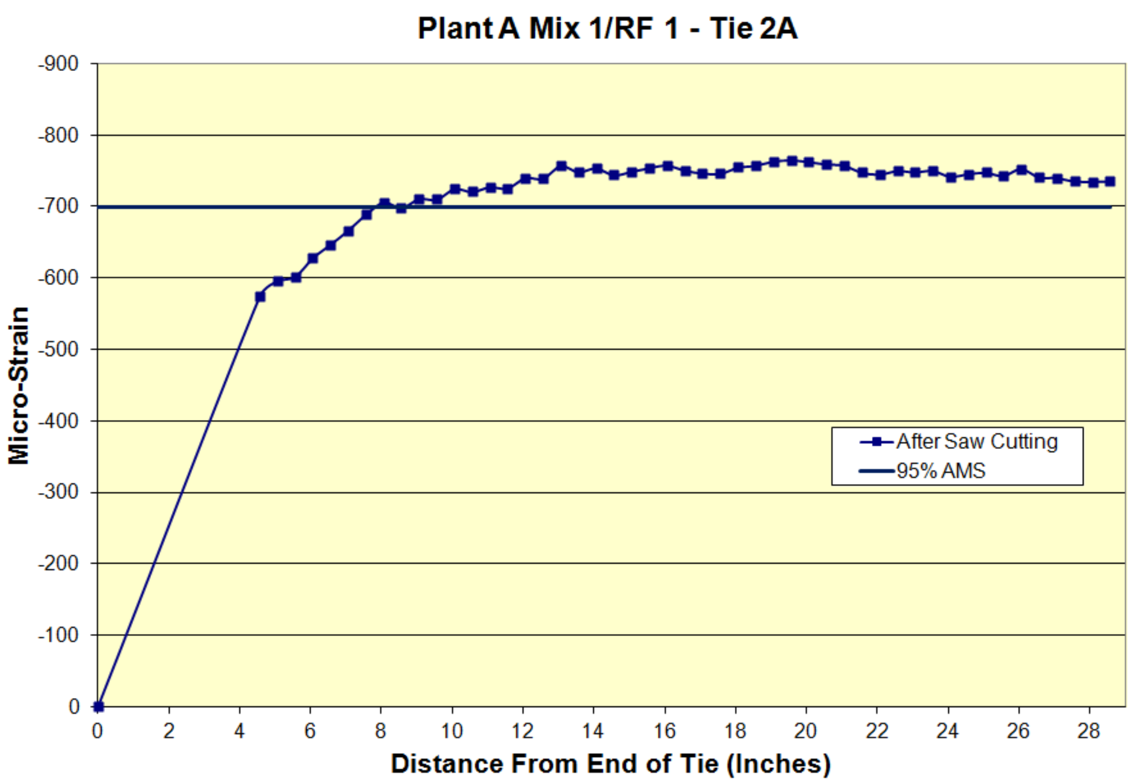

Figure A.2 Transfer length of Plant A Mix 1/RF 1 Tie 2A

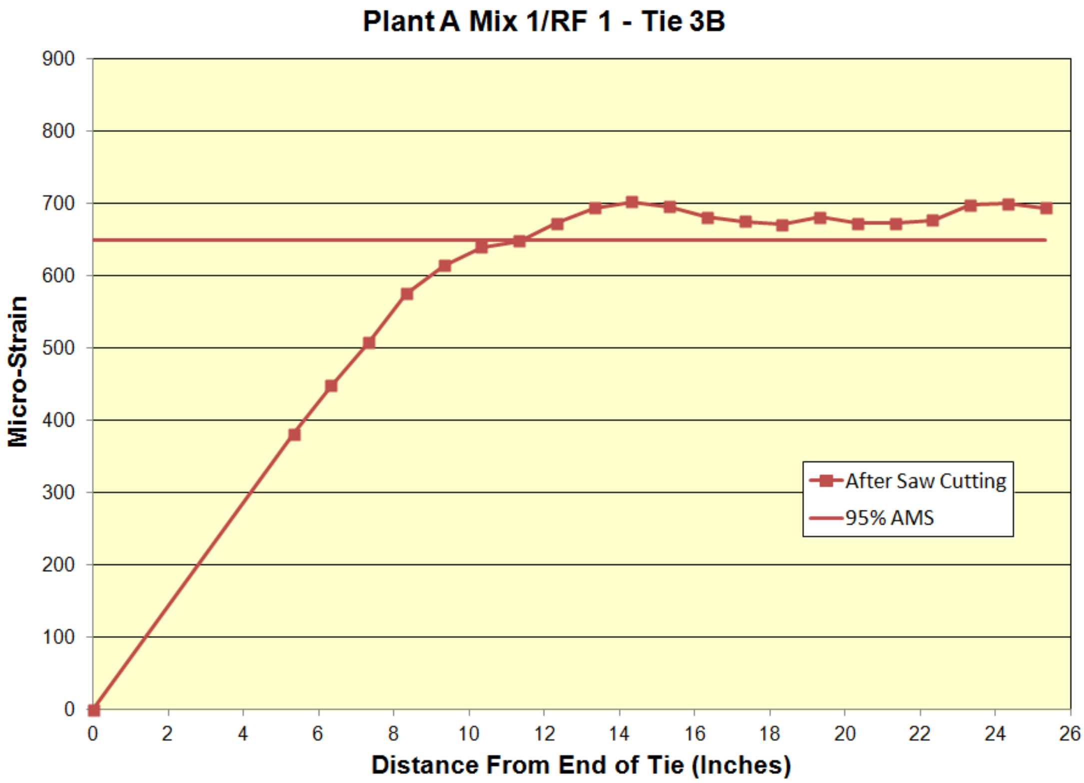

Figure A.3 Transfer length of Plant A Mix 1/RF 1 Tie 3B

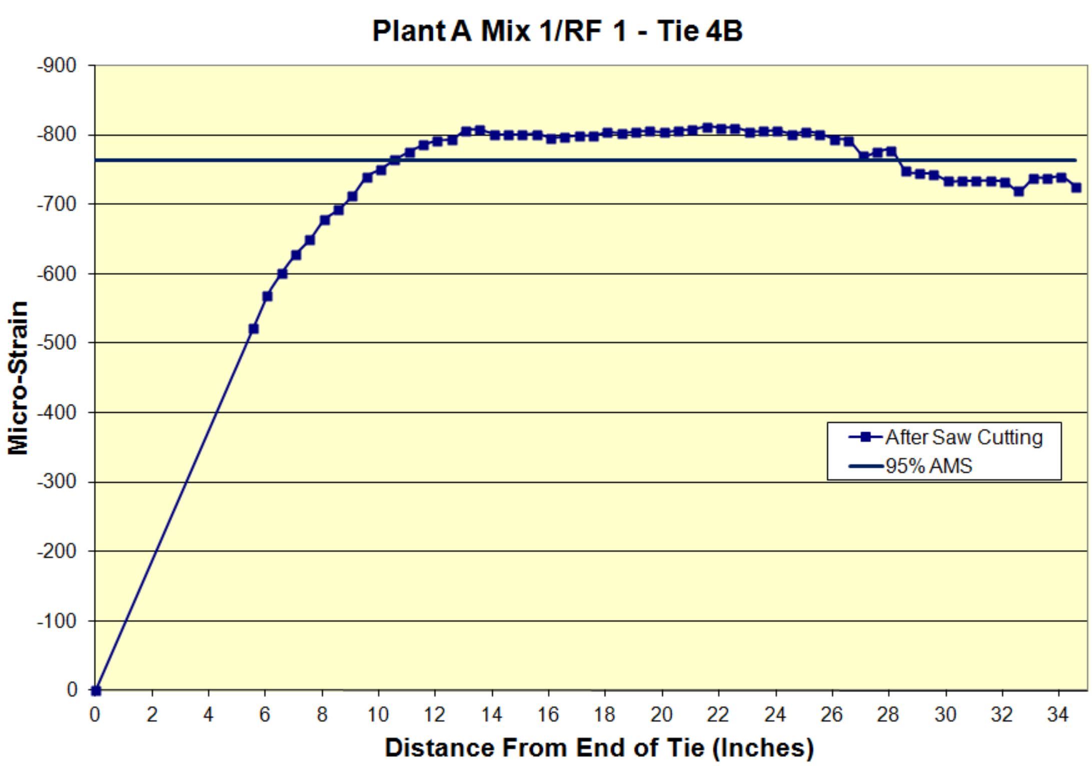

Figure A.4 Transfer length of Plant A Mix 1/RF 1 Tie 4B

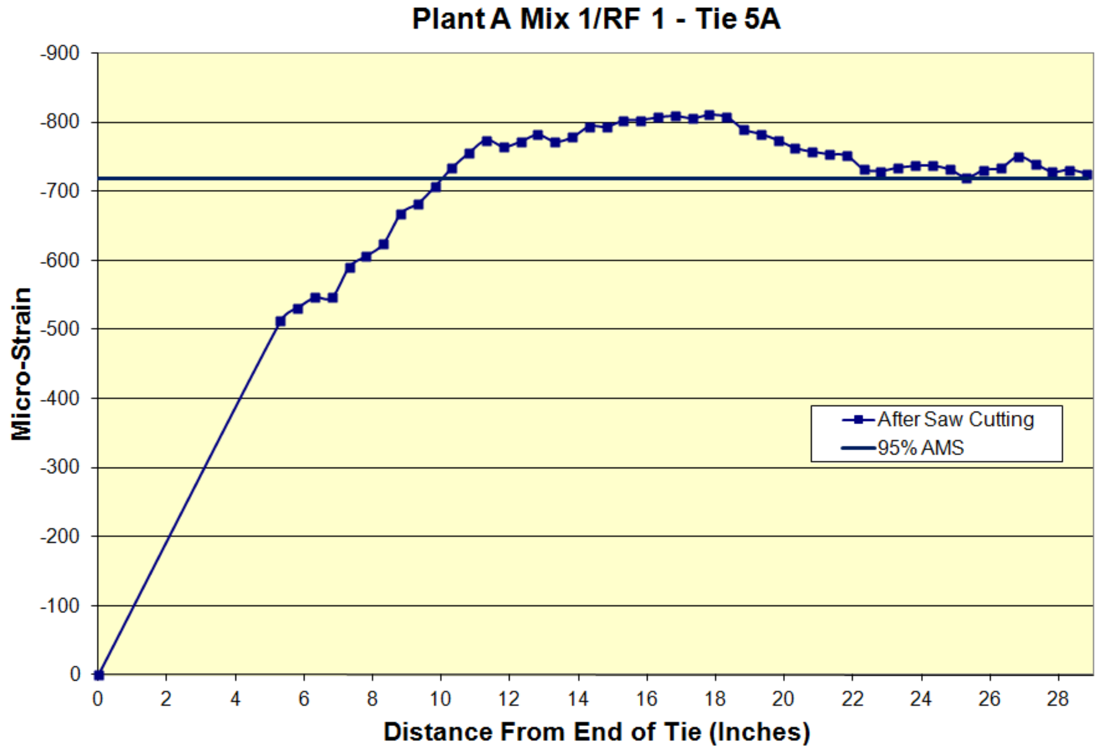

Figure A.5 Transfer length of Plant A Mix 1/RF 1 Tie 5A

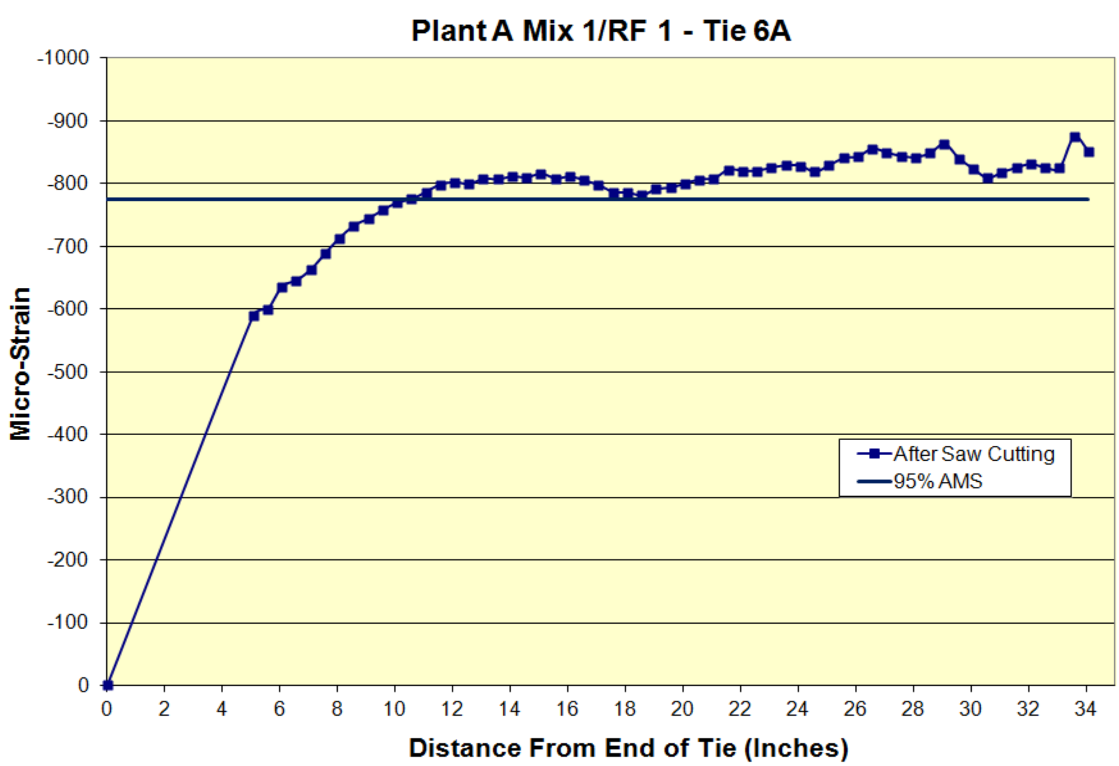

Figure A.6 Transfer length of Plant A Mix 1/RF 1 Tie 6A

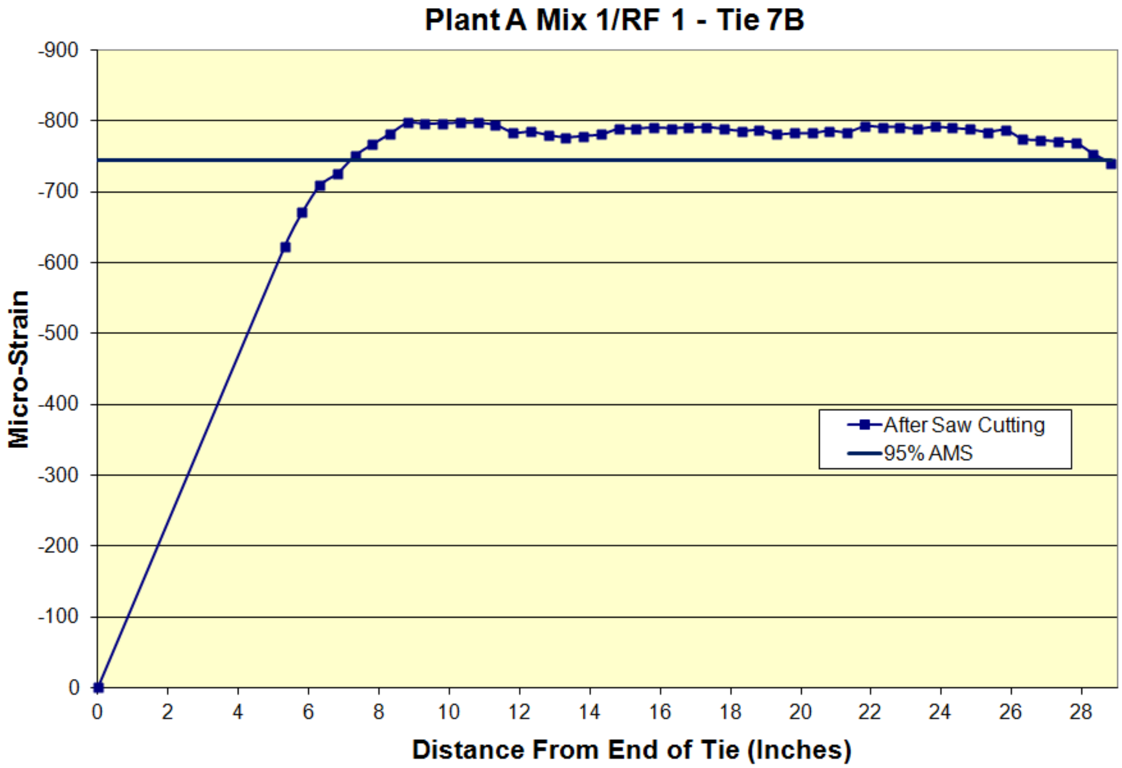

Figure A.7 Transfer length of Plant A Mix 1/RF 1 Tie 7B

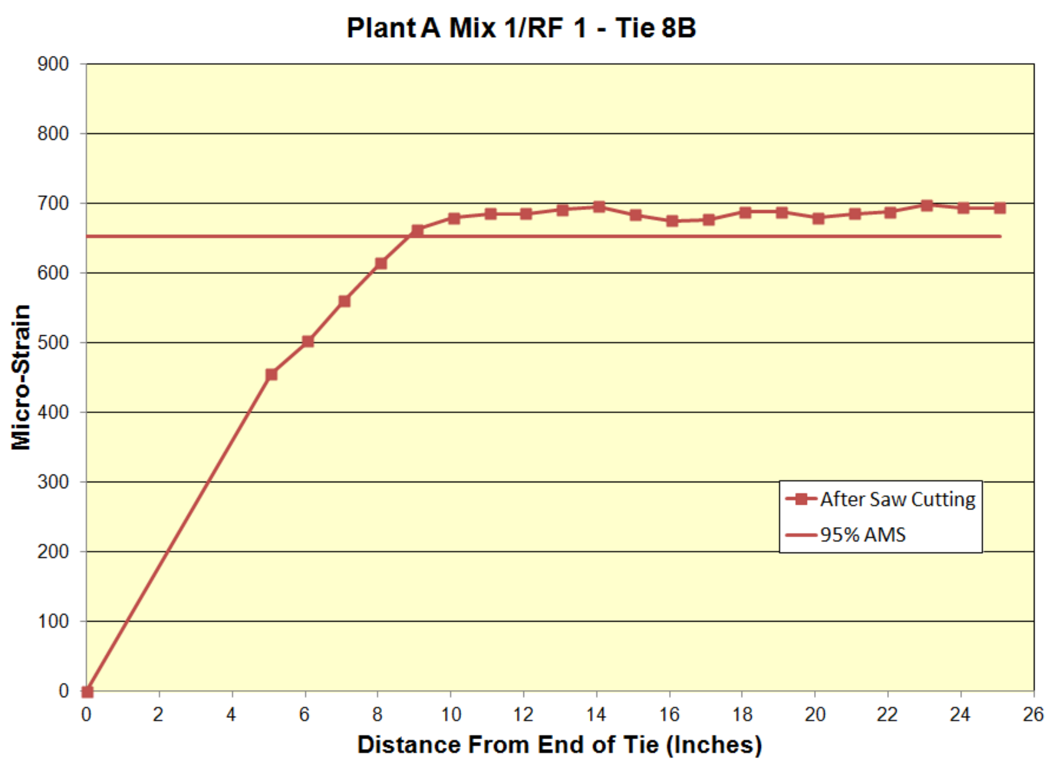

Figure A.8 Transfer length of Plant A Mix 1/RF 1 Tie 8B

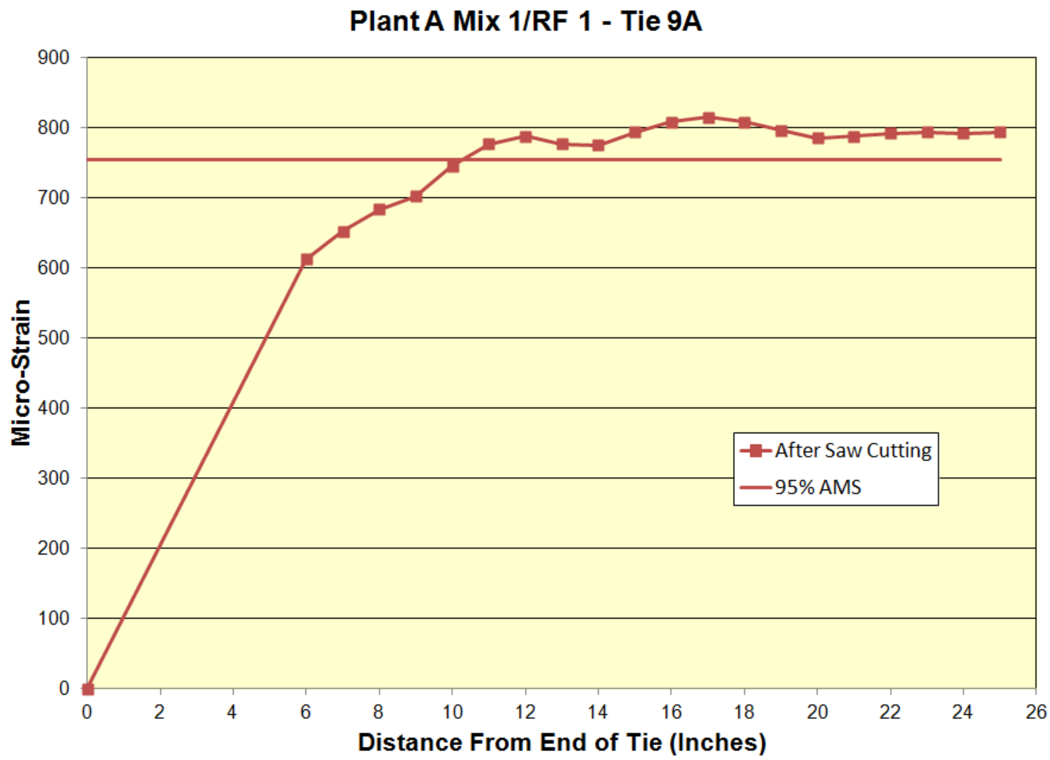

Figure A.9 Transfer length of Plant A Mix 1/RF 1 Tie 9A

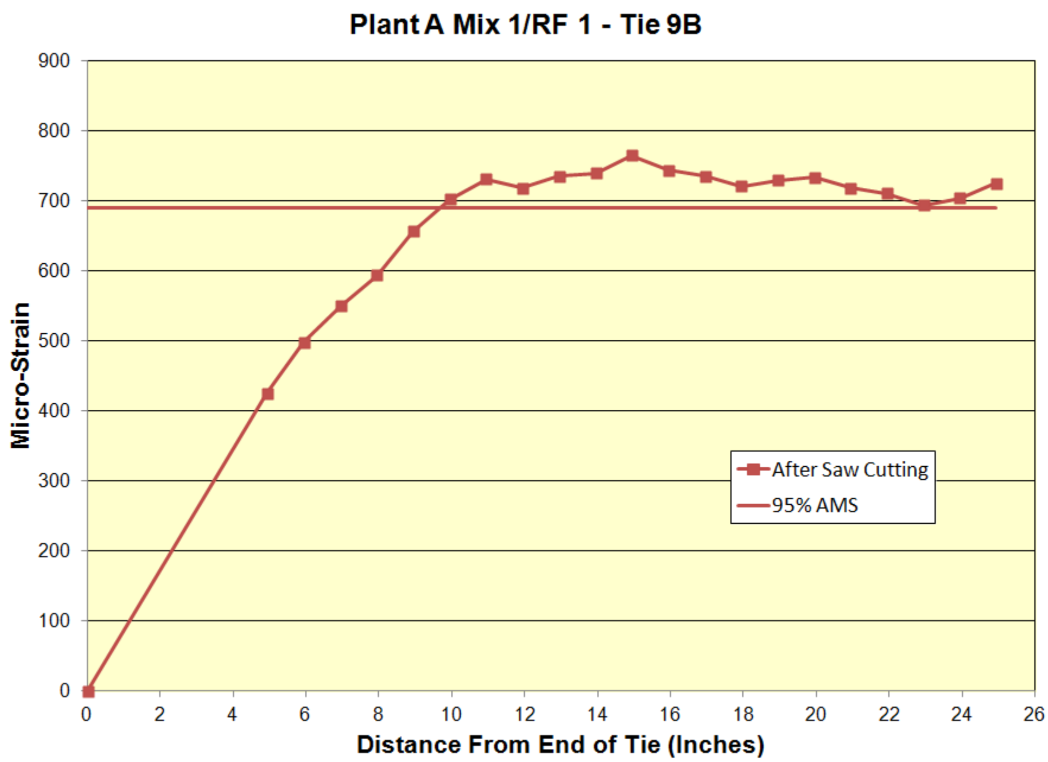

Figure A.10 Transfer length of Plant A Mix 1/RF 1 Tie 9B

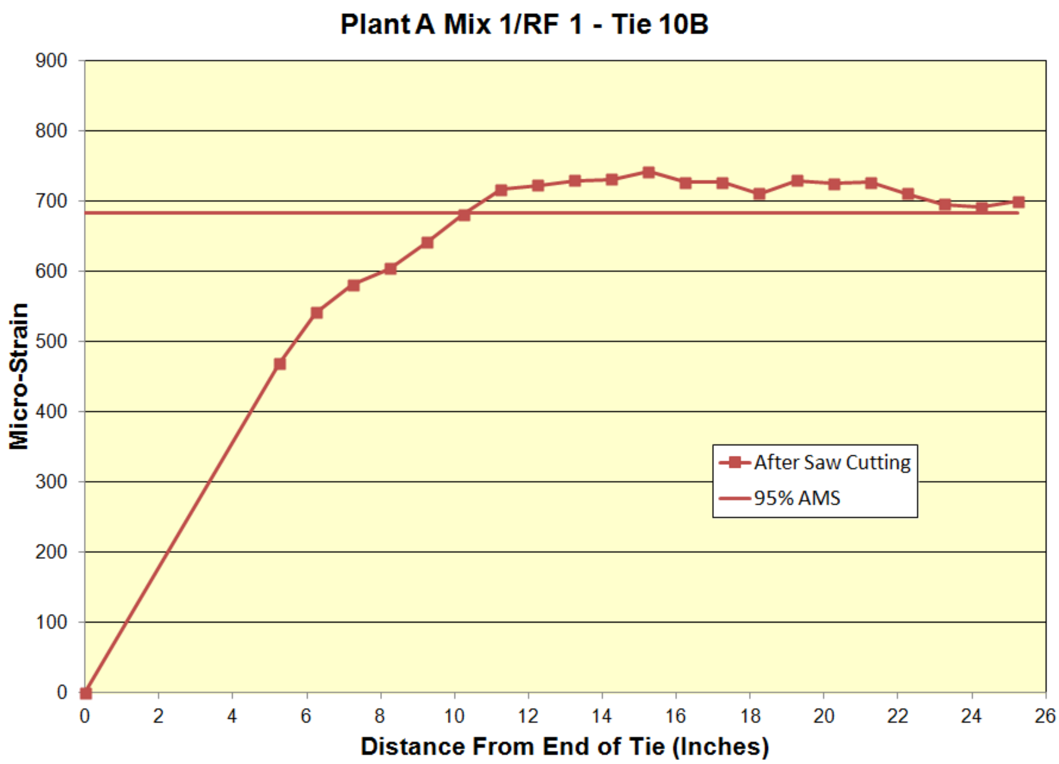

Figure A.11 Transfer length of Plant A Mix 1/RF 1 Tie 10B

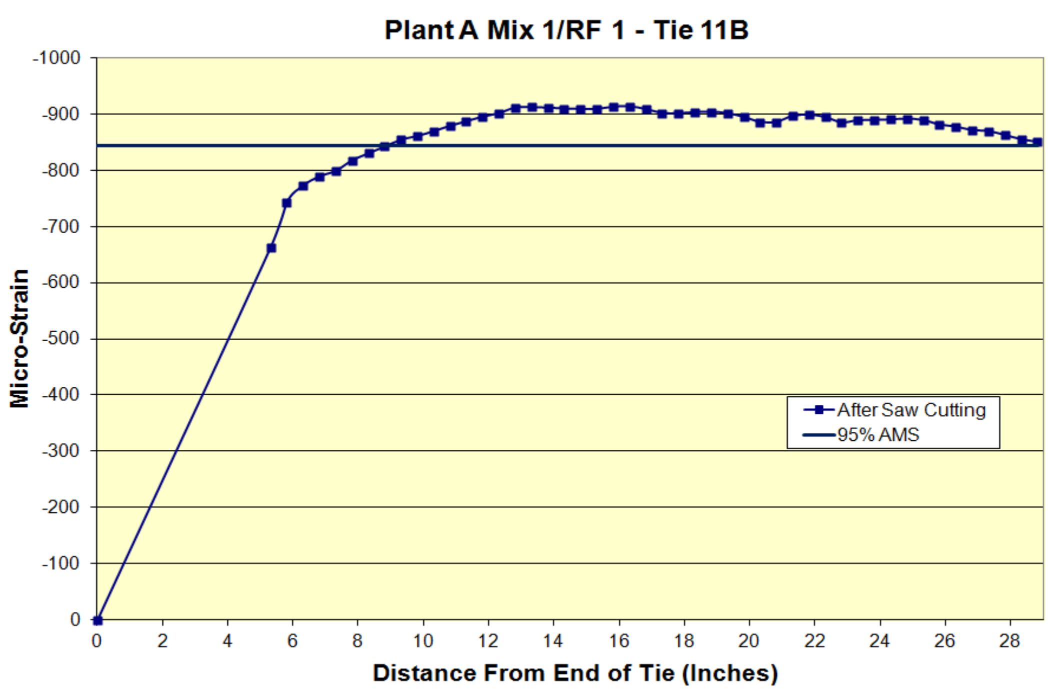

Figure A.12 Transfer length of Plant A Mix 1/RF 1 Tie 11B

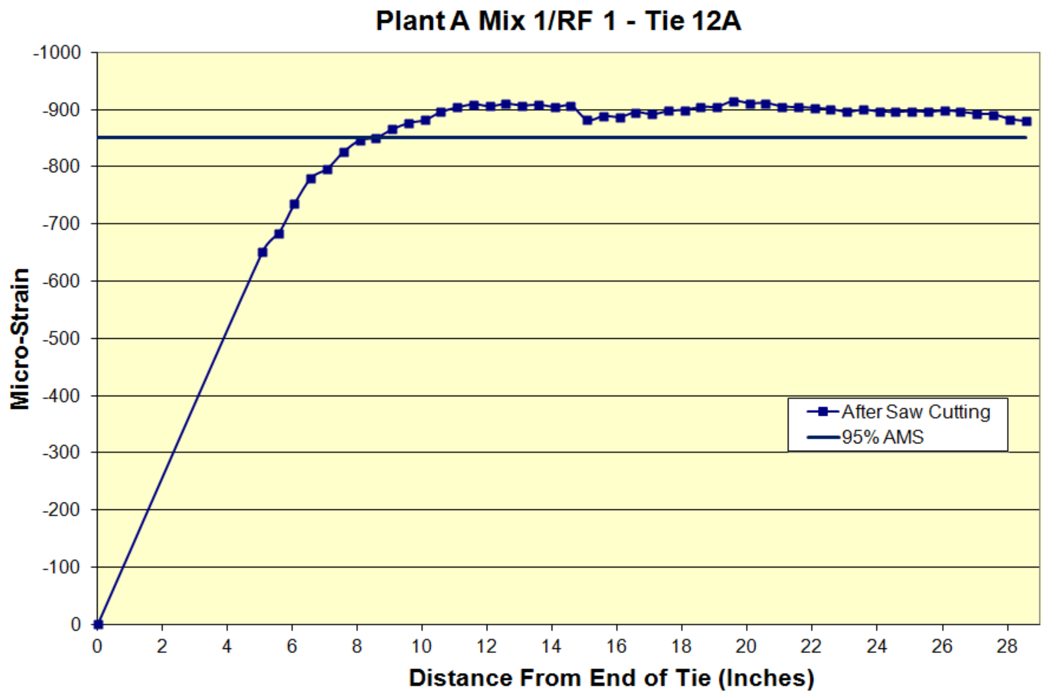

Figure A.13 Transfer length of Plant A Mix 1/RF 1 Tie 12A

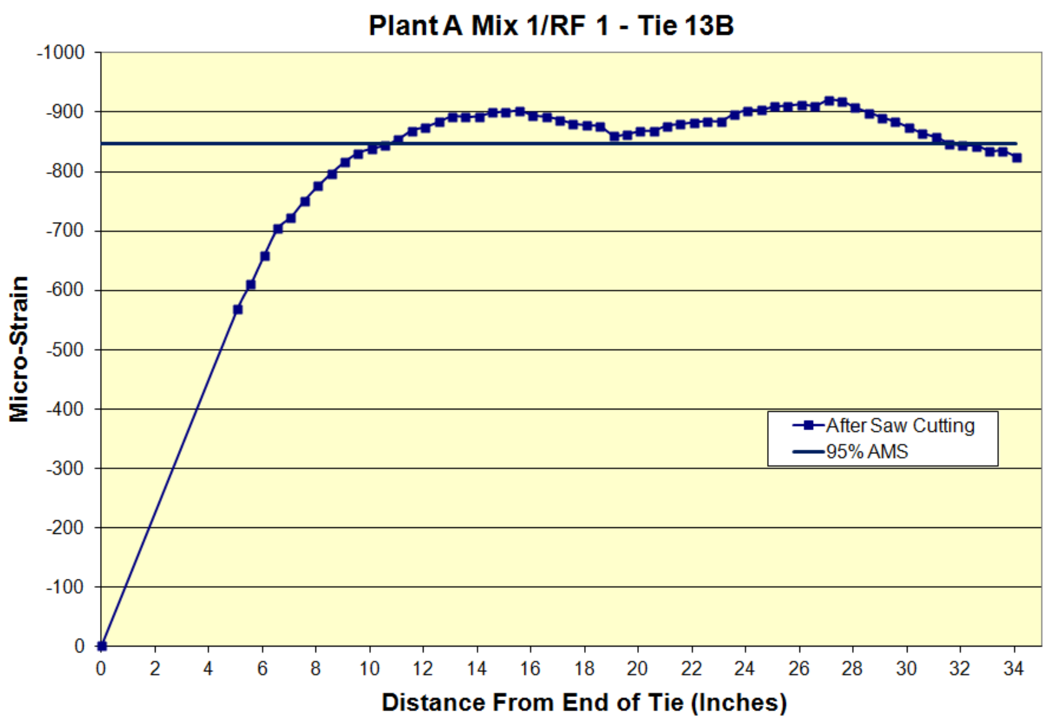

Figure A.14 Transfer length of Plant A Mix 1/RF 1 Tie 13B

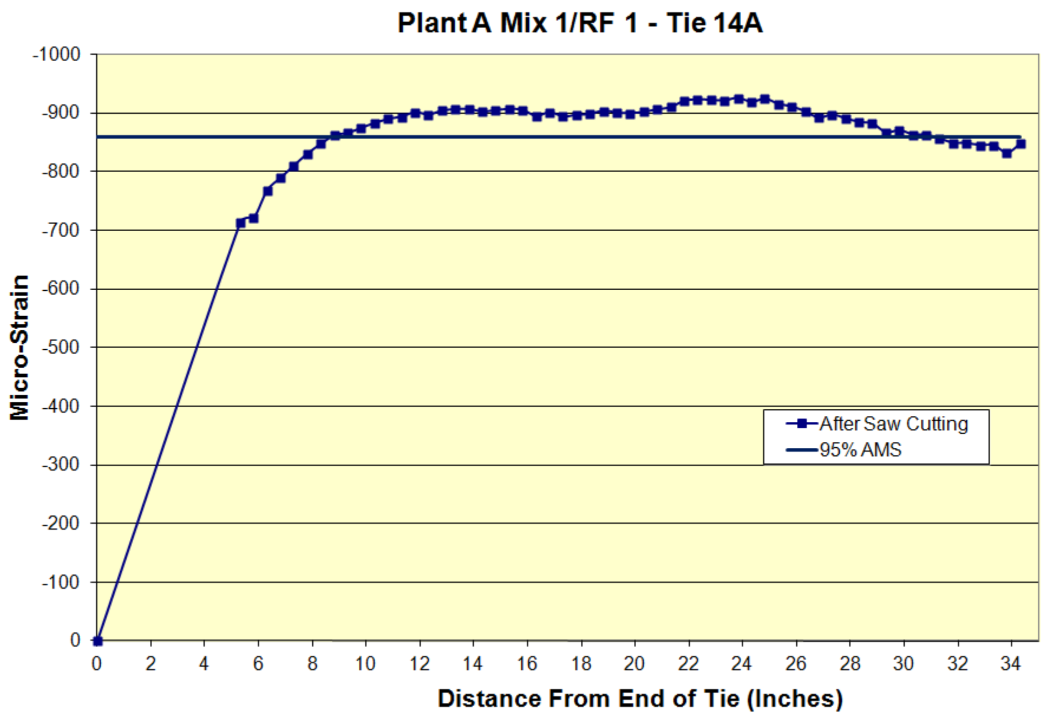

Figure A.15 Transfer length of Plant A Mix 1/RF 1 Tie 14A

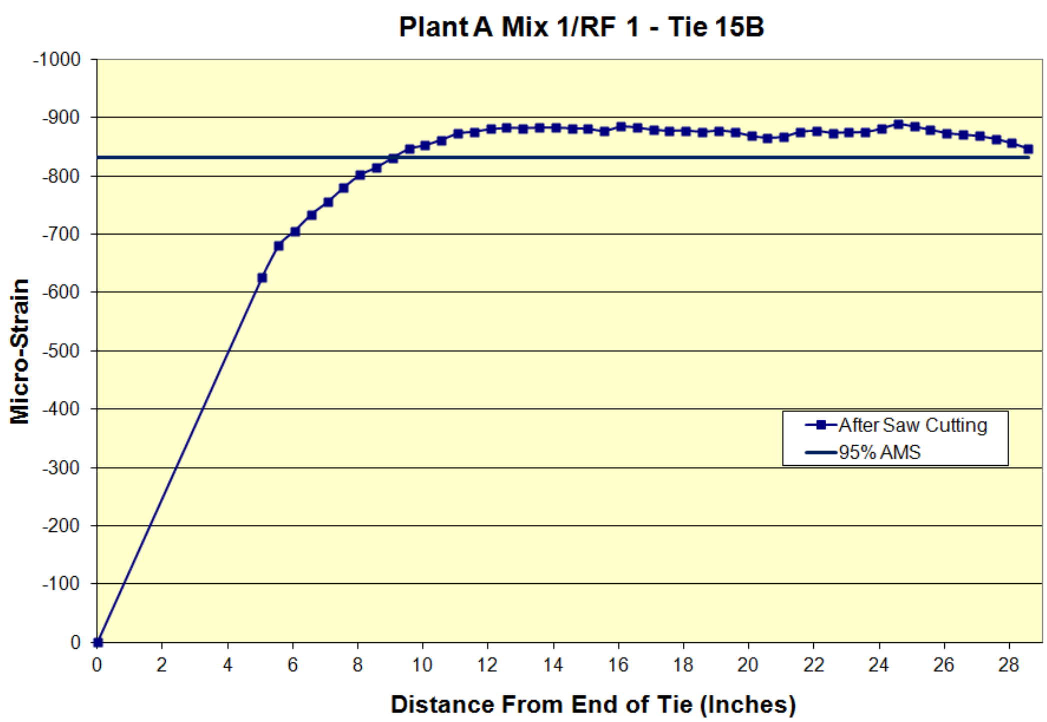

Figure A.16 Transfer length of Plant A Mix 1/RF 1 Tie 15B

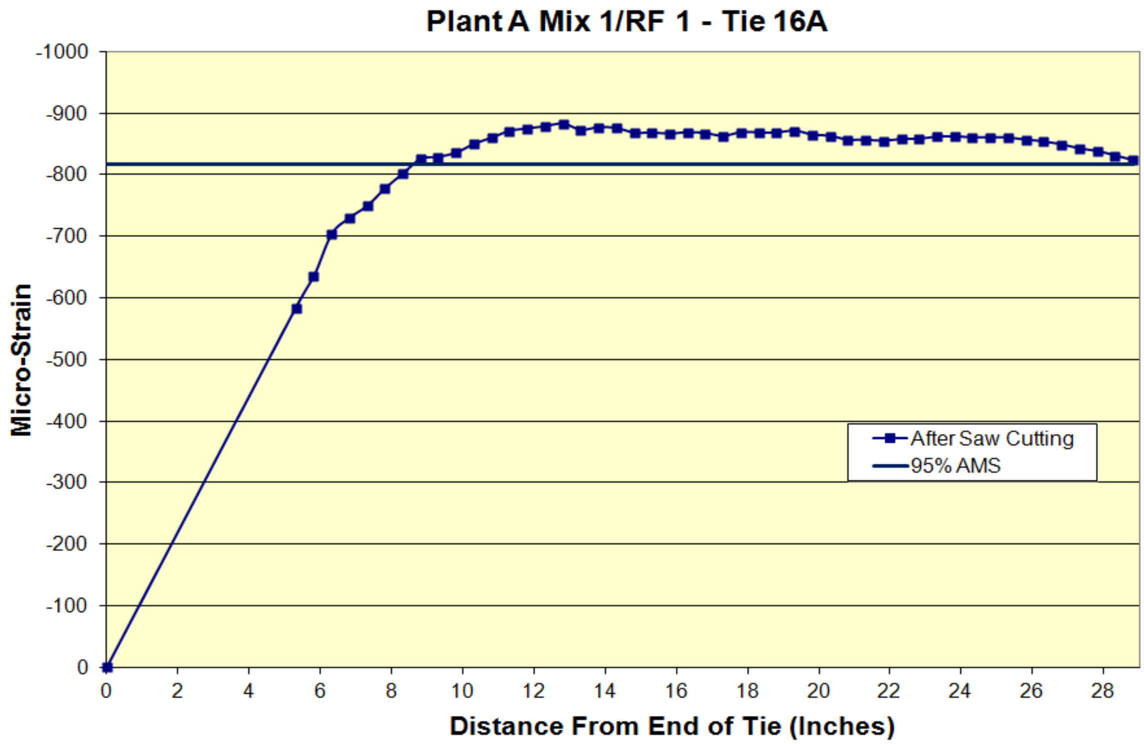

Figure A.17 Transfer length of Plant A Mix 1/RF 1 Tie 16A

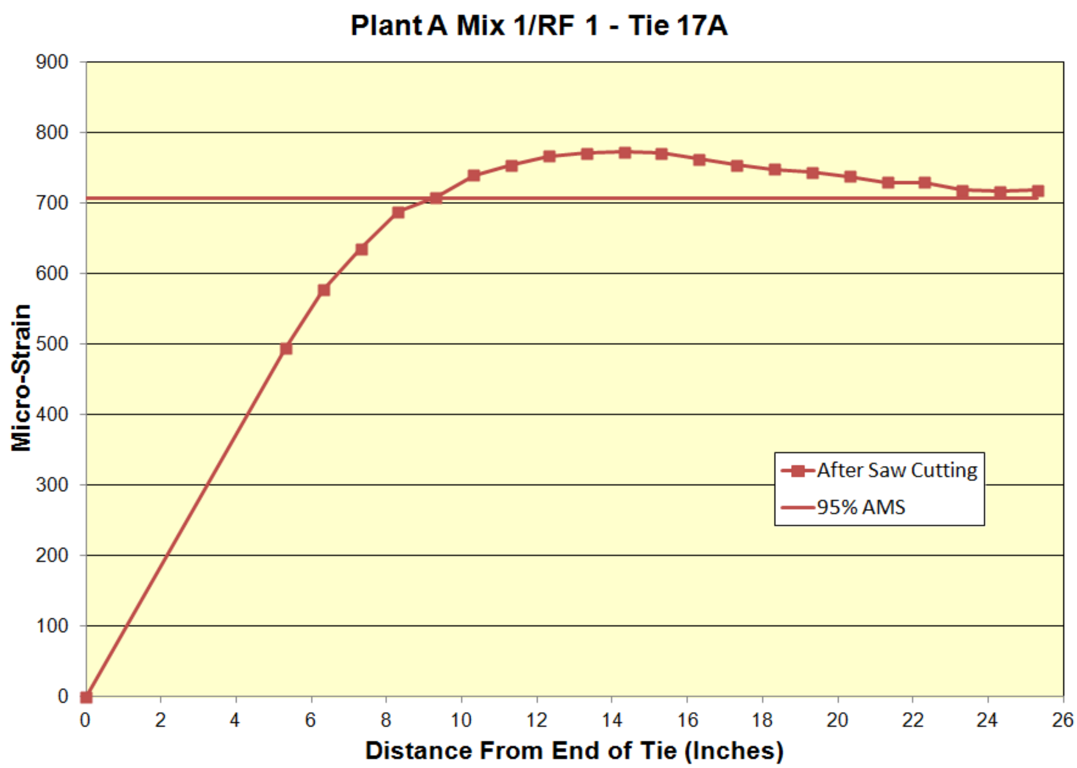

Figure A.18 Transfer length of Plant A Mix 1/RF 1 Tie 17A

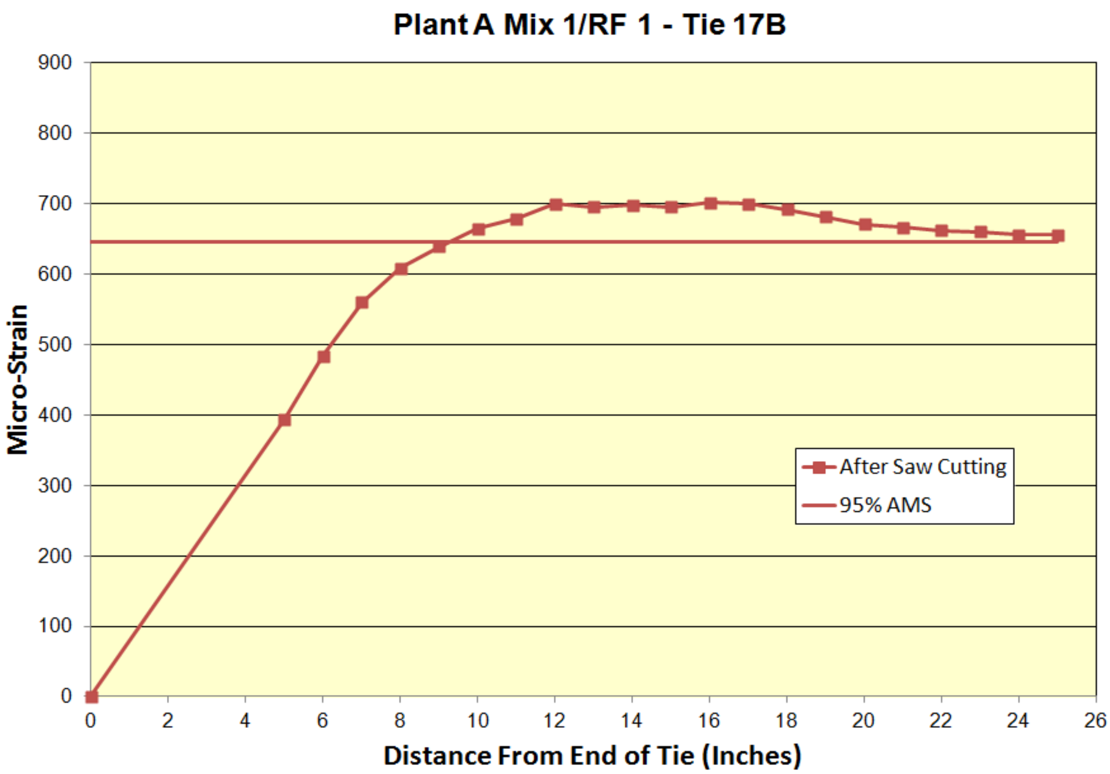

Figure A.19 Transfer length of Plant A Mix 1/RF 1 Tie 17B

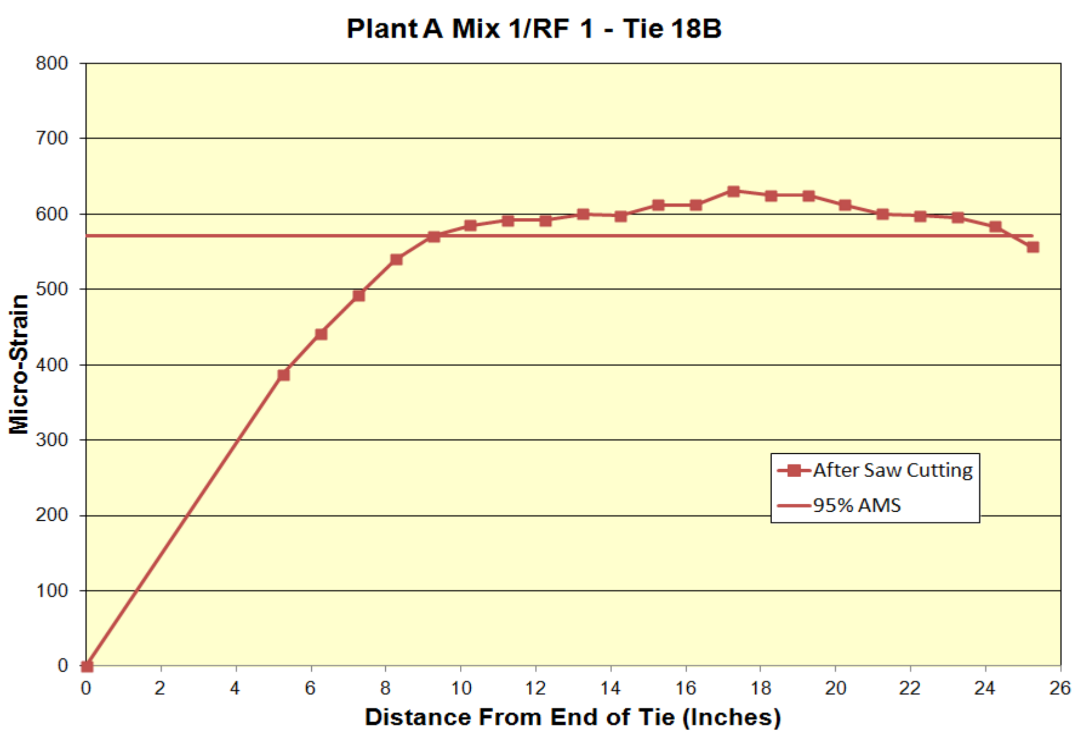

Figure A.20 Transfer length of Plant A Mix 1/RF 1 Tie 18B

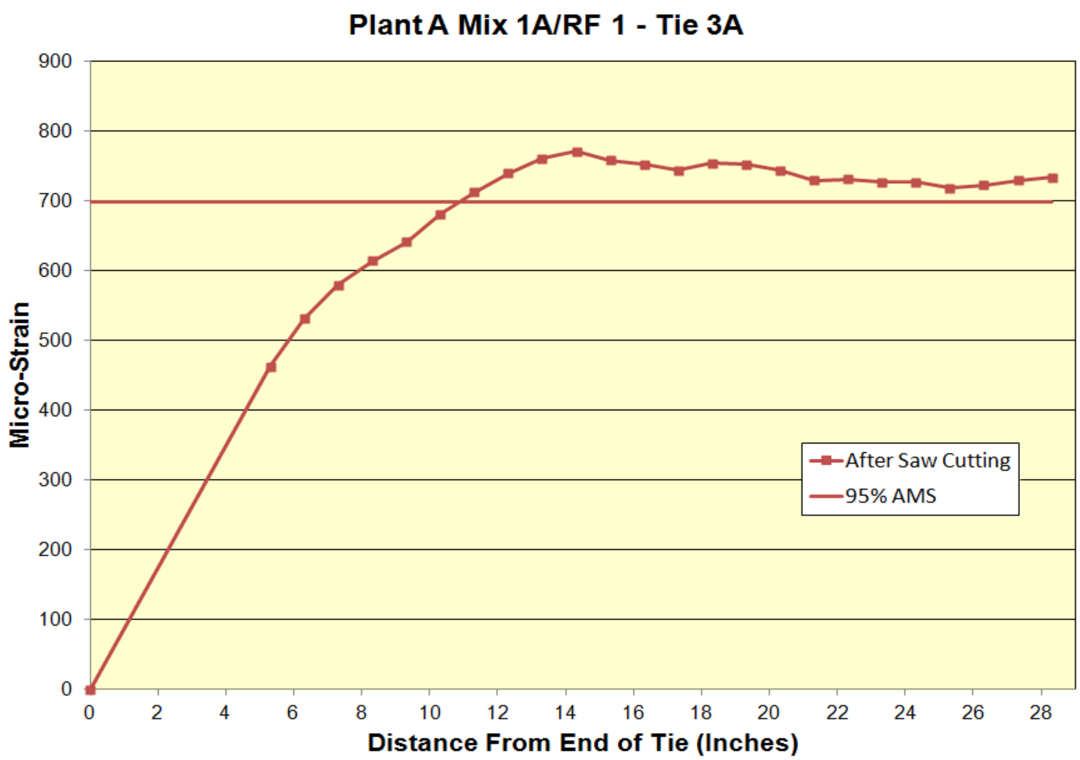

Figure A.21 Transfer length of Plant A Mix 1A/RF 1 Tie 3A

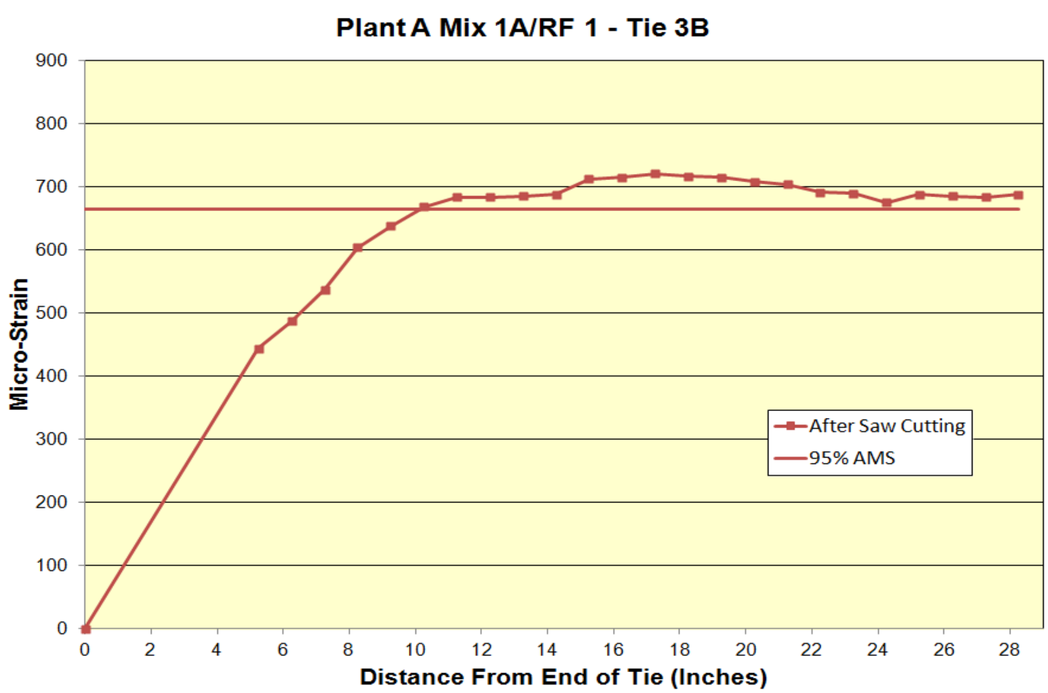

Figure A.22 Transfer length of Plant A Mix 1A/RF 1 Tie 3B

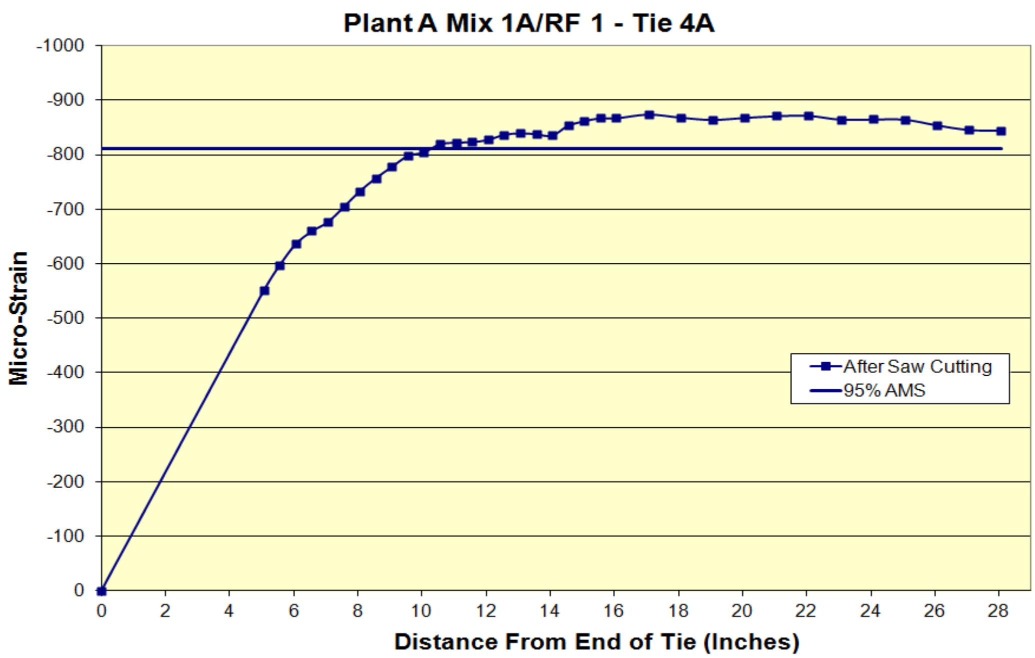

Figure A.23 Transfer length of Plant A Mix 1A/RF 1 Tie 4A

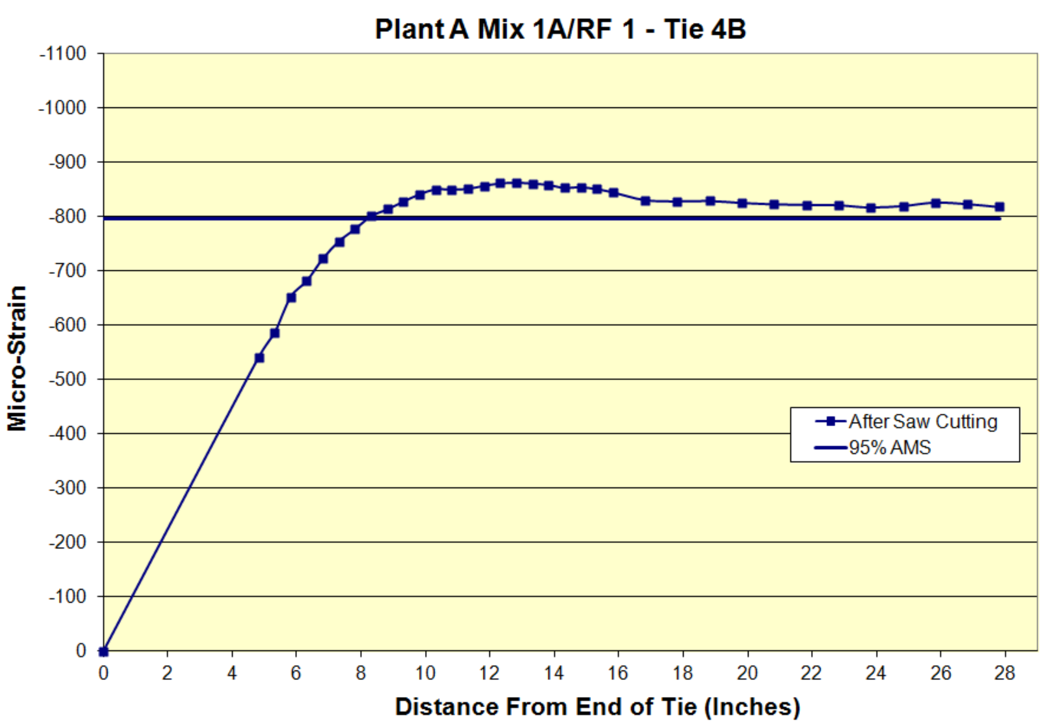

Figure A.24 Transfer length of Plant A Mix 1A/RF 1 Tie 4B

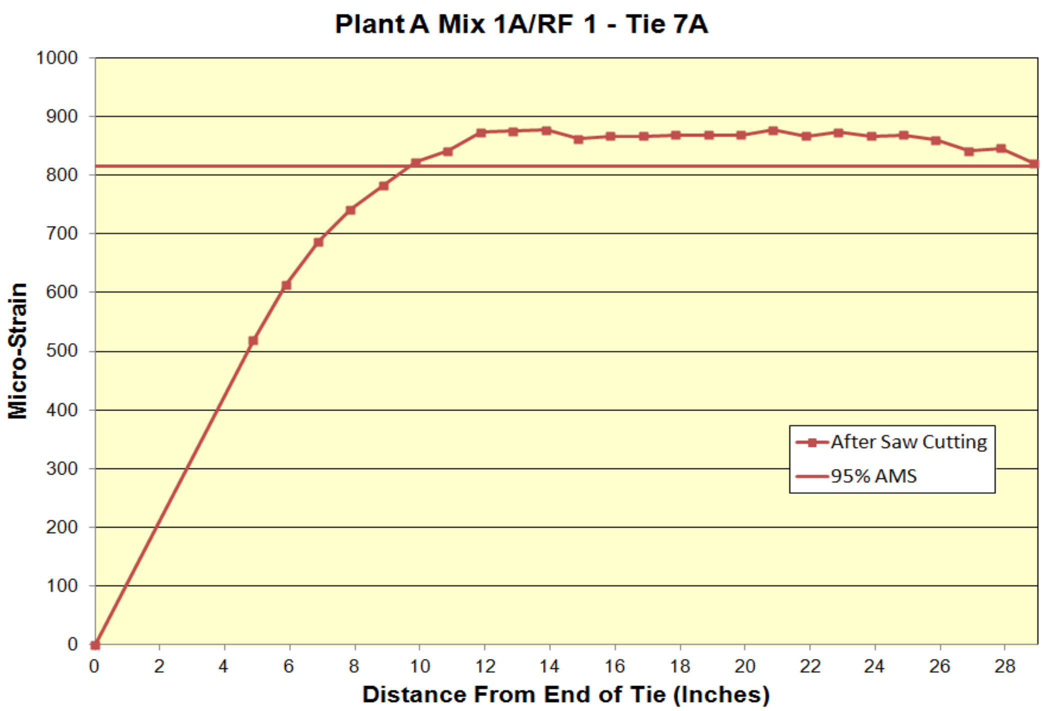

Figure A.25 Transfer length of Plant A Mix 1A/RF 1 Tie 7A

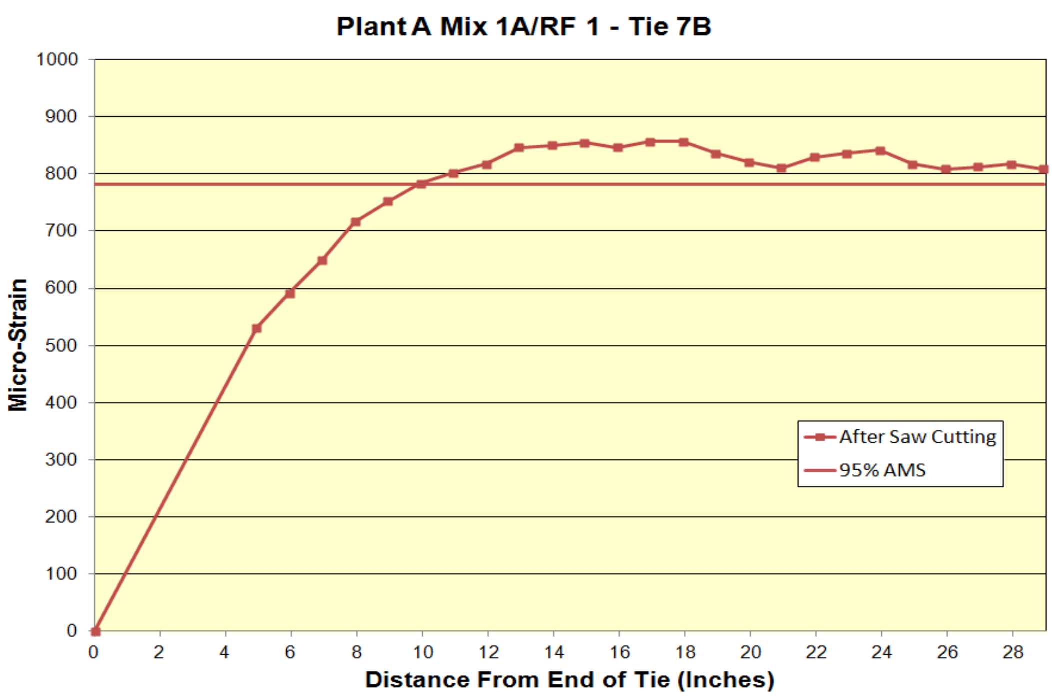

Figure A.26 Transfer length of Plant A Mix 1A/RF 1 Tie 7B

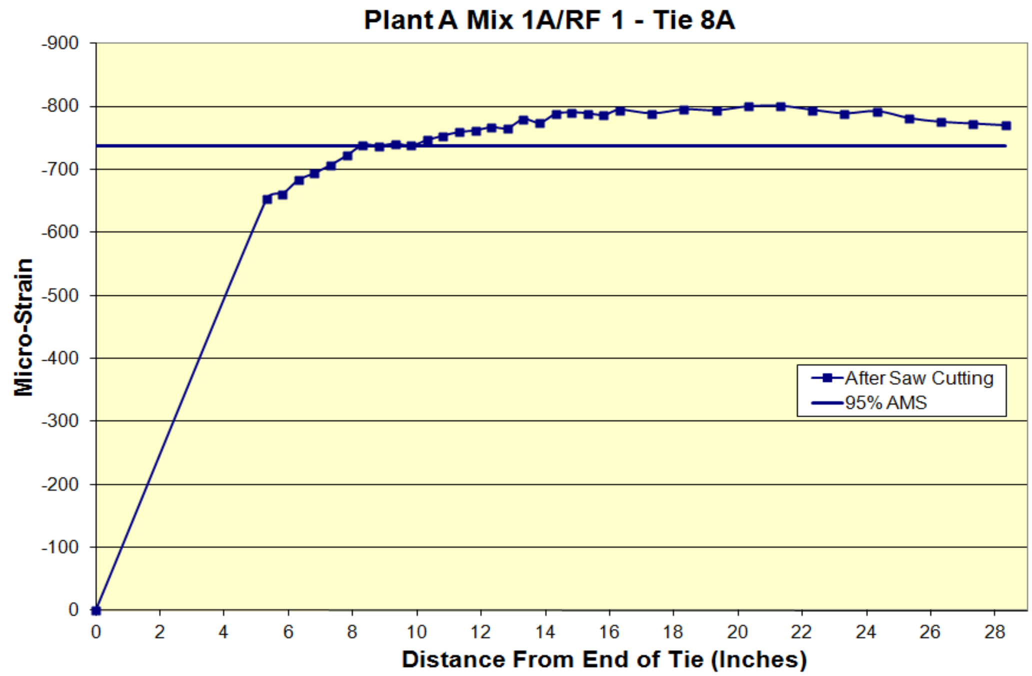

Figure A.27 Transfer length of Plant A Mix 1A/RF 1 Tie 8A

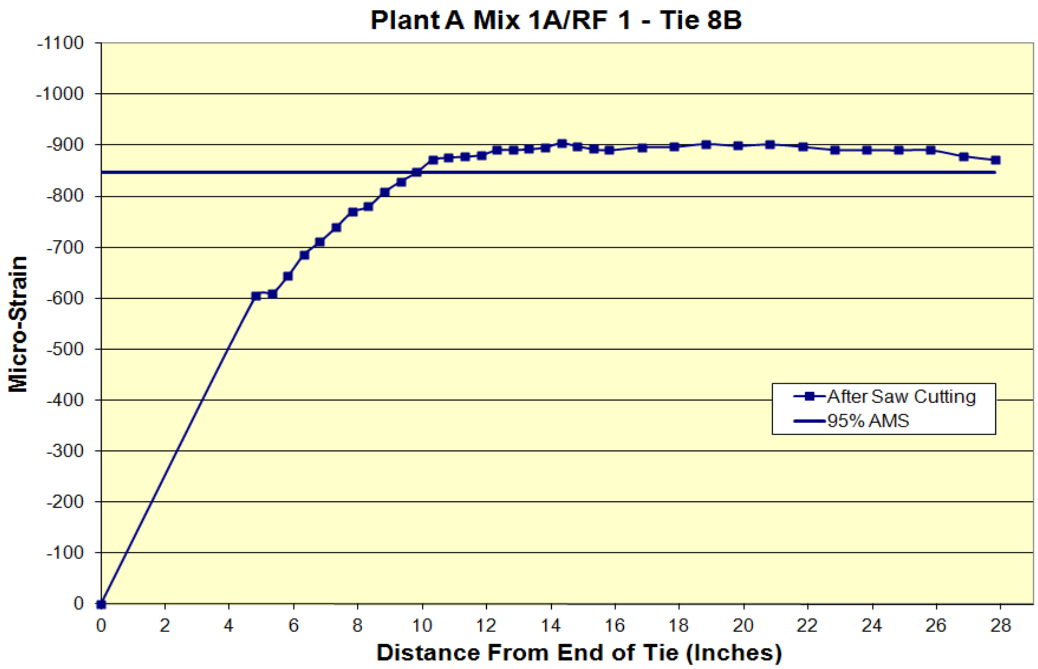

Figure A.28 Transfer length of Plant A Mix 1A/RF 1 Tie 8B

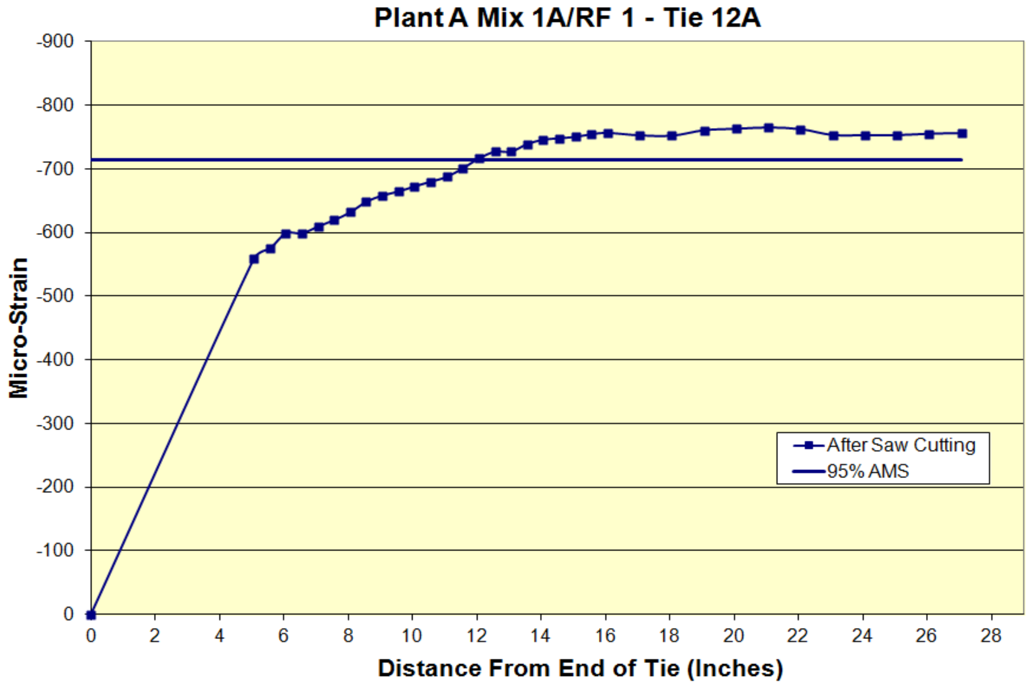

Figure A.29 Transfer length of Plant A Mix 1A/RF 1 Tie 12A

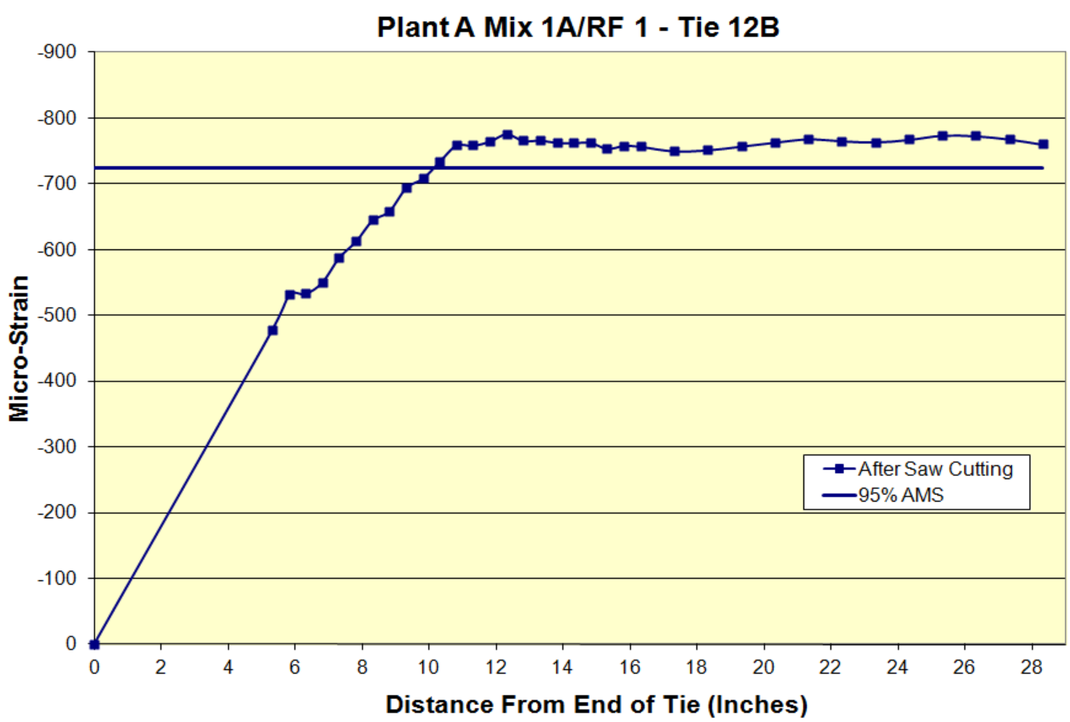

Figure A.30 Transfer length of Plant A Mix 1A/RF 1 Tie 12B

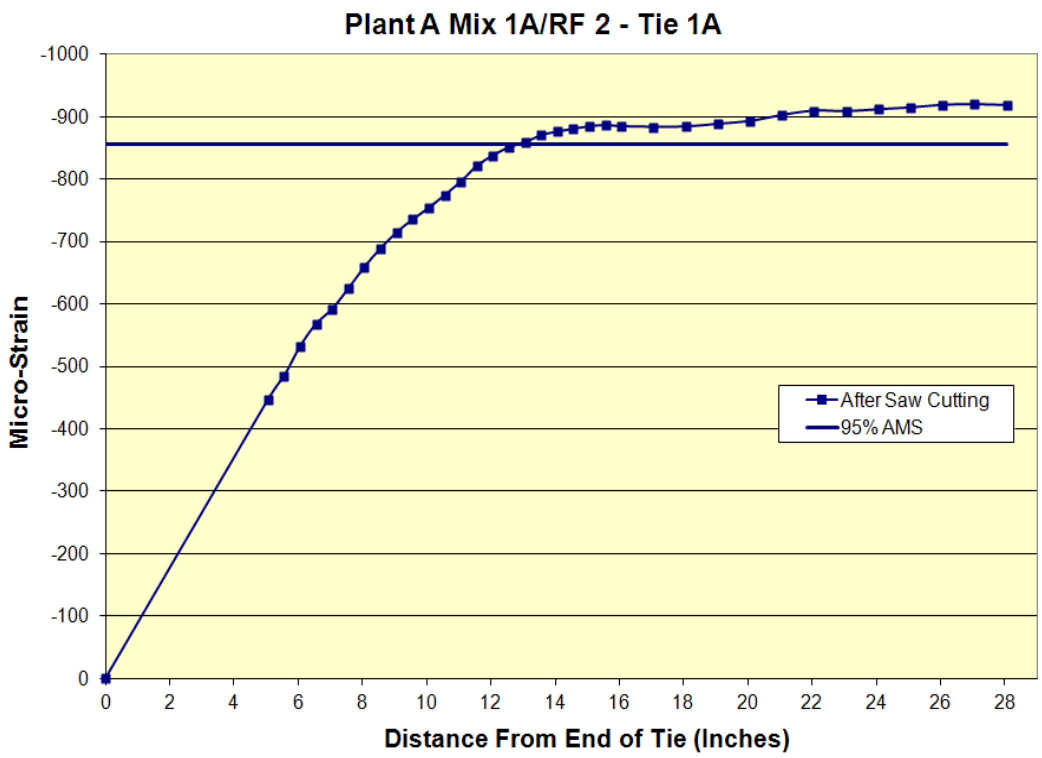

Figure A.31 Transfer length of Plant A Mix 1A/RF 2 Tie 1A

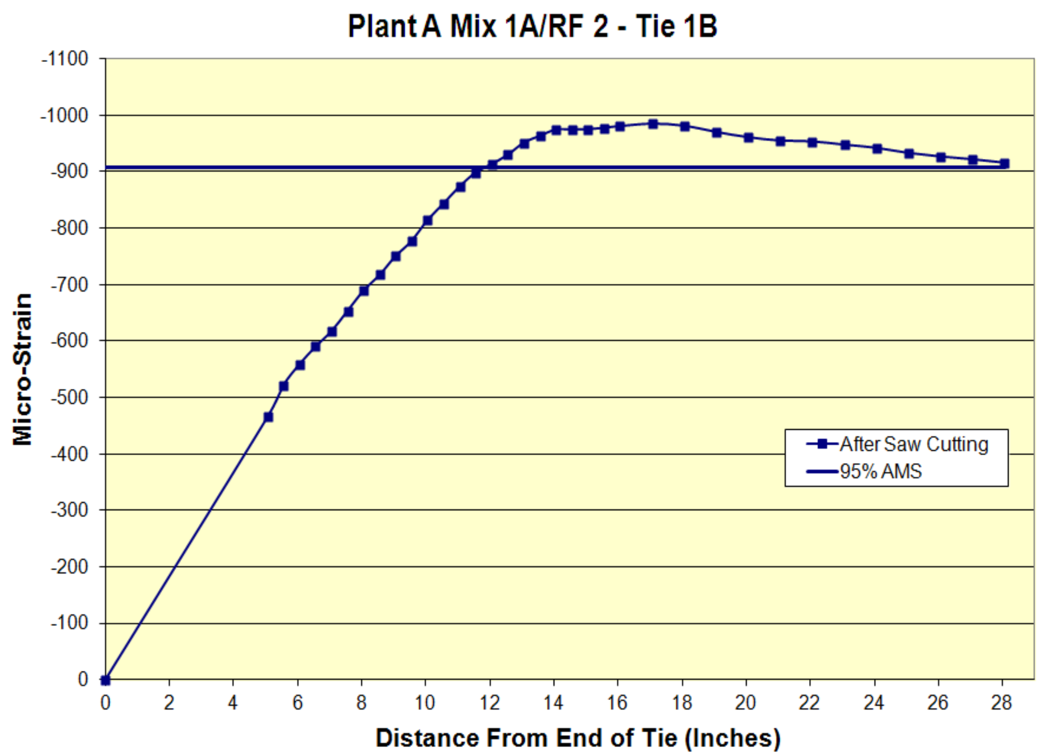

Figure A.32 Transfer length of Plant A Mix 1A/RF 2 Tie 1B

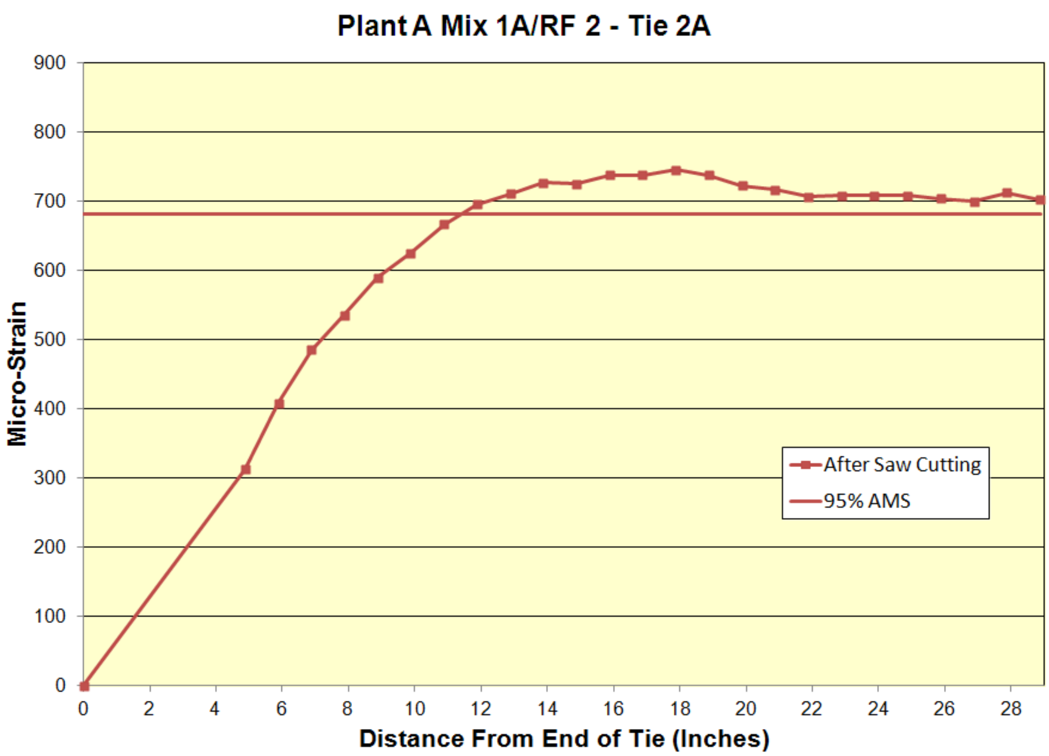

Figure A.33 Transfer length of Plant A Mix 1A/RF 2 Tie 2A

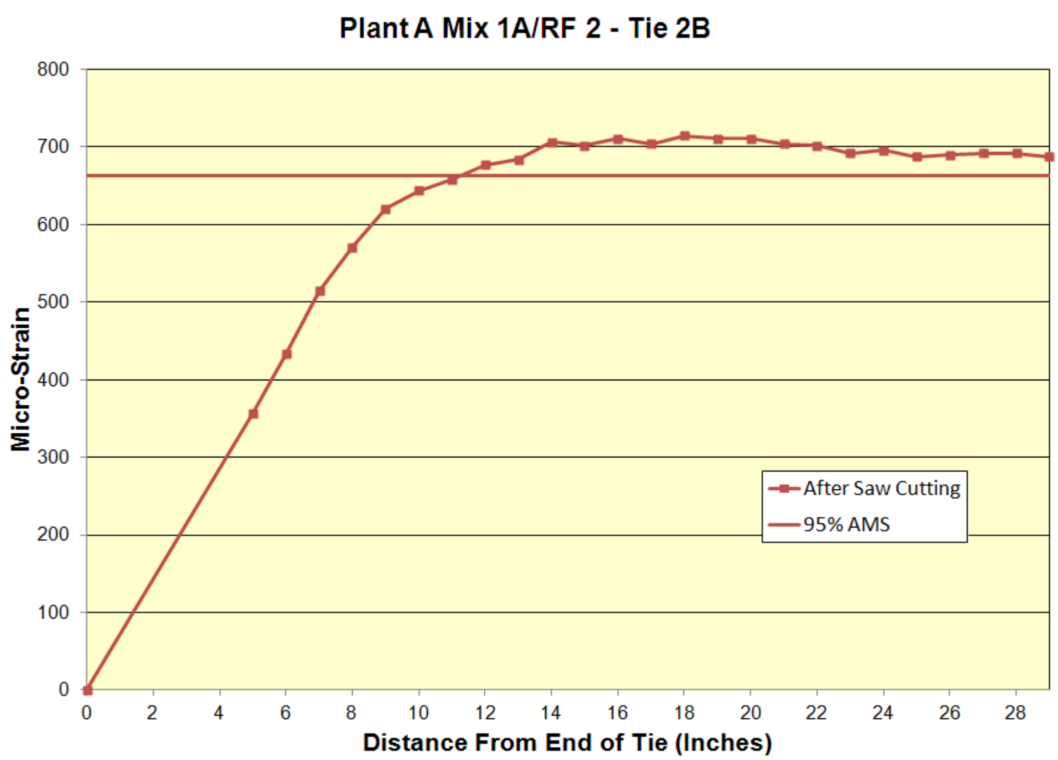

Figure A.34 Transfer length of Plant A Mix 1A/RF 2 Tie 2B

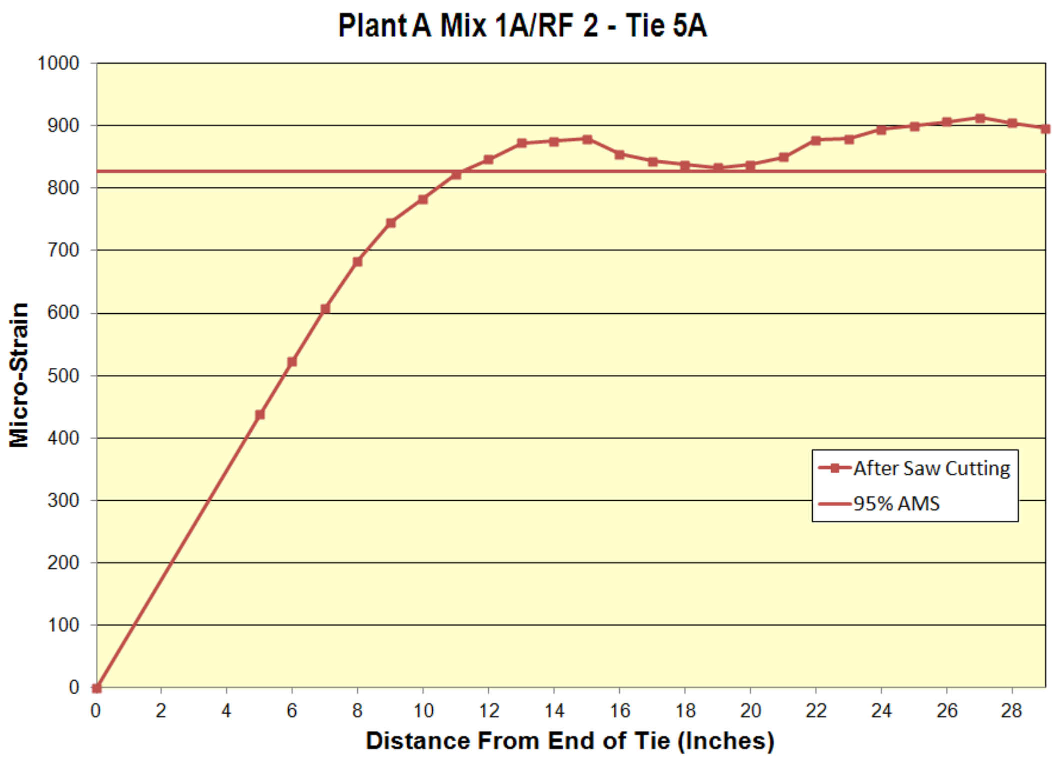

Figure A.35 Transfer length of Plant A Mix 1A/RF 2 Tie 5A

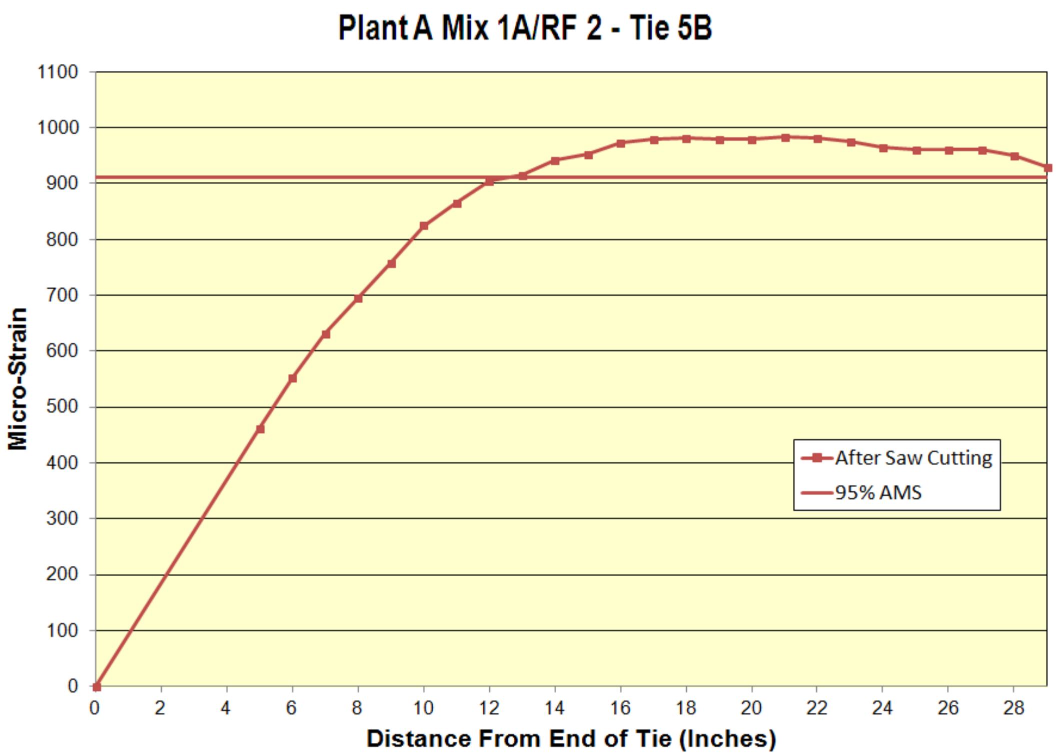

Figure A.36 Transfer length of Plant A Mix 1A/RF 2 Tie 5B

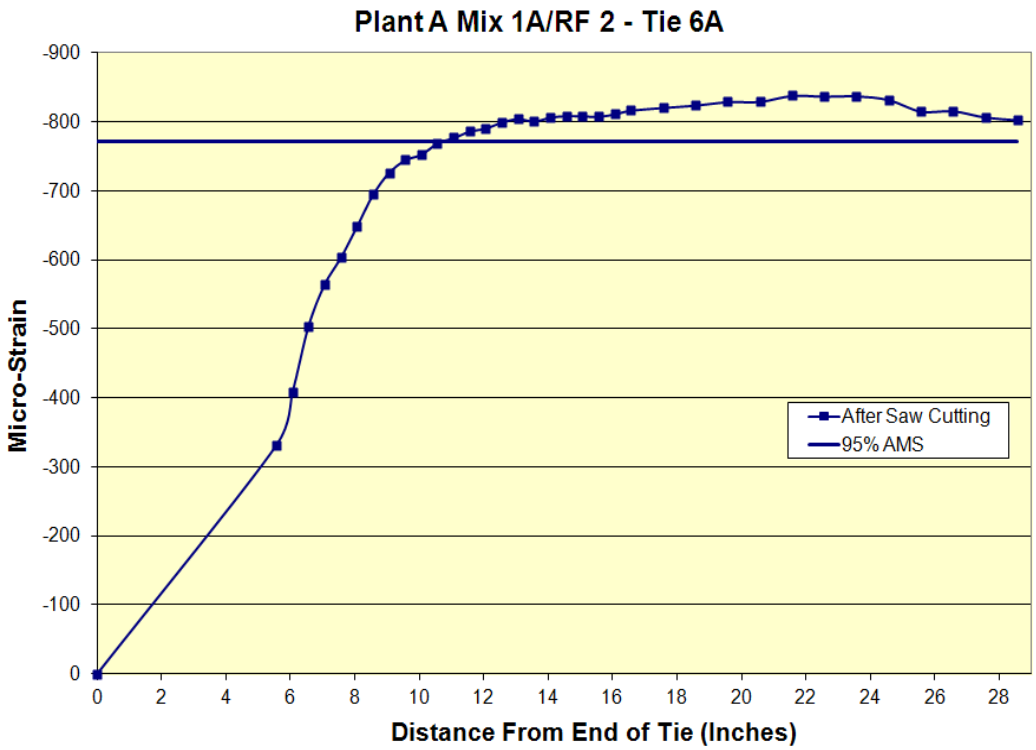

Figure A.37 Transfer length of Plant A Mix 1A/RF 2 Tie 6A

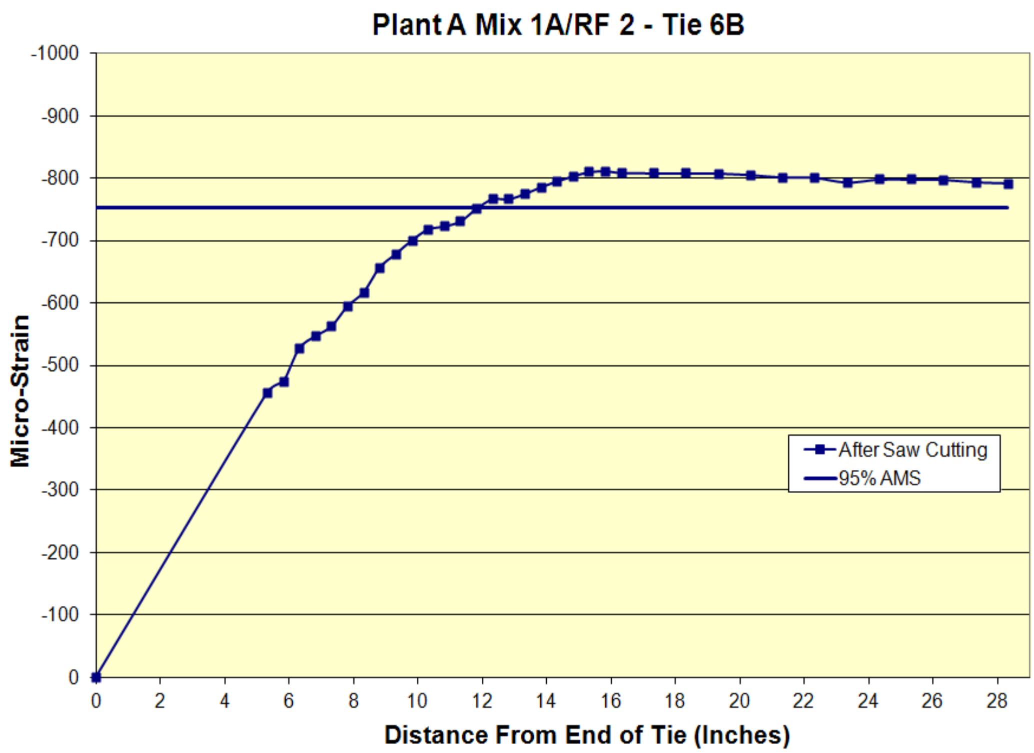

Figure A.38 Transfer length of Plant A Mix 1A/RF 2 Tie 6B

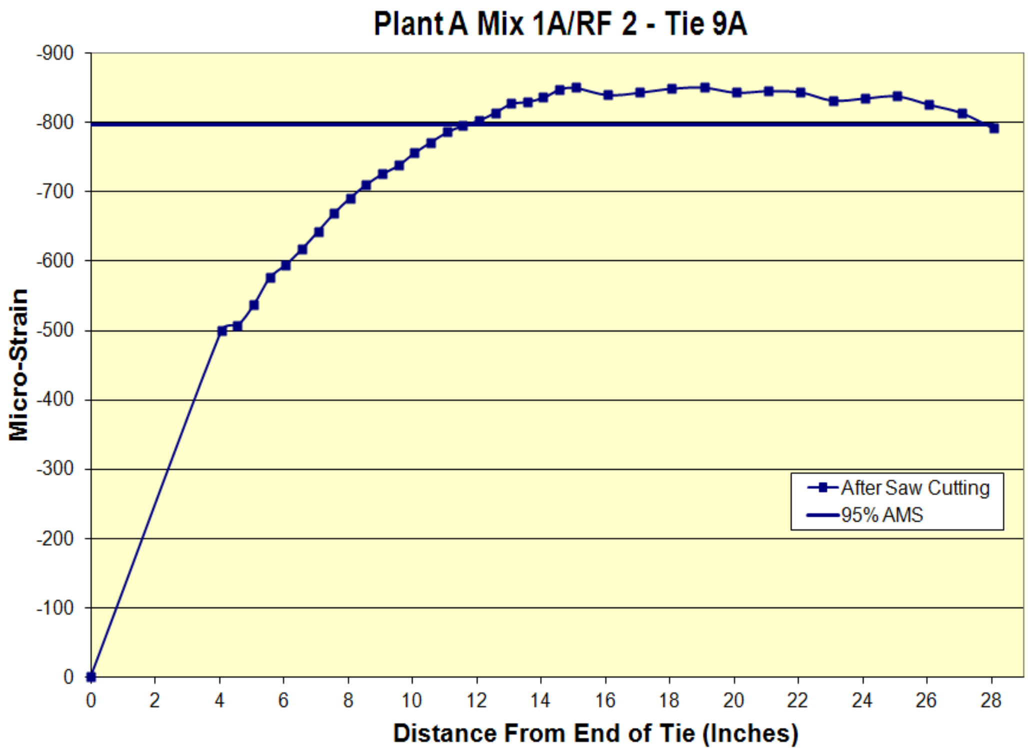

Figure A.39 Transfer length of Plant A Mix 1A/RF 2 Tie 9A

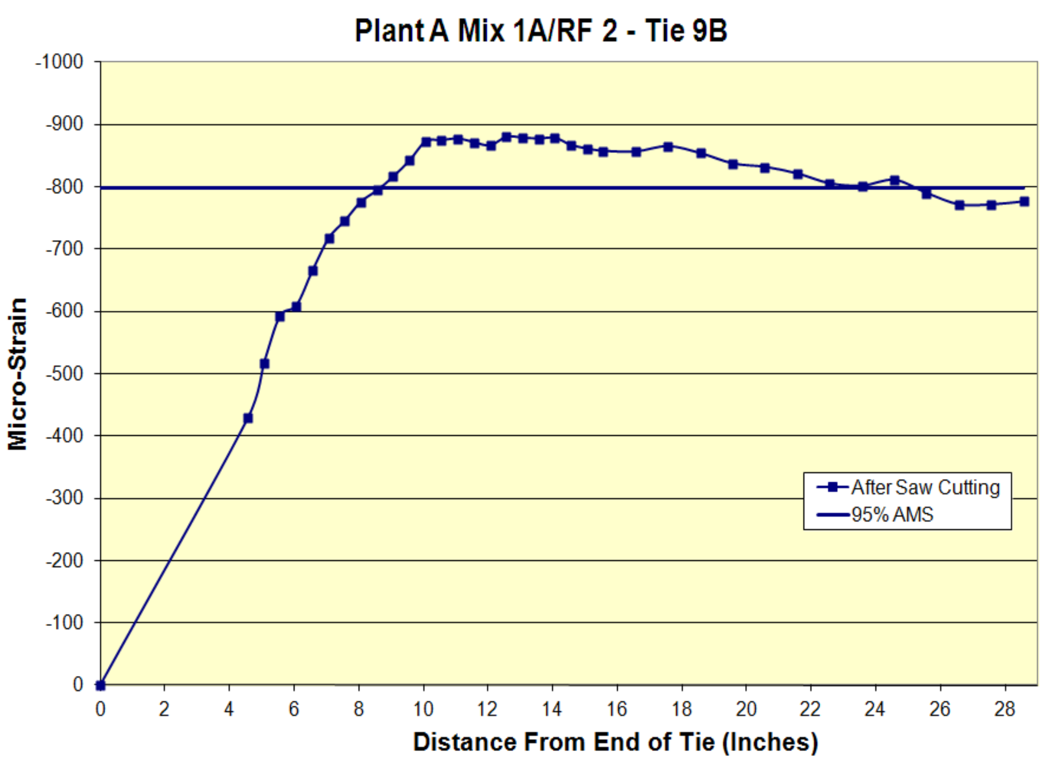

Figure A.40 Transfer length of Plant A Mix 1A/RF 2 Tie 9B

A.2 Long-term Transfer Lengths

Table A.2 Long-term transfer length data for Plant A Mix 1A/RF 1

Plant A Mix 1A/RF 1				
	Transfer Length (in.)			
Time of Reading	Tie 3A	Tie 3B	Tie 7A	Tie 7B
After Saw Cutting	10.8	10.1	9.7	10
40 Days After Pour	10.6	10.1	10.1	10.2
90 Days After Pour	10.6	10.4	10.4	10.3
120 Days After Pour	10.8	10.5	10.6	10.4
270 Days After Pour	10.8	10.6	10.6	11.2

Table A.3 Long-term transfer length data for Plant A Mix 1A/ RF 2

Plant A Mix 1A/RF 2				
	Transfer Length (in.)			
Time of Reading	Tie 2A	Tie 2B	Tie 5A	Tie 5B
After Saw Cutting	11.3	11.4	11.2	12.3
40 Days After Pour	11.1	11.2	11.3	13
90 Days After Pour	11.5	11.7	12.4	13.1
120 Days After Pour	11.6	11.6	12	13
270 Days After Pour	11.7	13.2	12.8	13.7

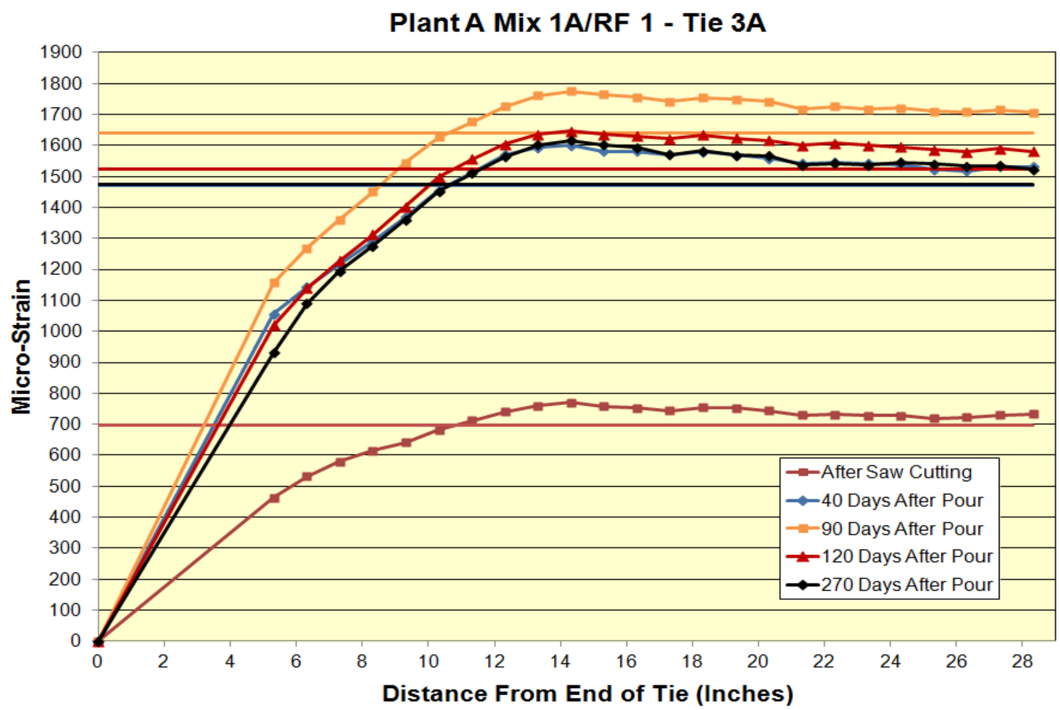

Figure A.41 Transfer length of Plant A Mix 1A/RF 1 Tie 3A

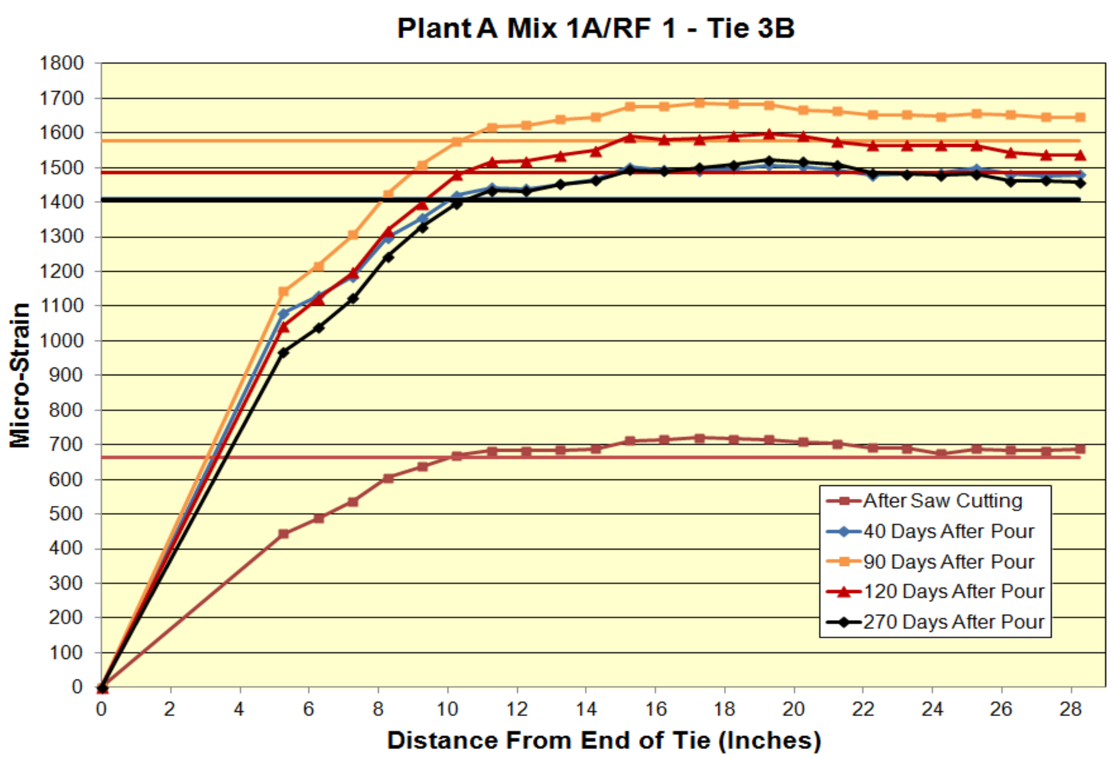

Figure A.42 Transfer length of Plant A Mix 1A/RF 1 Tie 3B

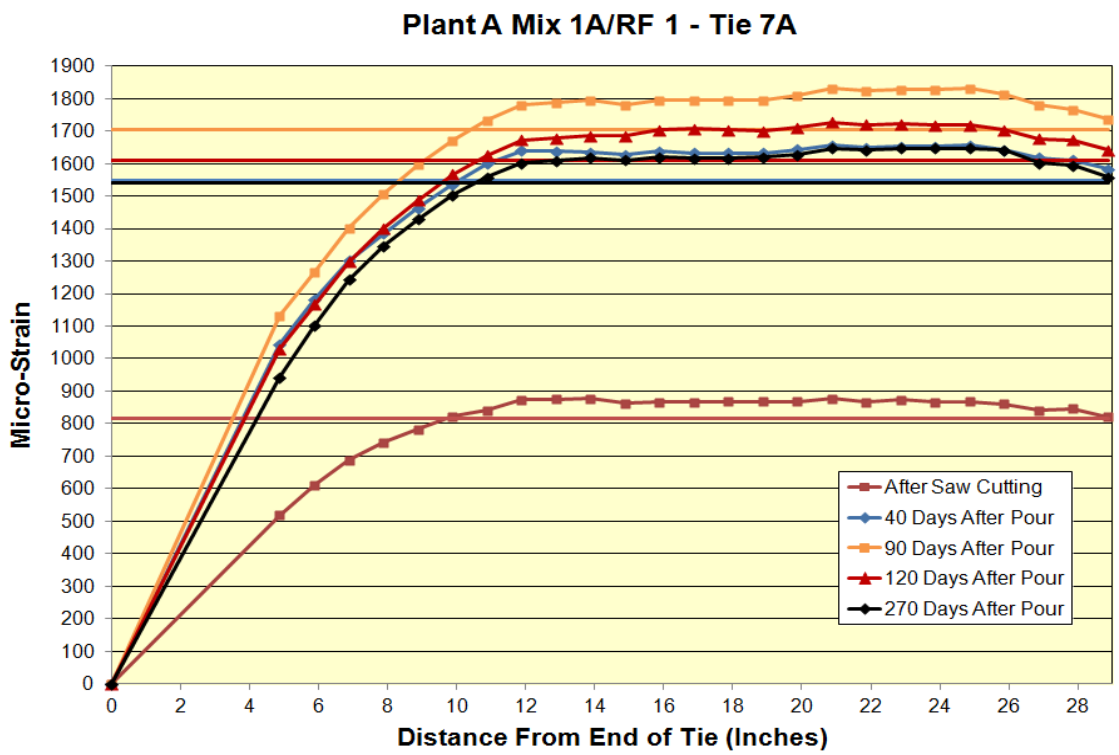

Figure A.43 Transfer length of Plant A Mix 1A/RF 1 Tie 7A

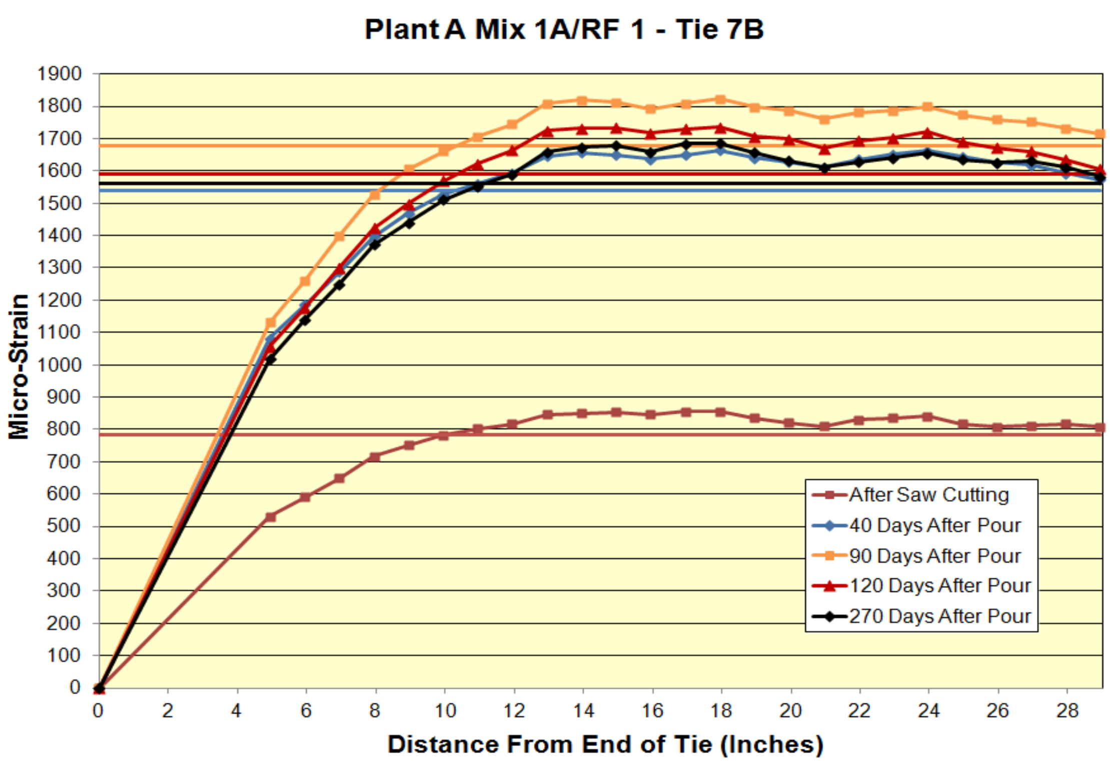

Figure A.44 Transfer length of Plant A Mix 1A/RF 1 Tie 7B

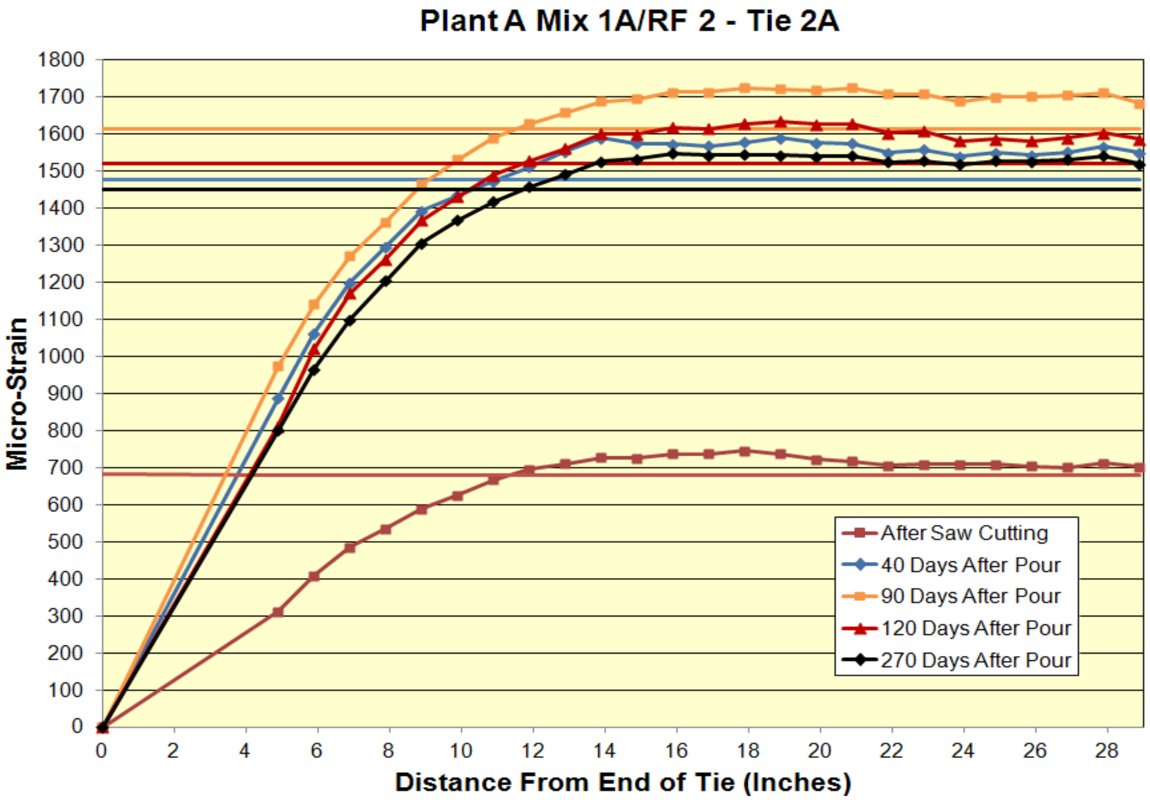

Figure A.45 Transfer length of Plant A Mix 1A/RF 2 Tie 2A

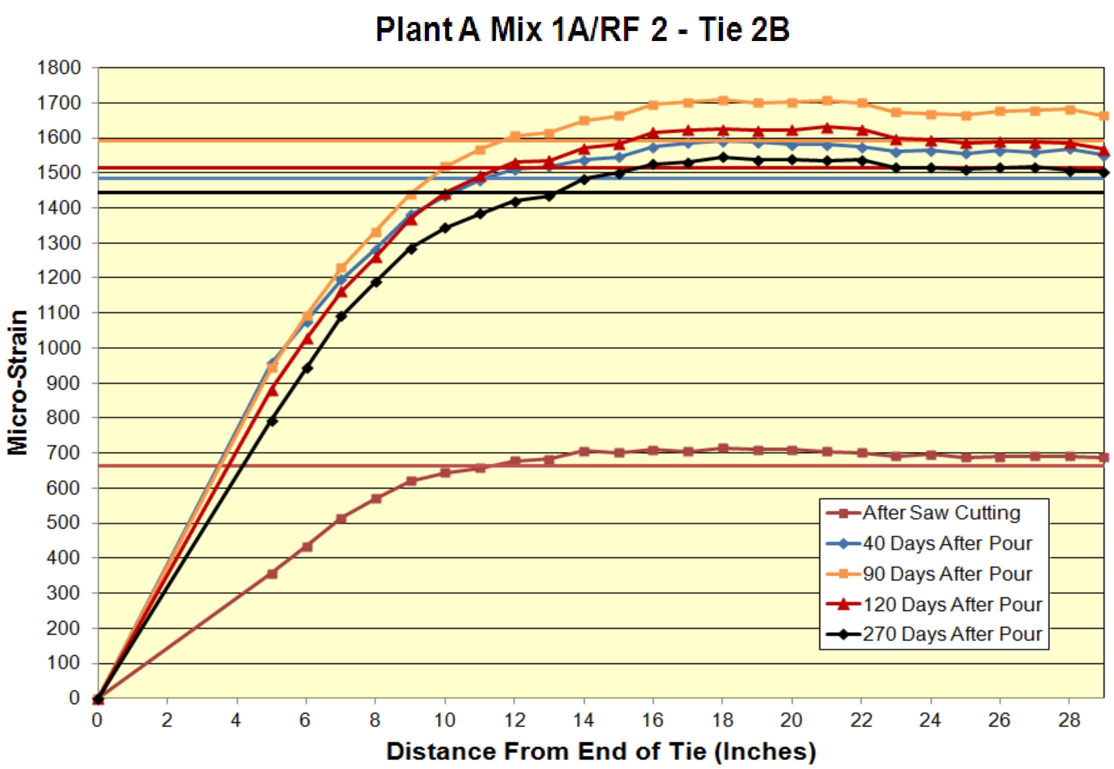

Figure A.46 Transfer length of Plant A Mix 1A/RF 2 Tie 2B

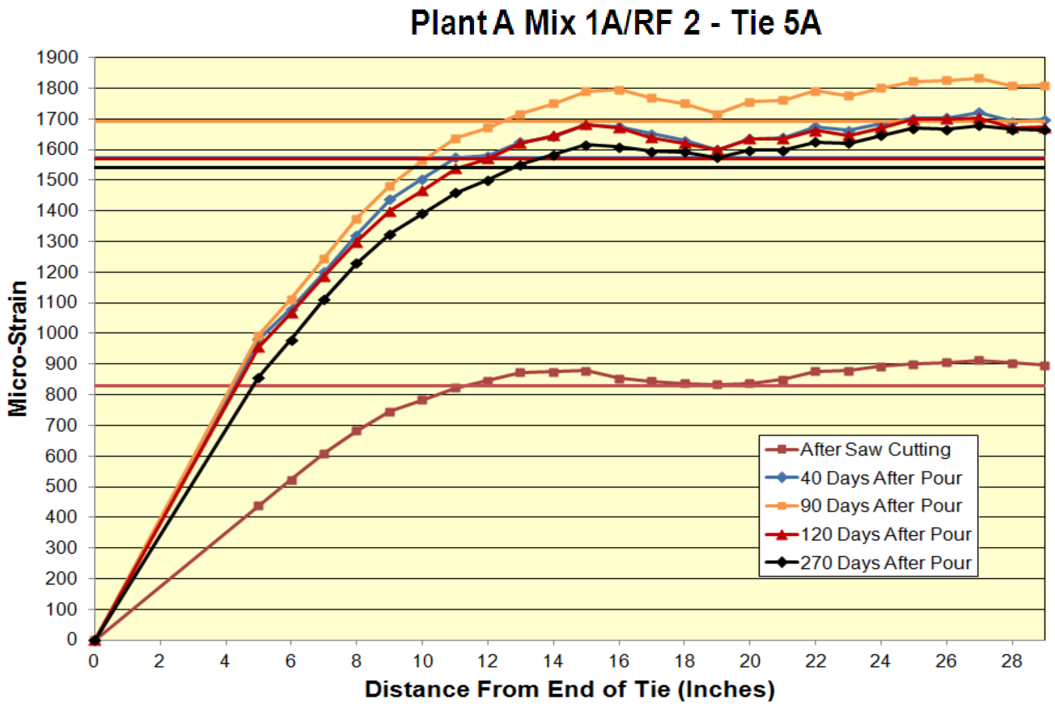

Figure A.47 Transfer length of Plant A Mix 1A/RF 2 Tie 5A

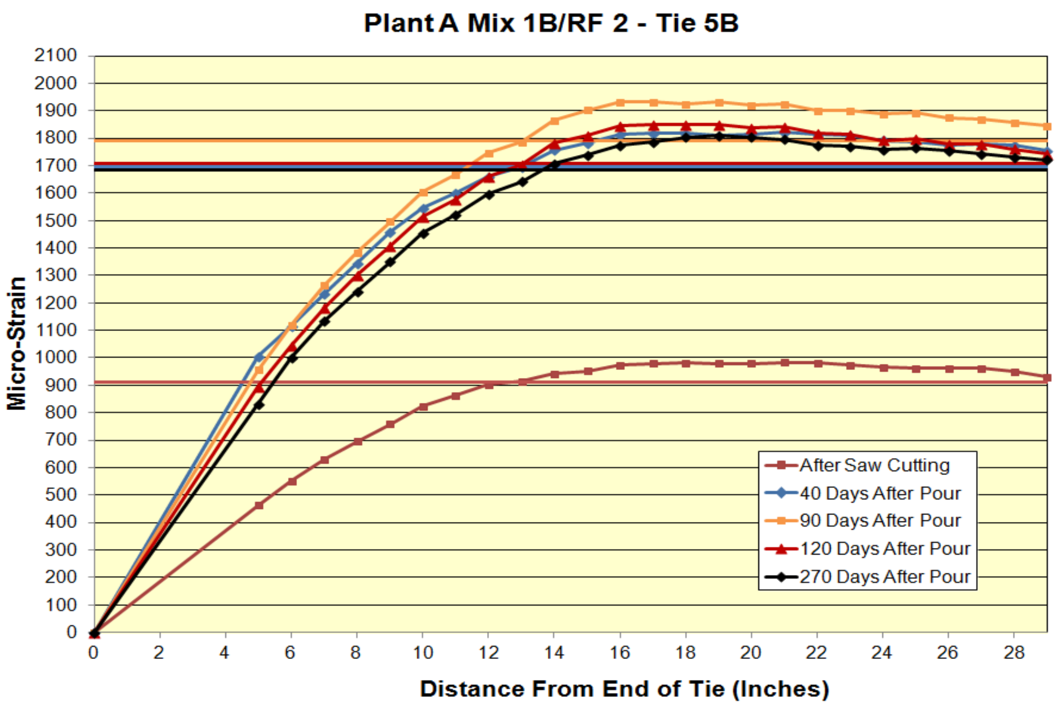

Figure A.48 Transfer length of Plant A Mix 1A/RF 2 Tie 5B

Appendix B Plant B Transfer Lengths

B.1 Short-term Transfer Lengths

Table B.1 Plant B transfer length data

	Tie Label	Measurement Method	Transfer Length (in.)
Plant B Mix 2/RF 3	1A	Laser Speckle	20.7
	1B	Laser Speckle	19.1
	3A	Laser Speckle	21.8
	4A	Whittemore Gage	20.4
	4B	Whittemore Gage	26.8
	5B	Laser Speckle	25.9
	6A	Laser Speckle	18.1
	6B	Laser Speckle	21.8
	7A	Laser Speckle	20.4
	7B	Laser Speckle	20
	9A	Whittemore Gage	18.3
	9B	Whittemore Gage	20.5
	11A	Laser Speckle	15
	13A	Laser Speckle	17
	13B	Laser Speckle	15.4
	14A	Whittemore Gage	18.8
	14B	Whittemore Gage	17.5
	15B	Laser Speckle	15.5
Plant B Mix 3/RF 3	17A	Whittemore Gage	14.3
	17B	Whittemore Gage	14.9
	18A	Laser Speckle	11
	18B	Laser Speckle	13.3
	19A	Laser Speckle	17.4
	19B	Laser Speckle	13.4
	20A	Laser Speckle	14.5
	20B	Laser Speckle	18.3
	21A	Laser Speckle	15
	21B	Laser Speckle	15.8
	23A	Whittemore Gage	12.6
	23B	Whittemore Gage	15
	24A	Laser Speckle	18
	25A	Whittemore Gage	14.3
	25B	Whittemore Gage	14.5
	26A	Laser Speckle	13.5
	26B	Laser Speckle	13.8
	27A	Laser Speckle	14
	27B	Laser Speckle	15
	28A	Laser Speckle	12.5
	28B	Laser Speckle	14.5

Note: Side A = Dead-end of tie

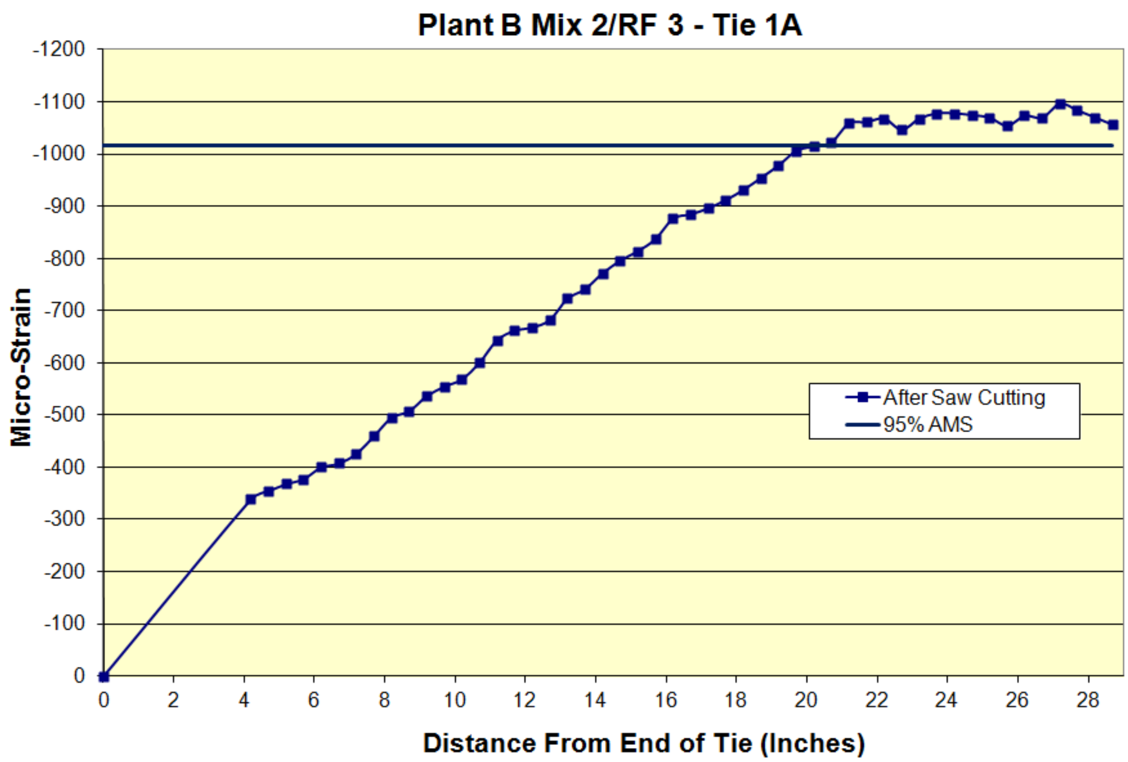

Figure B.1 Transfer length of Plant B Mix 2/RF 3 Tie 1A

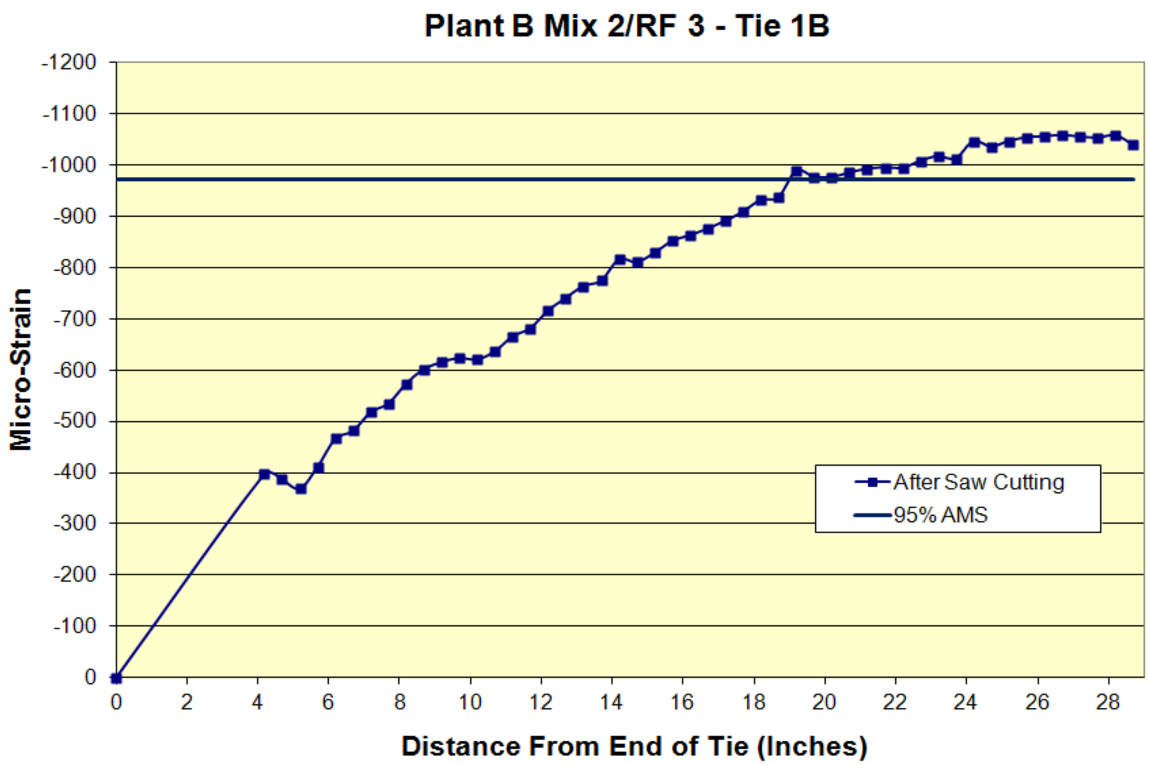

Figure B.2 Transfer length of Plant B Mix 2/RF 3 Tie 1B

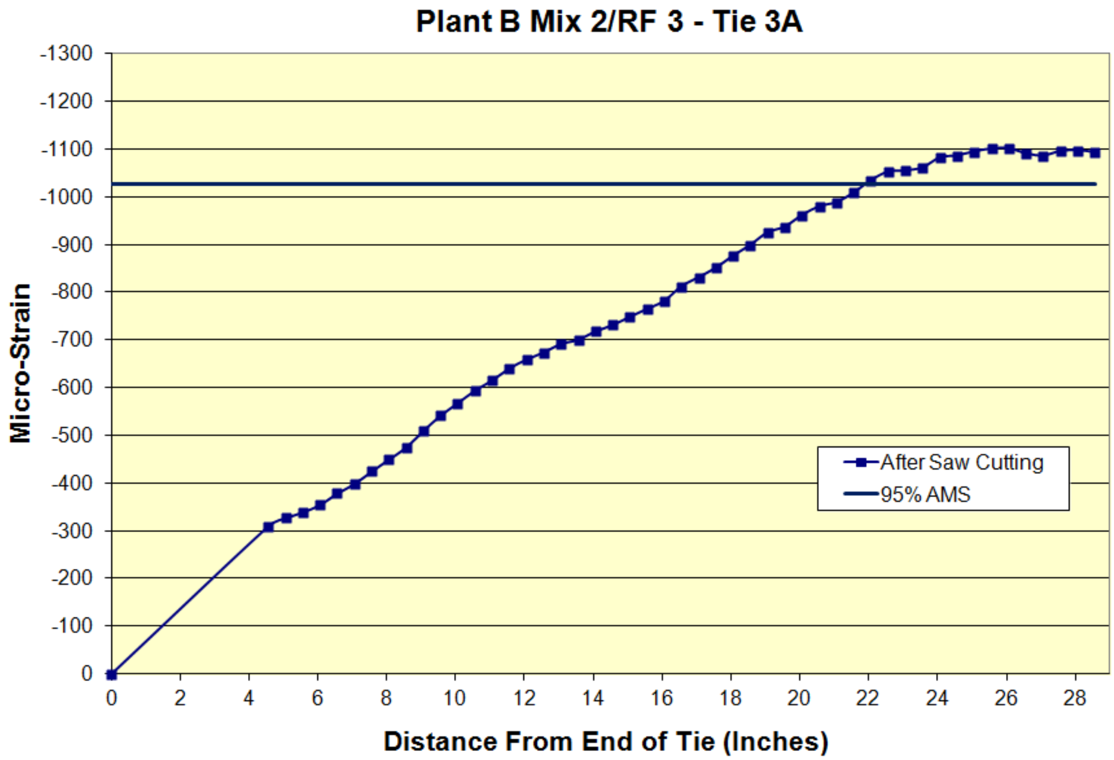

Figure B.3 Transfer length of Plant B Mix 2/RF 3 Tie 3A

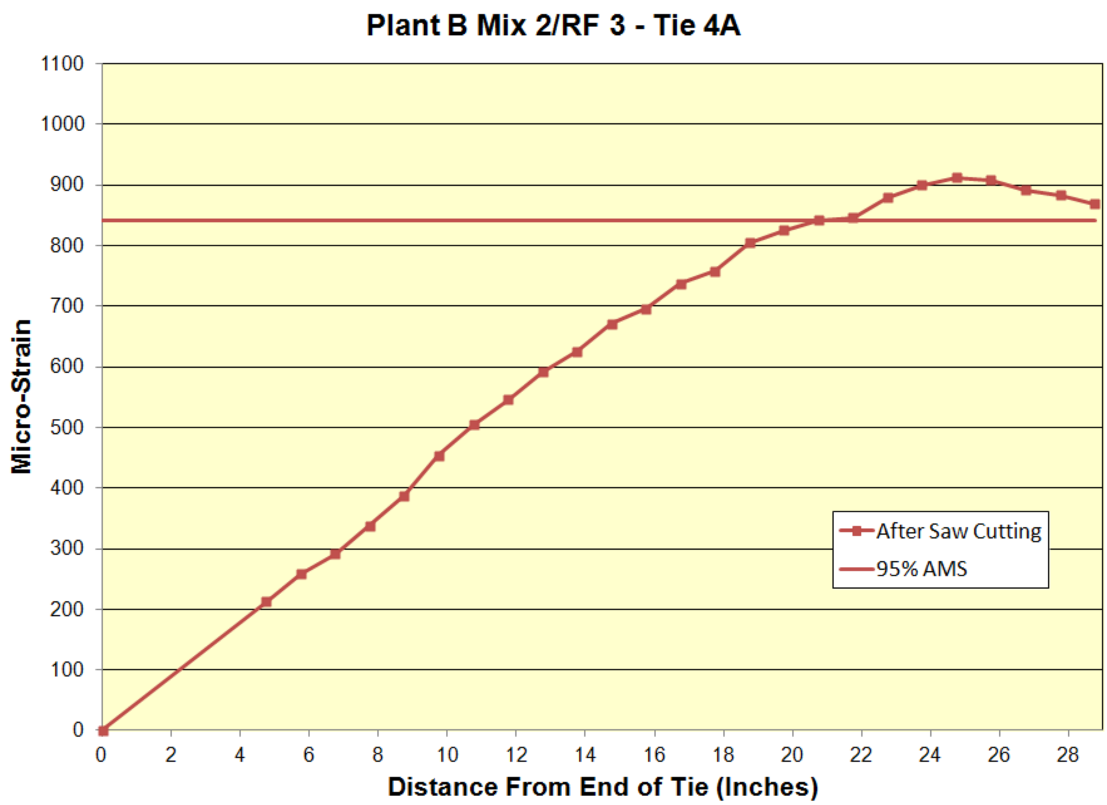

Figure B.4 Transfer length of Plant B Mix 2/RF 3 Tie 4A

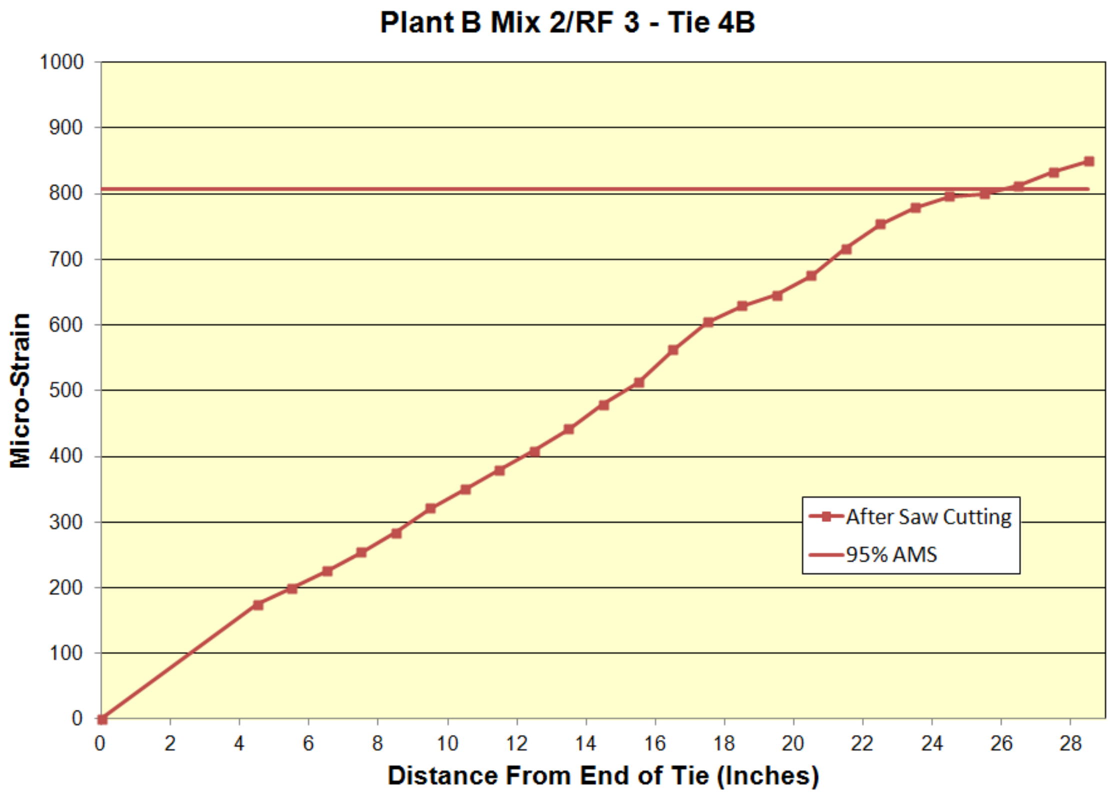

Figure B.5 Transfer length of Plant B Mix 2/RF 3 Tie 4B

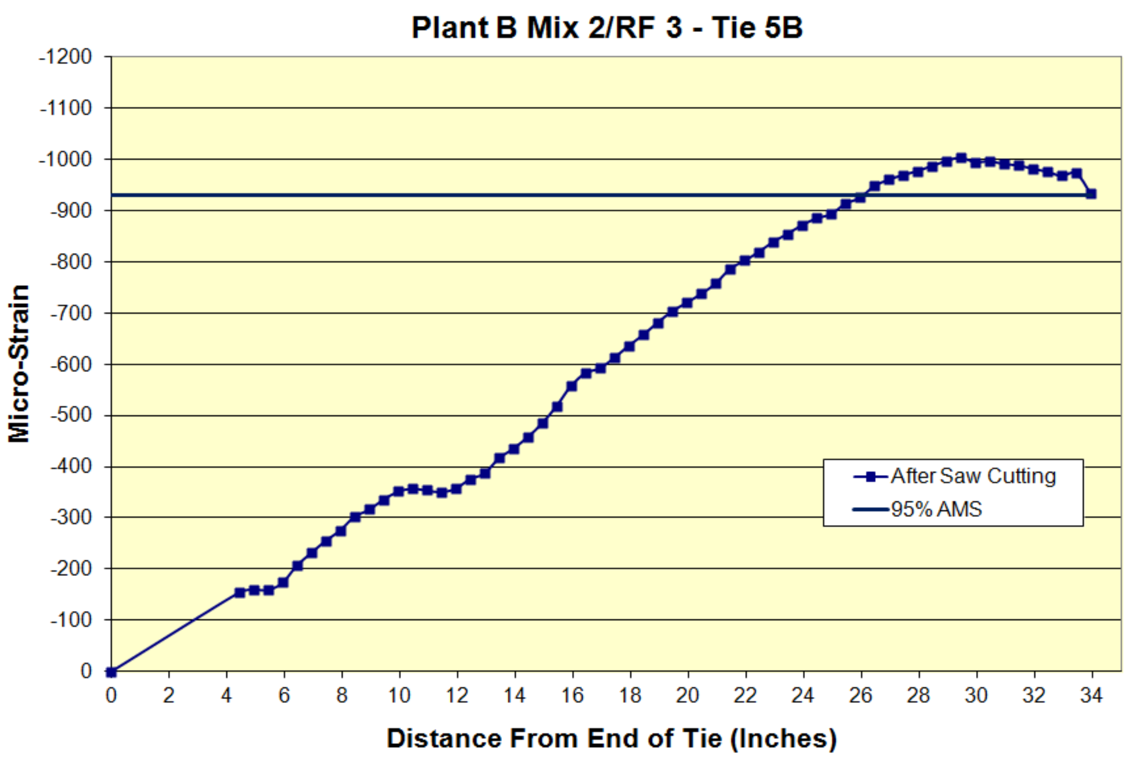

Figure B.6 Transfer length of Plant B Mix 2/RF 3 Tie 5B

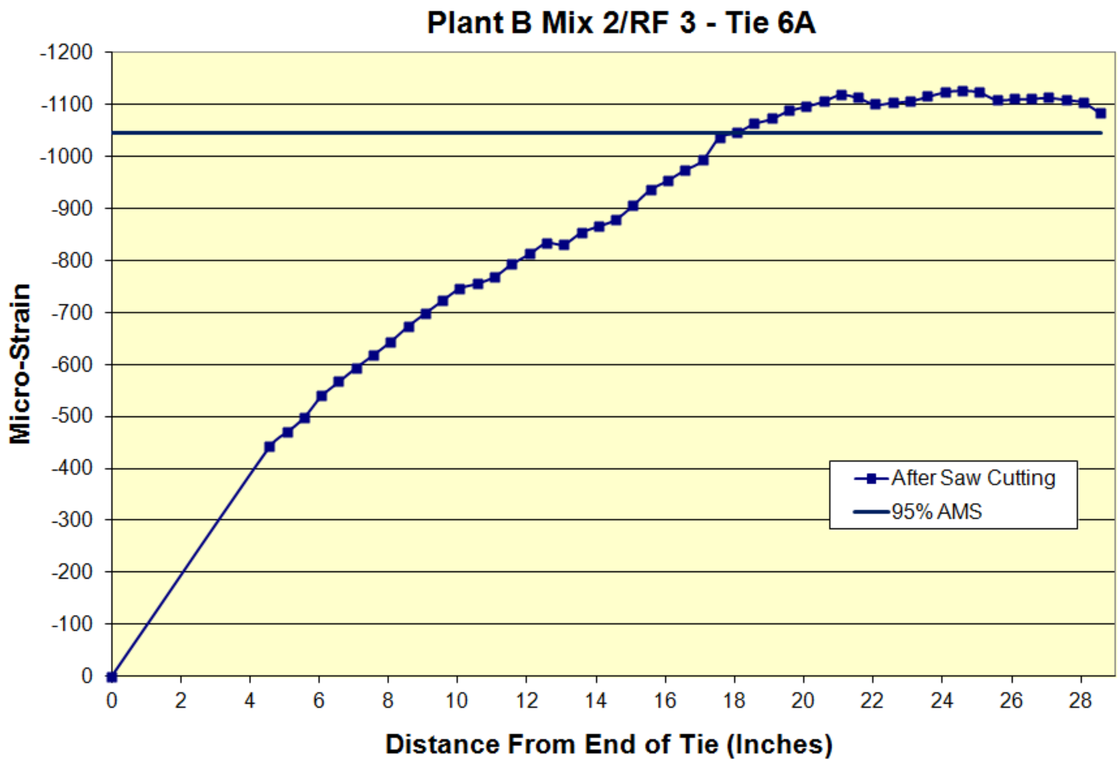

Figure B.7 Transfer length of Plant B Mix 2/RF 3 Tie 6A

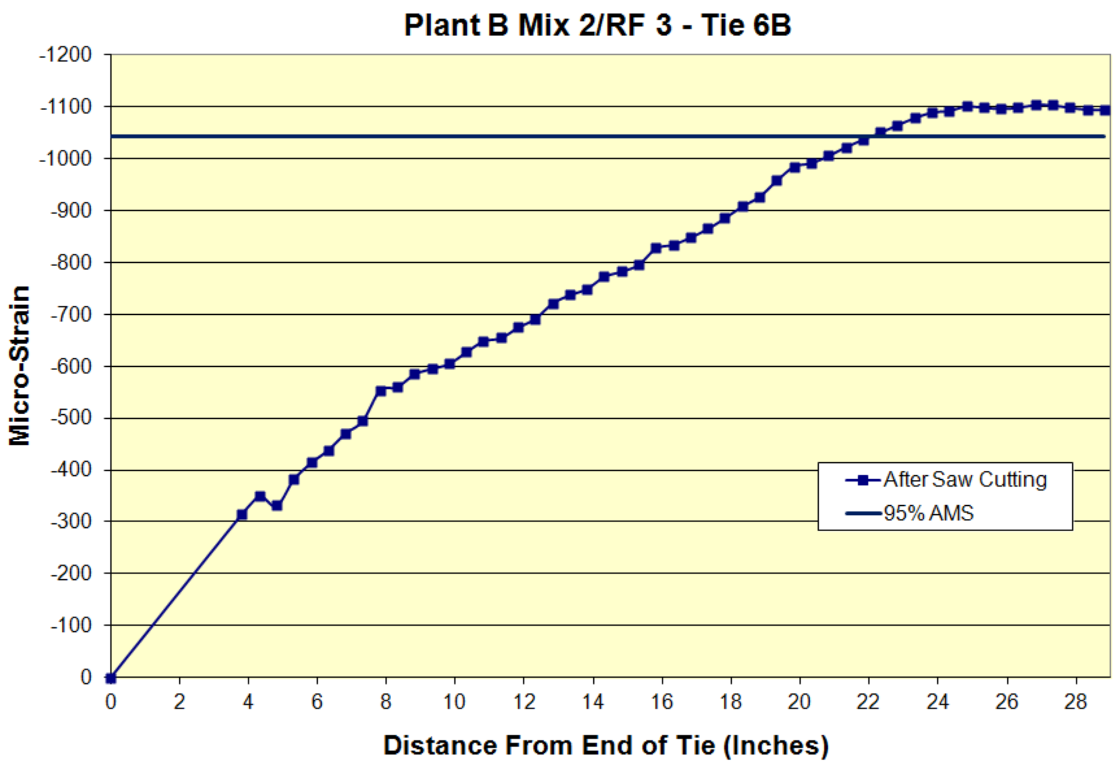

Figure B.8 Transfer length of Plant B Mix 2/RF 3 Tie 6B

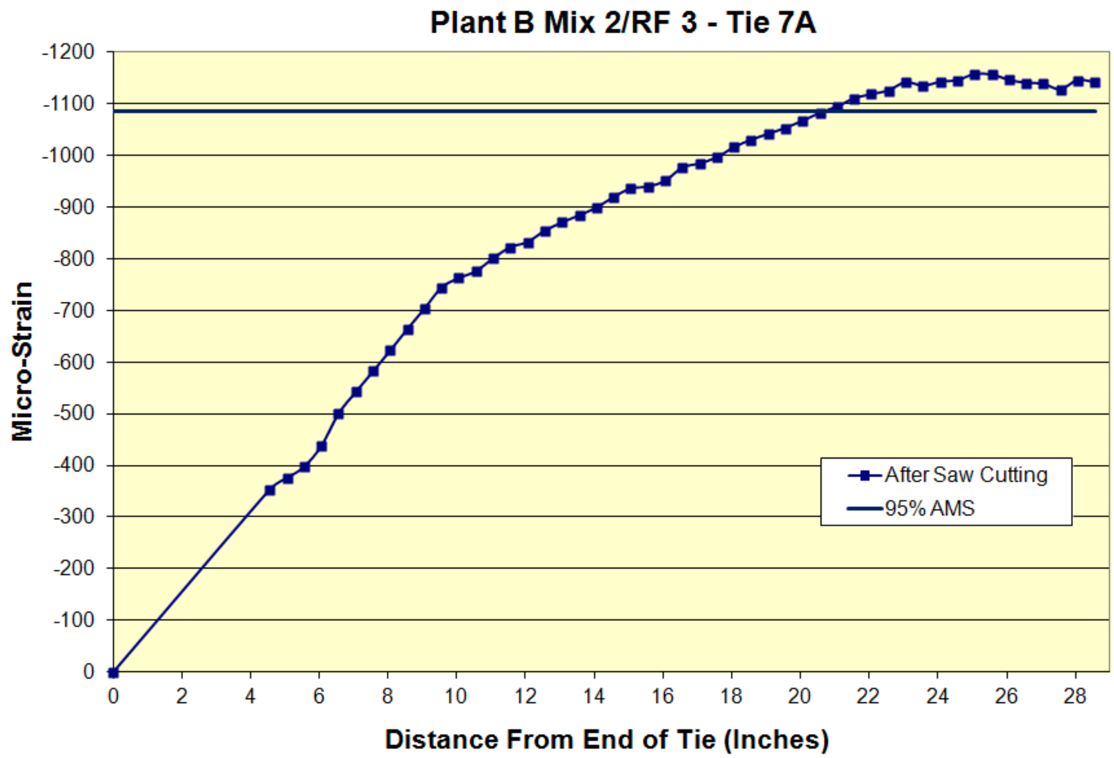

Figure B.9 Transfer length of Plant B Mix 2/RF 3 Tie 7A

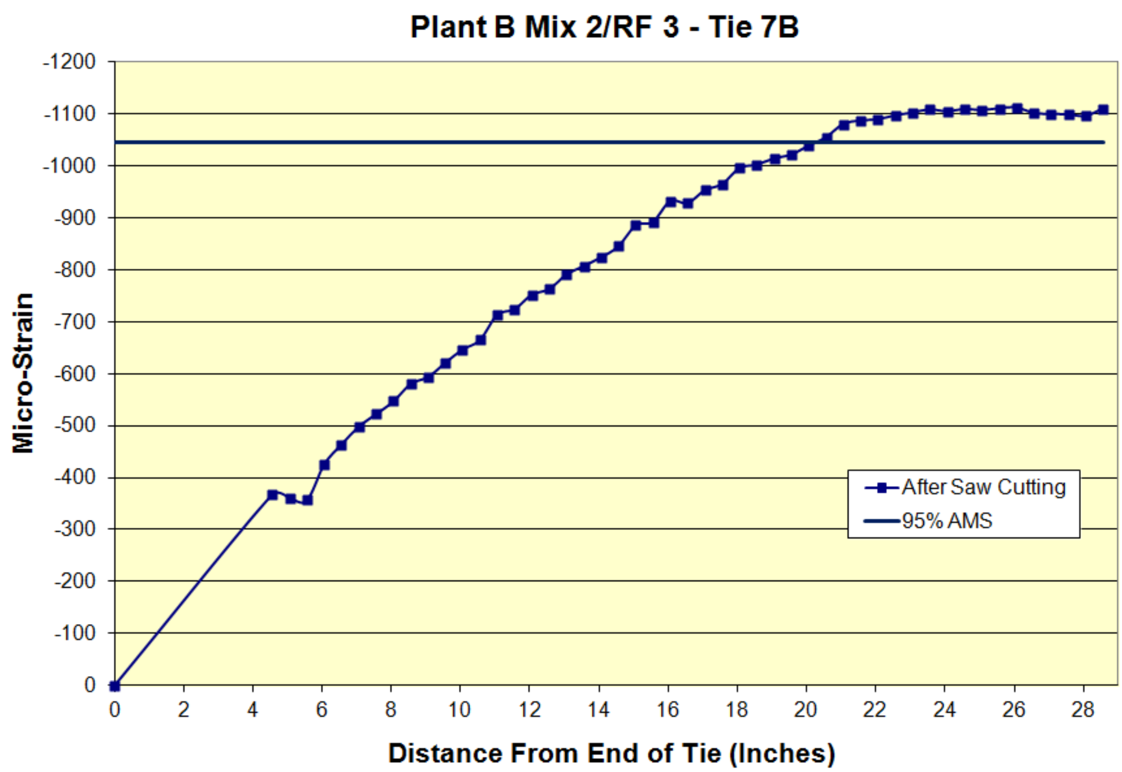

Figure B.10 Transfer length of Plant B Mix 2/RF 3 Tie 7B

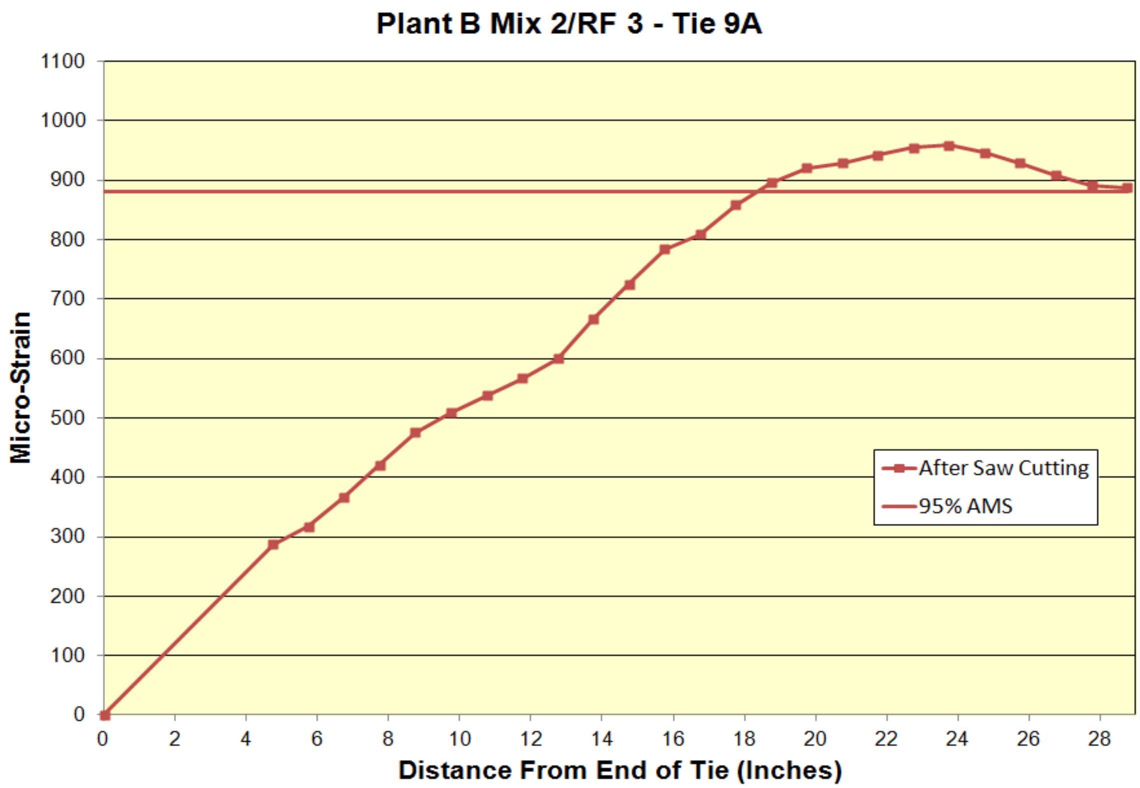

Figure B.11 Transfer length of Plant B Mix 2/RF 3 Tie 9A

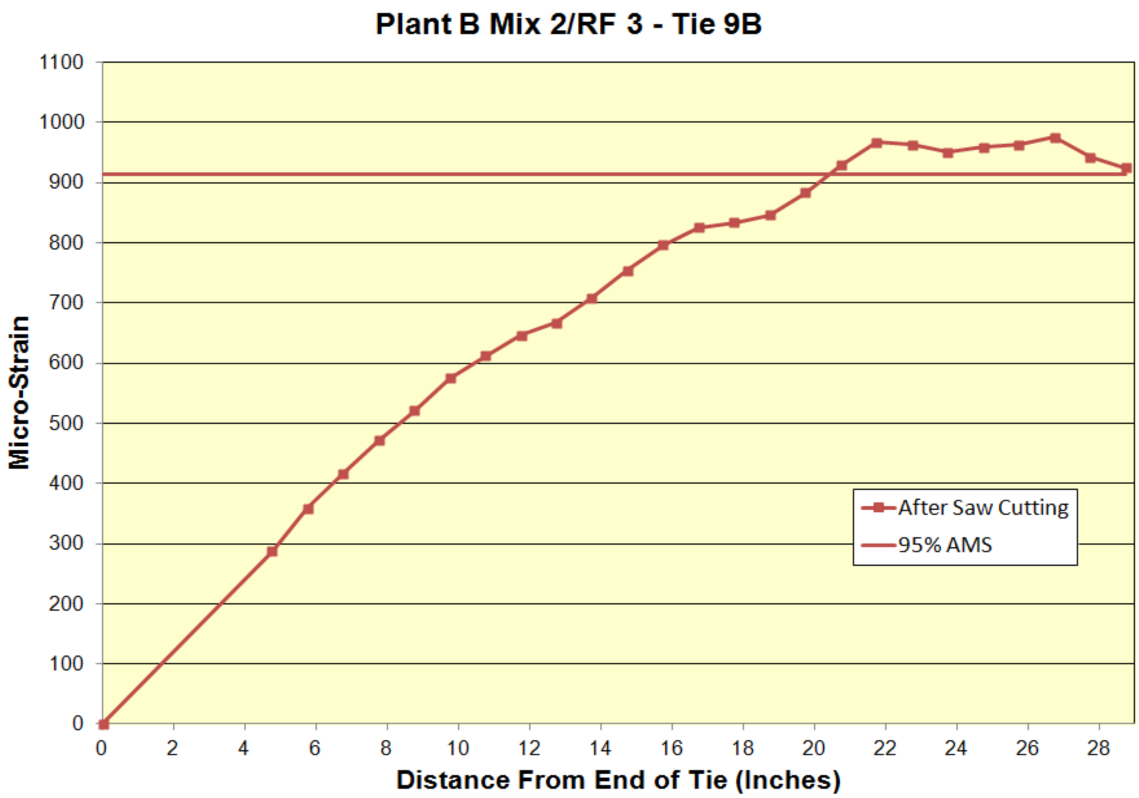

Figure B.12 Transfer length of Plant B Mix 2/RF 3 Tie 9B

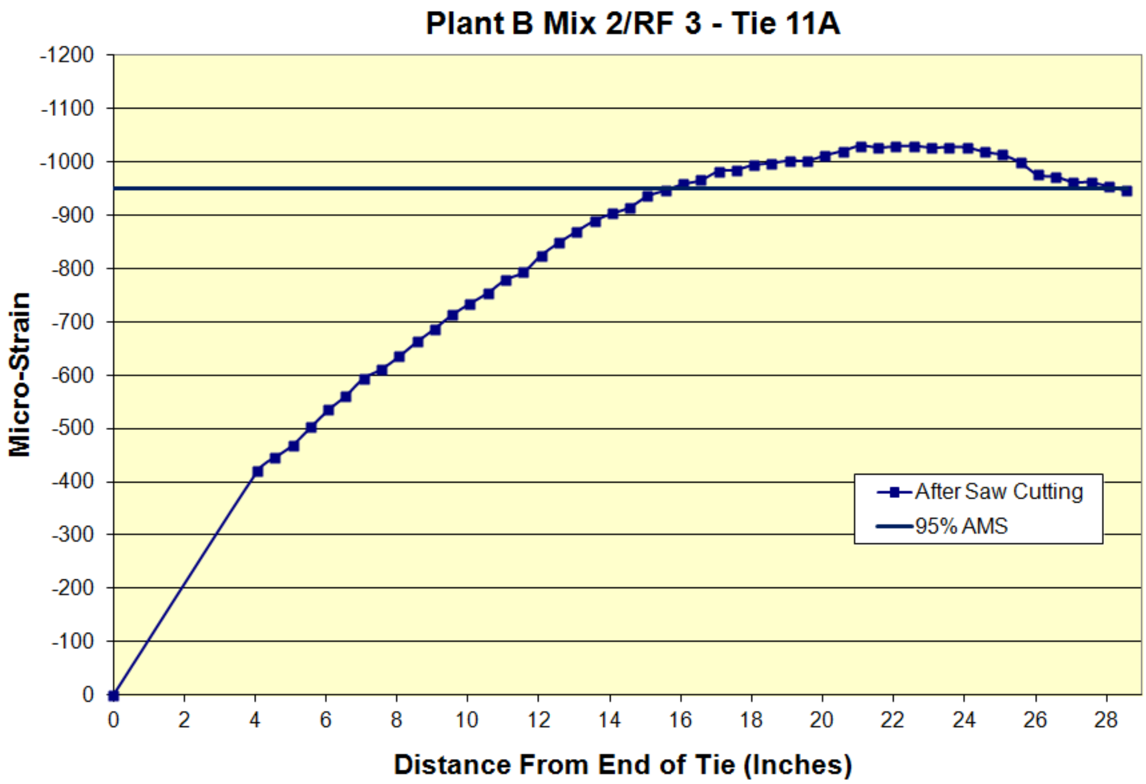

Figure B.13 Transfer length of Plant B Mix 2/RF 3 Tie 11A

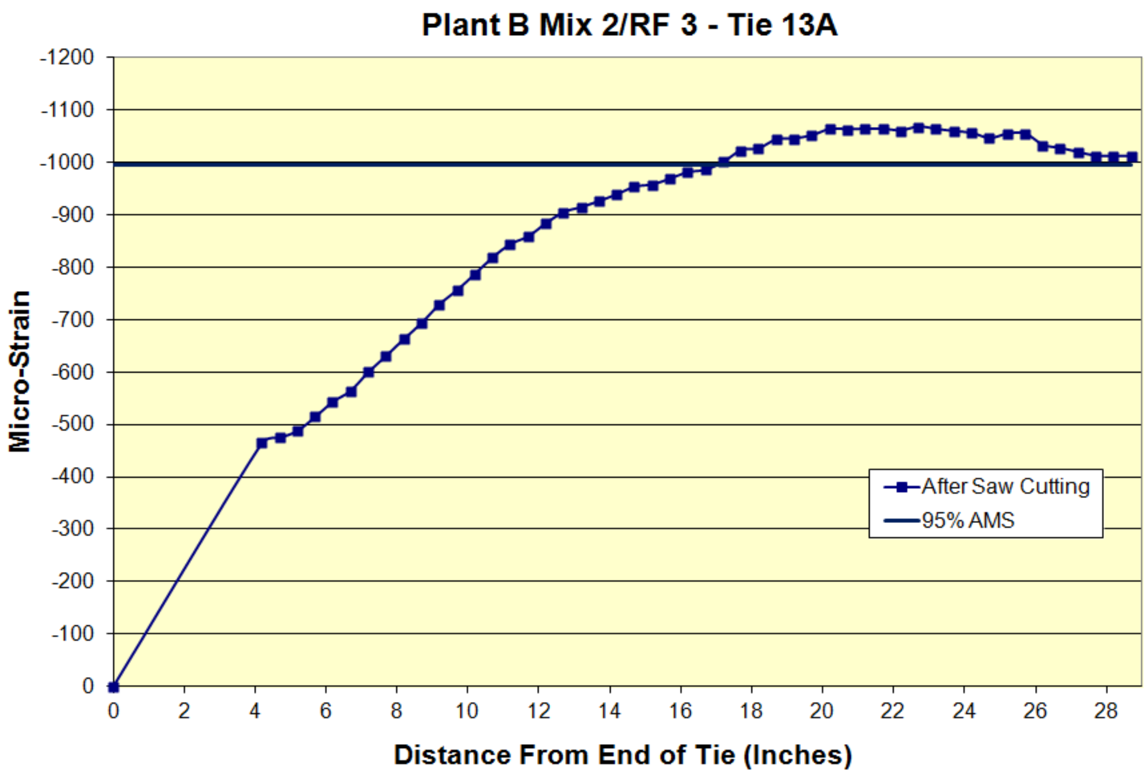

Figure B.14 Transfer length of Plant B Mix 2/RF 3 Tie 13A

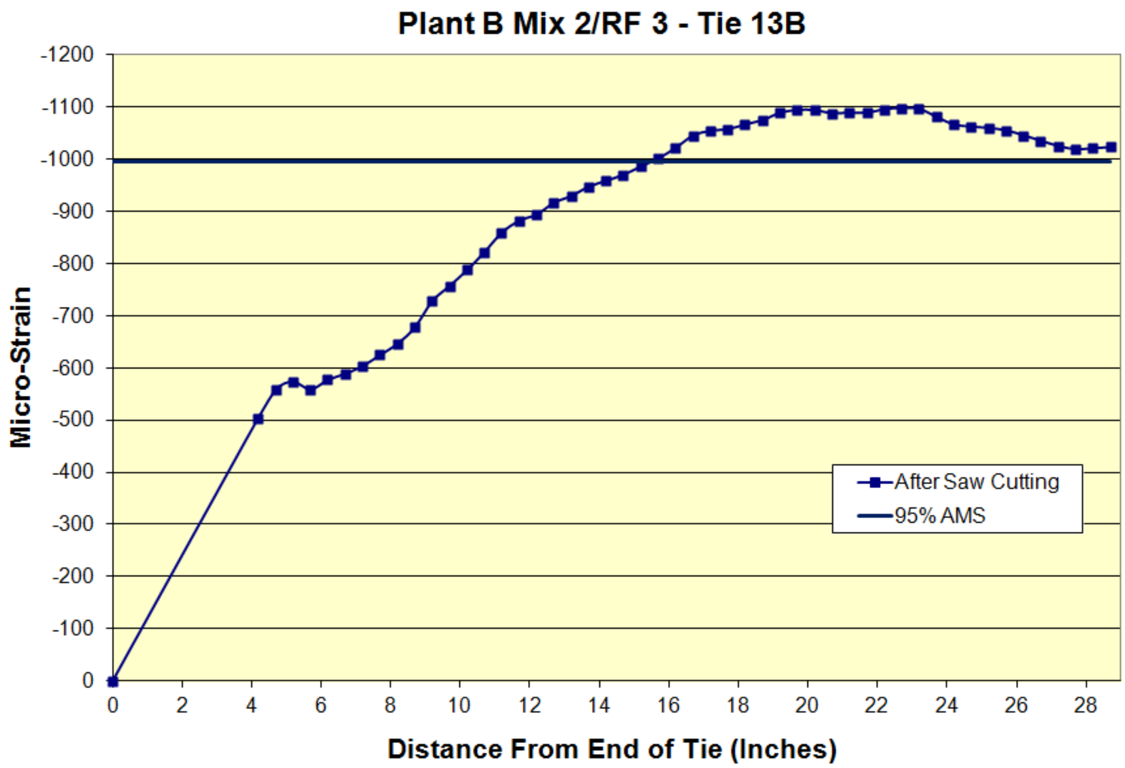

Figure B.15 Transfer length of Plant B Mix 2/RF 3 Tie 13B

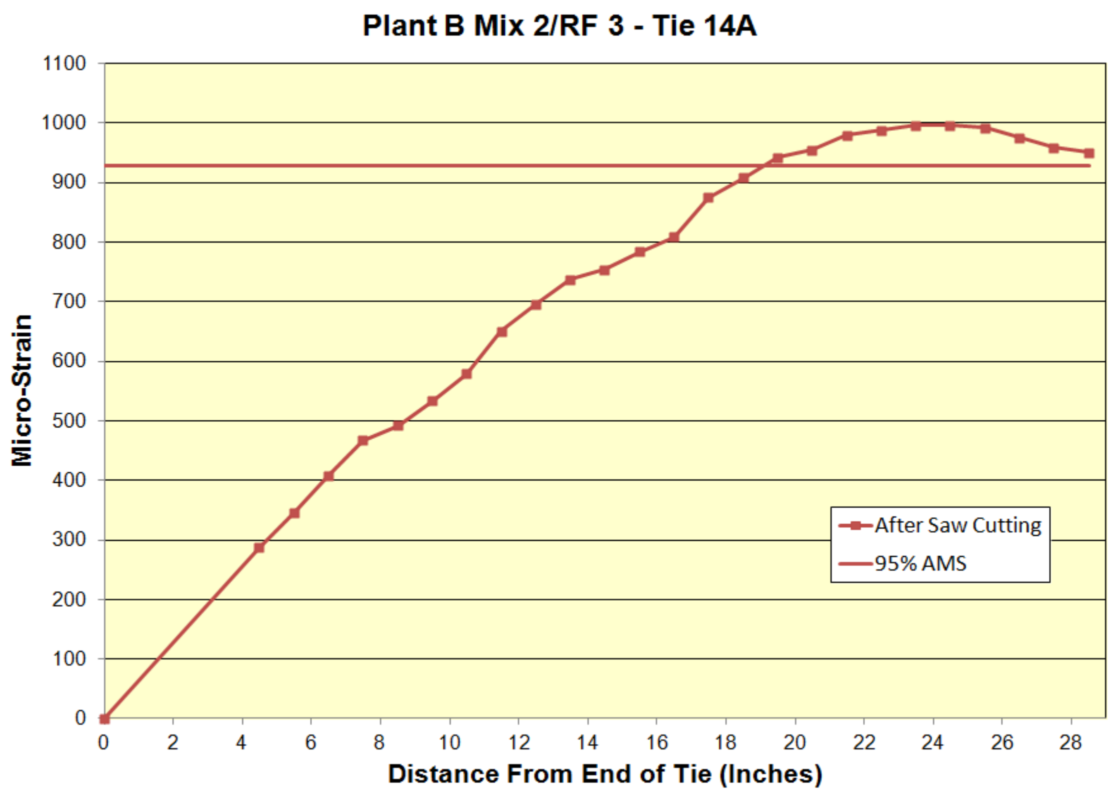

Figure B.16 Transfer length of Plant B Mix 2/RF 3 Tie 14A

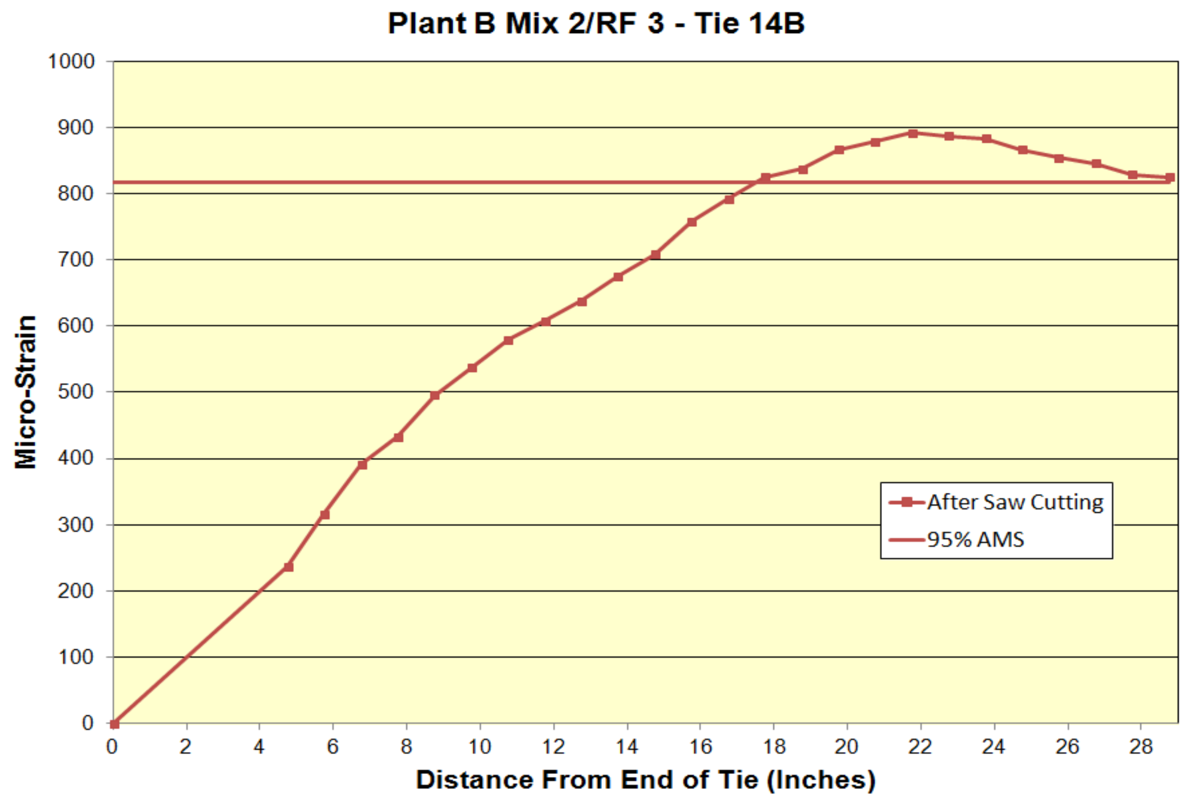

Figure B.17 Transfer length of Plant B Mix 2/RF 3 Tie 14B

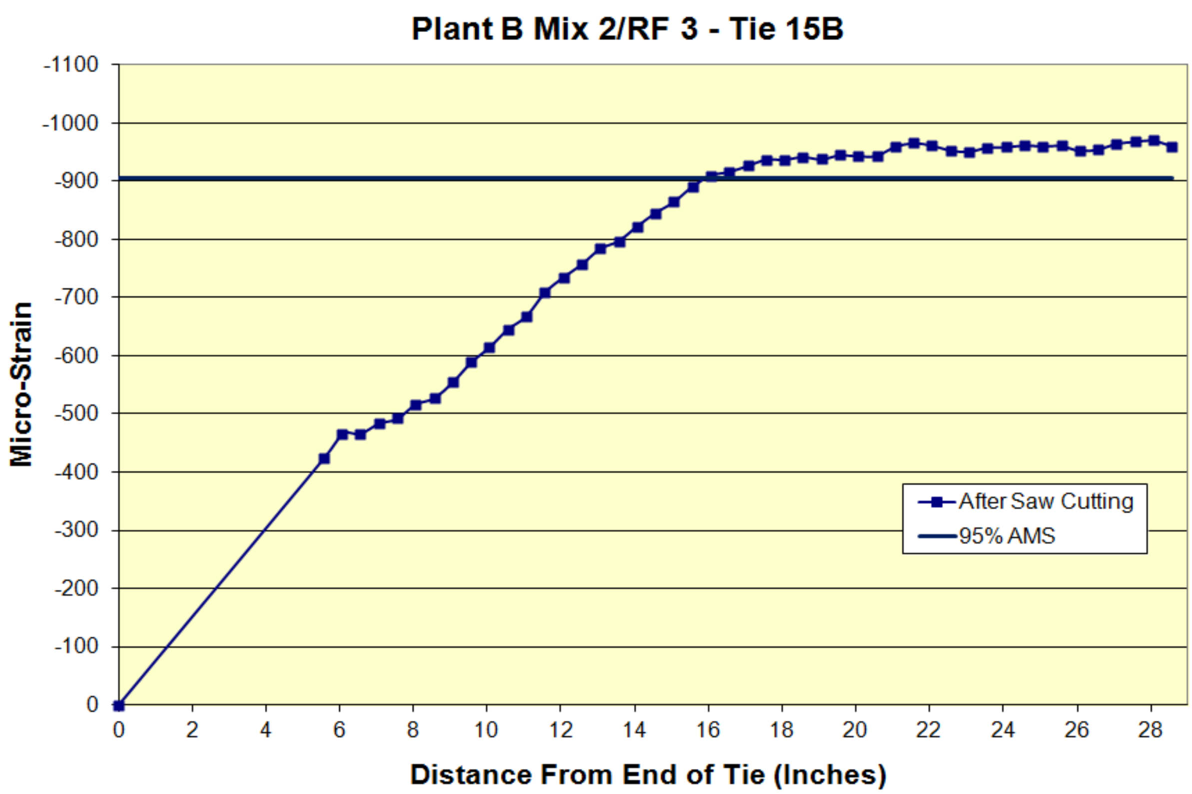

Figure B.18 Transfer length of Plant B Mix 2/RF 3 Tie 15B

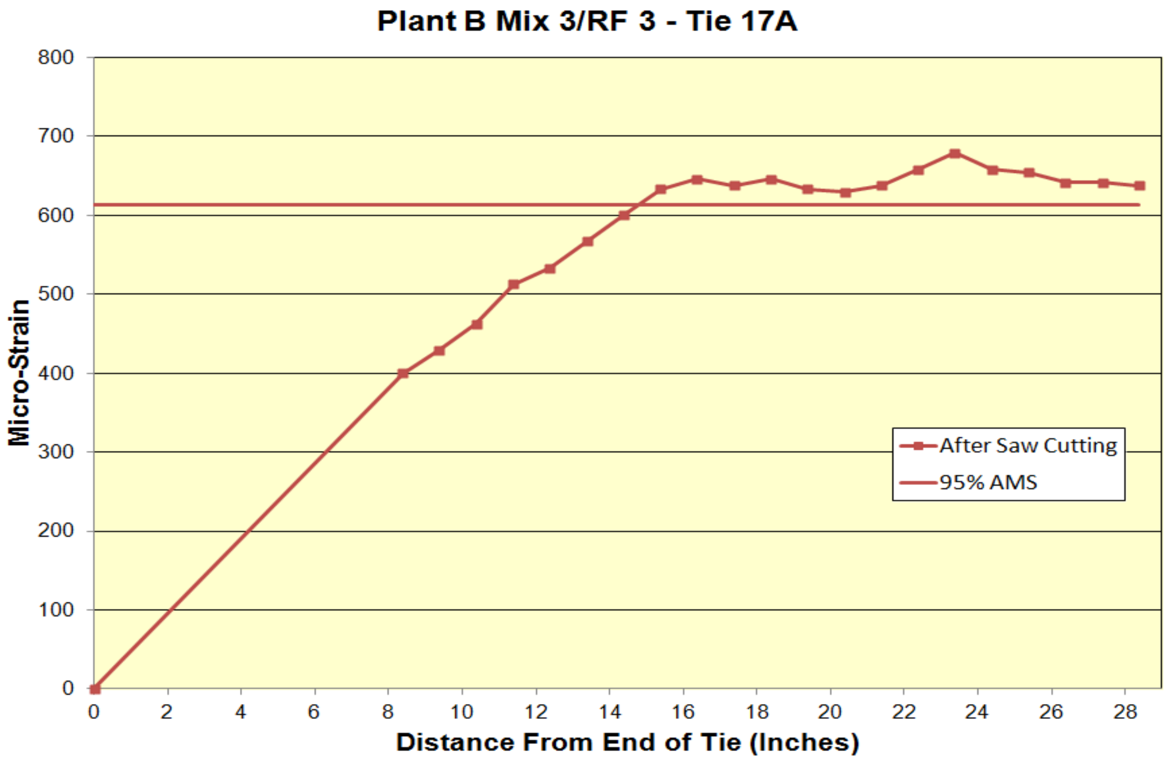

Figure B.19 Transfer length of Plant B Mix 3/RF 3 Tie 17A

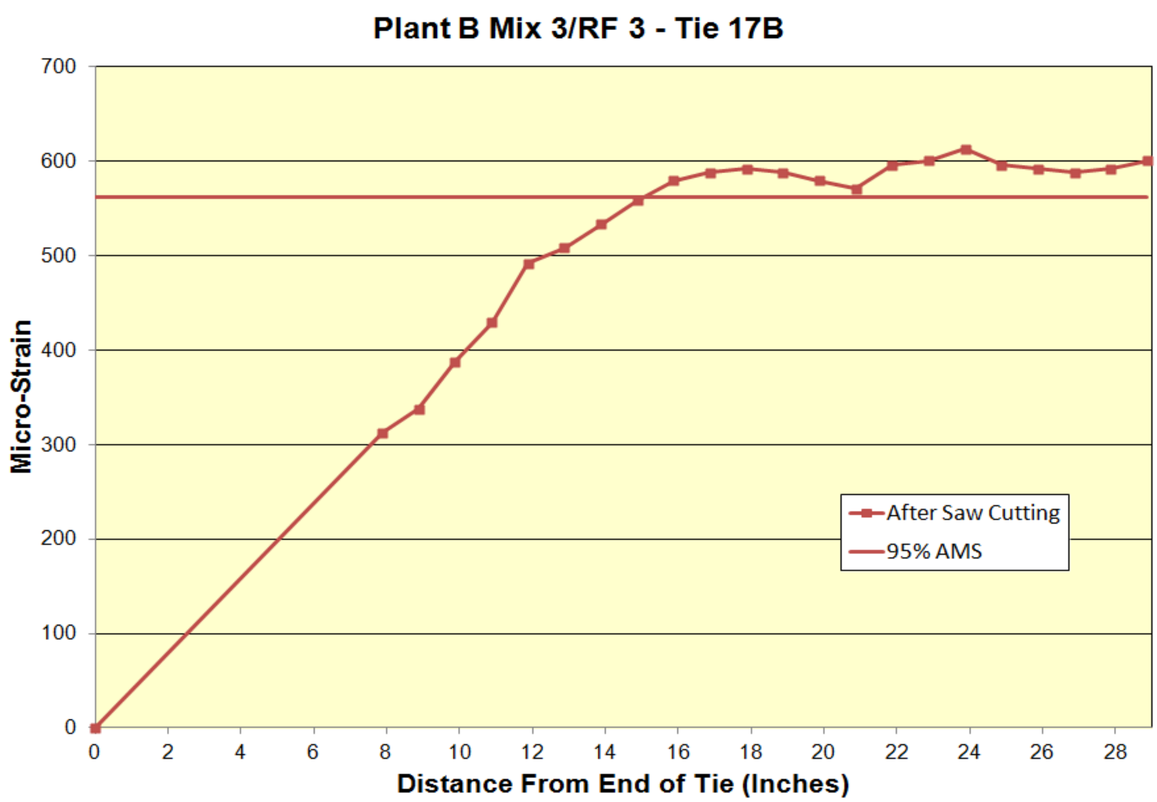

Figure B.20 Transfer length of Plant B Mix 3/RF 3 Tie 17B

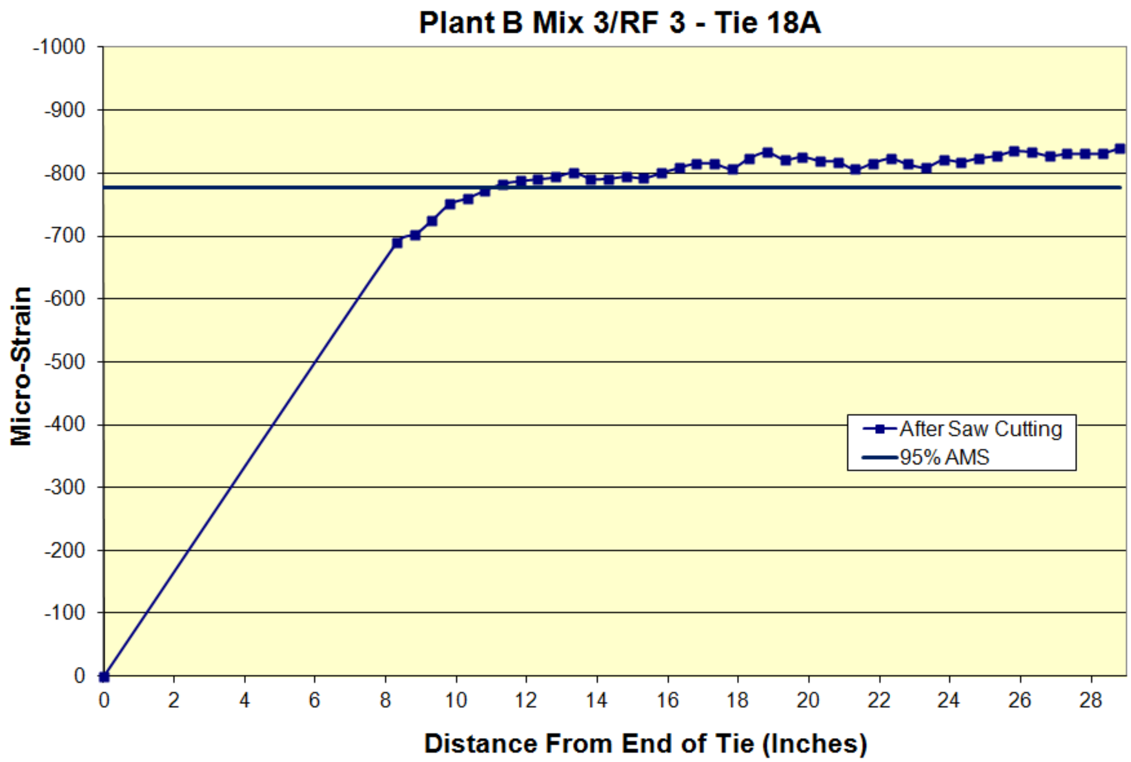

Figure B.21 Transfer length of Plant B Mix 3/RF 3 Tie 18A

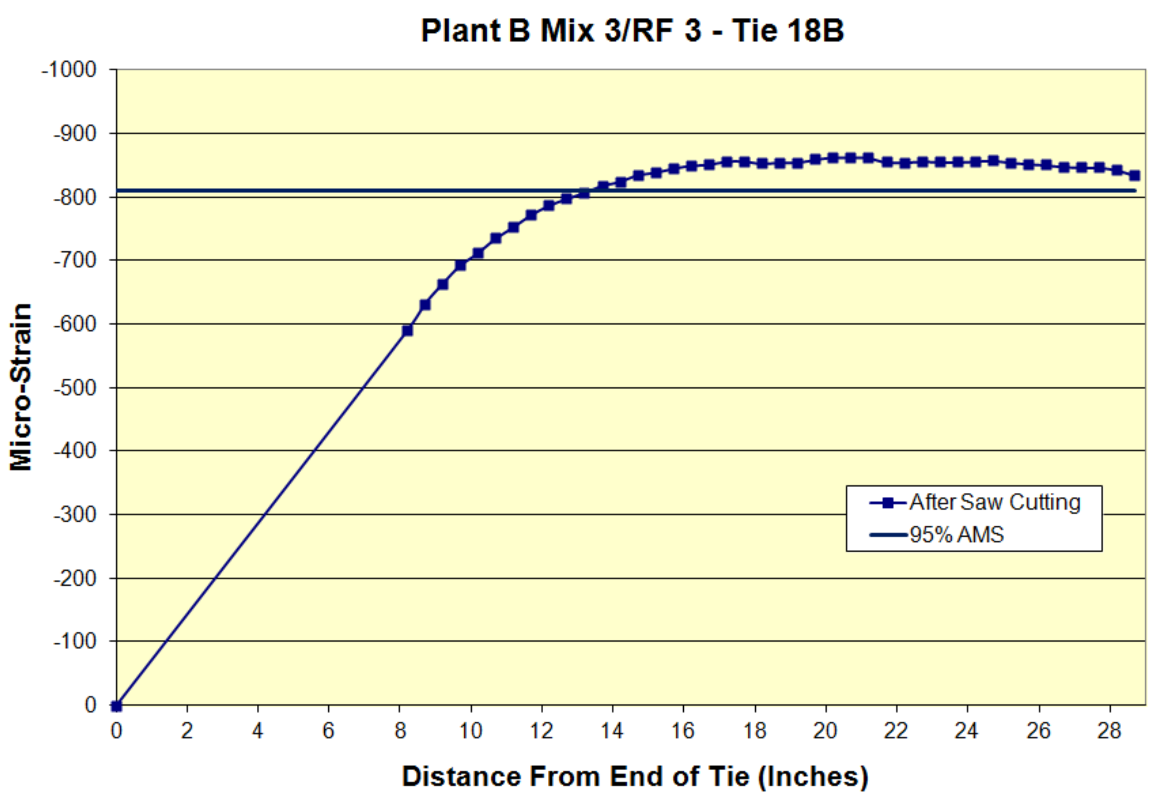

Figure B.22 Transfer length of Plant B Mix 3/RF 3 Tie 18B

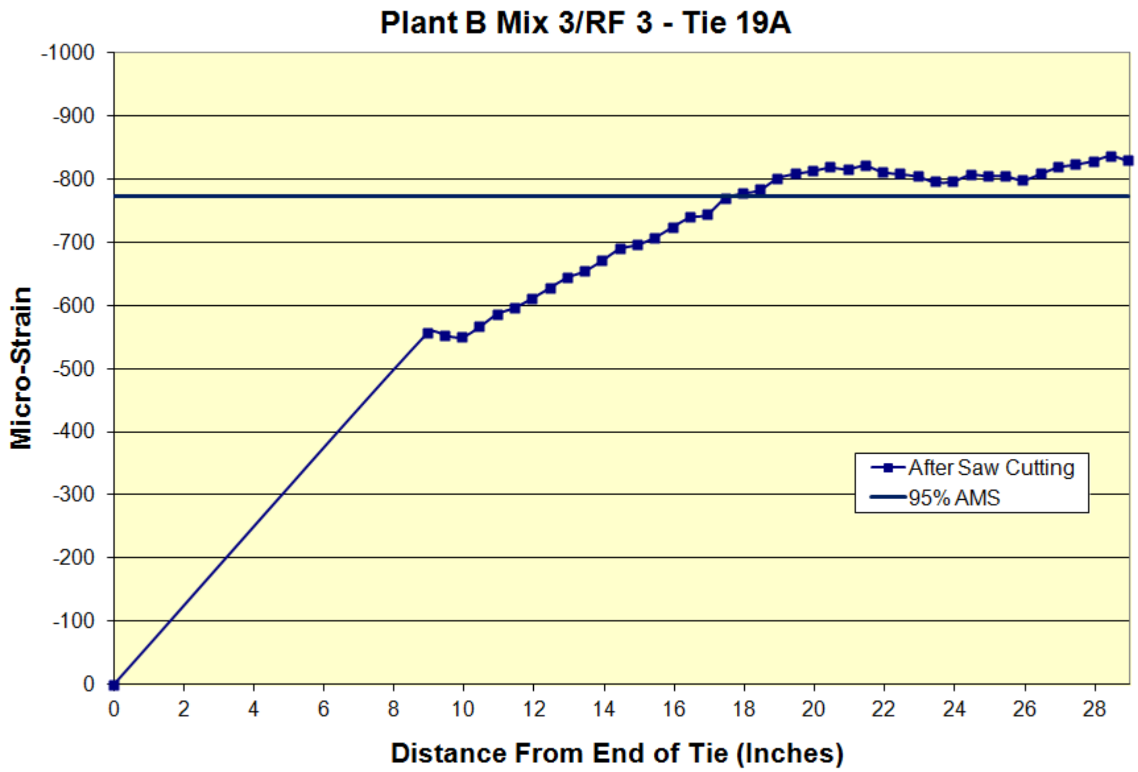

Figure B.23 Transfer length of Plant B Mix 3/RF 3 Tie 19A

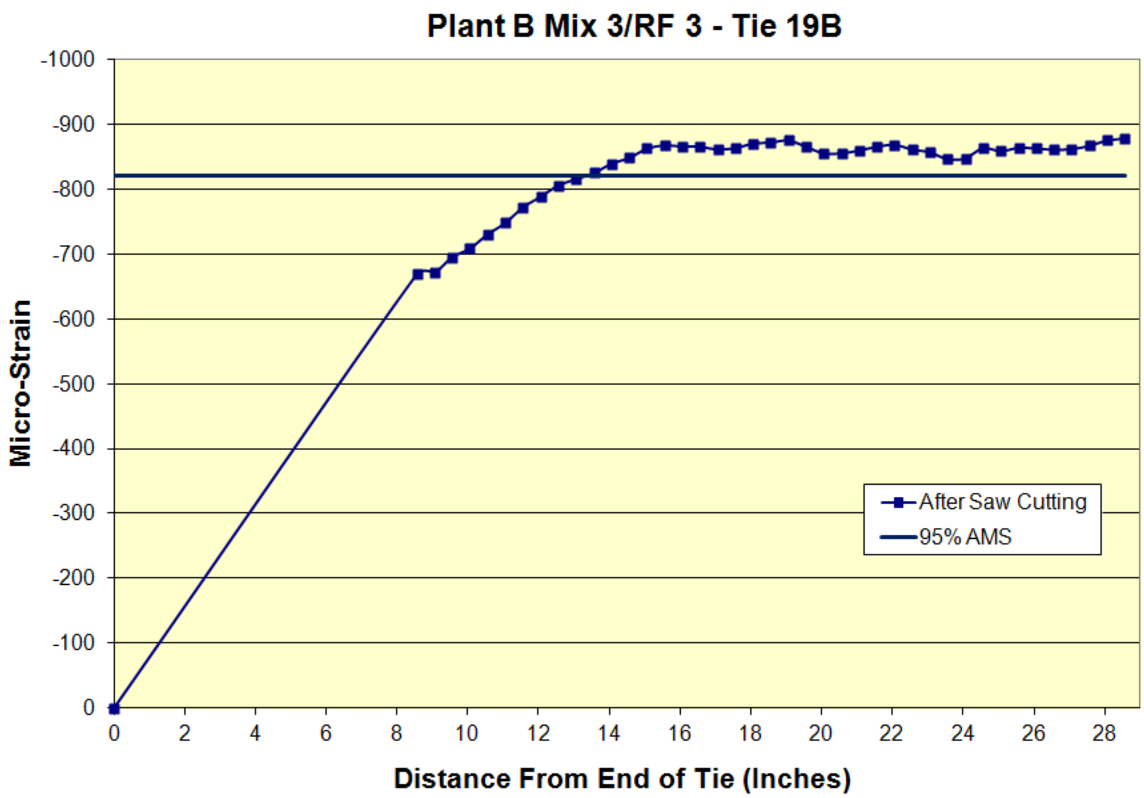

Figure B.24 Transfer length of Plant B Mix 3/RF 3 Tie 19B

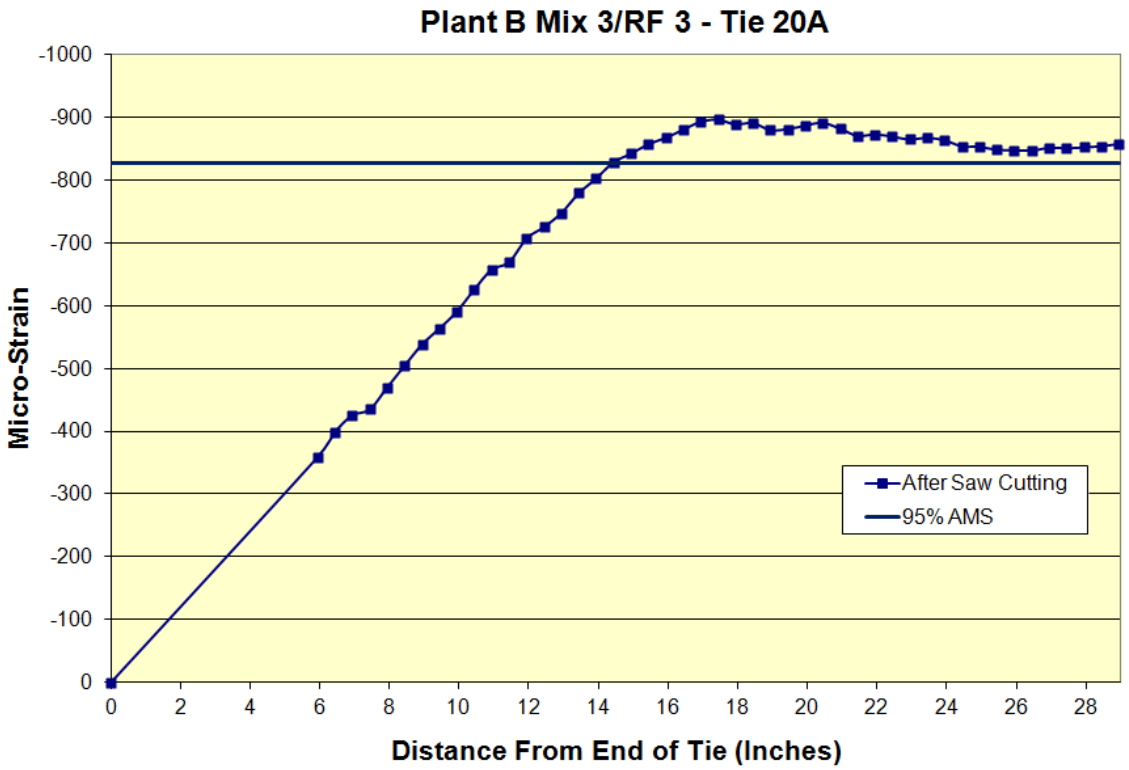

Figure B.25 Transfer length of Plant B Mix 3/RF 3 Tie 20A

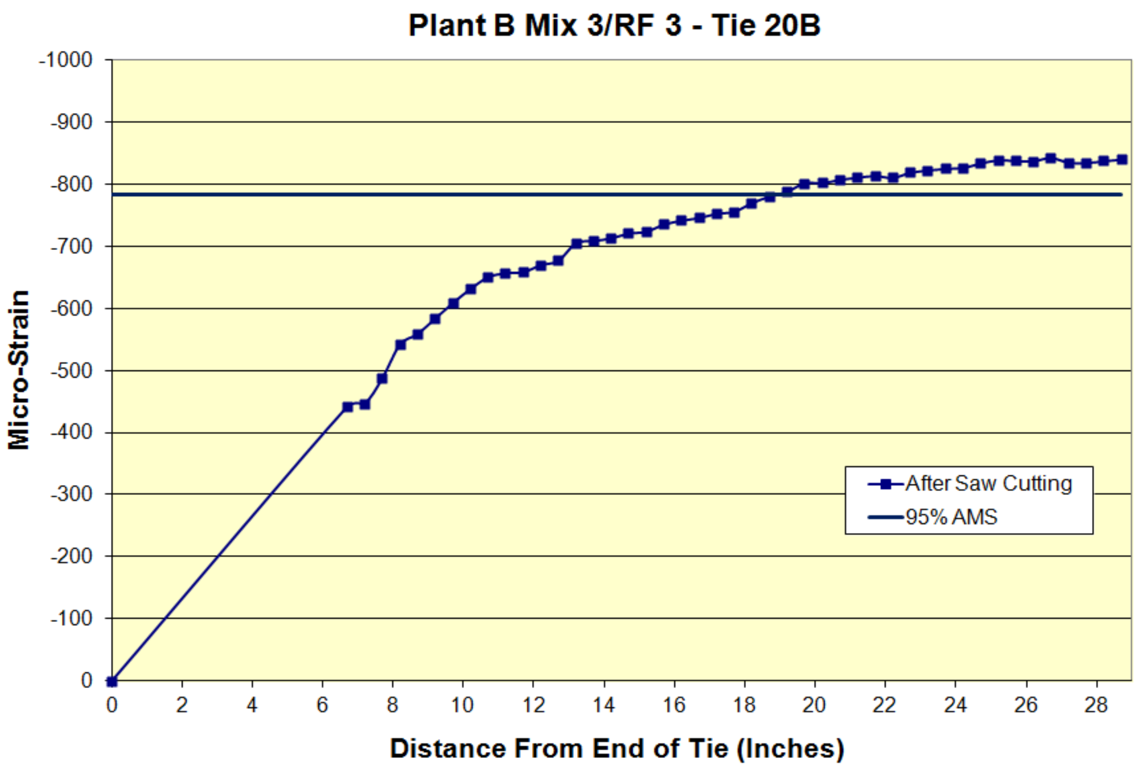

Figure B.26 Transfer length of Plant B Mix 3/RF 3 Tie 20B

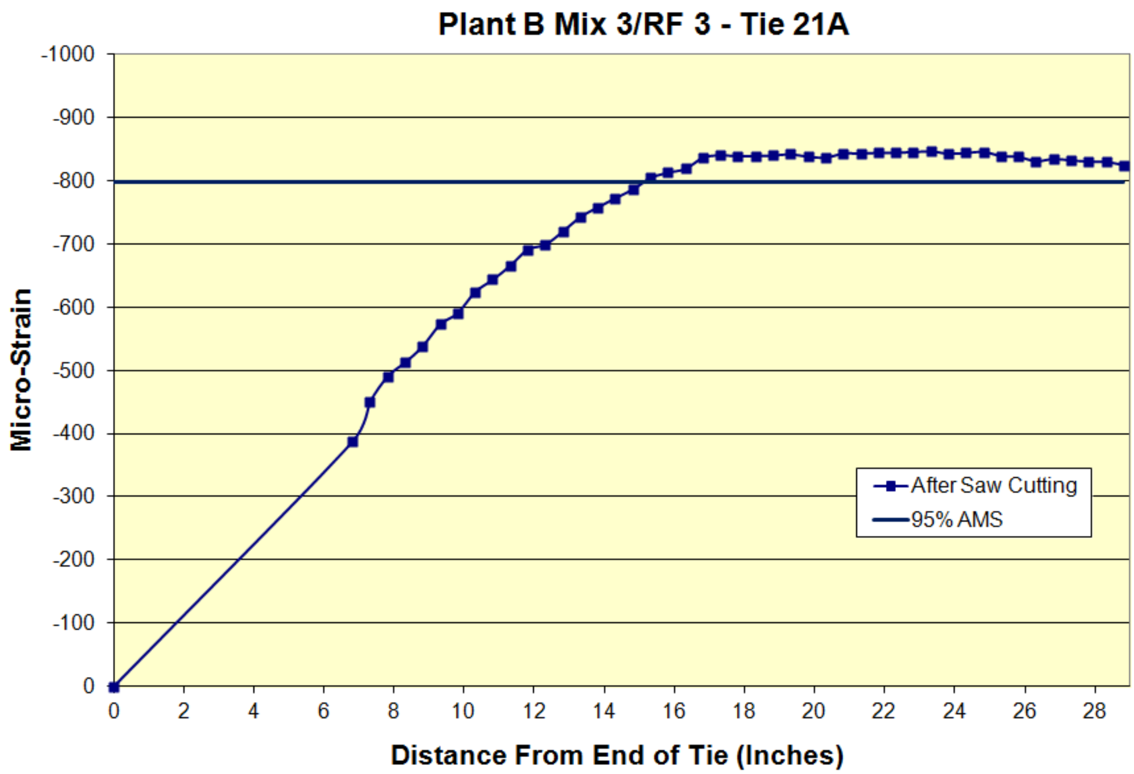

Figure B.27 Transfer length of Plant B Mix 3/RF 3 Tie 21A

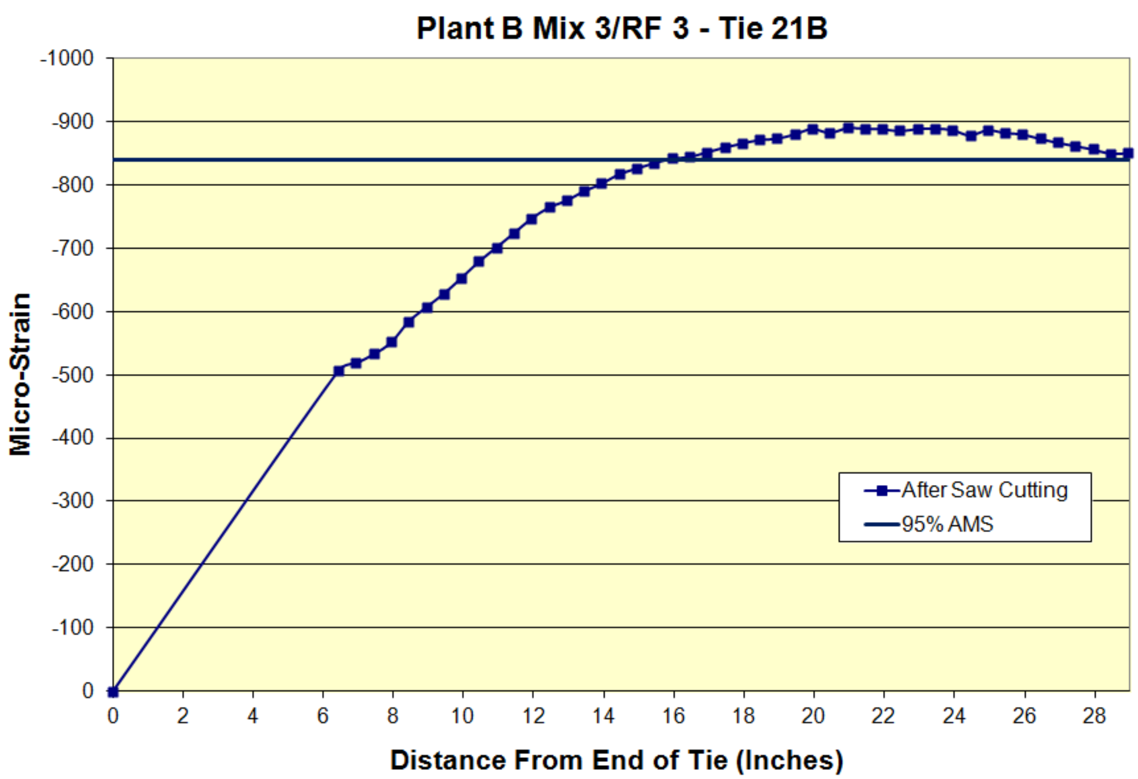

Figure B.28 Transfer length of Plant B Mix 3/RF 3 Tie 21B

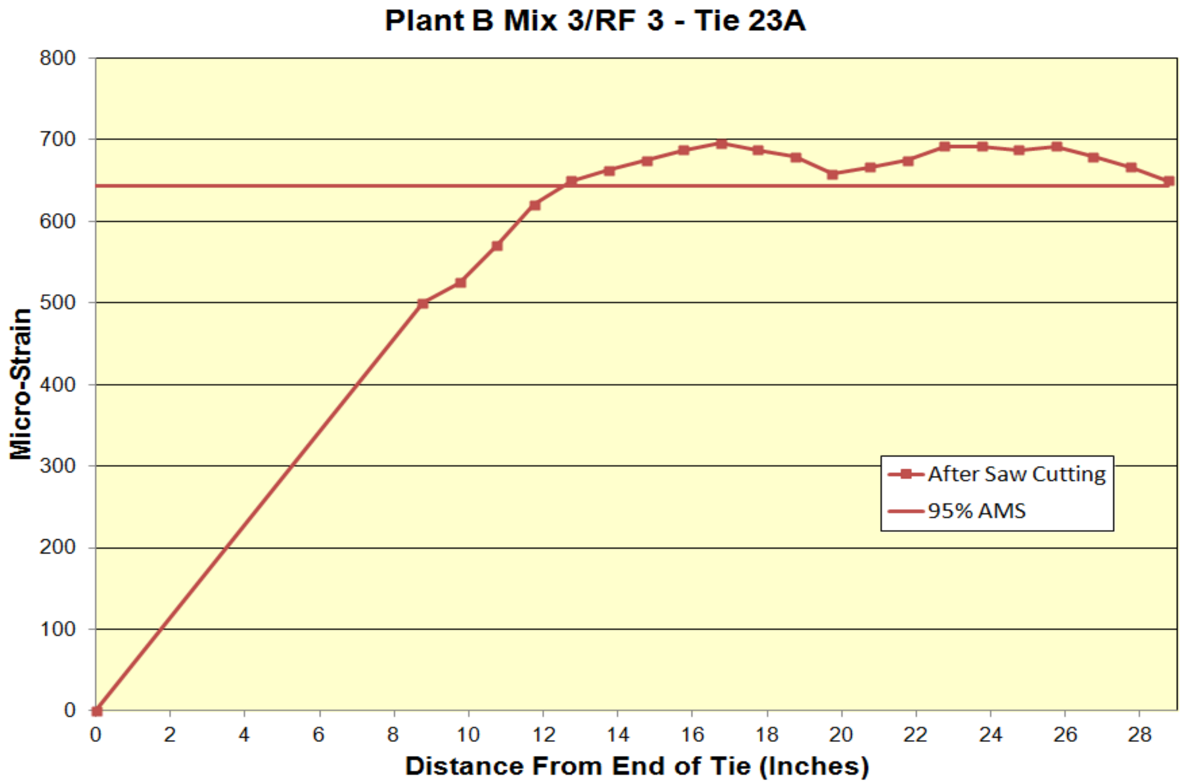

Figure B.29 Transfer length of Plant B Mix 3/RF 3 Tie 23A

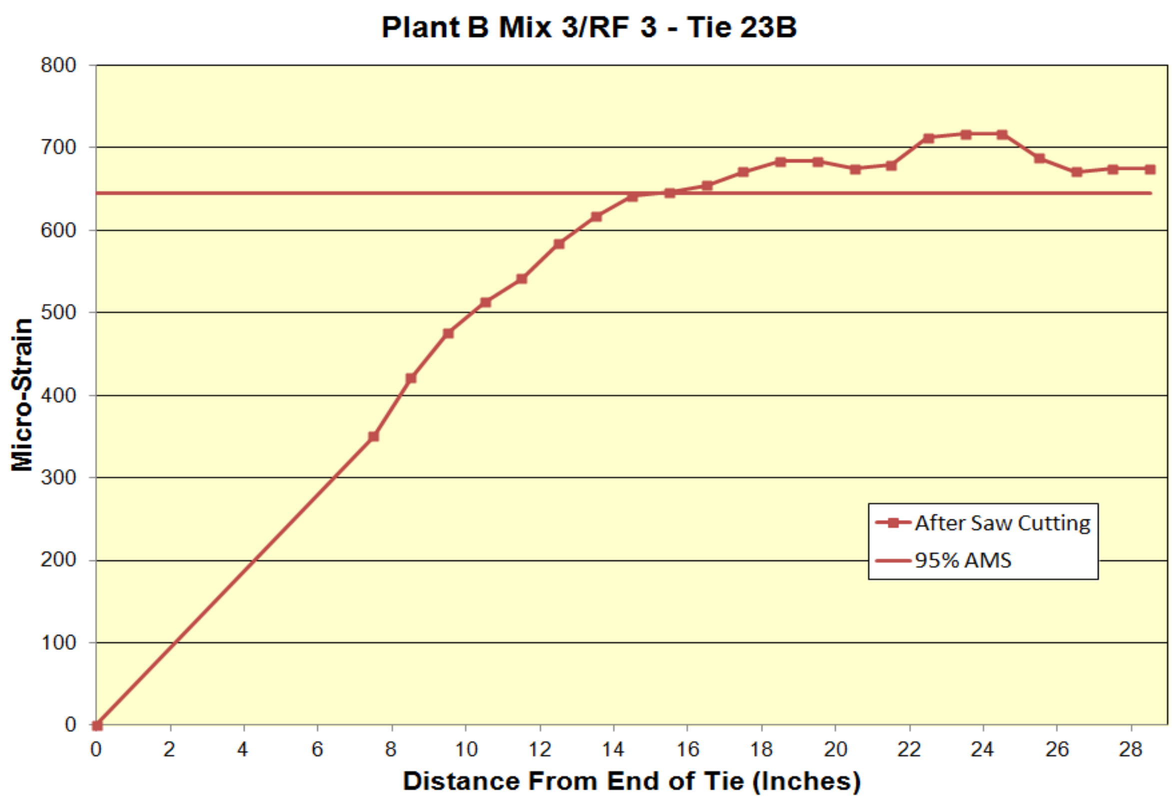

Figure B.30 Transfer length of Plant B Mix 3/RF 3 Tie 23B

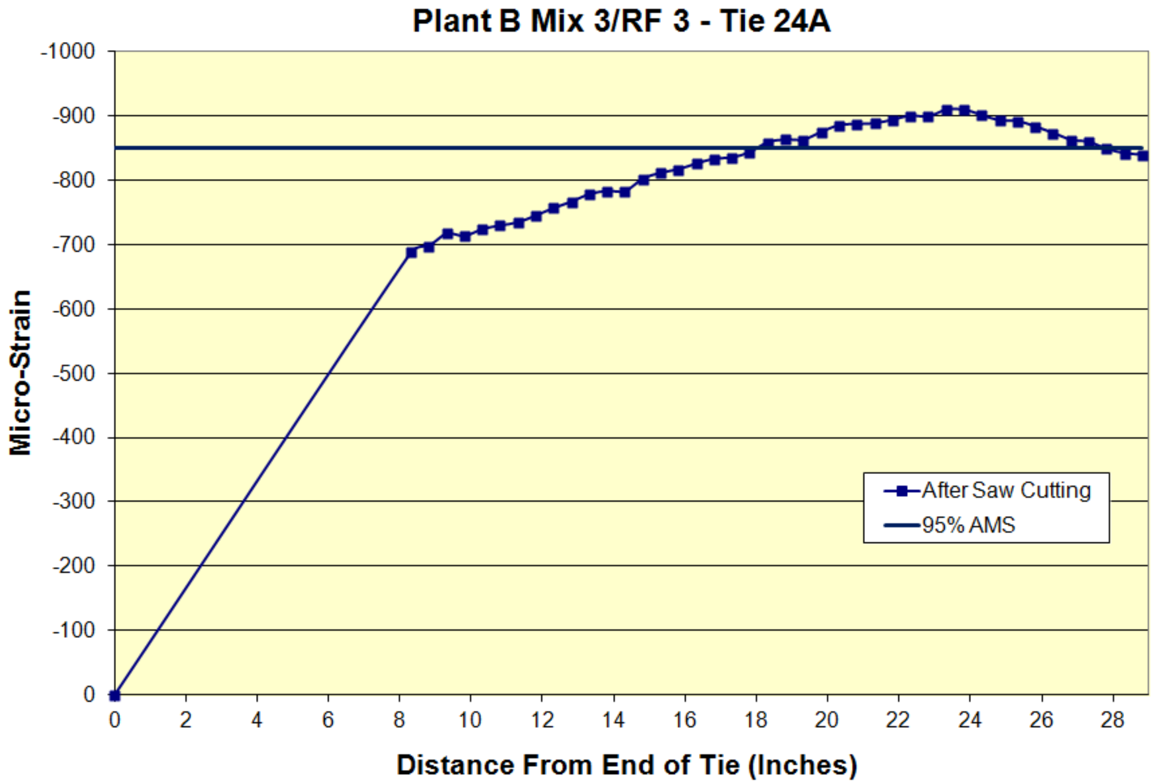

Figure B.31 Transfer length of Plant B Mix 3/RF 3 Tie 24A

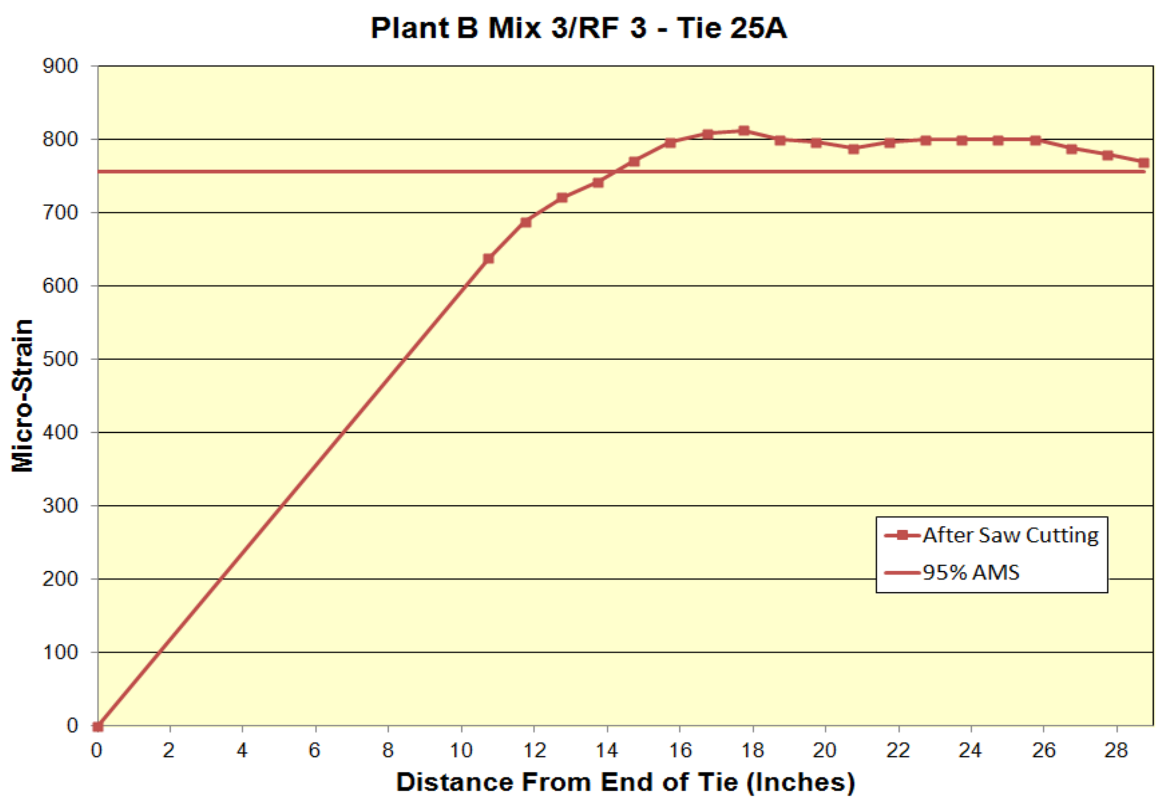

Figure B.32 Transfer length of Plant B Mix 3/RF 3 Tie 25A

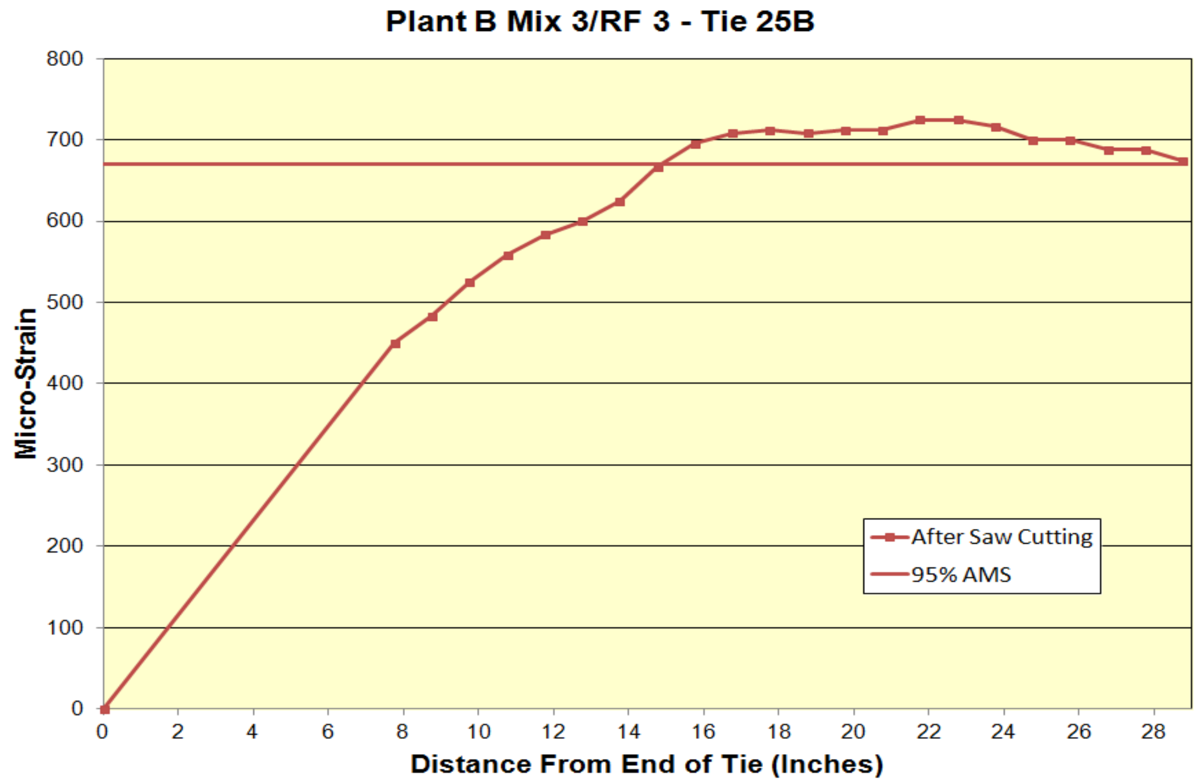

Figure B.33 Transfer length of Plant B Mix 3/RF 3 Tie 25B

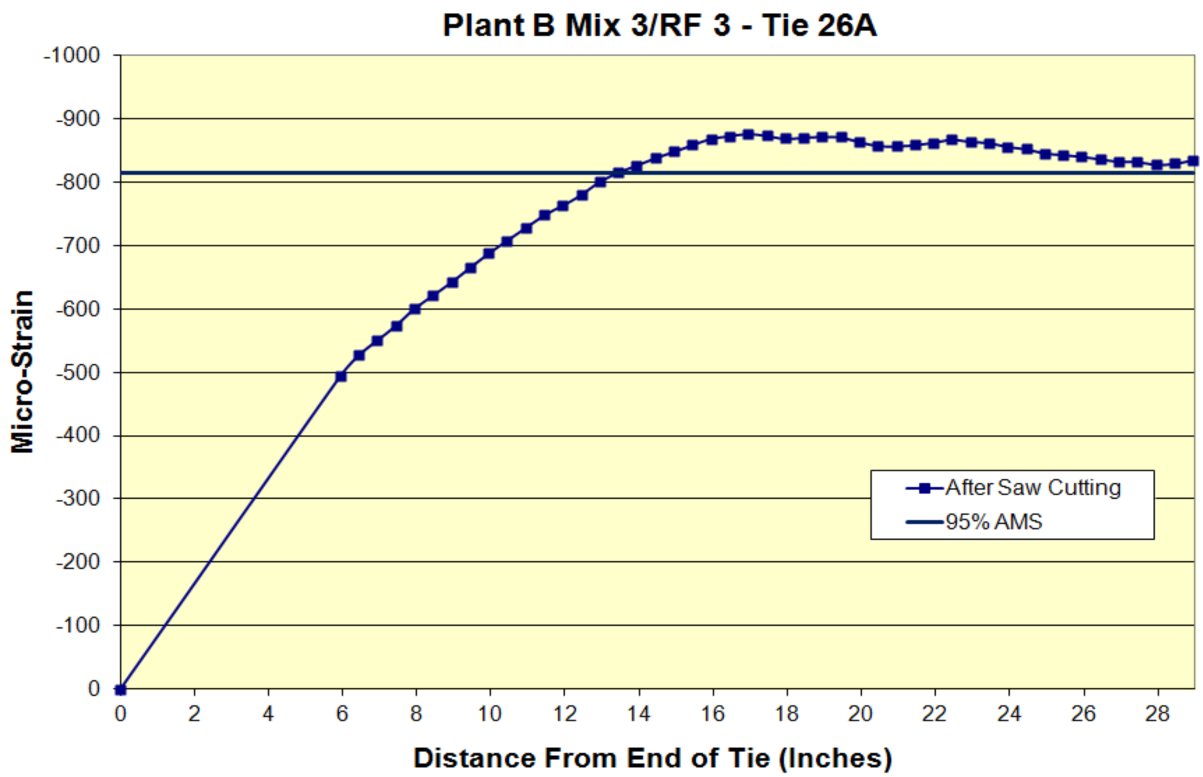

Figure B.34 Transfer length of Plant B Mix 3/RF 3 Tie 26A

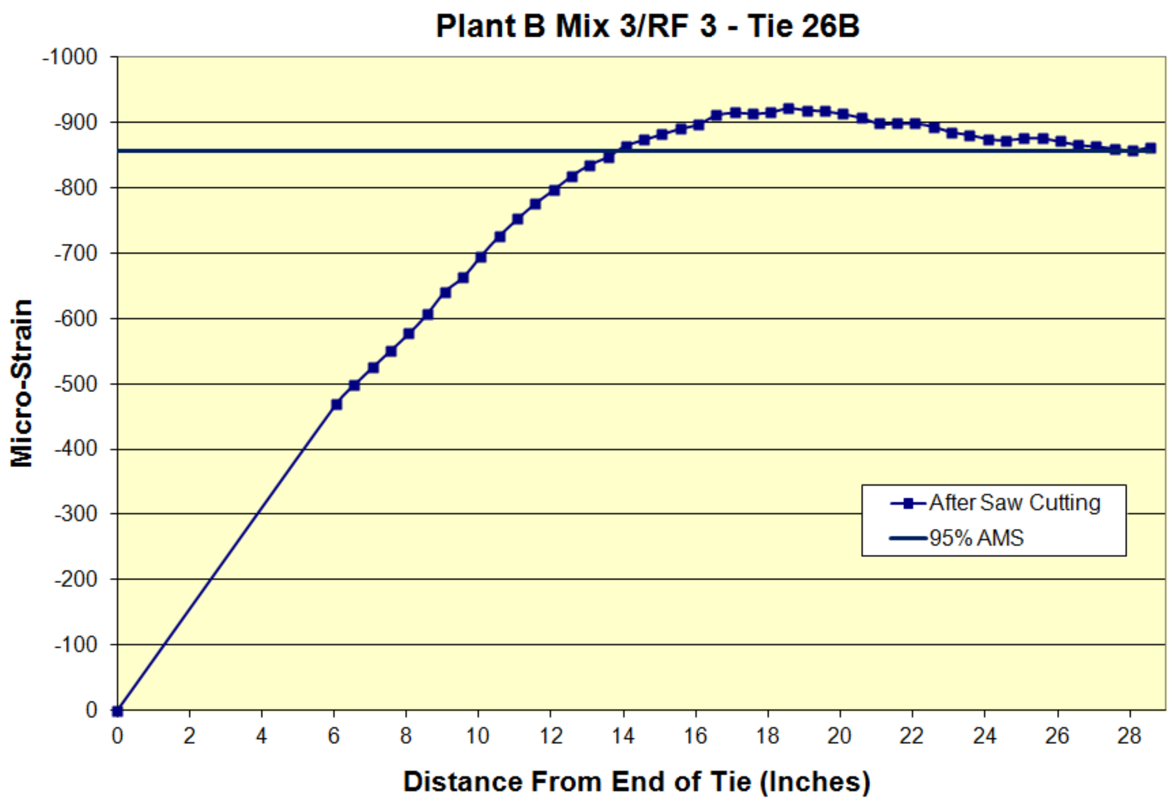

Figure B.35 Transfer length of Plant B Mix 3/RF 3 Tie 26B

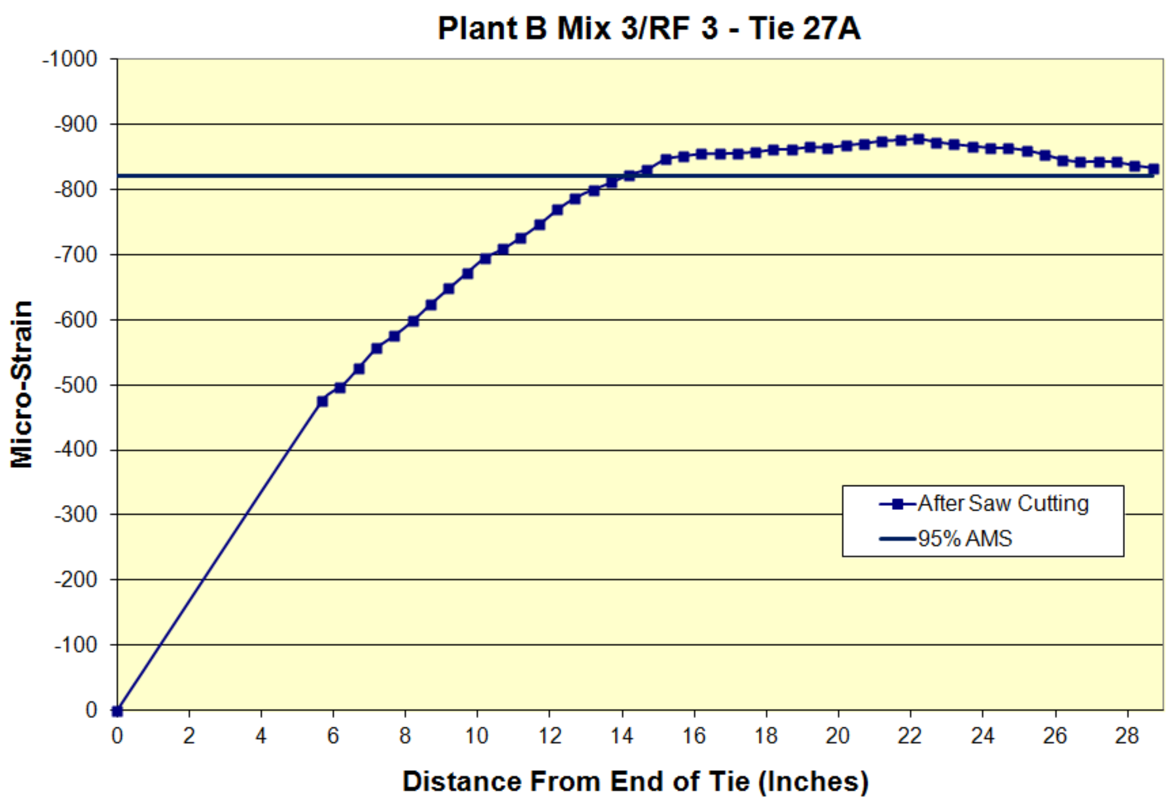

Figure B.36 Transfer length of Plant B Mix 3/RF 3 Tie 27A

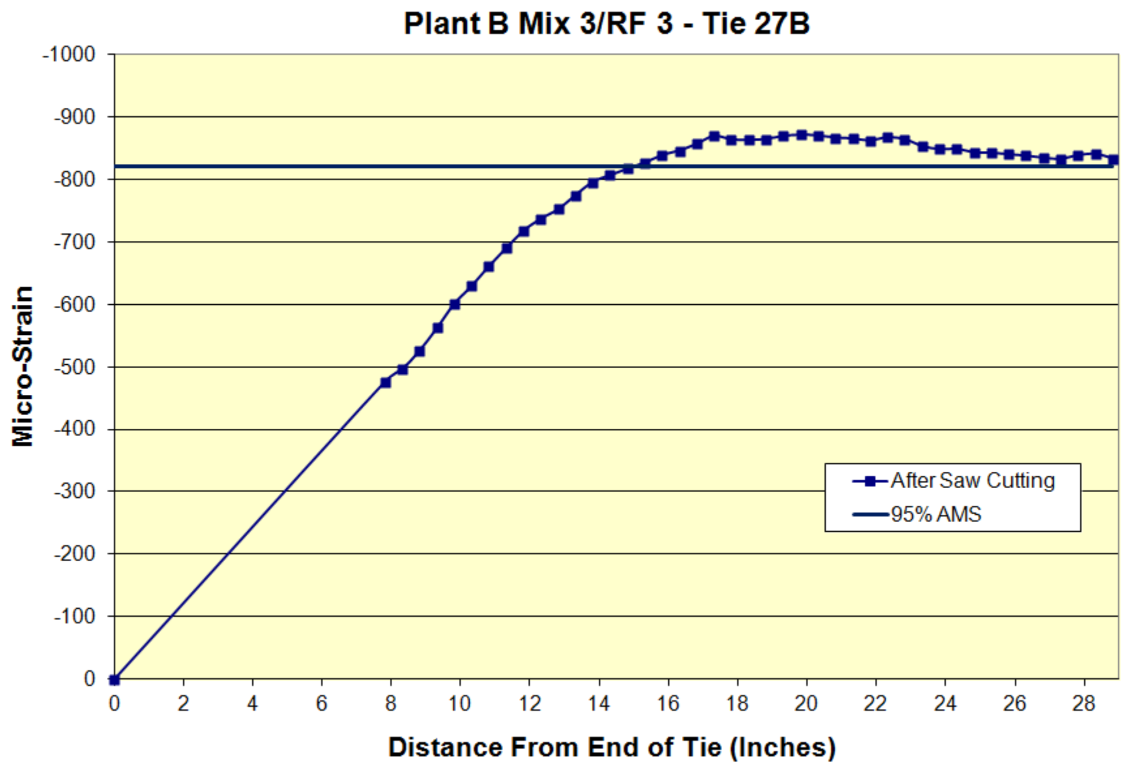

Figure B.37 Transfer length of Plant B Mix 3/RF 3 Tie 27B

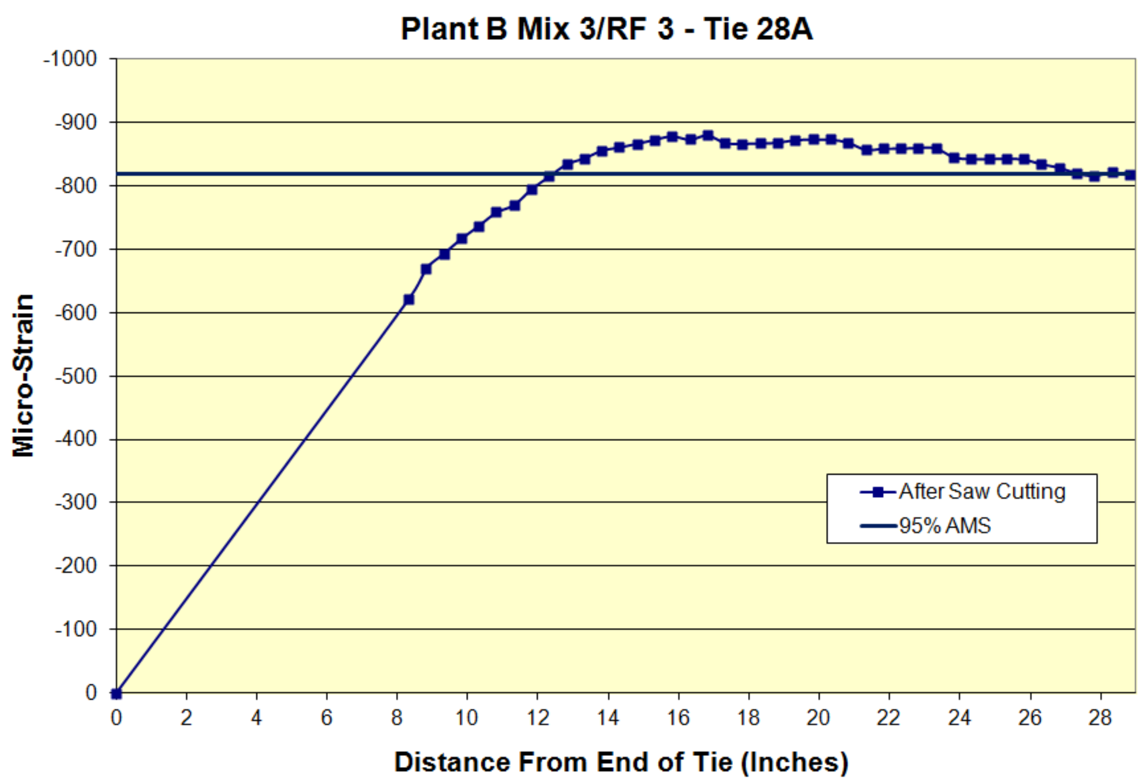

Figure B.38 Transfer length of Plant B Mix 3/RF 3 Tie 28A

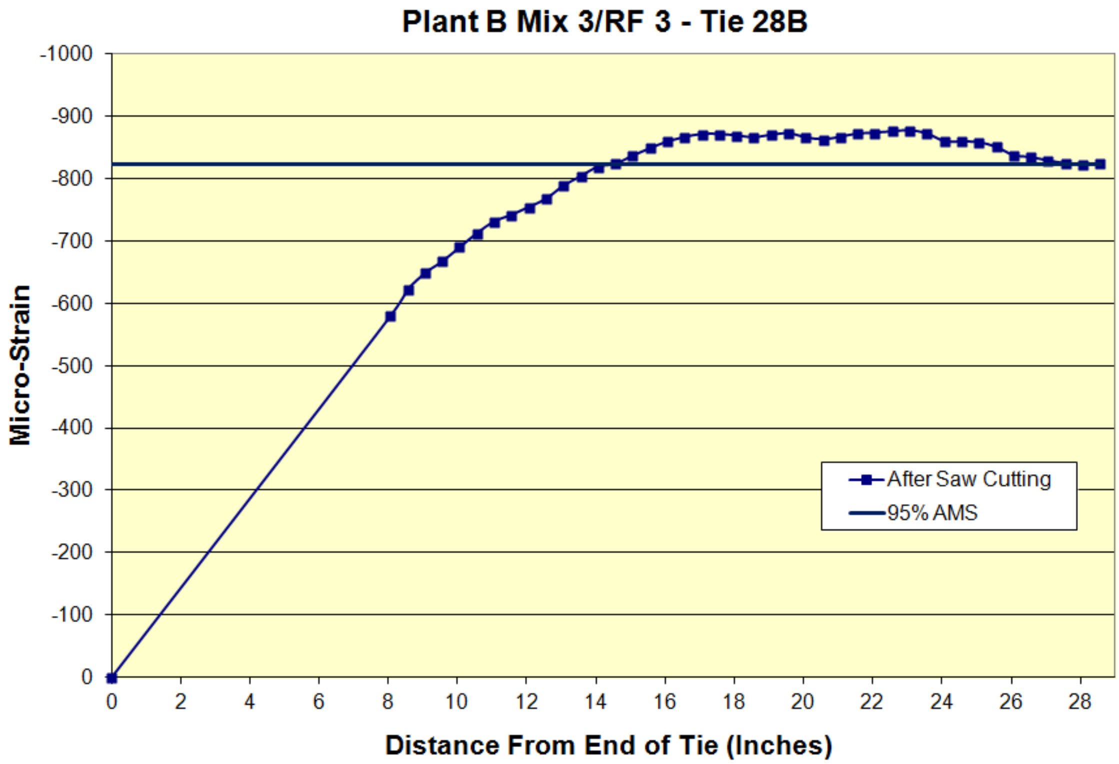

Figure B.39 Transfer length of Plant B Mix 3/RF 3 Tie 28B

B.2 Long-term Transfer Lengths

Table B.2 Long-term transfer length data for Plant B Mix 2/RF 3

Plant B Mix 2/RF 3					
	Transfer Length (in.)				
Time of Reading	Tie 4A	Tie 9A	Tie 9B	Tie 14A	Tie 14B
After Saw Cutting	20.4	18.3	20.5	18.8	17.5
15 Days After Pour	21.1	18.4	20.5	18.9	18.9
30 Days After Pour	21.3	18.5	20.6	19.1	18.9
90 Days After Pour	21.6	19.1	20.5	18.9	18.4

Table B.3 Long-term transfer length data for Plant B Mix 3/RF 3

Plant B Mix 3/RF 3						
	Transfer Length (in.)					
Time of Reading	Tie 17A	Tie 17B	Tie 23A	Tie 23B	Tie 25A	Tie 25B
After Saw Cutting	14.8	14.9	12.6	14.4	14.3	14.5
15 Days After Pour	15.2	14.9	13	15.8	14.9	14.6
30 Days After Pour	15.9	14.7	12.8	15.7	14.8	14.7
90 Days After Pour	15.3	14.6	13.5	14.4	15	14.7

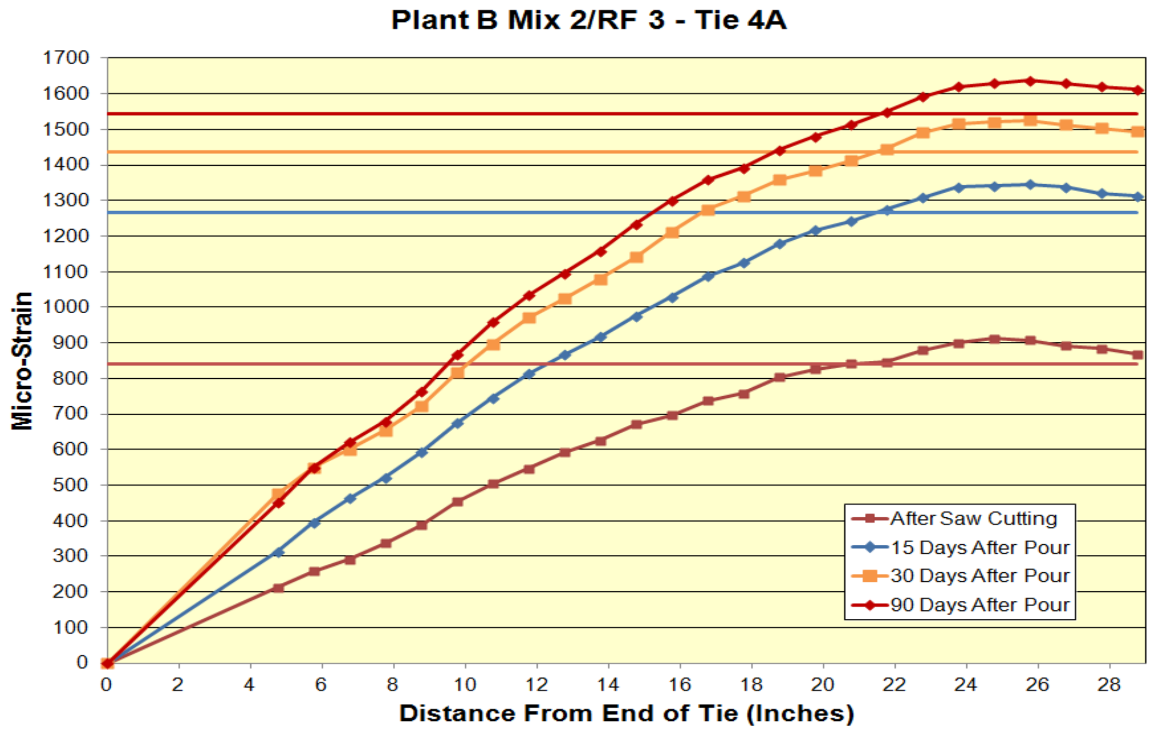

Figure B.40 Long-term transfer length of Plant B Mix 2/RF 3 Tie 4A

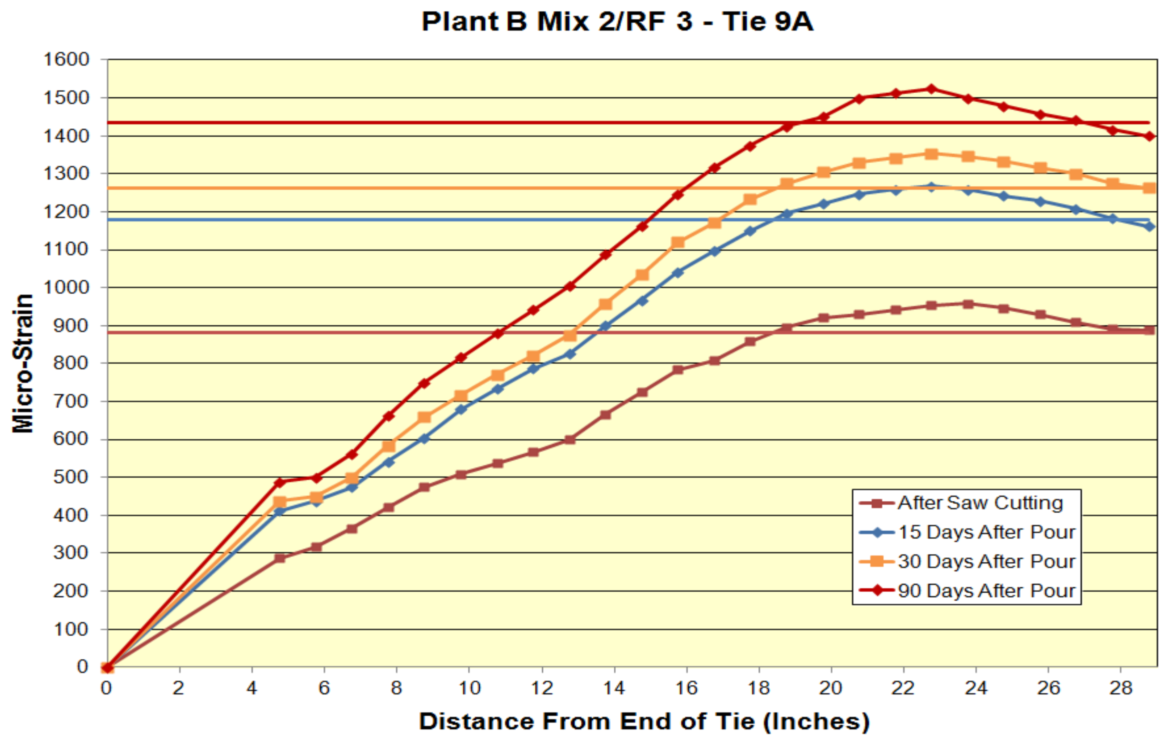

Figure B.41 Long-term transfer length of Plant B Mix 2/RF 3 Tie 9A

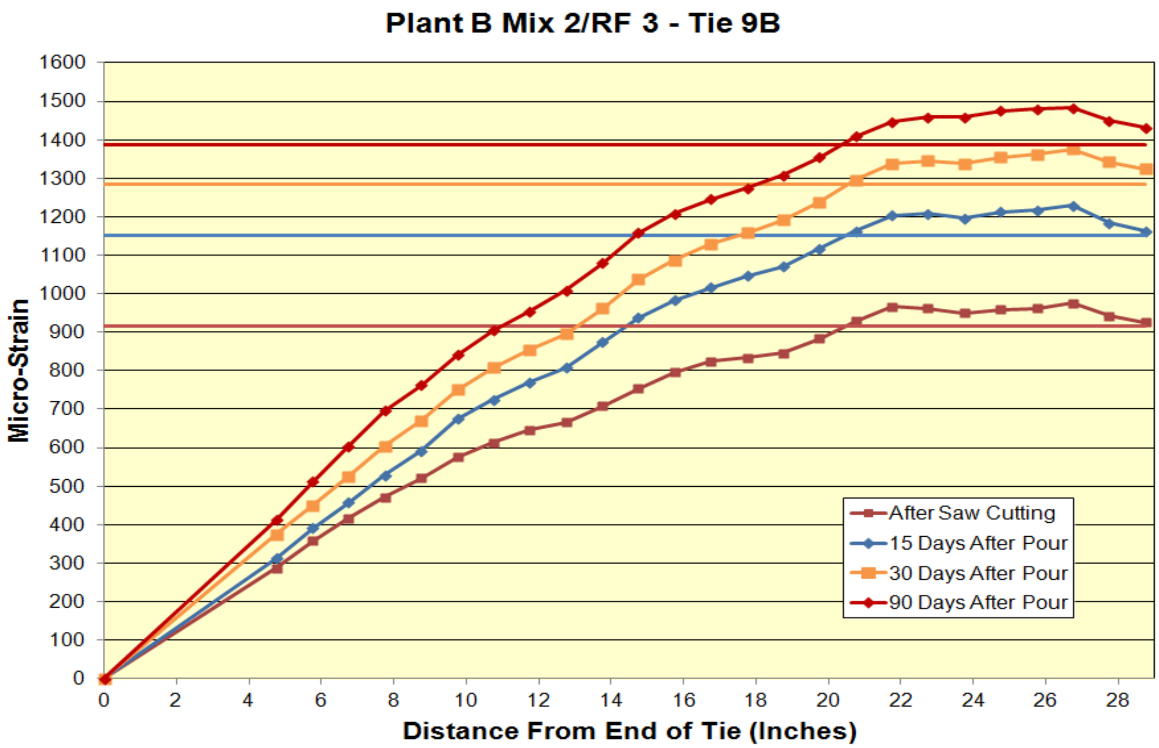

Figure B.42 Long-term transfer length of Plant B Mix 2/RF 3 Tie 9B

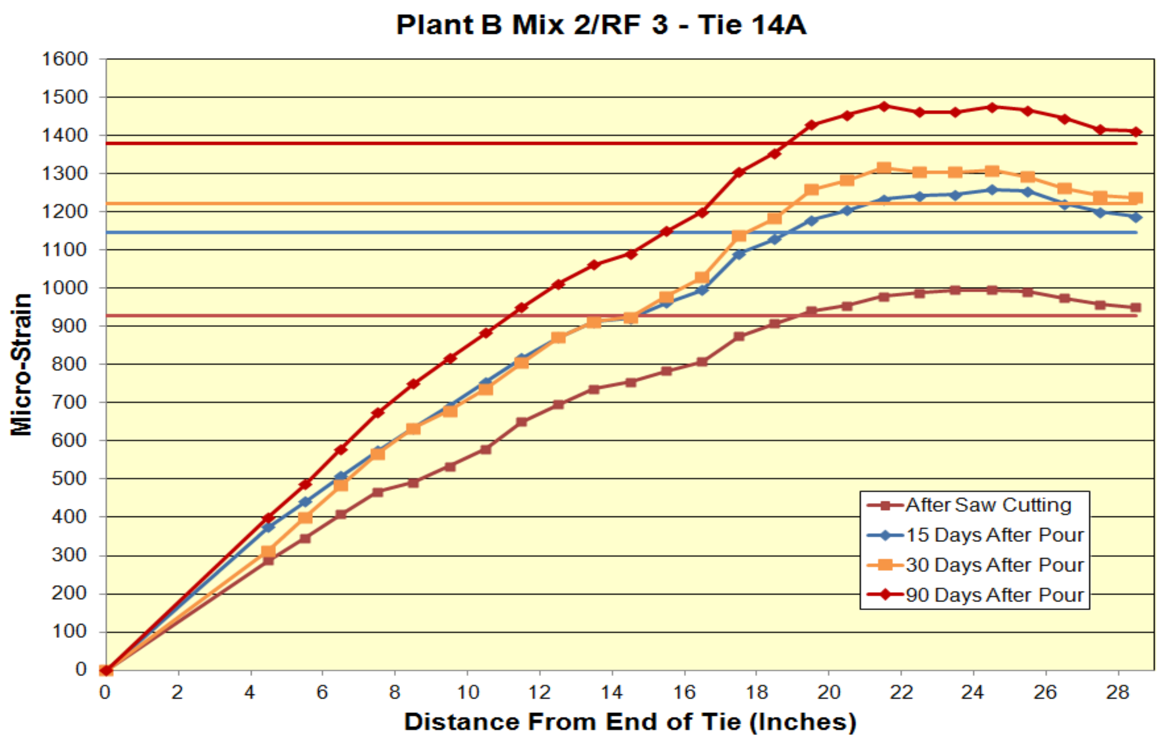

Figure B.43 Long-term transfer length of Plant B Mix 2/RF 3 Tie 14A

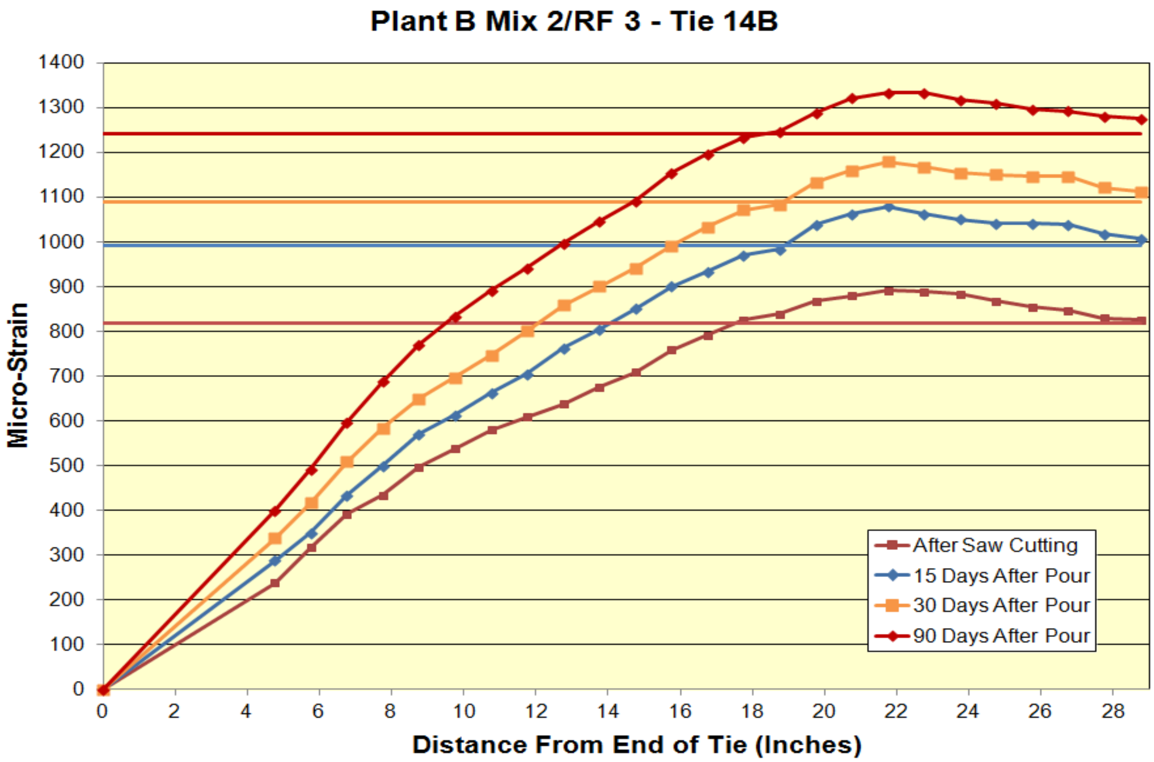

Figure B.44 Long-term transfer length of Plant B Mix 2/RF 3 Tie 14B

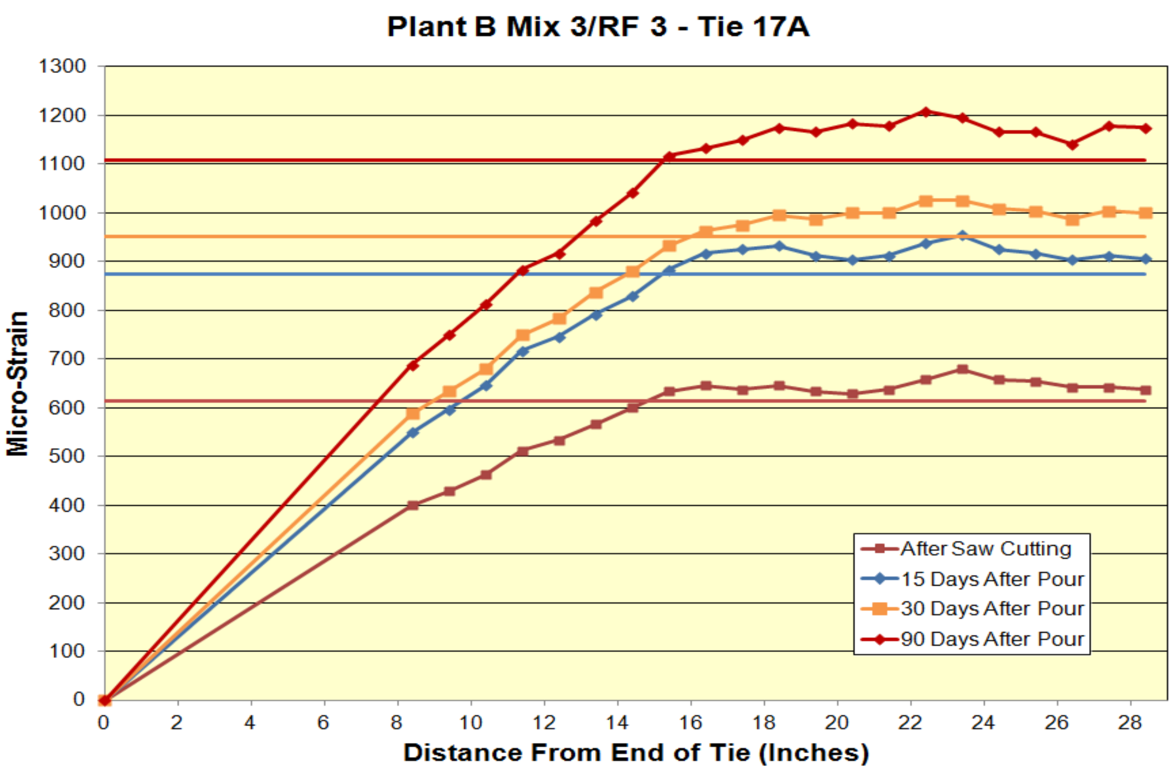

Figure B.45 Long-term transfer length of Plant B Mix 3/RF 3 Tie 17A

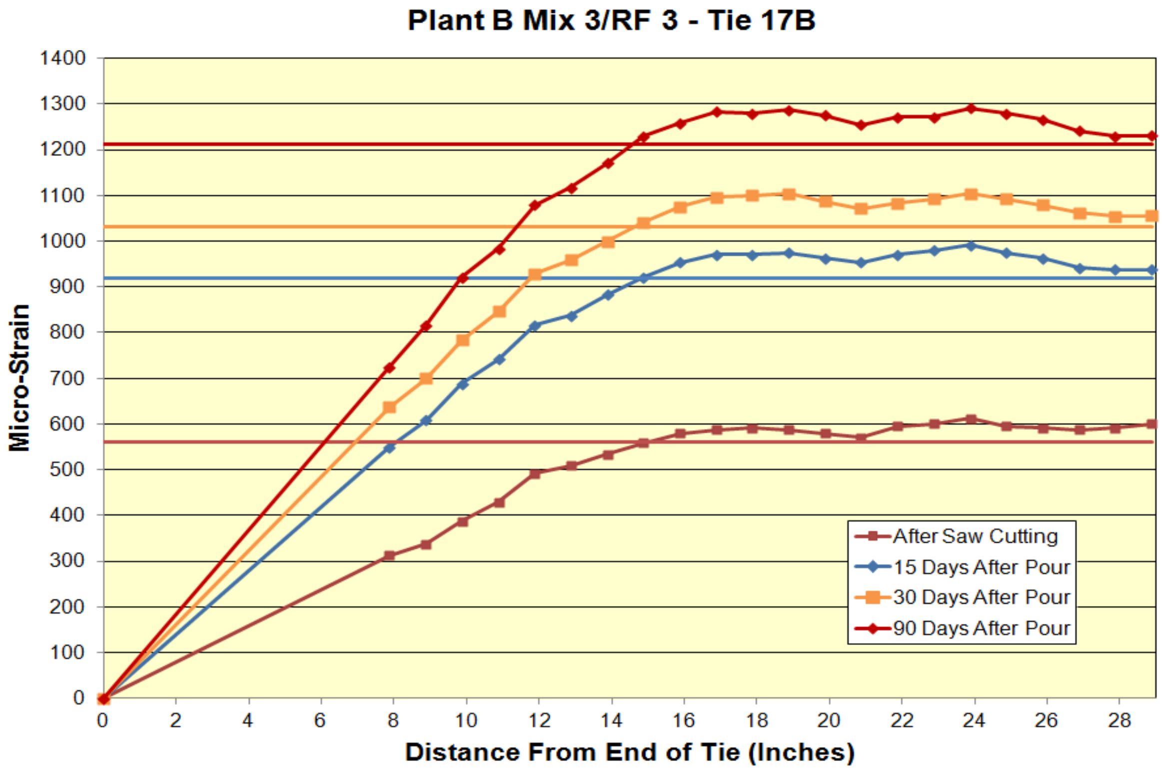

Figure B.46 Long-term transfer length of Plant B Mix 3/RF 3 Tie 17B

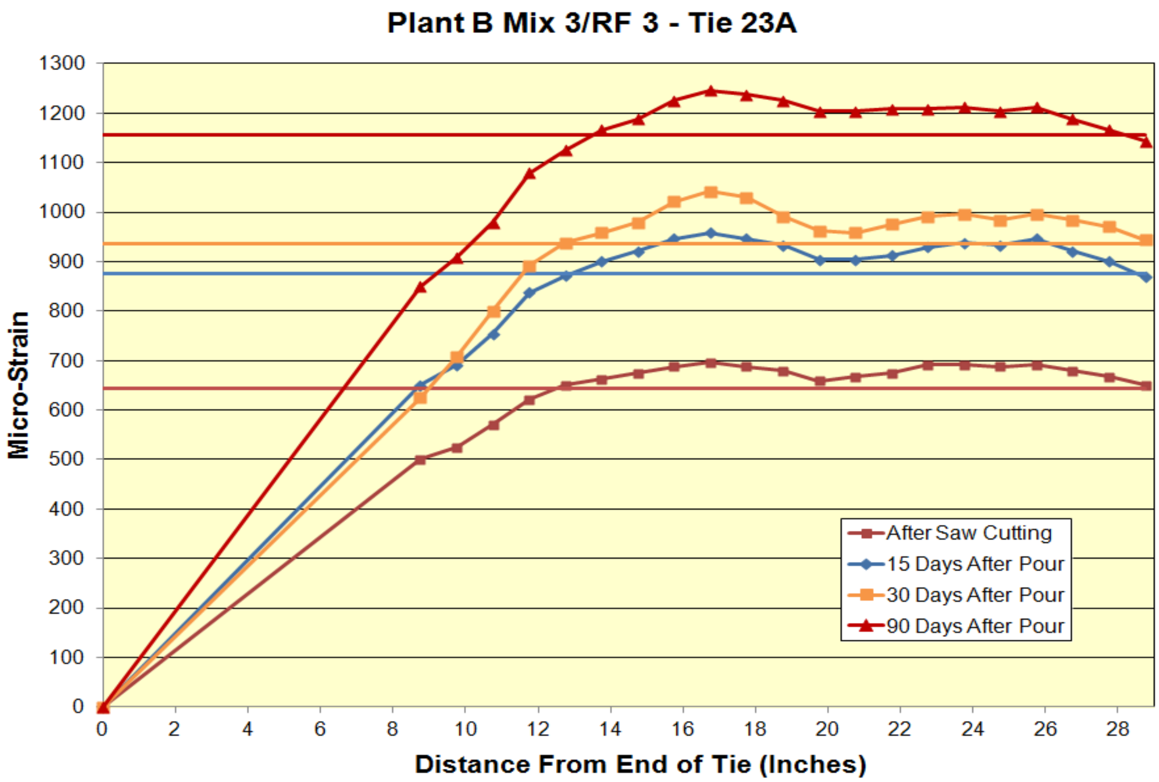

Figure B.47 Long-term transfer length of Plant B Mix 3/RF 3 Tie 23A

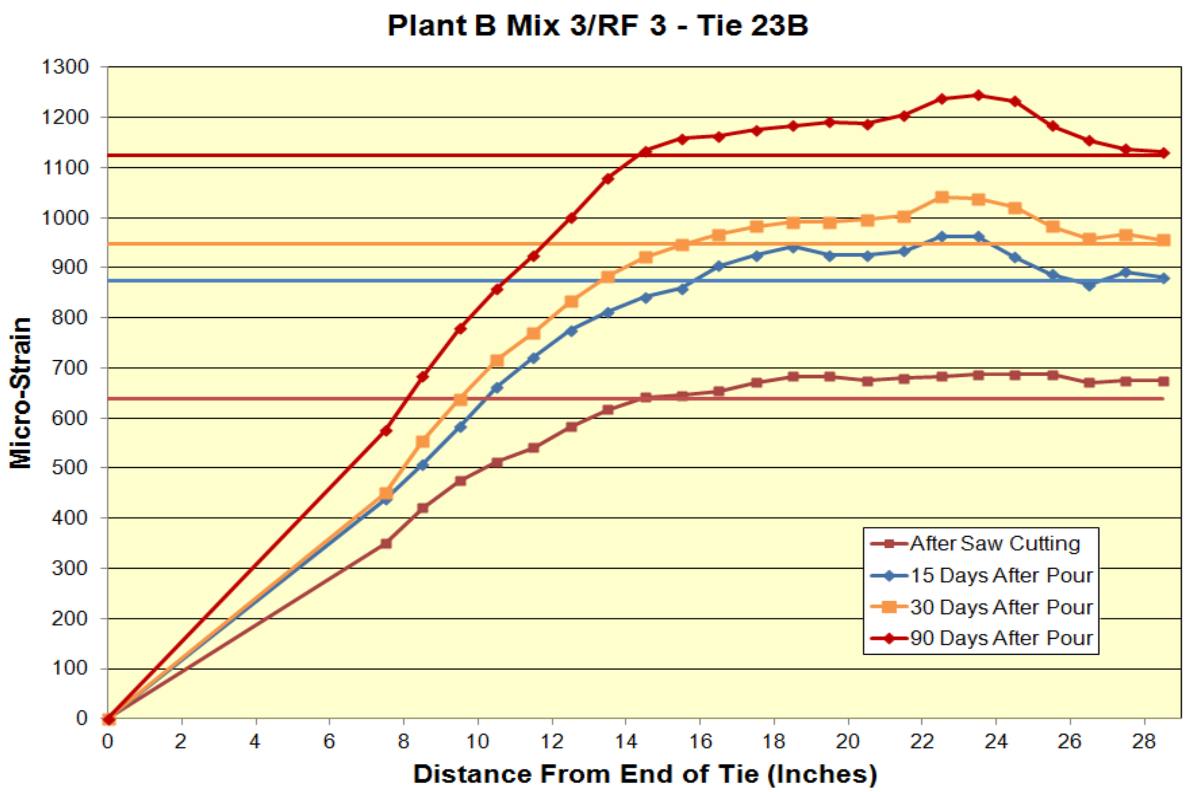

Figure B.48 Long-term transfer length of Plant B Mix 3/RF 3 Tie 23B

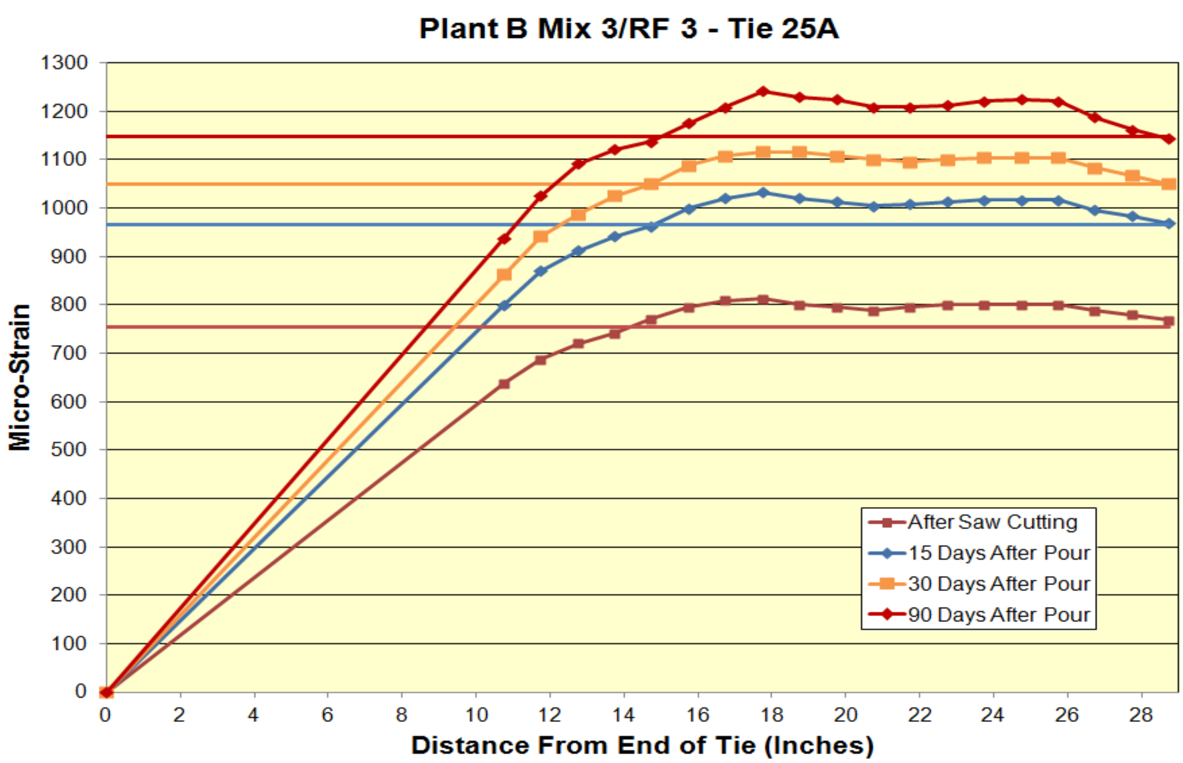

Figure B.49 Long-term transfer length of Plant B Mix 3/RF 3 Tie 25A

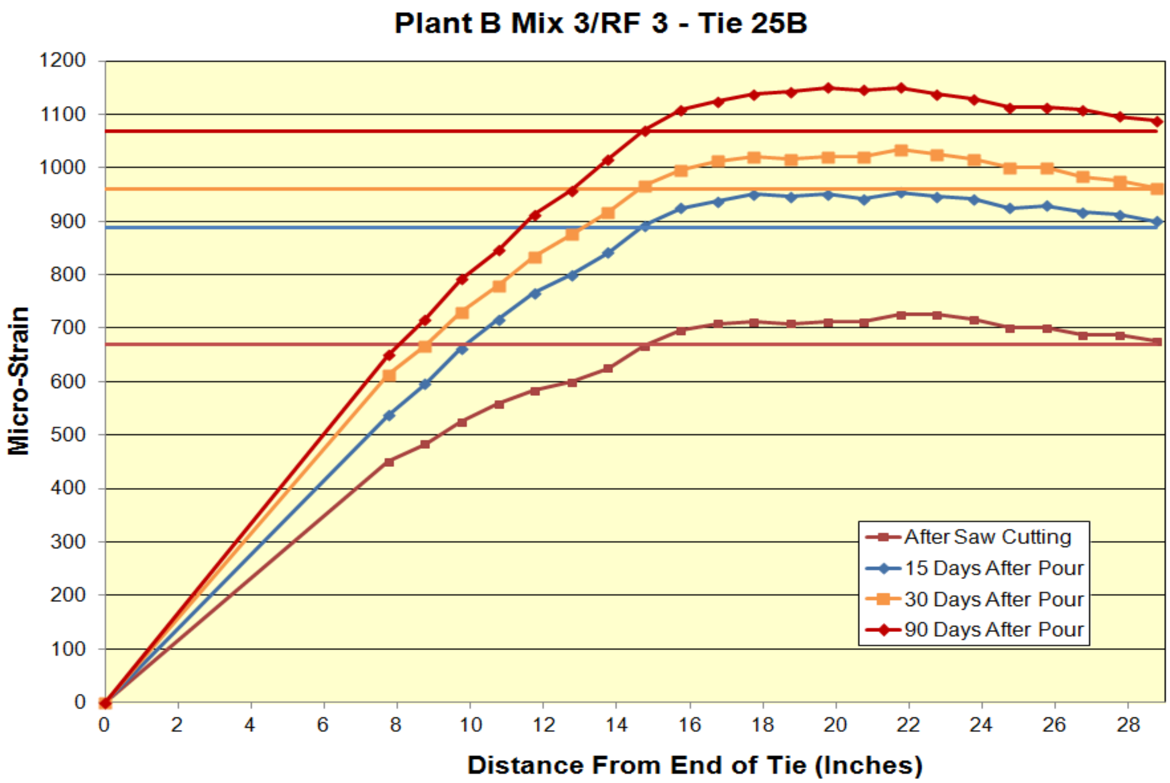

Figure B.50 Long-term transfer length of Plant B Mix 3/RF 3 Tie 25B

Appendix C Plant C Transfer Lengths

C.1 Short-term Transfer Lengths

Table C.1 Plant C transfer length data

	Tie Label	Measurement Method	Transfer Length (in.)
Plant C Mix 4/RF 4 Cast 1	1A	Whittemore Gage	7
	1B	Whittemore Gage	7.6
	2A	Whittemore Gage	7.8
	2B	Whittemore Gage	7.3
	3A	Whittemore Gage	6.3
	3B	Whittemore Gage	9.5
Plant C Mix 4/RF 4 Cast 2	1A	Laser Speckle	6.5
	2A	Laser Speckle	6
	2B	Laser Speckle	6.5
	3A	Laser Speckle	6
	3B	Laser Speckle	6.5
	4A	Laser Speckle	6.5
	4B	Laser Speckle	8

Note: For Cast 1, Side A = Dead-end of tie

For Cast 2, Side A = Live-end of tie

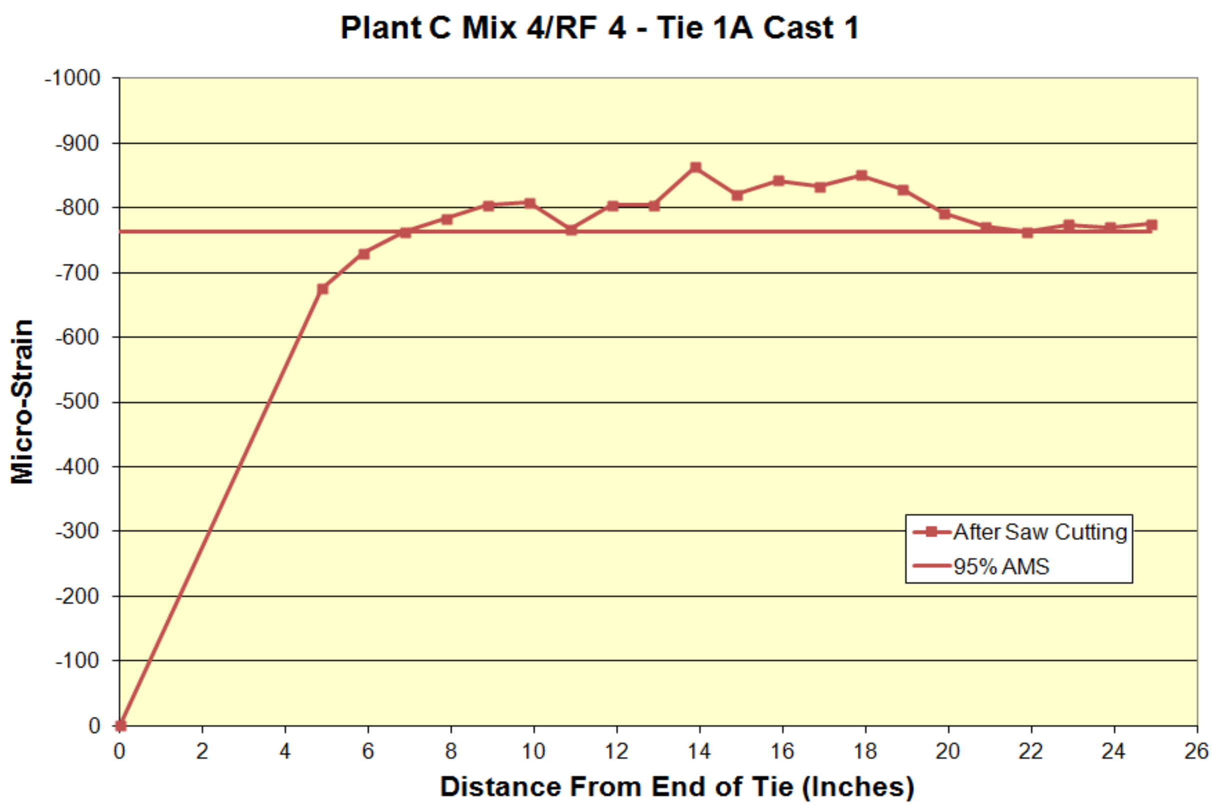

Figure C.1 Transfer length of Plant C Mix 4/RF 4 Tie 1A Cast 1

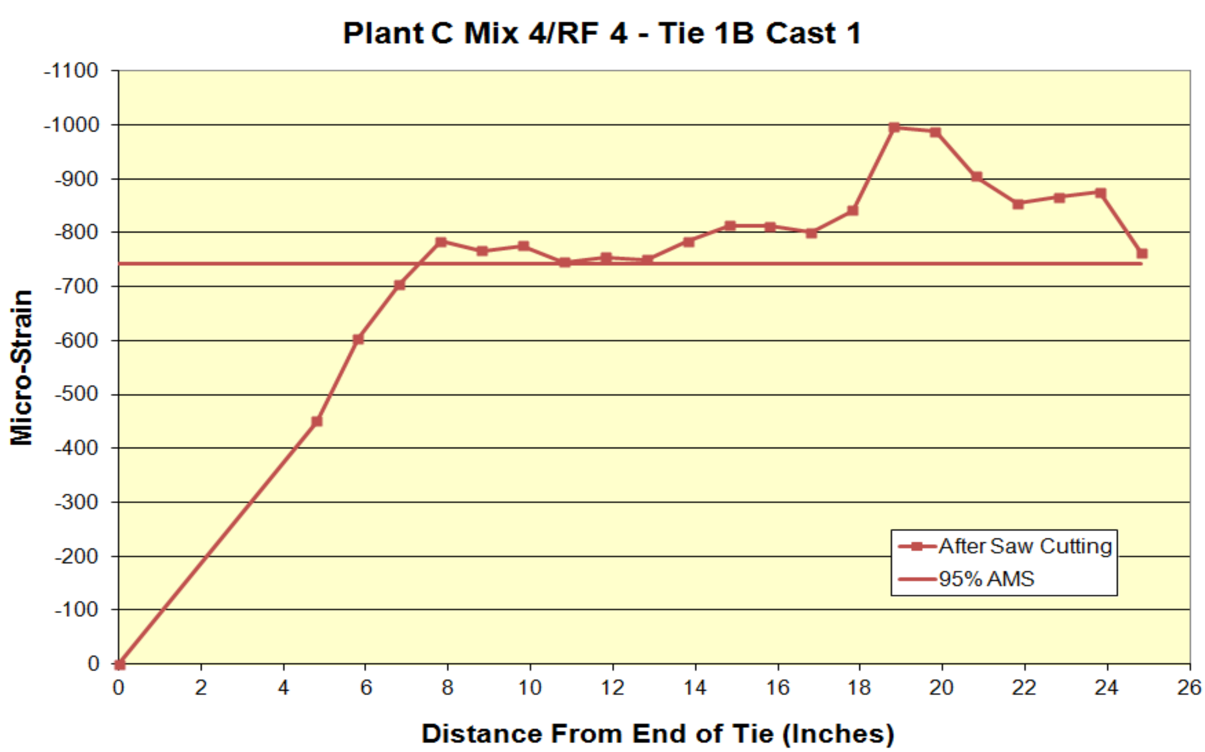

Figure C.2 Transfer length of Plant C Mix 4/RF 4 Tie 1B Cast 1

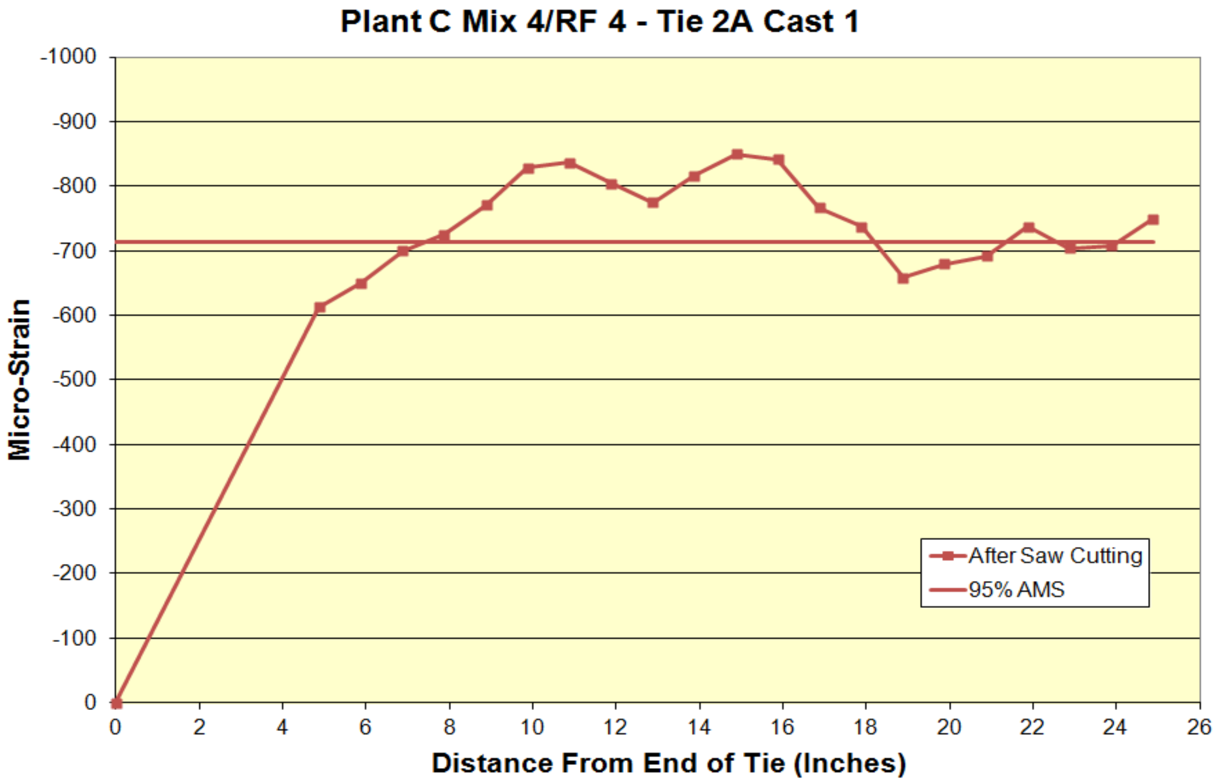

Figure C.3 Transfer length of Plant C Mix 4/RF 4 Tie 2A Cast 1

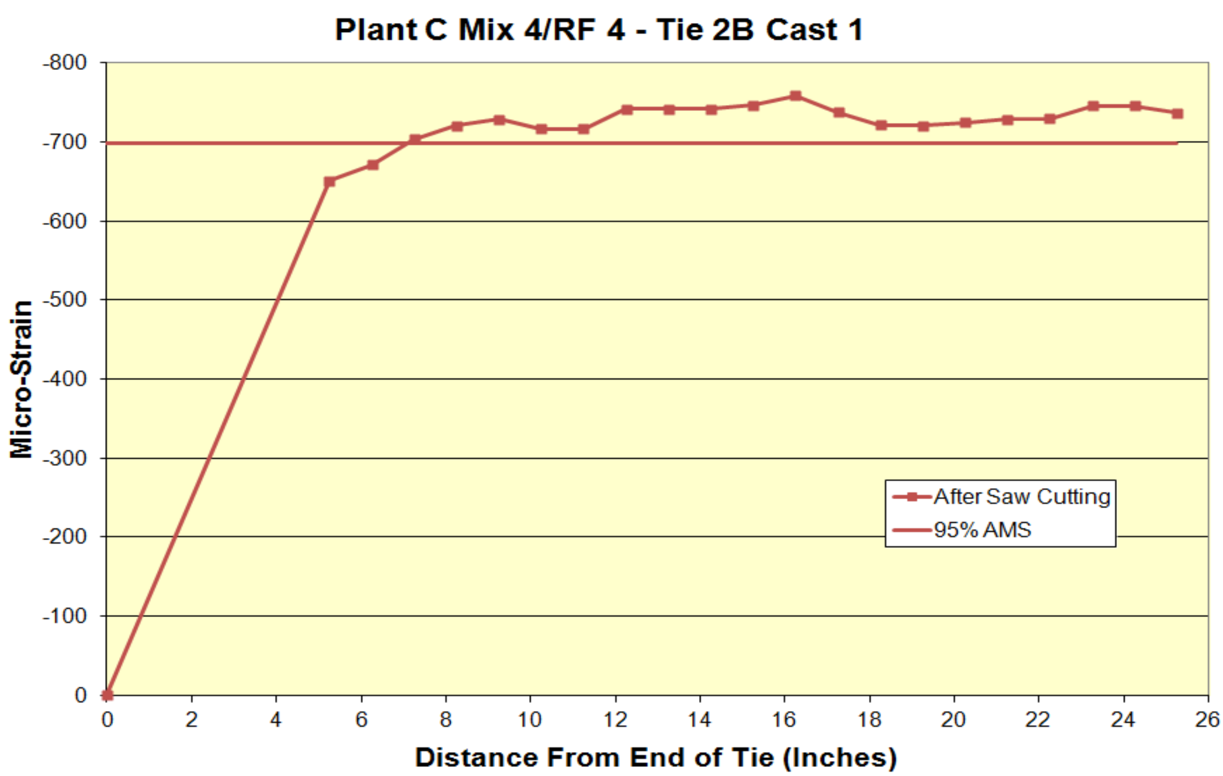

Figure C.4 Transfer length of Plant C Mix 4/RF 4 Tie 2B Cast 1

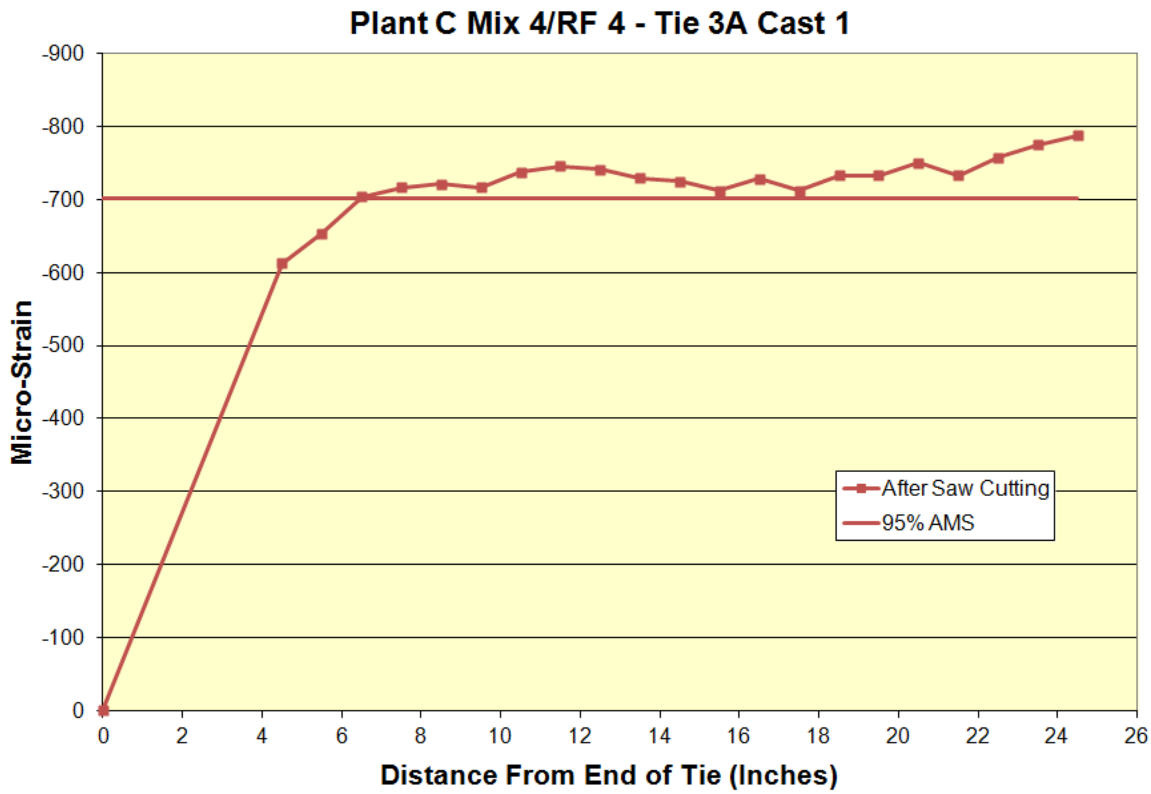

Figure C.5 Transfer length of Plant C Mix 4/RF 4 Tie 3A Cast 1

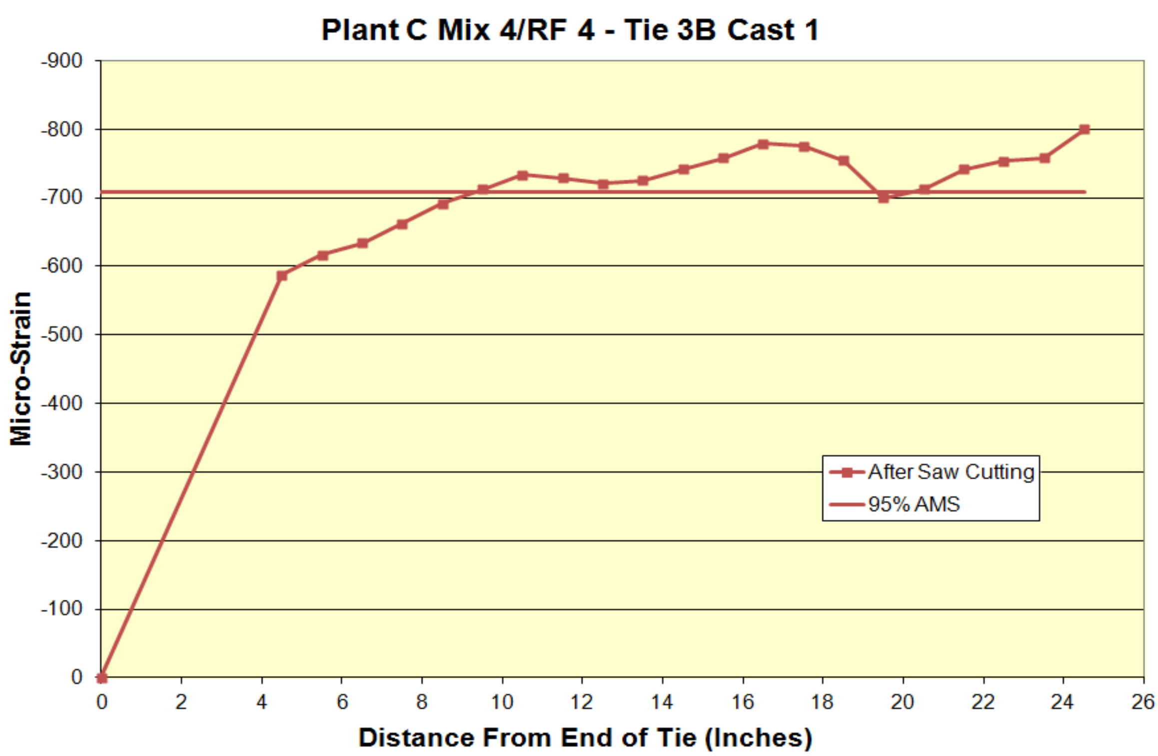

Figure C.6 Transfer length of Plant C Mix 4/RF 4 Tie 3B Cast 1

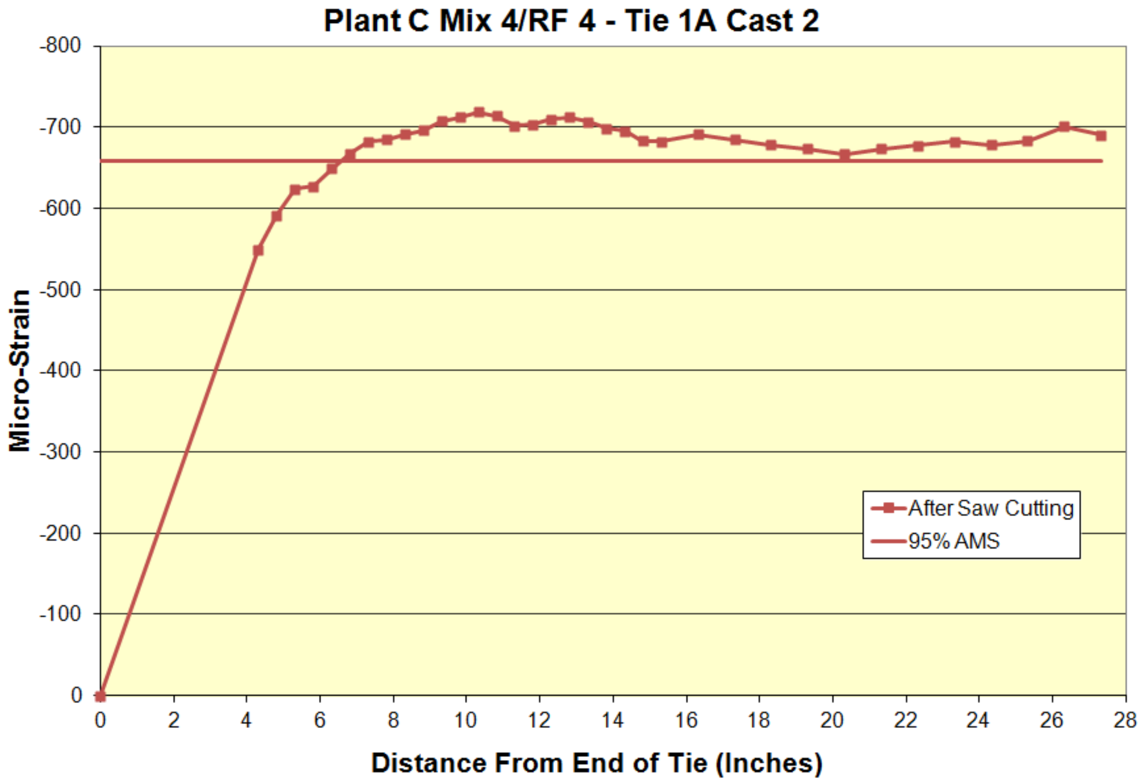

Figure C.7 Transfer length of Plant C Mix 4/RF 4 Tie 1A Cast 2

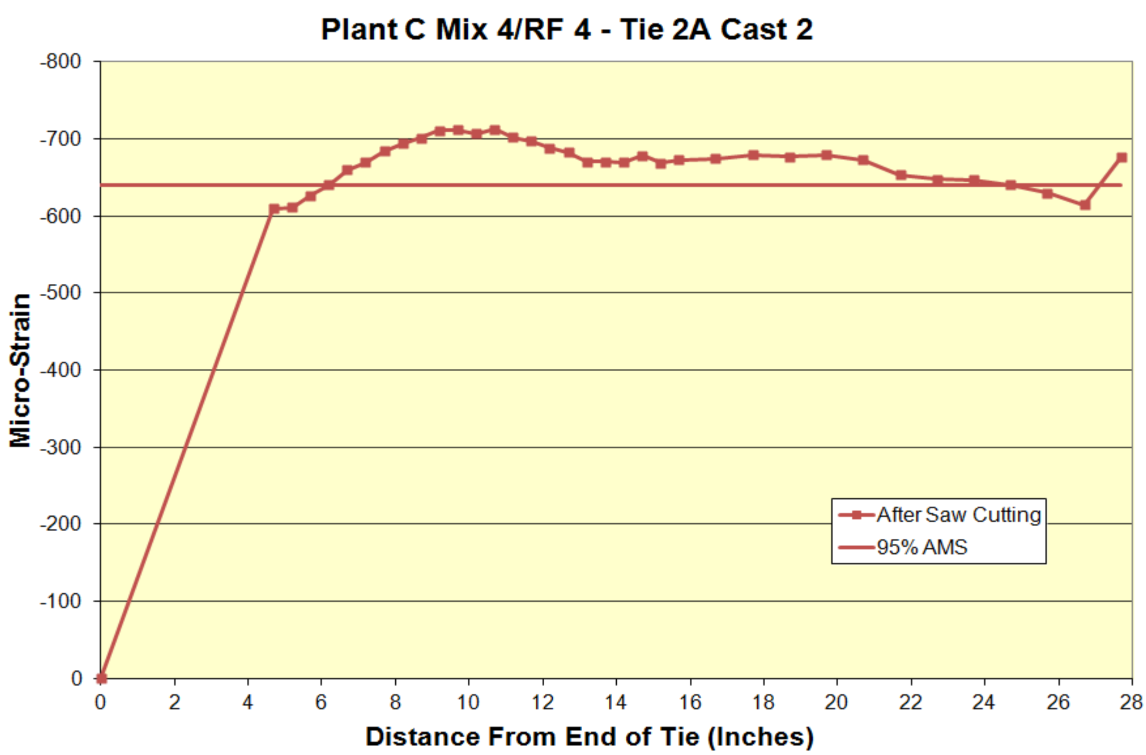

Figure C.8 Transfer length of Plant C Mix 4/RF 4 Tie 2A Cast 2

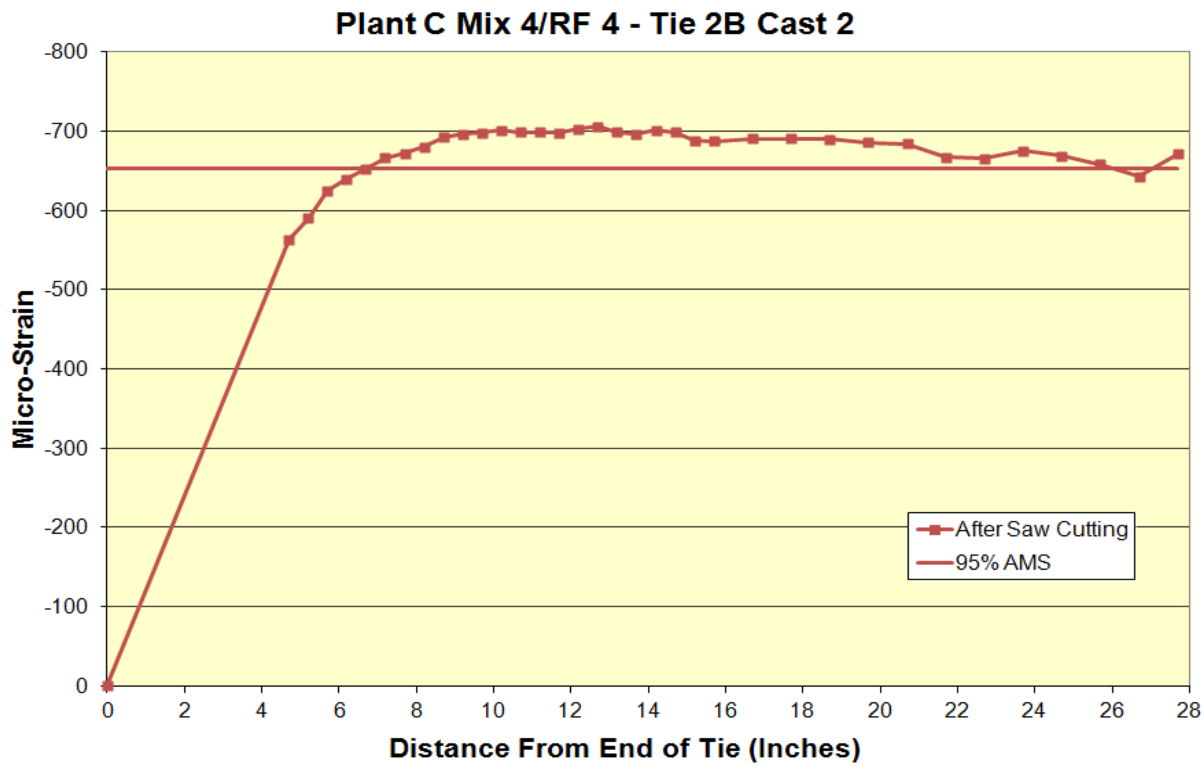

Figure C.9 Transfer length of Plant C Mix 4/RF 4 Tie 2B Cast 2

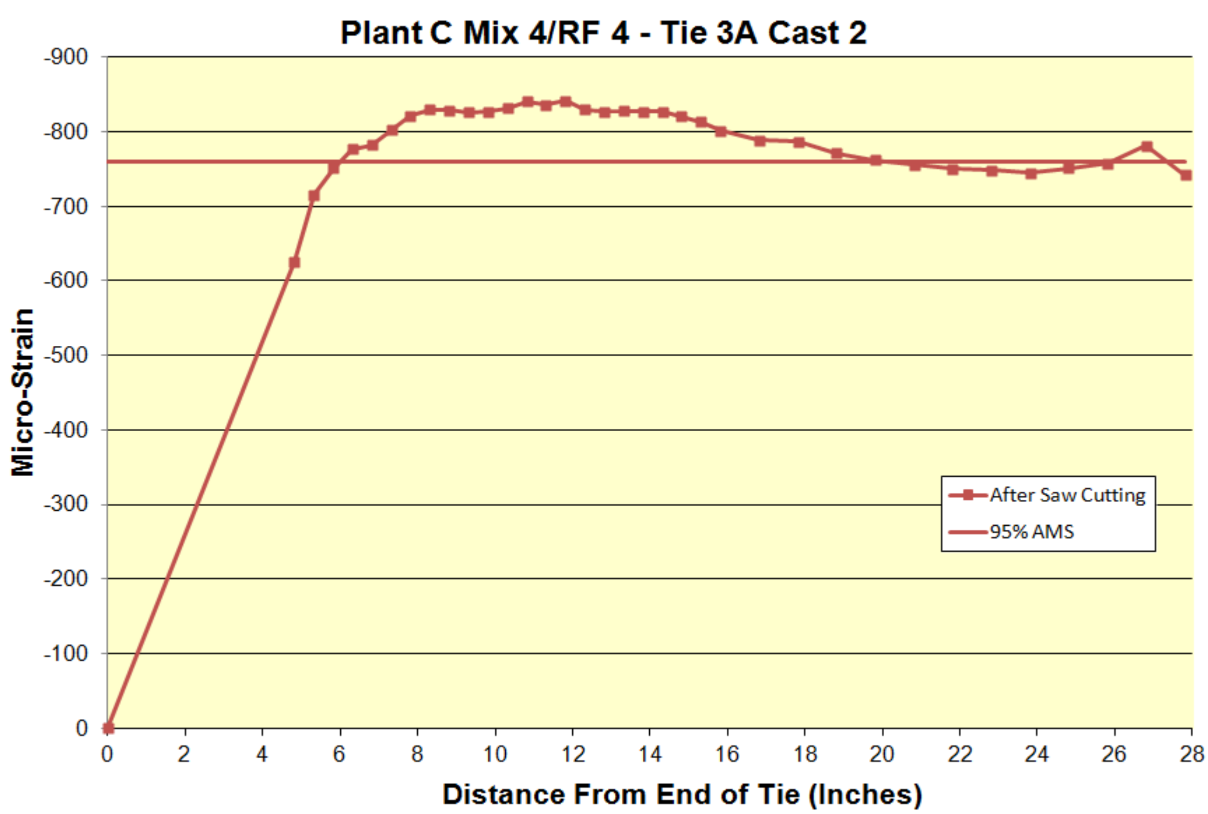

Figure C.10 Transfer length of Plant C Mix 4/RF 4 Tie 3A Cast 2

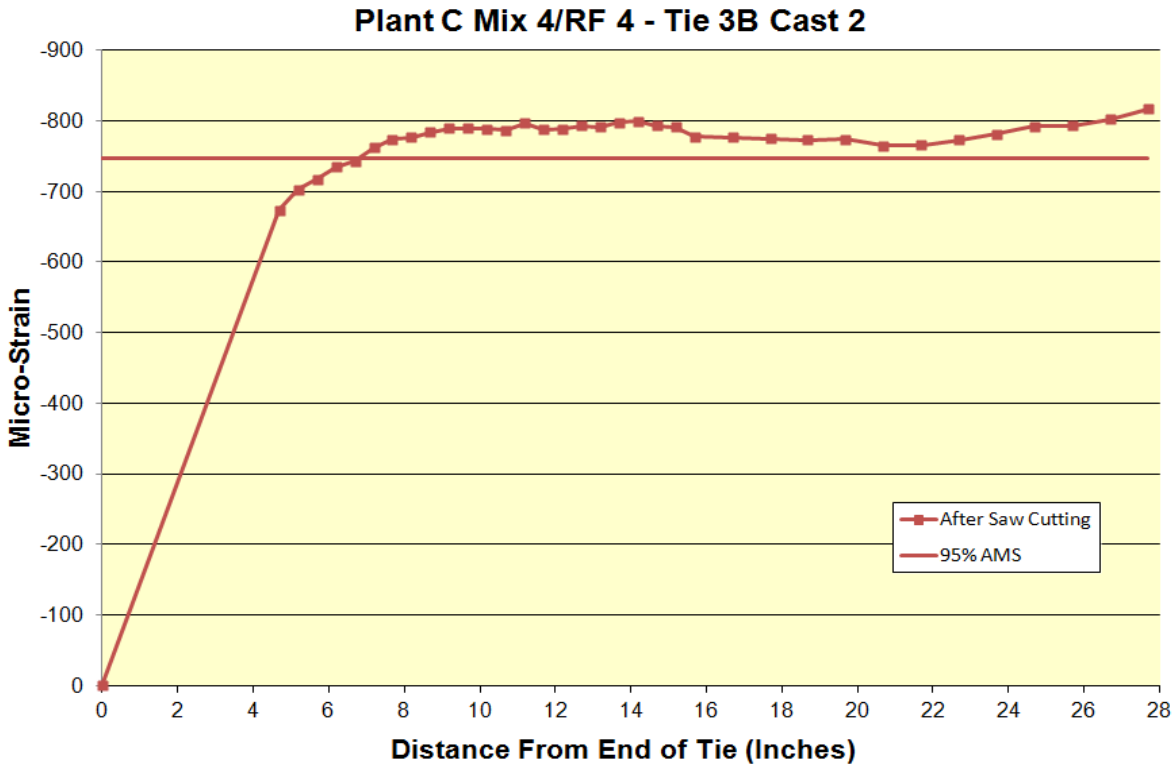

Figure C.11 Transfer length of Plant C Mix 4/RF 4 Tie 3B Cast 2

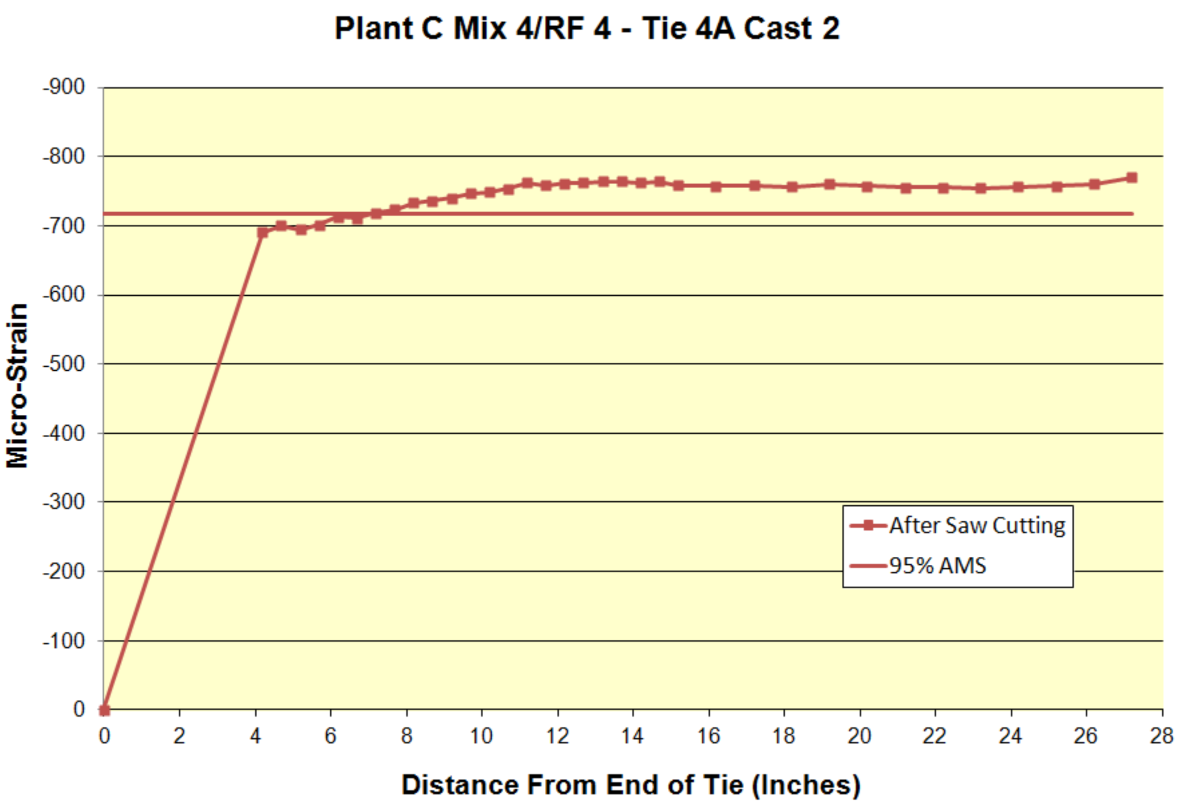

Figure C.12 Transfer length of Plant C Mix 4/RF 4 Tie 4A Cast 2

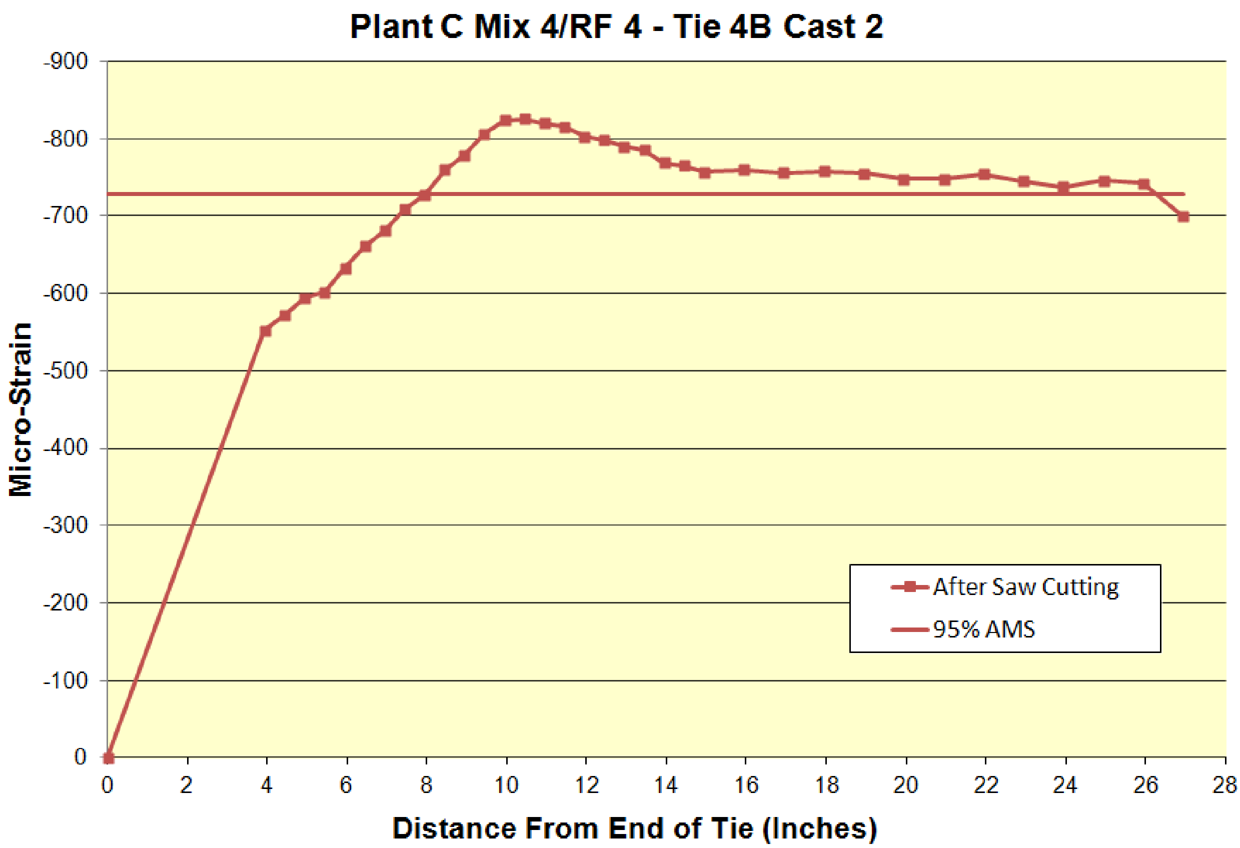

Figure C.13 Transfer length of Plant C Mix 4/RF 4 Tie 4B Cast 2

C.2 Long-term Transfer Lengths

Table C.2 Long-term transfer length data for Plant C Mix 4/RF 4 Cast 1

Plant C Mix 4/RF 4 Cast 1						
	Transfer Length (in.)					
Time of Reading	Tie 1A	Tie 1B	Tie 2A	Tie 2B	Tie 3A	Tie 3B
After Saw Cutting	7	7.6	7.8	6.3	6.8	9.5
20 Days After Pour	8	7.8	9	7.5	9.5	9.4
40 Days After Pour	8	7.6	8.3	8.8	9.5	9.7
90 Days After Pour	8	7.8	8.8	11	8.7	10
230 Days After Pour	8	9.3	9	10.2	8.5	9.7
470 Days After Pour	8.1	9.5	9.3	10.2	8.3	10.3

Table C.3 Long-term transfer length data for Plant C Mix 4/RF 4 Cast 2

Plant C Mix 4/RF 4 Cast 2					
	Transfer Length (in.)				
Time of Reading	Tie 1A	Tie 2A	Tie 2B	Tie 3A	Tie 3B
After Saw Cutting	6.5	6	6.5	6	6.5
10 Days After Pour	7	7.5	7.8	7.5	9.5
52 Days After Pour	7.5	8.5	8.5	9.2	10

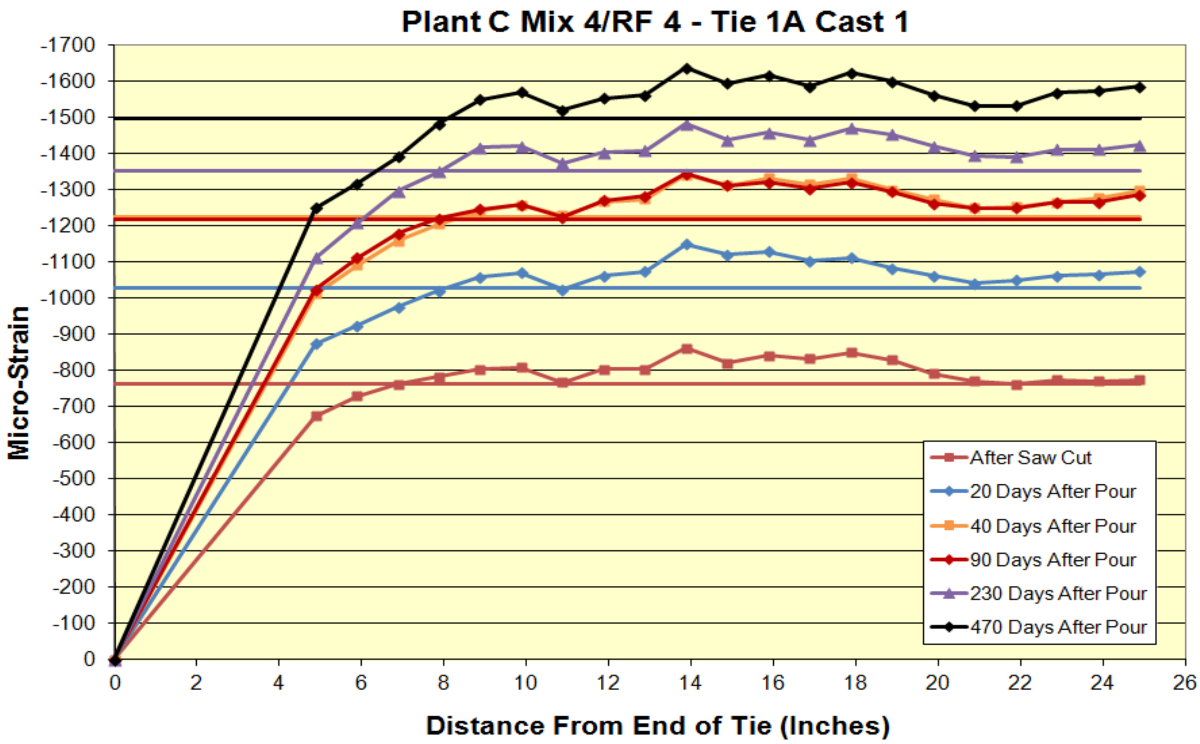

Figure C.14 Long-term transfer length of Plant C Mix 4/RF 4 Tie 1A Cast 1

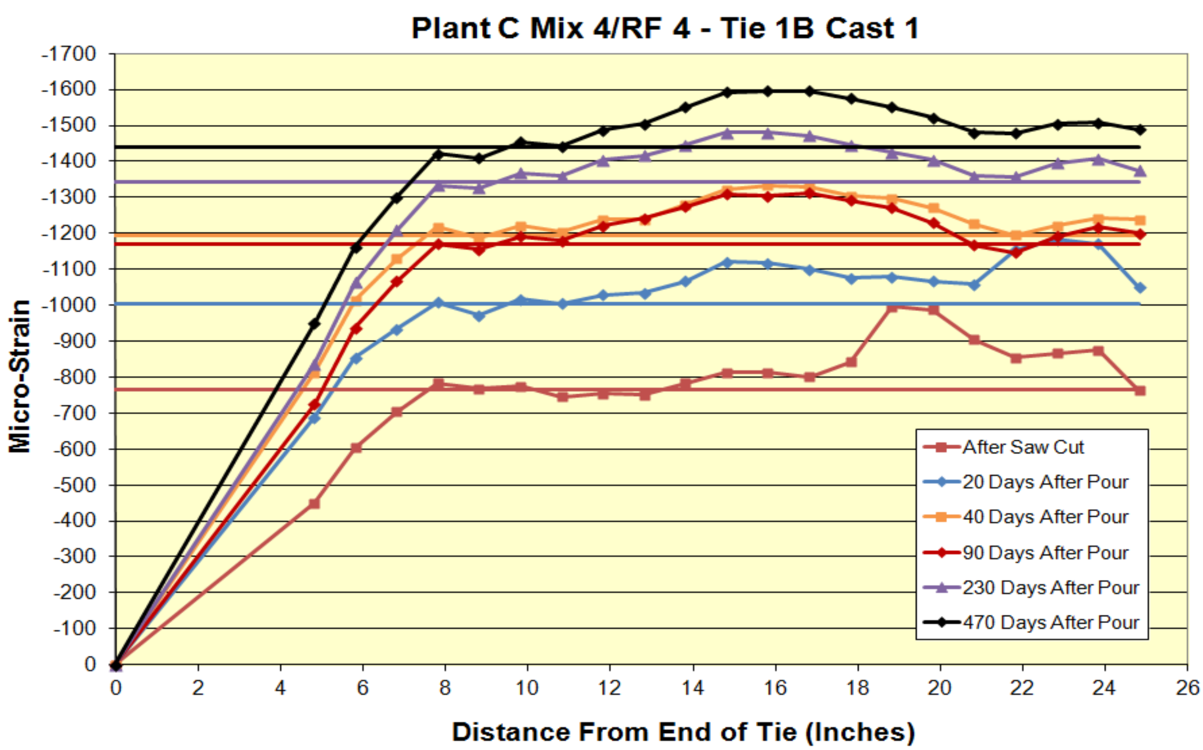

Figure C.15 Long-term transfer length of Plant C Mix 4/RF 4 Tie 1B Cast 1

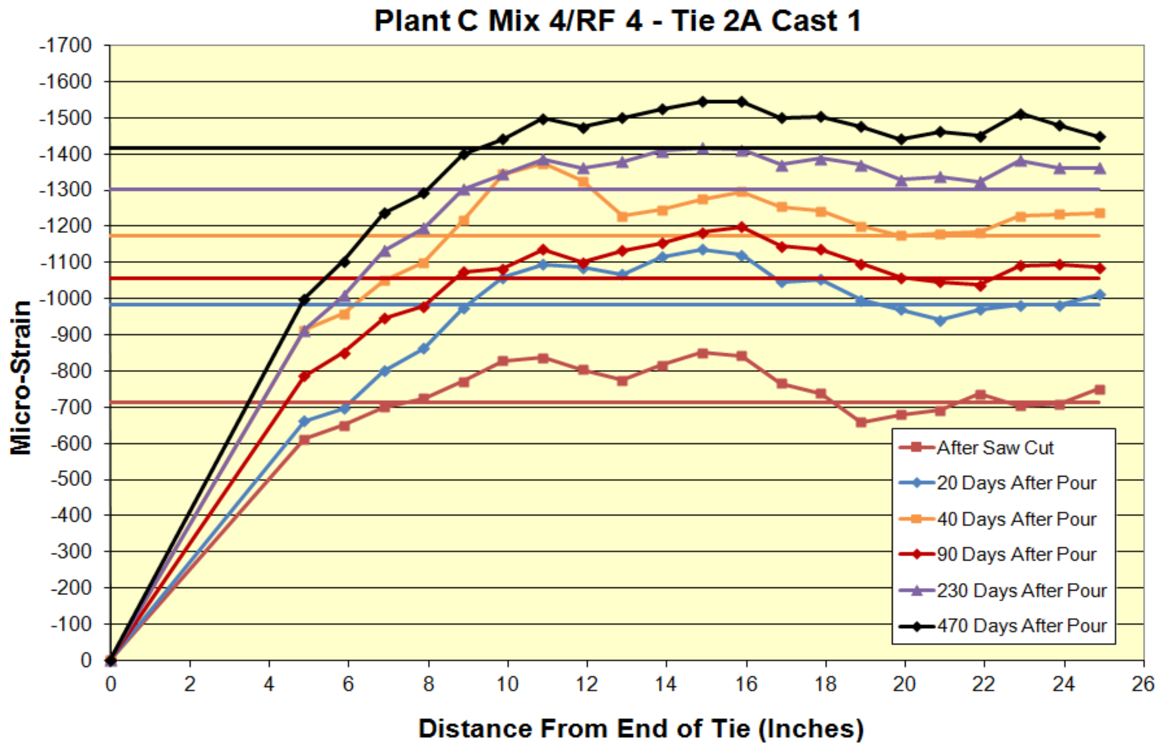

Figure C.16 Long-term transfer length of Plant C Mix 4/RF 4 Tie 2A Cast 1

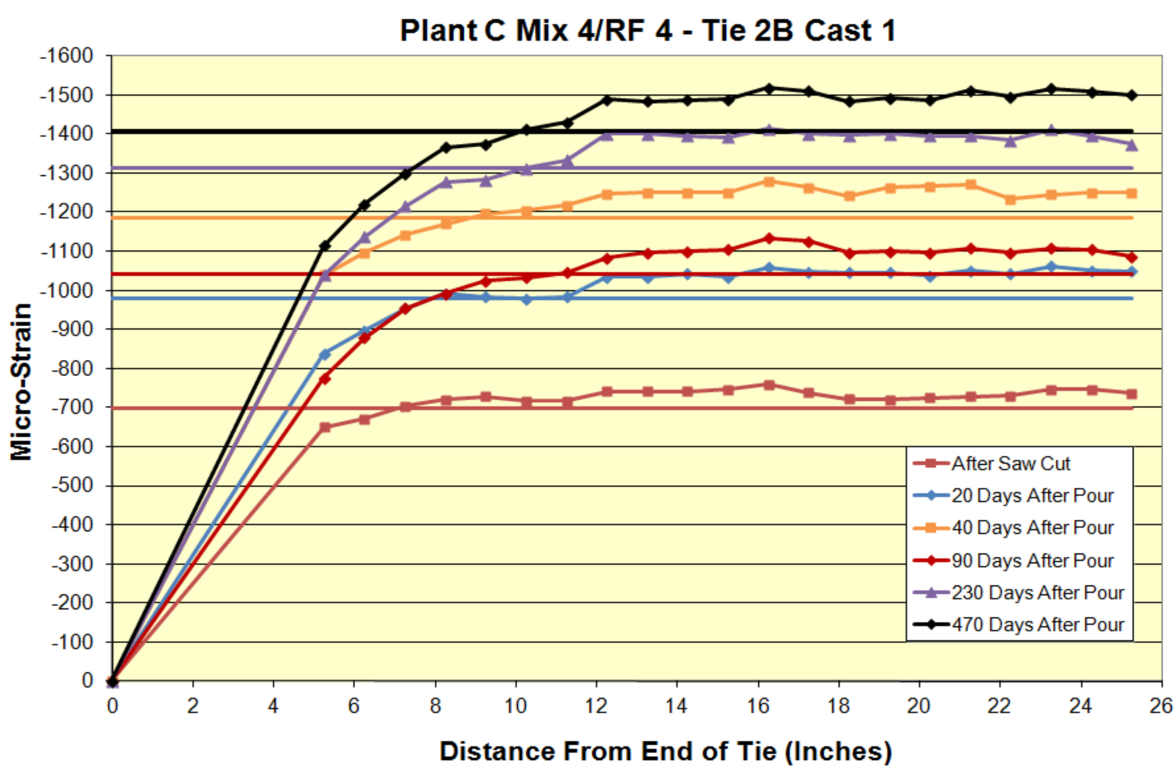

Figure C.17 Long-term transfer length of Plant C Mix 4/RF 4 Tie 2B Cast 1

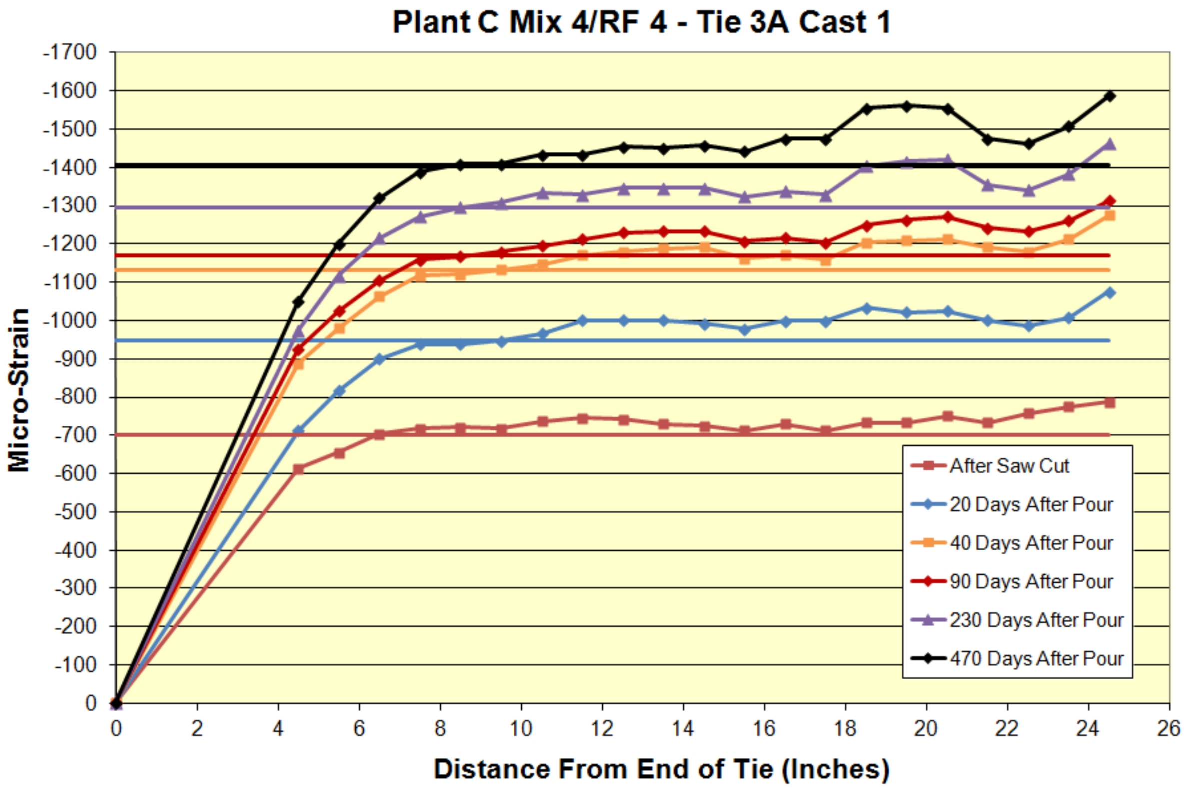

Figure C.18 Long-term transfer length of Plant C Mix 4/RF 4 Tie 3A Cast 1

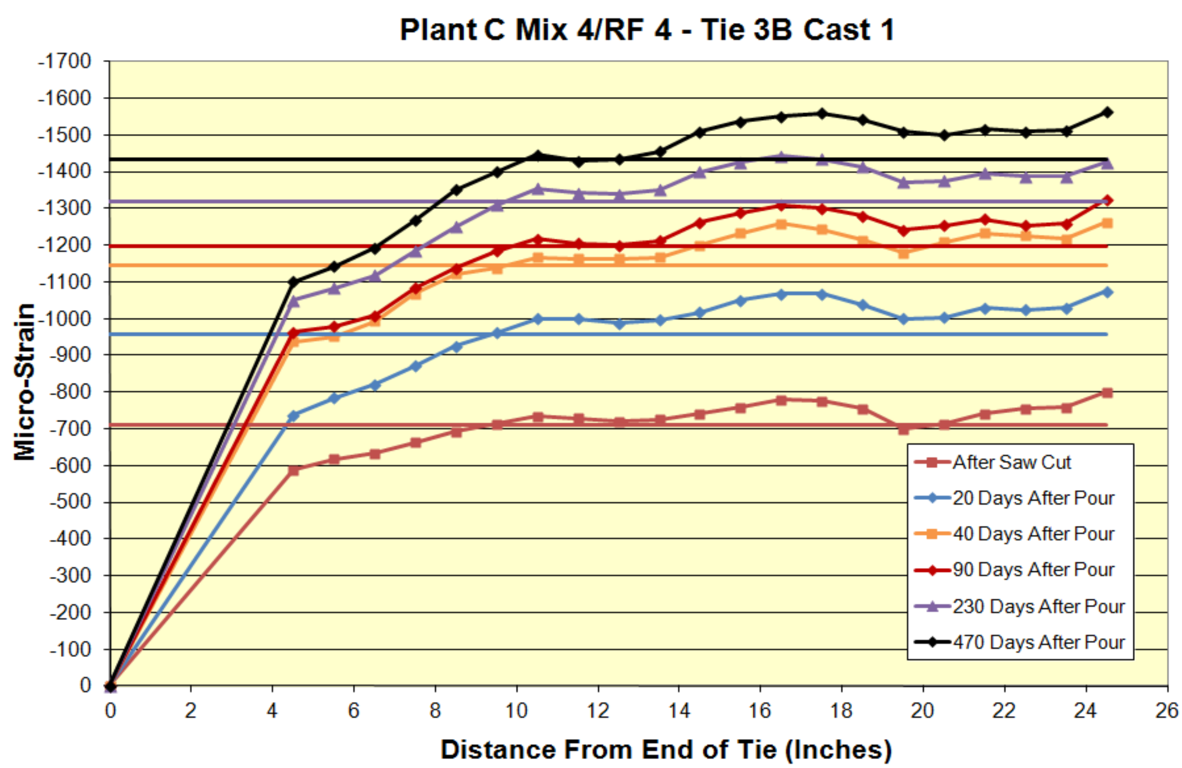

Figure C.19 Long-term transfer length of Plant C Mix 4/RF 4 Tie 3B Cast 1

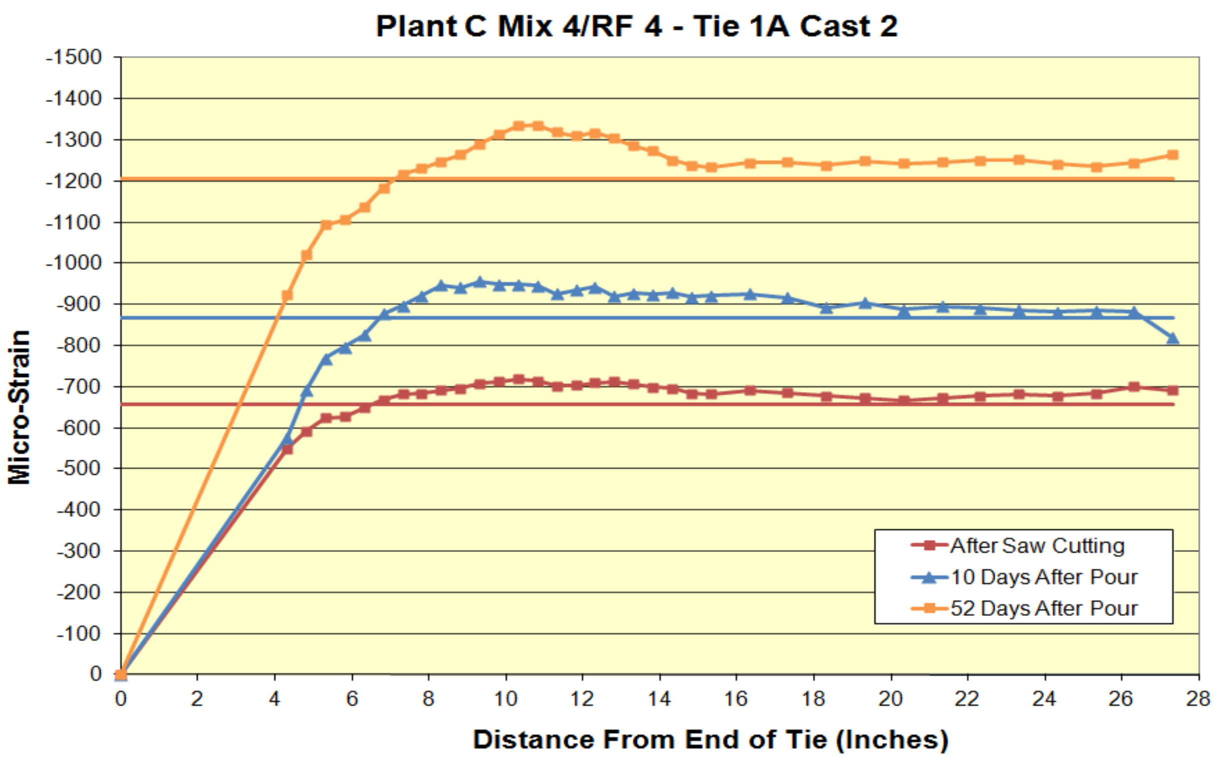

Figure C.20 Long-term transfer length of Plant C Mix 4/RF 4 Tie 1A Cast 2

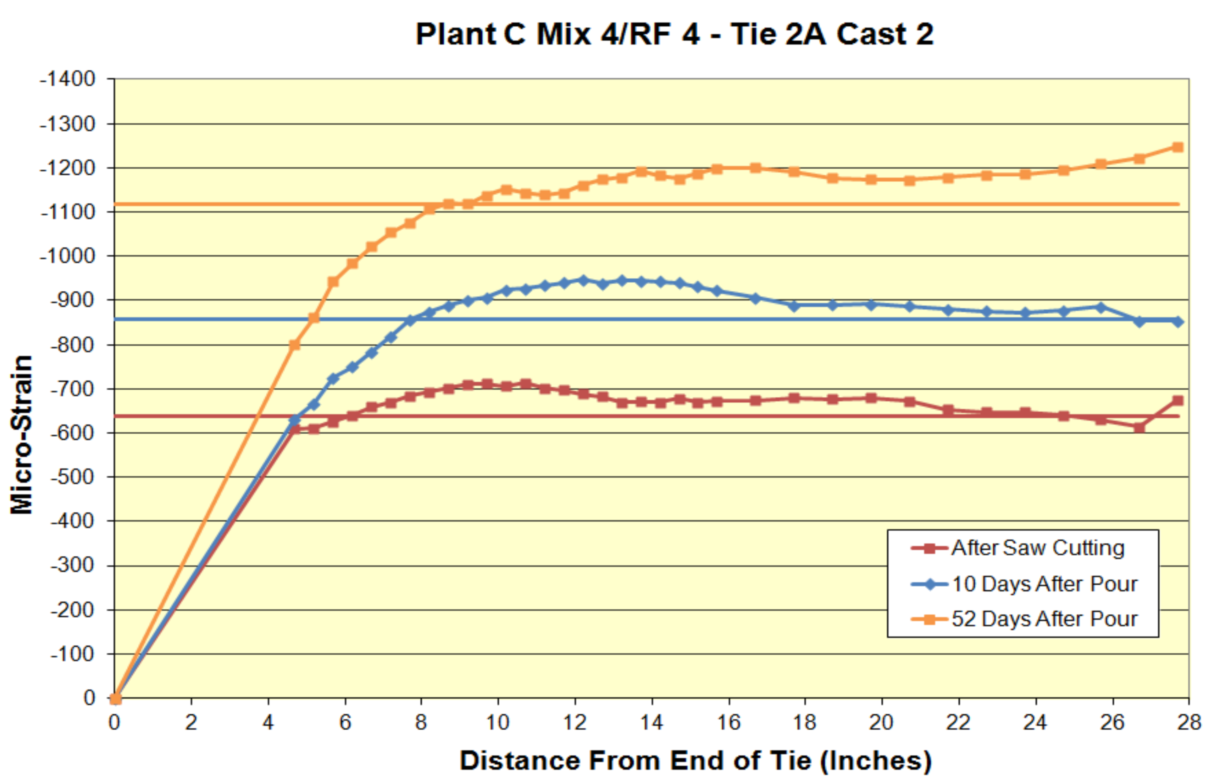

Figure C.21 Long-term transfer length of Plant C Mix 4/RF 4 Tie 2A Cast 2

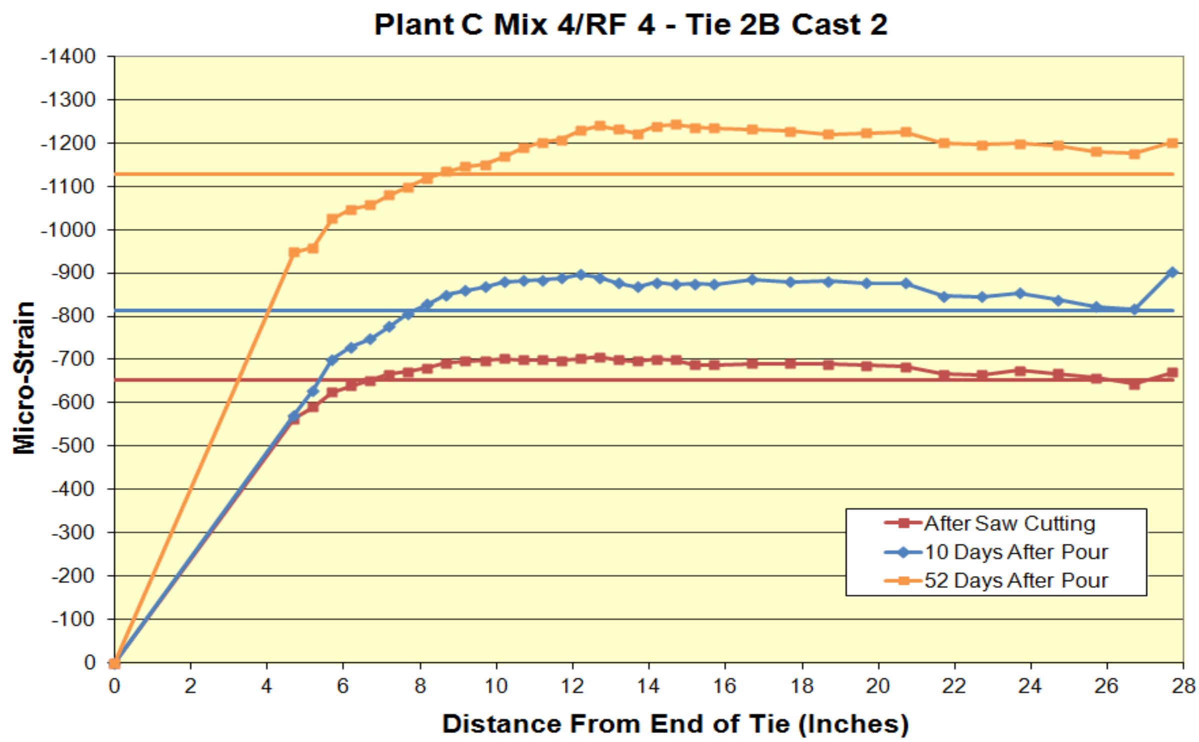

Figure C.22 Long-term transfer length of Plant C Mix 4/RF 4 Tie 2B Cast 2

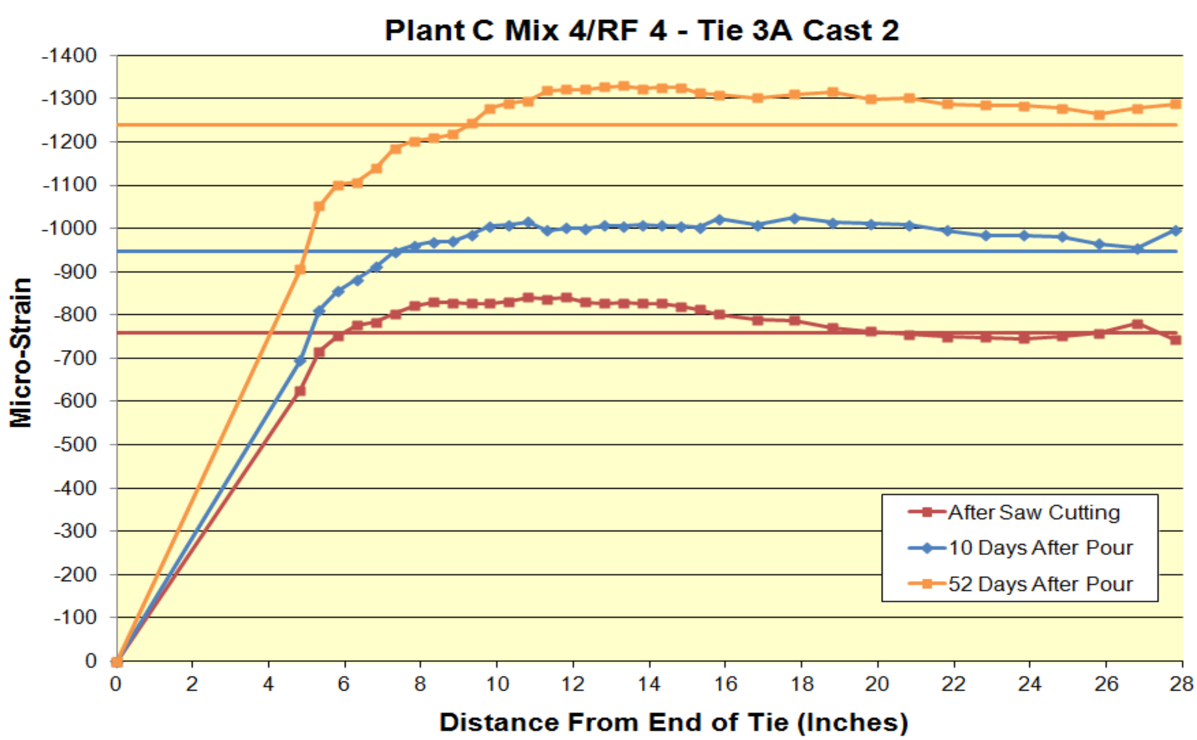

Figure C.23 Long-term transfer length of Plant C Mix 4/RF 4 Tie 3A Cast 2

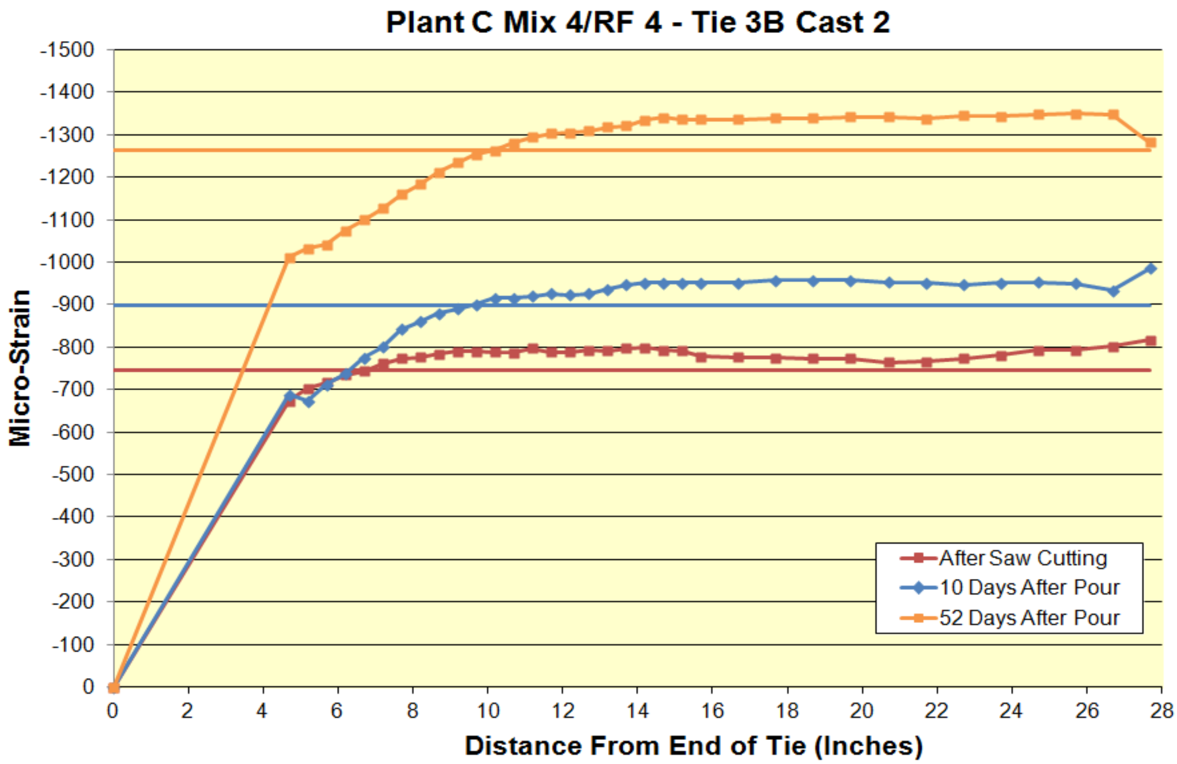

Figure C.24 Long-term transfer length of Plant C Mix 4/RF 4 Tie 3B Cast 2

Appendix D Plant D Transfer Lengths

D.1Short-term Transfer Lengths

Table D.1 Plant D transfer length data

	Tie Label	Measurement Method	Transfer Length (in.)
Plant D Mix 5/RF 5 Cast 1	1A	Whittemore Gage	9.1
	4A	Laser Speckle	11.6
	5A	Laser Speckle	11.6
	7A	Whittemore Gage	11.4
	7B	Whittemore Gage	10.1
	8A	Laser Speckle	9.7
	9A	Laser Speckle	11.9
	10A	Laser Speckle	11.1
Plant D Mix 5/RF 5 Cast 2	12A	Laser Speckle	10.1
	12B	Whittemore Gage	8.5
	13A	Laser Speckle	12.2
	14A	Laser Speckle	12
	14B	Laser Speckle	12.8
	15A	Laser Speckle	10.1
	15B	Laser Speckle	12.1
	16A	Laser Speckle	11.1
	16B	Laser Speckle	12.1
	19A	Whittemore Gage	11.5
	19B	Whittemore Gage	11.2
	22A	Laser Speckle	16.3
	22B	Laser Speckle	11.7

Table D.1 Plant D transfer length data (cont'd.)

	Tie Label	Measurement Method	Transfer Length (in.)
Plant D Mix 5/RF 6 Cast 3	23A	Whittemore Gage	9.5
	23B	Laser Speckle	12.5
	24B	Laser Speckle	13.1
	25A	Laser Speckle	10.7
	25B	Laser Speckle	11.9
	26A	Laser Speckle	10.1
	27A	Laser Speckle	8.2
	28A	Laser Speckle	10.3
	29A	Whittemore Gage	10.2
	29B	Whittemore Gage	9.7
	30A	Laser Speckle	12.2
	30B	Laser Speckle	13.3
	31A	Laser Speckle	14.7
	31B	Laser Speckle	14
	32A	Laser Speckle	11.6
	32B	Laser Speckle	10.2
	33A	Laser Speckle	12.3
	33B	Laser Speckle	13
	34A	Laser Speckle	11.2
	34B	Laser Speckle	15.3
Plant D Mix 5/RF 6 Cast 4	35A	Whittemore Gage	9.3
	35B	Laser Speckle	12.1
	36A	Laser Speckle	11.1
	36B	Laser Speckle	10.2
	37B	Laser Speckle	10.8
	38A	Laser Speckle	7.7
	38B	Laser Speckle	13.5
	39B	Laser Speckle	10.8
	40A	Laser Speckle	10.7
	40B	Laser Speckle	10
	41A	Whittemore Gage	10.6
	41B	Whittemore Gage	11.2
	42A	Laser Speckle	13.3
	42B	Laser Speckle	12.7
	43A	Laser Speckle	11.4
	43B	Laser Speckle	15.3
	44A	Laser Speckle	16.1
	44B	Laser Speckle	13.8
	45B	Laser Speckle	16.4
	46A	Laser Speckle	11.4
	46B	Laser Speckle	16.1

Note: Side A = Dead-end of tie

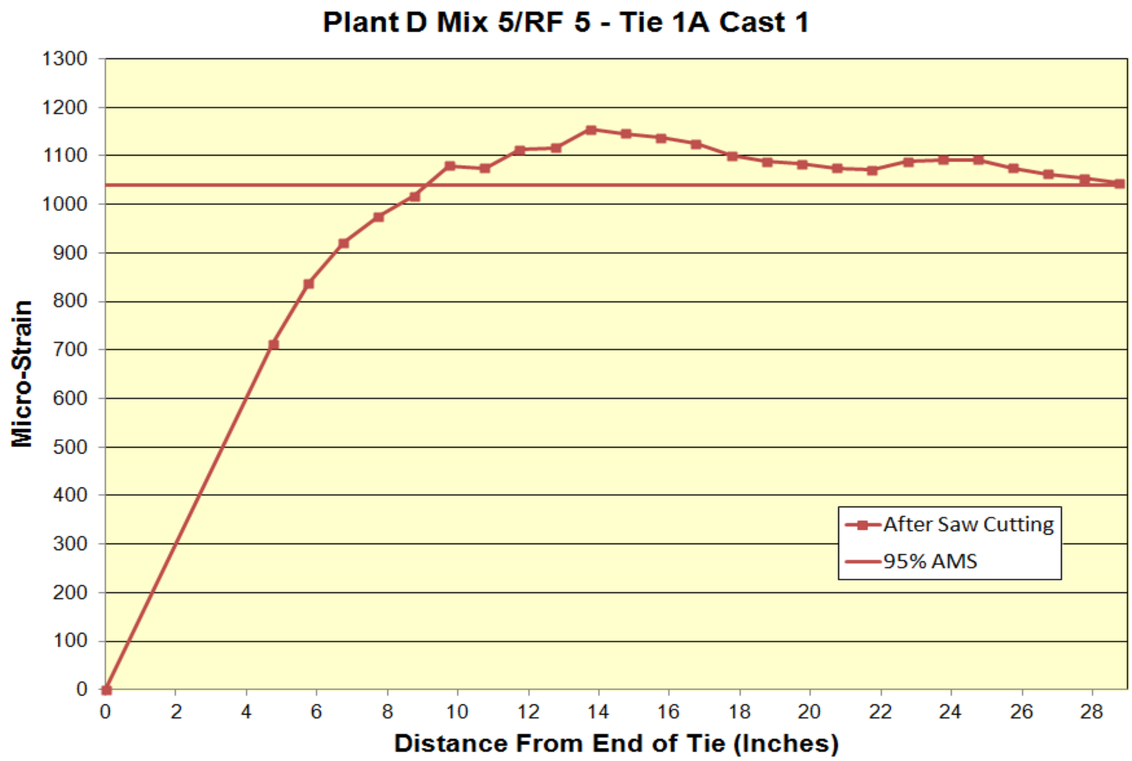

Figure D.1 Transfer length of Plant D Mix 5/RF 5 Tie 1A Cast 1

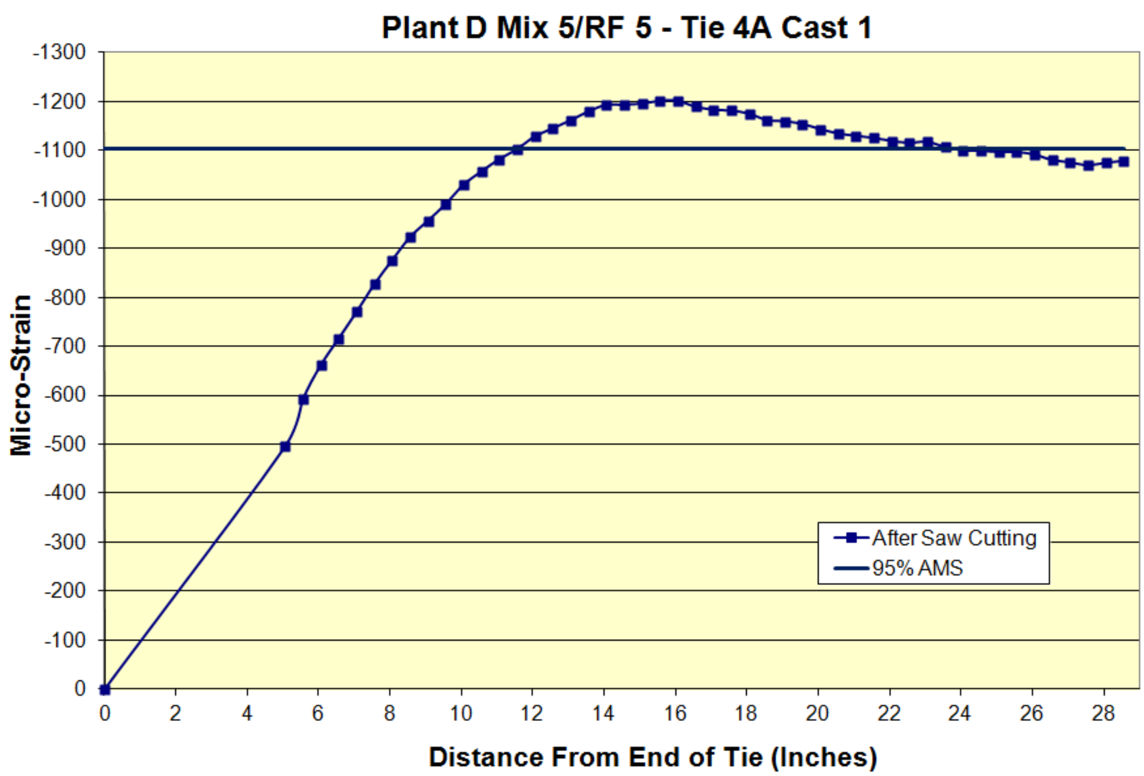

Figure D.2 Transfer length of Plant D Mix 5/RF 5 Tie 4A Cast 1

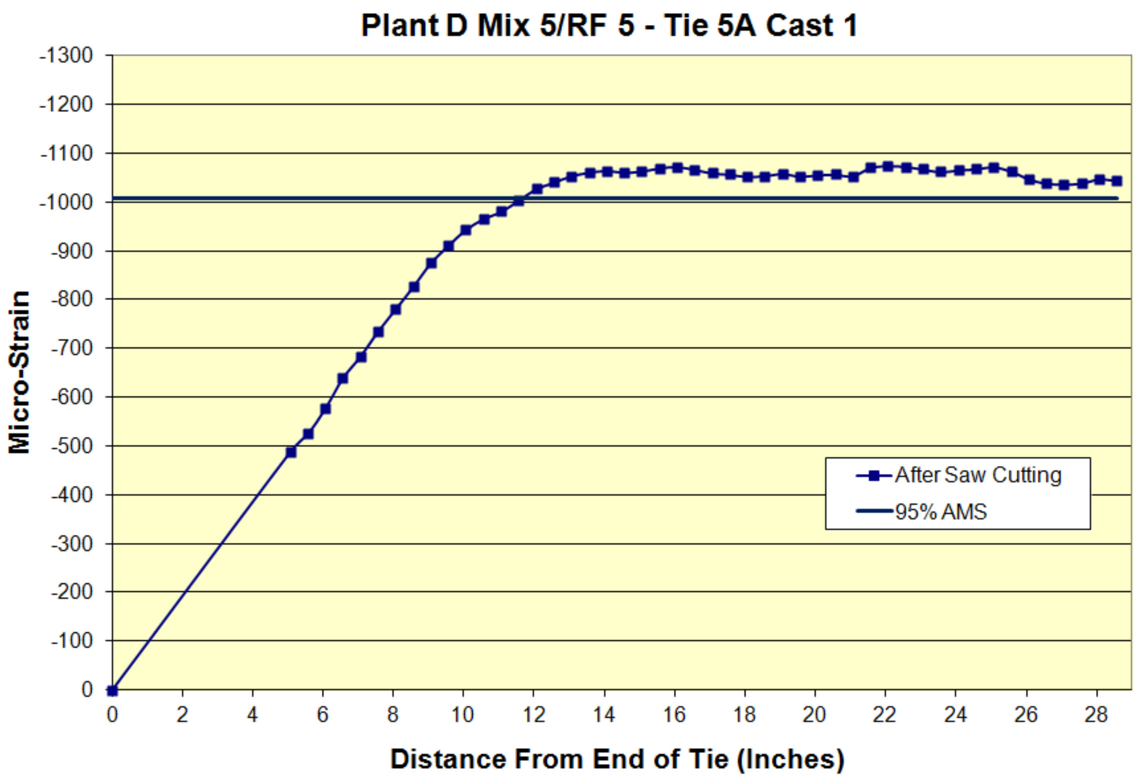

Figure D.3 Transfer length of Plant D Mix 5/RF 5 Tie 5A Cast 1

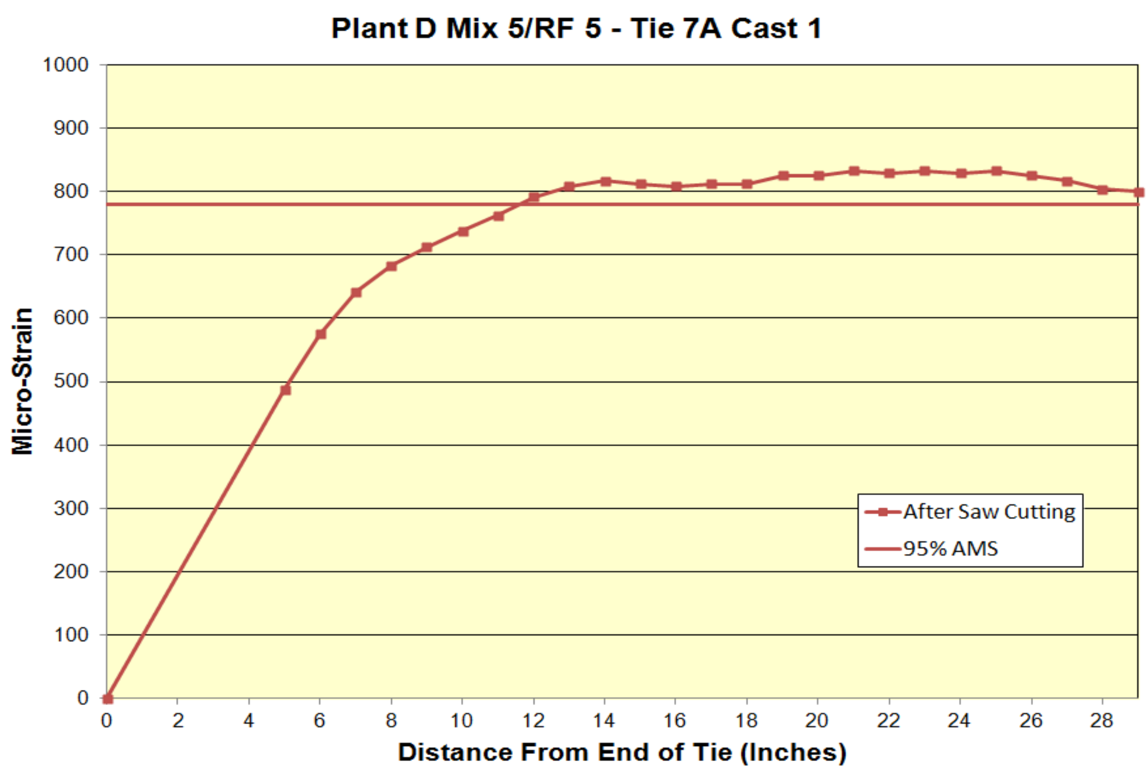

Figure D.4 Transfer length of Plant D Mix 5/RF 5 Tie 7A Cast 1

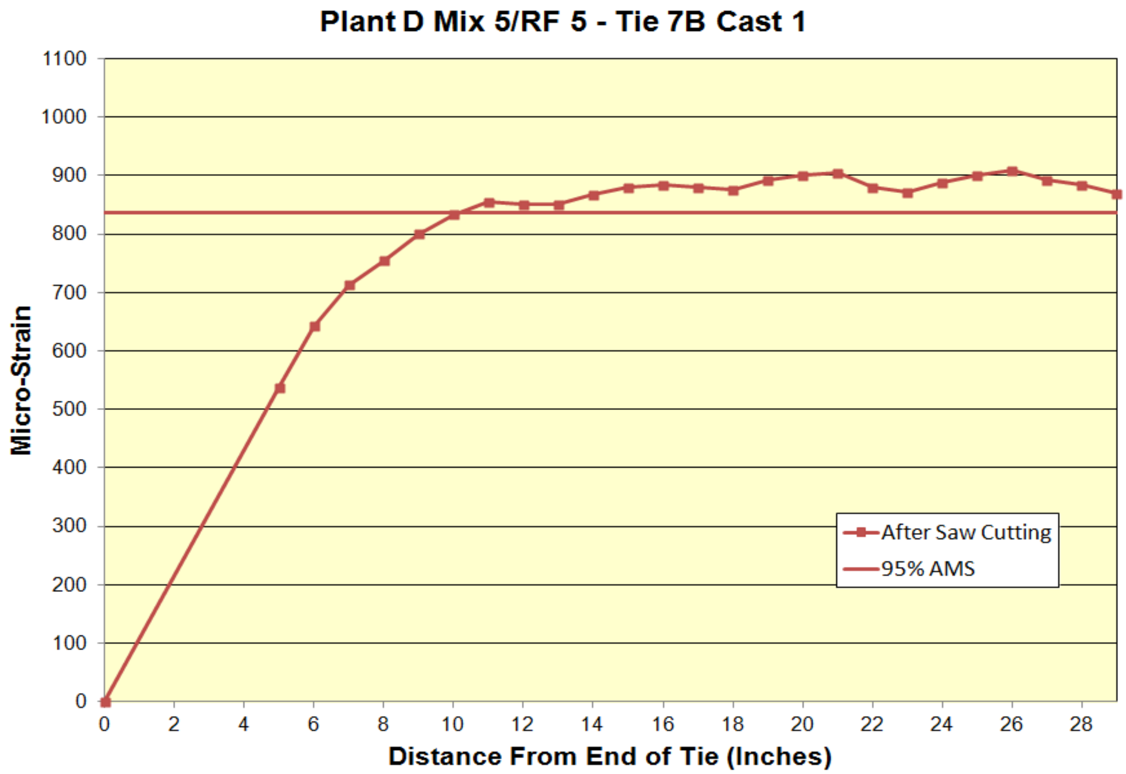

Figure D.5 Transfer length of Plant D Mix 5/RF 5 Tie 7B Cast 1

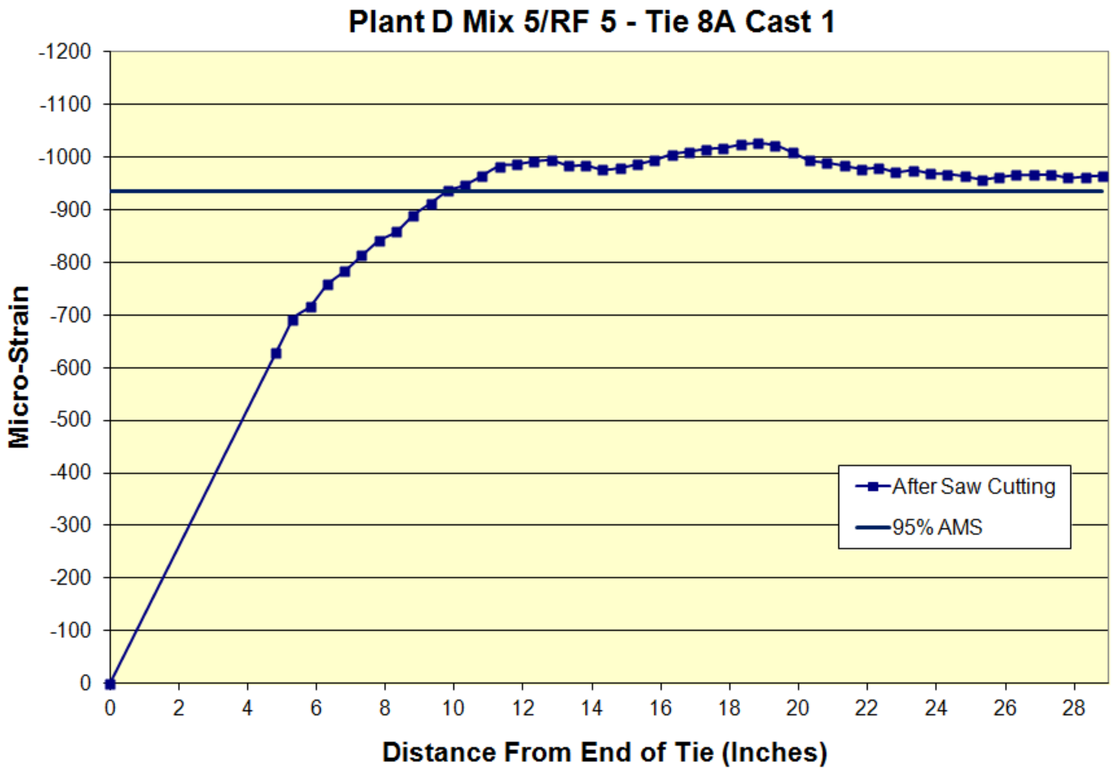

Figure D.6 Transfer length of Plant D Mix 5/RF 5 Tie 8A Cast 1

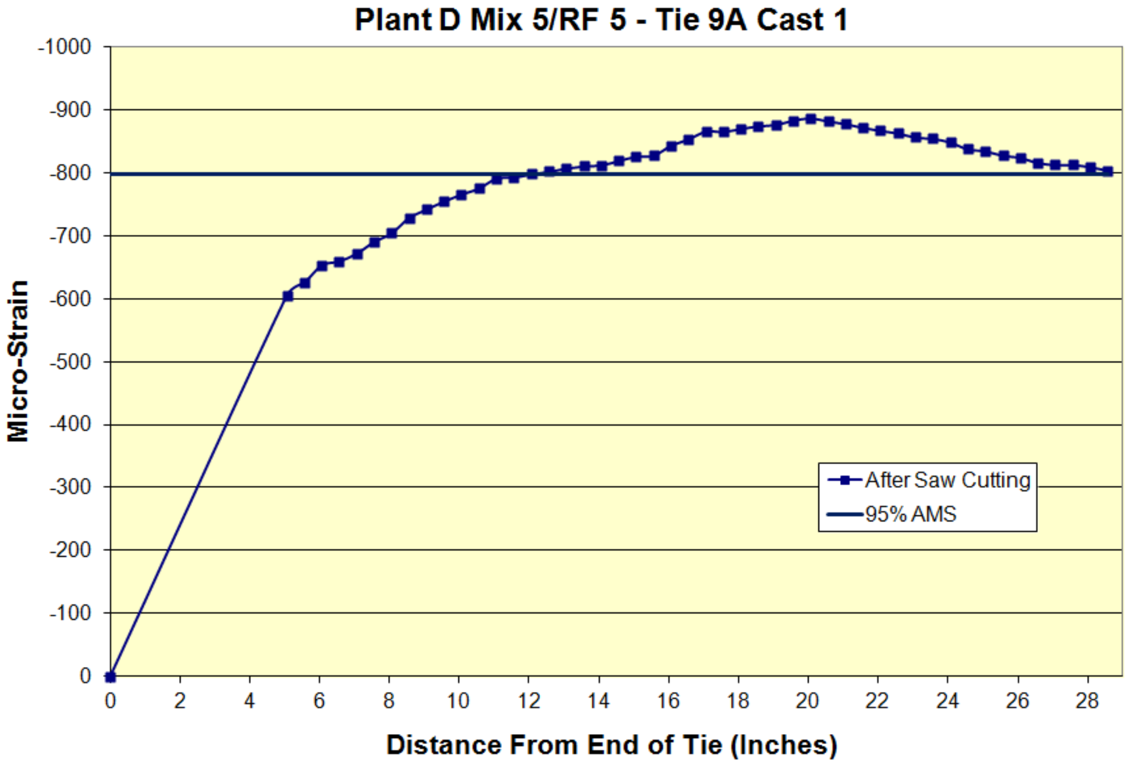

Figure D.7 Transfer length of Plant D Mix 5/RF 5 Tie 9A Cast 1

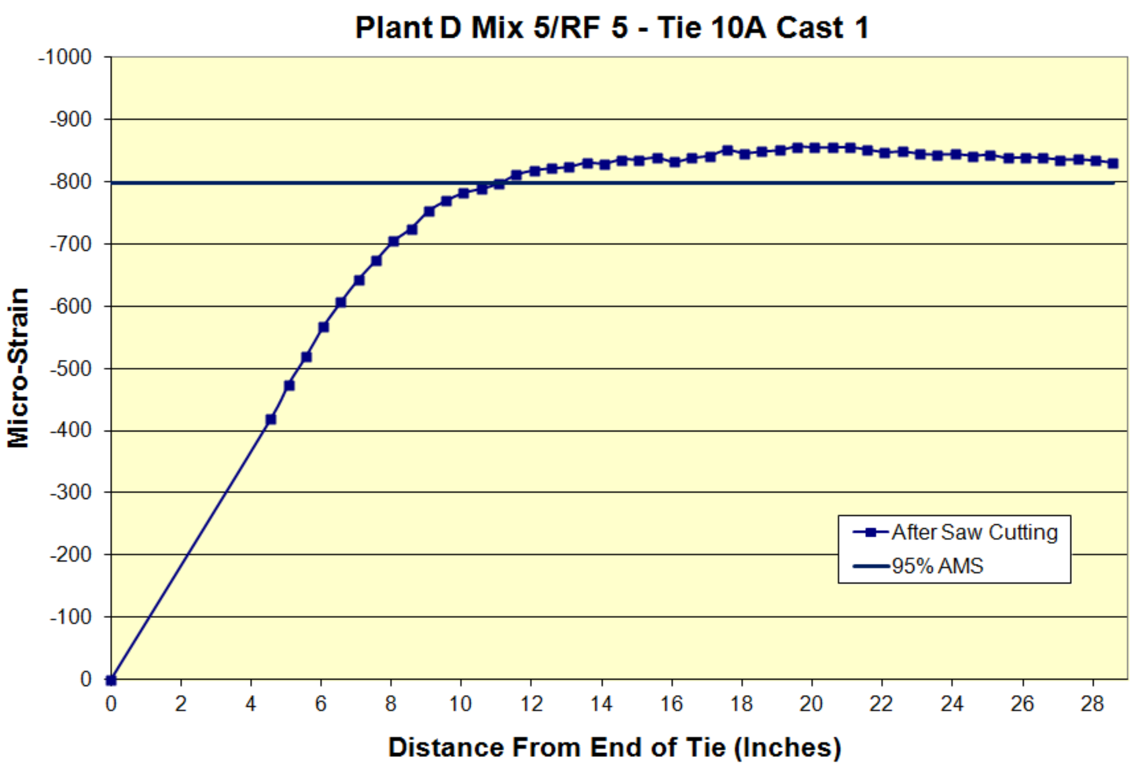

Figure D.8 Transfer length of Plant D Mix 5/RF 5 Tie 10A Cast 1

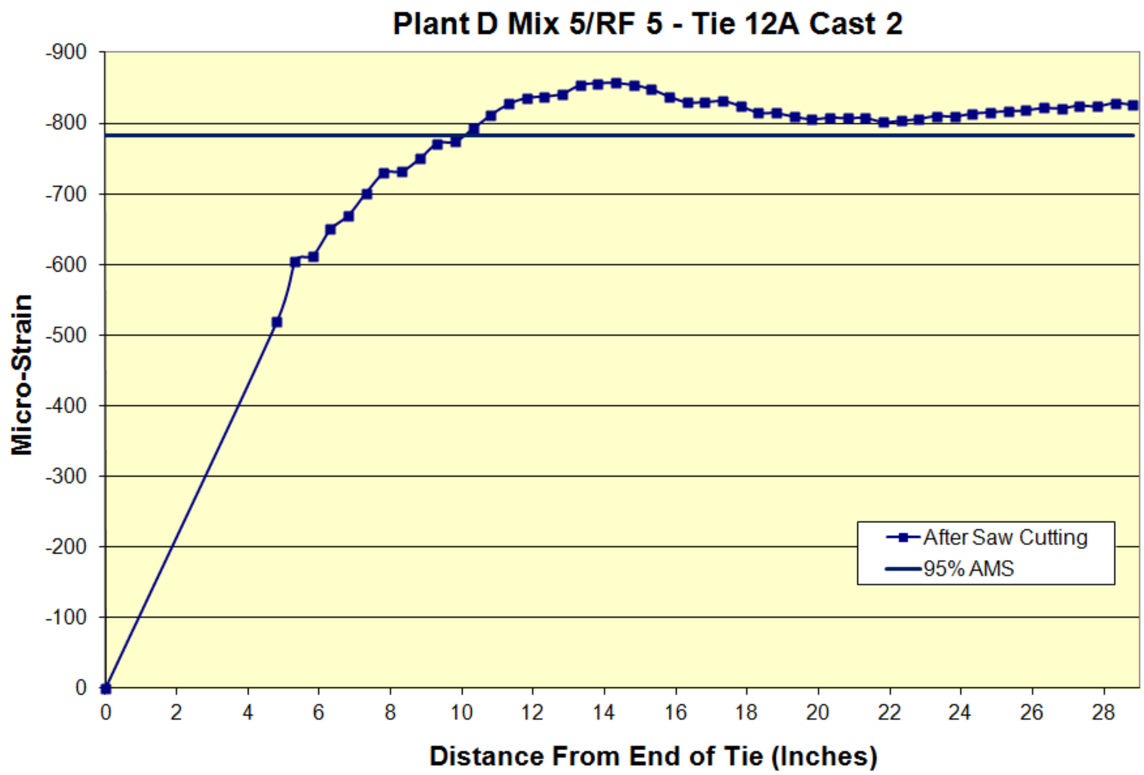

Figure D.9 Transfer length of Plant D Mix 5/RF 5 Tie 12A Cast 2

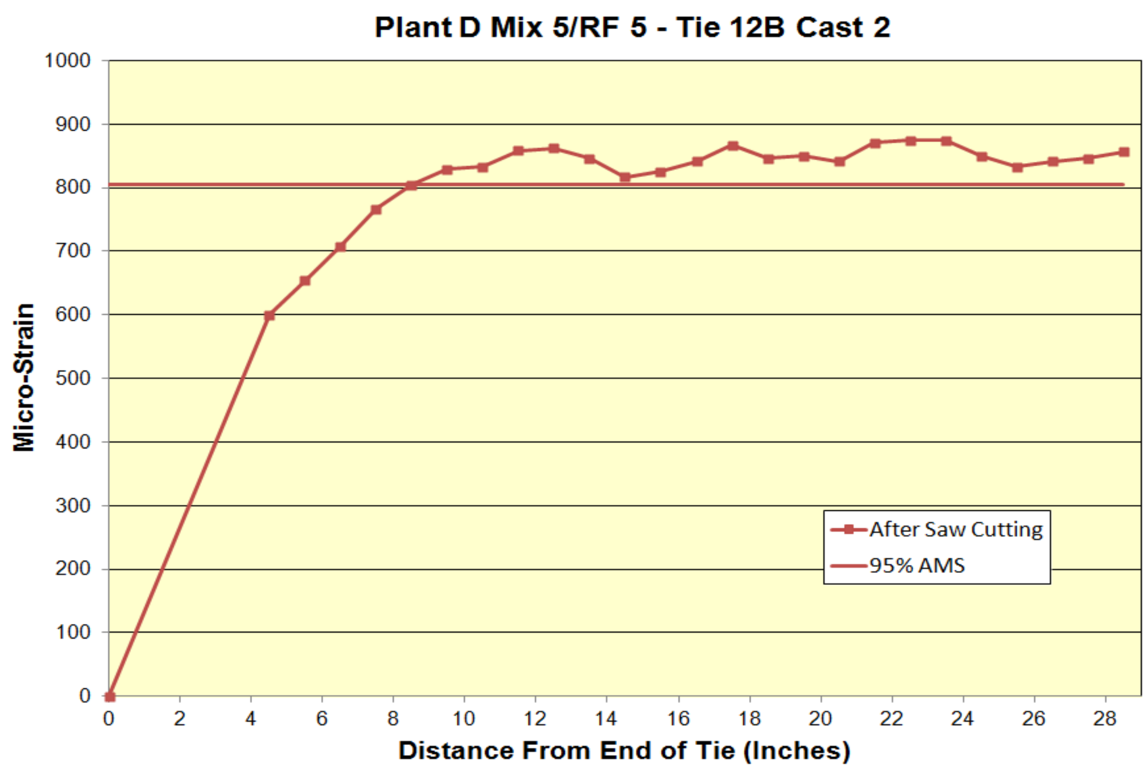

Figure D.10 Transfer length of Plant D Mix 5/RF 5 Tie 12B Cast 2

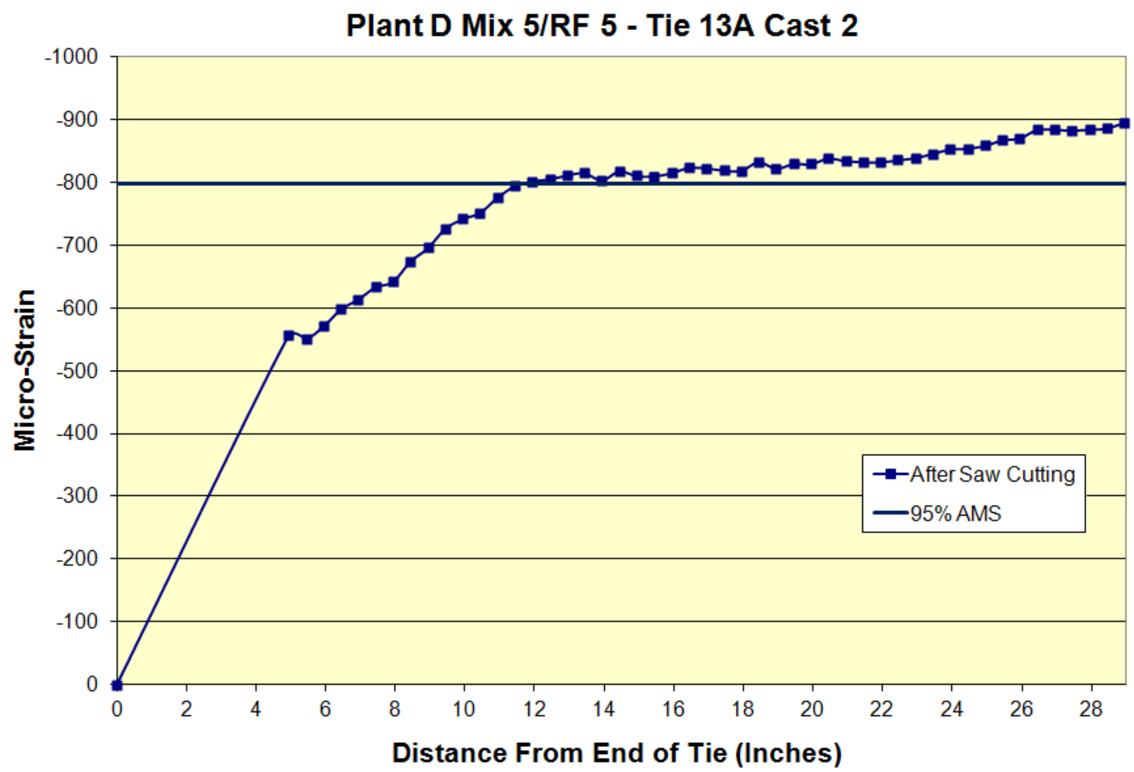

Figure D.11 Transfer length of Plant D Mix 5/RF 5 Tie 13A Cast 2

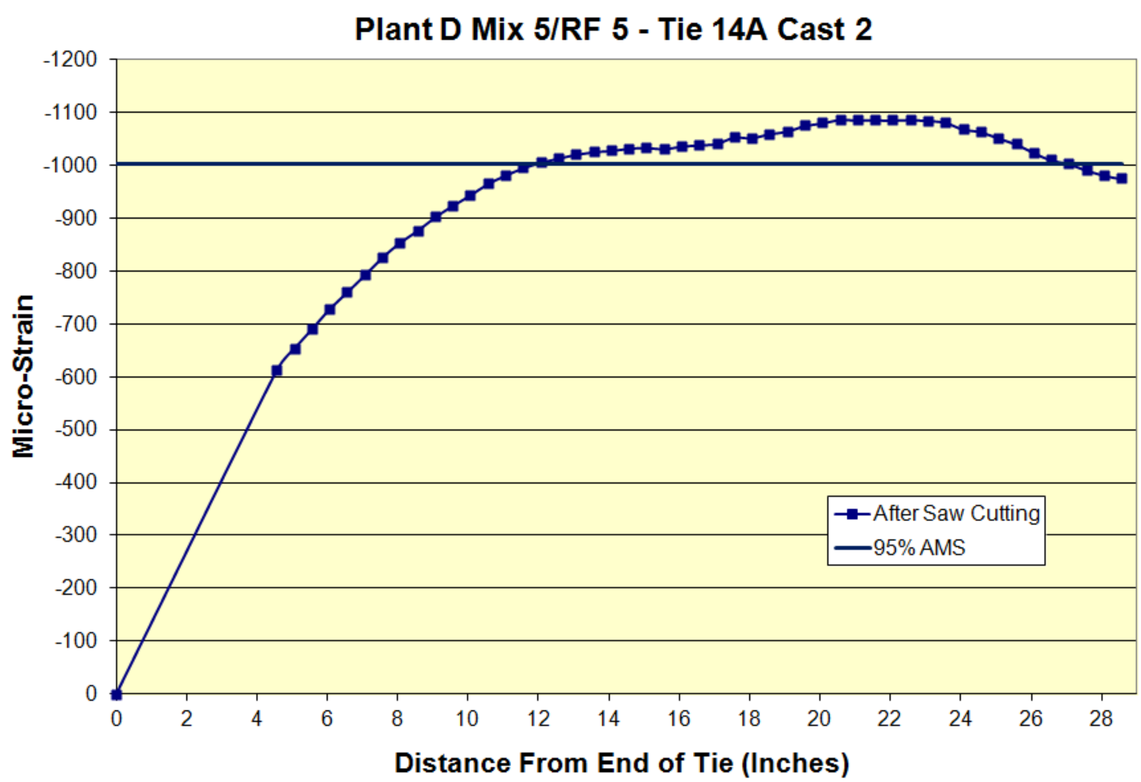

Figure D.12 Transfer length of Plant D Mix 5/RF 5 Tie 14A Cast 2

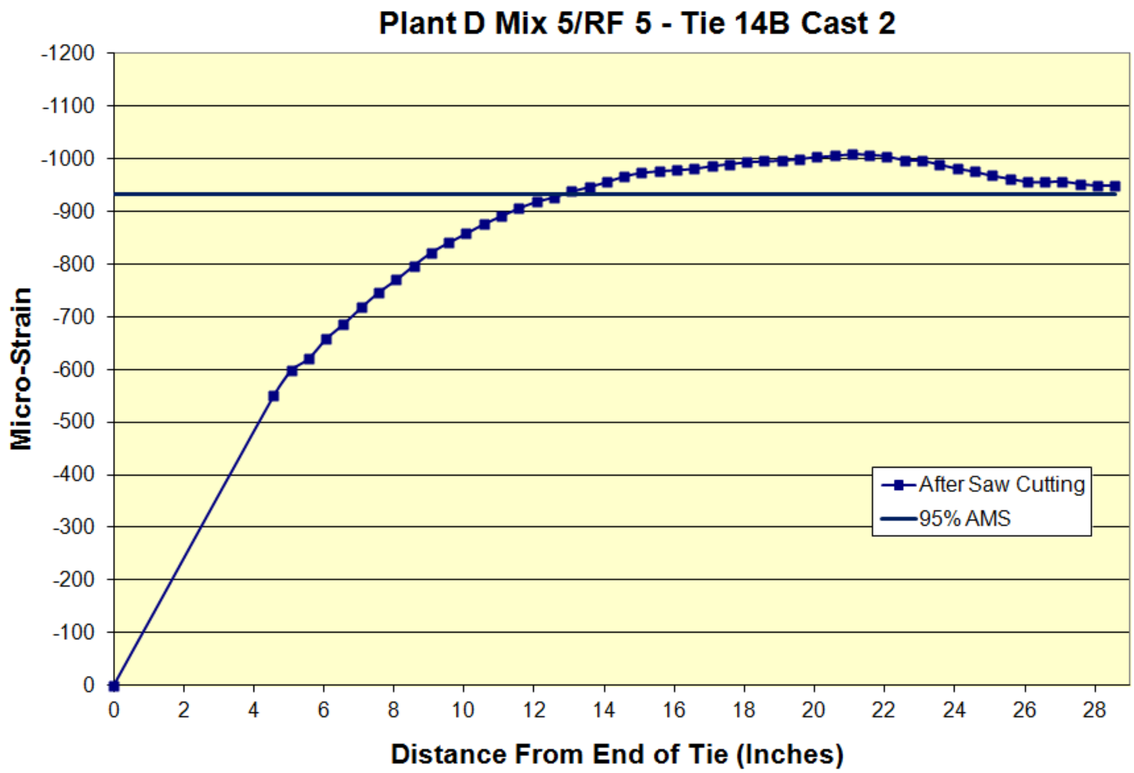

Figure D.13 Transfer length of Plant D Mix 5/RF 5 Tie 14B Cast 2

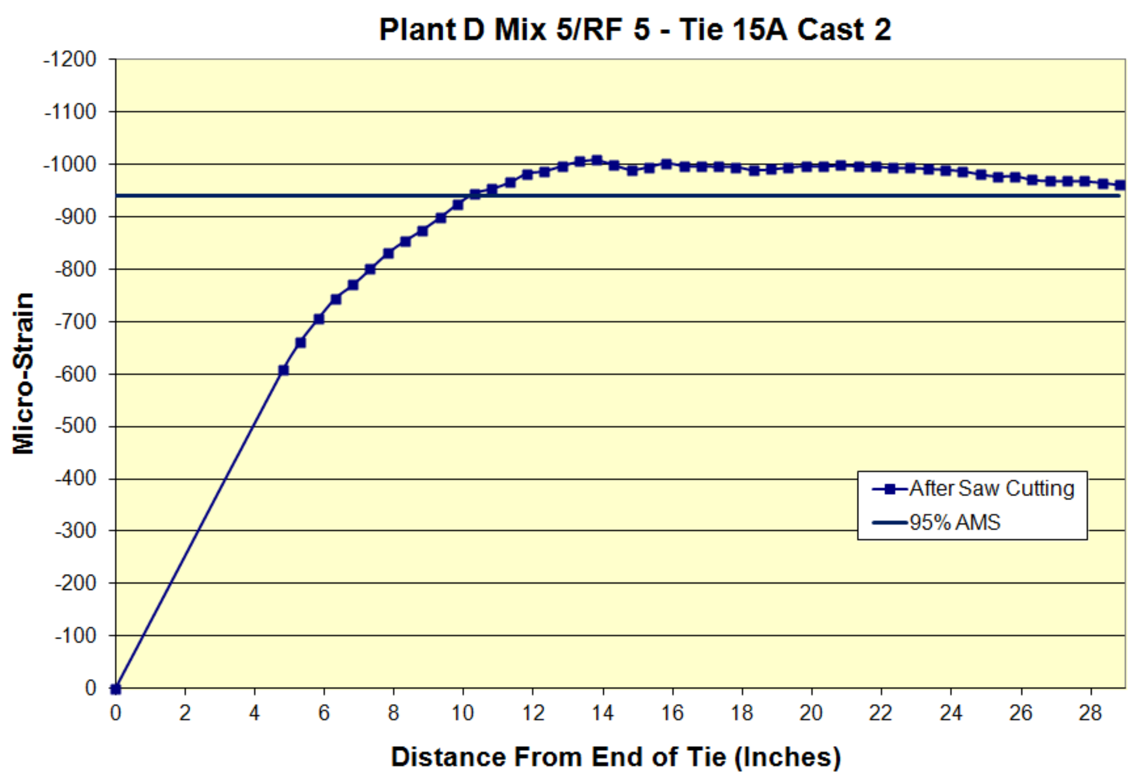

Figure D.14 Transfer length of Plant D Mix 5/RF 5 Tie 15A Cast 2

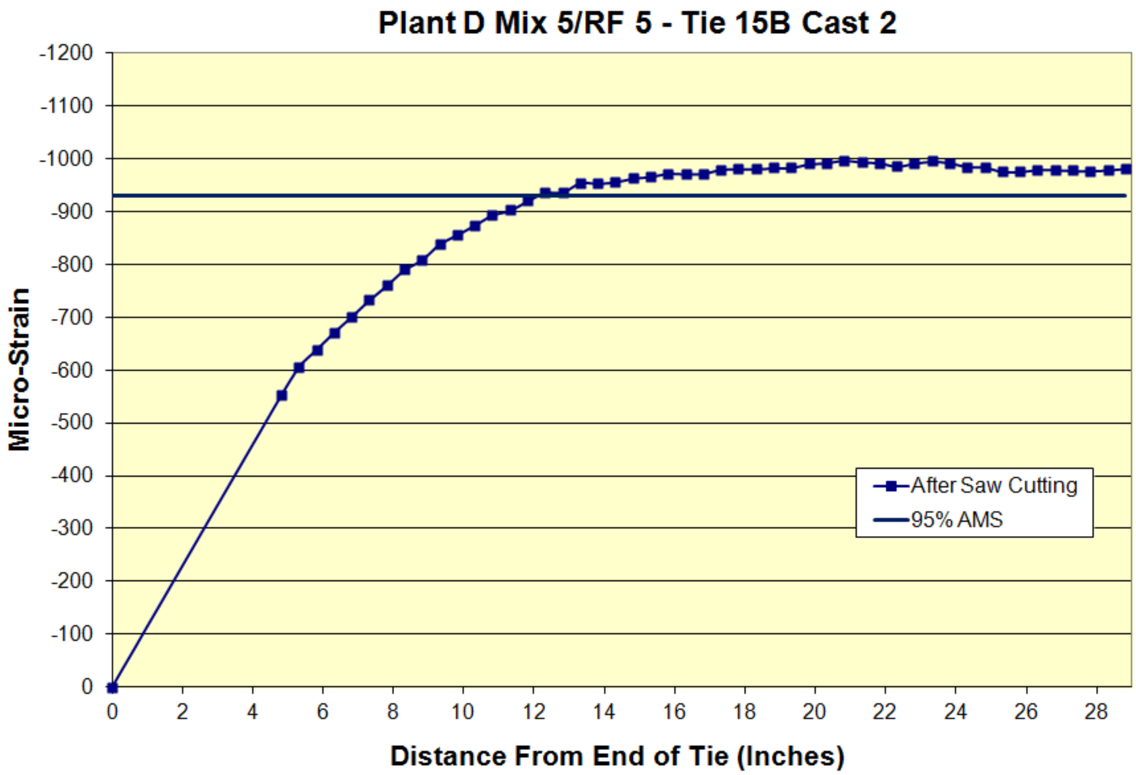

Figure D.15 Transfer length of Plant D Mix 5/RF 5 Tie 15B Cast 2

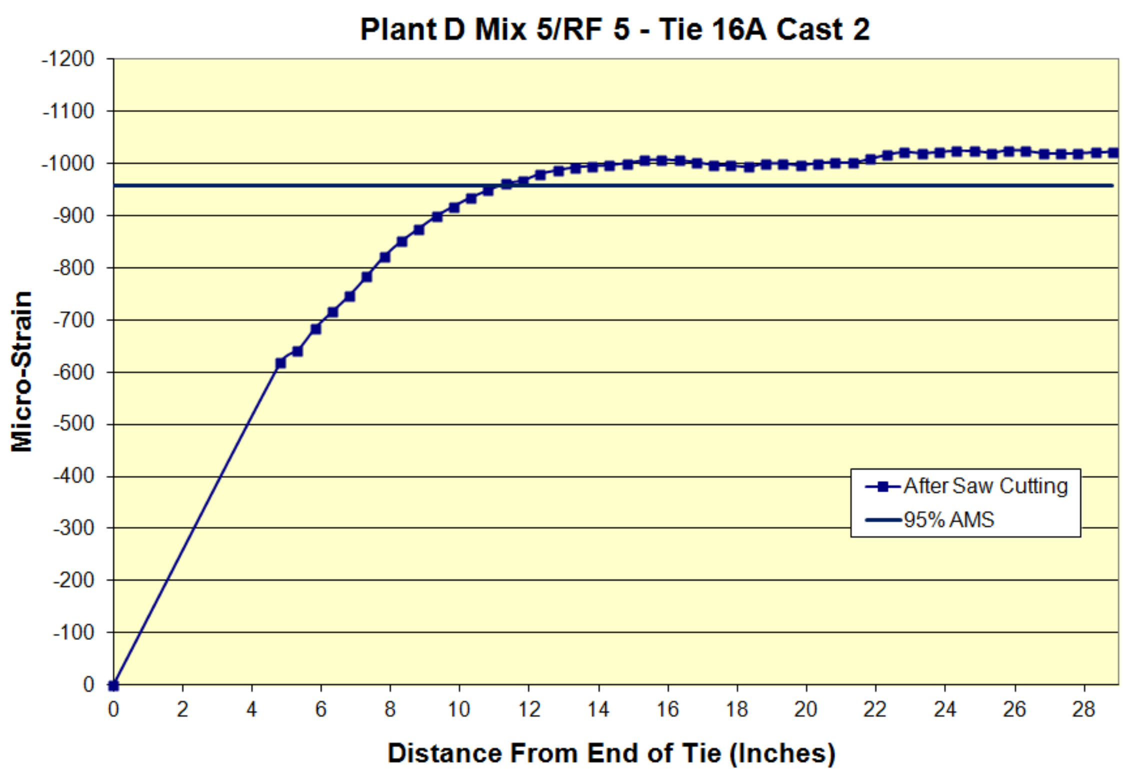

Figure D.16 Transfer length of Plant D Mix 5/RF 5 Tie 16A Cast 2

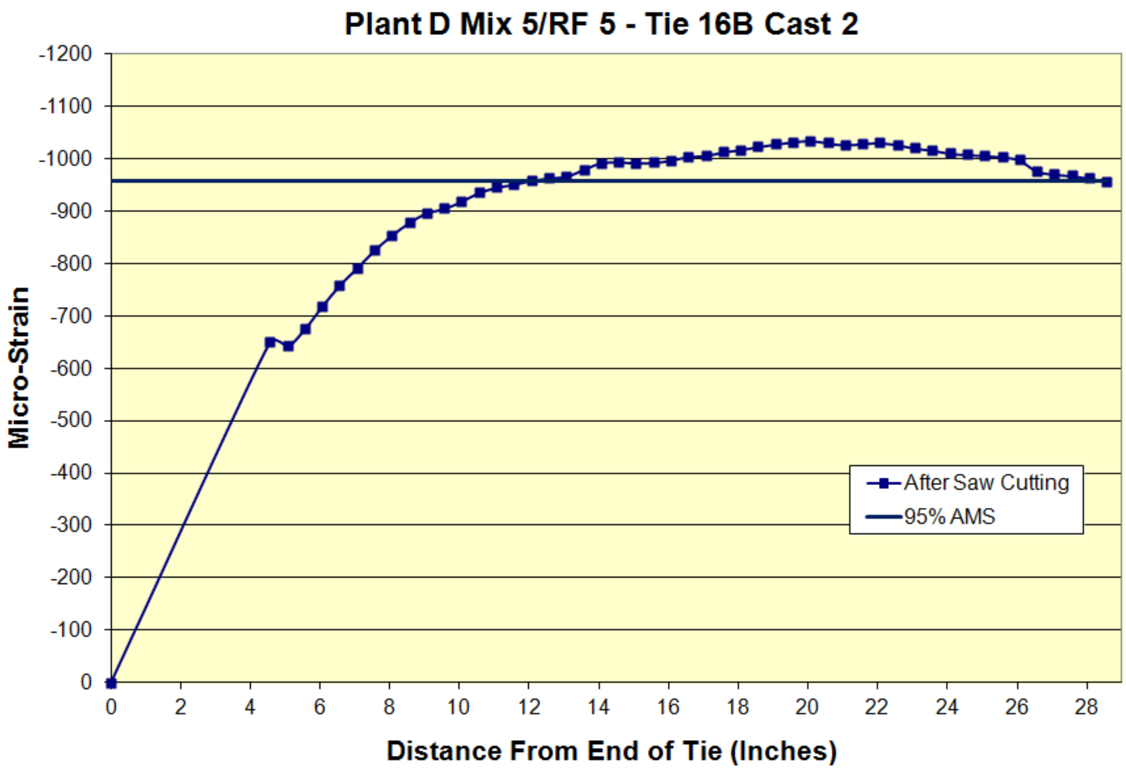

Figure D.17 Transfer length of Plant D Mix 5/RF 5 Tie 16B Cast 2

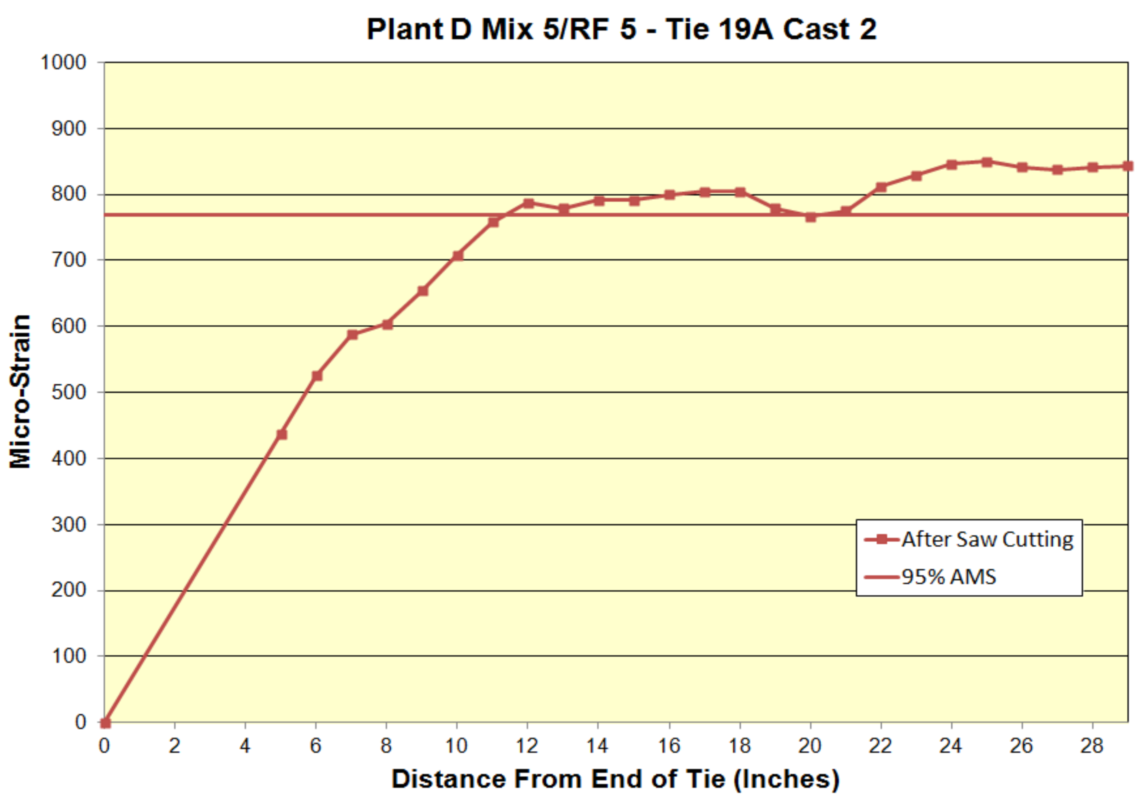

Figure D.18 Transfer length of Plant D Mix 5/RF 5 Tie 19A Cast 2

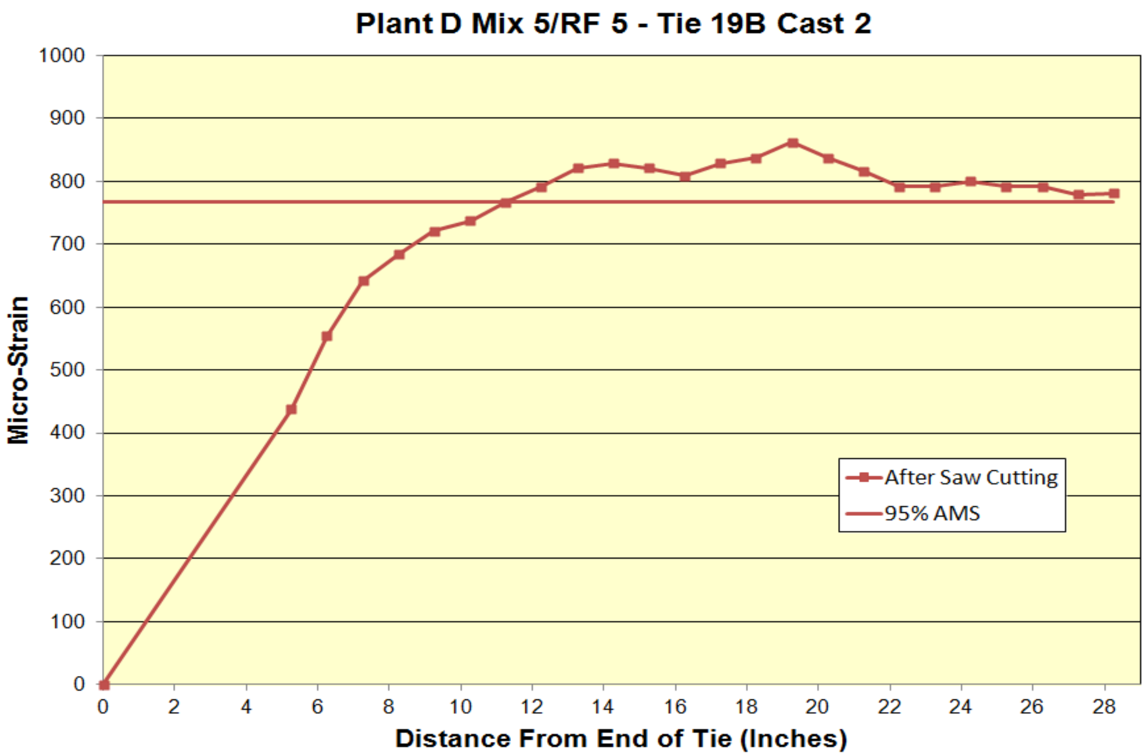

Figure D.19 Transfer length of Plant D Mix 5/RF 5 Tie 19B Cast 2

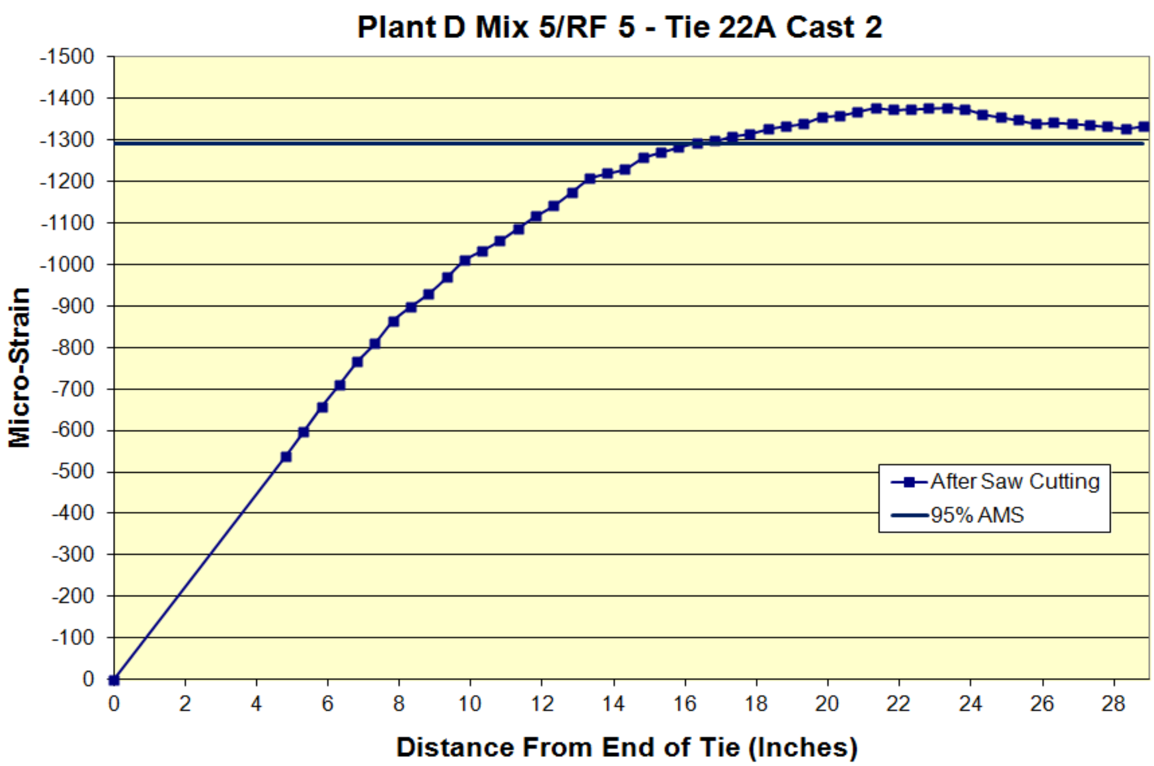

Figure D.20 Transfer length of Plant D Mix 5/RF 5 Tie 22A Cast 2

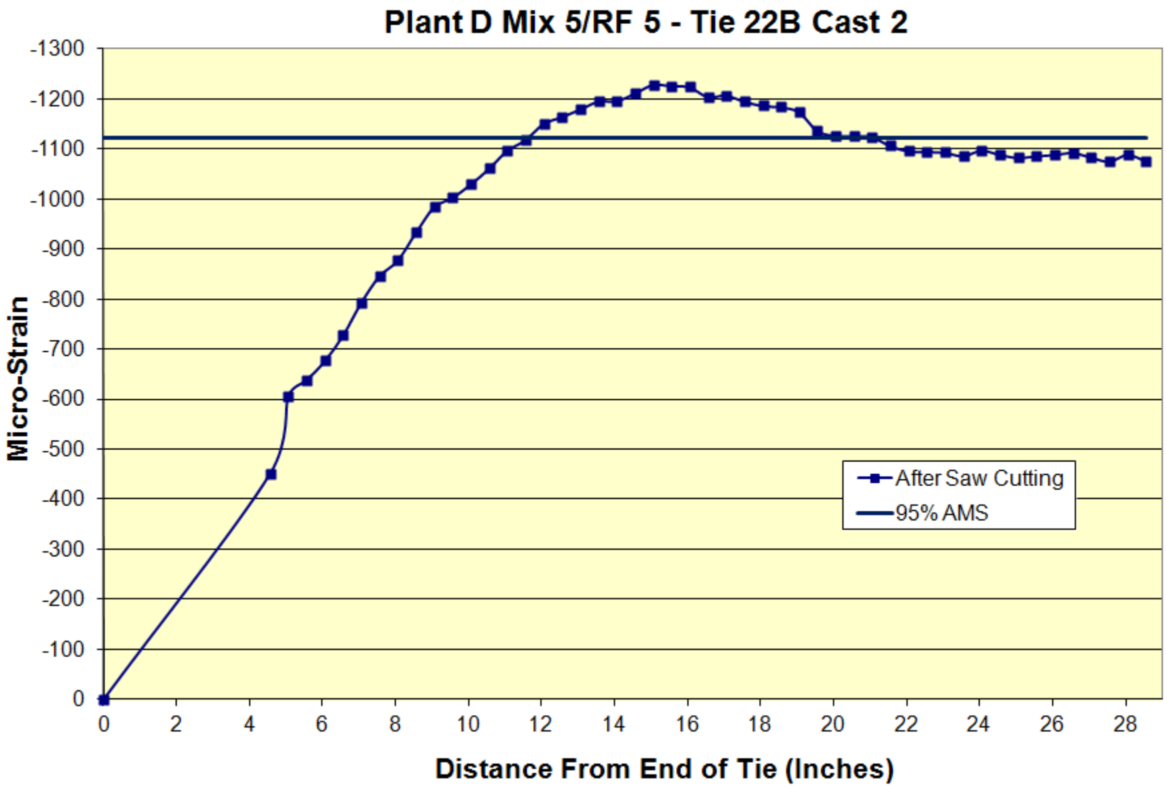

Figure D.21 Transfer length of Plant D Mix 5/RF 5 Tie 22B Cast 2

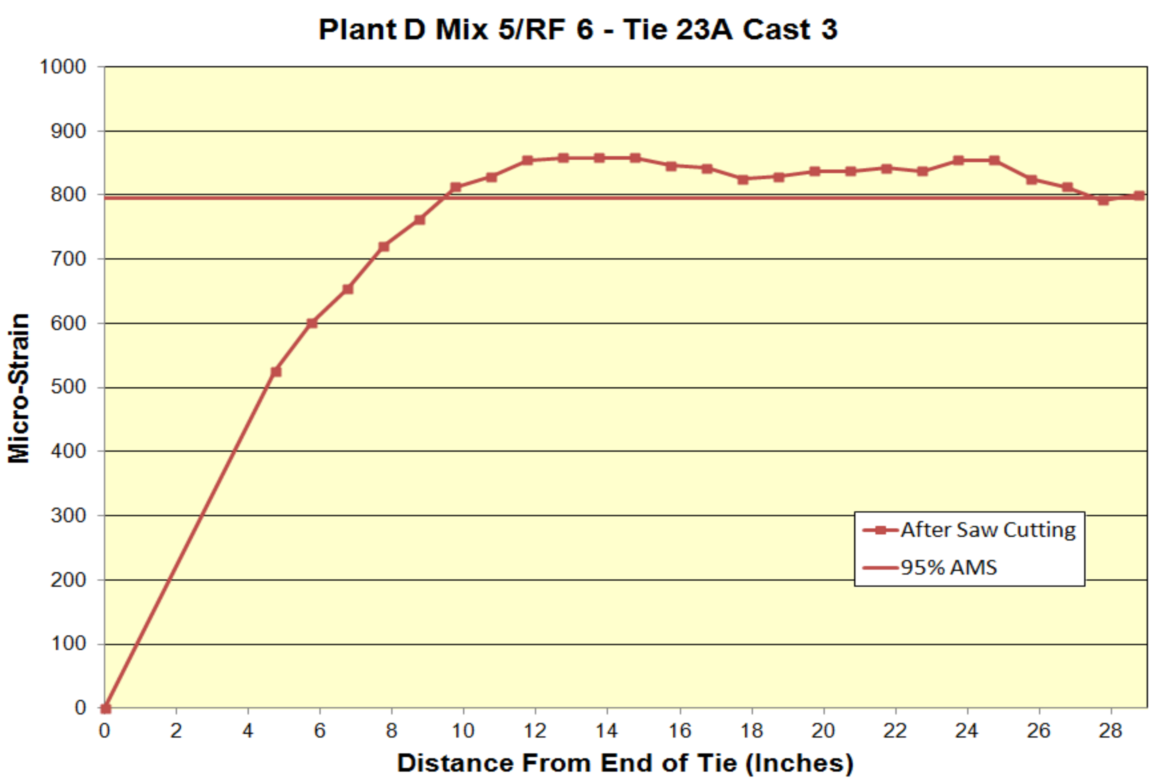

Figure D.22 Transfer length of Plant D Mix 5/RF 6 Tie 23A Cast 3

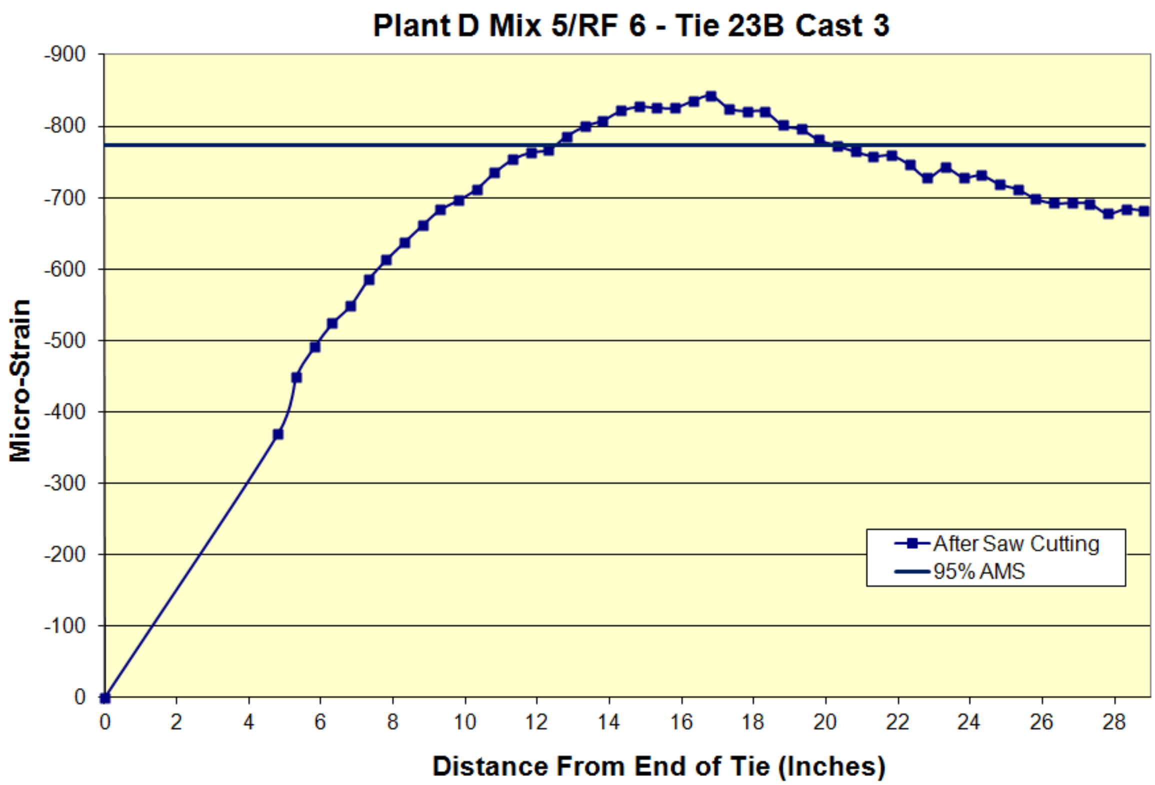

Figure D.23 Transfer length of Plant D Mix 5/RF 6 Tie 23B Cast 3

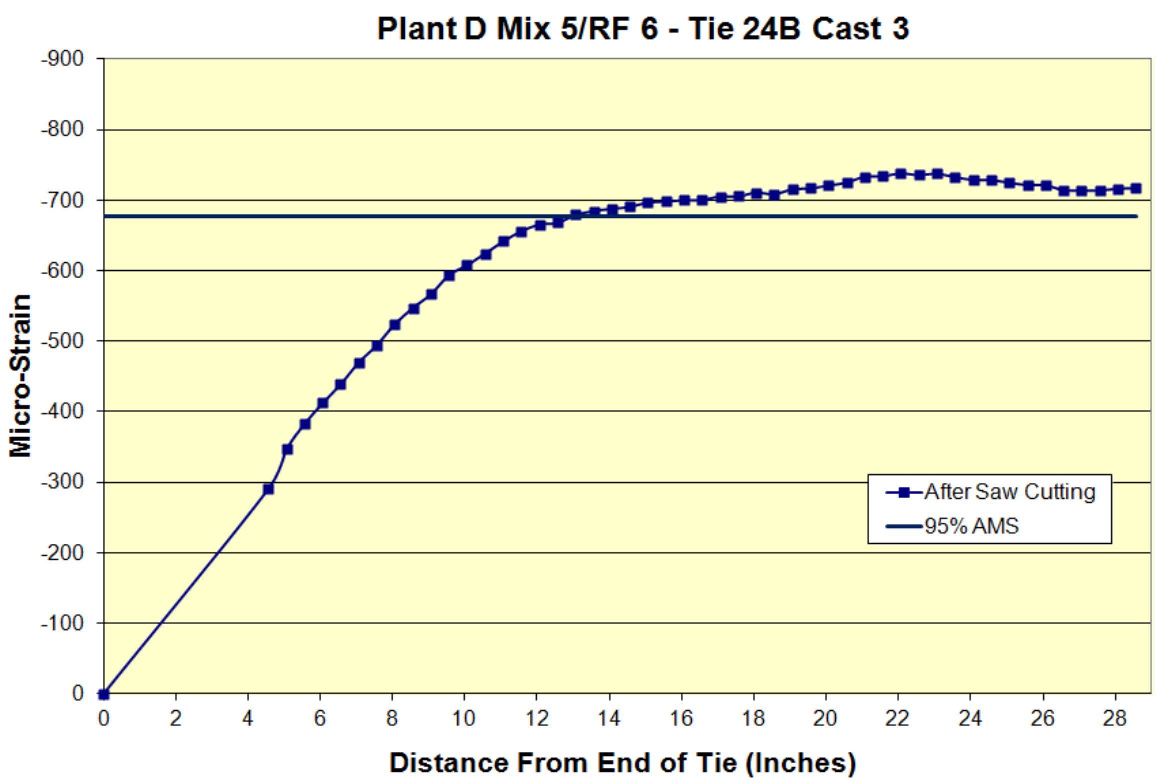

Figure D.24 Transfer length of Plant D Mix 5/RF 6 Tie 24B Cast 3

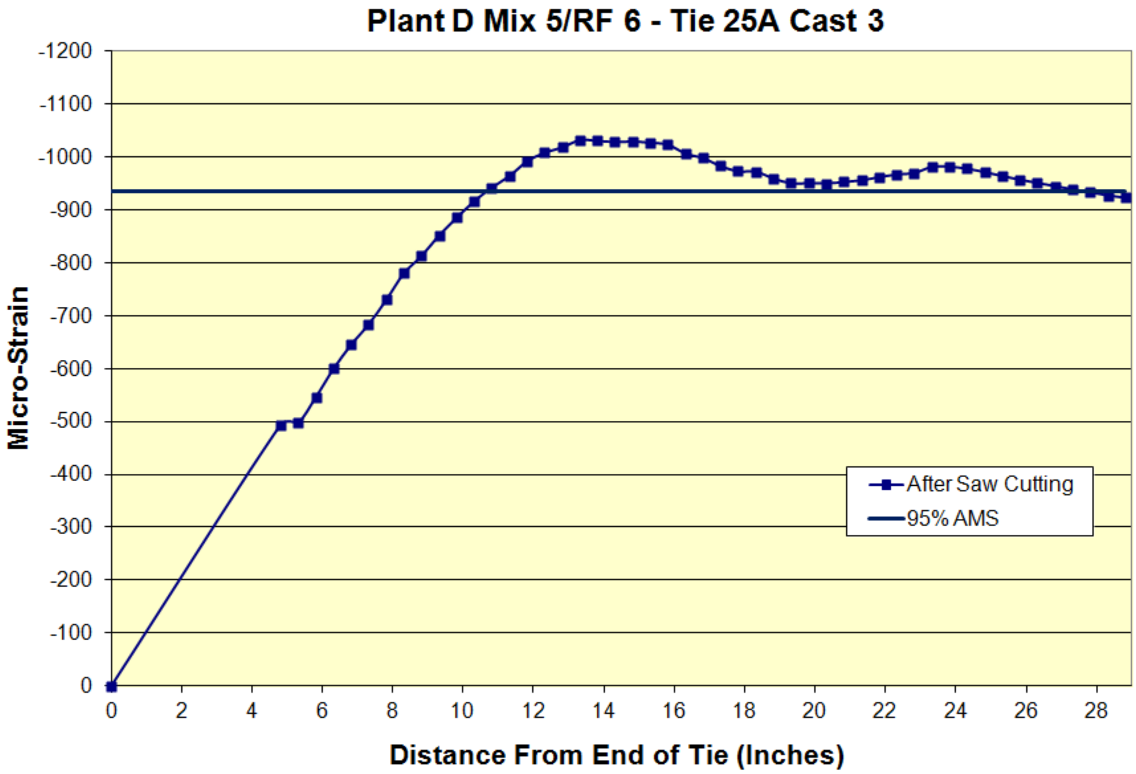

Figure D.25 Transfer length of Plant D Mix 5/RF 6 Tie 25A Cast 3

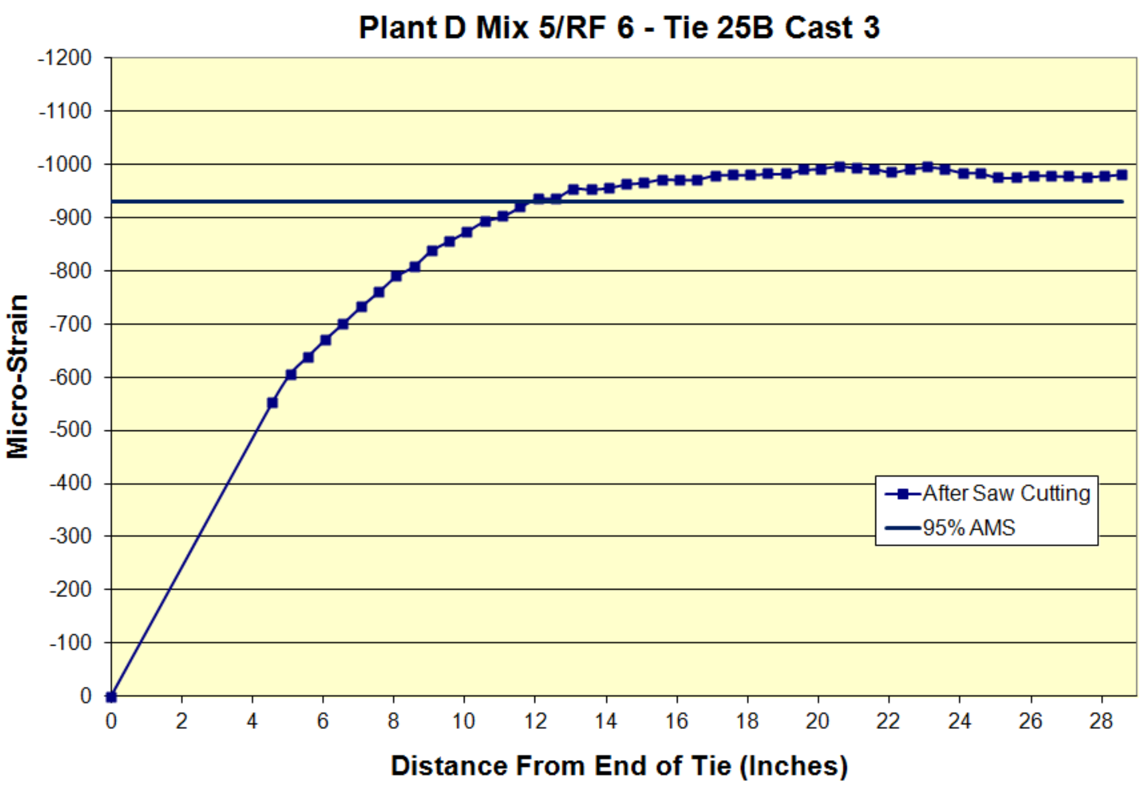

Figure D.26 Transfer length of Plant D Mix 5/RF 6 Tie 25B Cast 3

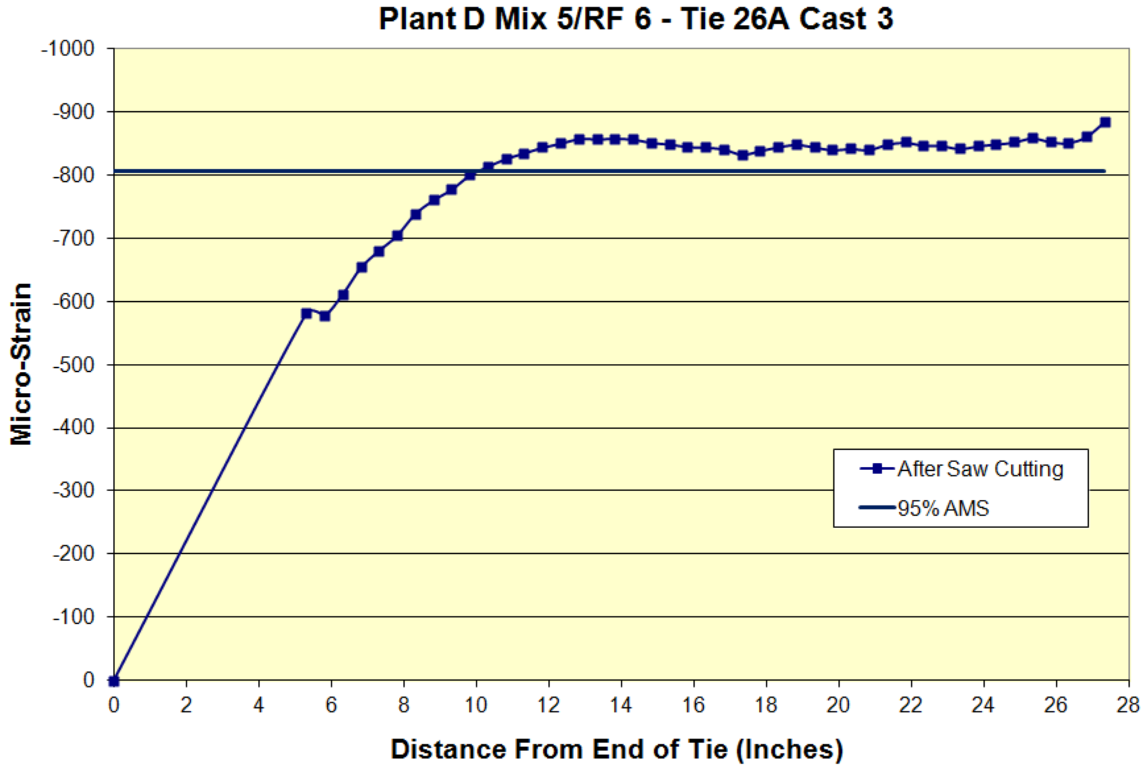

Figure D.27 Transfer length of Plant D Mix 5/RF 6 Tie 26A Cast 3

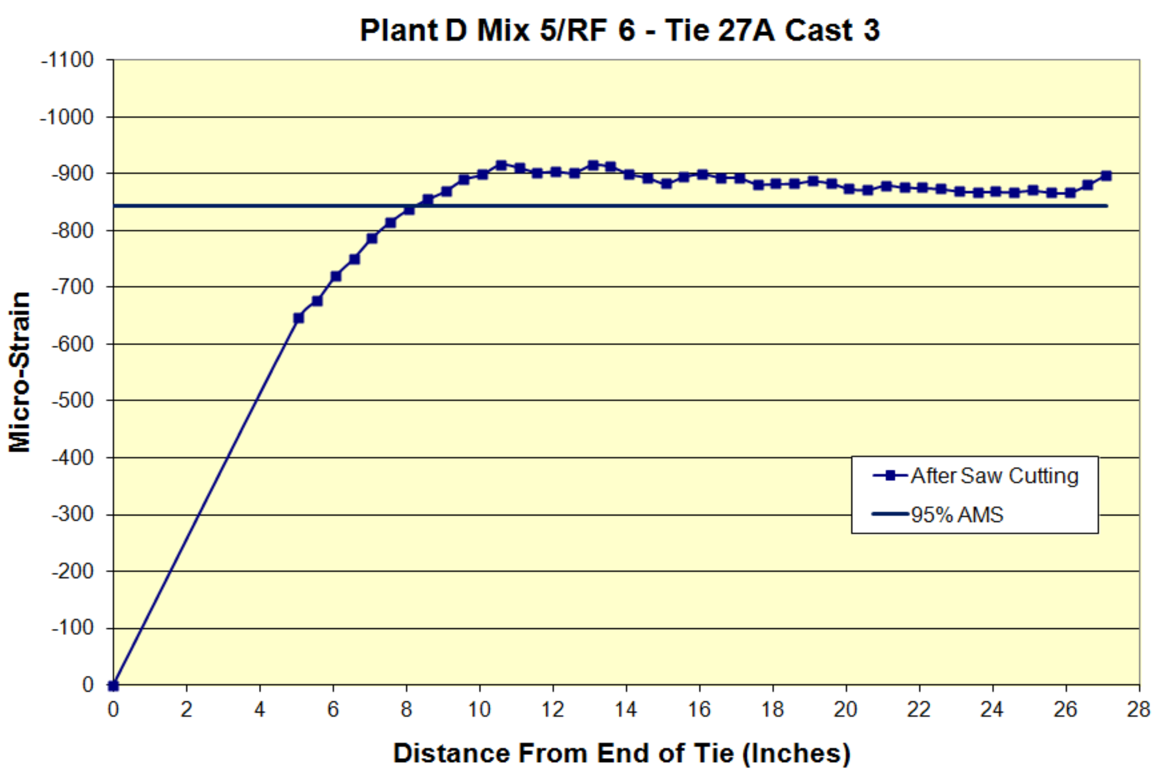

Figure D.28 Transfer length of Plant D Mix 5/RF 6 Tie 27A Cast 3

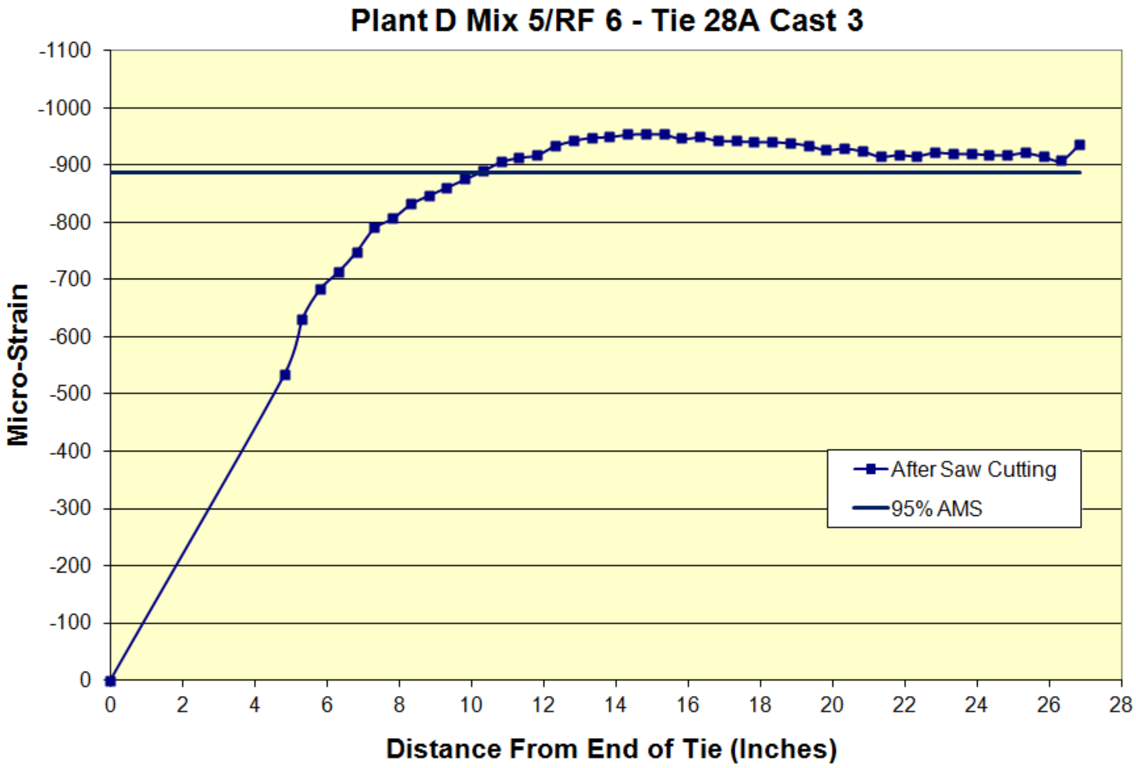

Figure D.29 Transfer length of Plant D Mix 5/RF 6 Tie 28A Cast 3

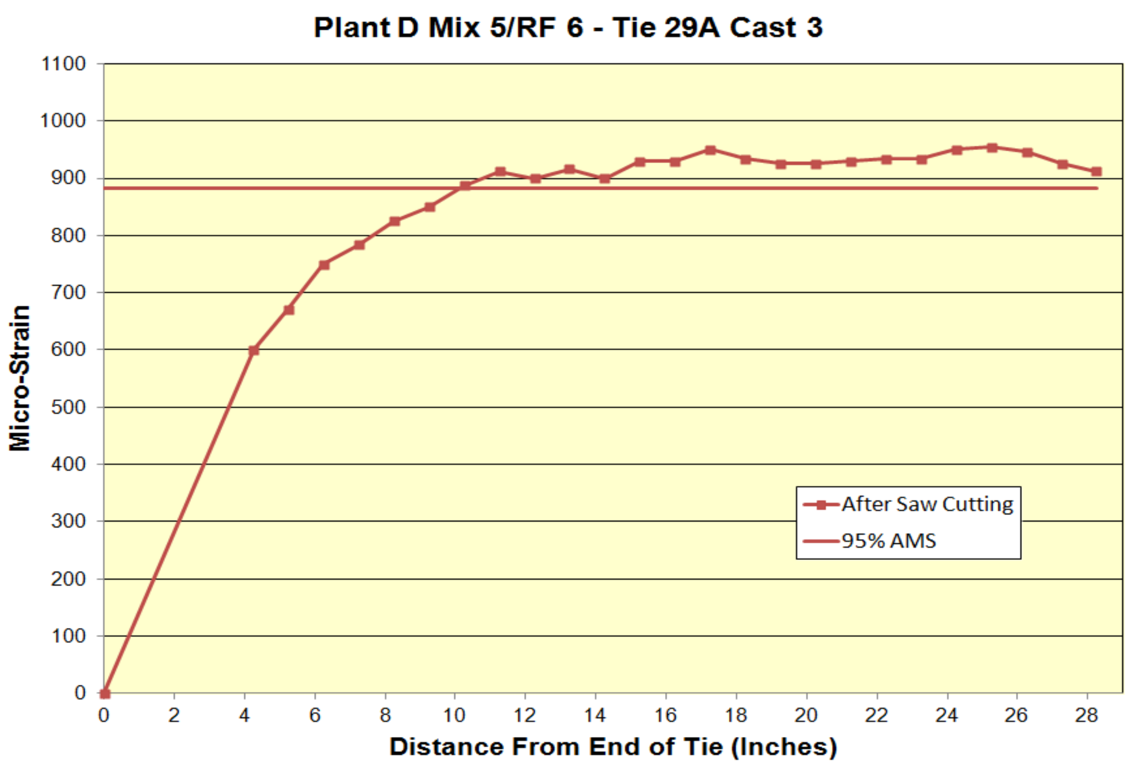

Figure D.30 Transfer length of Plant D Mix 5/RF 6 Tie 29A Cast 3

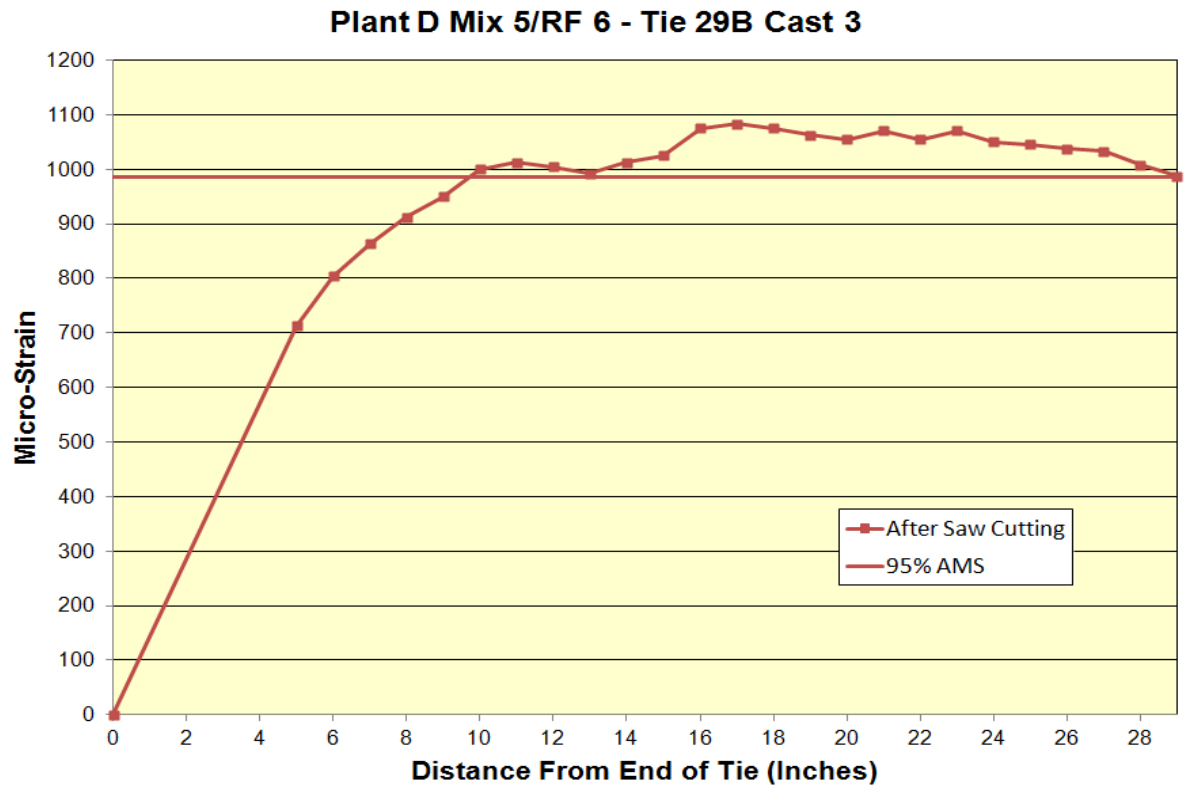

Figure D.31 Transfer length of Plant D Mix 5/RF 6 Tie 29B Cast 3

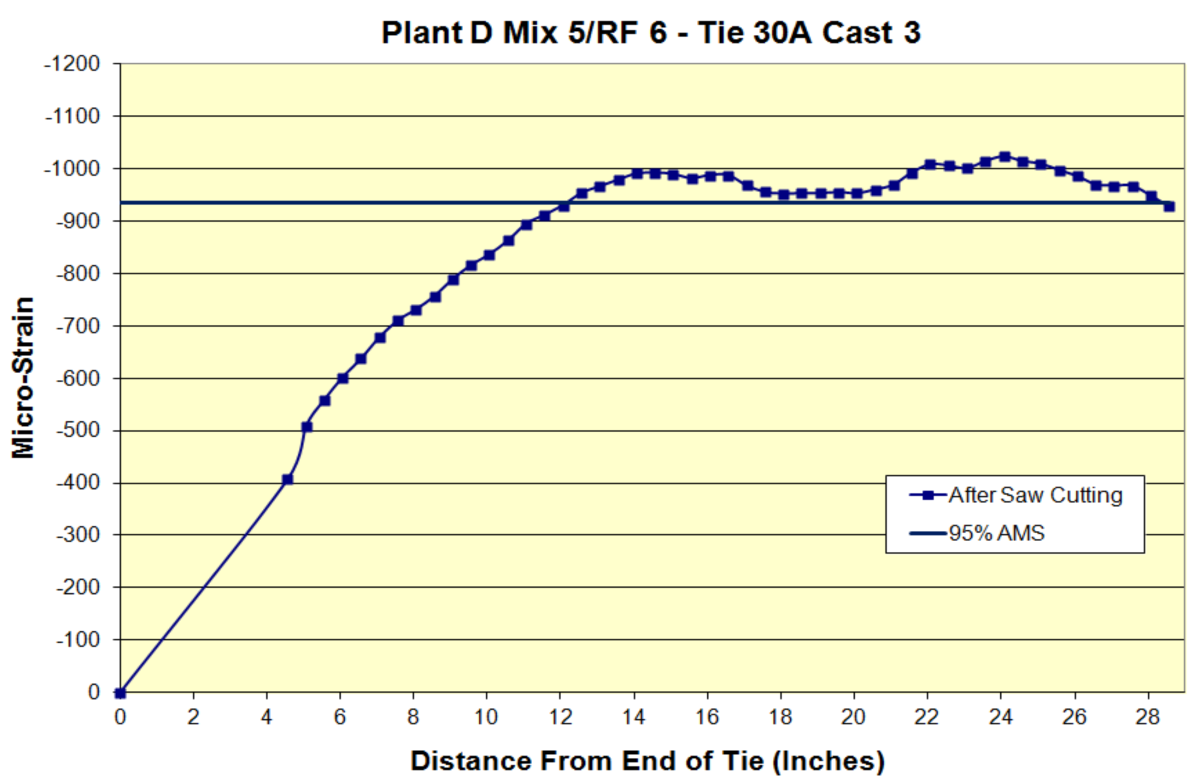

Figure D.32 Transfer length of Plant D Mix 5/RF 6 Tie 30A Cast 3

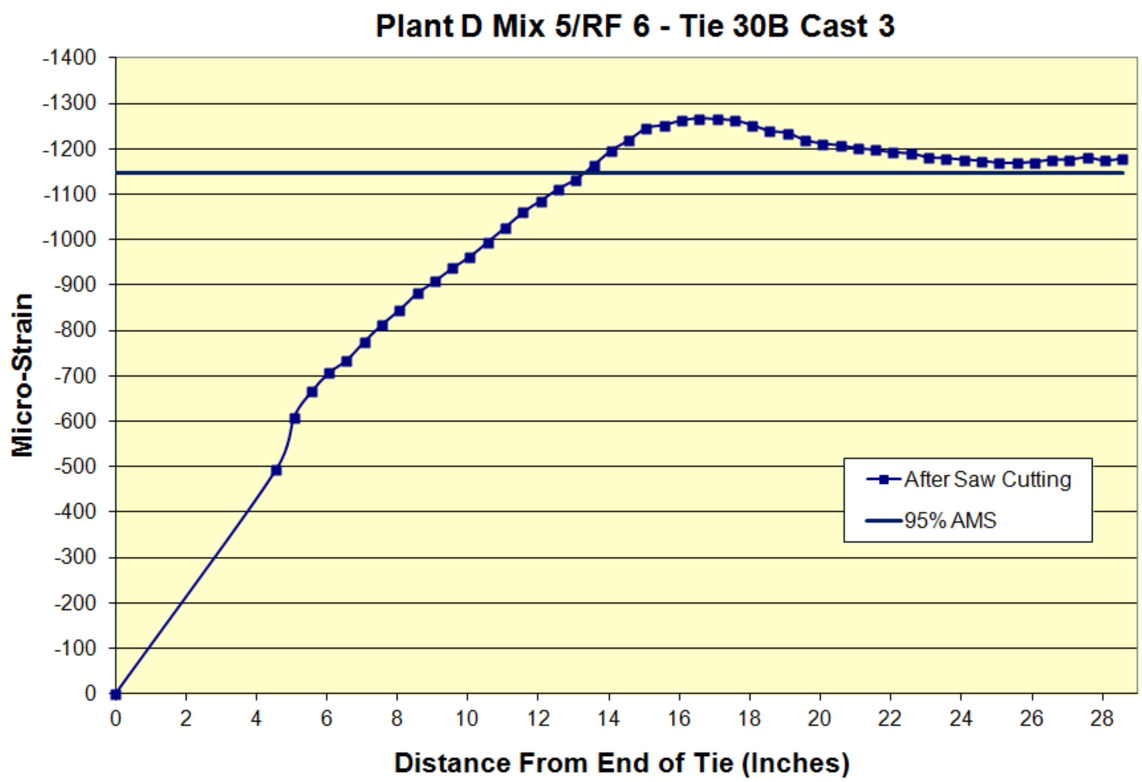

Figure D.33 Transfer length of Plant D Mix 5/RF 6 Tie 30B Cast 3

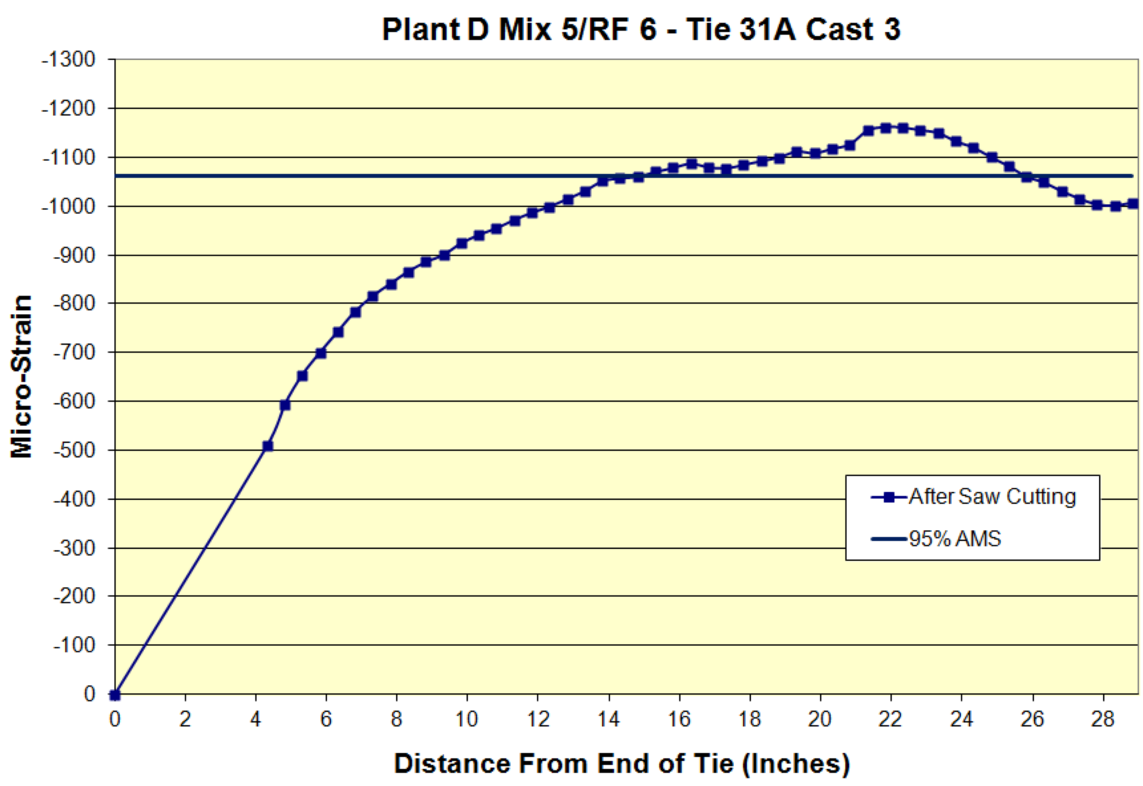

Figure D.34 Transfer length of Plant D Mix 5/RF 6 Tie 31A Cast 3

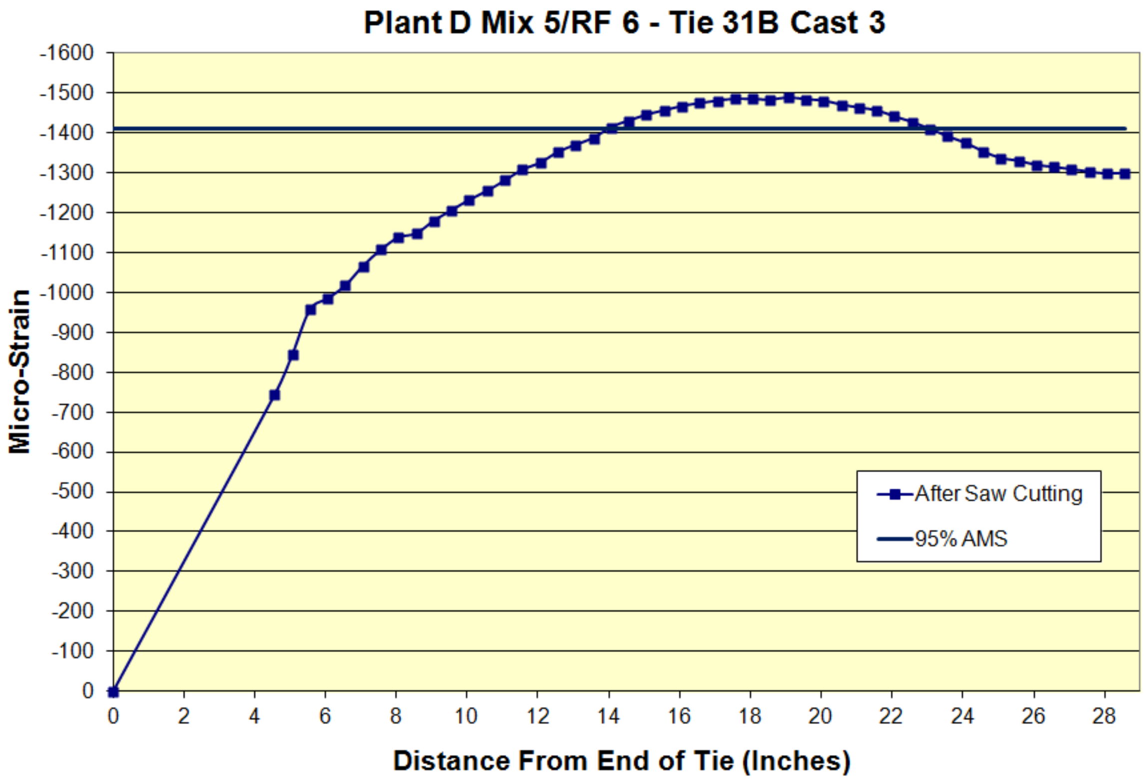

Figure D.35 Transfer length of Plant D Mix 5/RF 6 Tie 31B Cast 3

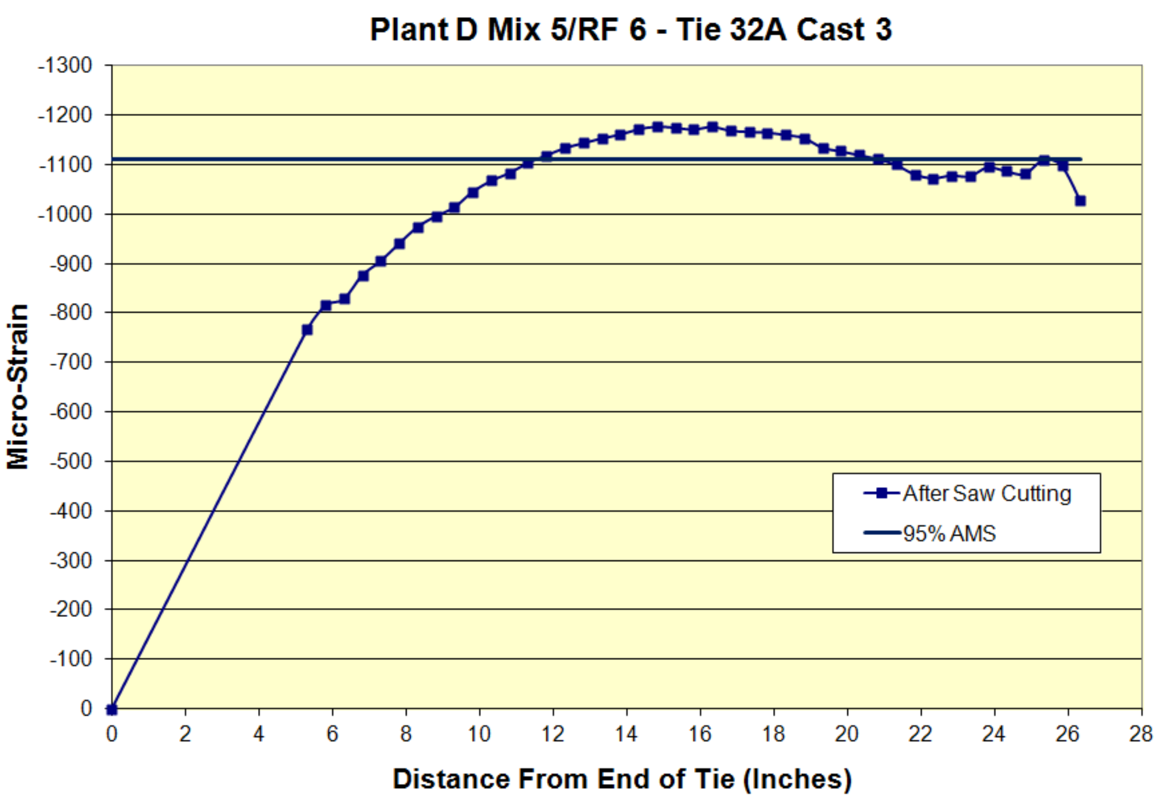

Figure D.36 Transfer length of Plant D Mix 5/RF 6 Tie 32A Cast 3

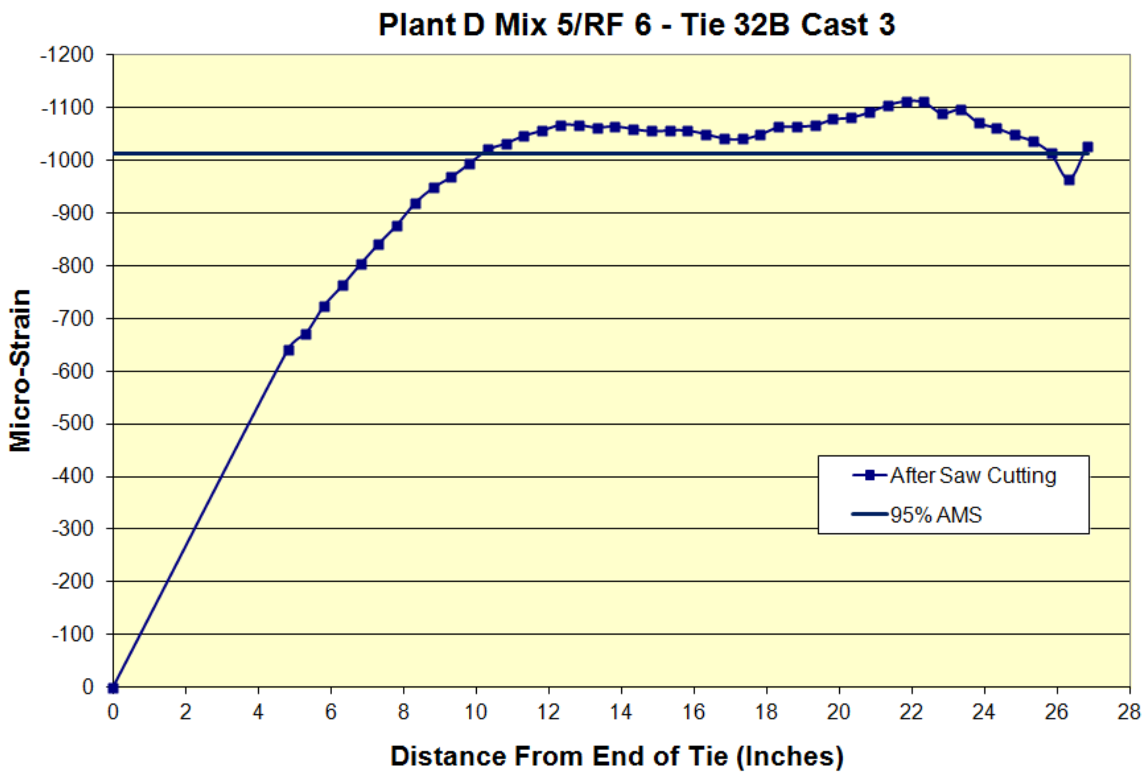

Figure D.37 Transfer length of Plant D Mix 5/RF 6 Tie 32B Cast 3

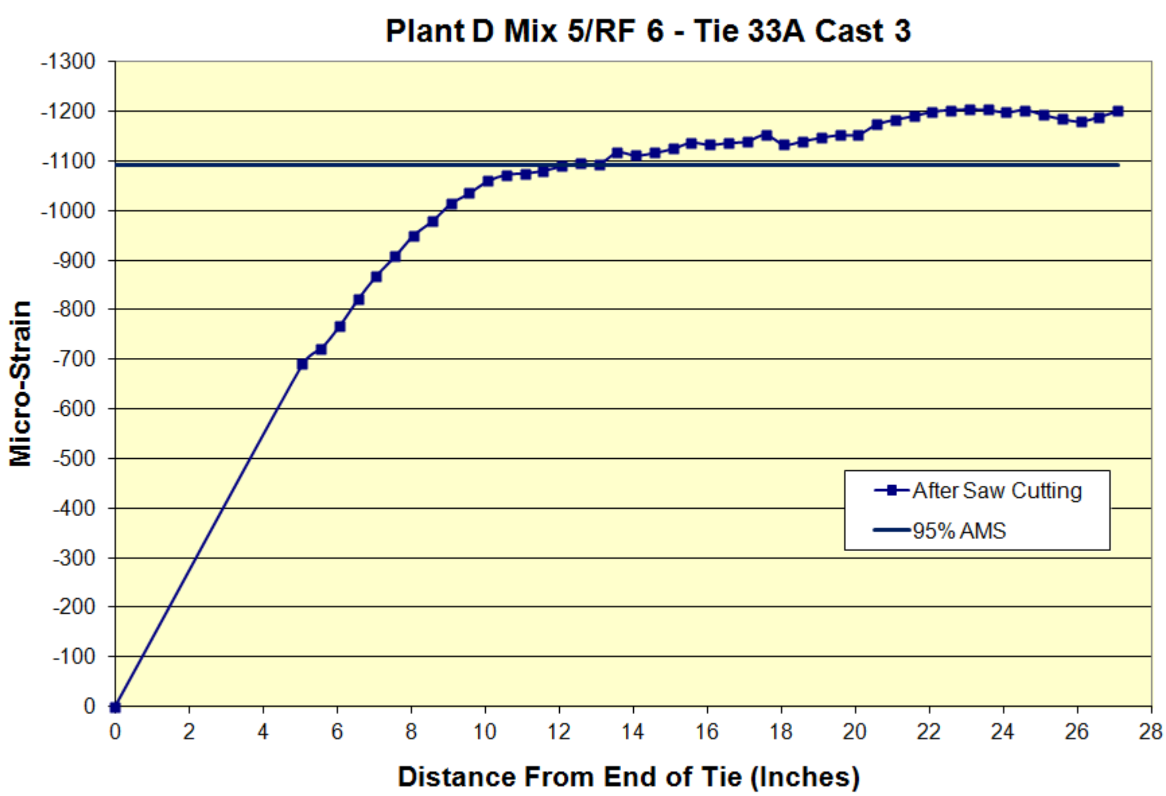

Figure D.38 Transfer length of Plant D Mix 5/RF 6 Tie 33A Cast 3

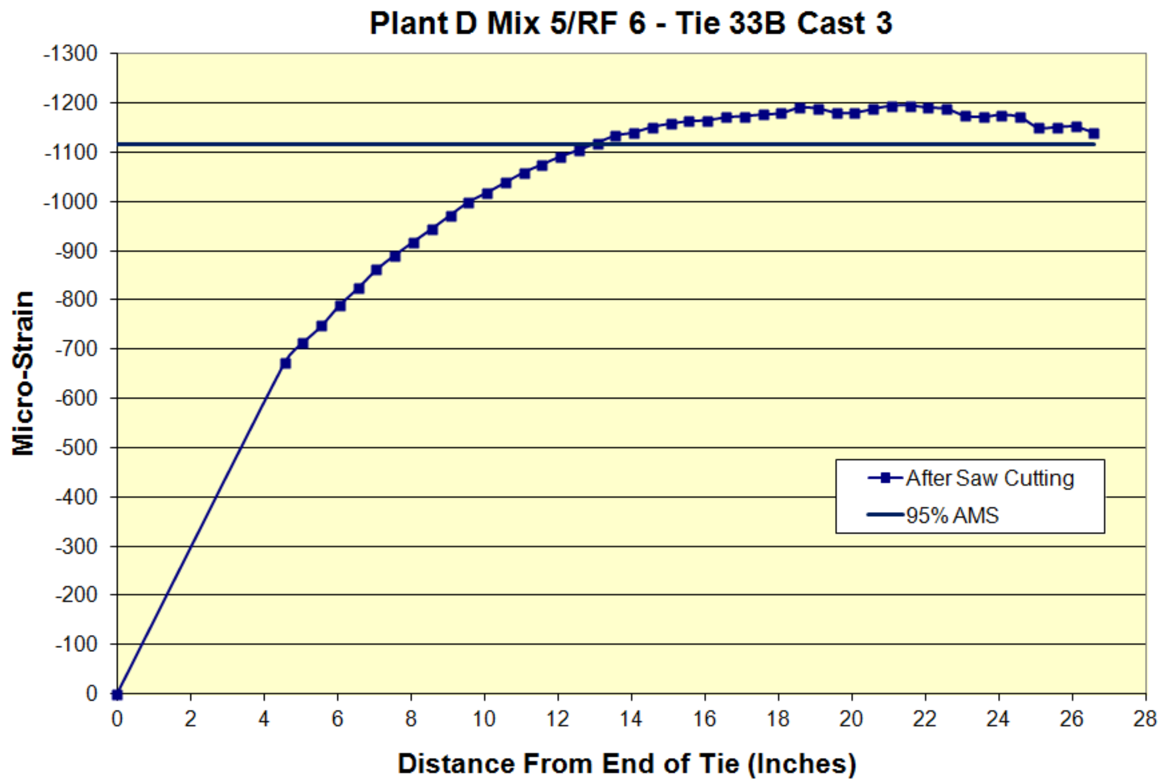

Figure D.39 Transfer length of Plant D Mix 5/RF 6 Tie 33B Cast 3

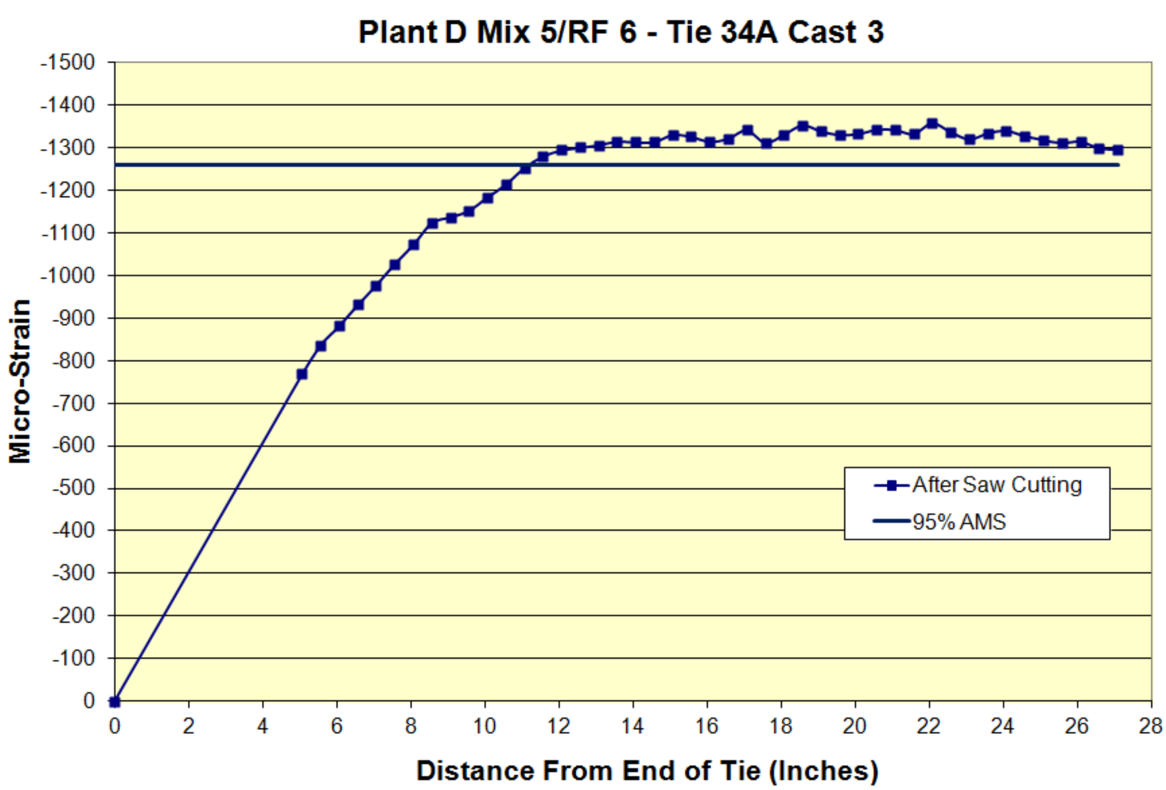

Figure D.40 Transfer length of Plant D Mix 5/RF 6 Tie 34A Cast 3

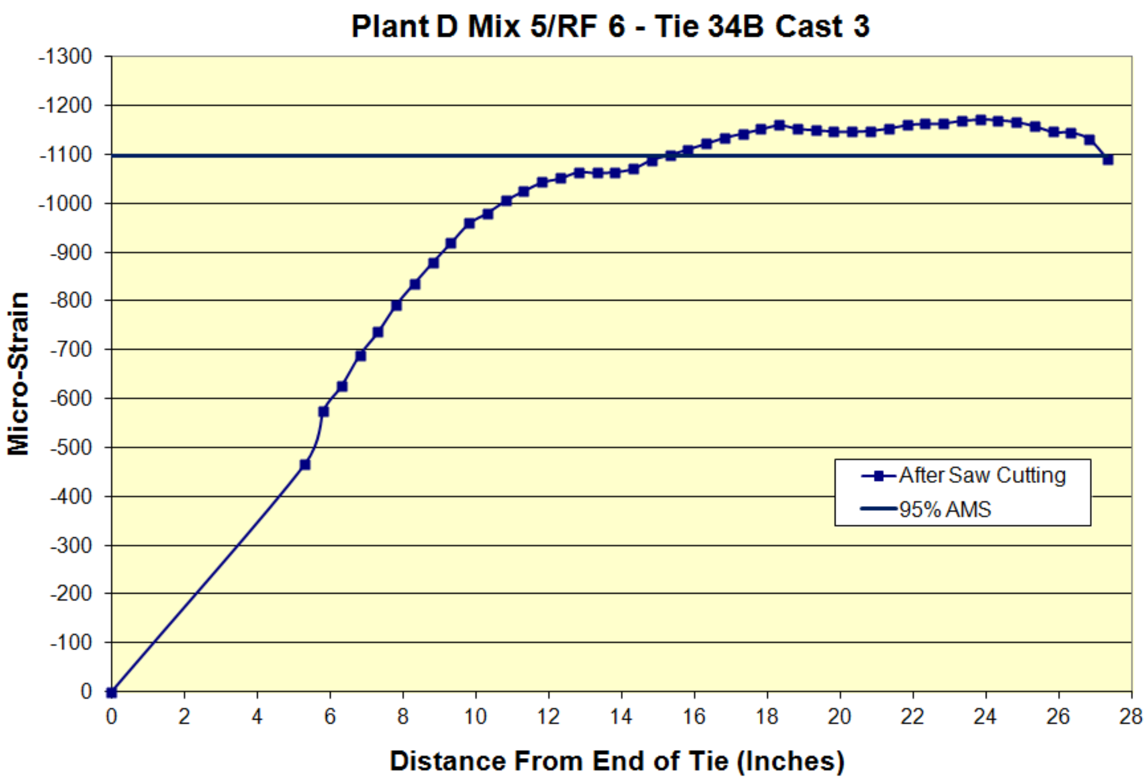

Figure D.41 Transfer length of Plant D Mix 5/RF 6 Tie 34B Cast 3

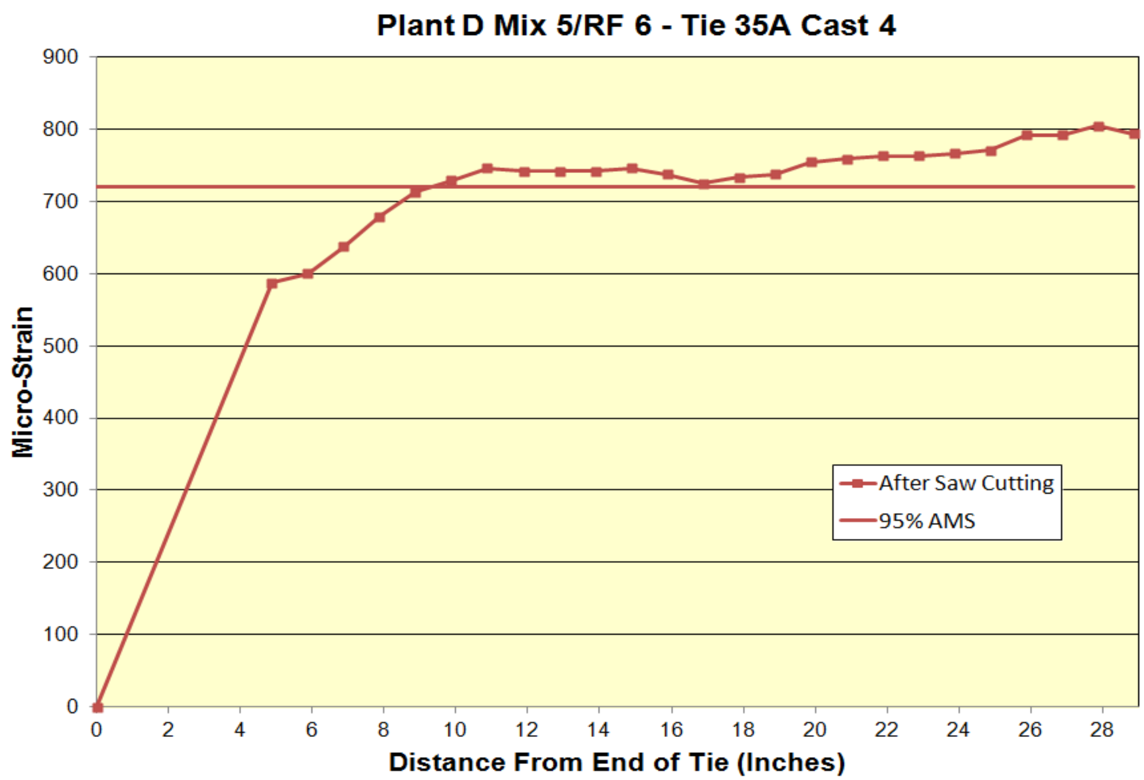

Figure D.42 Transfer length of Plant D Mix 5/RF 6 Tie 35A Cast 4

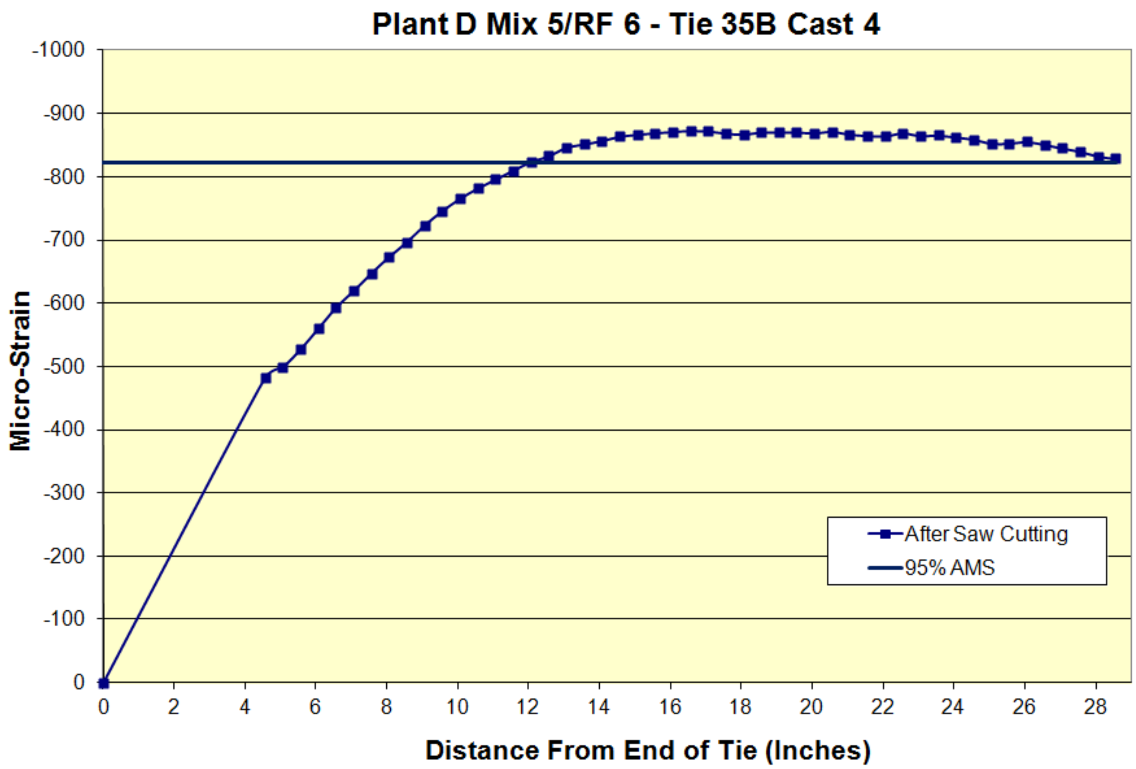

Figure D.43 Transfer length of Plant D Mix 5/RF 6 Tie 35B Cast 4

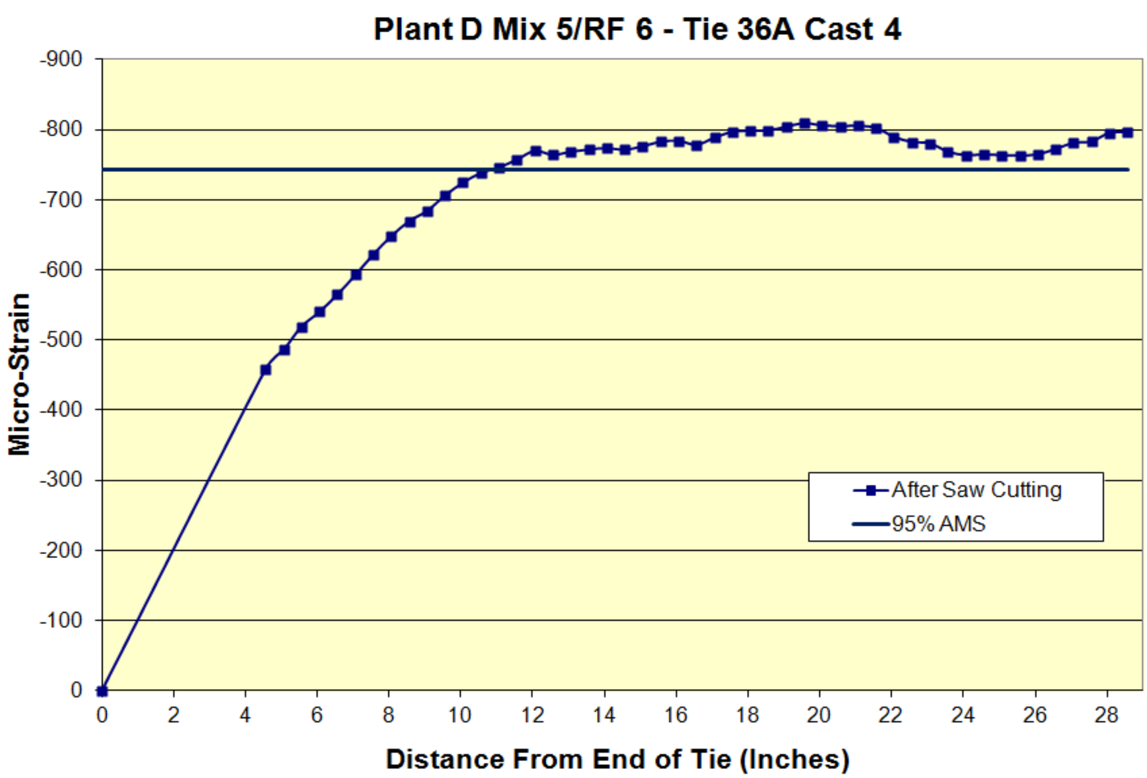

Figure D.44 Transfer length of Plant D Mix 5/RF 6 Tie 36A Cast 4

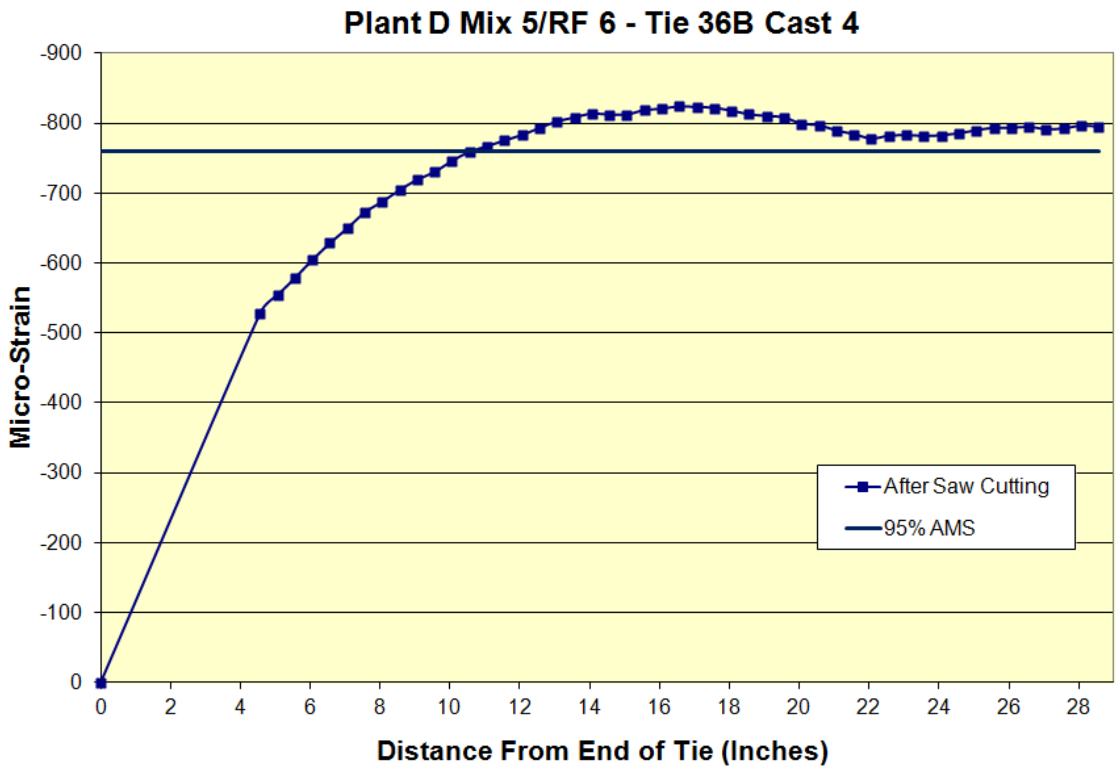

Figure D.45 Transfer length of Plant D Mix 5/RF 6 Tie 36B Cast 4

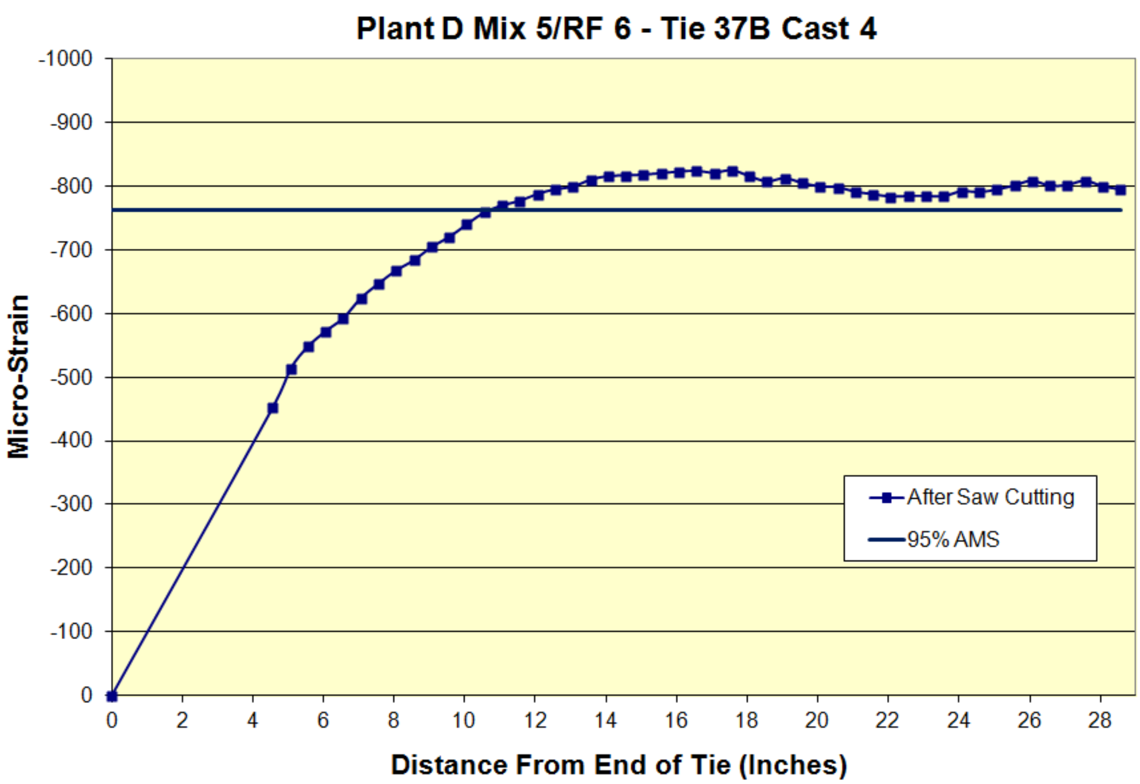

Figure D.46 Transfer length of Plant D Mix 5/RF 6 Tie 37B Cast 4

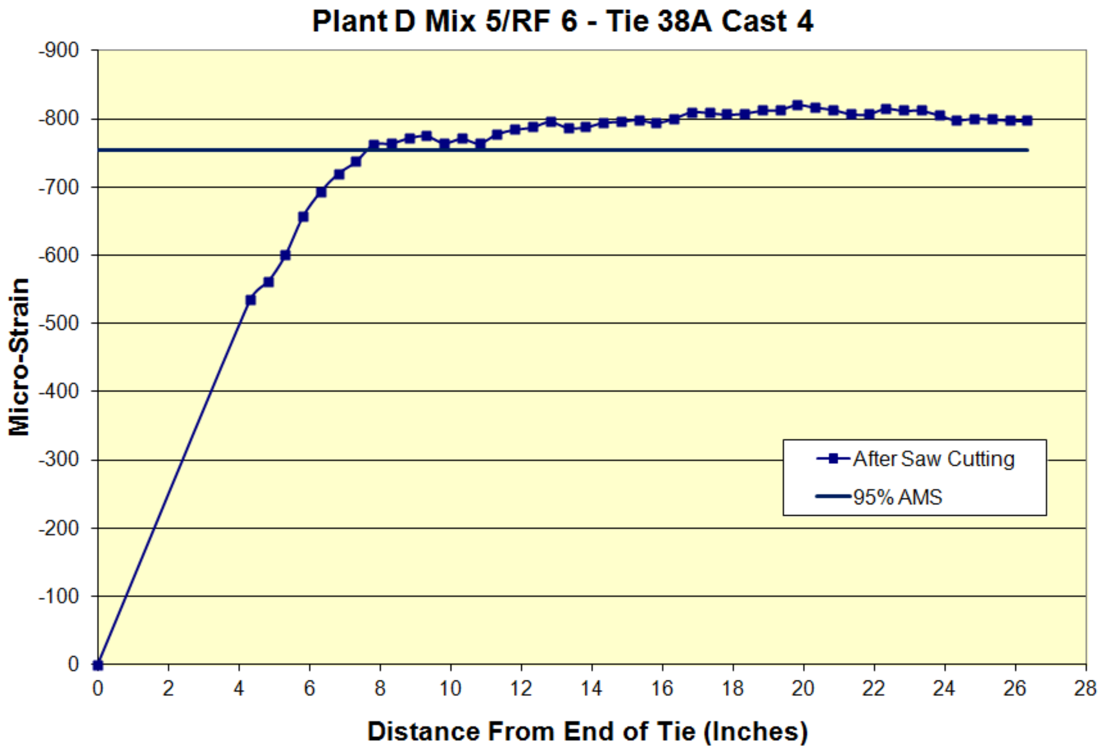

Figure D.47 Transfer length of Plant D Mix 5/RF 6 Tie 38A Cast 4

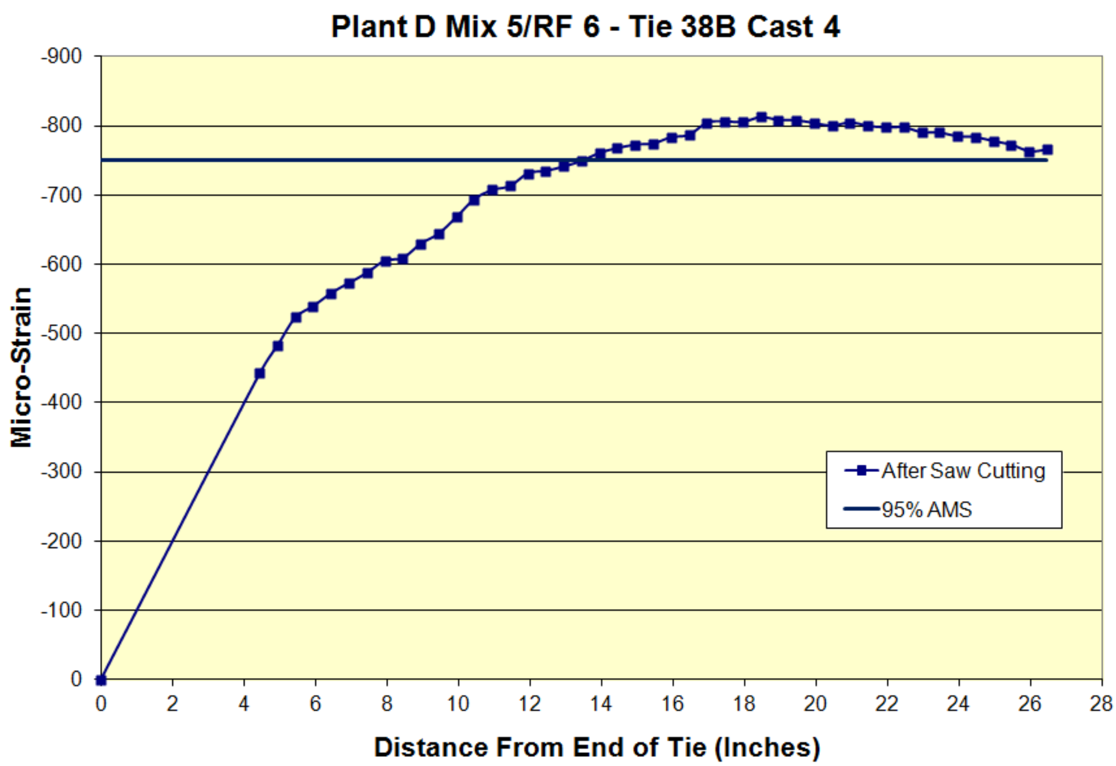

Figure D.48 Transfer length of Plant D Mix 5/RF 6 Tie 38B Cast 4

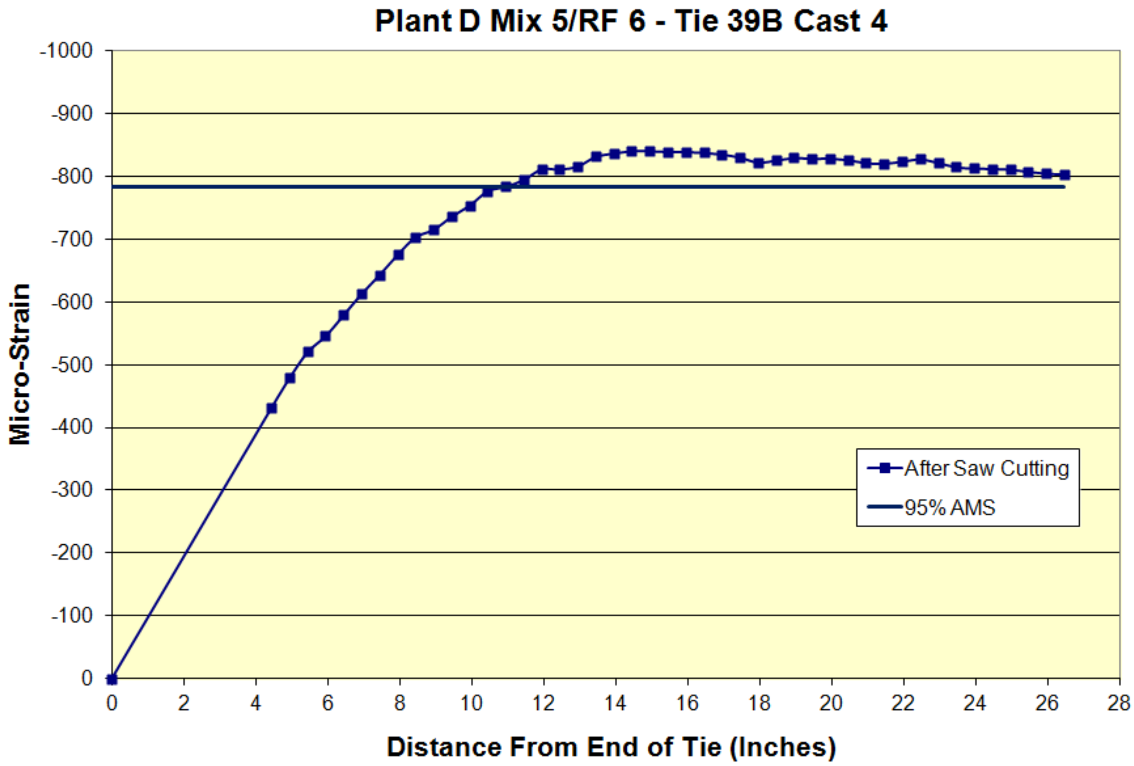

Figure D.49 Transfer length of Plant D Mix 5/RF 6 Tie 39B Cast 4

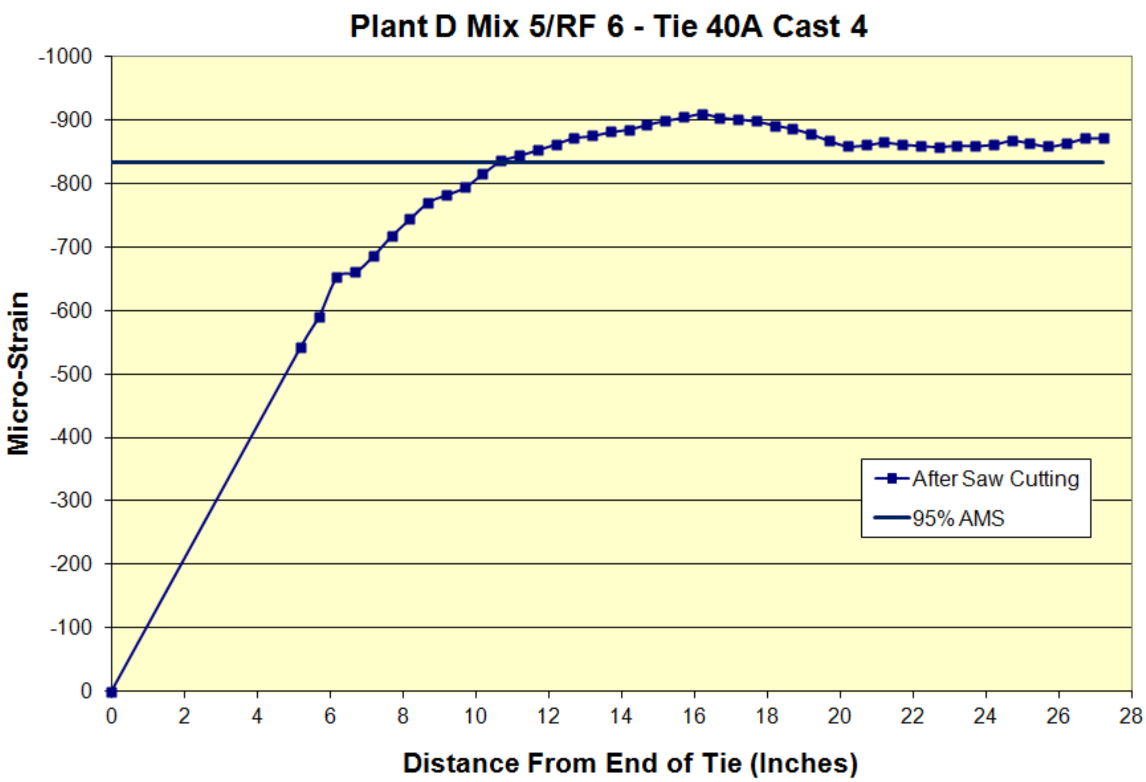

Figure D.50 Transfer length of Plant D Mix 5/RF 6 Tie 40A Cast 4

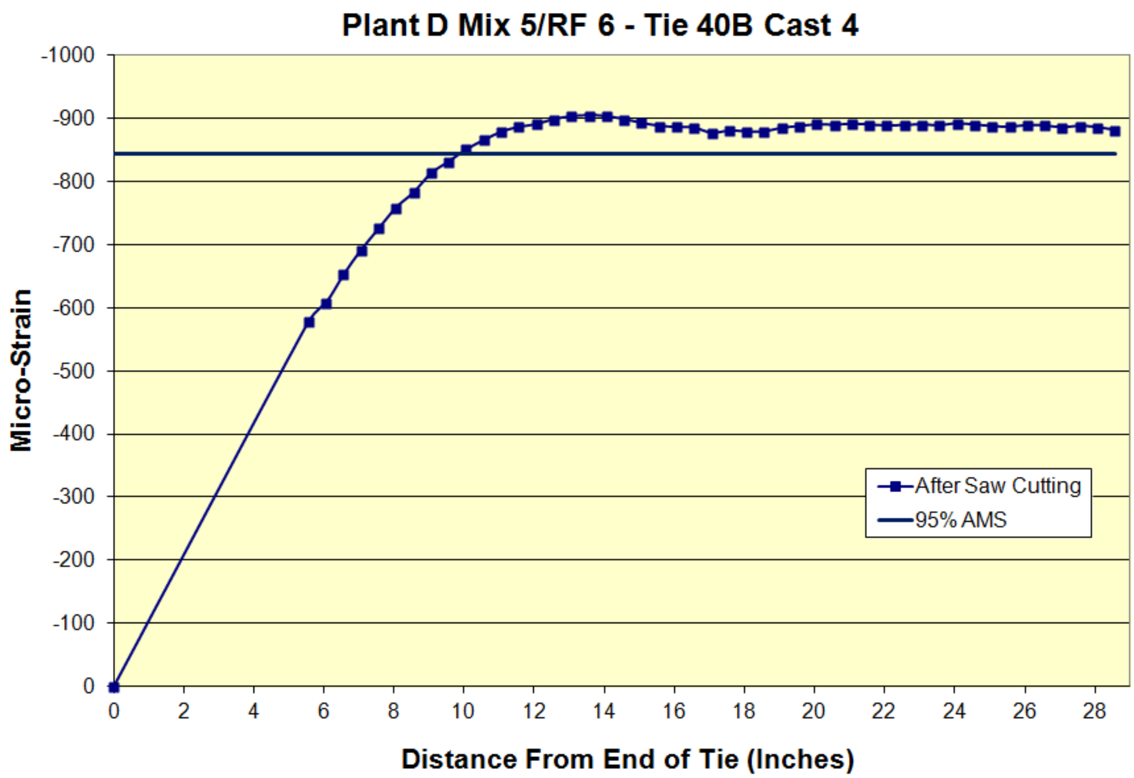

Figure D.51 Transfer length of Plant D Mix 5/RF 6 Tie 40B Cast 4

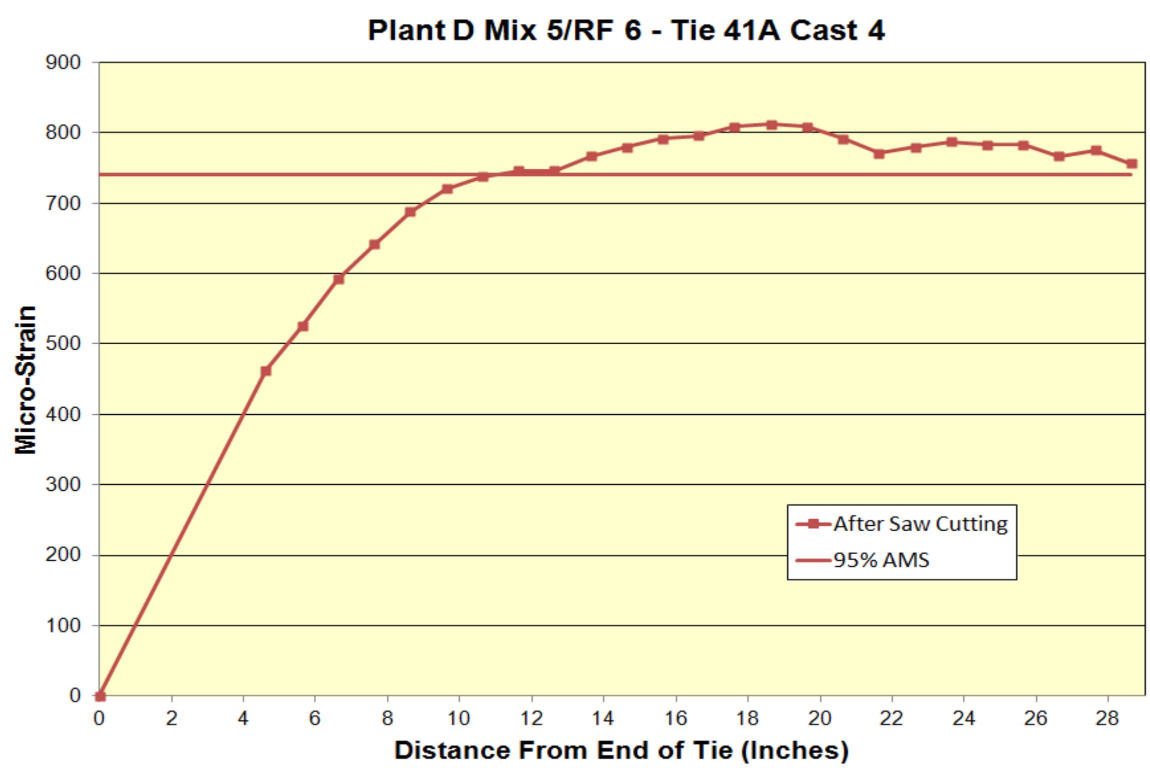

Figure D.52 Transfer length of Plant D Mix 5/RF 6 Tie 41A Cast 4

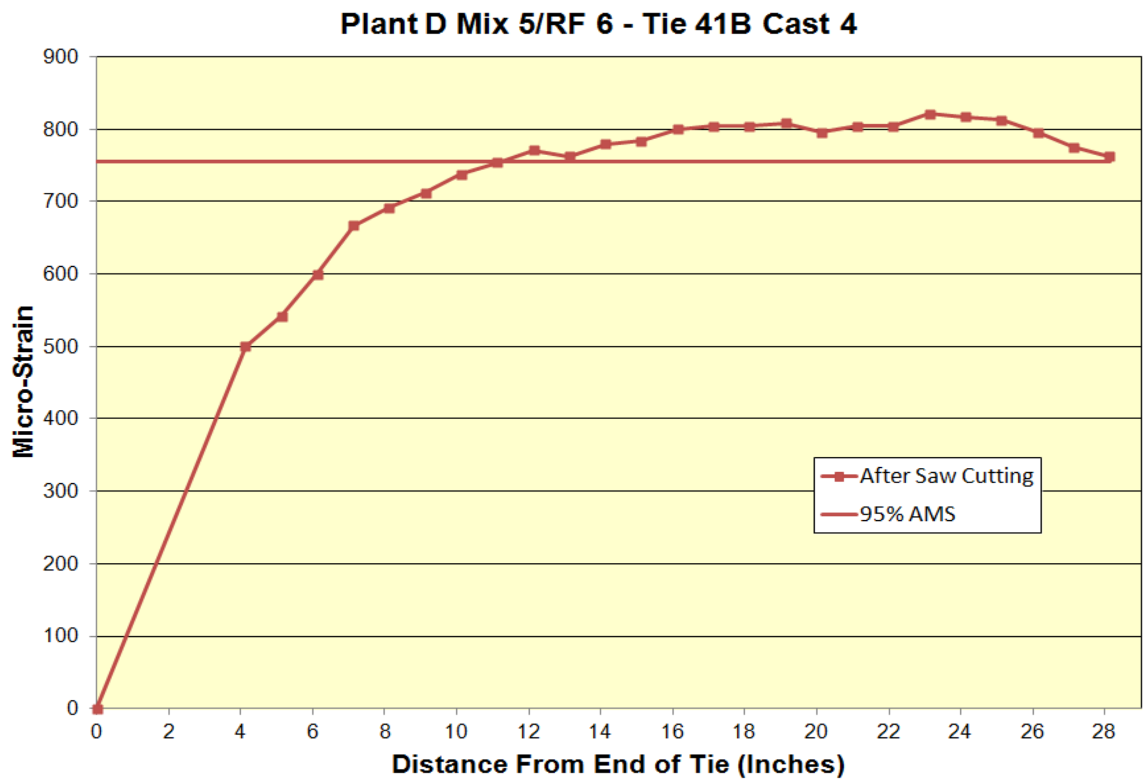

Figure D.53 Transfer length of Plant D Mix 5/RF 6 Tie 41B Cast 4

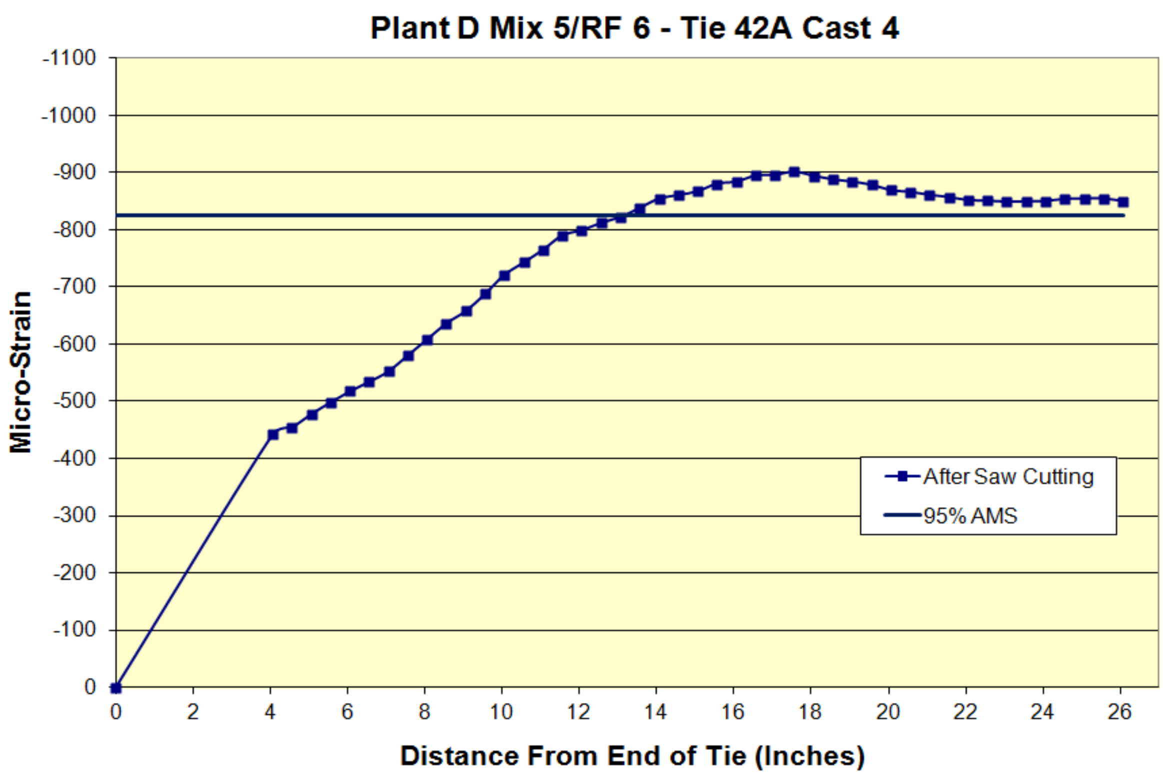

Figure D.54 Transfer length of Plant D Mix 5/RF 6 Tie 42A Cast 4

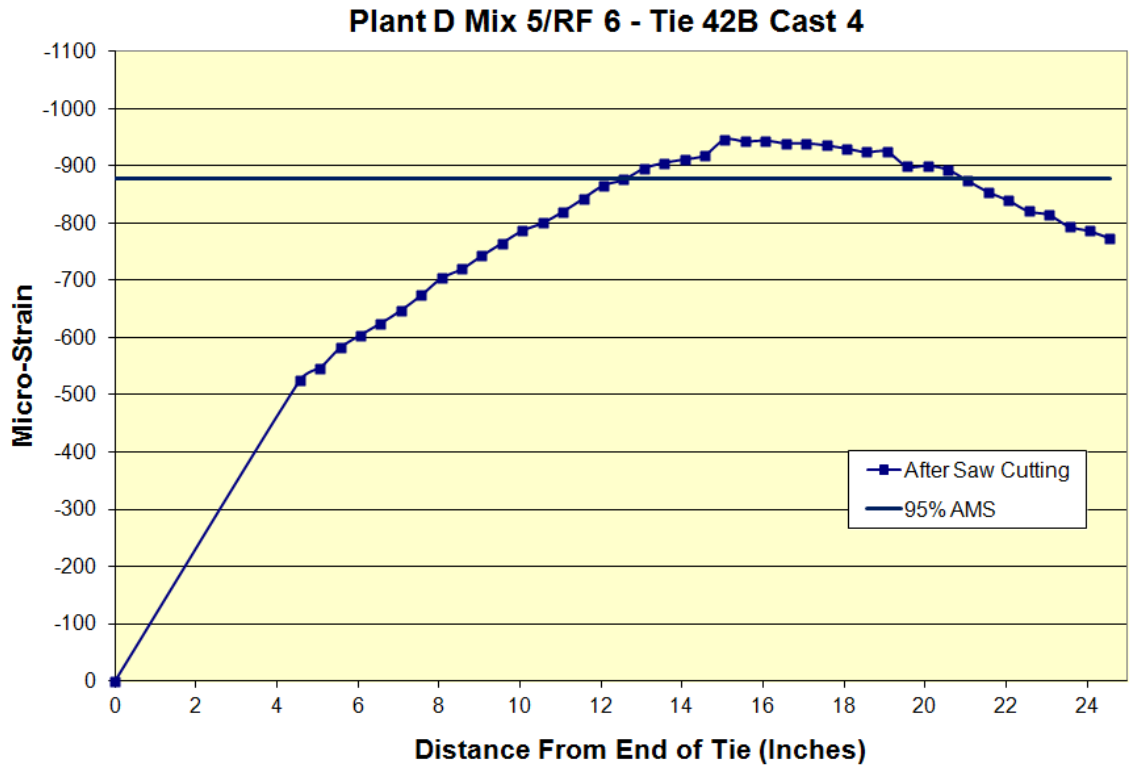

Figure D.55 Transfer length of Plant D Mix 5/RF 6 Tie 42B Cast 4

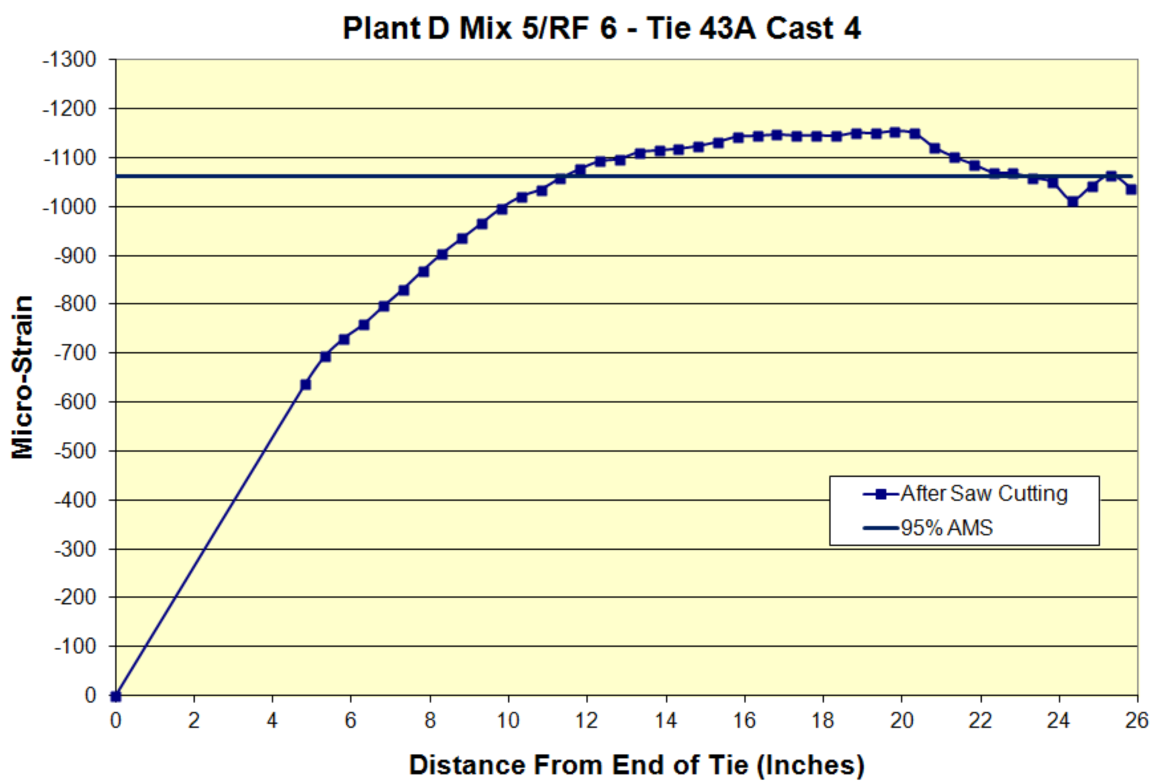

Figure D.56 Transfer length of Plant D Mix 5/RF 6 Tie 43A Cast 4

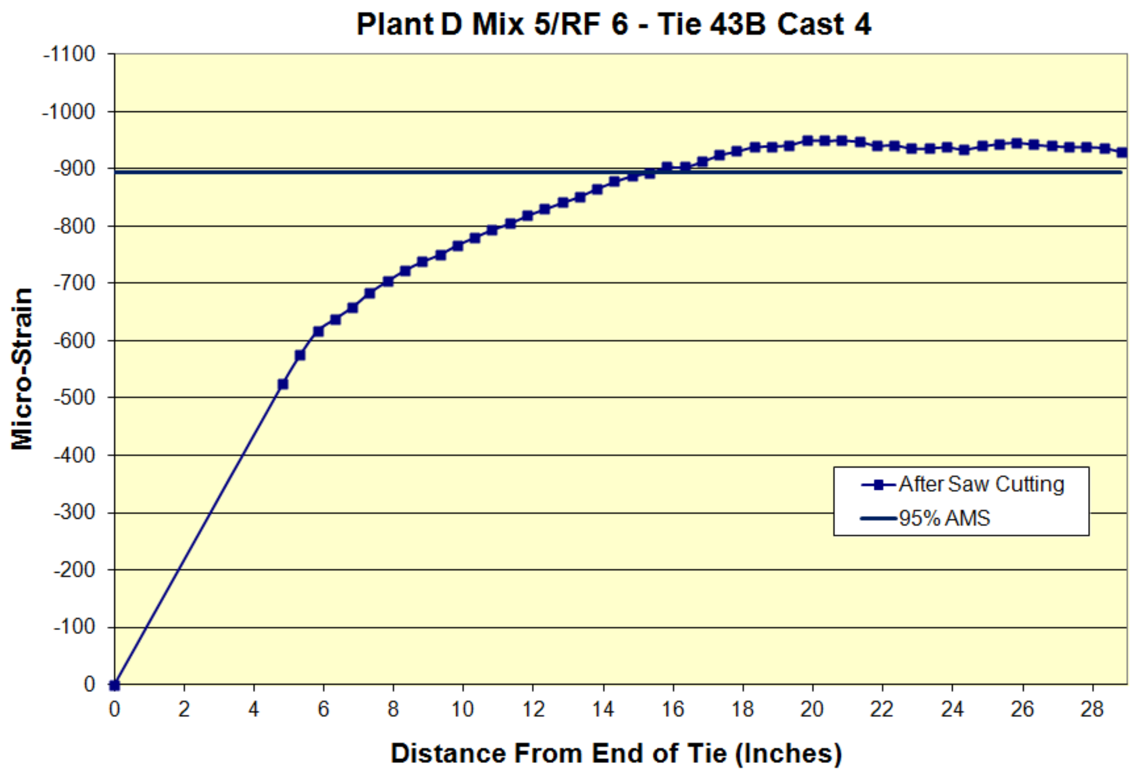

Figure D.57 Transfer length of Plant D Mix 5/RF 6 Tie 43B Cast 4

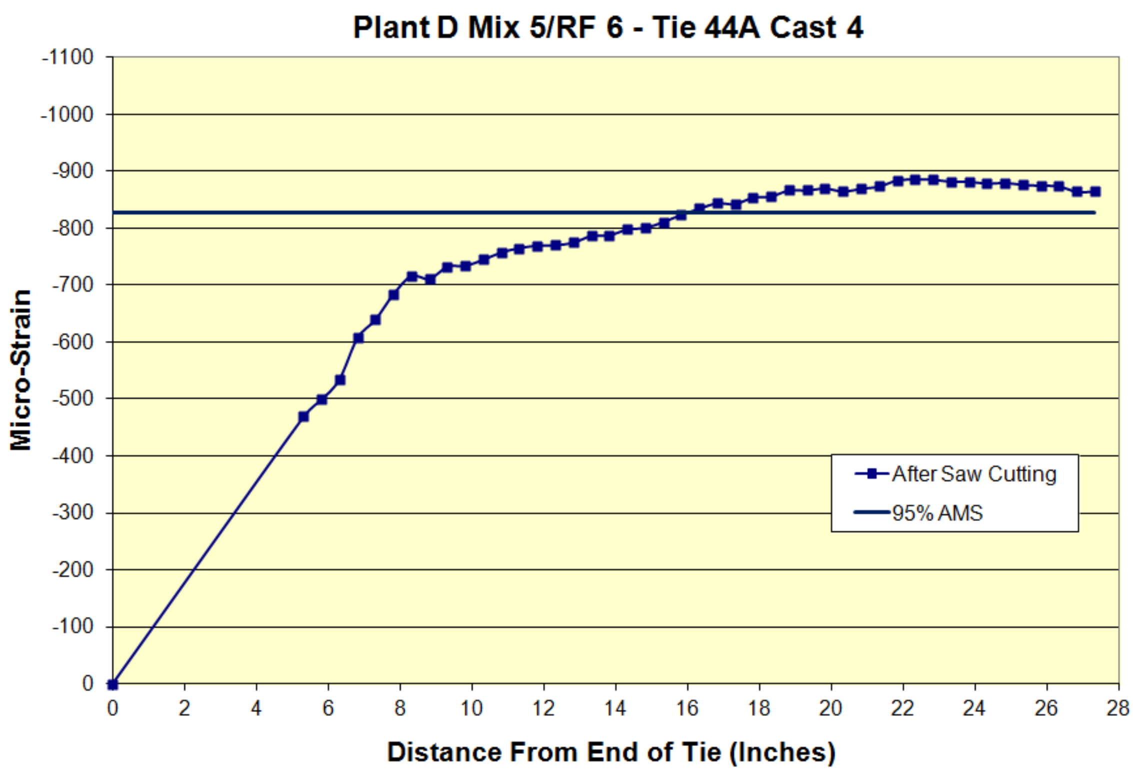

Figure D.58 Transfer length of Plant D Mix 5/RF 6 Tie 44A Cast 4

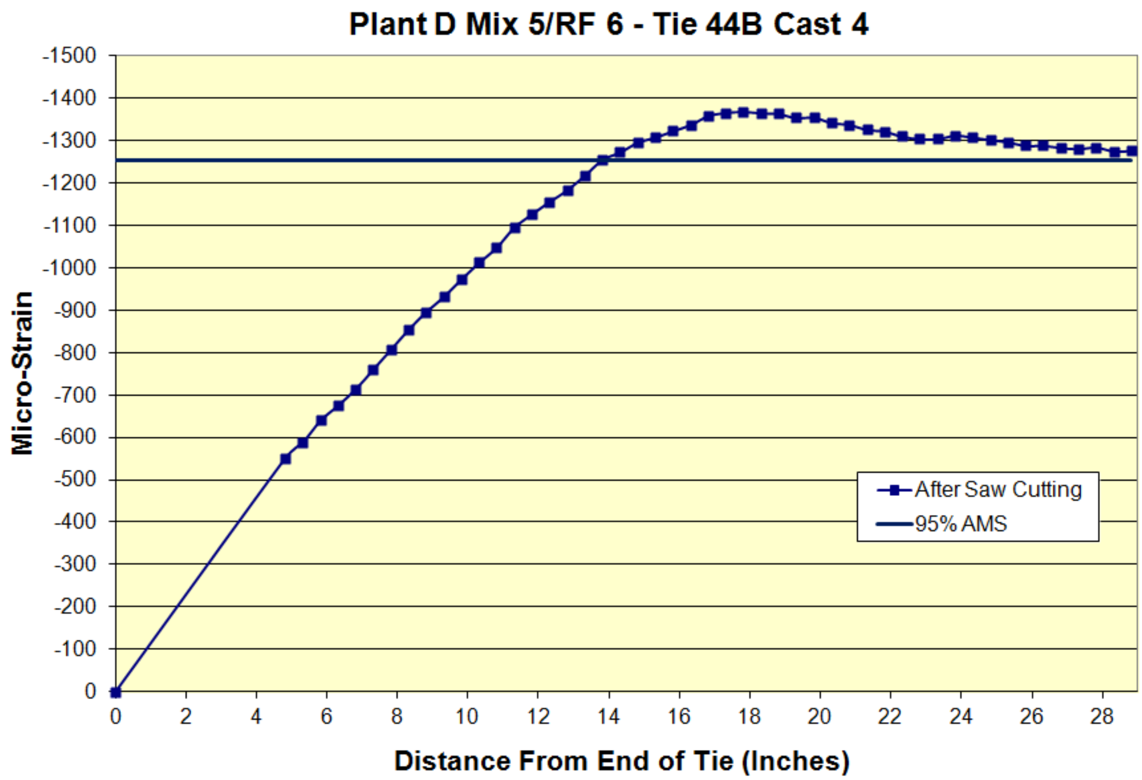

Figure D.59 Transfer length of Plant D Mix 5/RF 6 Tie 44B Cast 4

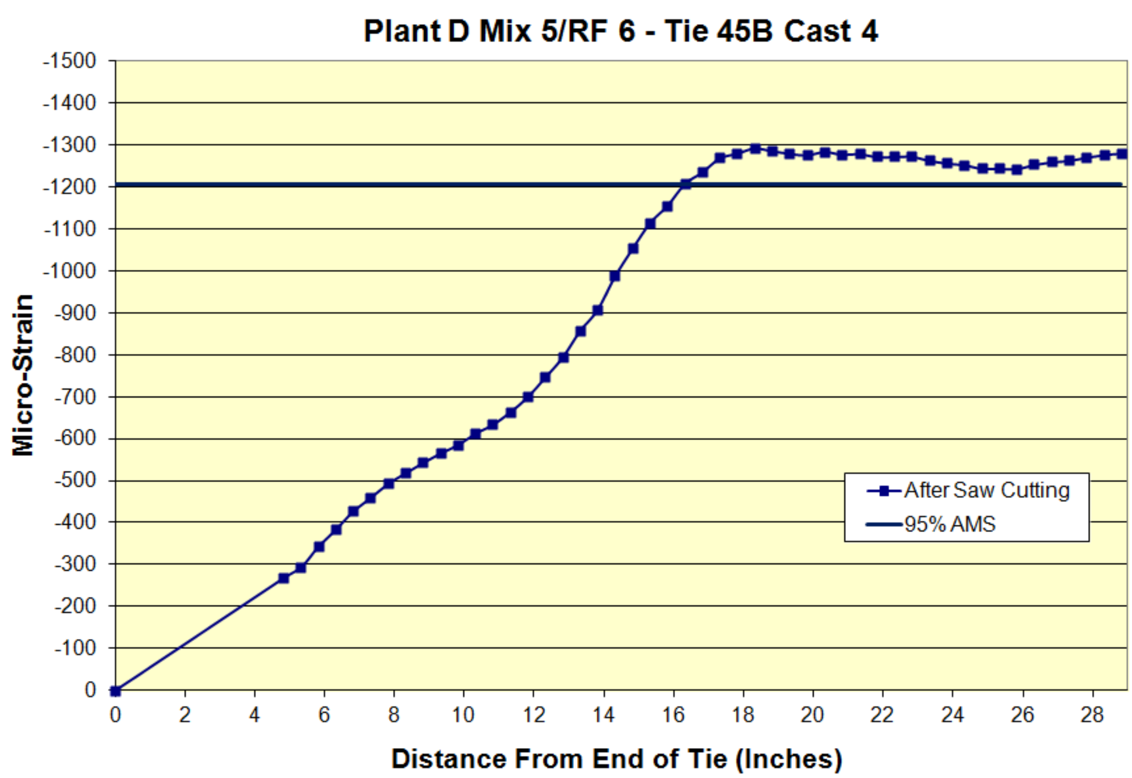

Figure D.60 Transfer length of Plant D Mix 5/RF 6 Tie 45B Cast 4

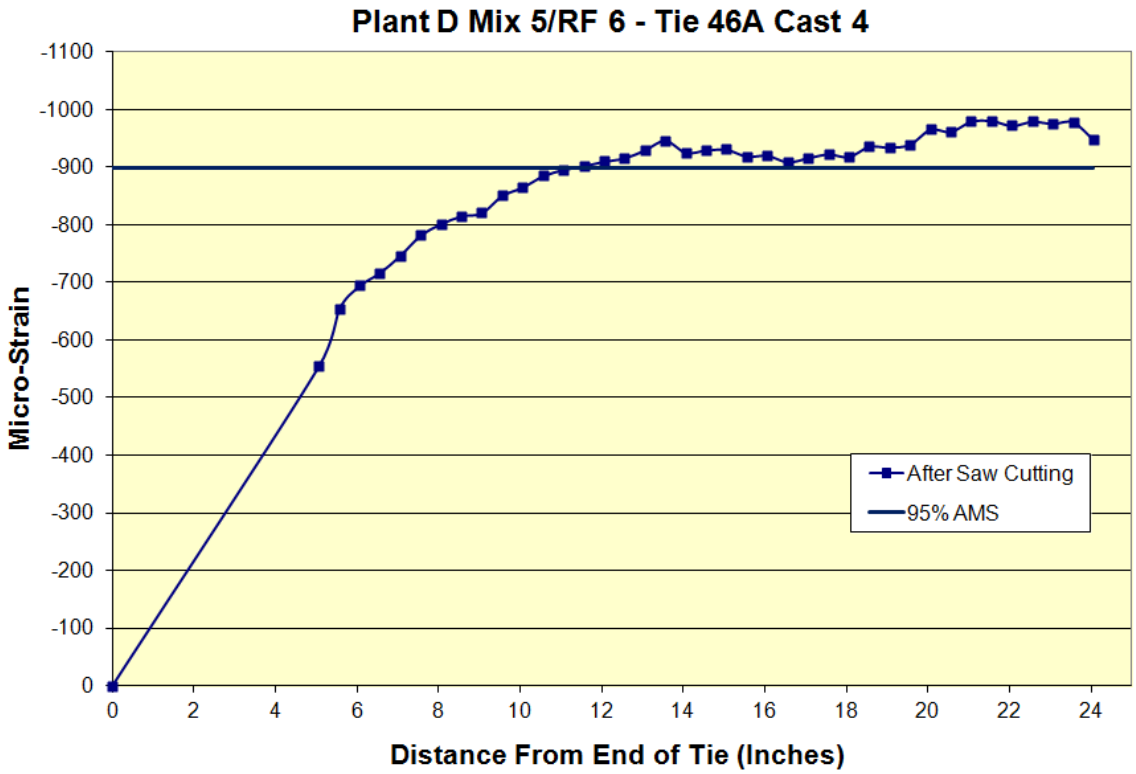

Figure D.61 Transfer length of Plant D Mix 5/RF 6 Tie 46A Cast 4

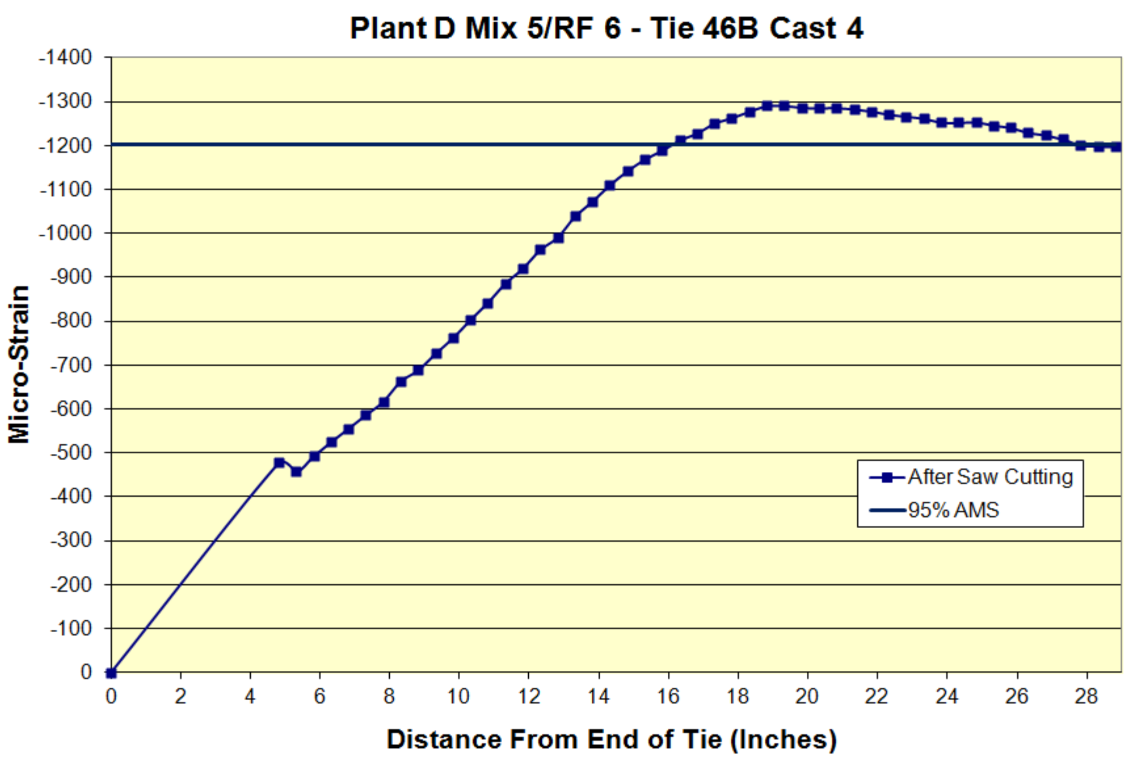

Figure D.62 Transfer length of Plant D Mix 5/RF 6 Tie 46A Cast 4

D.2 Long-term Transfer Lengths

Table D.2 Long-term transfer length data for Plant D Mix 5/RF 5 Cast 1

Plant D Mix 5/RF 5 Cast 1			
	Transfer Length (in.)		
Time of Reading	Tie 1A	Tie 7A	Tie 7B
After Saw Cutting	9.1	11.4	10.1
15 Days After Pour	10.9	10.9	9.8
35 Days After Pour	10.6	10.7	10.5
60 Days After Pour	11	11.6	10.9

Table D.3 Long-term transfer length data for Plant D Mix 5/RF 5 Cast 2

Plant D Mix 5/RF 5 Cast 2			
	Transfer Length (in.)		
Time of Reading	Tie 12B	Tie 19A	Tie 19B
After Saw Cutting	8.5	11.5	11.2
15 Days After Pour	10.6	13.5	11.6
35 Days After Pour	10	13.2	11.7
60 Days After Pour	9.9	13.4	11.9

Table D.4 Long-term transfer length data for Plant D Mix 5/RF 6 Cast 3

Plant D Mix 5/RF 6 Cast 3			
	Transfer Length (in.)		
Time of Reading	Tie 23A	Tie 29A	Tie 29B
After Saw Cutting	9.5	10.2	9.7
15 Days After Pour	10.2	11.8	11.9
35 Days After Pour	10	11.5	10.8
60 Days After Pour	10.2	11.2	10.9

Table D.5 Long-term transfer length data for Plant D Mix 5/RF 6 Cast 4

Plant D Mix 5/RF 6 Cast 4			
	Transfer Length (in.)		
Time of Reading	Tie 35A	Tie 41A	Tie 41B
After Saw Cutting	9.3	10.6	11.2
15 Days After Pour	10.5	10.9	10.9
35 Days After Pour	10.4	11.6	11
60 Days After Pour	10.5	12	11.4

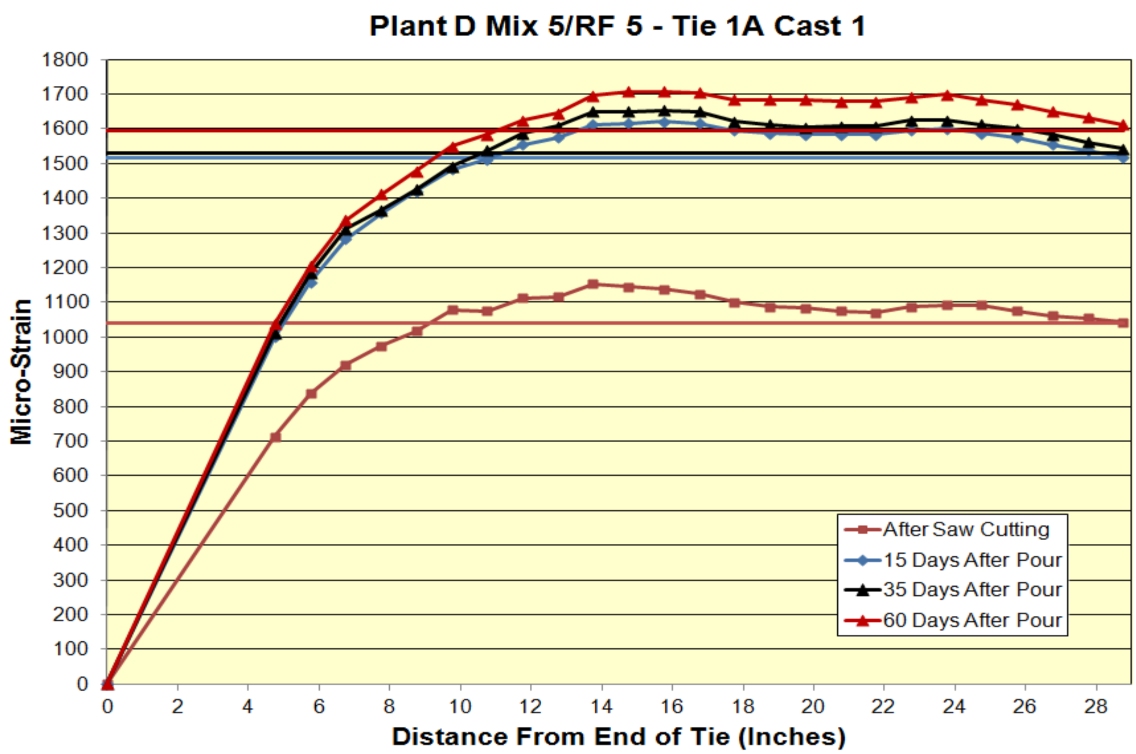

Figure D.63 Long-term transfer length of Plant D Mix 5/RF 5 Tie 1A Cast 1

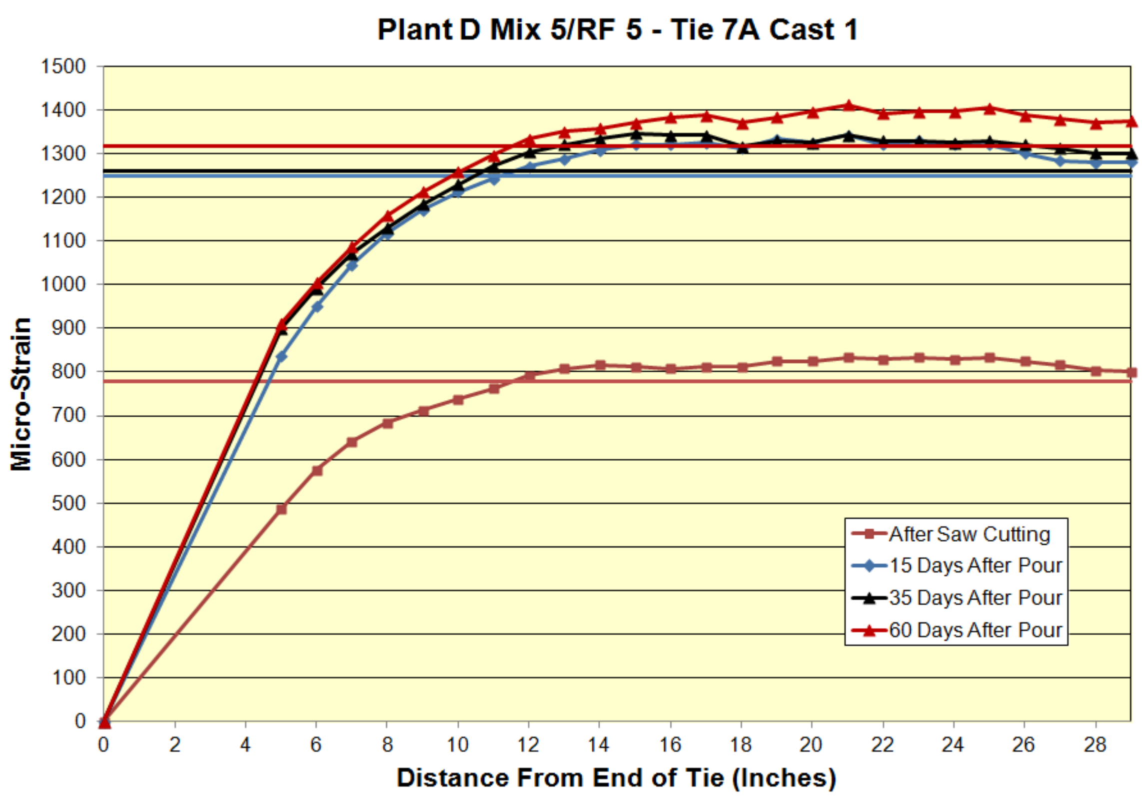

Figure D.64 Long-term transfer length of Plant D Mix 5/RF 5 Tie 7A Cast 1

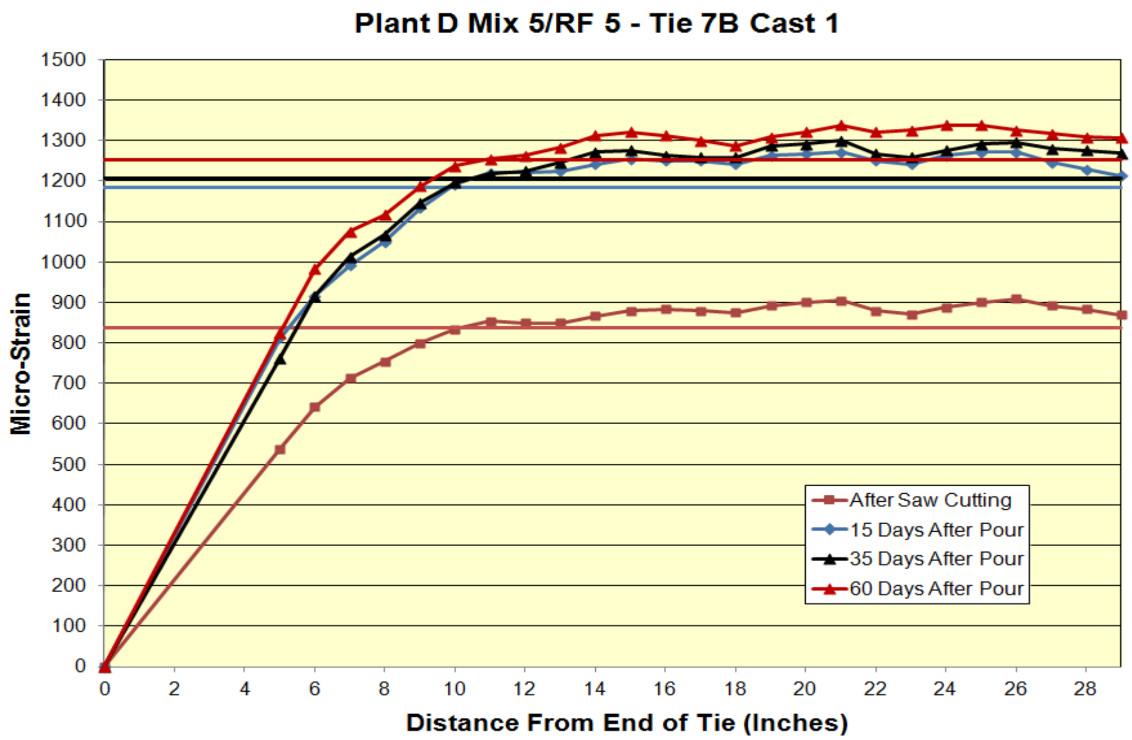

Figure D.65 Long-term transfer length of Plant D Mix 5/RF 5 Tie 7B Cast 1

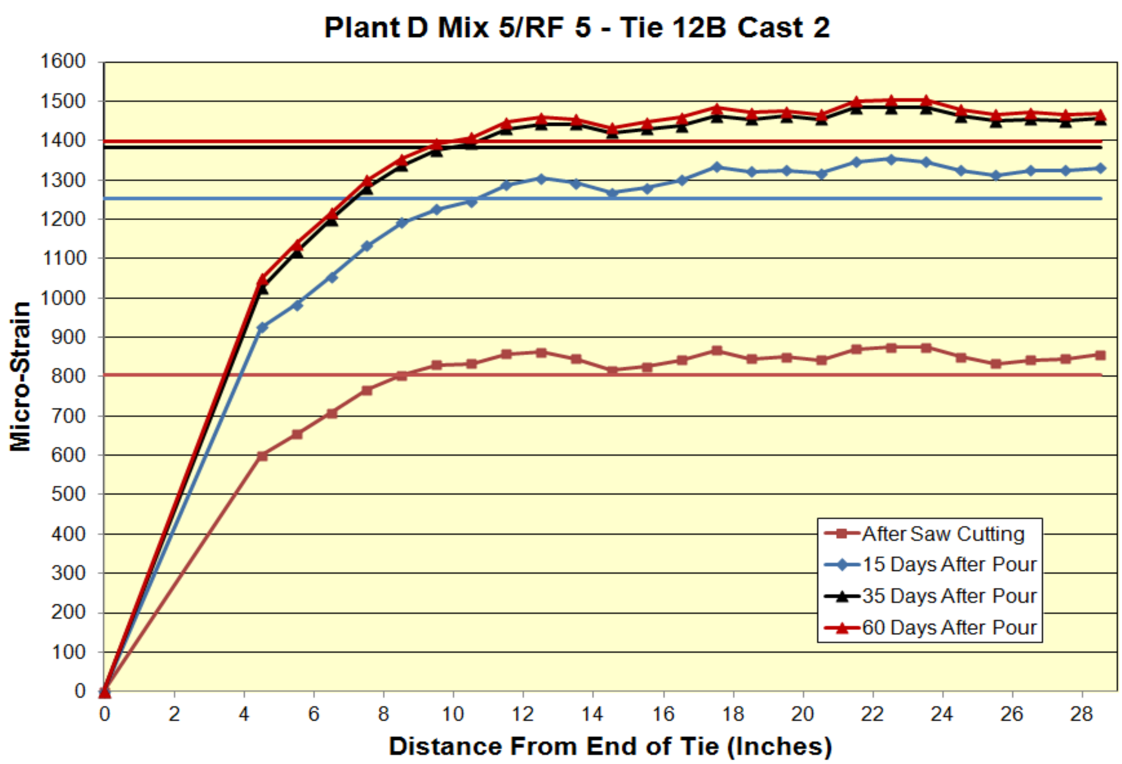

Figure D.66 Long-term transfer length of Plant D Mix 5/RF 5 Tie 12B Cast 2

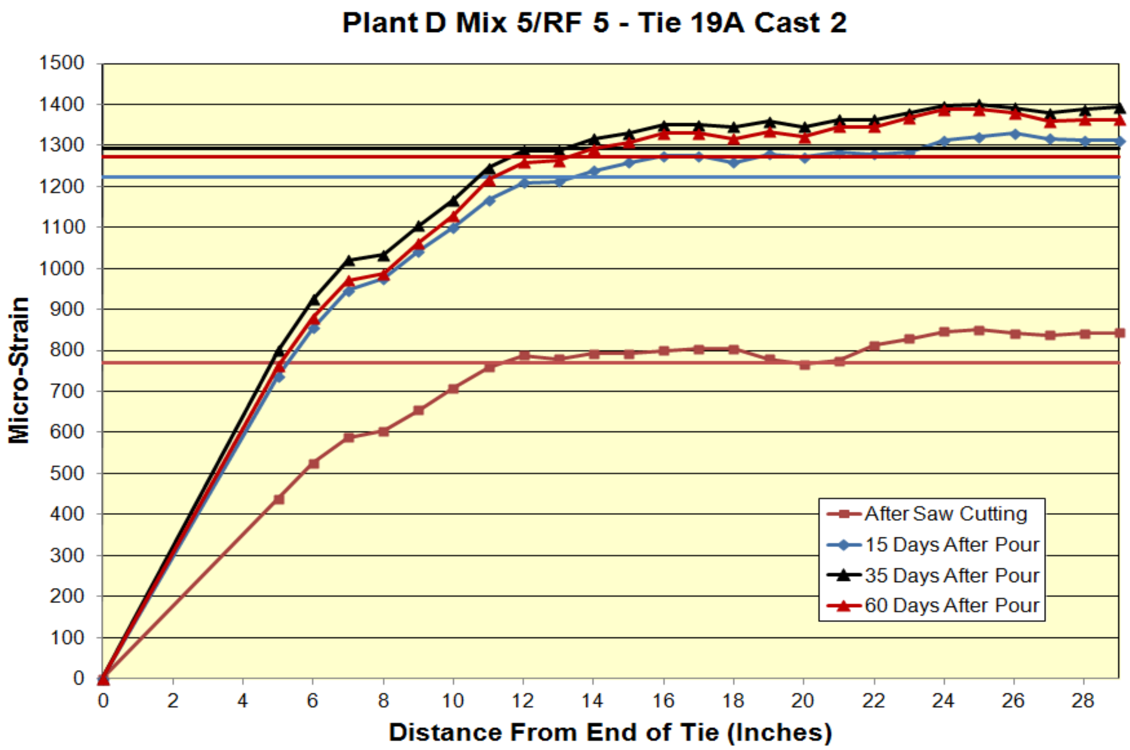

Figure D.67 Long-term transfer length of Plant D Mix 5/RF 5 Tie 19A Cast 2

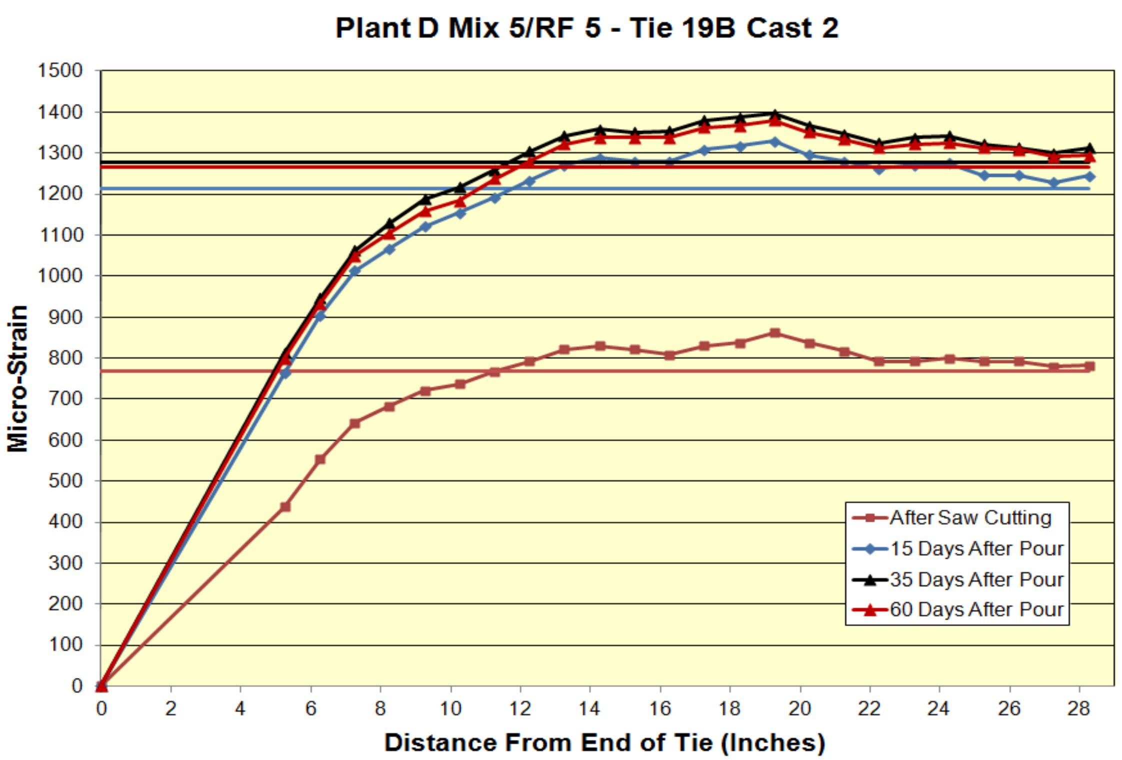

Figure D.68 Long-term transfer length of Plant D Mix 5/RF 5 Tie 19B Cast 2

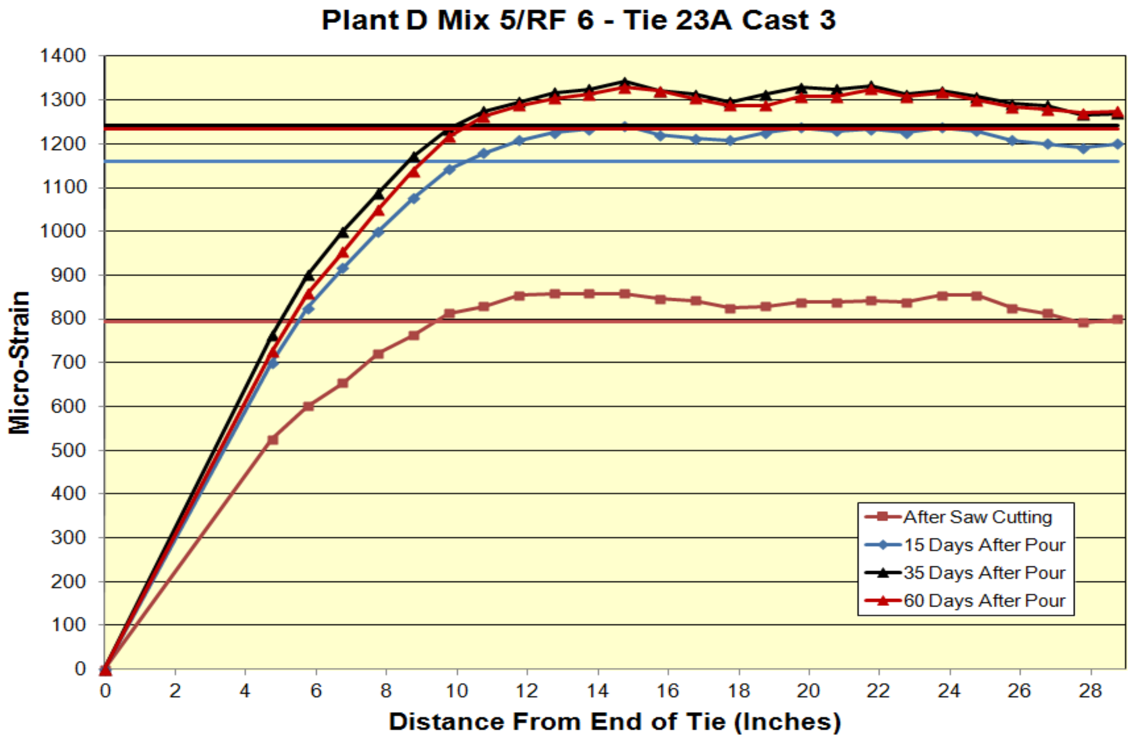

Figure D.69 Long-term transfer length of Plant D Mix 5/RF 6 Tie 23A Cast 3

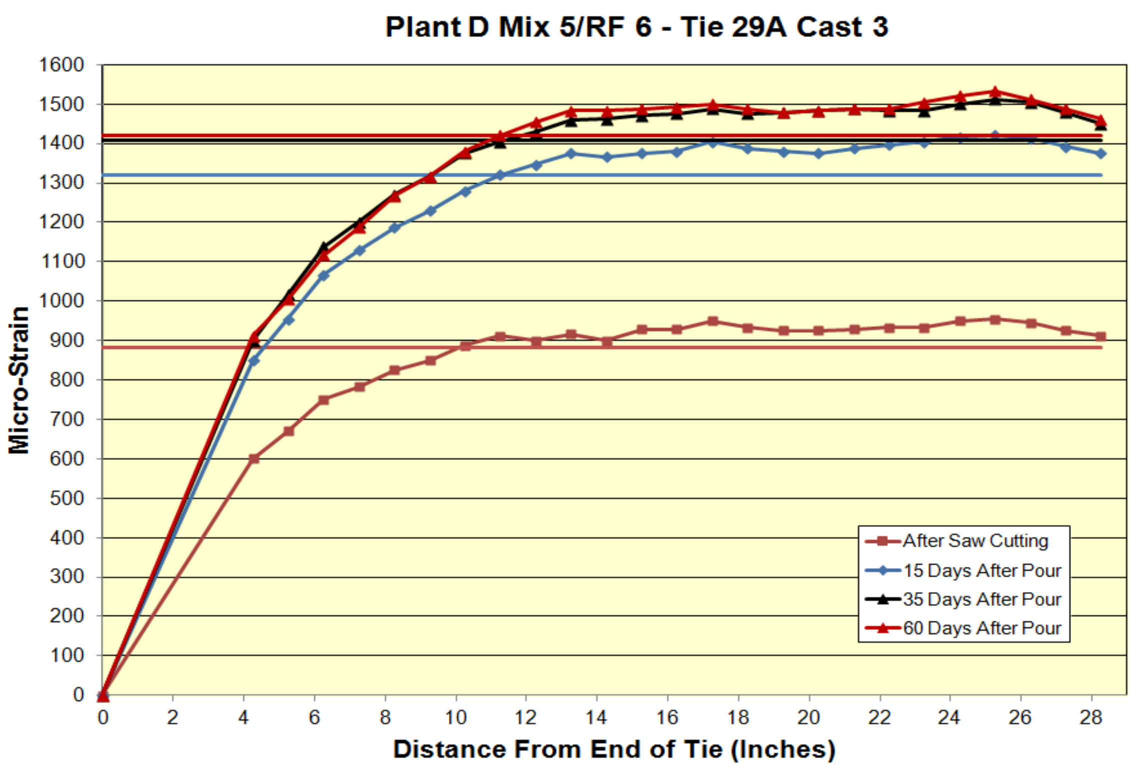

Figure D.70 Long-term transfer length of Plant D Mix 5/RF 6 Tie 29A Cast 3

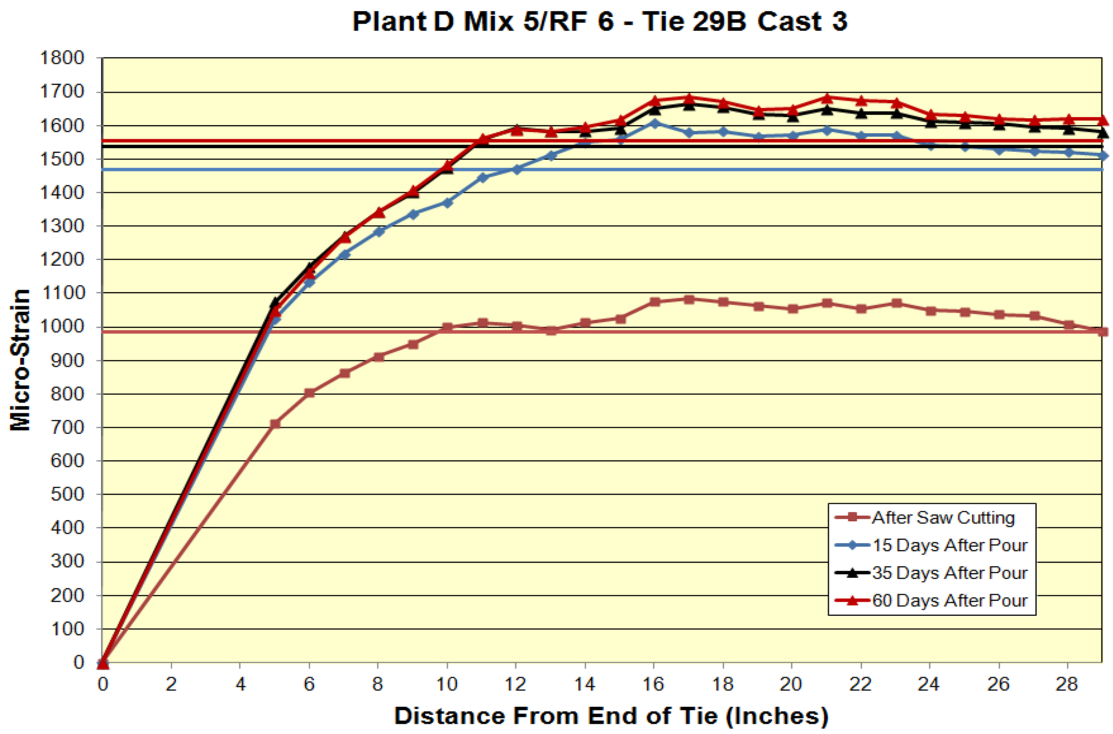

Figure D.71 Long-term transfer length of Plant D Mix 5/RF 6 Tie 29B Cast 3

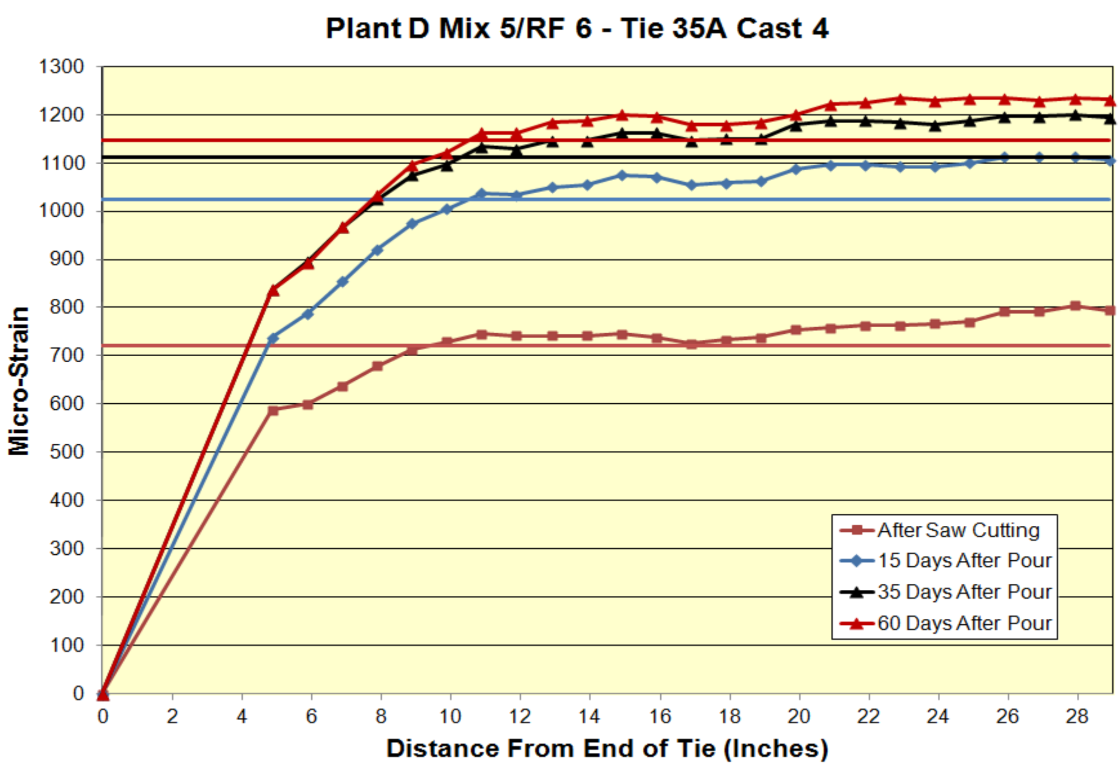

Figure D.72 Long-term transfer length of Plant D Mix 5/RF 6 Tie 35A Cast 4

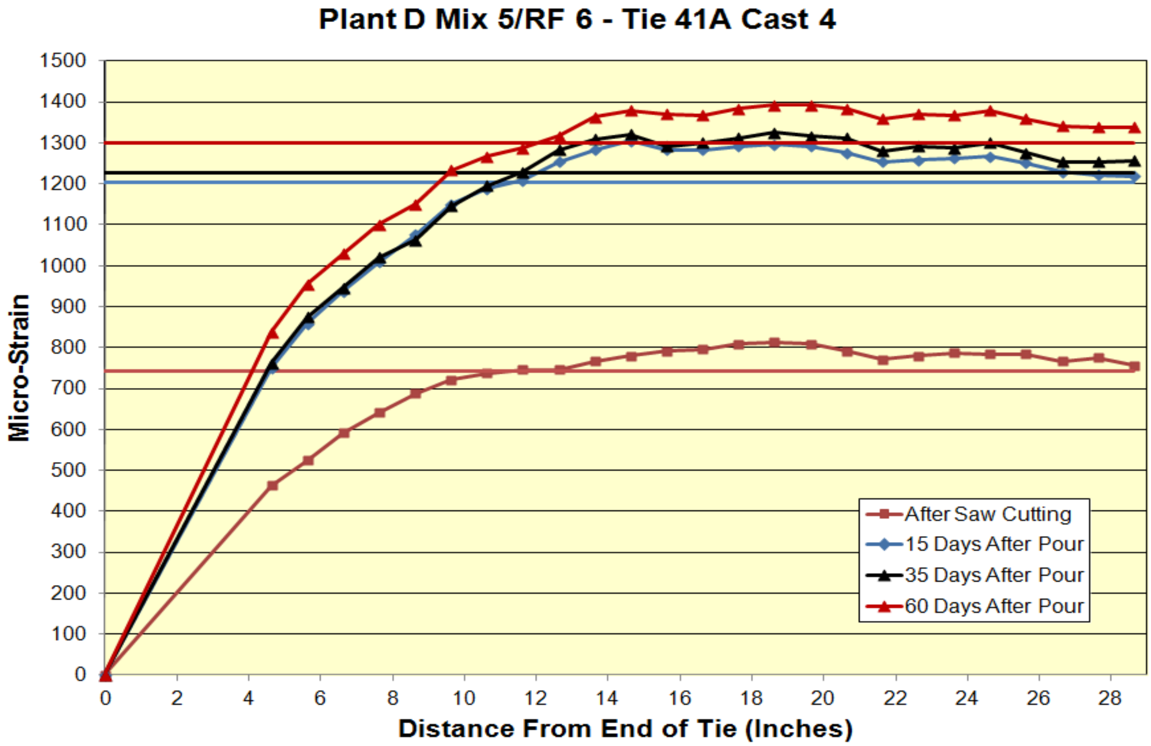

Figure D.73 Long-term transfer length of Plant D Mix 5/RF 6 Tie 41B Cast 4

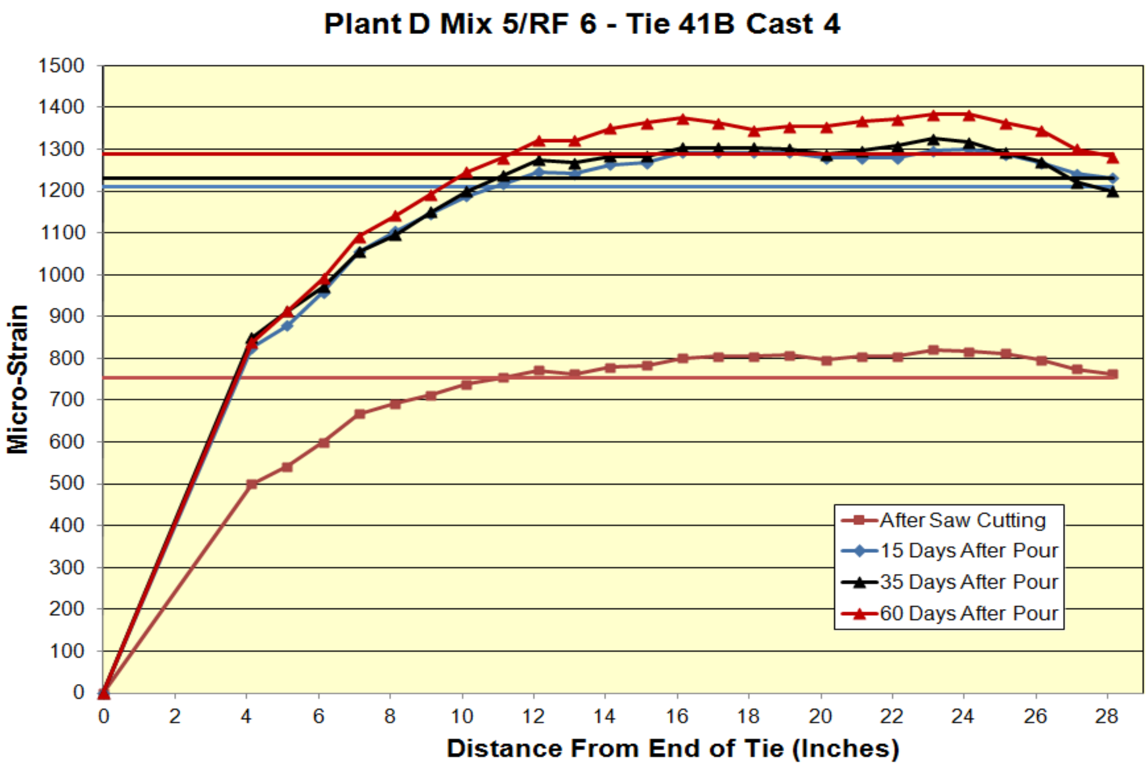

Figure D.74 Long-term transfer length of Plant D Mix 5/RF 6 Tie 41A Cast 4

Appendix E Plant E Transfer Lengths

E.1Short-term Transfer Lengths

Table E.1 Plant E transfer length data

	Tie Label	Measurement Method	Transfer Length (in.)
Plant E Mix 6/RF 7	1A	Laser Speckle	18.5
	1B	Laser Speckle	21
	2A	Laser Speckle	18
	2B	Laser Speckle	19
	3A	Laser Speckle	19
	3B	Laser Speckle	17.5
	5A	Laser Speckle	20.5
	5B	Laser Speckle	16
	6A	Laser Speckle	17.5
	6B	Laser Speckle	19
	7A	Whittemore Gage	19.8
	7B	Whittemore Gage	16.7
	8A	Whittemore Gage	18.3
	8B	Whittemore Gage	19.2
Plant E Mix 7/RF 7	9A	Whittemore Gage	22.2
	9B	Whittemore Gage	15
	10A	Whittemore Gage	15
	10B	Whittemore Gage	16.4
	11A	Laser Speckle	17.5
	11B	Laser Speckle	19
	12A	Laser Speckle	18
	12B	Laser Speckle	22.4
	13A	Laser Speckle	20
	13B	Laser Speckle	17
	14A	Laser Speckle	18
	15A	Laser Speckle	18.5
	15B	Laser Speckle	17
	16A	Laser Speckle	19
	16B	Laser Speckle	22.8
	17A	Whittemore Gage	19
	17B	Whittemore Gage	14.4

Note: Side A = Dead-end of tie

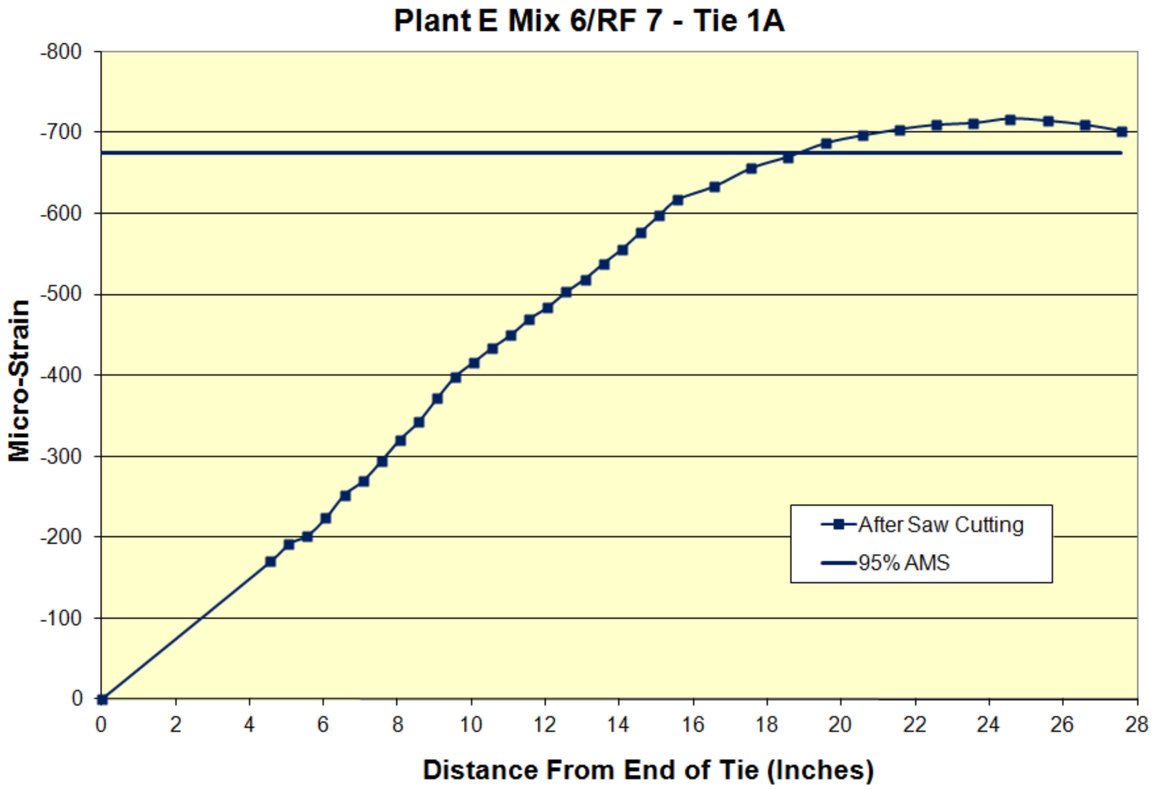

Figure E.1 Transfer length of Plant E Mix 6/RF 7 Tie 1A

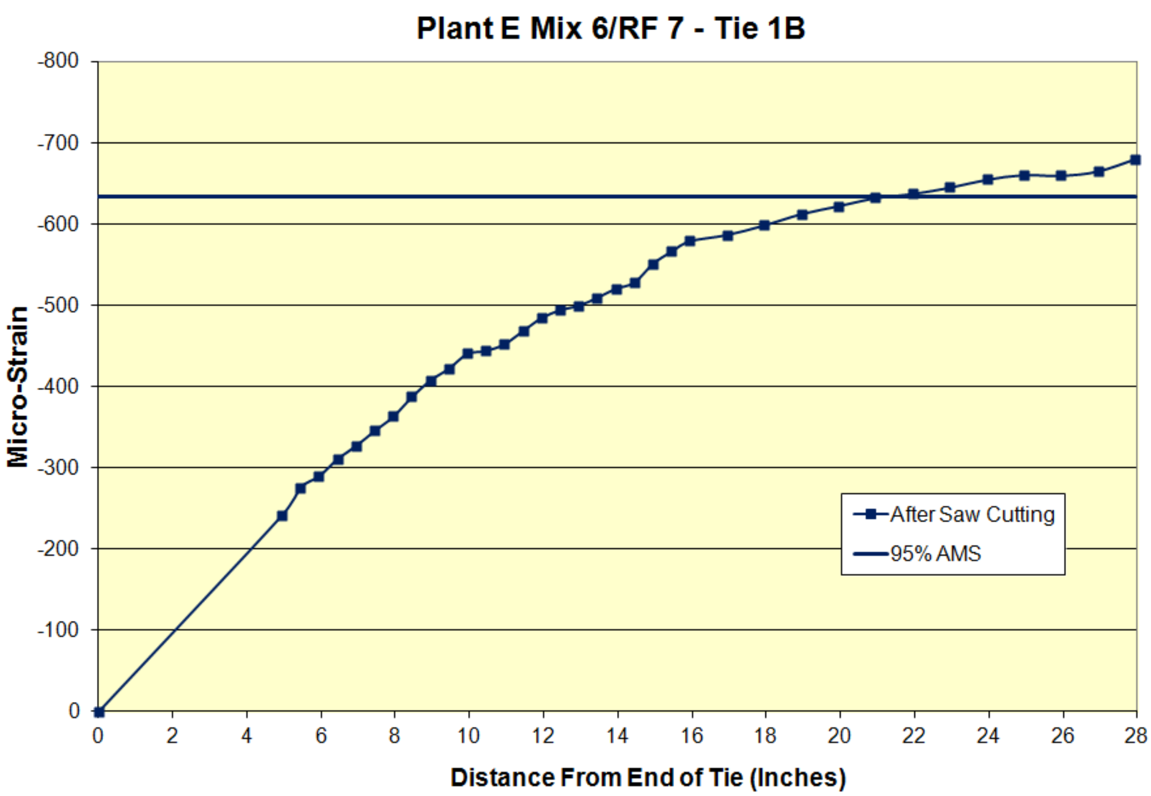

Figure E.2 Transfer length of Plant E Mix 6/RF 7 Tie 1B

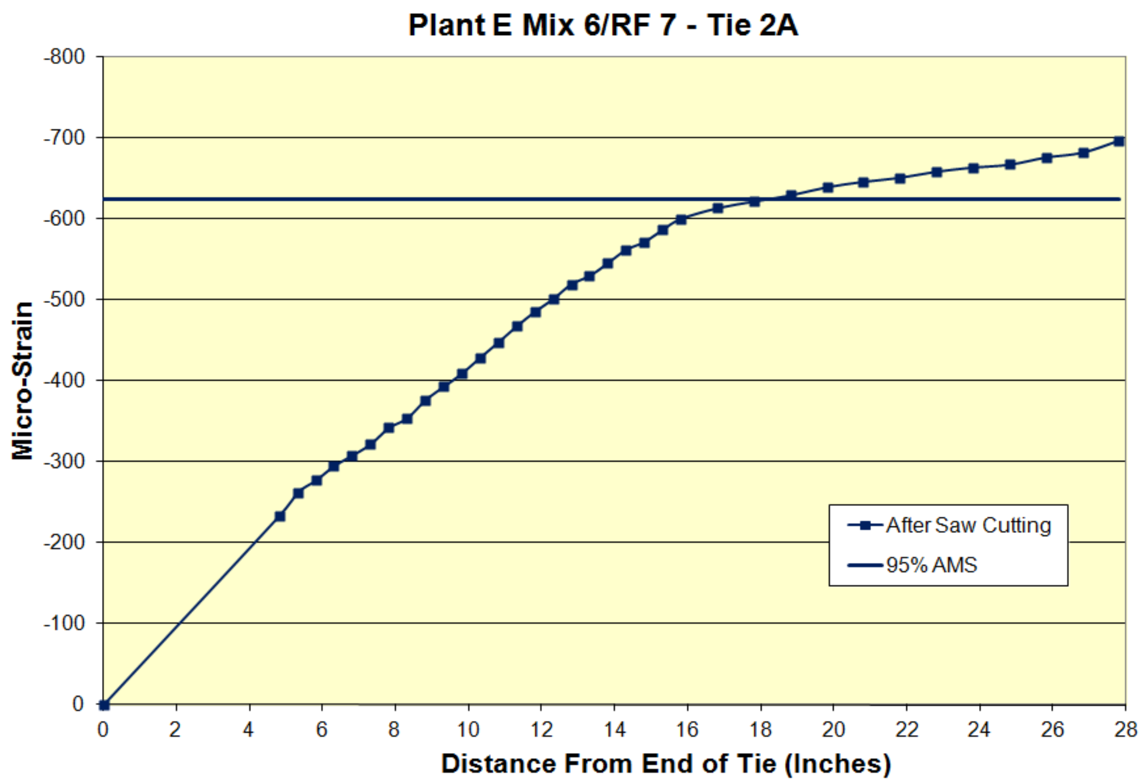

Figure E.3 Transfer length of Plant E Mix 6/RF 7 Tie 2A

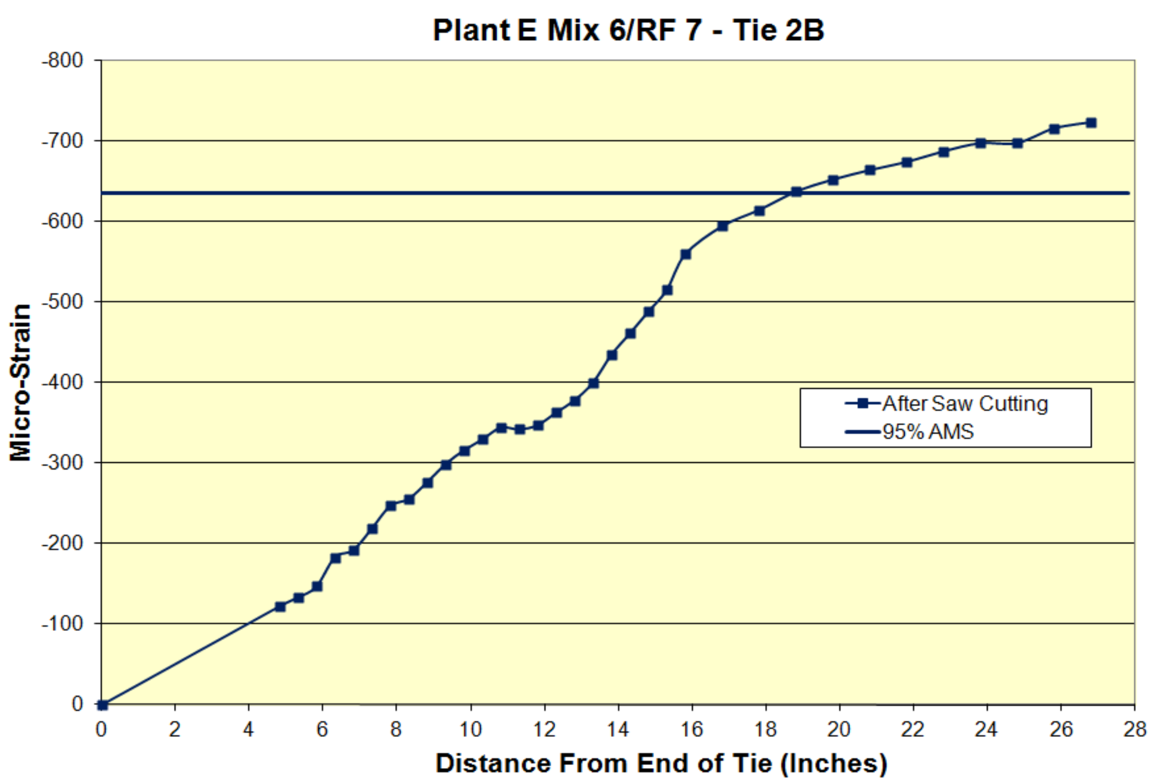

Figure E.4 Transfer length of Plant E Mix 6/RF 7 Tie 2B

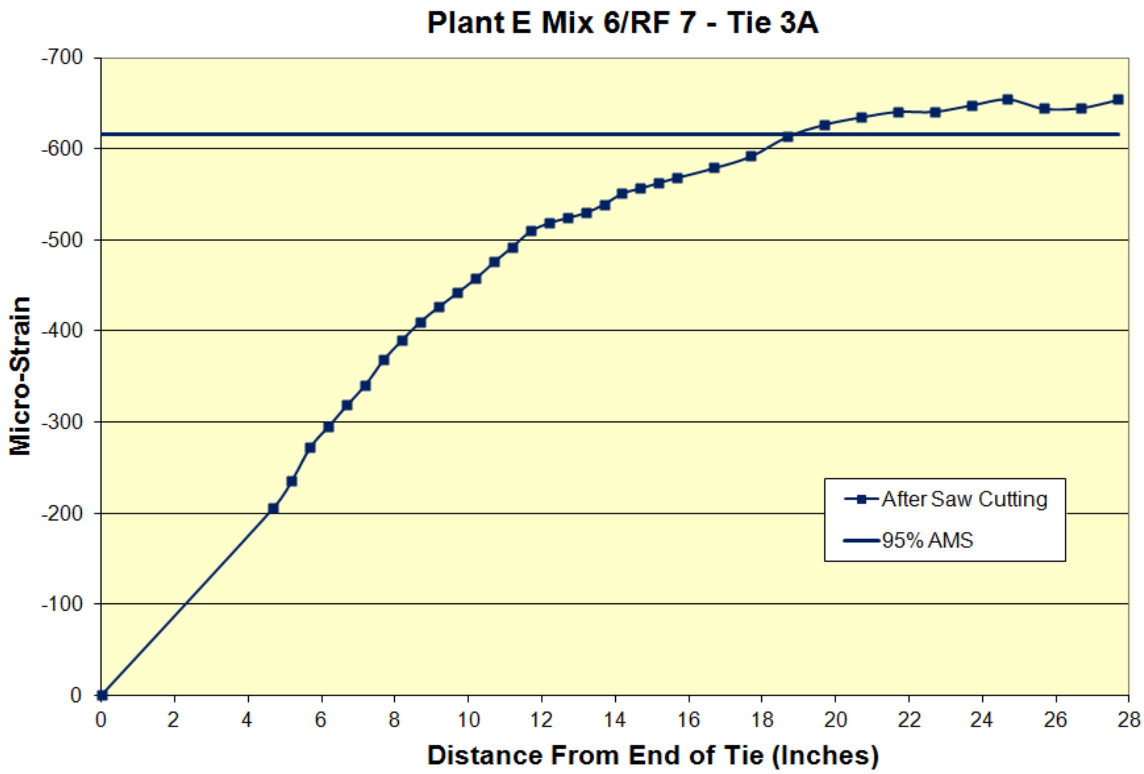

Figure E.5 Transfer length of Plant E Mix 6/RF 7 Tie 3A

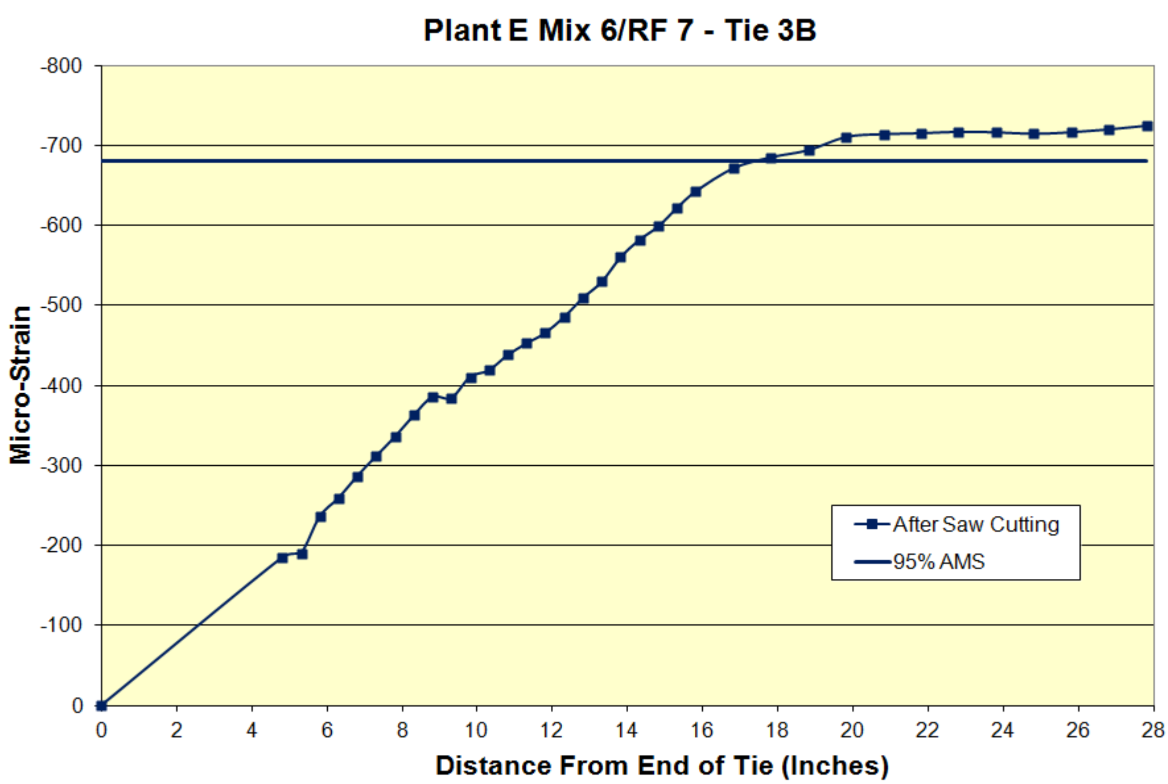

Figure E.6 Transfer length of Plant E Mix 6/RF 7 Tie 3B

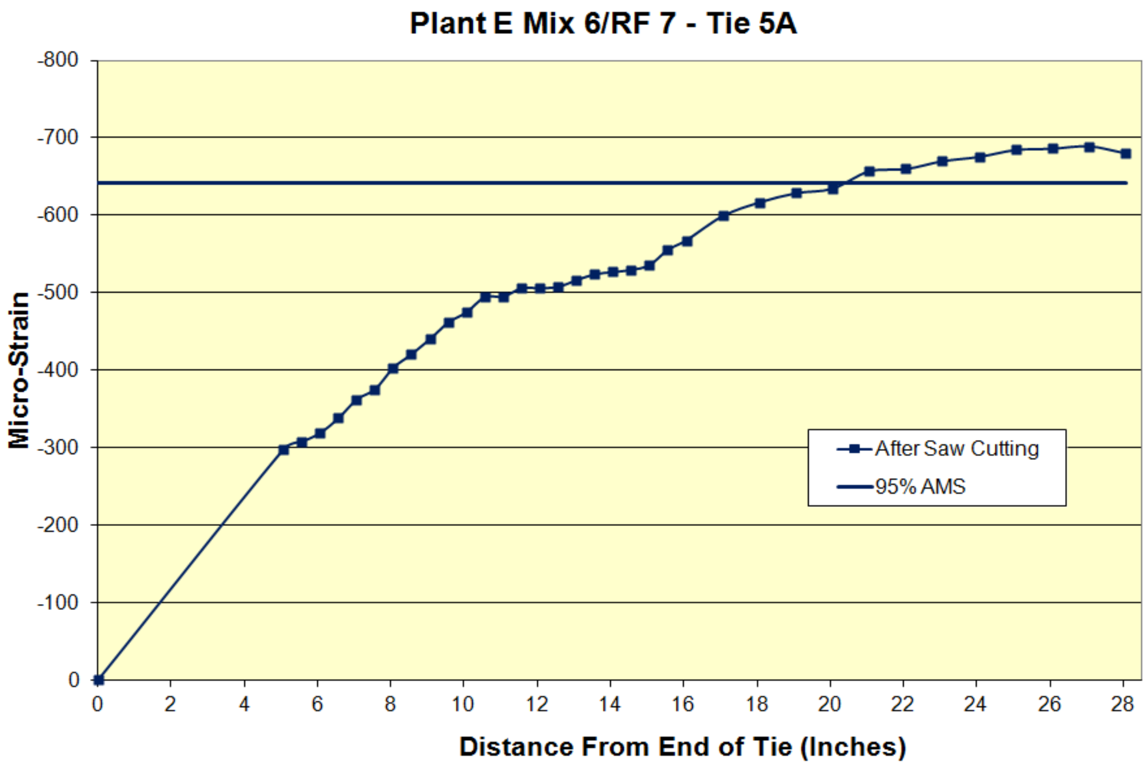

Figure E.7 Transfer length of Plant E Mix 6/RF 7 Tie 5A

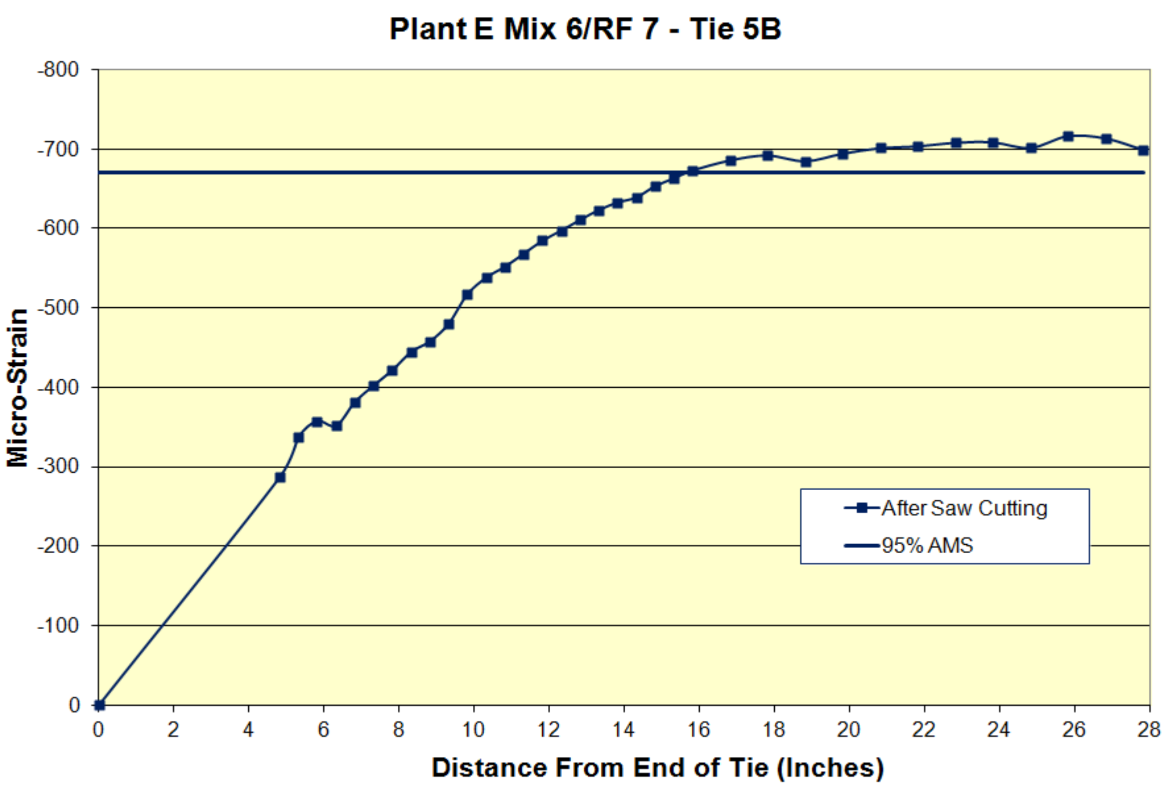

Figure E.8 Transfer length of Plant E Mix 6/RF 7 Tie 5B

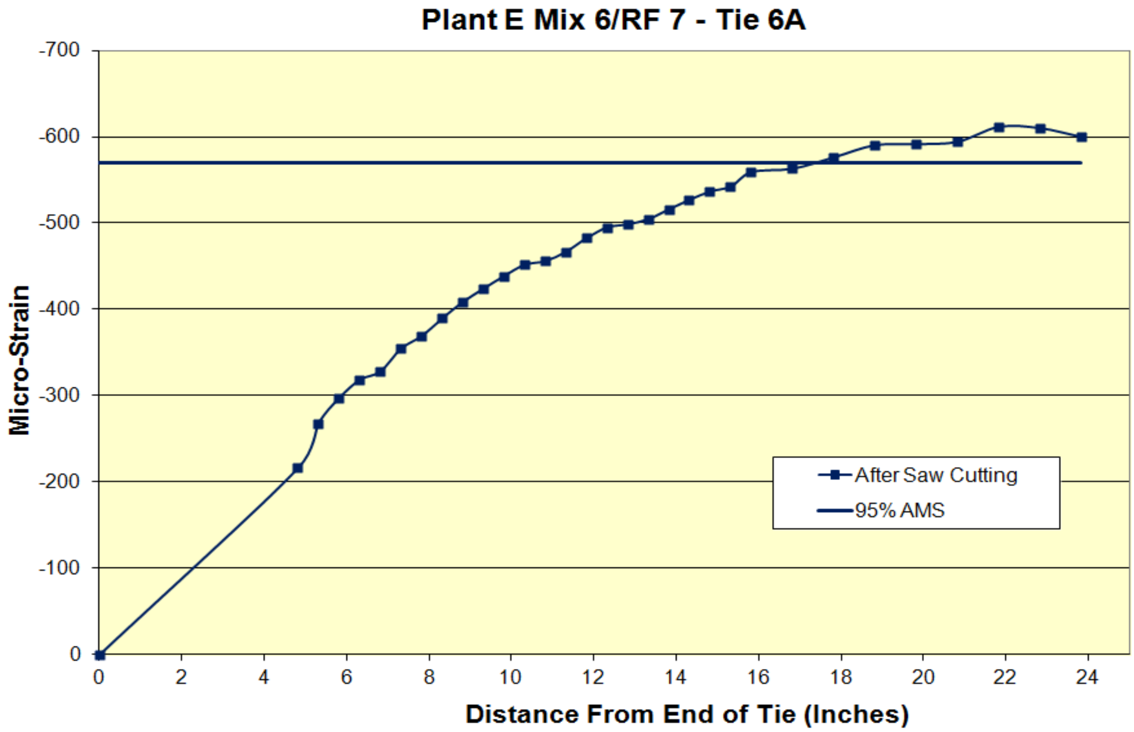

Figure E.9 Transfer length of Plant E Mix 6/RF 7 Tie 6A

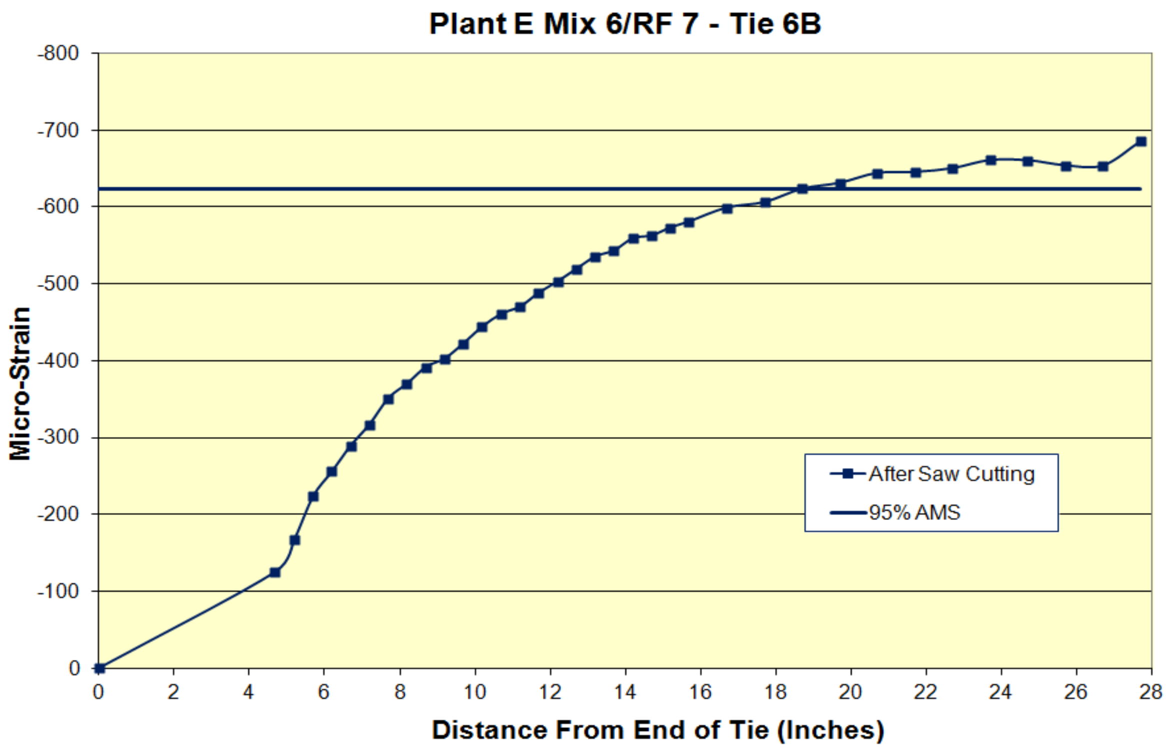

Figure E.10 Transfer length of Plant E Mix 6/RF 7 Tie 6B

Figure E.11 Transfer length of Plant E Mix 6/RF 7 Tie 7A

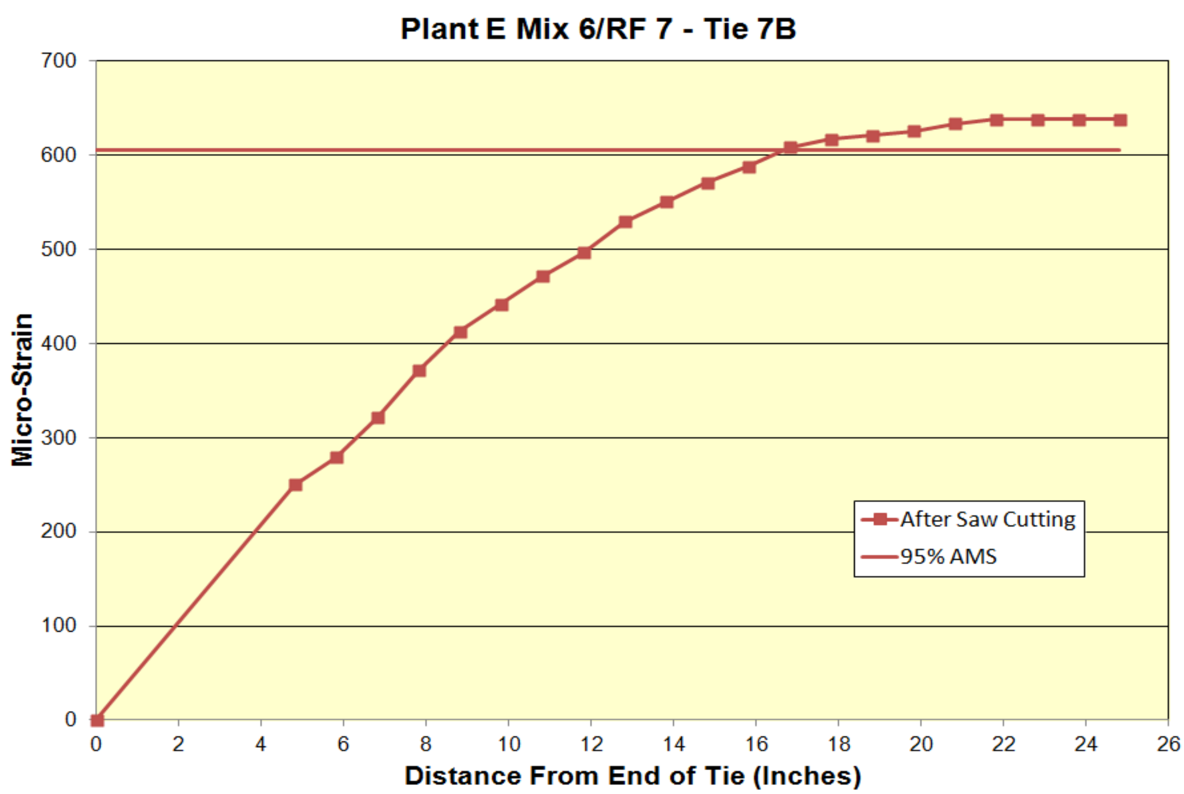

Figure E.12 Transfer length of Plant E Mix 6/RF 7 Tie 7B

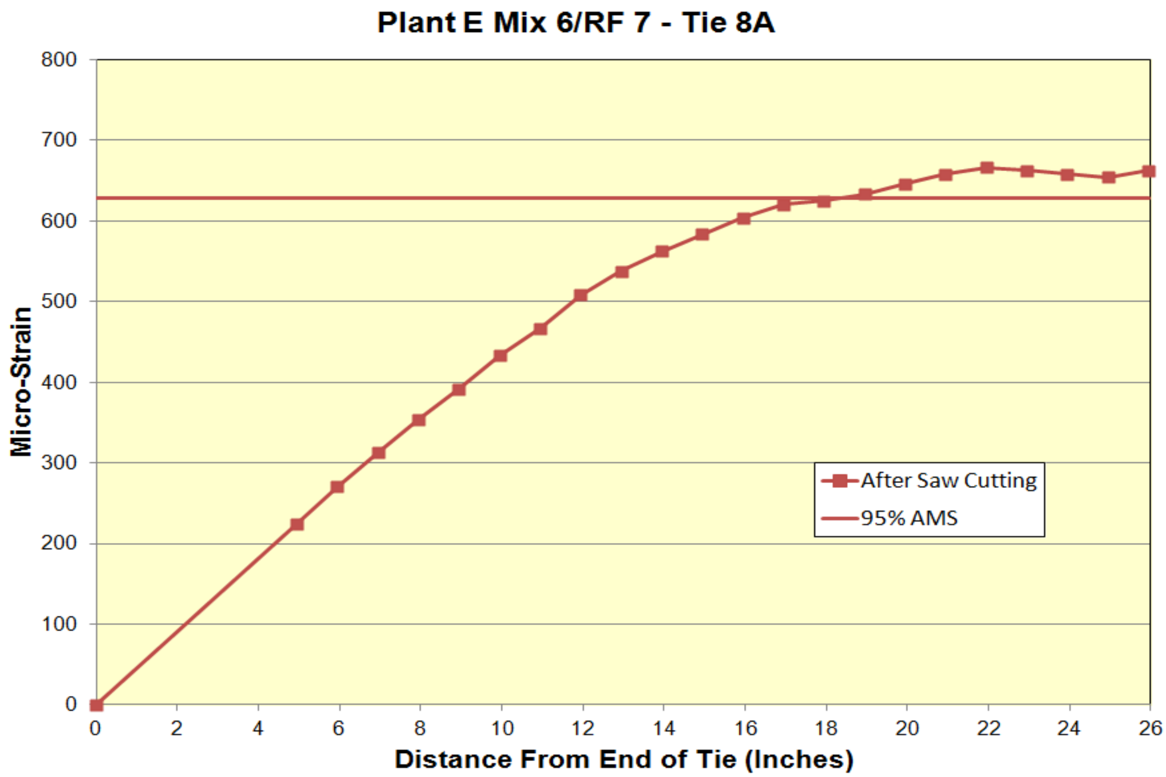

Figure E.13 Transfer length of Plant E Mix 6/RF 7 Tie 8A

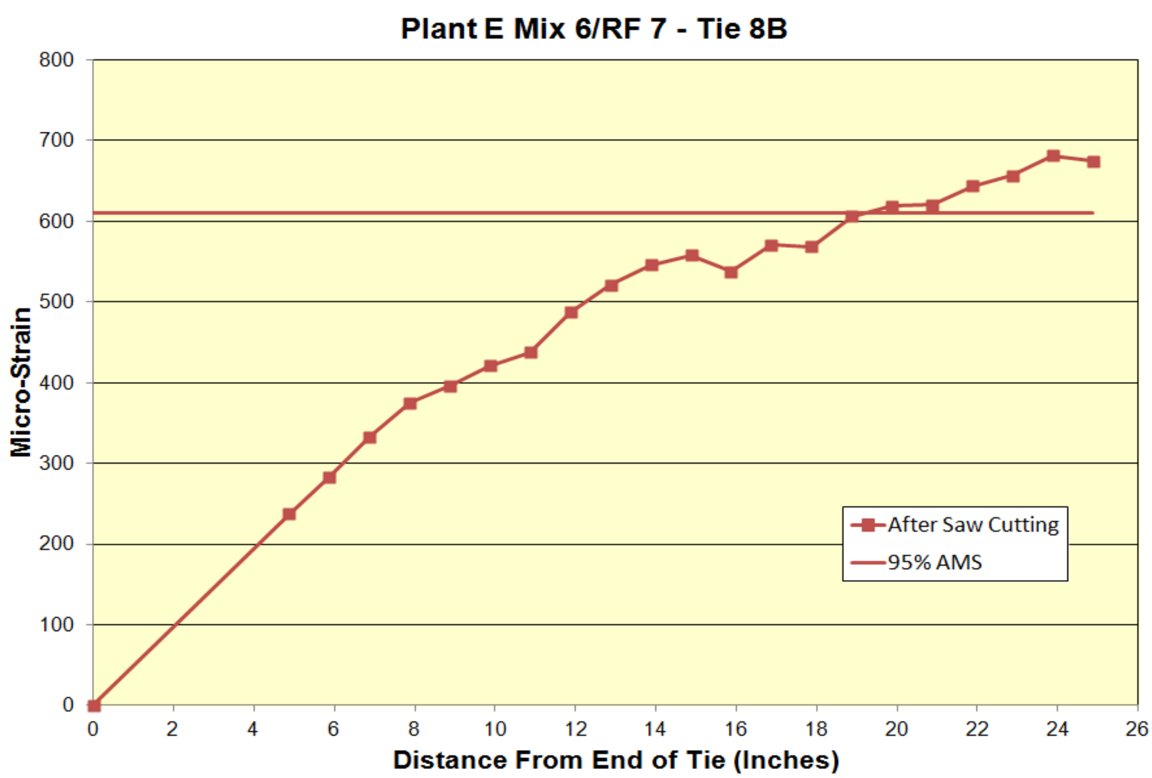

Figure E.14 Transfer length of Plant E Mix 6/RF 7 Tie 8B

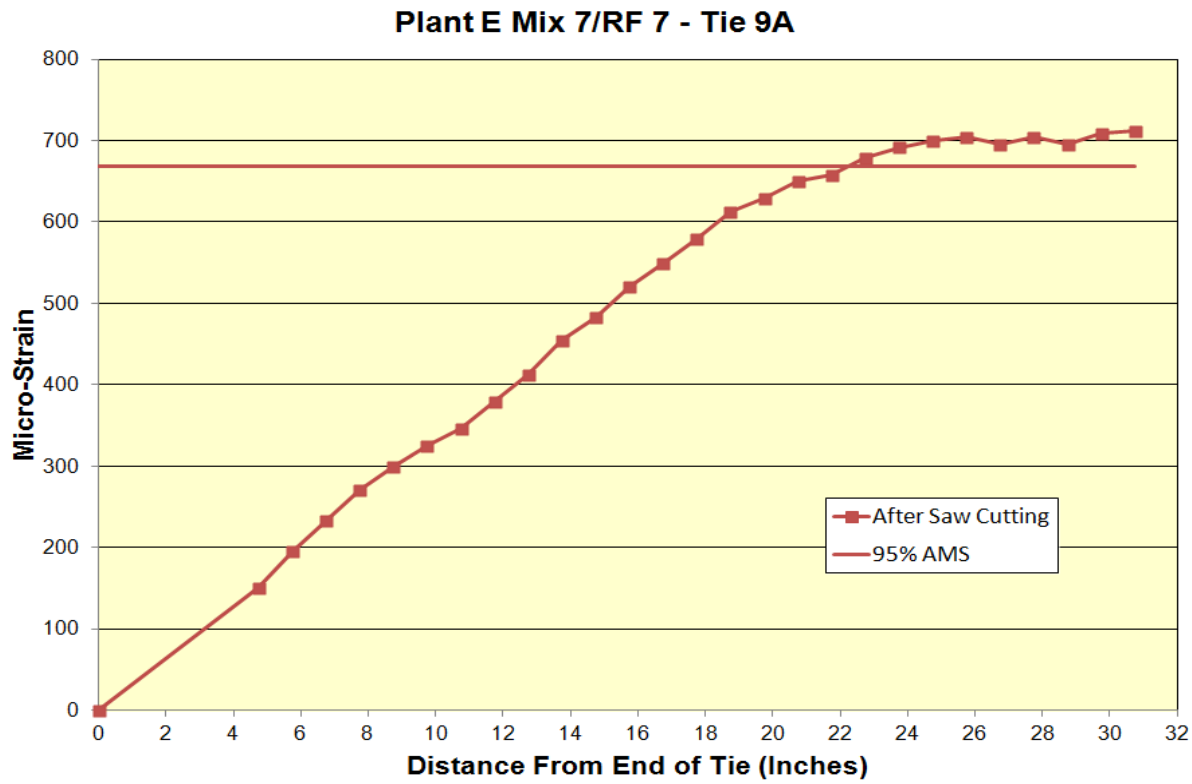

Figure E.15 Transfer length of Plant E Mix 7/RF 7 Tie 9A

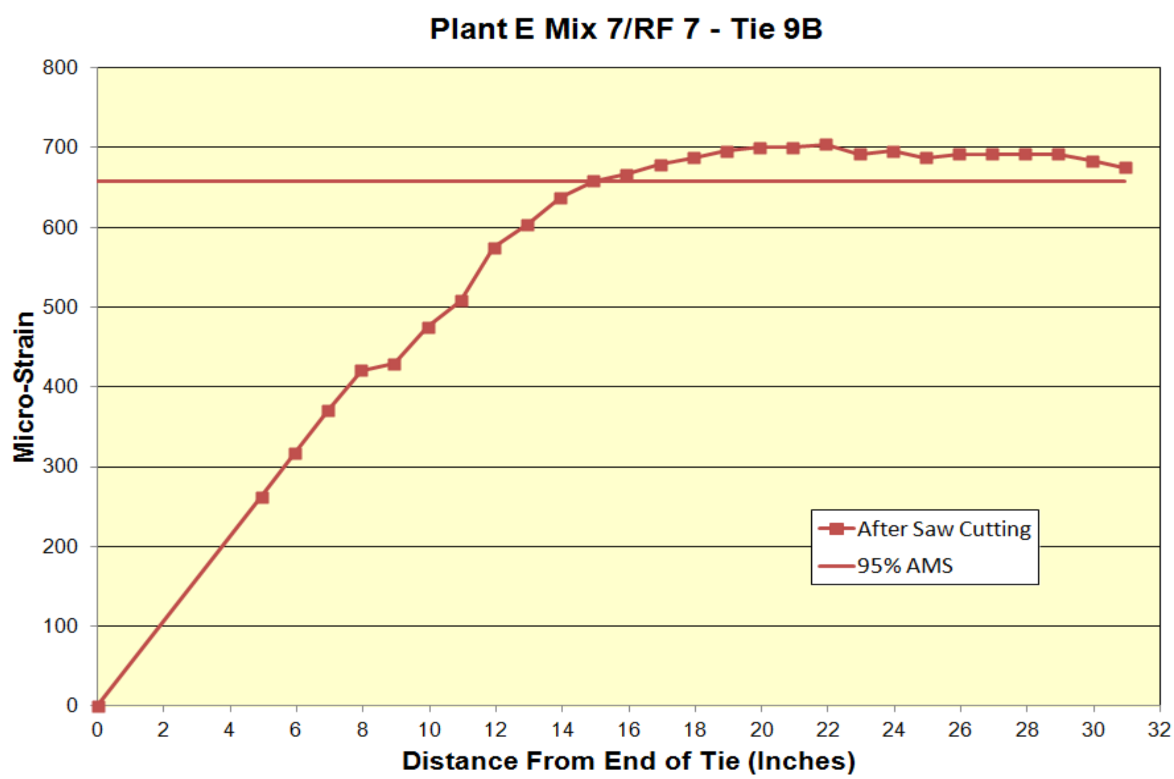

Figure E.16 Transfer length of Plant E Mix 7/RF 7 Tie 9B

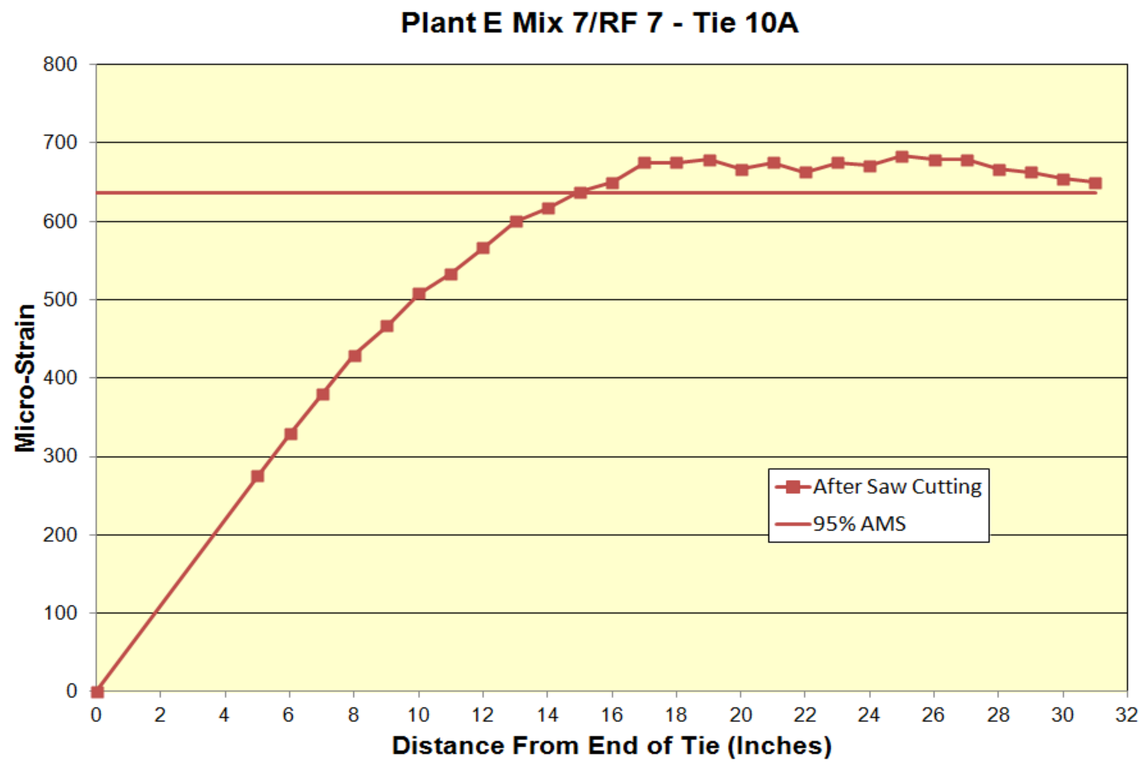

Figure E.17 Transfer length of Plant E Mix 7/RF 7 Tie 10A

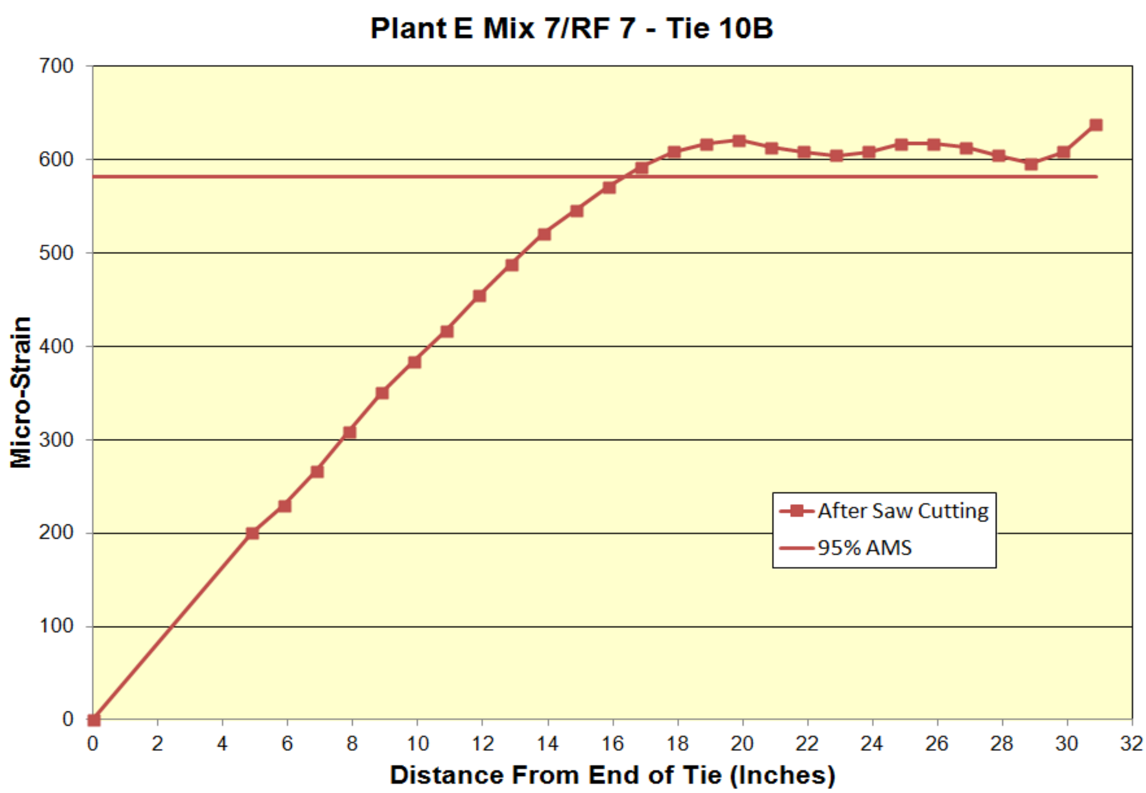

Figure E.18 Transfer length of Plant E Mix 7/RF 7 Tie 10B

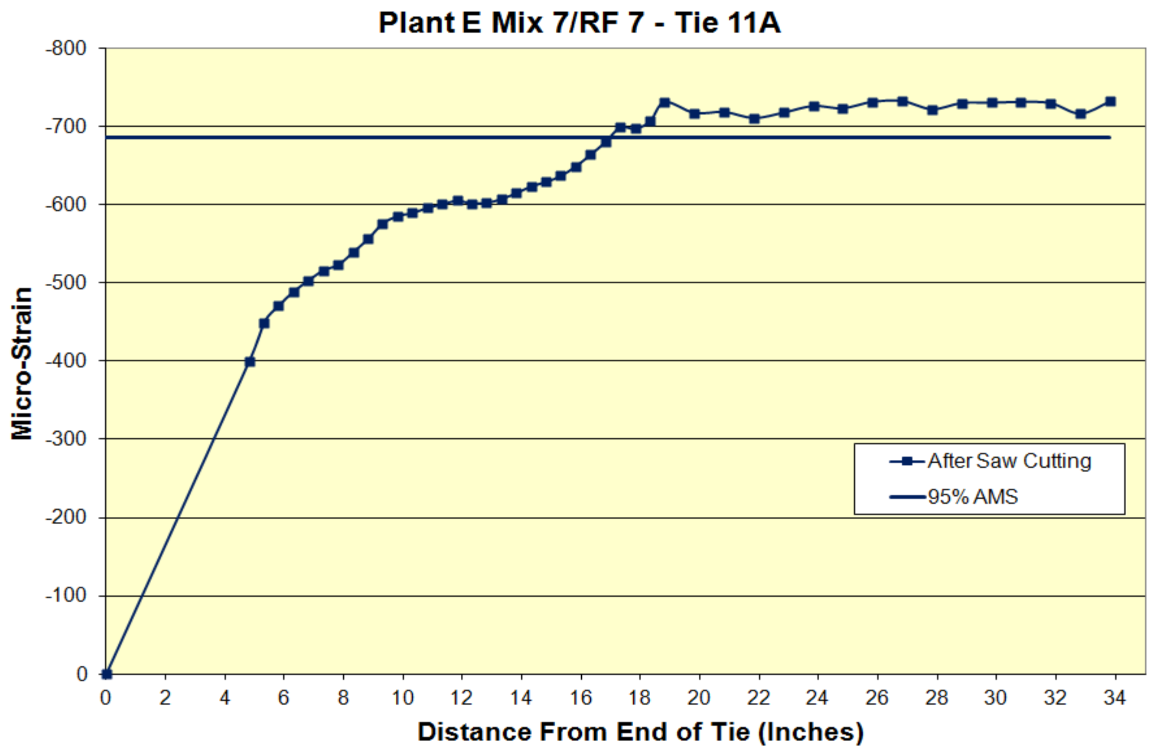

Figure E.19 Transfer length of Plant E Mix 7/RF 7 Tie 11A

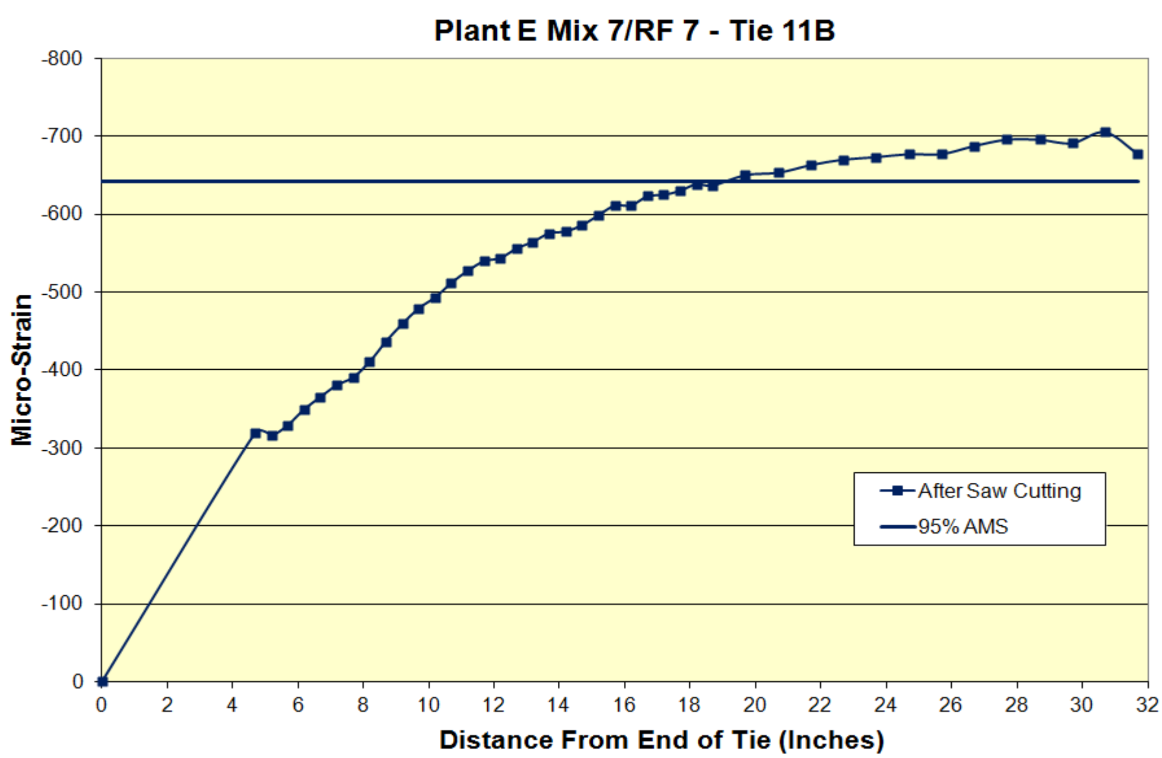

Figure E.20 Transfer length of Plant E Mix 7/RF 7 Tie 11B

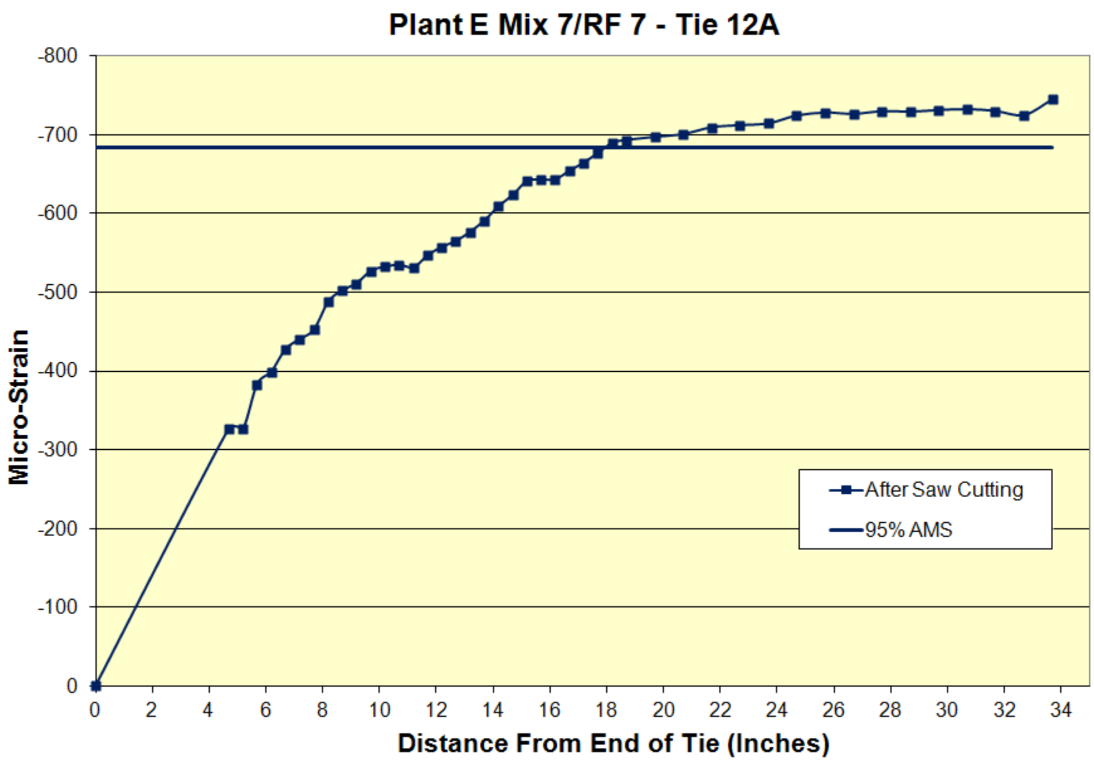

Figure E.21 Transfer length of Plant E Mix 7/RF 7 Tie 12A

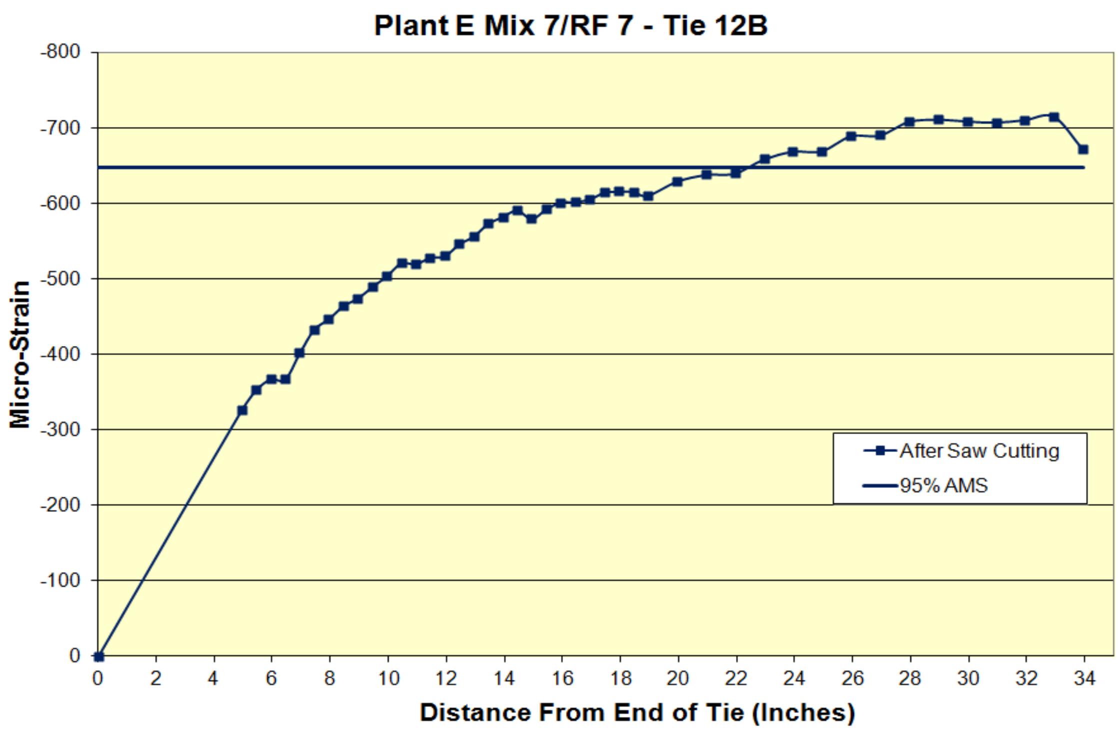

Figure E.22 Transfer length of Plant E Mix 7/RF 7 Tie 12B

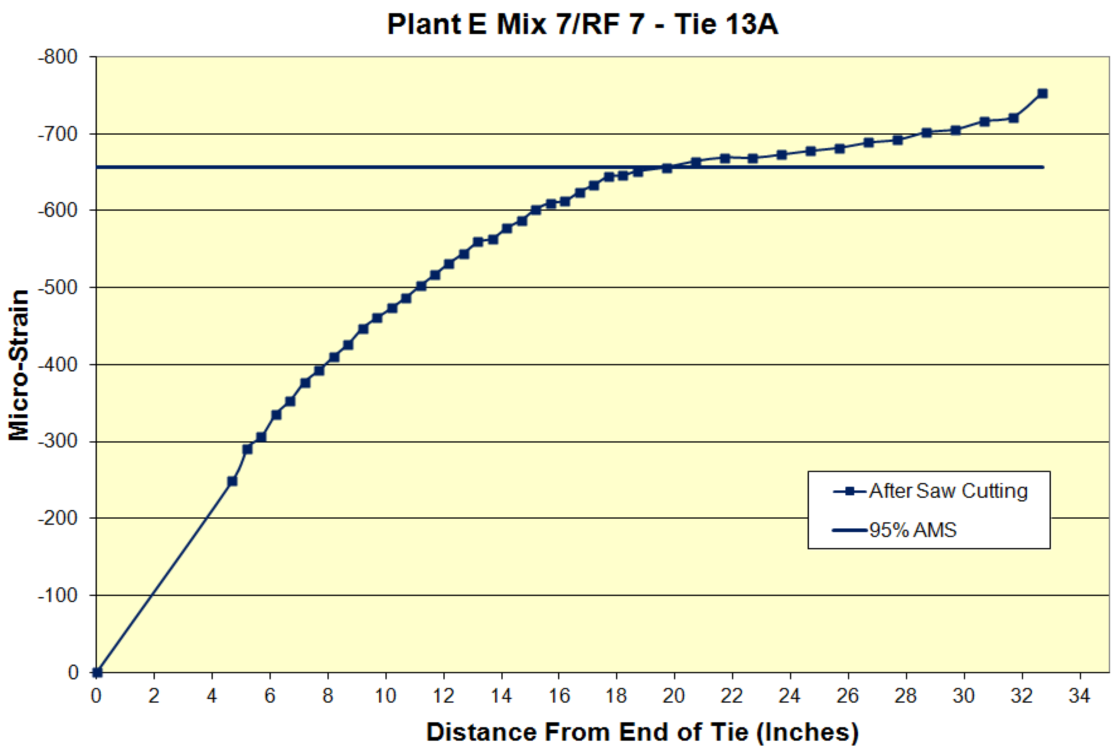

Figure E.23 Transfer length of Plant E Mix 7/RF 7 Tie 13A

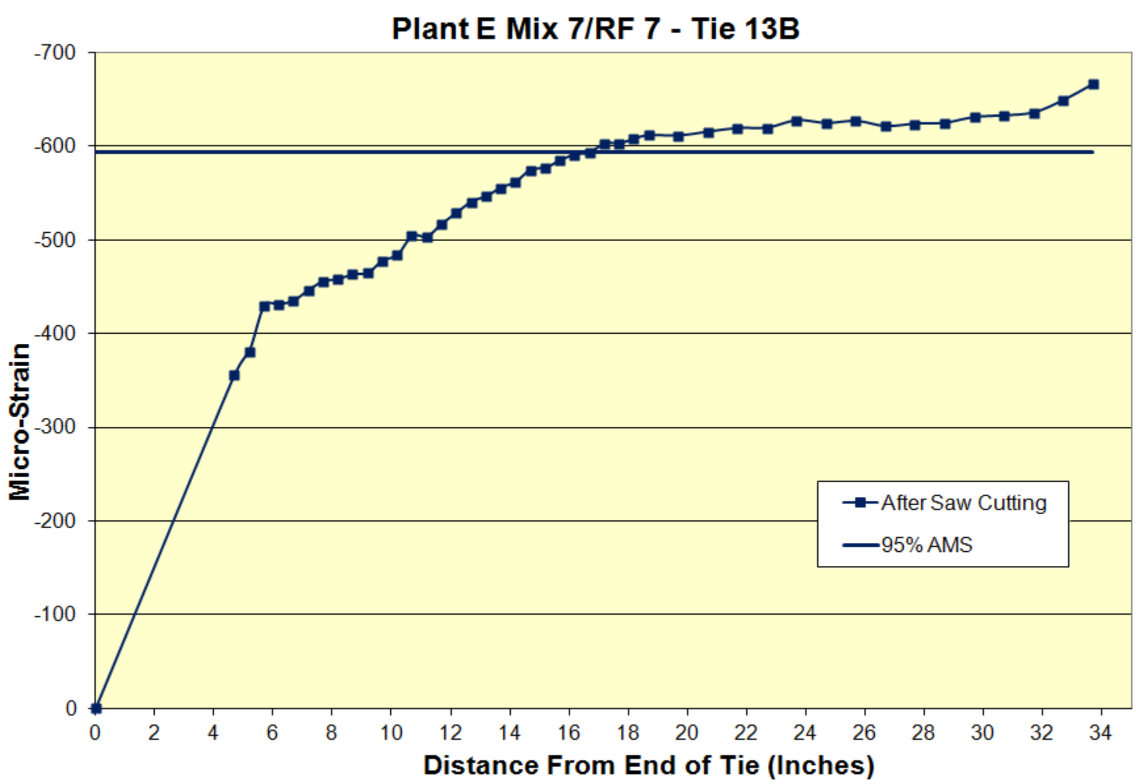

Figure E.24 Transfer length of Plant E Mix 7/RF 7 Tie 13B

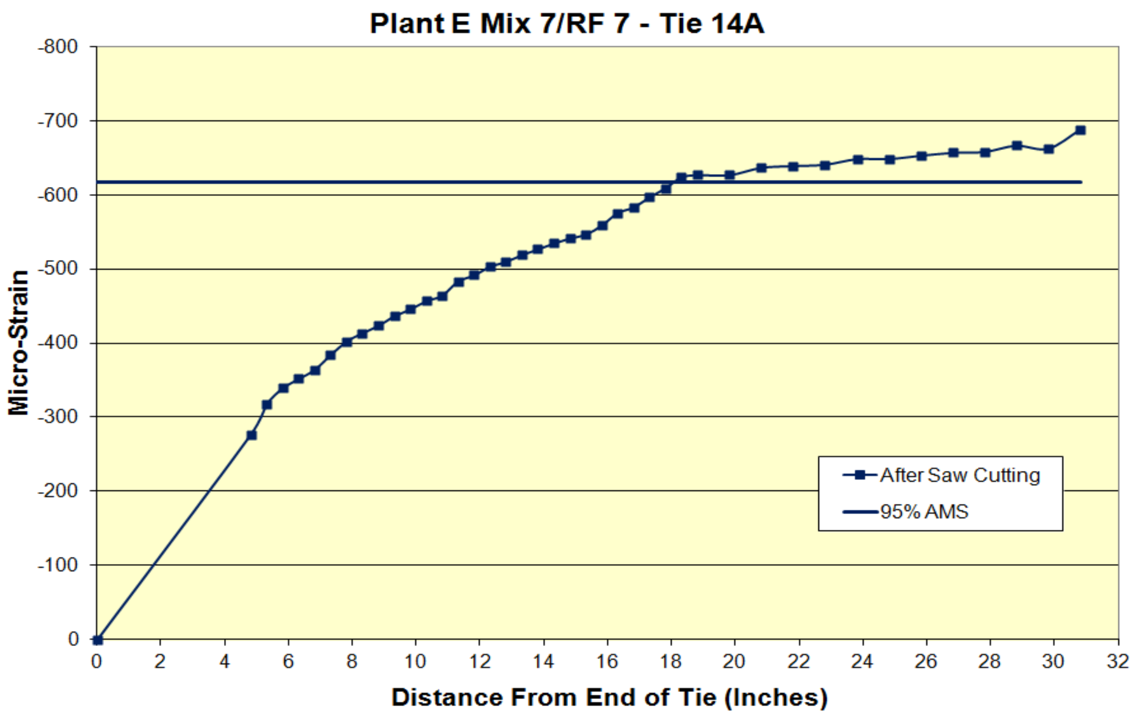

Figure E.25 Transfer length of Plant E Mix 7/RF 7 Tie 14A

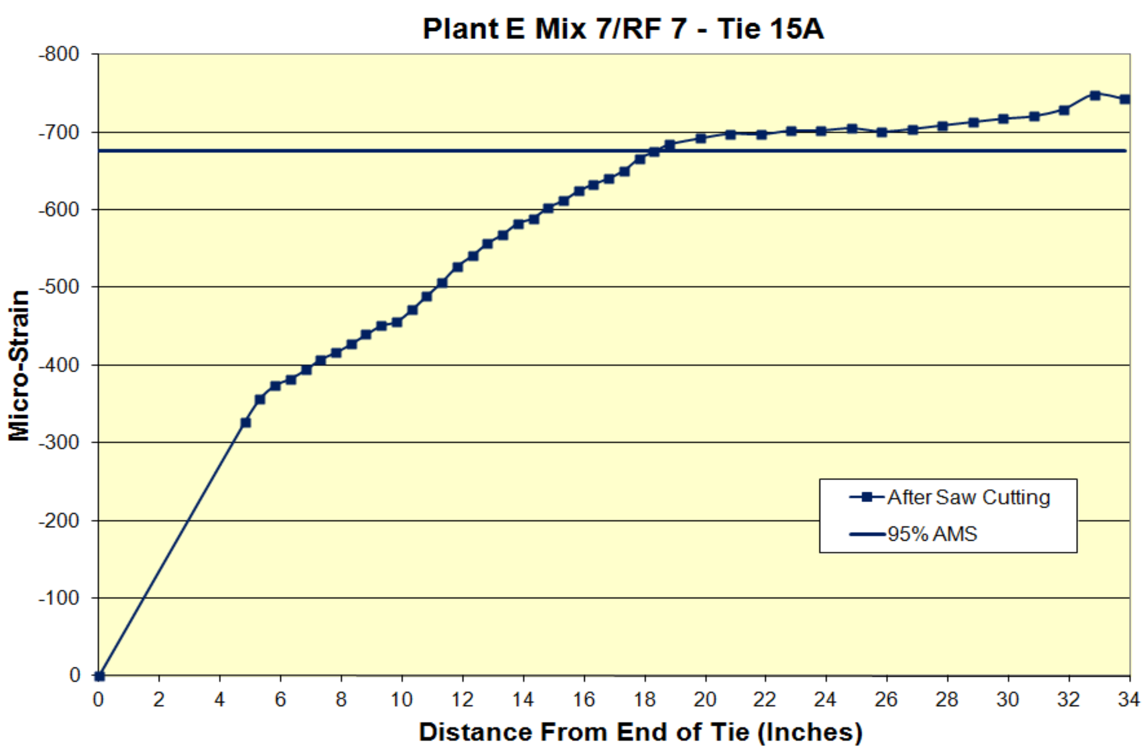

Figure E.26 Transfer length of Plant E Mix 7/RF 7 Tie 15A

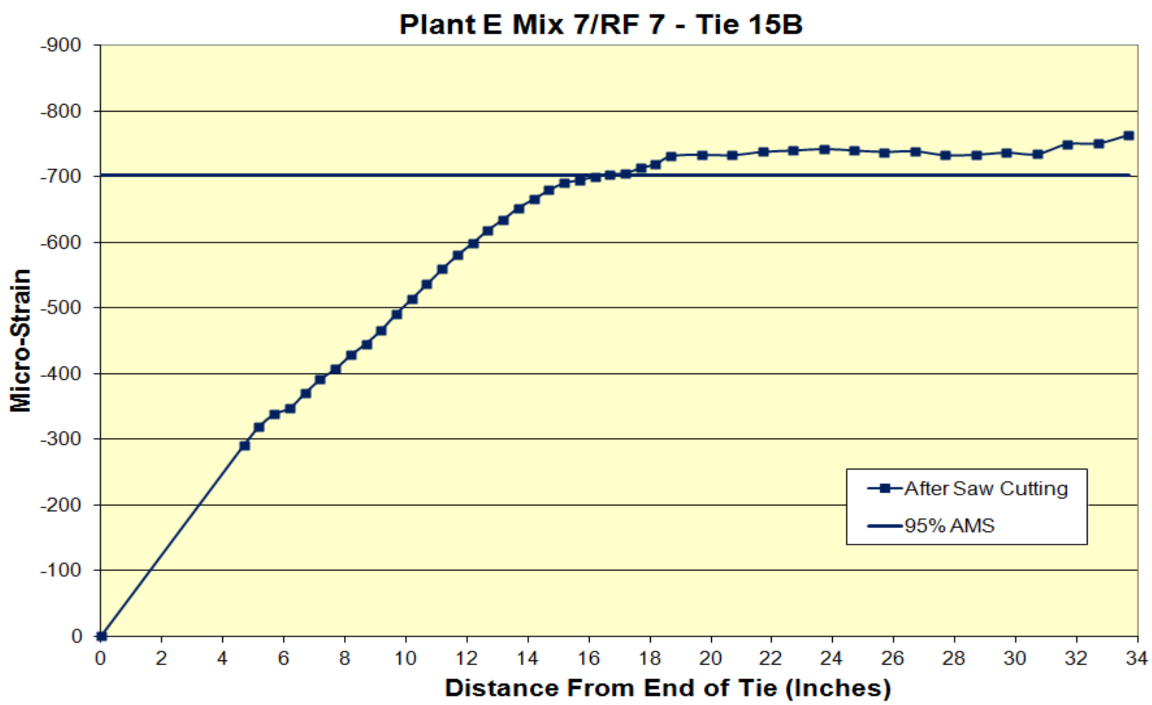

Figure E.27 Transfer length of Plant E Mix 7/RF 7 Tie 15B

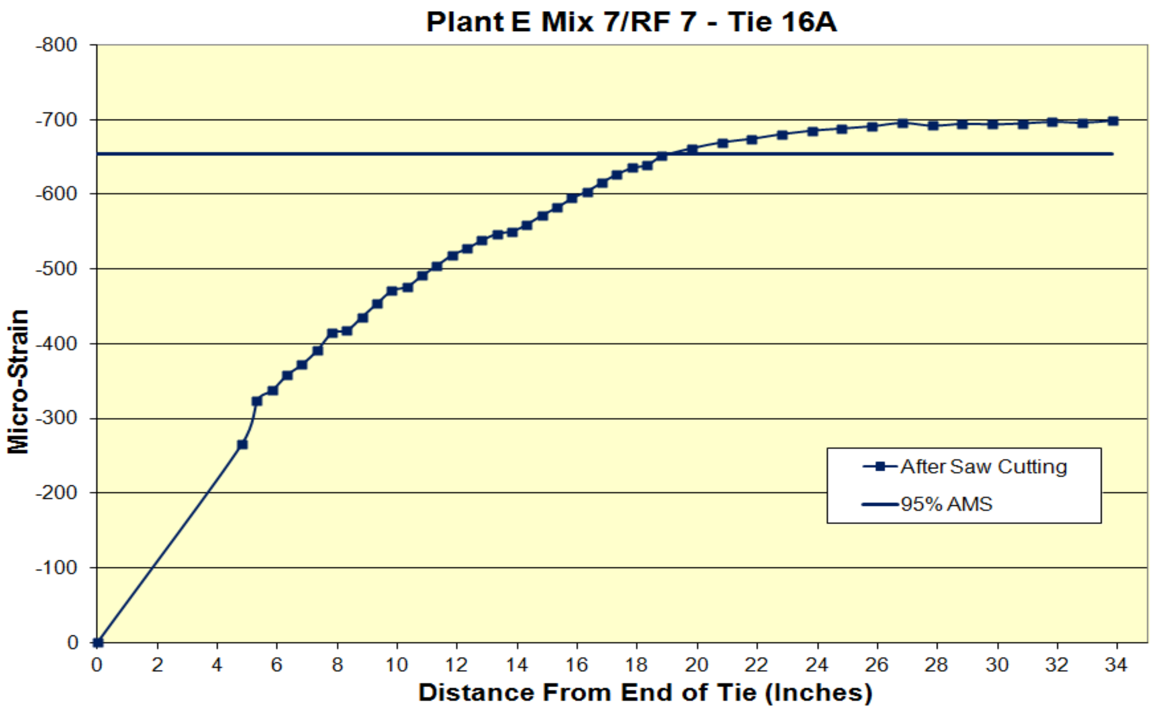

Figure E.28 Transfer length of Plant E Mix 7/RF 7 Tie 16A

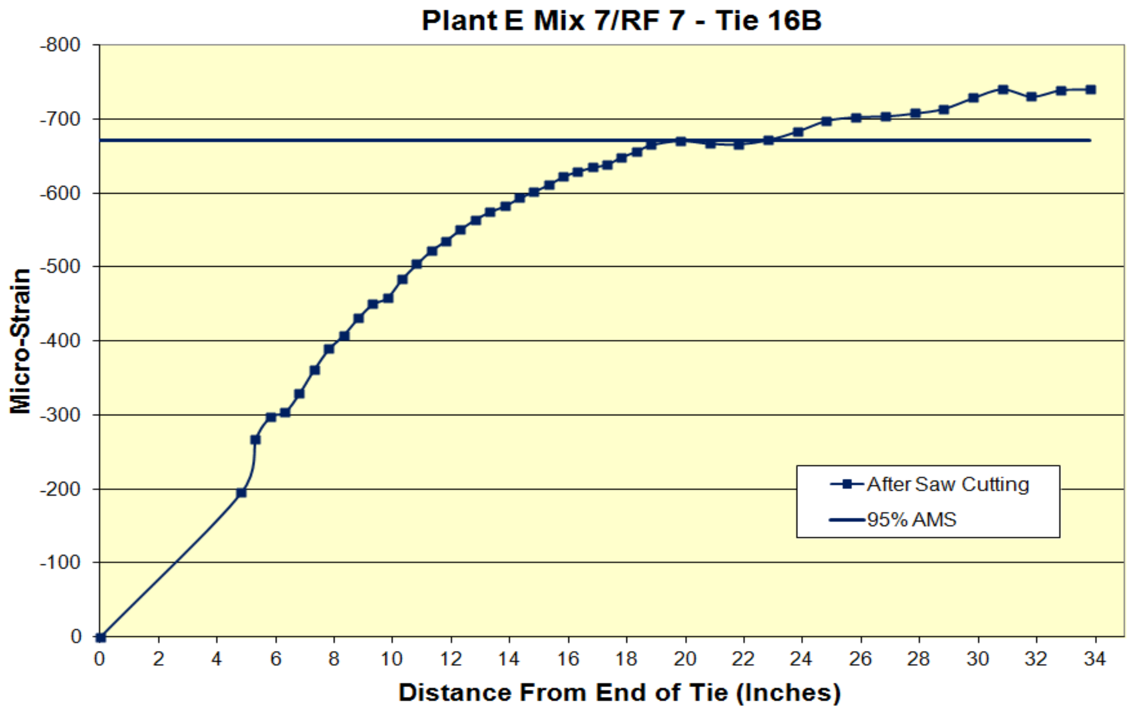

Figure E.29 Transfer length of Plant E Mix 7/RF 7 Tie 16B

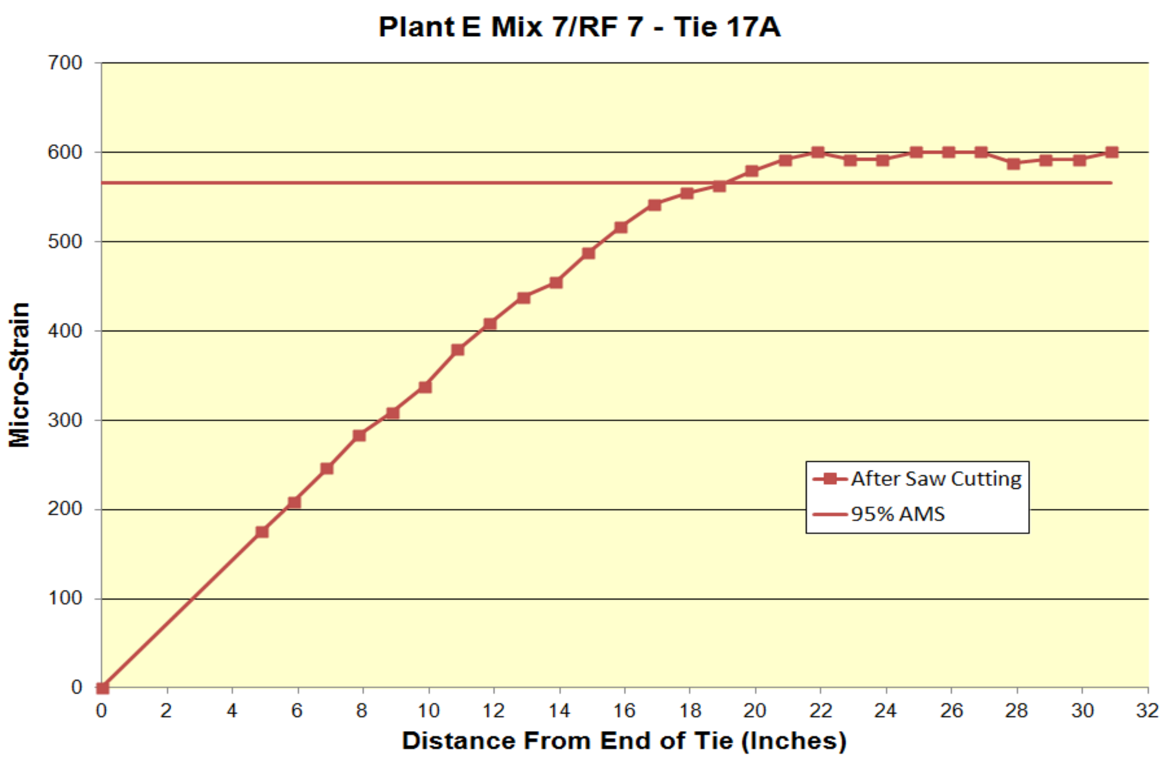

Figure E.30 Transfer length of Plant E Mix 7/RF 7 Tie 17A

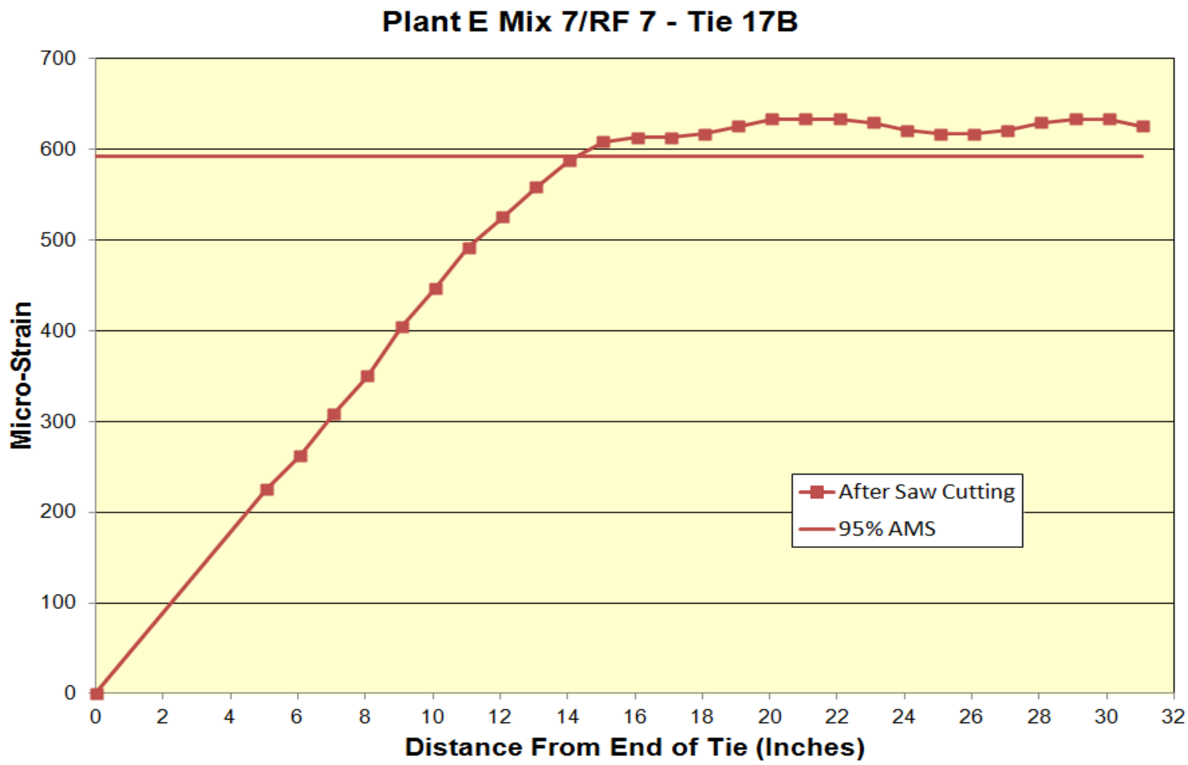

Figure E.31 Transfer length of Plant E Mix 7/RF 7 Tie 17B

E.2 Long-term Transfer Lengths

Table E.2 Long-term transfer length data for Plant E Mix 7/RF 7

Plant E Mix 7/RF 7				
	Transfer Length (in.)			
Time of Reading	Tie 9A	Tie 9B	17A	17B
After Saw Cutting	22.2	15	19	14.4
315 Days After Pour	22.6	15.2	19.4	14.9

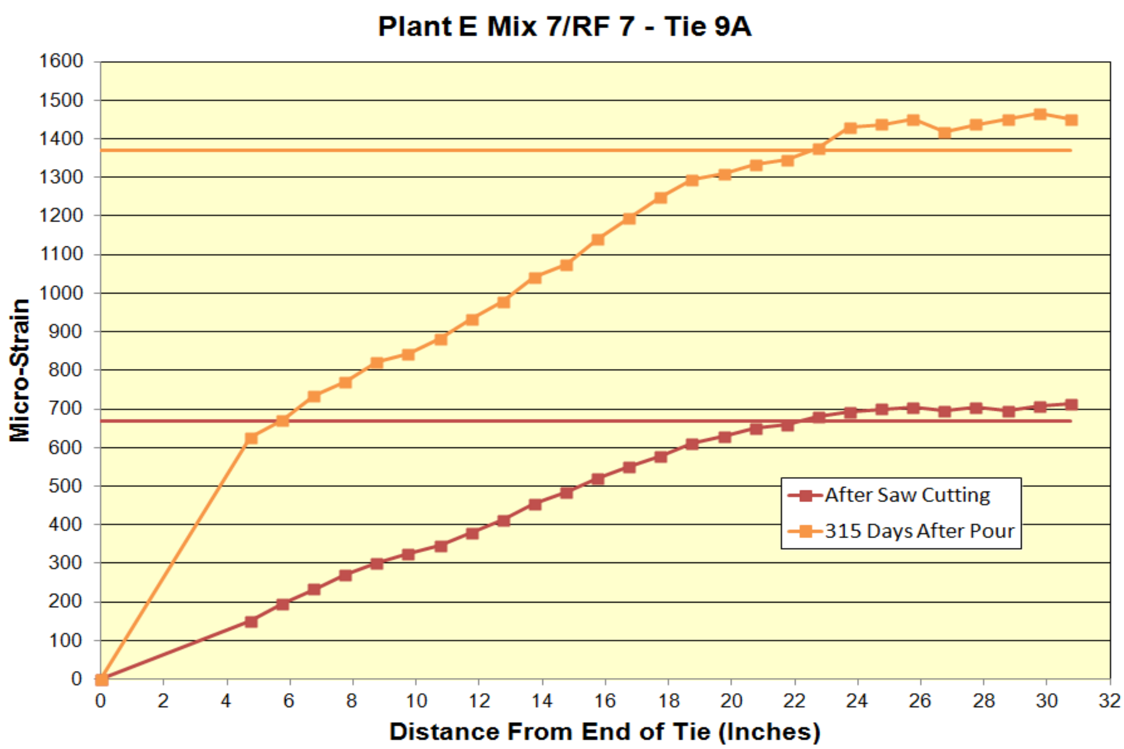

Figure E.32 Long-term transfer length of Plant E Mix 7/RF 7 Tie 9A

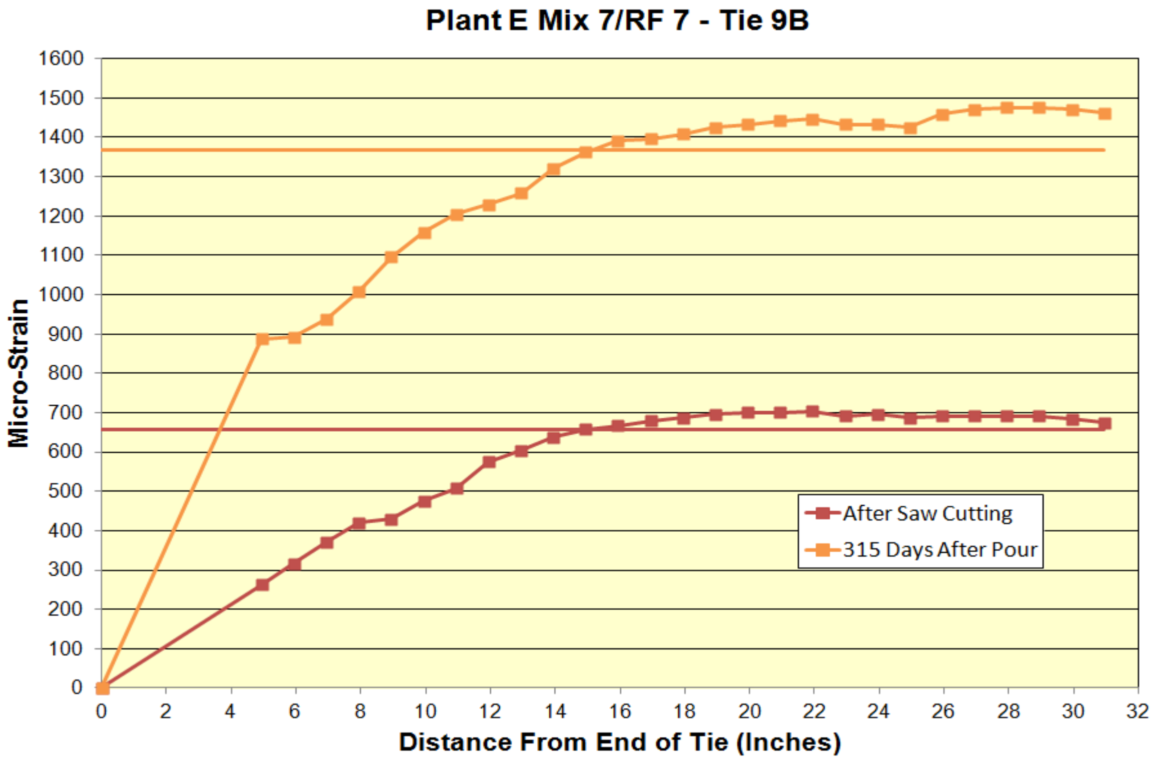

Figure E.33 Long-term transfer length of Plant E Mix 7/RF 7 Tie 9B

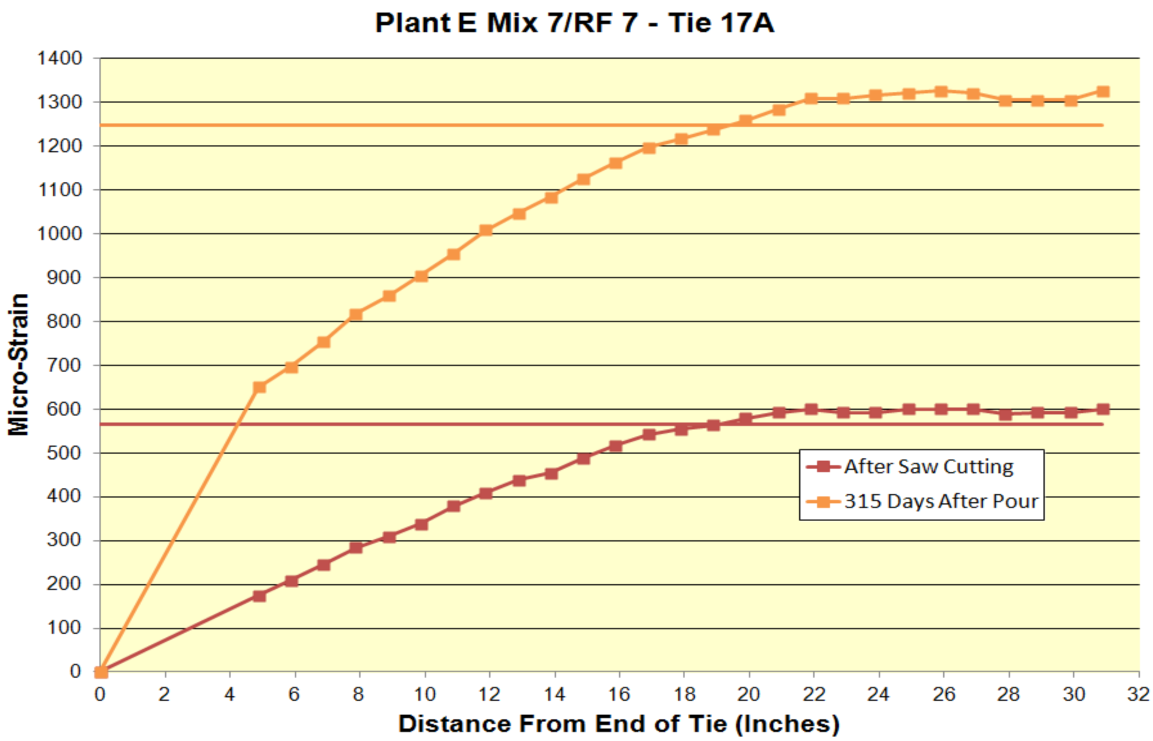

Figure E.34 Long-term transfer length of Plant E Mix 7/RF 7 Tie 17A

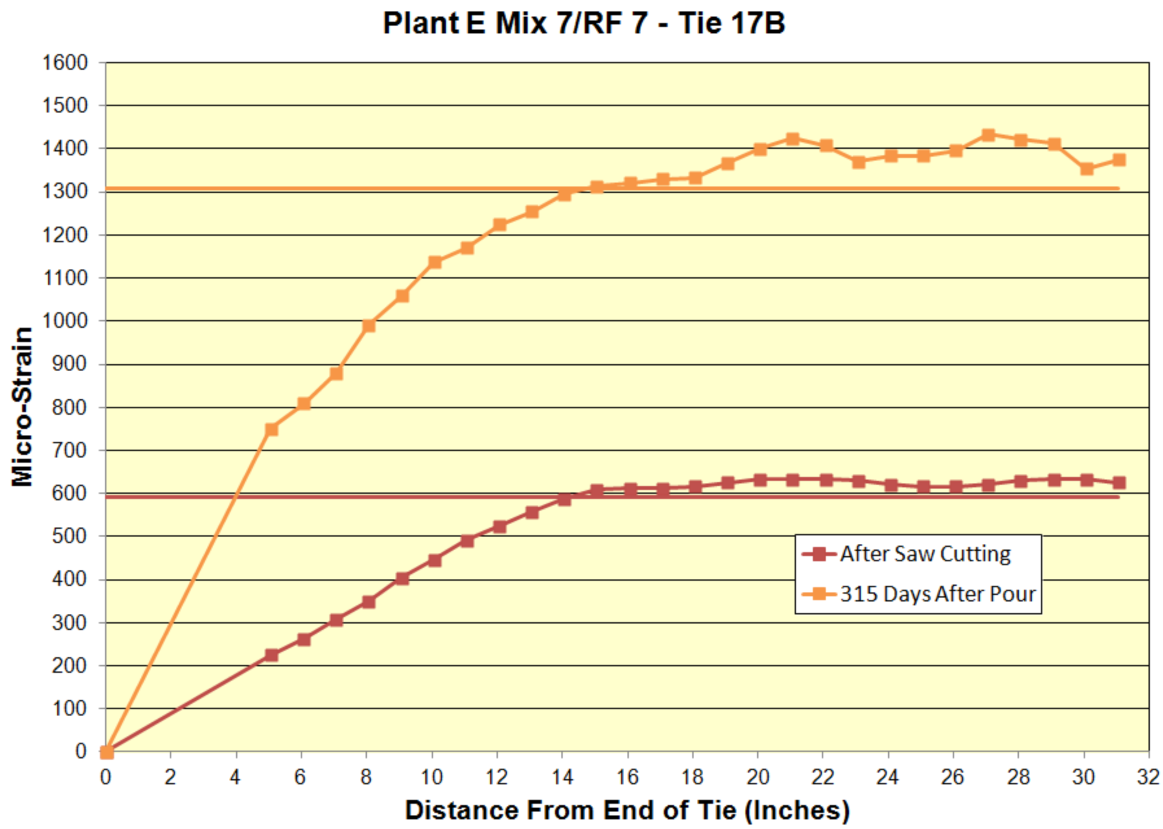

Figure E.35 Long-term transfer length of Plant E Mix 7/RF 7 Tie 17B

Appendix F Plant F Transfer Lengths

F.1 Short-term Transfer Lengths

Table F.1 Plant F transfer length data

	Tie Label	Measurement Method	Transfer Length (in.)
Plant F Mix 8/RF 8	1A	Laser Speckle	10
	1B	Laser Speckle	14
	2A	Laser Speckle	8
	2B	Laser Speckle	4.5
	3A	Laser Speckle	6
	3B	Laser Speckle	9.8
	4A	Whittemore Gage	9.3
	4B	Whittemore Gage	12.2
	5A	Whittemore Gage	11
Plant F Mix 8/RF 9	1A	Laser Speckle	9
	1B	Laser Speckle	9.6
	2A	Laser Speckle	14.7
	2B	Laser Speckle	9.5
	3A	Laser Speckle	7.5
	3B	Laser Speckle	7.5
	4A	Whittemore Gage	7.4
	4B	Whittemore Gage	9.3
	5A	Whittemore Gage	9.8
Plant F Mix 8/RF 10	1B	Laser Speckle	7
	2A	Laser Speckle	7.5
	2B	Laser Speckle	8.3
	3A	Laser Speckle	5.2
	3B	Laser Speckle	8
	4A	Whittemore Gage	9.7
	4B	Whittemore Gage	8.7
	5A	Whittemore Gage	7.8
Plant F Mix 9/RF 10	1A	Laser Speckle	5.1
	1B	Laser Speckle	8
	2A	Laser Speckle	11
	2B	Laser Speckle	10.5
	3A	Laser Speckle	7.5
	3B	Laser Speckle	8.5
	4A	Whittemore Gage	7.3
	4B	Whittemore Gage	6.8
	5A	Whittemore Gage	8.3

Note: Side A = Dead-end of tie

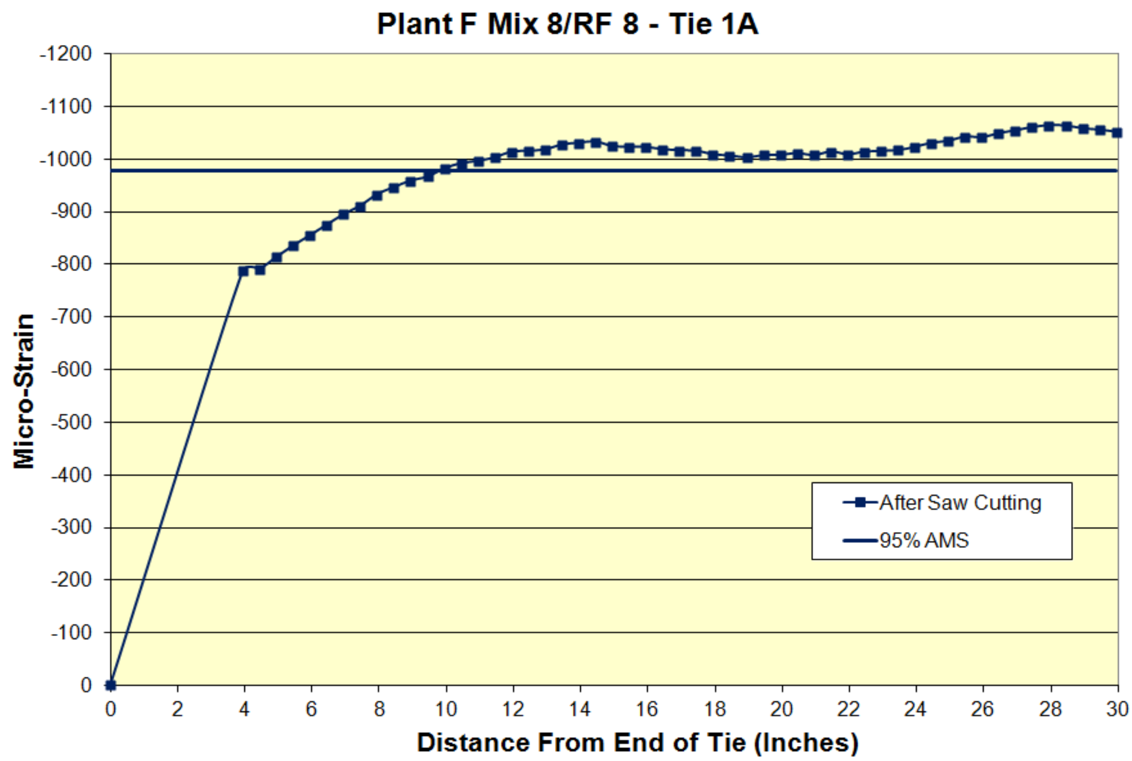

Figure F.1 Transfer length of Plant F Mix 8/RF 8 Tie 1A

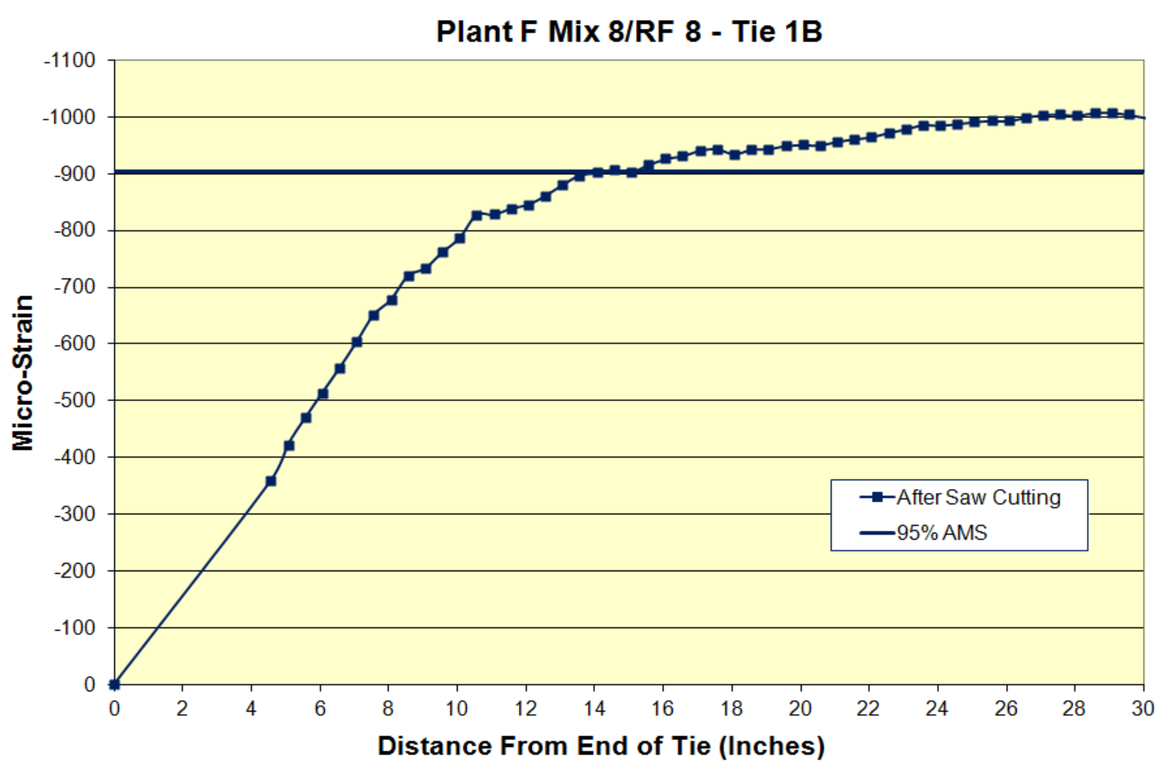

Figure F.2 Transfer length of Plant F Mix 8/RF 8 Tie 1B

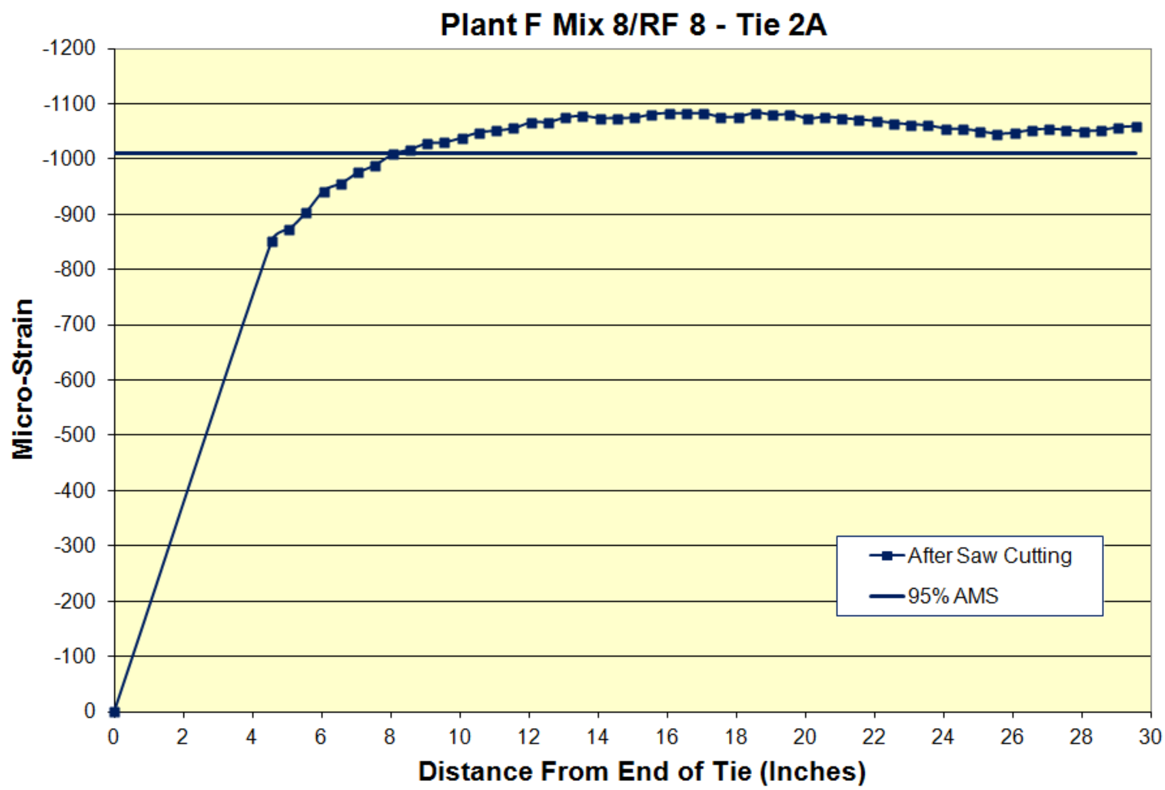

Figure F.3 Transfer length of Plant F Mix 8/RF 8 Tie 2A

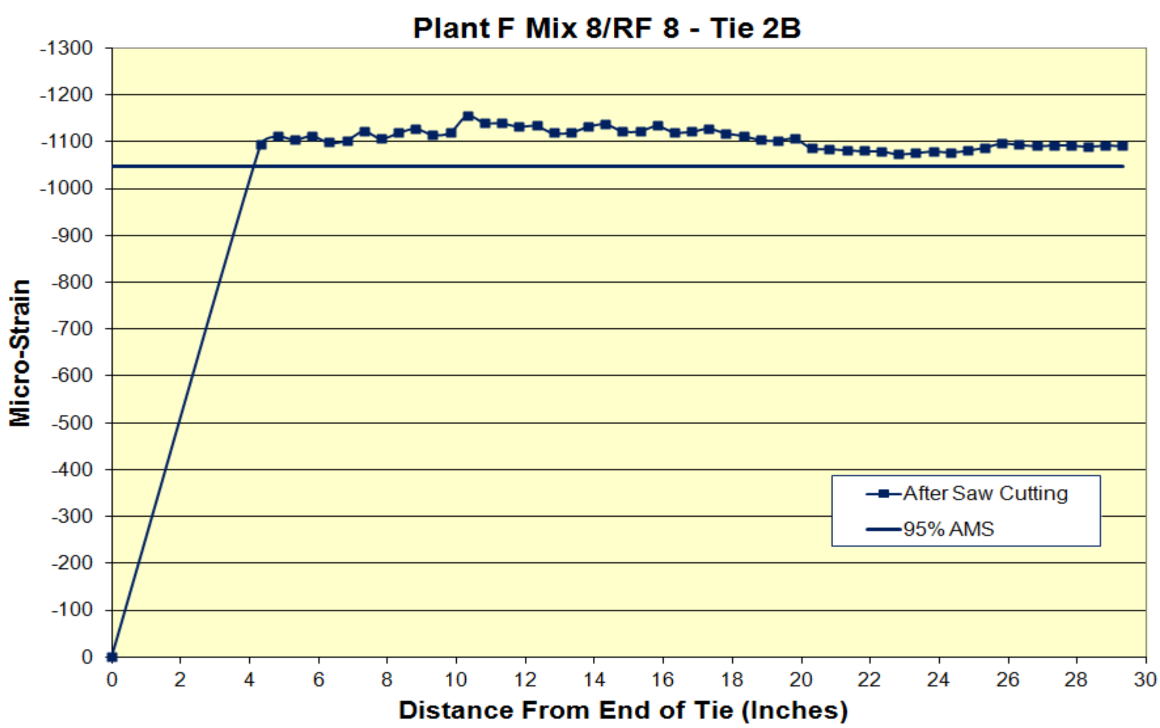

Figure F.4 Transfer length of Plant F Mix 8/RF 8 Tie 2B

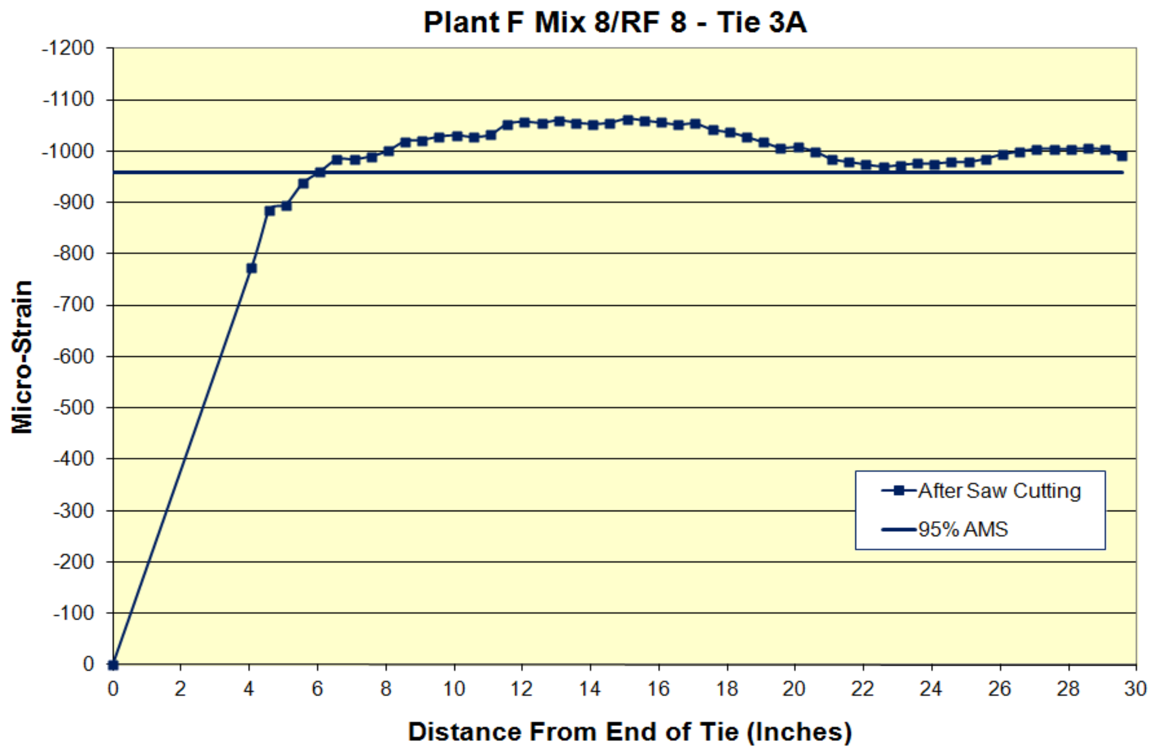

Figure F.5 Transfer length of Plant F Mix 8/RF 8 Tie 3A

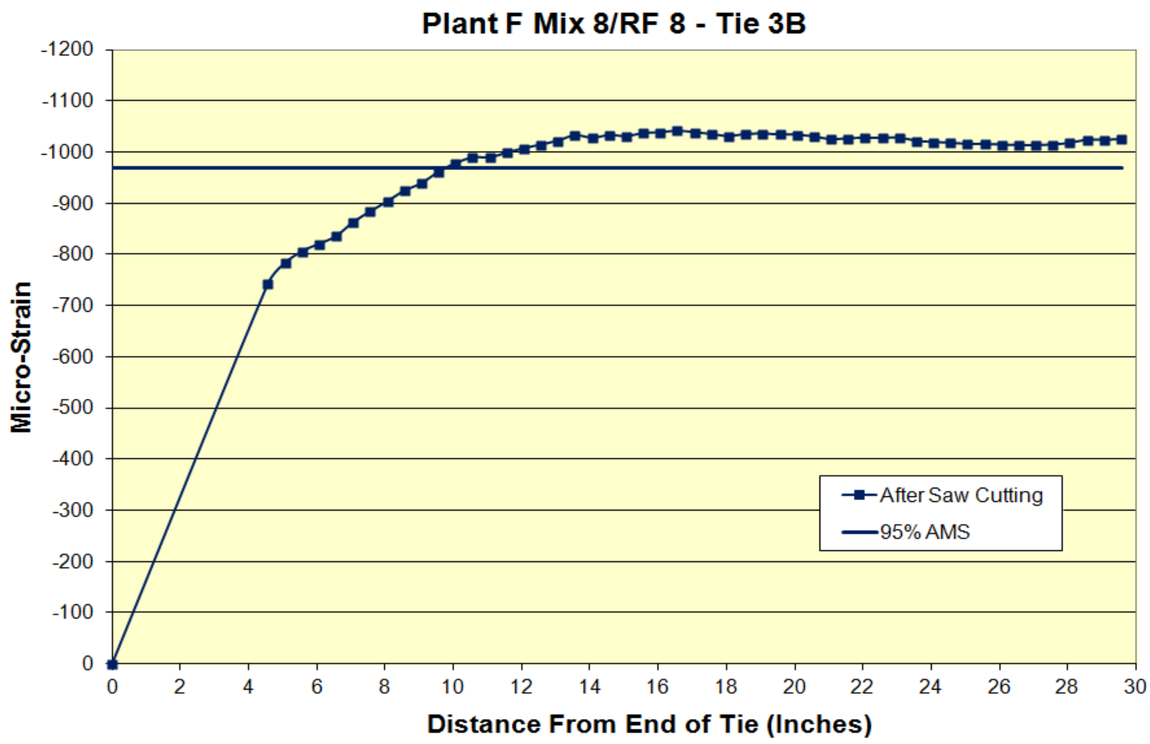

Figure F.6 Transfer length of Plant F Mix 8/RF 8 Tie 3B

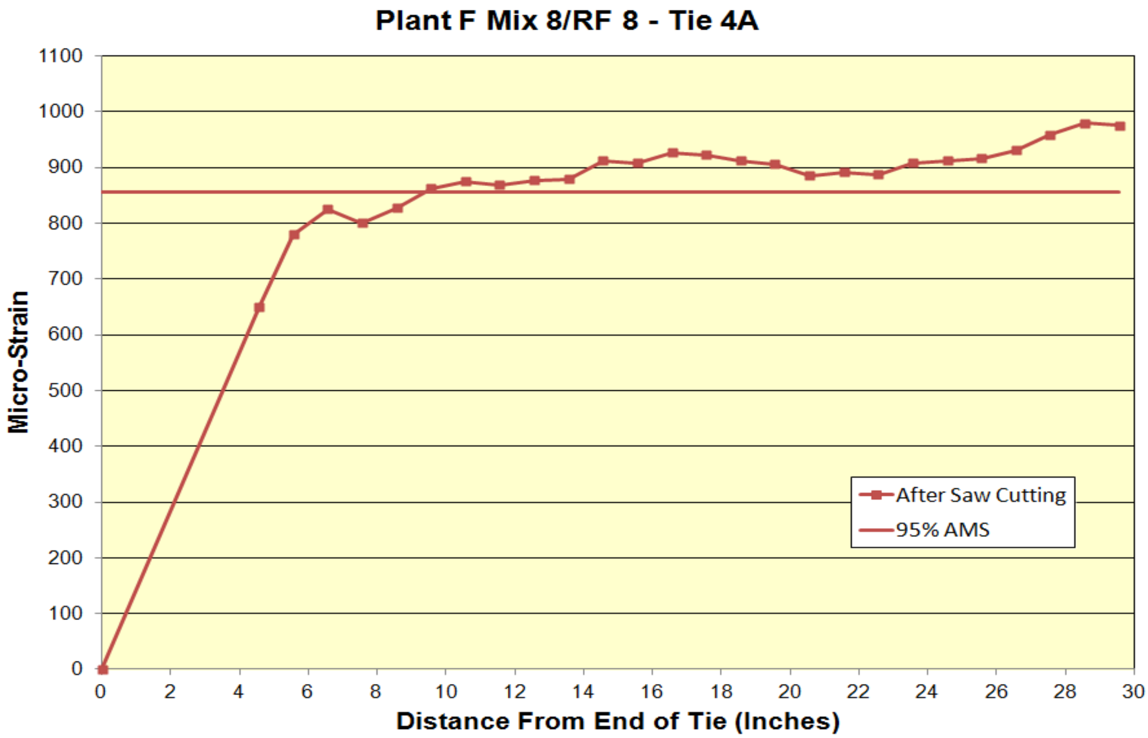

Figure F.7 Transfer length of Plant F Mix 8/RF 8 Tie 4A

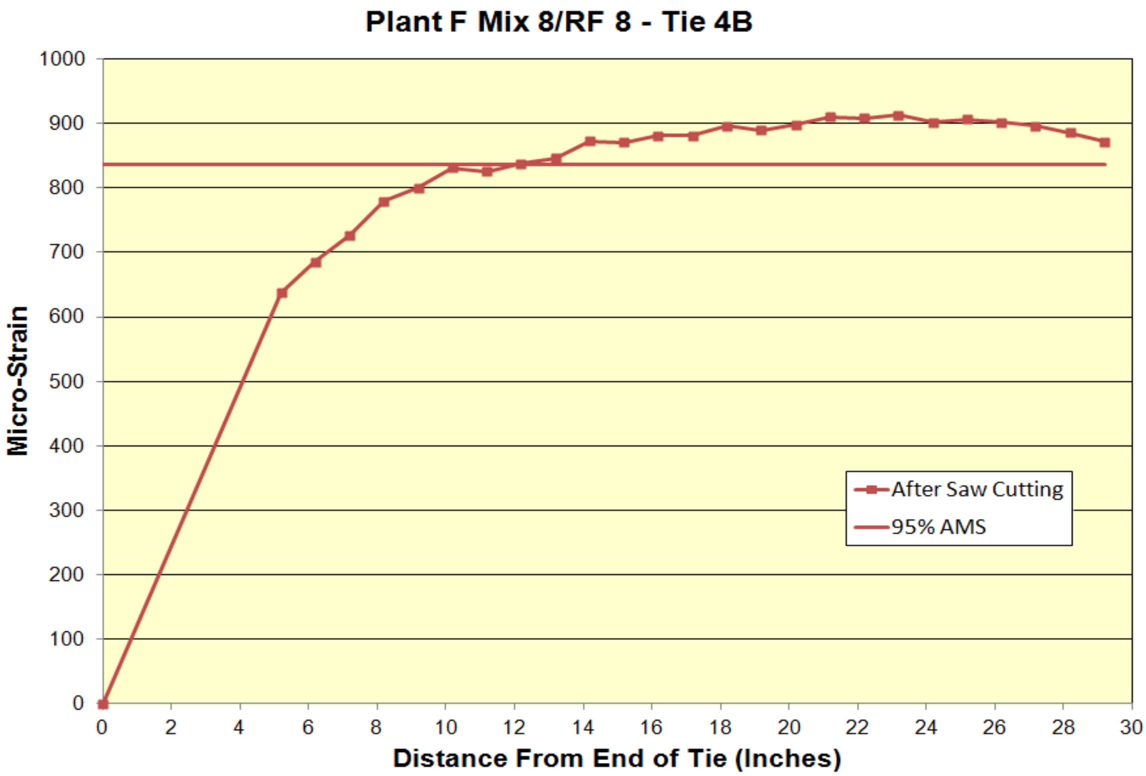

Figure F.8 Transfer length of Plant F Mix 8/RF 8 Tie 4B

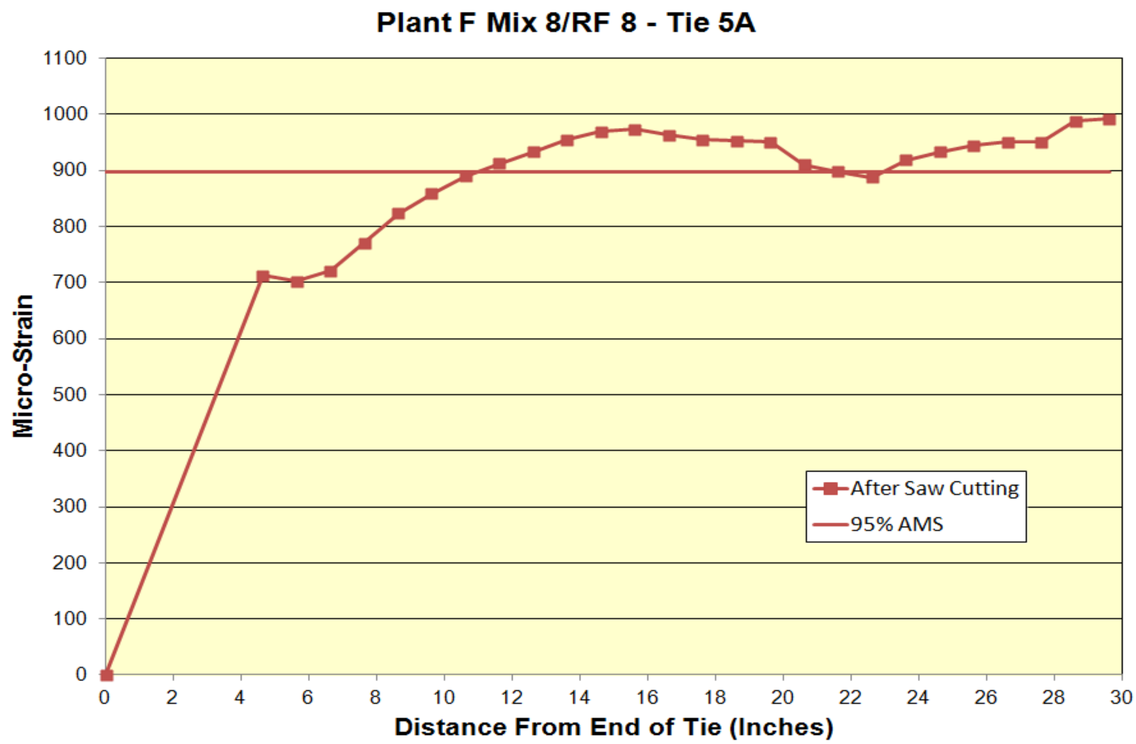

Figure F.9 Transfer length of Plant F Mix 8/RF 8 Tie 5A

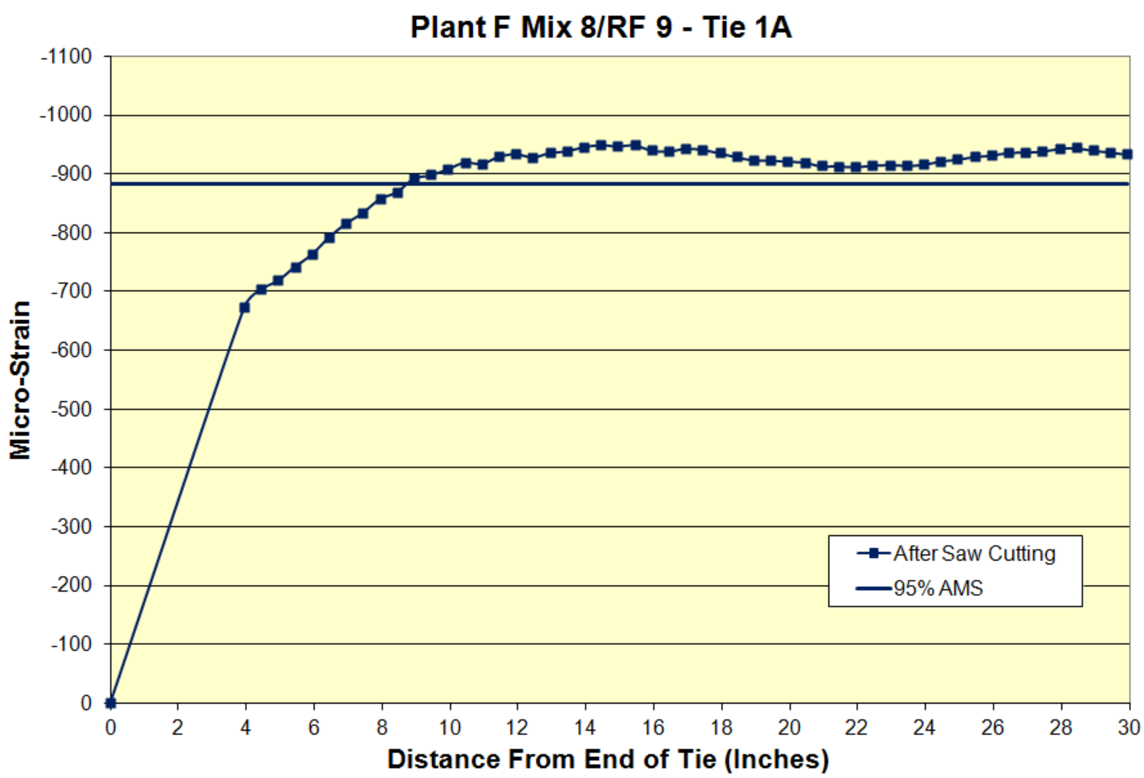

Figure F.10 Transfer length of Plant F Mix 8/RF 9 Tie 1A

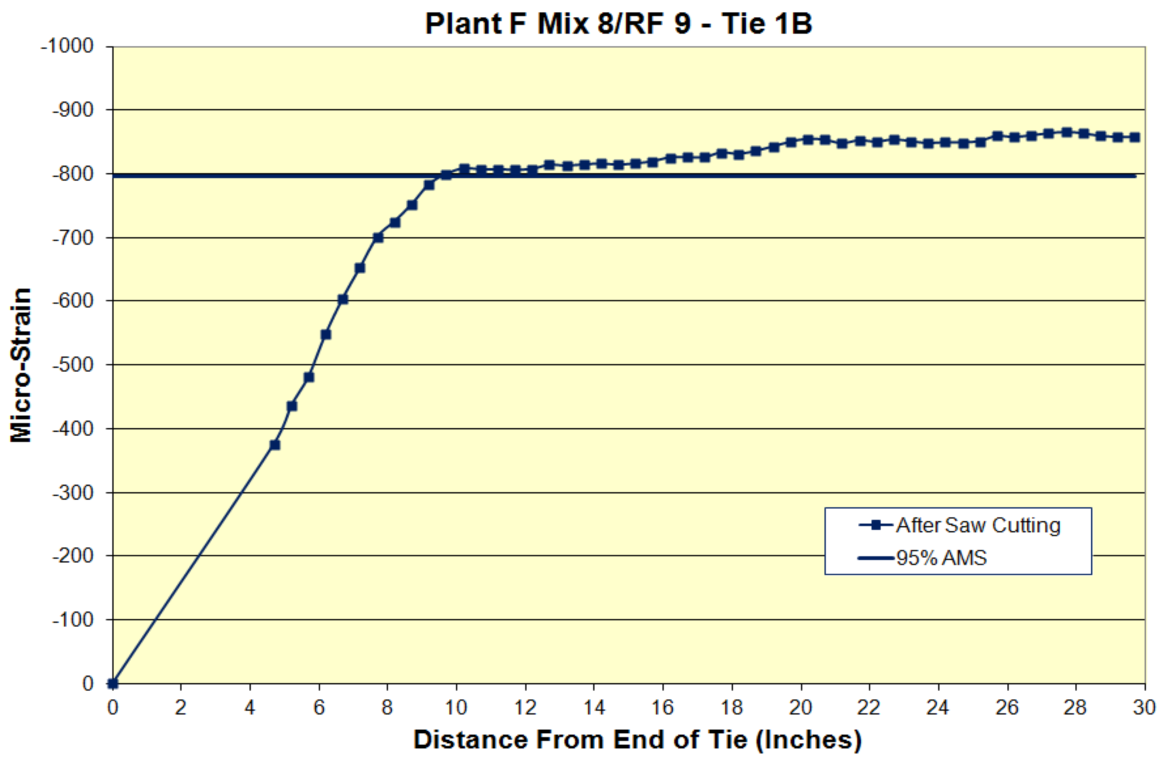

Figure F.11 Transfer length of Plant F Mix 8/RF 9 Tie 1B

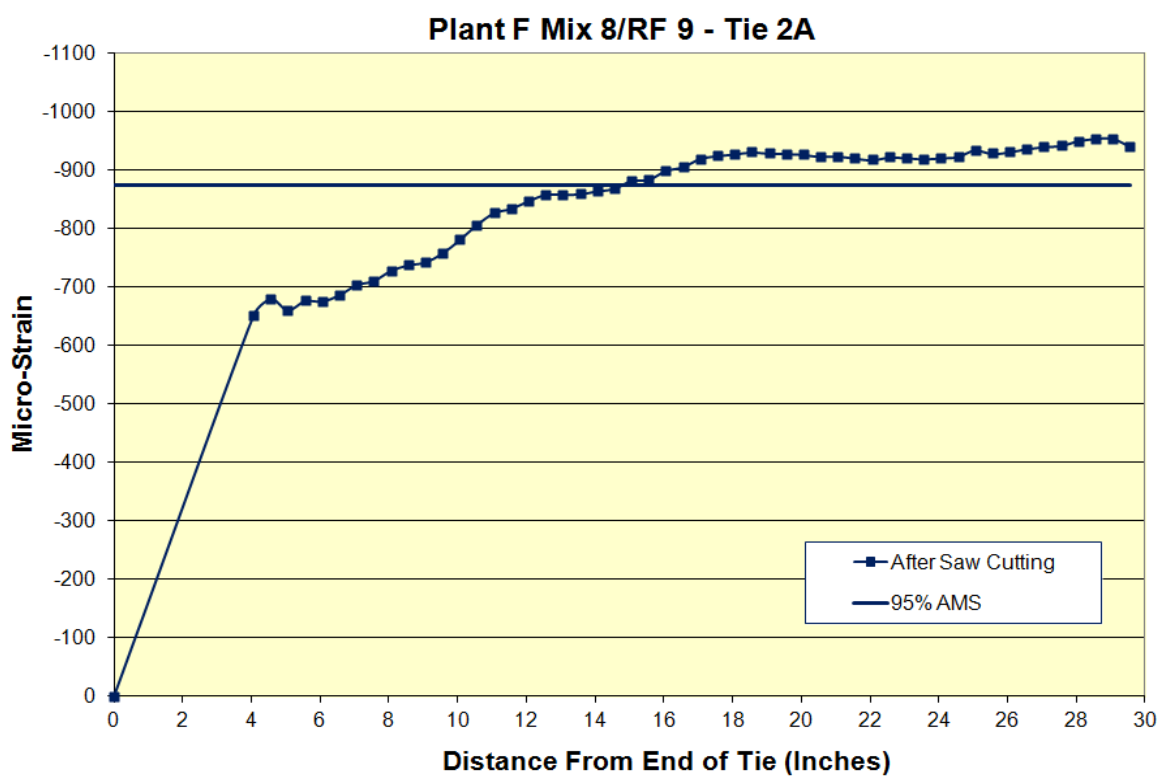

Figure F.12 Transfer length of Plant F Mix 8/RF 9 Tie 2A

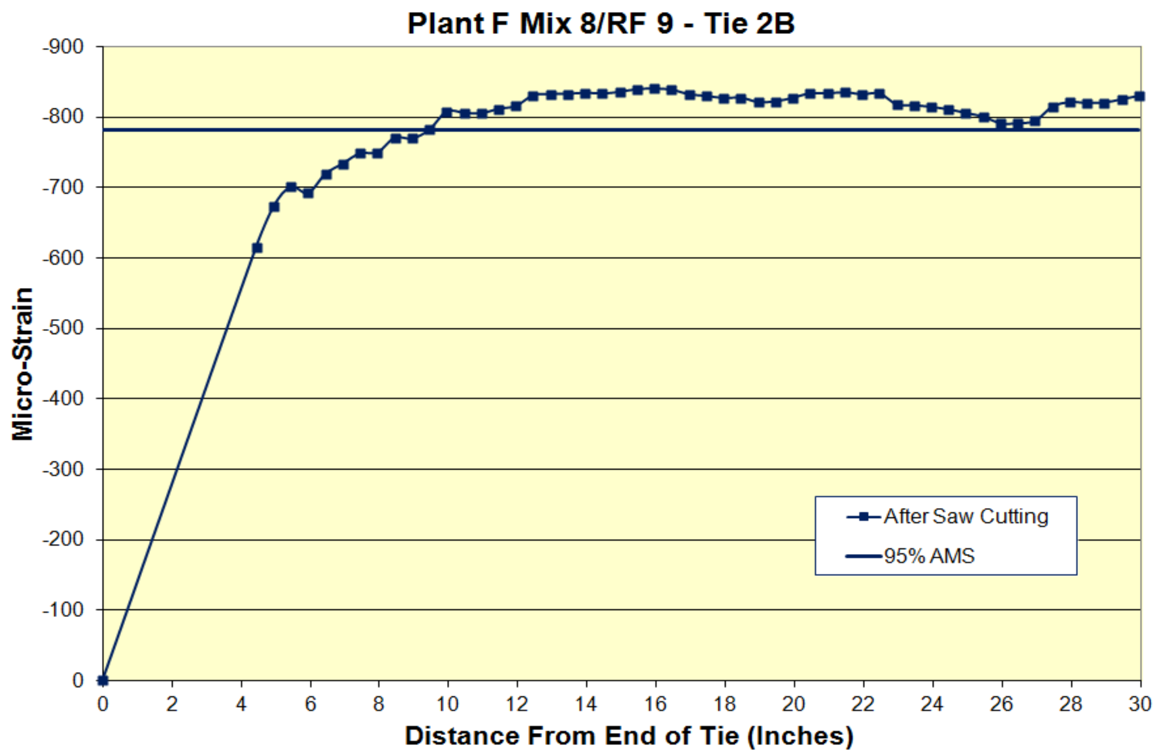

Figure F.13 Transfer length of Plant F Mix 8/RF 9 Tie 2B

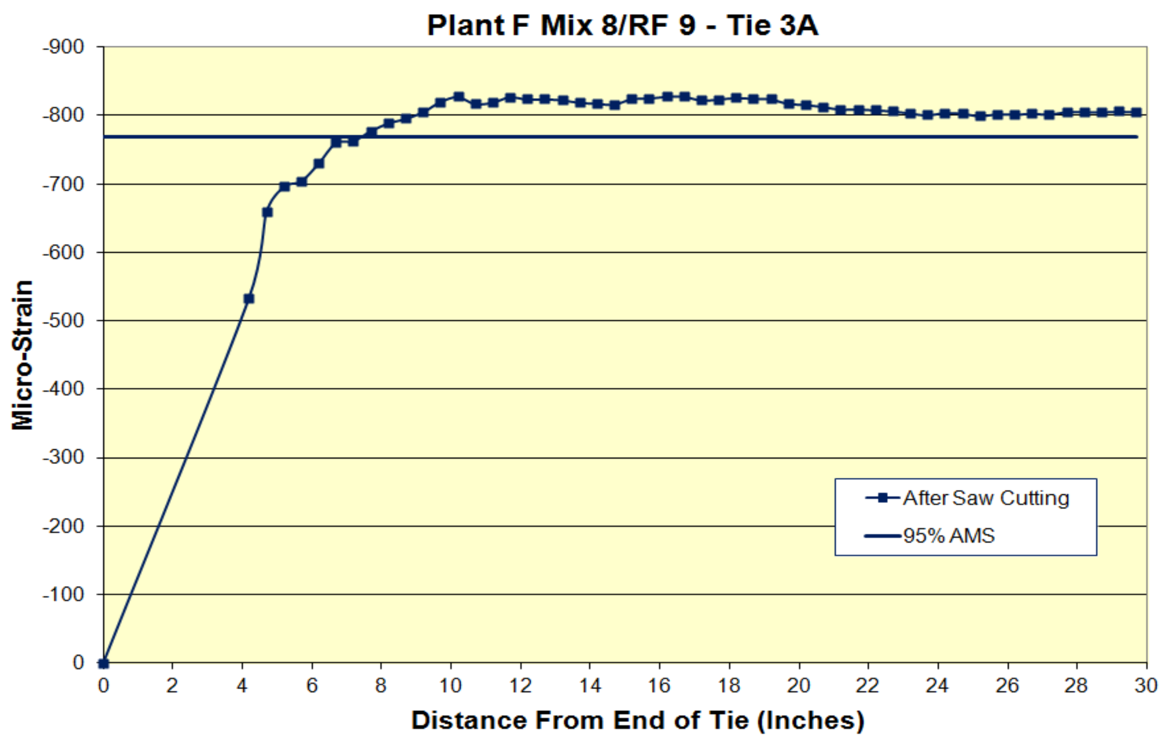

Figure F.14 Transfer length of Plant F Mix 8/RF 9 Tie 3A

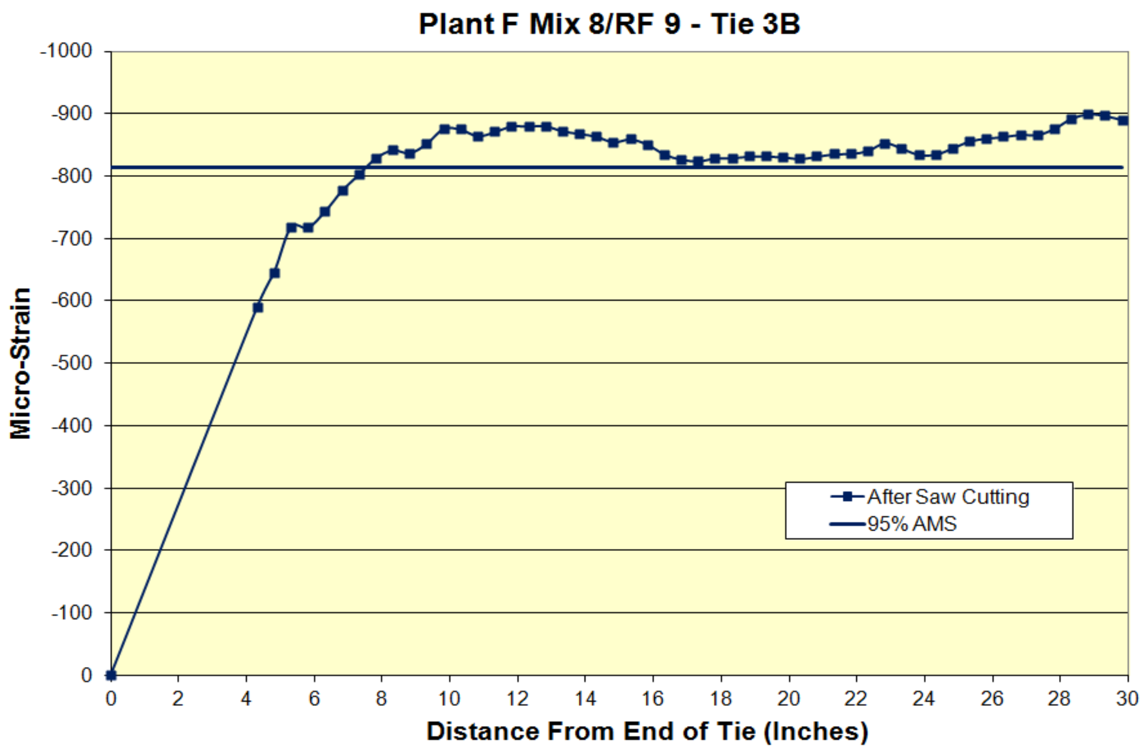

Figure F.15 Transfer length of Plant F Mix 8/RF 9 Tie 3B

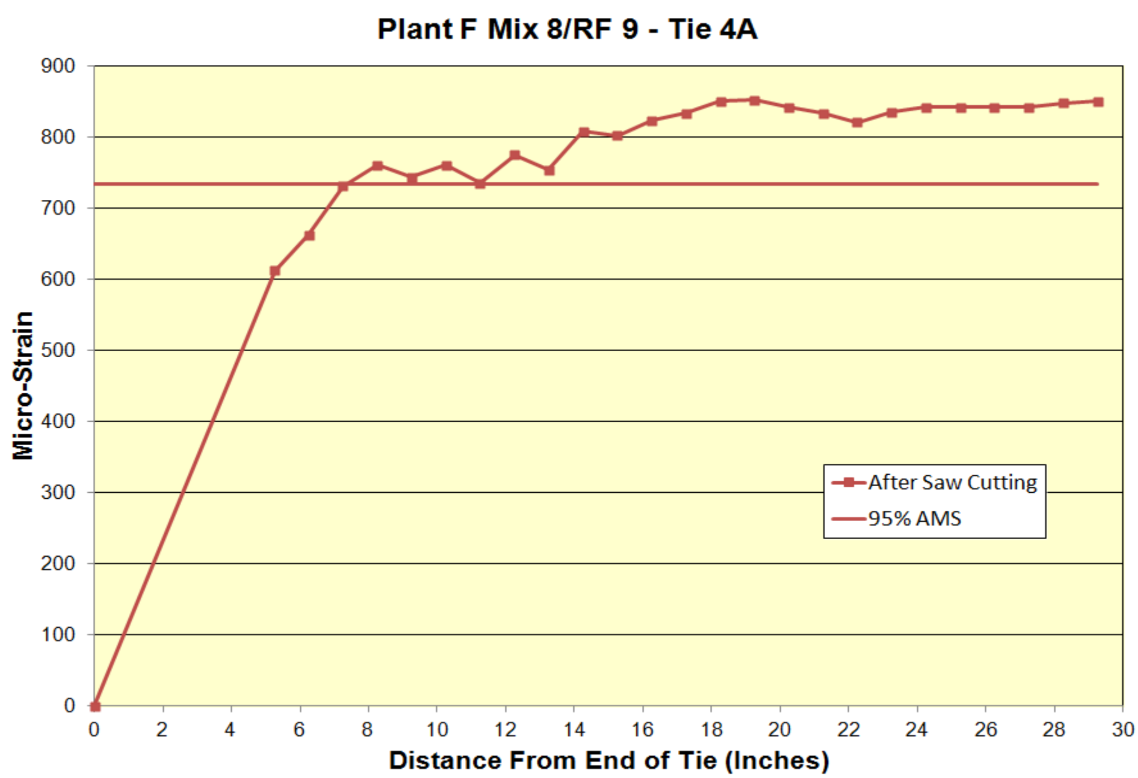

Figure F.16 Transfer length of Plant F Mix 8/RF 9 Tie 4A

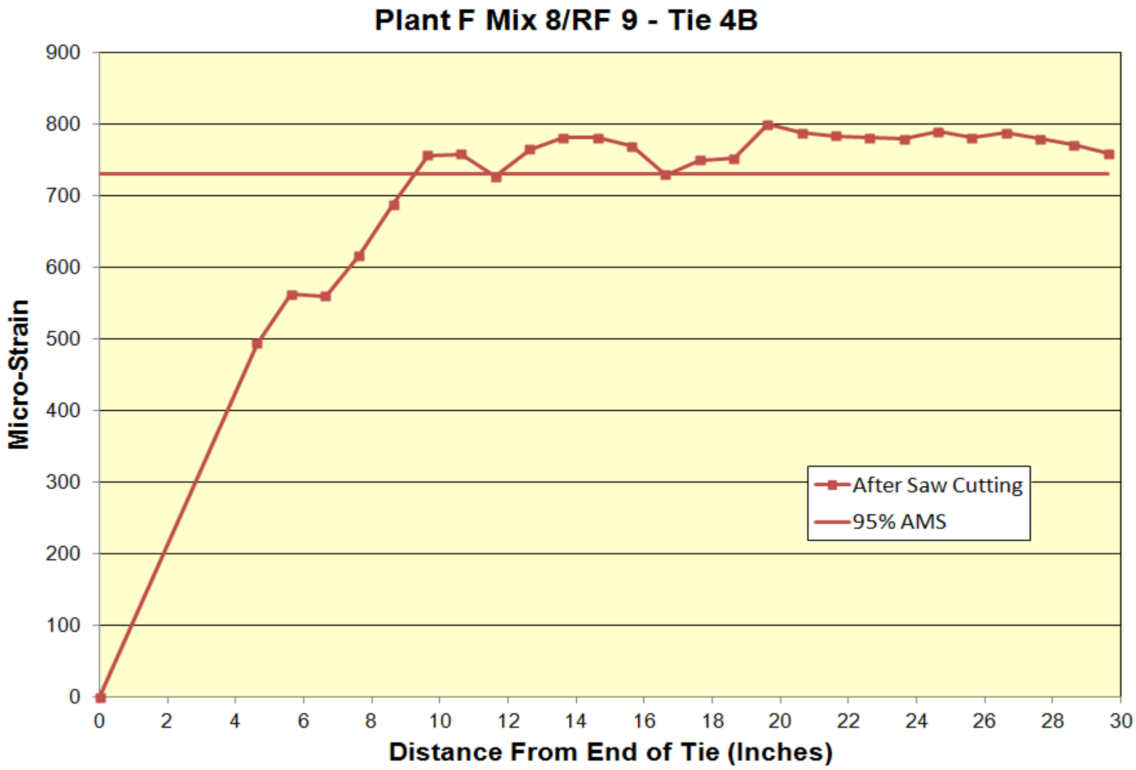

Figure F.17 Transfer length of Plant F Mix 8/RF 9 Tie 4B

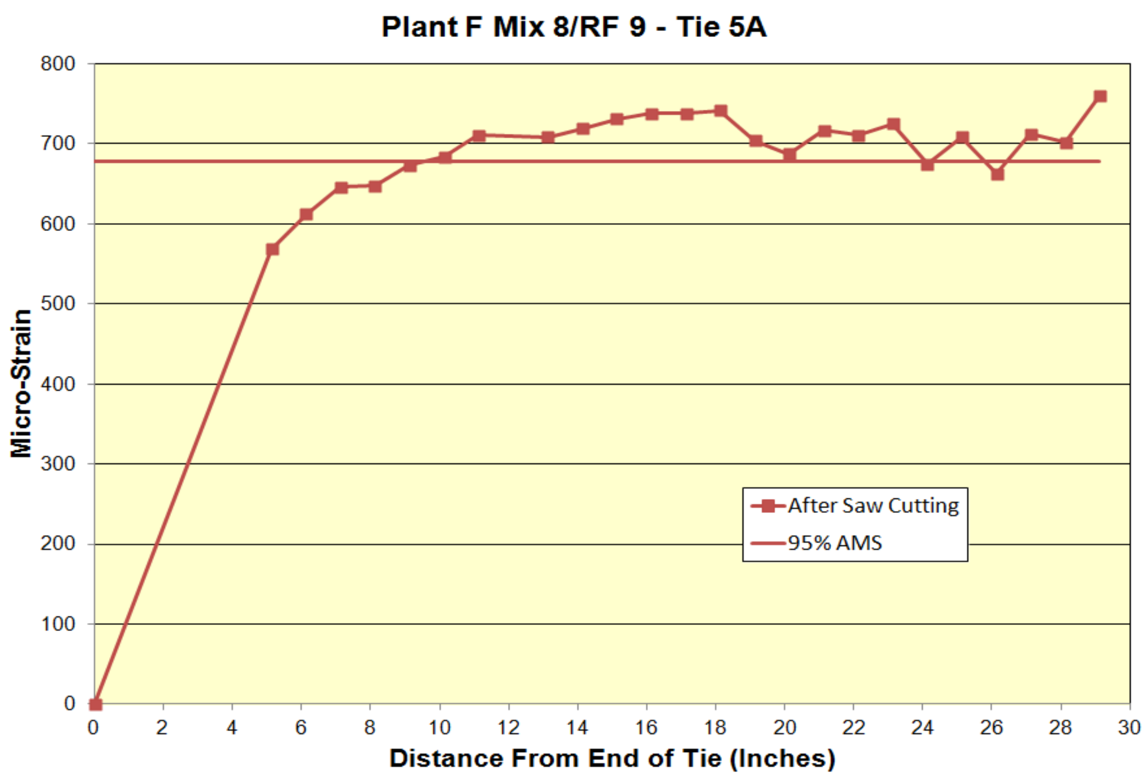

Figure F.18 Transfer length of Plant F Mix 8/RF 9 Tie 5A

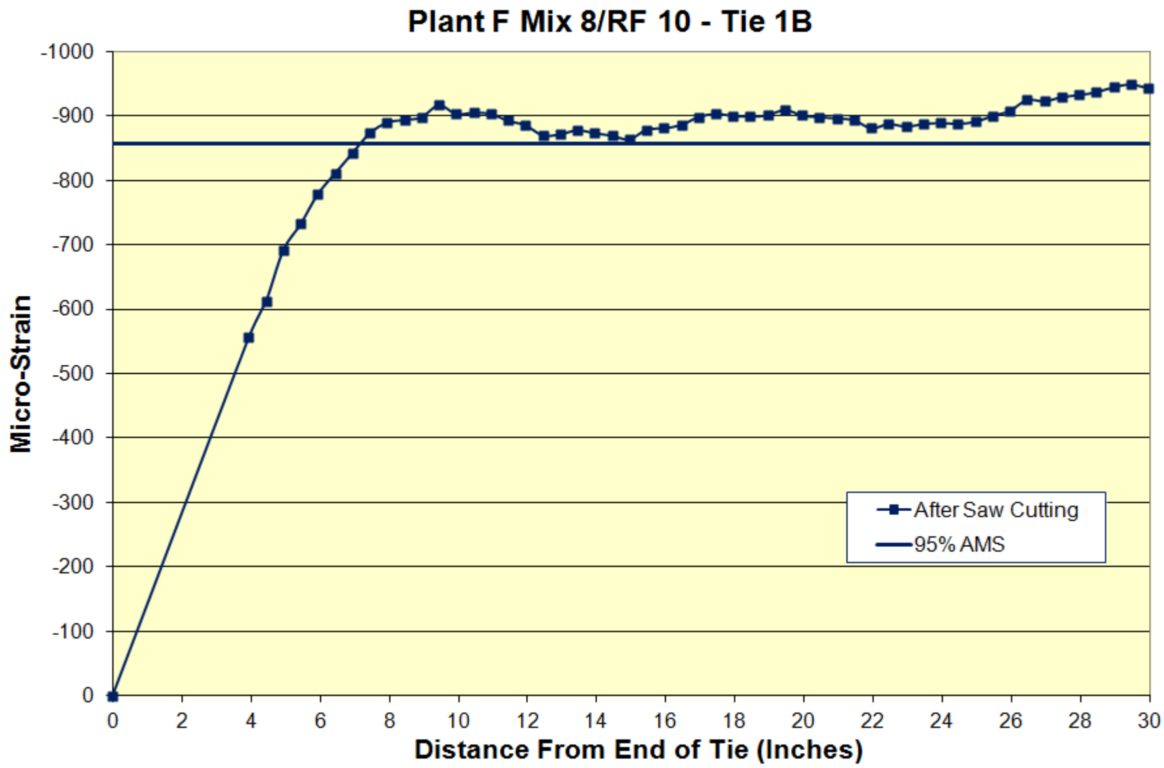

Figure F.19 Transfer length of Plant F Mix 8/RF 10 Tie 1B

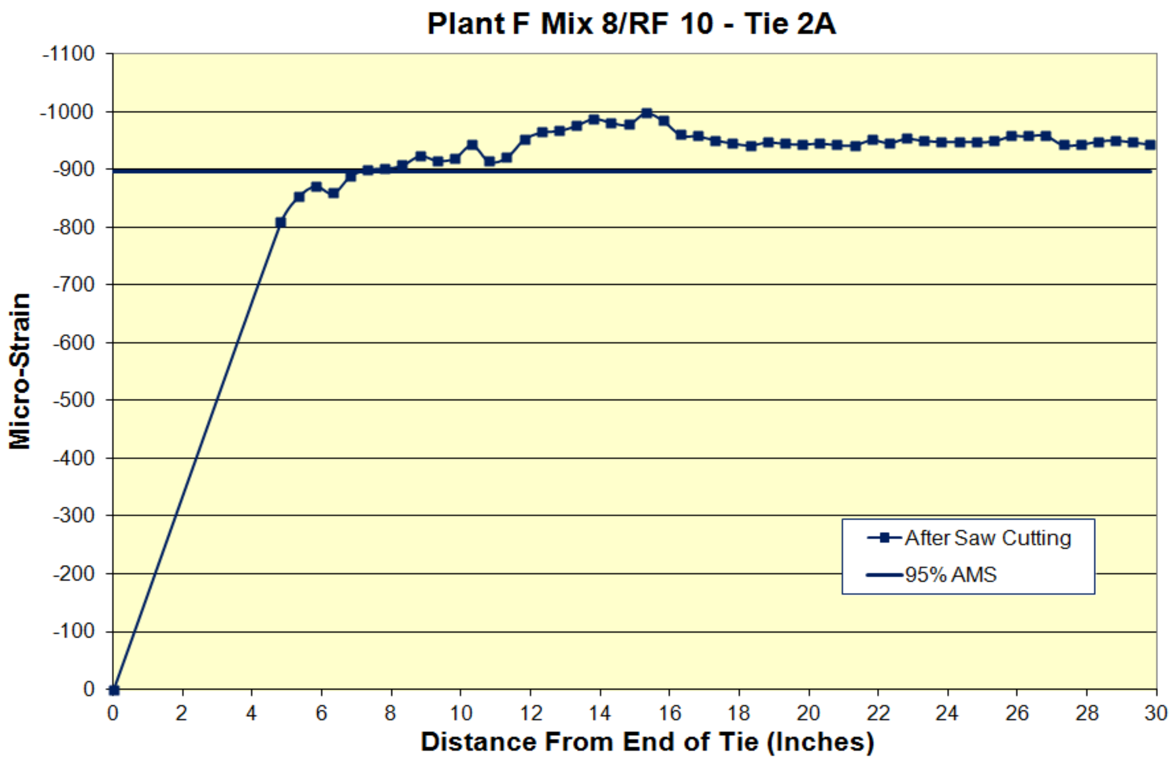

Figure F.20 Transfer length of Plant F Mix 8/RF 10 Tie 2A

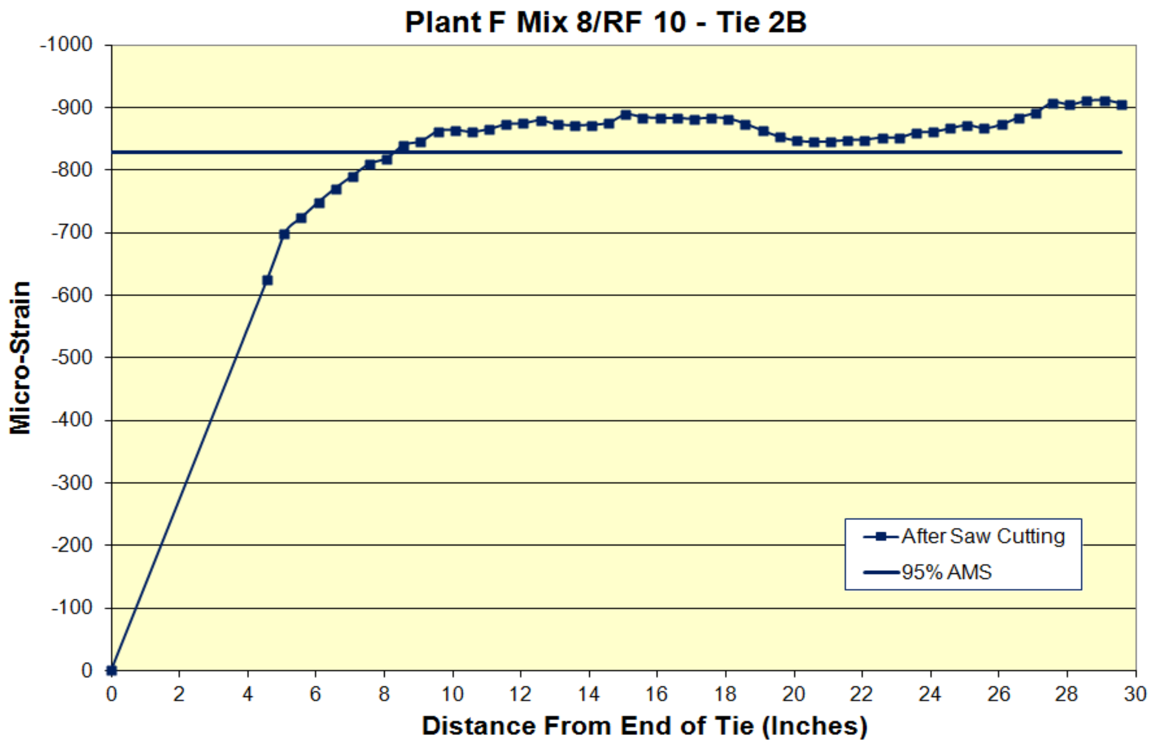

Figure F.21 Transfer length of Plant F Mix 8/RF 10 Tie 2B

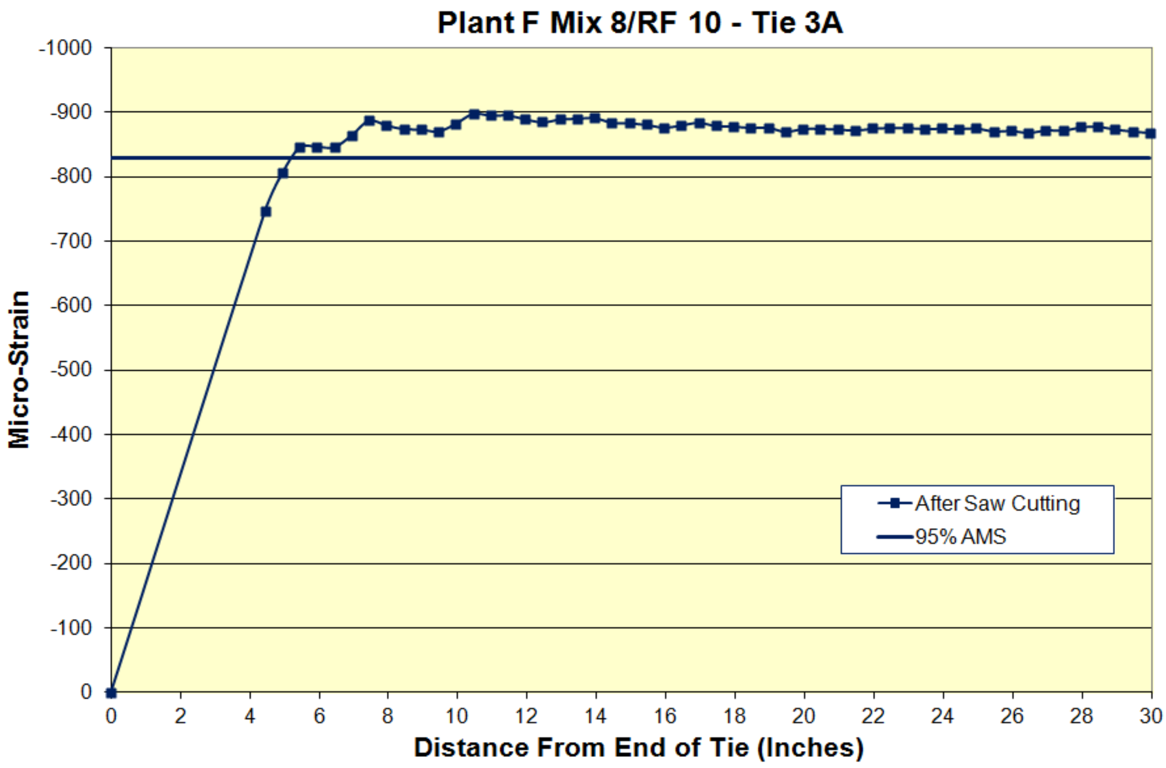

Figure F.22 Transfer length of Plant F Mix 8/RF 10 Tie 3A

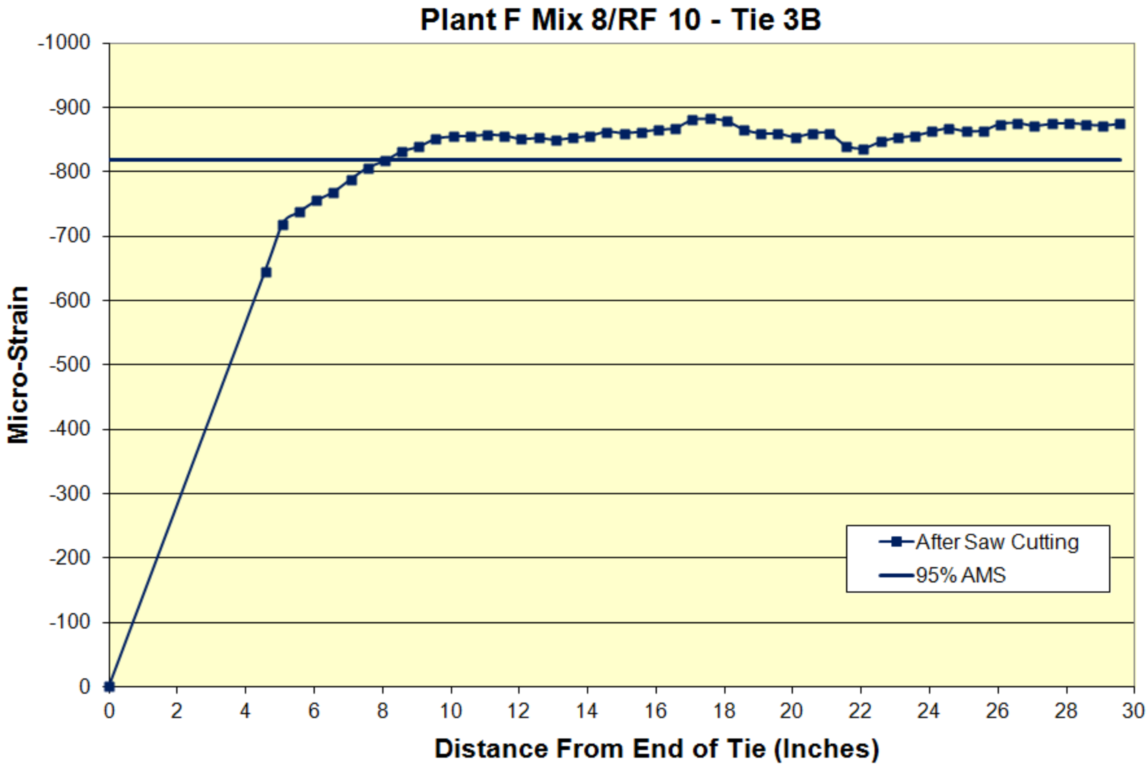

Figure F.23 Transfer length of Plant F Mix 8/RF 10 Tie 3B

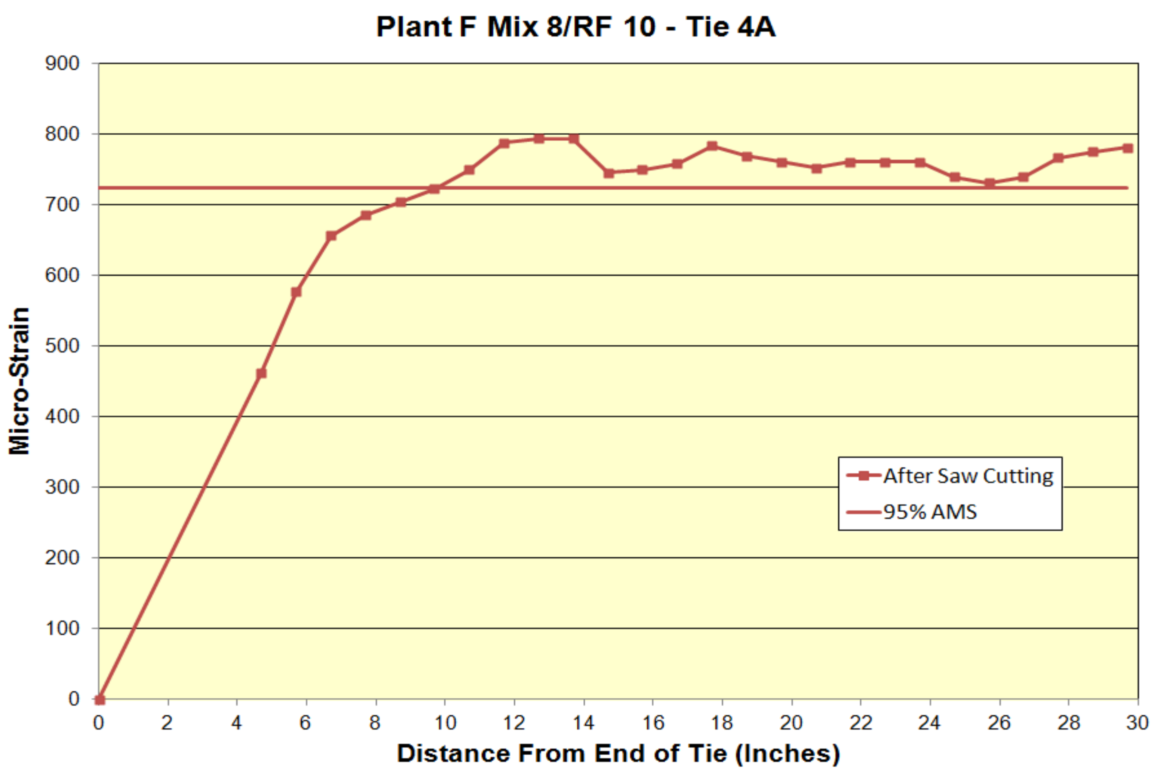

Figure F.24 Transfer length of Plant F Mix 8/RF 10 Tie 4A

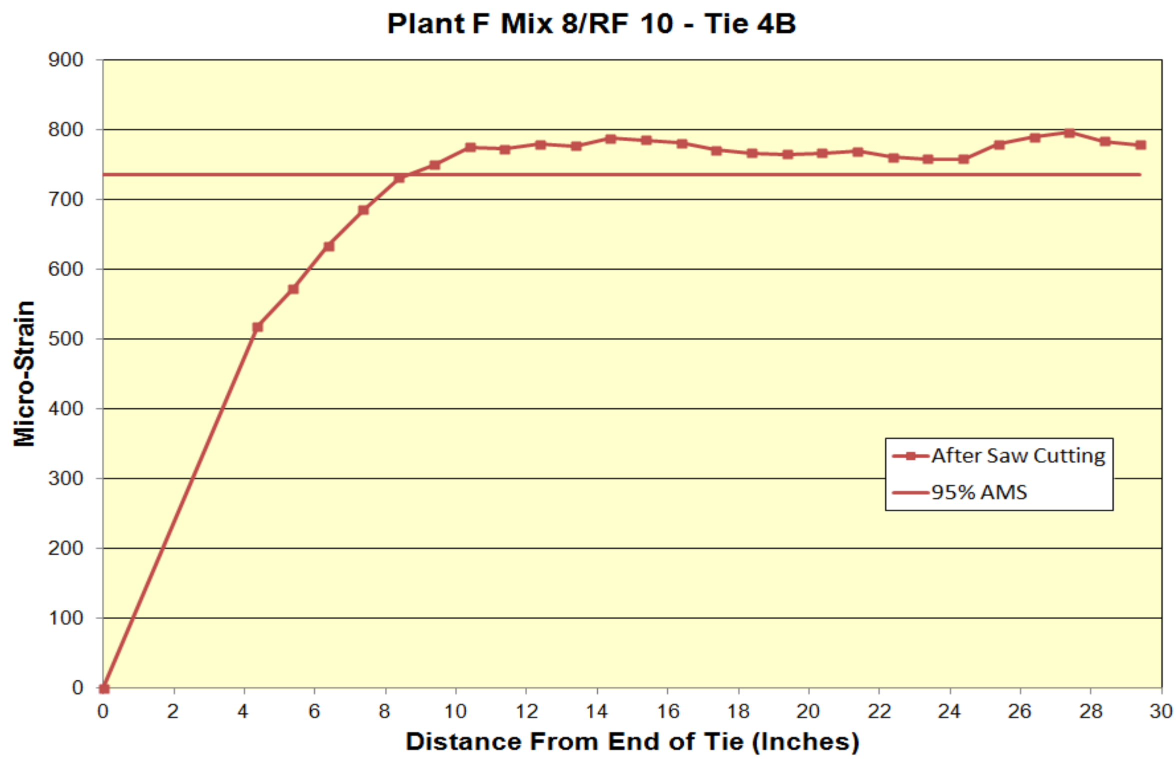

Figure F.25 Transfer length of Plant F Mix 8/RF 10 Tie 4B

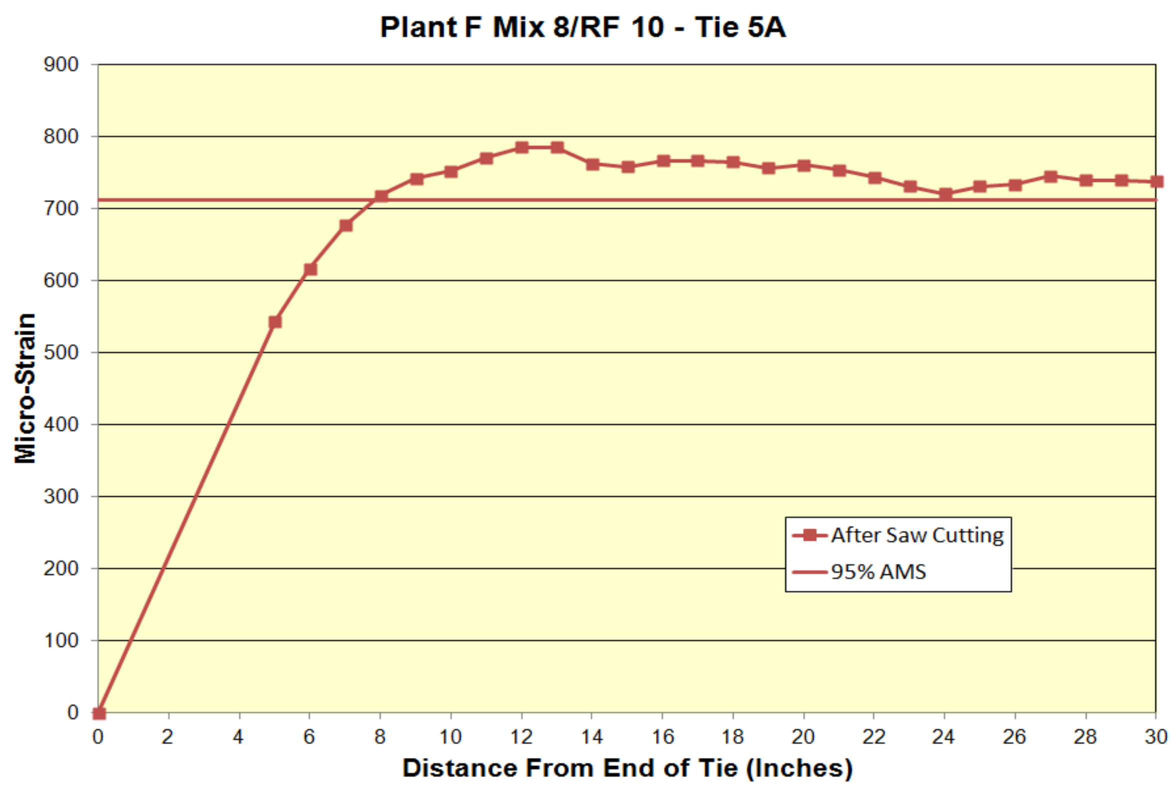

Figure F.26 Transfer length of Plant F Mix 8/RF 10 Tie 5A

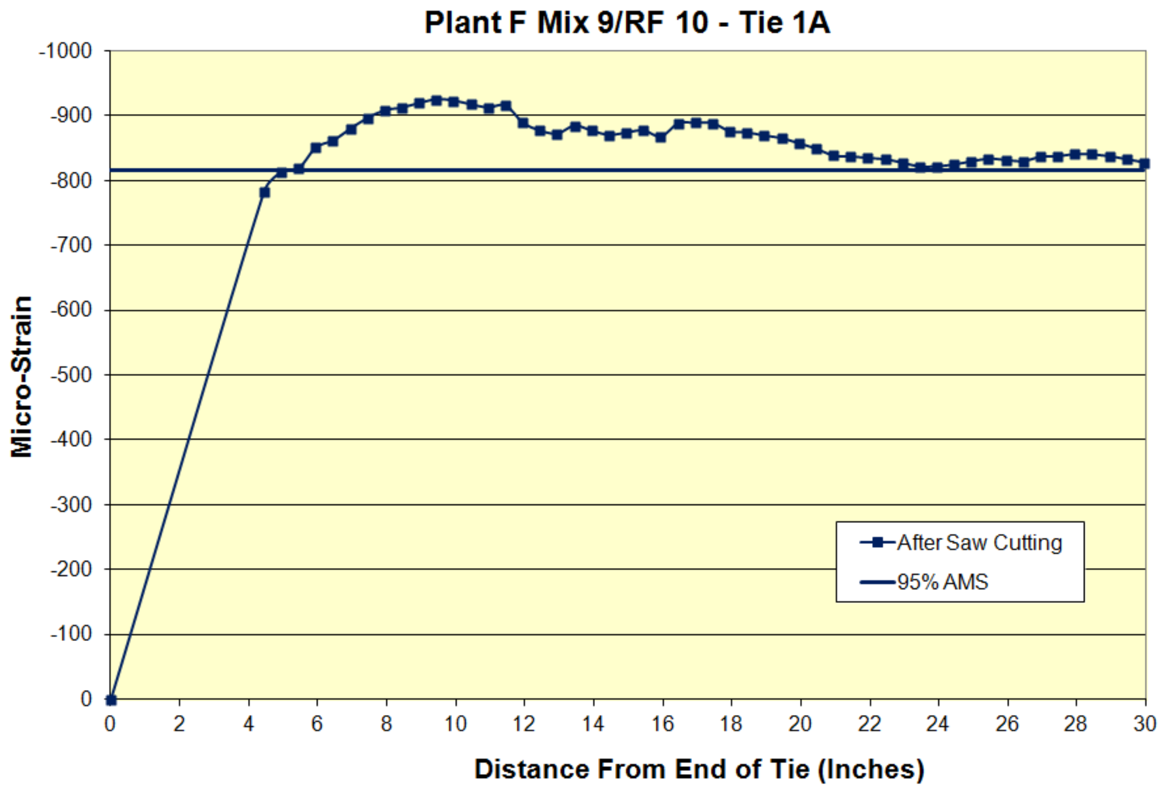

Figure F.27 Transfer length of Plant F Mix 9/RF 10 Tie 1A

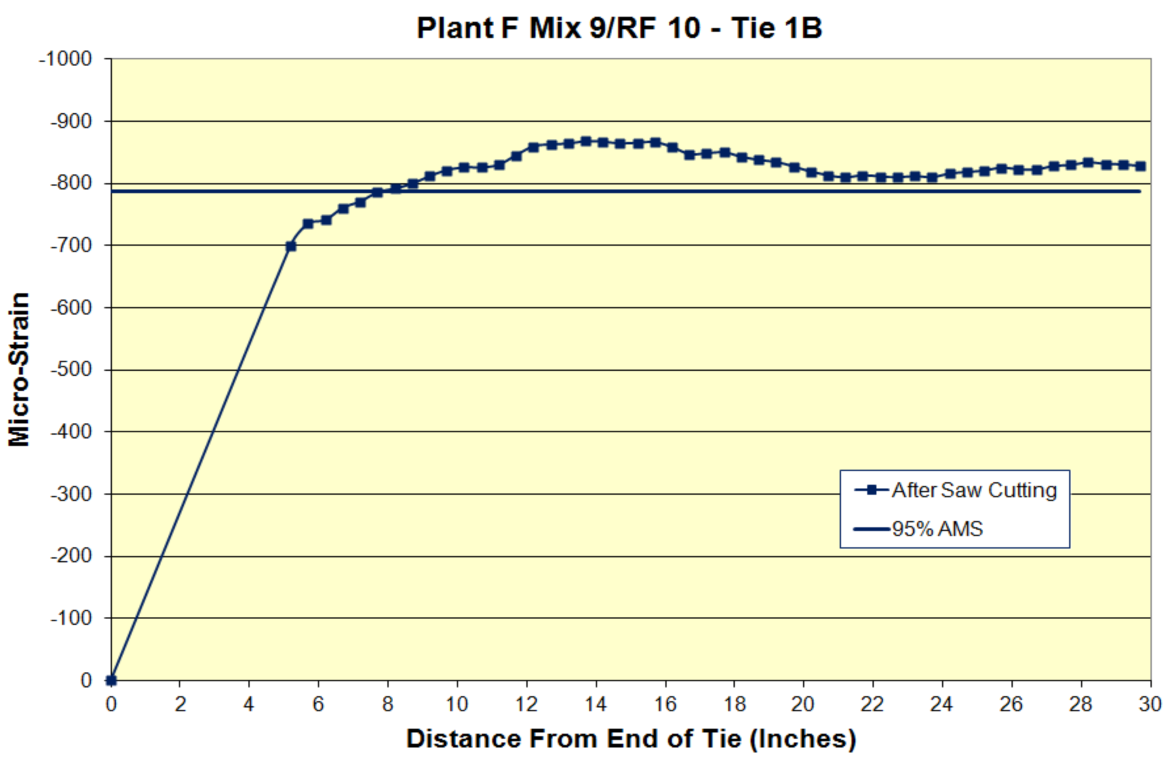

Figure F.28 Transfer length of Plant F Mix 9/RF 10 Tie 1B

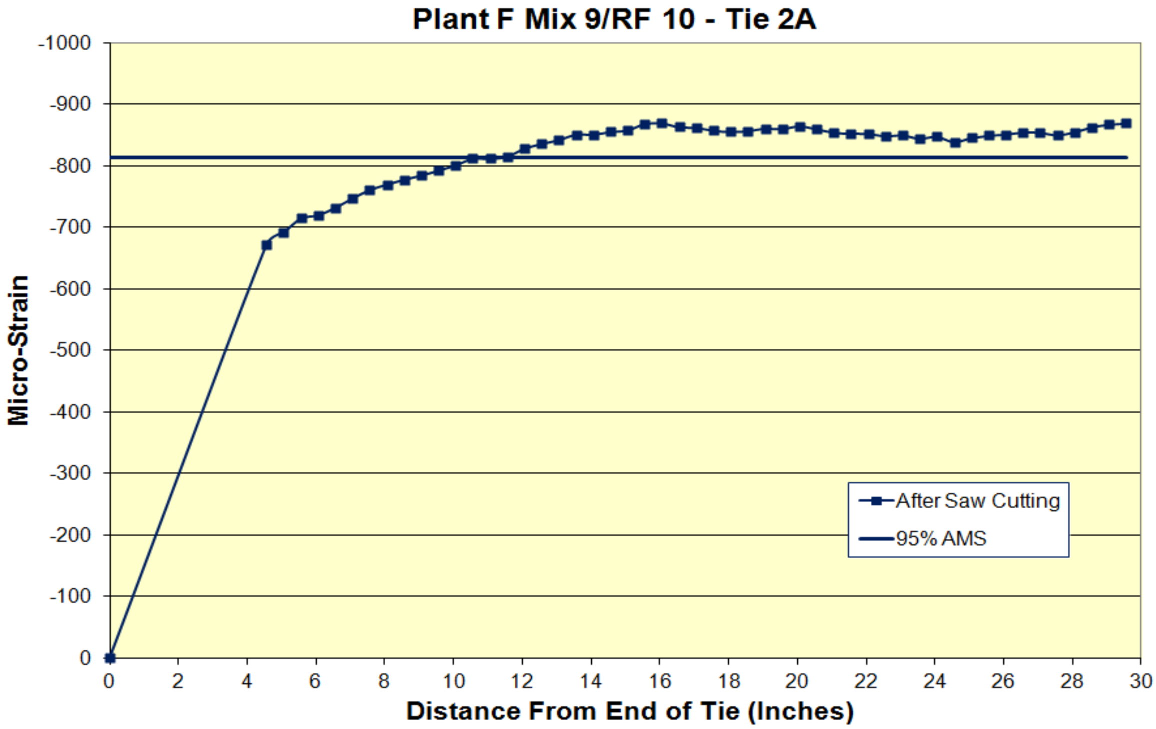

Figure F.29 Transfer length of Plant F Mix 9/RF 10 Tie 2A

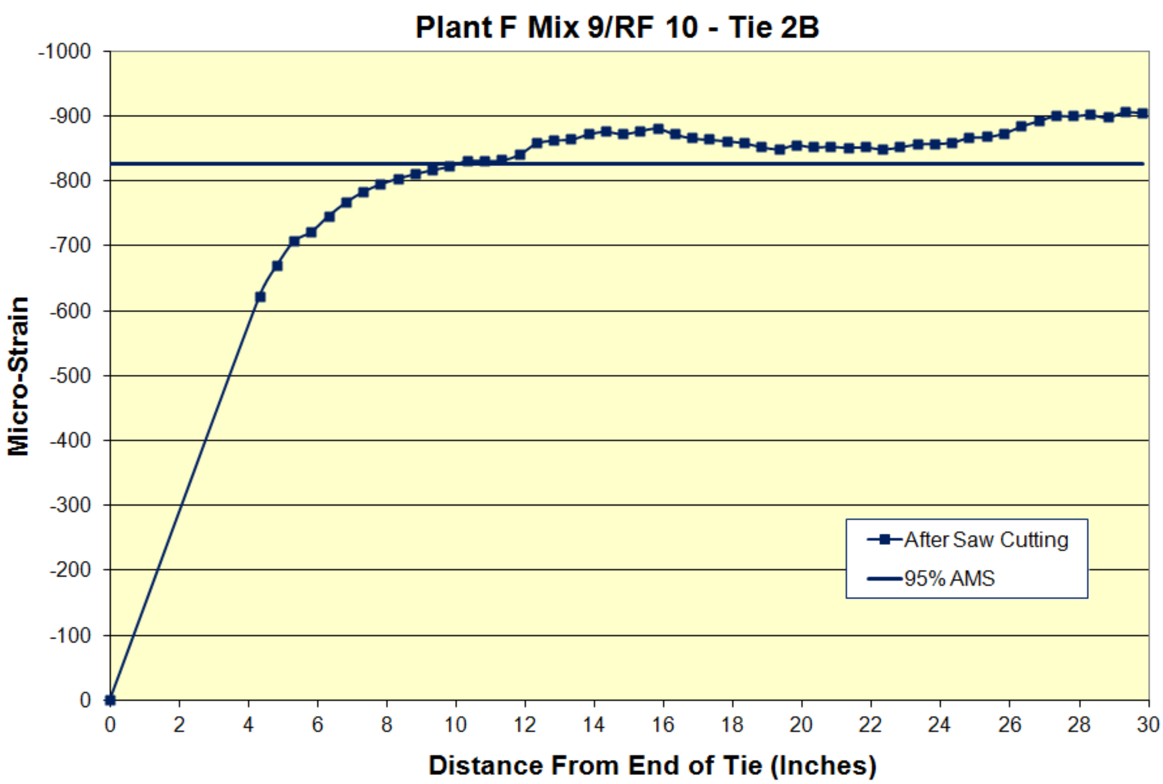

Figure F.30 Transfer length of Plant F Mix 9/RF 10 Tie 2B

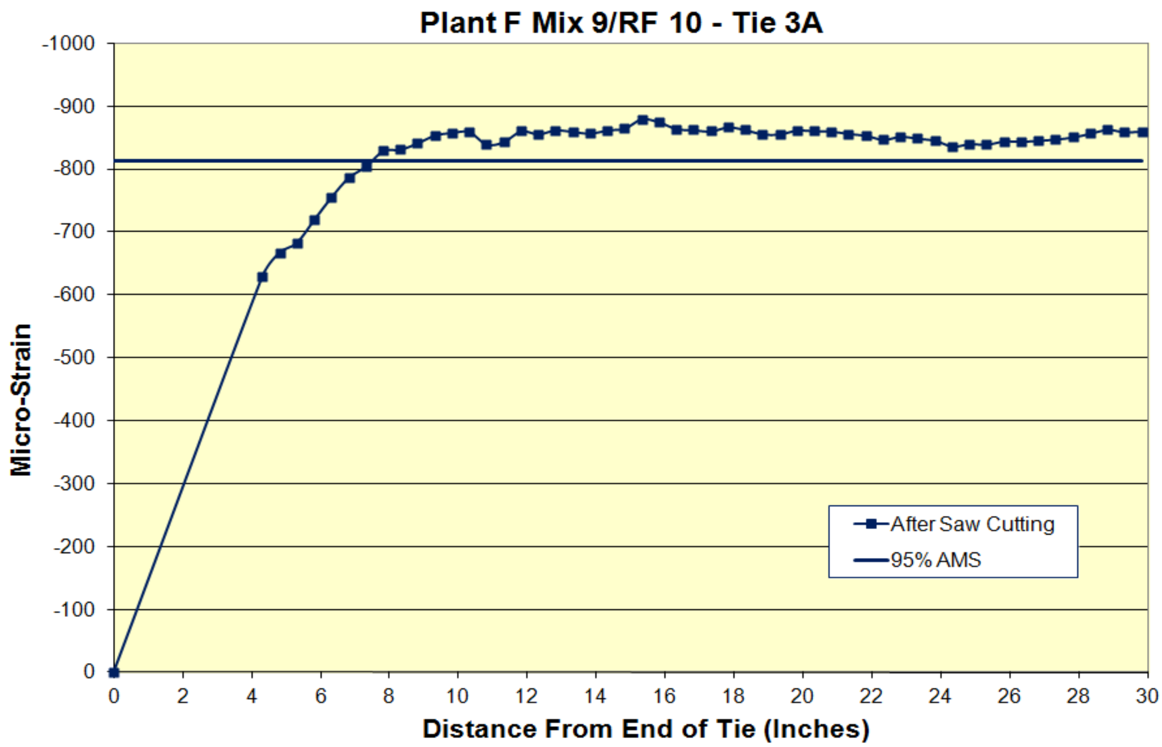

Figure F.31 Transfer length of Plant F Mix 9/RF 10 Tie 3A

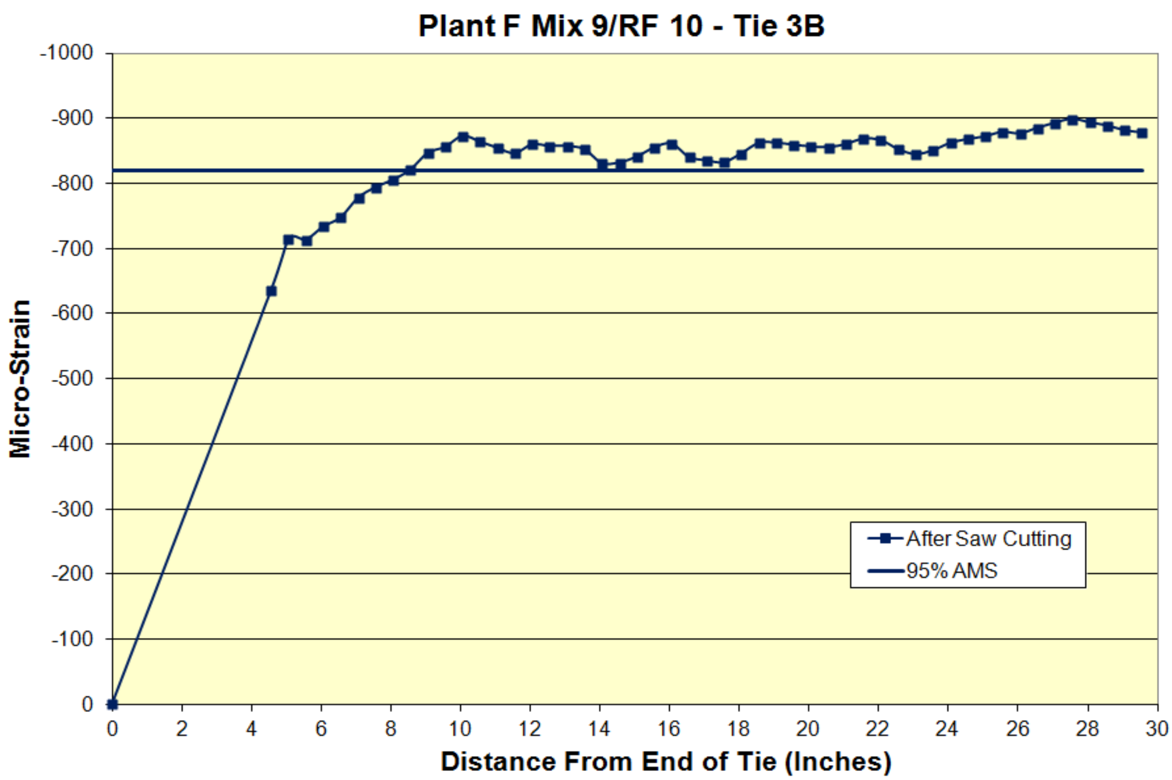

Figure F.32 Transfer length of Plant F Mix 9/RF 10 Tie 3B

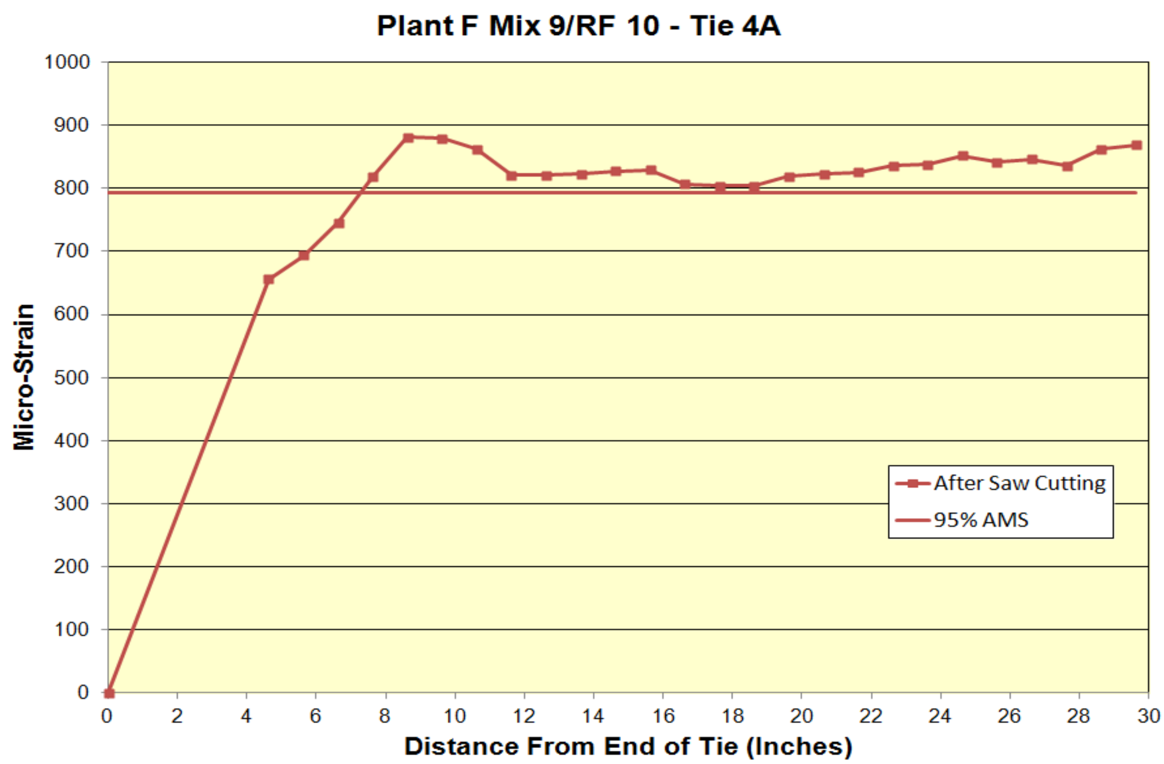

Figure F.33 Transfer length of Plant F Mix 9/RF 10 Tie 4A

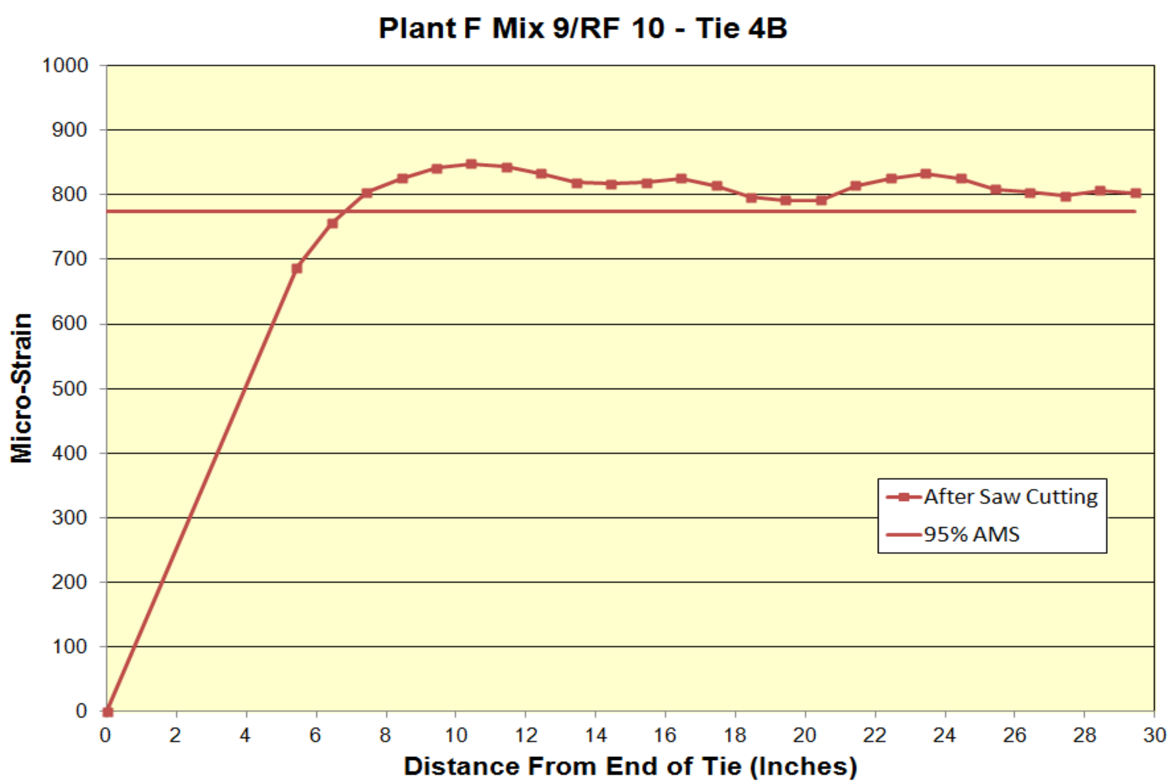

Figure F.34 Transfer length of Plant F Mix 9/RF 10 Tie 4B

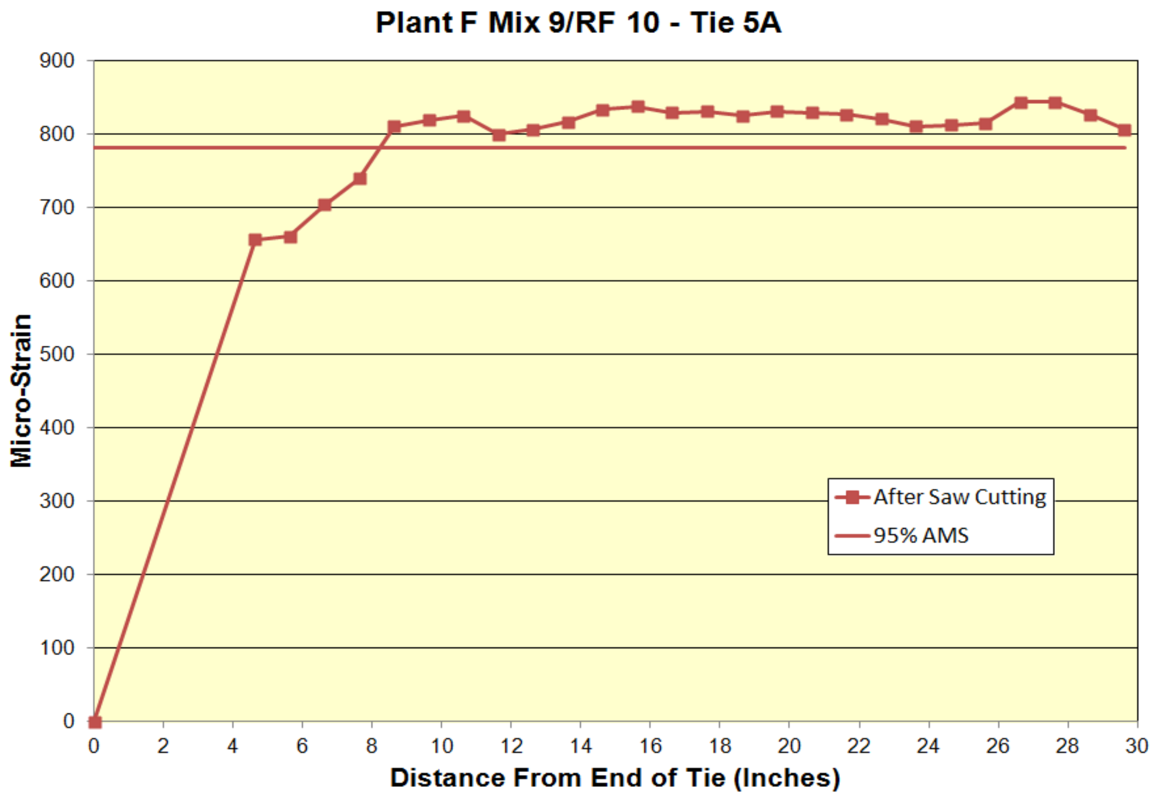

Figure F.35 Transfer length of Plant F Mix 9/RF 10 Tie 5A

F.2 Long-term Transfer Lengths

Table F.2 Long-term transfer length data for Plant F Mix 8/RF 8

Plant F Mix 8/RF 8		
	Transfer Length (in.)	
Time of Reading	Tie 4A	Tie 4B
After Saw Cutting	9.3	12.2
40 Days After Pour	11.6	13.2
90 Days After Pour	12	12.9
160 Days After Pour	12	12.9
270 Days After Pour	11.8	12.5

Table F.3 Long-term transfer length data for Plant F Mix 8/RF 9

Plant F Mix 8/RF 9		
	Transfer Length (in.)	
Time of Reading	Tie 4A	Tie 4B
After Saw Cutting	7.4	9.3
40 Days After Pour	9.8	9.7
90 Days After Pour	9.7	10
160 Days After Pour	9.9	10.5
270 Days After Pour	10.9	12.4

Table F.4 Long-term transfer length data for Plant F Mix 8/RF 10

Plant F Mix 8/RF 10		
	Transfer Length (in.)	
Time of Reading	Tie 4A	Tie 4B
After Saw Cutting	9.7	8.7
40 Days After Pour	10.1	9.8
90 Days After Pour	9.8	10.1
160 Days After Pour	10.2	10
270 Days After Pour	10.4	10.1

Table F.5 Long-term transfer length data for Plant F Mix 9/RF 10

Plant F Mix 9/RF 10		
	Transfer Length (in.)	
Time of Reading	Tie 4A	Tie 4B
After Saw Cutting	7.3	6.8
40 Days After Pour	8.3	8.4
90 Days After Pour	8.2	9.2
160 Days After Pour	8.3	9
270 Days After Pour	8.3	8.7

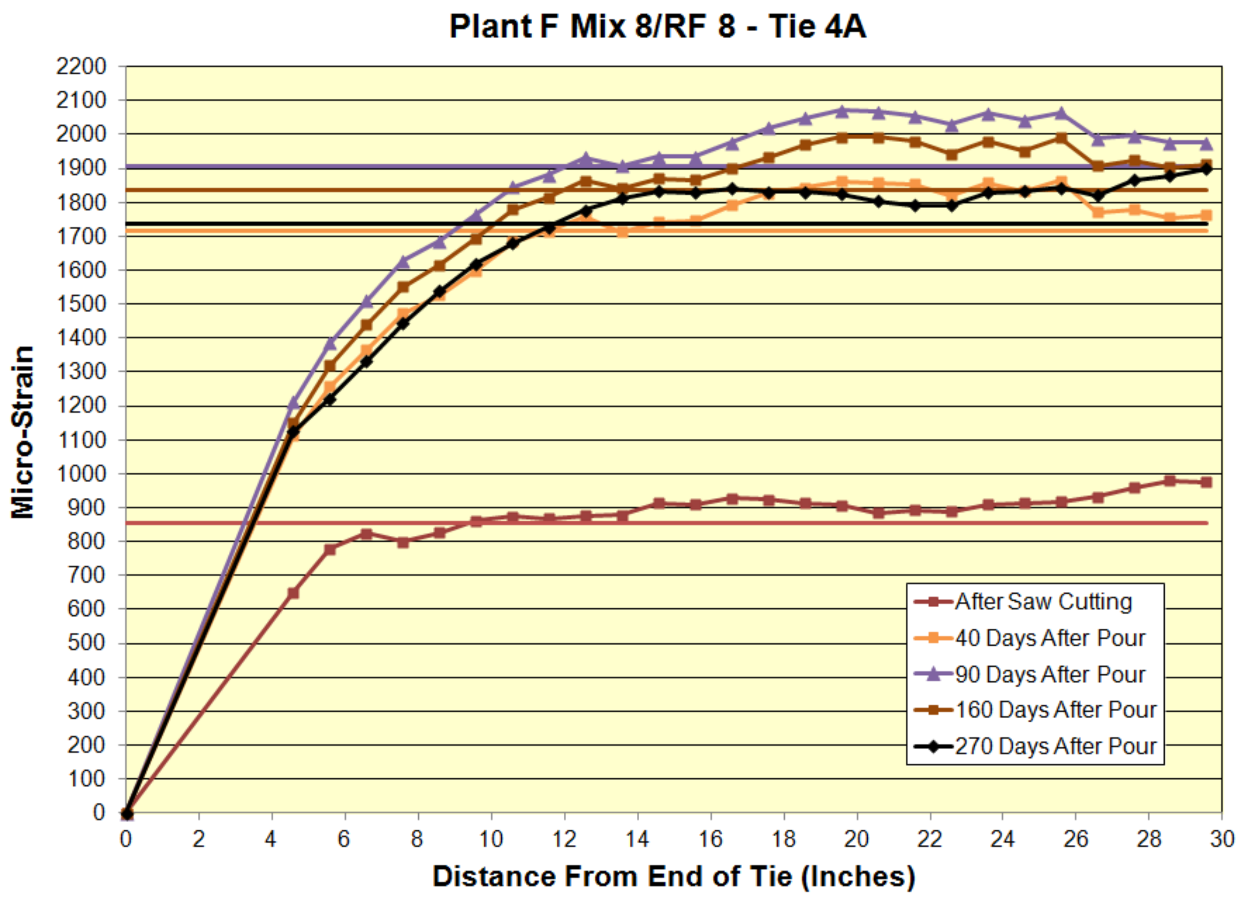

Figure F.36 Long-term transfer length of Plant F Mix 8/RF 8 Tie 4A

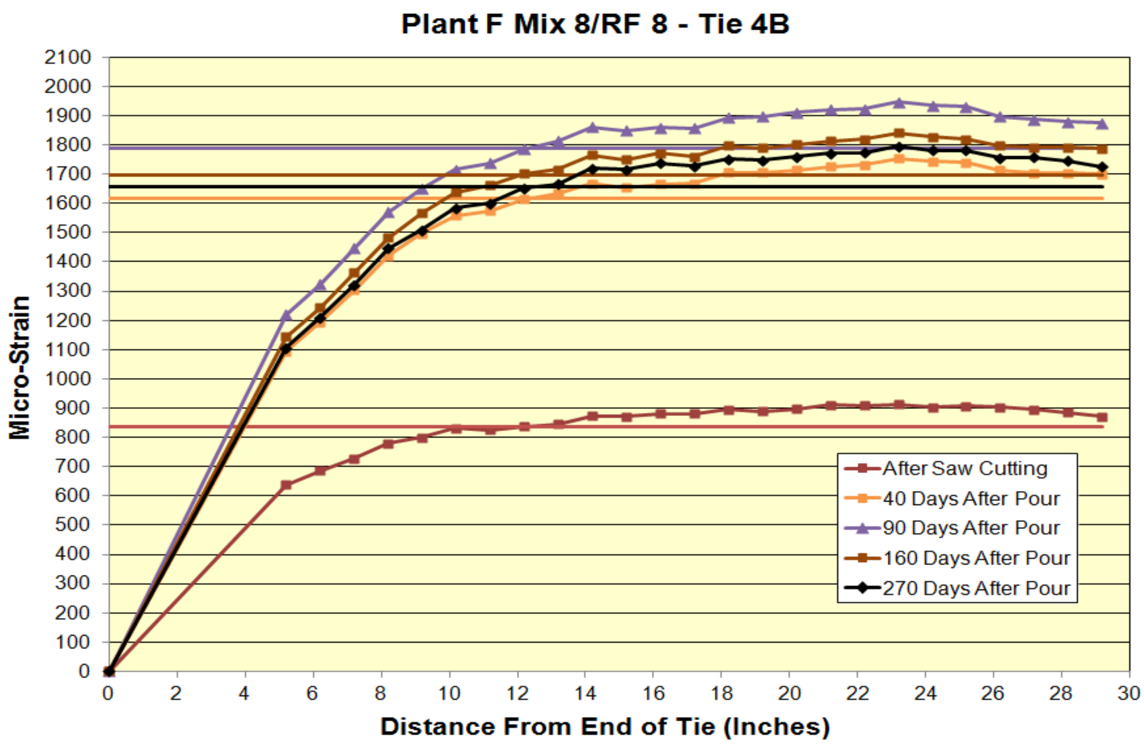

Figure F.37 Long-term transfer length of Plant F Mix 8/RF 8 Tie 4B

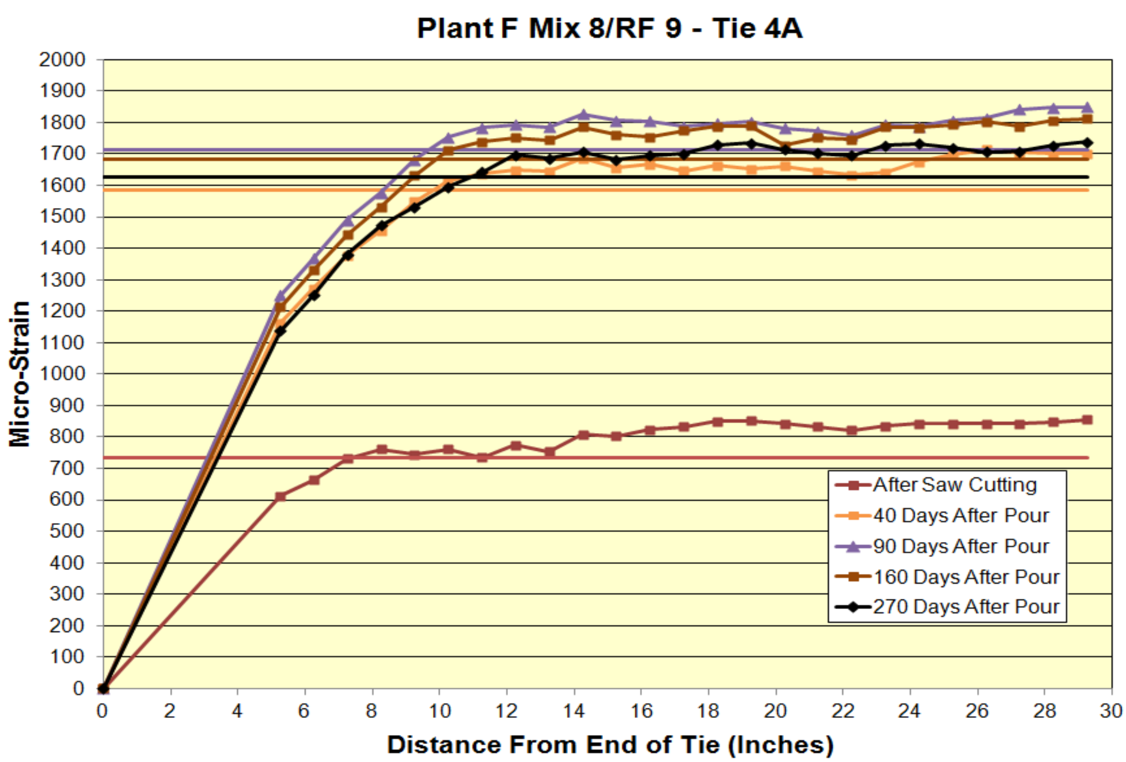

Figure F.38 Long-term transfer length of Plant F Mix 8/RF 9 Tie 4A

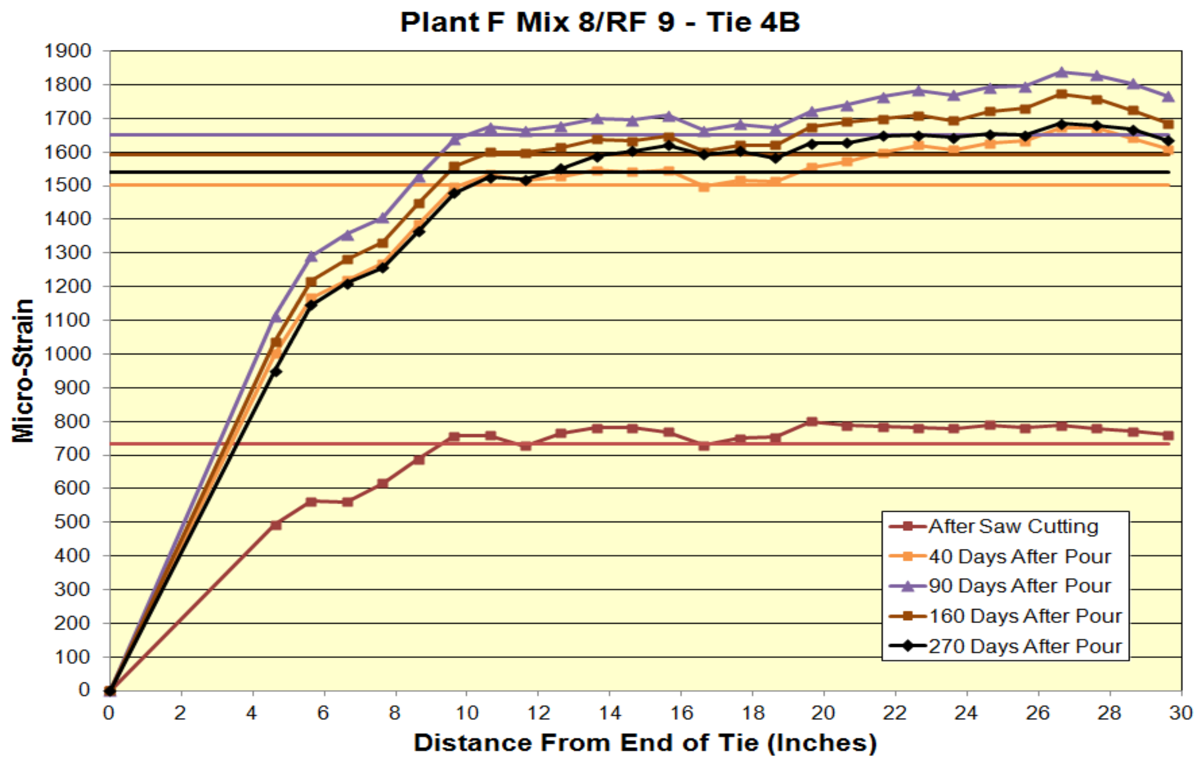

Figure F.39 Long-term transfer length of Plant F Mix 8/RF 9 Tie 4B

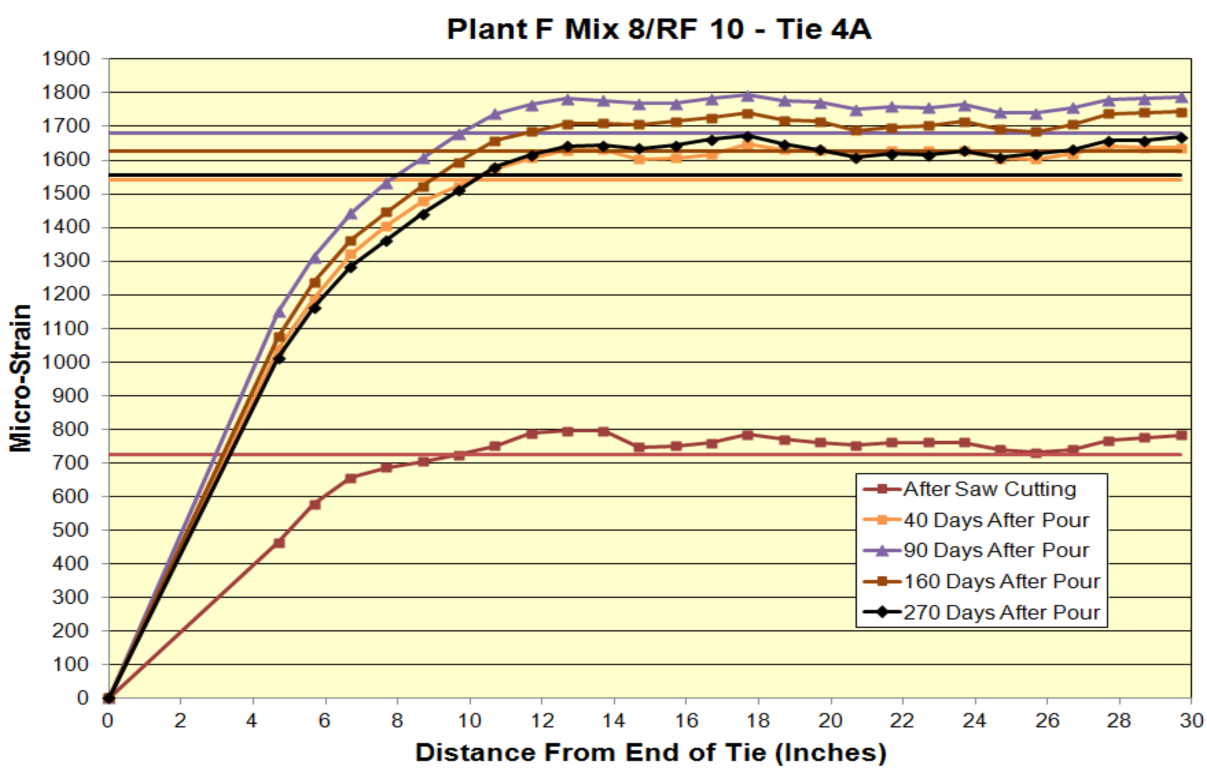

Figure F.40 Long-term transfer length of Plant F Mix 8/RF 10 Tie 4A

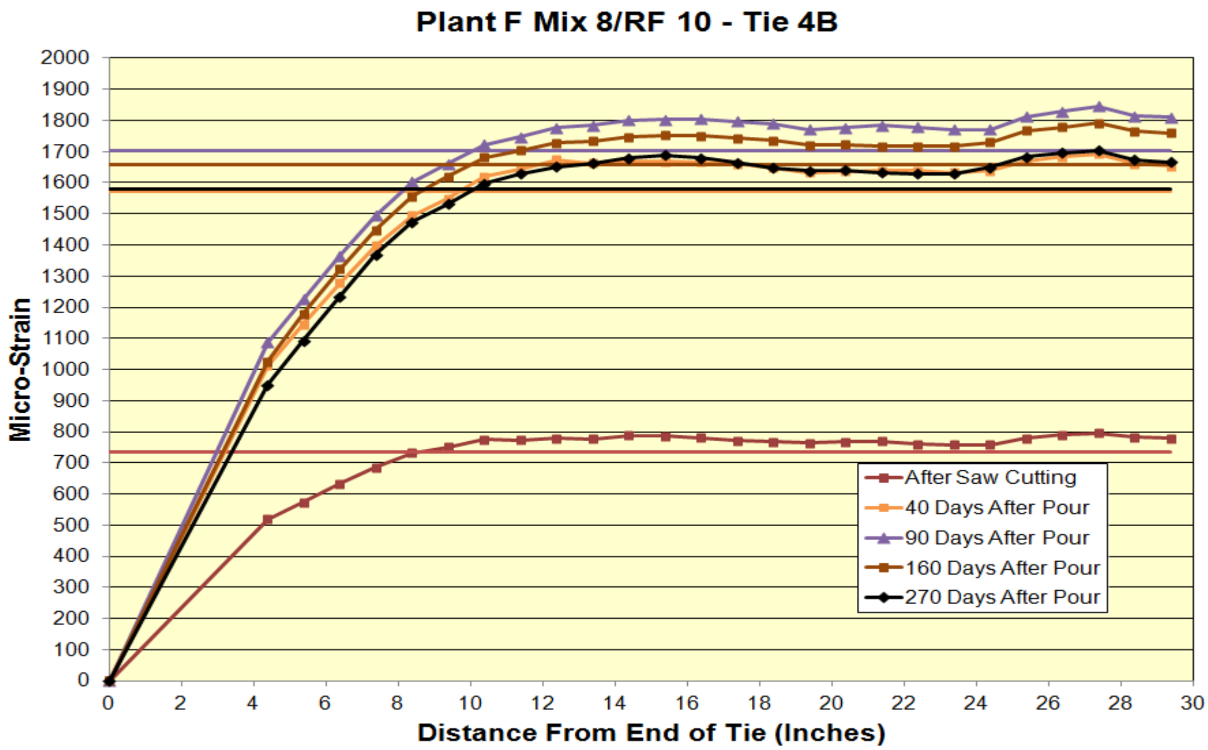

Figure F.41 Long-term transfer length of Plant F Mix 8/RF 10 Tie 4B

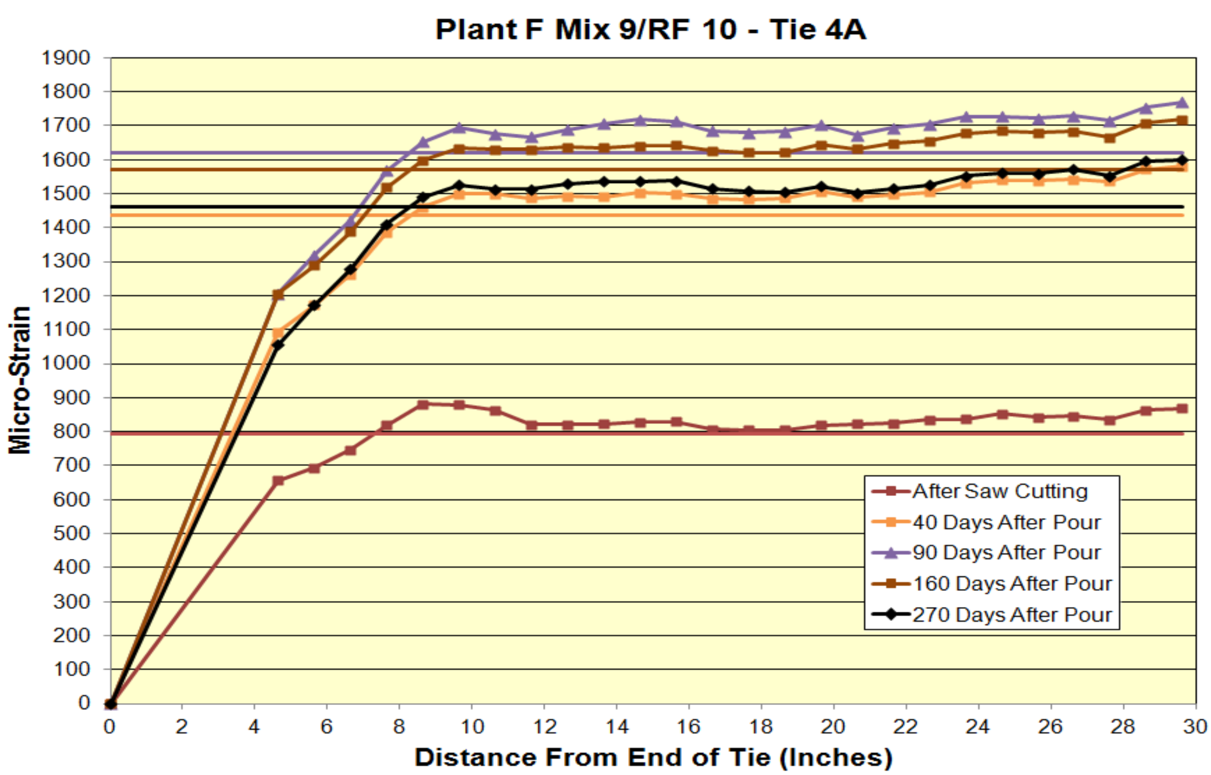

Figure F.42 Long-term transfer length of Plant F Mix 9/RF 10 Tie 4A

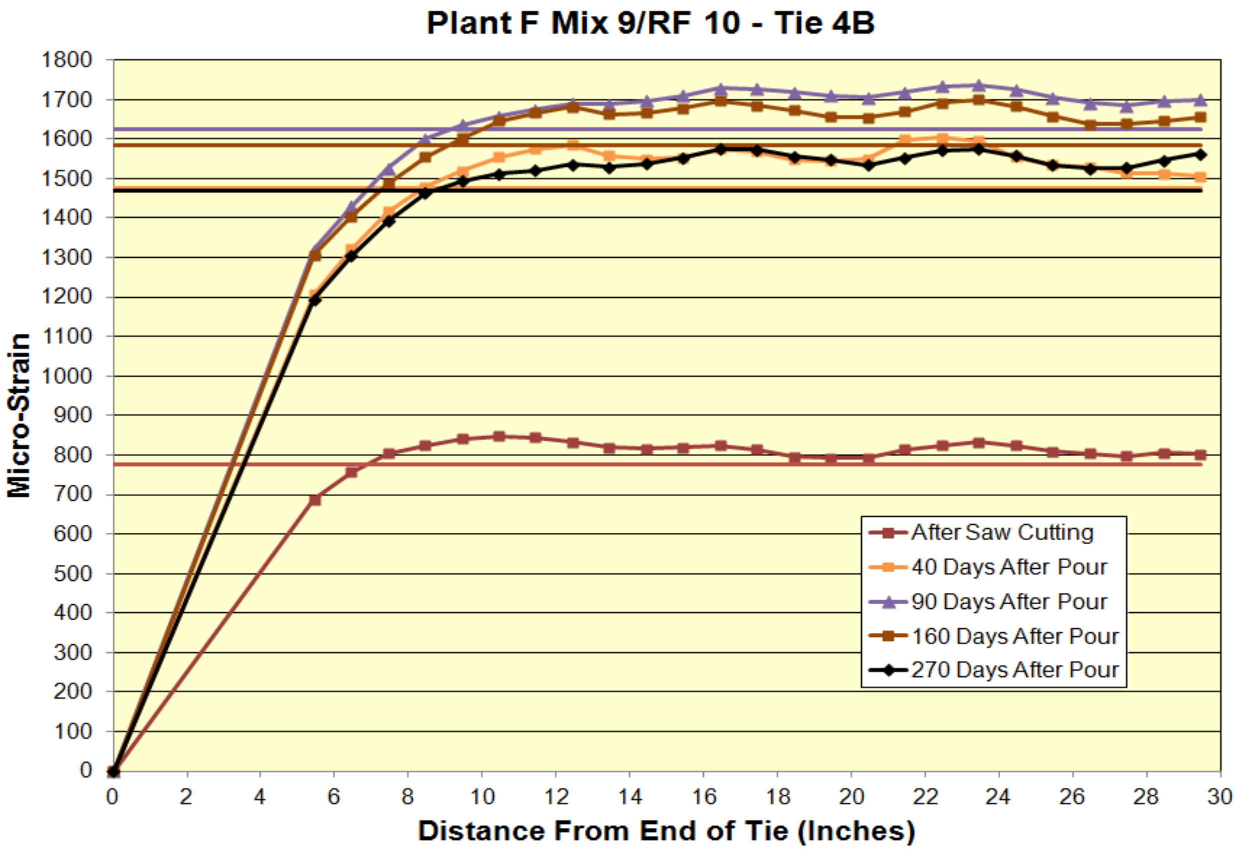

Figure F.43 Long-term transfer length of Plant F Mix 9/RF 10 Tie 4B